Multi-carrier CDMA using convolutional coding and interference cancellation

Maxey, Joshua James

Award date:
1997

Awarding institution:
University of Bath

MULTI-CARRIER DS-CDMA USING CONVOLUTIONAL CODING AND INTERFERENCE CANCELLATION

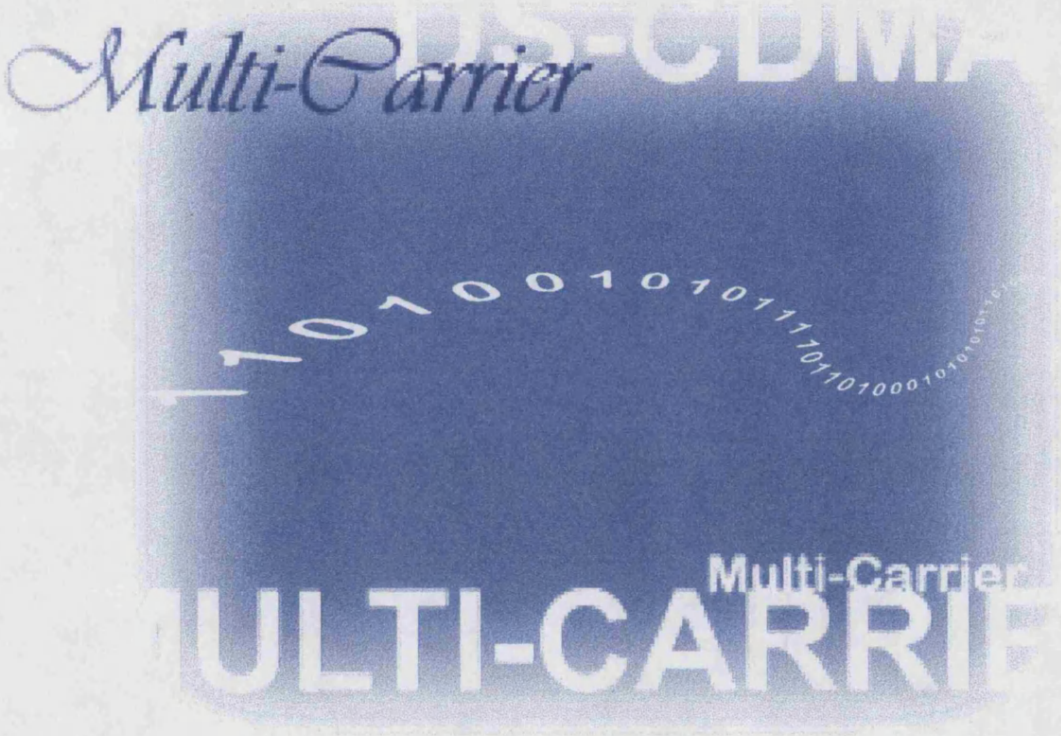

Joshua James Maxey

BATH UNIVERSITY

November 1997

MULTI-CARRIER CDMA USING CONVOLUTIONAL CODING AND INTERFERENCE CANCELLATION

Submitted by

Joshua James Maxey

for the degree of PhD

of The University of Bath

1997

COPYRIGHT

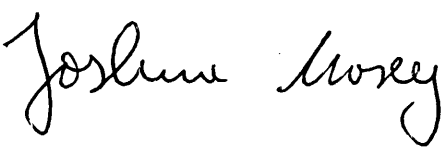

ProQuest LLC
789 East Eisenhower Parkway
P.O. Box 1346
Ann Arbor, MI 48106-1346

ACKNOWLEDGEMENTS

Many thanks are owed to my supervisor Dr. Richard Ormondroyd for the continuing encouragement throughout the duration of my postgraduate study, his friendly approach and morale boosting fruitful discussions on the field of wireless communications.

I also wish to thank Mr. Keith Edwards from NORTEL for his provision of sponsorship for this project and his invaluable insight into alternative applications of such a diverse field.

Finally, thanks go to all my other friends, both within the University of Bath and outside who are too numerous to list here, but who have made my years of research an enjoyable and entirely worthwhile experience.

PUBLICATIONS & PATENTS

The author has published the following papers and patents as part of the work presented in this thesis:

1) Maxey, J J and Ormondroyd, R F, "Performance of Low-Rate Orthogonal Convolutional Codes in DS-CDMA Applications", *IEEE Transactions on Vehicular Technology*, Vol. 46, No.2, May 1997

2) Maxey, J J, and Ormondroyd, R F, "Optimisation of orthogonal low-rate convolutional codes in a DS-CDMA system", *IEEE/URSI Conference Proceedings of ISSSE'95*, Vol. 95TH8047, pp. 493-496, 1995

3) Maxey, J J, and Ormondroyd, R F, "A high performance CDMA cellular radio system based on orthogonal low-rate convolutional coding", *IEE International Conference on Radio Receivers and Associated Systems*, Conference Proc. Vol.414, pp.17-21, 1995

4) Maxey, J J, and Ormondroyd, R F, "Low-Rate Orthogonal Convolutional Coded DS-CDMA using Non-Coherent Multi-Carrier Modulation over the AWGN and Rayleigh Faded Channel", *IEEE Conference Proceedings of ISSSTA'96*, Vol. 2, pp.575-579, 1996

5) Maxey, J J, Ormondroyd, R F and Edwards, K, "Evaluation of a fixed wireless access DS-CDMA system employing low-rate orthogonal convolutional codes", *5th European Conference on Fixed Radio Systems and Networks*, Bologna, Italy, 14-17th May, pp. 277-282, 1996

6) Maxey, J J, and Ormondroyd, R F, "Non-coherent differential encoded multi-carrier SS modulation schemes using low-rate orthogonal convolutional coding in frequency selective Rayleigh fading", *IEEE 47th International Vehicular Technology Conference (VTC'97)*, May 1997

7) Ormondroyd, R F, Maxey, J J, and Alsusa, E, "COFDM - An Alternative Multiple Access Strategy for next-generation mobile communications", *IEE Colloquium on Mobile*

Communications Towards the Next Millennium and Beyond, Vol. 1996/115, pp.8/1-8/6, May 1996

8) Ormondroyd, R F, and Maxey, J J, "Comparison of time guard-band and coding strategies for OFDM digital cellular radio in multipath fading", *IEEE 47th International Vehicular Technology Conference (VTC'97)*, May 1997

9) Maxey, J J, and Ormondroyd, R F, "Multi-Carrier CDMA using Convolutional Coding and Interference Cancellation over Fading Channels", *IEEE First International Workshop on Multi-Carrier Spread-Spectrum, DLR Oberpfaffenhofen*, Germany, April 24-25, 1997

10) Maxey, J J, and Ormondroyd, R F, "A Downlink and Uplink performance comparison of Multi-Carrier DS-CDMA Systems using Coding and Interference Cancellation", *2. OFDM Fachgespräch*, Braunschweig, Germany, September 1997

11) Maxey, JJ, "An adaptive constraint length hyper-orthogonal convolutional coding scheme", *US Patent Pending # 08/961107, October 30, 1997*

The full versions of all published papers are presented at the end of this thesis.

SUMMARY

The work in this thesis has been motivated by the challenges of third generation mobile communication systems and fixed wireless applications using high data rates. In particular, we have investigated receiver structures that employ the relevant coding techniques and channel equalisation strategies in multi-carrier CDMA systems and multipath faded channels.

In fixed wireless access (FWA) and mobile cellular systems it has been shown that the correlation statistics on the link level between the subscriber and basestation can have dramatic effects on the inter-cell interference. The use of highly directional antennas and stationary users has shown that the effects of shadowing depend heavily on the correlation of the fading signals on the uplink. The anticipated inter-cell frequency re-use factor for realistic values of decay index (2 to 4) will unlikely drop below 0.85. For mobile cellular applications it has been found that this value can be as low as 0.2, therefore having a significant effect on the overall cellular capacity.

The performance of low-rate orthogonal convolutional codes and novel low-rate hyper-orthogonal codes has been studied in a single-user and multi-user AWGN environment and multipath Rayleigh faded channels. Considerable performance improvements have been found for both coding strategies compared to conventional rate ½ convolutional coding strategies.

The simulation of a rate 1/32, constraint length 5 low-rate orthogonal convolutional coding scheme in a 4-path Rayleigh faded channel with a Doppler of 300Hz has shown to provide extremely good coding gains. Compared to uncoded faded channels, a coding gain in the order of 6dB was found for bit-error rates of 10^{-5} using low-rate orthogonal convolutional coding structures with BPSK modulation. Using low-rate hyper-orthogonal coding with a constraint length of 8 and rate 1/64 has shown to increase the coding gain to over 10dB at bit-error rates of 10^{-6}. Of course, this is achieved at the expense of increased hardware complexity.

The primary advantage of MC-CDMA is its ability to operate in a high user rate system that has only a limited system bandwidth available for spreading. Because MC-CDMA strategically tries to reduce the effects of multi-user interference through sub-carriers and guard intervals, MC-CDMA does not become less efficient in terms of bits/s/Hz when the spreading factor is reduced, as in DS-CDMA systems. Therefore, the goal of MC-CDMA is to address the area of weakness of the DS-CDMA system by supporting higher data-rates. Since a MC-CDMA system

is able to adjust the number of sub-carriers per user signal, MC-CDMA is highly flexible with respect to variable rate traffic. This thesis has analysed and simulated the effects of imperfect channel estimation, convolutional coding, time and frequency diversity requirements, equalisation, time-guard bands and interference cancellation using MC-CDMA on the uplink and downlink.

The use of guard bands has shown that the irreducible bit-error rate dominates the performance degradation in a multipath faded channel when using convolutional coding and insufficient time-guard band lengths. The use of interference cancellation schemes may only provide reasonable capacity gains on the uplink if the channel parameters can be estimated accurately and when the level of interference from other users is relatively low. On the downlink, however, the use of interference cancellation presents little problem and serves to improve the capacity at all levels of E_b/N_o and full user capacity.

CONTENTS

1. INTRODUCTION 1

1.1 FUTURE MOBILE COMMUNICATIONS 2
1.2 MULTIPLE ACCESS TECHNIQUES 4
1.3 MAIN AREAS OF ORIGINAL WORK 8
1.4 TEXT OUTLINE 9
1.5 REFERENCES 11

2. CHANNEL MODEL AND CHARACTERISTICS 14

2.1 THE MOBILE PROPAGATION ENVIRONMENT 15
2.2 FAST FADING 17
2.3 SLOW FADING 20
2.4 CHARACTERISATION OF THE MOBILE RADIO CHANNEL 21
2.4.1 Time-selective fading 21
2.4.2 Frequency-selective multipath fading 23
2.4.3 Approximation of the delay power profiles by discrete taps 25
2.5 EQUIVALENT BASEBAND MODEL OF CHANNEL 28
2.6 A DISCRETE-TIME MODEL FOR A CHANNEL WITH ISI 28
2.7 SUMMARY 31
2.8 REFERENCES 33

3. CELLULAR APPLICATIONS 35

3.1 INTRODUCTION 36
3.2 INTRODUCTION TO FWA SYSTEMS 36
3.3 INTER-CELL INTERFERENCE ANALYSIS 39
3.4 FWA INTERFERENCE STATISTICS 43
3.4.1 Interference Rejection through Directional Antenna 43
3.4.2 Inter-Cell Interference Analysis including shadowing 46
3.5 CELLULAR MOBILE SYSTEMS 53
3.6 SUMMARY 56
3.7 REFERENCES 57

4. DIRECT-SEQUENCE SPREAD-SPECTRUM 61

4.1 INTRODUCTION 62
4.2 SIGNATURE WAVEFORM GENERATION 64
4.3 MODULATION SCHEMES 67
4.4 FORWARD ERROR CORRECTION CODING 68
4.4.1 Convolutional Codes 69
4.4.2 Low-Rate Orthogonal Convolutional Codes 73
4.4.3 Hyper-Orthogonal Codes and State Diagrams 81
4.5 DEMODULATION AND DECODING 87
4.5.1 Diversity RAKE Receivers 87
4.5.2 The Viterbi Algorithm 90
4.6 SUMMARY 91
4.7 REFERENCES 93

5. MULTI-USER DS-CDMA SYSTEMS 96

5.1 INTRODUCTION 97
5.2 DS-CDMA UPLINK ANALYSIS 97
5.2.1 DS-CDMA bit-error rate calculations 100
5.2.2 Bit-error probability in faded multi-user channels 105
5.2.3 The Near-Far Problem 108
5.2.4 Asymptotic multi-user efficiency 109
5.3 DS-CDMA DOWNLINK ANALYSIS 110
5.3.1 AWGN Channel Performance 112
5.3.2 Frequency Selective Fading Channel 112
5.4 TECHNIQUES TO COMBAT MULTI-USER INTERFERENCE 114
5.4.1 Power control 114
5.4.2 Diversity 115
5.4.3 Adaptive antennas 115
5.4.4 Interference cancellation 116
5.5 SUMMARY 117
5.6 REFERENCES 120

6. LOW-RATE ORTHOGONAL CONVOLUTIONAL CODES 123

6.1 INTRODUCTION 124
6.2 THEORETICAL BASIS 125
6.2.1 AWGN channels 125
6.2.2 LROCC performance in L-path Rayleigh fading 129
6.3 SIMULATION RESULTS 132
6.3.1 AWGN performance 132
6.3.2 Super- and Hyper-Orthogonal Convolutional Codes 134
6.3.3 Multi-user environment 136
6.3.4 Multipath Rayleigh faded channels 139
6.4 SUMMARY 142
6.5 REFERENCES 144

7. ORTHOGONAL FREQUENCY DIVISION MULTIPLEX 147

7.1 INTRODUCTION 148
7.2 THEORETICAL ANALYSIS 152
7.3 SPECTRAL EFFICIENCY 154
7.4 ORTHOGONAL BASIS FUNCTIONS 155
7.5 DISCRETE FOURIER TRANSFORM 156
7.6 LINEAR CHANNEL ANALYSIS 157
7.7 GUARD-BAND INTERVAL ANALYSIS 159
7.7.1 Convolutional Coding Techniques 164
7.8 ASYNCHRONOUS OFDM IN A FADING CHANNEL 167
7.9 ERROR PROBABILITY 170
7.10 OFDM CHANNEL ESTIMATION 172
7.11 SUMMARY 178
7.12 REFERENCES 180

8. MULTI-CARRIER CDMA SYSTEMS 184

8.1 INTRODUCTION 185
8.2 CURRENT SYSTEM PROPOSALS 186
8.3 COHERENT BPSK DESIGN 191

8.4 NON-COHERENT DPSK DESIGN 193
8.5 SIMULATION APPROACH 197
8.6 SYSTEM AND CHANNEL CONFIGURATION 198
8.7 PERFORMANCE RESULTS 198
8.8 SUMMARY 201
8.9 REFERENCES 204

9. MULTI-USER MC-CDMA SYSTEMS 207

9.1 INTRODUCTION 208
9.2 INDEPENDENT FADING CHANNEL 208
9.3 MULTI-USER MC-CDMA SYSTEM 210
9.4 EQUALISATION AND DETECTION 212
9.4.1 Equal Gain Combining (EGC) *212*
9.4.2 Zero-Forcing (ZF) *213*
9.4.3 Controlled Equalisation (CE) *213*
9.4.4 Maximum Ratio Combining (MRC) *214*
9.4.5 Minimum Mean-Square Error (MMSE) Detection *216*
9.4.6 Maximum Likelihood Detection (MLD) *217*
9.5 SUCCESSIVE INTERFERENCE CANCELLATION 218
9.6 PARALLEL INTERFERENCE CANCELLATION 221
9.6.1 Downlink Model *221*
9.6.2 Uplink Model *229*
9.7 SUMMARY 234
9.8 REFERENCES 237

10. CAPACITY ANALYSIS 241

10.1 OVERVIEW 242
10.1.1 Adaptive Time Divison Multiple Access (ATDMA) *243*
10.1.2 Capacity of an Adaptive TDMA FWA System *246*
10.1.3 Capacity of a DS-CDMA FWA System *250*
10.2 SUMMARY 254
10.3 REFERENCES 257

11. CONCLUSIONS & FUTURE WORK 261

11.1 CONCLUSIONS 262
11.1.1 Low-Rate Hyper-Orthogonal Convolutional Coding: Rationale *262*
11.1.2 Low-Rate Hyper-Orthogonal Convolutional Coding: Performance *263*
11.1.3 Multi-Carrier CDMA: Rationale *264*
11.1.4 Multi-Carrier CDMA: Performance *266*
11.2 CONCLUDING REMARKS 269
11.3 FUTURE WORK 271
11.3.1 Synchronisation *271*
11.3.2 Reduction of the Crest Factor *271*
11.3.3 Wavelet Based Transmission *272*
11.3.4 Decoding Strategies *272*
11.3.5 Channel Estimation *272*
11.4 REFERENCES 274

APPENDIX A 275

APPENDIX B 279

APPENDIX C 284

APPENDIX D.....288

PUBLISHED PAPERS.....291

LIST OF ABBREVIATIONS

AMPS	Advanced Mobile Phone Service
ATDMA	Advanced (or Adaptive) Time Division Multiple Access
AWGN	Additive White Gaussian Noise
BER	Bit-Error Rate
BPSK	Binary Phase Shift Keying
BS	Basestation
CC	Convoltuional Coding
CCI	Co-Channel Interference
CDMA	Code Division Multiple Access
CE	Controlled Equalisation
COFDM	Coded Orthogonal Frequency Division Multiplex
COST	Committee of Standards
CSI	Channel State Information
DAB	Digital Audio Broadcast
DCS1800	Digital Communication System
DFT	Discrete Fourier Transform
DMC	Discrete Memoryless Channel
DPSK	Differential Phase Shift Keying
DS	Direct Sequence
DS-CDMA	Direct-Sequence Code-Division Multiple Access
DTTB	Digital Terrestrial Television Broadcasting
DWT	Discrete Walsh Transform
EGC	Equal Gain Combining
FDMA	Frequency Division Multiple Access

FEC	Forward Error Correction
FFT	Fast Fourier Transform
FPLMTS	Future Public Land Mobile Telecommunications System
FWA	Fixed Wireless Access
GSM	Global System for Mobile Communications
GWSSUS	Gaussian Wide-Sense Stationary Uncorrelated Scattering
IC	Interference Cancellation
ICI	Inter-Carrier Interference
IDFT	Inverse Discrete Fourier Transform
IFFT	Inverse Fast Fourier Transform
ISDN	International Standard for Digital Networks
ISI	Inter-Symbol Interference
LCC	Lost Call Cleared
LCH	Lost Call Held
LOS	Line Of Sight
LPF	Low-Pass Filter
LRHOCC	Low-Rate Hyper Orthogonal Convolutional Coding
LROCC	Low-Rate Orthogonal Convolutional Codes
MAI	Multiple Access Interference
MAIC	Multiple Access Interference Cancellation
MC	Multi-Carrier
MC-CDMA	Multi-Carrier Code Division Multiple Access
MCM	Multi-Carrier Modulation
MC-SS	Multi-Carrier Spread Spectrum
MLD	Maximum Likelihood Detection
MMSE	Minimum Mean Square Error
MRC	Maximum Ratio Combining
MT-CDMA	Multi-Tone Code Division Multiple Access

NMT	Nordic Mobile Telephone
OFDM	Orthogonal Frequency Division Multiplex
PCS	Personal Communication Services
PDA	Personal Digital Assistant
PDC	Personal Digital Communications
PMR	Private Mobile Radio
PN	Pseudo-Random Noise Sequence
PRMA	Packet Reservation Multiple Access
PSK	Phase Shift Keying
QAM	Quadrature Amplitude Modulation
QPSK	Quaternary Phase Shift Keying
SNR	Signal to Noise Ratio
SS	Spread-Spectrum
SSMA	Spread-Spectrum Multiple Access
TACS	Total Access Communications System
TDMA	Time Division Multiple Access
UMTS	Universal Mobile Telecommunications System
VA	Viterbi Algorithm
WSS	Wide-Sense Stationary
ZF	Zero-forcing

LIST OF SYMBOLS

Chapter 2: Channel Model and Characteristics

V	Vehicle speed
λ	Wavelength of signal
T_g	Delay spread
R_D	Transmission rate
$r(t)$	Received signal
$A(t)$	Envelope of faded signal
$\theta(t)$	Phase of faded signal
w_o	Carrier frequency
T_c, T_s	Gaussian random processes
$p(x)$	Normal distribution of variable x
σ	Standard deviation of distribution
L	Number of propagation paths
ϕ_l	Phase of the lth path
w_l	Doppler shift of path l
v	Relative velocity of transmitter to receiver
γ_l	Arrival angle of the lth ray
$p(r)$	Rayleigh distribution of varaible r
$p(z)$	Ricean distribution of variable z
$I_o(x)$	Modified Bessel function of zero order and the first kind
K	Ratio of power in LOS component to scattered signal components
y	Standard normal distribution
$y2$	Log-normal distribution
f_d	Maximum Doppler frequency shift
$R(\tau)$	Auto-correlation function at delay τ
c	Speed of light
f_o	Frequency of the transmitted signal
$S(f)$	Doppler spectrum at frequency f
τ_c	Coherence time (correlation time)
A	Threshold value for a fade
$\bar{t}$	Average duration of a fade below threshold level A

$P_m(\tau_l)$	Average power delay profile
τ_l	Propagation delay from the transmitter to receiver
d_m	Mean excess delay
τ_A	First arrival delay
s_m	RMS delay spread
Δf	Coherence bandwidth
$h(t)$	Channel impulse response
α_l	Amplitude of path l
$\overline{\tau^2}$	Mean-square excess delay
T_b	Data bit rate
$g(t)$	Transmitter impulse response
$c(t)$	Channel impulse response
s_k	Discrete-time information sequence
y_k	Discrete-time output sequence of channel
η_k	Noise sequence
N_o	Noise power spectral density
f_s	Sampling frequency

Chapter 3: Cellular Applications

$R_{i,j}$	Distance of mobile j to unwanted basestation i
$r_{i,j}$	Distance of mobile j to wanted basestation i
D	Distance between basestations
$P_{i,j}$	Transmitted power from ith subscriber to basestation j
P	Total power received at basestation
N_u	Number of active users
α	Decay index
$I_{i,j}$	Interference from ith user to jth basestation
r_d	Radius of cell
θ	Angle between $R_{i,j}$ and $r_{i,j}$
A	Area of cell
N_c	Total number of cells
F	Interference degradation factor
N_o	Noise power spectral density
E_b	Energy per bit
W	Bandwidth occupied by signal

R_b	Data rate of user
φ	Angle of antenna pattern
G_A	Antenna gain
Erl	Erlang traffic capacity
R	Code rate of convolutional encoder
K	Constraint length of convolutional encoder
N	Number of available channels
P_{ber}	Bit-error probability
N_{out}	Number of antenna ouputs
L	Difference in path loss
r_1	Distance of interfering subscriber to its own basestation
r_2	Distance of interfering subscriber to wanted basestation
m	Frequency re-use pattern
C	Carrier Power
I	Interference/noise power
P_r	Received power
P_t	Transmitted power
ϕ	Gaussian randomly distributed variable
μ	Mean value
σ	Standard deviation
ξ	Shadowing component common to all basestations
a,b	Constants representing correlation statistics
R_l	Largest radius of hexagon
R_N	Arbitrary radius level for a given θ
$N_{density}$	User density for hexagonal cell
γ	Valid integrand angle
I_s	Total outer-cell interference including effects of shadowing
I_{total}	Total outer-cell interference from one cell in hexagonal cell structure
$h(t)$	Channel impulse response
k	Re-use distance ratio
$\sigma_{i,r}$	Sum of the possible first interfering active paths for cell i
ε	TDMA efficiency gain
P_b	Probability of a blocked call
λ/μ	Erlang statistics
V	Voice activity factor
T	Antenna diversity at the basestation

S_{av}	Minimum required average power level in threshold condition
B	Boltzman constant
T_o	Environmental temperature
F_N	Noise figure of the receiver
F_m	Inter-cell degradation factor excluding shadowing effects
F	Inter-cell degradation factor including shadowing effects

Chapter 4: DS-CDMA Systems

N_u	Number of active users
τ	Time delay
$R(\tau)$	Auto-correlation function at delay τ
N	Spreading sequence length
$2t_u$	Length of auto-correlation peak
m	Order of maximal length sequence
$\boldsymbol{a}, \boldsymbol{b}$	m-sequences
$t(m)$	Off-peak auto correlation functions
n	Number of chip durations
K	Constraint length of convolutional code
R	Code rate
Y	Information input sequence
X	Encoder output sequence
g	Encoder impulse response
D	Unit delay
d_{free}	Free distance of convolutional code
P_z	Probability of error for path length z
c_z	Weight measurement for path length z
p	Probability of error
T	Data bit duration
k	Order of Hadamard matrix
A	Amplitude of signal
$S(w)$	Frequency response at frequency w
T_s	Symbol period
$r(t)$	Modulated signal
$d(t)$	Bipolar data transmitted at time t
w_o	Carrier frequency
T_b	Data bit period

$d'(t)$ Differentially encoded data stream

T_c Chip duration

T_m Maximum delay spread

Δf Coherence bandwidth

$\delta(.)$ Unit impulse

$p(t)$ User signature waveform

e_l Signal strength estimate of lth path

γ_l Average SNR for lth path

α_l Magnitude of path l

L Number of multipath

P_e Bit-error probability

$r_i(t)$ Input sequence at depth i in the trellis

$s_j(t)$ jth expected output sequence from Hadamard encoder

$v_{i,j}$ Metric increment at depth for state j

B State transition due to input of one

W Weight measurement of state transition

$T(W,B)$ Generating transfer function

H_k Hadamard matrix of order k

K_T Total constraint length of hyper-orthogonal encoder

Chapter 5: Multi-User DS-CDMA Systems

N_u Number of active users

$d_i(t)$ Data sequence of user i

T_s Symbol period

$p_i(t)$ Spreading sequence of user i

T_c Chip period

N Spreading sequence length

$r(t)$ Broadband received signal

$g_i(t)$ Matched filter output of user i

$s_i(t)$ Transmitted signal of user i

w_o Carrier frequency

P_i Transmitted power of user i

θ_i Random phase of the ith carrier

A_i Received signal amplitude of user i

τ_i Transmission delay associated with the ith user

$n(t)$	Additive white Gaussian noise
L	Number of multipath components
α_l	Amplitude of the lth element in an impulse response
ϕ_l	Phase of the lth element in an impulse response
$\delta(t)$	Impulse at time t
$h_i(t)$	Lowpass equivalent complex channel impulse response of ith user
P_e	Bit-error probability
E_b	Energy per bit
N_o	Noise power spectral density
$Q(.)$	Gaussian integral function
A	Bipolar matched filter output
I	Magnitude of multiple access interference
P_{BER}	Bit-error rate
$U(.)$	Unit step function
$b_{i,n}$	nth random data bit of the ith user
$C_{i,j}$	Cross-correlation between signature waveforms i and j
I_o	Modified Bessel function of zero order
J_o	Sum of the square of all interfering cross-correlation terms
ρ	Minimising variable of Chernoff bound
$\delta(\cdot)$	Dirac impulse
$y_i(t)$	Channel output sequence
$Z_{i,l}$	Decision statistic of receiver i locked onto lth path
$R_{l,i}(\tau_{l,i})$	Continuous time partial cross-correlation of the ith and 1st spectral waveforms
P_{sig}	Average signal power
T_b	Data bit duration
P_{noise}	Gaussian noise power
σ^2_{int}	Variance of other user interference
$\sigma_{l,i}^2$	Power of lth faded Ricean path of user i
c^2	Power of LOS component
P_b	Bit-error probability
K_f	Ratio of power in LOS component to scattered signal components
K_{Max}	Maximum number of users that can be supported
ξ_i	Multiuser asymptotic efficiency for user i
η	Thermal noise power
Δf	Coherence bandwidth
γ	SNR per bit

Chapter 6: LROCC Performance

K	Constraint length
R	Code Rate
d_{free}	Free distance of convolutional code
P_z	Path bit-error probability
C_z	Path distance function in trellis
P_{BER}	Bit-error rate
B	Trellis transition caused by data input of one
W	Weight measurement for branch metric
Z	Exponential of the signal-to-noise ratio
I, Q	Real and Imaginary components of the channel
Y_I, Y_Q	Demodulated input variables, real and imaginary
L	Number of multipath components
λ	Amplitude of each independent Rayleigh faded path
$p(\lambda)$	Probability function of Rayleigh faded signal of amplitude λ
E_c	Chip Energy
σ	Standard deviation of the fading process
E_{avg}	Average chip energy
M	Mean signal power
J	Number of symbols per data bit in the Hadamard shift register
$P_c(z)$	Probability of a correct signal
$P_I(z)$	Probability of an incorrect signal
E_s	Average symbol energy per path
E_b	Total energy per bit
I_o	Interference energy
x_d	Incorrect branch metric at depth d
y_d	Correct branch metric at depth d
P_d	Probability of wrong path decision at depth d
p	Minimising variable of the Chernoff function
U	Signal to noise ratio per path
K_1	Number of shift registers in front end of Hadamard encoder
K_2	Number of shift registers directly linked to Hadamard encoder

Chapter 7: Orthogonal Frequency Division Multiplex

T_s	Symbol duration
N	Number of parallel sub-carriers
R	Input data rate
f_o	Lowest sub-carrier frequency
T_b	Effective OFDM block duration (data-bit period)
f_n	Frequency of the nth sub-carrier
$d_{n,i}$	Symbol of the nth sub-channel at time interval iT_b
$s(t)$	Multi-carrier transmitted signal
$p(t)$	Response of the transmitter filter
$S(f)$	Frequency spectrum of signal $s(t)$
B_{MC}	Bandwidth of baseband multi-carrier signal
$\varphi_n(t)$	Orthogonal basis function for the nth sub-carrier
$H(f)$	Linear channel transfer function
H_n	Magnitude of channel transfer function at frequency n
$\phi(n)$	Phase response of channel transfer function at frequency n
$r(t)$	Time domain received signal
z_i	Discrete time sampled ith output at the DFT
$\hat{d}_i$	ith data estimate
$\alpha(f)$	Slope of the magnitude of channel transfer function at frequency f
$t_{gn}(f)$	Group delay of the channel at frequency f
$h(t)$	Channel impulse response
$n(t)$	AWGN with power spectral density $N_o/2$
L	Number of multipath components
a_l	Amplitude of multipath component
τ_l	Time of arrival of multipath component
θ_l	Phase of multipath component
$R_{n,k}(\tau_l)$	Partial cross-correlation function of signals at frequency n and k at time τ_l
T_g	Guard interval
T_b'	Effective symbol duration with guard interval
Δf	Carrier separation
P_b	Bit-error probability
σ_{ISI}^2	Variance of inter-symbol interference
σ_{ICI}^2	Variance of inter-carrier interference
σ_{al}^2	Expected value of the amplitude of multipath component a_l
T	Number of grouped sub-carriers

M	Number of pilot sub-carriers
$X(k)$	OFDM modulated signal at sub-carrier k
s_k	Sampled transmitted sequence
$H(k)$	FFT of the baseband equivalent channel transfer function
$I(k)$	ICI component in received signal
$W(k)$	Fourier transform of the AWGN component
$Y(k)$	Sampled output of the FFT in the receiver
c	Pilot signal stregth
$G_M(p)$	Transform domain signal at 'frequency' p of length M
$G_M'(p)$	Low-pass filtered transform domain signal at 'frequency' p of length M
$G_N'(p)$	Zero padded to length N version of $G_M'(p)$
p	Transform-domain index
p_c	Cut-off 'frequency' of transform domain filter

Chapter 8: MC-CDMA Systems

N	Number of sub-carriers
T_b	Data bit duration
t	Time
d_i	Data bit of user i
c_i	Spreading code assigned to user i
f_o	Lowest sub-carrier frequency
$s_i(t)$	Continous time-domain output signal for user i
$s_i(n)$	Discrete-time output signal for user i
$g_i(n)$	Equaliser co-efficients of user i
K	Constraint length of convolutional code
T_s	Symbol period
T_c	Chip duration
$y(n)$	Output chip sequence of LROCC
$x(k)$	Output sequence at sub-carrier k
f_n	Sub-carrier frequency
Δt	Arbitrary time-interval
t_k	Time after k time intervals
$h(n)$	Complex channel fading sequence
$p(n)$	Rayleigh distributed attenuation co-efficient
$\phi(n)$	Uniformly distributed phase distortion
$H(k)$	Channel frequency response at sub-carrier k

$\mu(n)$ Complex Gaussian noise

$Y(k)$ Frequency-domain signal of $y(n)$

$g(n)$ FFT demodulator input

$g'(n)$ DPSK demodulator output

f_d Doppler frequency

L Number of multipath components

Chapter 9: OFDM-CDMA Systems

N Number of sub-carriers

Δ Length of guard interval (cyclic extension)

$\boldsymbol{d}$ Data bit vector

$\boldsymbol{S}$ Transmitted sequence vector after coding

$\boldsymbol{c}$ Code vector of length N

$\boldsymbol{s}$ Modulated multi-carrier signal (complex vector)

$\boldsymbol{H}$ Discrete time channel transfer function

$\boldsymbol{n}$ Complex AWGN vector

$\boldsymbol{r}$ Faded but noiseless received signal vector

$\boldsymbol{g}$ Received complex signal vector

$\boldsymbol{u}$ Demodulated signal vector

$\boldsymbol{y}$ Detected signal vector

$\boldsymbol{G}$ Complex equalisation matrix

$s(t)$ Complex time-domain transmitted signal

f_l Sub-carrier at frequency l

d_l lth data bit

c_l Spreading code sequence lth chip

f_o Lowest sub-carrier frequency

T_s Symbol duration

N_u Number of active users

M Spreading sequence length

Q Number of blocks per user per OFDM symbol

D Number of grouped blocks per OFDM symbol

$h_{l,l}$ Diagonal matrix value of channel transfer matrix $\boldsymbol{H}$

$g_{l,l}$ Diagonal matrix value of equaliser matrix $\boldsymbol{G}$

p_{thres} Threshold level for controlled equalisation

E_b Energy per bit

N_o Noise power spectral density

σ_n^2	Variance of AWGN
σ_a^2	Variance of transmitted data symbol
δ_i^2	Euclidean distance of sequence i
$d_i'(t)$	Data bit estimate of stage i
$y(i)$	Discrete time sampled ith signal estimate
R	Code rate of convolutional encoder
T_{cod}	Encoded symbol duration
N_B	Maximum capacity of the basestation
d	Sub-grouping block index
$\boldsymbol{e}$	Encoded symbol sequence vector
$\boldsymbol{S_d}$	Transmission vector for block d
$\boldsymbol{V}$	Complex vector sequence after OFDM modulation
$x(t)$	Transmitted multi-carrier signal
$s_{q,d,l}$	lth component of $\boldsymbol{S_d}$ of the qth data bit
$y(t)$	Received time-domain multi-carrier signal
ρ	Attenuation of complex channel fading characteristic
ϕ	Phase shift of complex channel fading characteristic
$n(t)$	AWGN component
$\boldsymbol{N_d}$	Complex noise vector for dth block at the receiver
$\boldsymbol{R}'$	Complex signal vector before detection
$\boldsymbol{d}'$	Estimate of transmitted data bit
$y'(t)$	Estimated interference signal
$\boldsymbol{e}'$	Estimated encoded output sequence of $\boldsymbol{d}'$
T_c	Chip rate
K	Constraint length of convolutional encoder

CHAPTER 1:

INTRODUCTION

1.1 Future Mobile Communications

The demand for wireless communications is driving a rapid advance in the technologies that provide these services and has become a significant area of growth within the last decade. There is currently a diverse range of products and services on the market, but cellular and personal communication services (PCS) radio networks probably have the highest public profile. Some 750,000 new subscribers are joining the European digital networks every month [1] and nearly a million hours of calls are made daily. The future size of this fast expanding market is estimated at 100 million subscribers [1] in Europe alone by the end of the decade. For successful network operators and equipment suppliers rewards are potentially high and as a consequence, competition in the mobile communications market place is fierce.

At present, the cellular network comprises the 'first generation' analogue systems such as AMPS, TACS[1] and NMT, which are now being superseded by second generation digital systems, including D-AMPS, GSM, PDC, CDMA and DCS1800. The pan-European GSM (Global System for Mobile Communications) is typical of second generation systems, allowing the user to roam through most countries in Europe with the same handset in addition to providing limited paging, fax and data facilities. The American equivalent standard is based on the North American IS-54 access protocols. Analogue systems still account for the majority of market share with over a million subscribers to the two major network operators in the UK alone. However, within the next few years second generation systems are likely to dominate the market.

For the year 2000 and beyond, increased numbers of users and the growing demand for personal communication networks which can combine voice, data, fax and paging facilities into a single portable handset will require third generation mobile systems such as the Universal Mobile Telecommunications System (UMTS) in Europe and the equivalent IMT2000 in the United States. The progression from the initial first generation systems, launched in the UK in January 1985, to third generation has been expedious and spans less than two decades.

[1] The UK will in fact discontinue its analogue system by the end of 2005.

UMTS is a communications concept which will attempt to integrate the disparate services currently provided on private mobile radio (PMR), cordless systems, and cellular radio into a common standard. It is expected that UMTS will provide the following services to the user [2]:

- Existing mobile and fixed telecommunications services at data rates of up to 2 Mb/s.
- Pan-European mobile navigation, vehicle location and traffic information services.
- Handsets capable of being used anywhere; in rural areas, within urban office environments and which support transparent roaming from one European country to another and possibly global roaming at a later date.
- The range of UMTS receivers available will extend from low cost pocket handsets to sophisticated terminals supporting video and high data rate services.
- It could be likely that users will purchase bandwidth, rather than time, on the system, with low-rate voice communications at the bottom of the tariff range and video and data services the most expensive.
- Friendly inter-operator roaming will ensure that the user receives a single bill from their service provider, irrespective of which country and whose network they have been using.

The technological issues that must be resolved in order to provide the user with these services are extensive. The decision on which type of multiple access technique to employ in UMTS has now finally been completed, with a decision to use a similar system to the wideband CDMA (W-CDMA) as found in the NTT Japan standard and additionally paired with Time-Division CDMA (TD-CDMA).

One of the most daring ventures of the world-wide telecom industry is being launched before the end of the century. Indeed, several international consortia are planning to introduce satellite services with the ultimate telecommunications solution: global connectivity to and from any spot on the earth's surface. In the United States, the goals of IMT2000 are essentially the same as UMTS and a common spectrum of 230 MHz in the 1.885-2.200 GHz band has been allocated to the two systems. The similarity of IMT2000/UMTS opens up the possibility of

truly global wireless communications and several consortiums have to date been formed with the intention of offering global mobile satellite services. Iridium, ICO and Globalstar are all currently in operation[3,4], which all gravitate towards TDMA rather than CDMA.

Globalstar is a consortium that has Qualcomm Inc. of the United States and Vodafone (UK) amongst its many partners. The network is based on a constellation of 48 low Earth orbit satellites which will provide a communications pipeline from one part of the globe to another. Globalstar estimate that the final cost of their system will be $1.8 billion, with call costs roughly equal to that of current US cellular networks. Iridium is a more sophisticated system than Globalstar, as its 66 low Earth orbit satellites will have the capability to hand on calls from one satellite to another. Each satellite will effectively act as a mobile base station, encircling the earth in six low-earth orbital planes at 780km altitude. The consortium is headed by Motorola and has committed $800 million to the project. Inmarsat already operates a satellite communications network, including its Inmarsat C and Inmarsat M services, which have briefcase-sized terminals.

The change which wireless communications is about to undergo has been likened with that which personal computing underwent a few years ago [5]. In the early 1980s, personal computers supported a large number of features and a high degree of functionality, but the level of knowledge required to exploit these features to the full prohibited their use by the layman. With the advent of applications such as Microsoft's Windows, PCs suddenly became far more accessible and personal computing was revolutionised. In wireless communications many of the services that a user might wish for exist at the current time, but it will take a unifying concept, such as IMT2000, to make them accessible to everyone. Ultimately, this worldwide digital telecommunications system will offer wireless telephone and other digital services, such as data transmission, paging facsimile and position location. The phrase *Personal Digital Assistant* (PDA) has been coined to describe the portable device that will integrate all of these communications services.

1.2 Multiple Access Techniques

To provide an efficient service to a large number of simultaneous users places great importance on the multiple access capabilities of the system. Traditionally, each user of a multiple access system is provided with certain resources, such as frequency or time slots, or both, which are

disjoint from those of any other user. In this way, the multiple access channel reduces to a multiplicity of single point-to-point channels, assuming perfect isolation of each user's transmission resources from those of all other users. Each channel's capacity is limited only by the bandwidth and time allotted to it, the degradation caused by background noise, mostly of thermal origin, other-user noise through loss of orthogonality and propagation anomalies, which produce multipath fading and shadowing effects.

While broadcasting is a one-to-many channel, with one transmitter serving many users, multiple access is a many-to-one channel, with one terrestrial base-station or satellite hub station receiving from multiple users. Until the advent of cellular wireless mobile telephony, multiple access systems were limited to one cell. This cell covered either an urban area from a single base-station in a high place, or a larger geographical region (sometimes nation-wide) from a single satellite transponder accessed by only a few earth terminals. In fact, satellites are the "grandfather" of multiple access in wireless radio because they are a single frequency. With the arrival of cellular services, frequency re-use became central to realising multiple access for a much larger user population scattered over many, often contiguous, metropolitan areas.

Transmissions at different frequencies can be rendered mutually orthogonal by suitable frequency domain filtering. This is the most common of all methods of securing mutual orthogonality, and is the basis of frequency division multiple access (FDMA). In the frequency domain it has become commonplace for signals to hop (i.e. be modulated onto carriers which change frequency in discrete jumps in a pre-determined sequence) or chirp (i.e. be modulated onto carriers which change frequency in a continuous fashion with time).

Another method of achieving multiple access over a channel is to make use of sequency domain orthogonality. An extended binary sequence, such as a pseudo random sequence, can be orthogonal to another such if their integral over the sequence period is zero. Thus, if one sequence is made the carrier for a binary digital transmission it can be isolated by another such message by multiplying and integrating over the sequence period. This process of correlation is mathematically closely analogous to frequency domain filtering, which has led to some describing it as filtering in the sequency domain - a space so defined that each sequence has a unique identity within it. Because a sequence will in general require more than a single parameter to define it, the sequency domain is a hyperspace in its most general form. Each unique sequence may be identified as a point in this hyperspace. By contrast, since ordinarily

frequency may be uniquely specified by a single parameter, the frequency domain may be regarded as a one-space, in which each frequency is a point.

Sequency domain orthogonality is the basis of Code Division Multiple Access (CDMA), where a family of mutually orthogonal codes are used to carry messages independently of each other. There are many different variations of Spread-Spectrum Multiple Access (SSMA), but this thesis will only focus on the use of one particular scheme, namely Direct-Sequence Code Division Multiple Access (DS-CDMA).

DS-CDMA techniques are one way to separate all users transmitting in a common channel as long as some specific rules are adhered to. The potential resource used to define a DS-CDMA system is usually measured in terms of the *processing gain* available. In the white noise definition this is given by dividing the total bandwidth by the aggregate data-rate of the system. The orthogonal sequences introduced earlier may therefore be used to spread the bandwidth of the original data to a level proportional to the length of the orthogonal sequence length.

Since all users transmit in the same bandwidth using the same carrier frequency it is convenient to employ such systems for land-mobile wireless radio systems using a universal frequency for every cell, termed *universal frequency re-use*. Of course, for non-stationary channel conditions the problem of determining which basestation the user should be communicating to becomes a problem. As the size of the cells becomes consistently smaller, such as in micro-cellular applications, for example, the problem of hand-offs to neighbouring basestations dominates the capacity of these systems. Therefore, this may present an upper limit on the cell size.

The use of DS-CDMA techniques also requires every user to be received at the same power on the uplink. Otherwise, every user communicating to their own basestation in a cellular environment using the same frequency will "swamp" out the other users in the same cell by transmitting at power levels which may be too high. To determine the attenuation of the channel for every user, the basestation transmits a known pilot tone that is measured by the individual user to adjust their own transmitter power level.

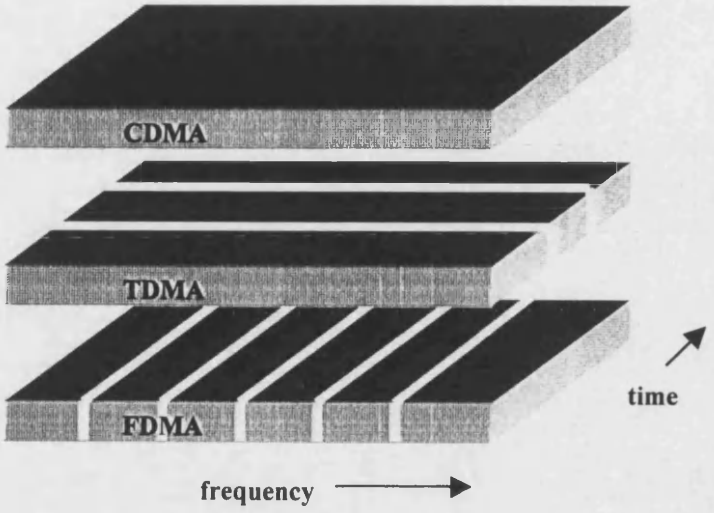

Figure 1-1. Multiple access techniques

Fundamental to the specification of any future mobile communications system is the multiple access technique that will be employed. Frequency division, time division and code division multiple access (FDMA, TDMA and CDMA respectively) have all been proposed at some stage or other for future systems. Each method has its proponents and antagonists, and the debate over which technique offers the greatest bandwidth efficiency, which will support the highest number of users and which has the lowest complexity will continue for some time.

In Europe the considerable effort and expenditure which went into the development of GSM and related standards, which utilise the TDMA access technique, means that many equipment manufacturers and network operators favour TDMA for future systems. It is indisputable, nevertheless, that the future UMTS network will require to support a high data-rate which is progressively seen to increase in future years. With greater mobility requirements of subscribers it will be difficult to satisfy both requirements using traditional methods, calling for more research into alternative and more complex strategies. The harshness of the channel and increased levels of inter-symbol interference are the limiting factor on the data-rates that can be accomplished. With second generation mobile systems, in particular, this requires more complex equalisation and coding strategies, and therefore this thesis pays particular attention to these issues. For next generation digital radio services it will be necessary to suggest simpler alternative solutions that will accomplish these tasks, and current research is focusing on

systems that will be simpler to implement in practice and at the same time provide adequate data throughput.

Multi-carrier orthogonal frequency division multiplexing (OFDM) systems are one alternative solution that is receiving considerable attention with regard to these current issues. These systems solve the problem of increased equaliser complexity by shifting the problem of ISI into the frequency domain, but it looks unlikely that these systems will be able to give any significant gains in high Doppler faded environments. The problem of frequency selectivity in faded channels presents a smaller problem to multi-carrier DS-CDMA (MC-CDMA) systems than conventional DS-CDMA systems, and a variety of papers have shown improved performance results using these methods [7-20]. In this thesis we will investigate some alternative methods to provide insight into what methods may be utilised to give a higher data throughput than conventional designs for fixed and mobile systems.

1.3 Main Areas of Original Work

- Cellular applications of CDMA for FWA systems. This includes a novel study on the correlation statistics of a FWA uplink using highly directional antenna in a hexagonal and circular cell layout.
- Low-rate orthogonal codes have been investigated in more detail for multiple access channels, introducing the concept of a switching matrix for different users.
- Hyper-orthogonal codes are introduced as an alternative method of encoding and spreading the data in a DS-CDMA system. These are simulated in different channel environments.
- The effects of guard-bands in a convolutionally coded OFDM system have been studied and investigated.
- A novel MC-CDMA system has been proposed, using LROCC coding and non-coherent demodulation techniques. Novel equalisation structures together with two-stage interference cancellation techniques have also been proposed for coherent downlink designs. The effects of coding, equalisation, interference cancellation and channel estimation techniques in this context are all novel areas of work.
- Capacity calculations using new results with regard to FWA systems are applied.

1.4 Text Outline

This thesis is concerned with the theory, design and implementation of multi-carrier DS-CDMA systems employing forward error correction techniques such as high-rate convolutional codes, low-rate orthogonal convolutional codes (LROCC) and a novel low-rate hyper-orthogonal convolutional coding scheme. The proposed schemes are intended to provide an alternative solution to conventional single-carrier DS-CDMA systems using pseudo-random noise (PN) spreading sequences and time-domain RAKE receivers.

Chapter 2 serves as an introduction to the mobile channel environment. The statistics of Rayleigh and Ricean fading are presented together with some more fundamental work on the properties of time and frequency selective fading. The categorisation of the different channel properties through the time-delay spread, Doppler spread, rms delay spread, number of taps and the different COST channel models is presented with an outline on how to simulate a continuous power delay profile in the discrete-time domain. A discrete-time model representing a multipath channel with ISI is also shown.

Chapter 3 gives an analysis of the effects of inter-cell interference on the system capacity of a mobile and fixed wireless access system. The use of highly directional antenna for fixed wireless access systems and their effect on the correlation statistics is presented with regards to cellular structures. A comparison between mobile omni-directional and directional antennas is made for different hexagonal and circular cell structures.

Chapter 4 is an introduction to conventional DS-CDMA mobile communications, with particular emphasis on the different convolutional coding techniques that may be employed. A description of the propagation mechanisms in the wireless environment is given for mobile and fixed channels, and in particular, the effect of these on communication through these channels. The relative merits of using coherent and non-coherent modulation and coding techniques are also outlined in this chapter.

In Chapter 5, the concept of using DS-CDMA techniques for multiple-access communications is introduced with some upper bounds on the bit-error rate performance for synchronous and asynchronous channels.

Chapter 6 gives a detailed analysis of the LROCC implementation for FEC techniques with particular emphasis on the natural attributes of such coding schemes within wideband spread-spectrum applications. A novel concept based on a hyper-orthogonal coding scheme is also simulated and shown in comparison to conventional coding techniques. Methods of achieving multiple access using LROCC for fading channels are presented.

Chapter 7 provides an introduction and detailed analysis of OFDM systems and their application to a variety of systems proposed to date. The concept of guard-band intervals, orthogonal basis functions and channel estimation is also introduced here.

Chapter 8 introduces the different implementations of OFDM in direct-sequence spread-spectrum systems and a summary of the different designs proposed to date. The application of OFDM together with DS-CDMA techniques is presented using non-coherent demodulation methods, and the relative merits and disadvantages of each system are outlined. A new multi-carrier DS-CDMA (MC-CDMA) concept is presented for future mobile wireless systems with considerable performance improvements in the bit-error rate. A comparison between high-rate convolutional encoded DS-CDMA and LROCC coding for MC-CDMA is also presented.

Chapter 9 presents simulation results for the uplink and downlink channel using MC-CDMA techniques in a multiple-access environment. The use of interference cancellation techniques for the removal of multiple access interference (MAI) within the same cell is also introduced in this chapter. The different equalisation strategies for coherent demodulation in the frequency domain are introduced and compared in the up- and downlink.

A detailed capacity analysis for FWA applications using MC-CDMA and conventional ATDMA designs in a wideband cellular environment is shown in chapter 10. This analysis concentrates in particular on the service provision of voice and ISDN.

Conclusions and recommendations for future work are then finally given in Chapter 11.

1.5 References

[1] "GSM: Europe's super-airway", *Land Mobile*, Vol. 2, No. 10, pp.9, Nov. 1995

[2] De Boer, H, "RACE mobile communications", *IEE Electronics and Communications Engineering Journal*, Vol. 5, pp. 157-158, June 1993

[3] Crosbie, D B, "The new space race, satellite mobile communications", *IEE Review*, pp. 111-114, May 1993

[4] "Will global mobile satellite services ever fly? ", *MTN*, October 1994

[5] Radley, P, "The time to change is now", *MTN*, p. 22, September 1993

[6] Krapf, E, "Get the bugs out – It's make-or-break time for CDMA", *America's Network*, pp.26-29, July 1996

[7] Reiners, C and Rohling, H, "Multicarrier Transmission Technique in Cellular Mobile Communications Systems", *IEEE Proc. VTC'94*, pp. 1645-1649

[8] Yee, N and Linnartz, J-P, "Wiener Filtering of Multi-carrier CDMA in Rayleigh Fading Channel", *IEEE Proc. PIMRC'94*, pp. 1344-1347

[9] Kaiser, S, "Analytical Performance Evaluation of OFDM-CDMA Mobile Radio Systems", *Proc. 1st European personal and Mobile Communications Conference (EPMCC'95)*, Bologna, Italy, November 1995, pp. 215-220

[10] Fazel, K, "Performance of CDMA/OFDM for mobile communication systems", *IEEE 2nd International Conference on Universal Personal Communications (ICUPC) Proc.*, October 1993

[11] Caswell, A C, "Multicarrier transmission in a mobile radio channel", *Electronics Letters*, pp. 1962-1963, October 1996

[12] Wiel, O and Vandendorpe, L, "Adaptive Equalisation for Multitone CDMA Systems", *IEEE Proc. PIMRC'94*, pp. 253-257

[13] Stirling-Gallacher, R A and Povey, G J R, "Different Channel Coding Strategies for OFDM-CDMA", *Proc. IEEE Veh. Technology*, Phoenix, Arizona, May 1997

[14] Stirling-Gallacher, R A and Povey, G J R, "Performance of an OFDM-CDMA System with orthogonal Convolutional Coding and Interference Cancellation", *Proc. IEEE Veh. Technology*, Phoenix, Arizona, May 1997

[15] Weinstein, S B and Ebert, P M, "Data Transmission by Frequency-Division Multiplexing Using the Discrete Fourier Transform", *IEEE Trans. on Comm. Tech.*, Vol. COM-19, No. 5, Oct. 1971, pp.628-634

[16] Kondo, S and Milstein, L B, "Performance of Multicarrier DS CDMA Systems", *IEEE Trans. on Comms.*, Vol. 44, No. 2, Feb. 1996, pp. 238-246

[17] Sanada, Y and Nakagawa, M, "A Multiuser interference Cancellation Technique Utilizing Convolutional Codes and orthogonal Multicarrier Modulation for Wireless Indoor Communications", *IEEE Journal on Selected Areas in Comm.*, Vol. 14, No. 8, Oct. 1996, pp. 1500-1509

[18] Zou, W Y and Wu, Y, "COFDM: An Overview", *IEEE Trans. on Broadcasting*, Vol. 41, No.1, March 1995

[19] Floch, B, Alard, M and Berrou, C, "Coded Orthogonal Frequency Division Multiplex", *Proc. of the IEEE*, Vol. 83, No. 6, June 1995, pp. 982-996

[20] Sourour, E and Nakagawa, M, "A modified Multi-Stage Co-Channel Interference Cancellation in Asynchronous CDMA systems", *PIMRC'94*, pp. 425-429

[21] Zheng, F and Barton, S, "Near-Far Resistant Detection of CDMA Signals via Isolation Bit Insertion", *IEEE Trans. on Comms.*, Vol. 43, No. 2/3/4, Feb/Mar/April 1995, pp. 1313-1317

[22] Bhargava, V, "High Rate Data Transmission in Mobile and Personal Communications", *PIMRC'94*, pp. 1106-1113

[23] Wu, K T and Tsaur, S A, "Error performance for diversity DS-SSMA communications in fading channels", *IEE Proc. Commun.*, Vol. 141, No. 5, pp. 357-363, Oct. 1994

[24] Laurenson, D I and Povey, G J R, "Channel Modelling for a Predictive RAKE Receiver System", *PIMRC'94*, pp. 715-719

[25] Turin, G L, "Introduction to spread-spectrum antimultipath techniques and their application to urban digital radio", *Proc. of the IEEE*, Vol. 68, pp. 328-353, March 1980

CHAPTER 2:

CHANNEL MODEL AND CHARACTERISTICS

2.1 The Mobile Propagation Environment

Propagation through a mobile channel environment presents a variety of obstacles for a successful communications link. For typical carrier frequencies of 900 MHz or above, the local geographic region may lead to a variety of different signal arrival mechanisms in the urban environment. Figure (2-1) shows the distribution of scatters in the mobile radio environment, ranging from line-of-sight (LOS) paths, diffraction shadowing to reflections and scattering. This results in the received signal being received by several different paths, causing multipath fading.

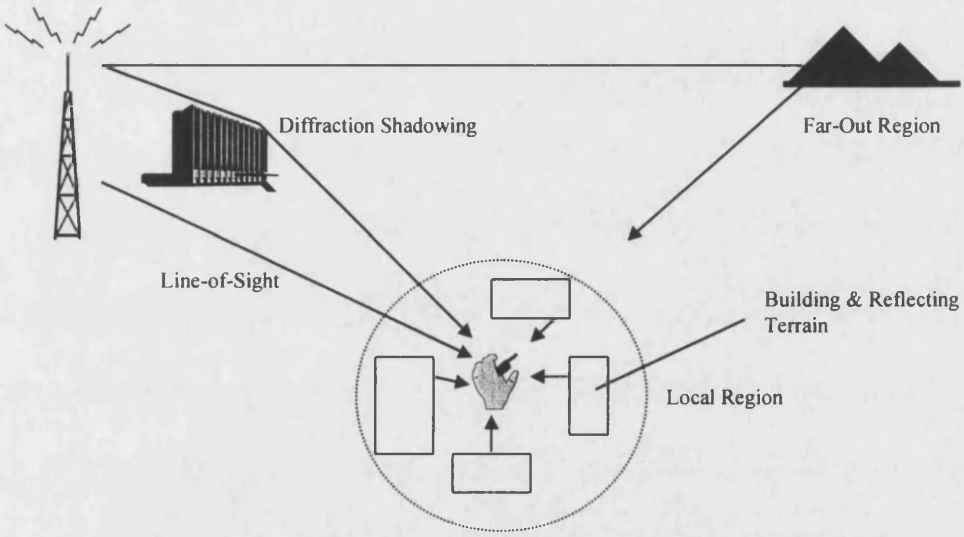

Figure 2-1. Distribution of scatters in a mobile radio environment

Each ray has a different amplitude, time delay and phase, causing the combined received signal to fade by up to 40dB below the mean signal level. This problem is intensified when the mobile unit moves through the environment, causing a significant rapid fade in the signal level. This is dependent on the speed of the subscriber unit. The average duration of fades of a Rayleigh faded signal in the time domain as well as the level crossing rates (lcr), measured at 10dB below the average power of a signal, is a function of vehicle speed V and wavelength λ, given as [1]:

$$\text{fade duration} = 0.132\left(\frac{\lambda}{V}\right) \text{ sec}$$
$$\text{lcr} = 0.75\left(\frac{V}{\lambda}\right) \text{crossings/sec} \qquad (2\text{-}1)$$

For a carrier frequency of 1.6 GHz and a speed of 60 km/h the average fade duration obtained from (2-1) is 1.485 ms and the level crossing rate is 67 crossings per second.

As described earlier, a single symbol transmitted from one end and received at the other end in a mobile environment receives not only its own symbol but also many echoes of its symbol. This

phenomenon occurs if a time dispersive channel is present and can be measured by the time delay spread of the channel. The time delay spread intervals, which are measured from the first symbol to the last detectable echo, are different in different built environments. The average time delay spread due to the local scatterers in suburban areas is 0.5μs and in urban areas it is 3μs. These local scatterers are in the near-end region, as shown in figure (2-1), and the time delay spread corresponding to this region is illustrated in figure (2-2).

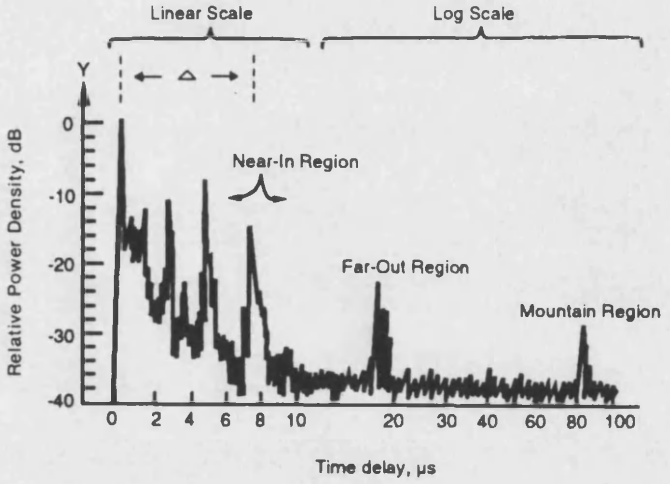

Figure 2-2. An illustration of time delay spread

As this figure shows, there are other types of time delay spreads. One type of delayed wave is caused by the reflection of high-rise buildings (far out region), and another kind by reflection from mountains. In certain mountain areas the time delay spread can be up to 100μs. These time delay spreads would cause inter-symbol interference (ISI) for data transmission. To avoid ISI, the transmission rate R_D should not exceed the inverse value of the mean delay spread T_g if the mobile unit is at a standstill (non-fading case):

$$R_D < \frac{1}{T_g} \tag{2-2}$$

or R_D should not exceed the inverse value of $2\pi T_g$ if the mobile unit is in motion (fading case):

$$R_D < \frac{1}{2\pi T_g} \tag{2-3}$$

If the transmission rate, R_D, is higher than that given in equation (2-2) and equation (2-3), both FDMA and TDMA need equalisers capable of reducing ISI to some degree depending on the complication of the time delay spread length and the wave arrival distribution. An FDMA system always requires a slower transmission rate than a TDMA system when both systems offer the same radio capacity. Usually, an FDMA system can overcome the need for

equalisation as long as its transmission rate does not rise too high above 10 ksamples/sec. CDMA systems do not need an equaliser, but can use sophisticated RAKE receivers and correlators if the chip rate is sufficiently high to allow the multipath spread to be resolved.

In the event that there are fixed scatters or signal reflectors in the medium, in addition to randomly moving scatters, the impulse response can no longer be modelled as having zero mean. In this case, the envelope has a Rice distribution and the channel is said to be a *Ricean fading channel*. When the impulse response is modelled as a zero-mean complex valued Gaussian process, the envelope at any instant t is Rayleigh distributed. In this case the channel is said to be a *Rayleigh fading channel*.

2.2 Fast fading

The received signal in the mobile environment is the resultant of the line-of-sight and all multipath components at the receiver location, as shown in figure (2-3).

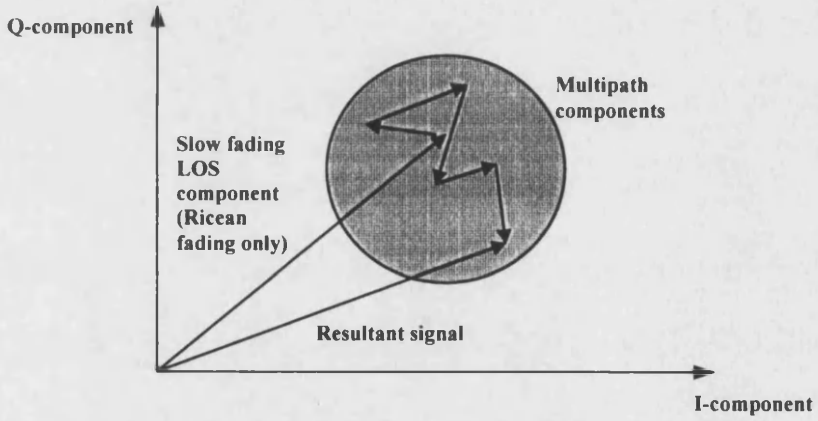

Figure 2-3. Phasor addition of received signal components

The received signal, *r(t)*, undergoing fading is given as:

$$r(t) = A(t)\cos(w_0 t + \theta(t)) \tag{2-4}$$

where $A(t)$ and $\theta(t)$ are the envelope and phase of $r(t)$ respectively, and w_0 is the carrier frequency. Rice [2] has shown that equation (2-4) can be expressed as:

$$r(t) = T_c \cos(w_0 t) - T_s \sin(w_0 t) \tag{2-5}$$

where T_c and T_s are the envelopes of a narrowband Gaussian random process with zero mean (i.e. no line-of-sight signal component exists) and equal variance. These represent the real and

imaginary components of the received signal and have probability distributions described by the normal distribution:

$$p(x) = \frac{1}{\sqrt{2\pi\sigma^2}} \exp\left(-\frac{x^2}{2\sigma^2}\right) \tag{2-6}$$

The variables T_c and T_s can be expressed as:

$$\begin{aligned} T_c(t) &= \sum_{l=1}^{L} C_l \cos(w_l(t) + \phi_l) \\ T_s(t) &= \sum_{l=1}^{L} C_l \sin(w_l(t) + \phi_l) \end{aligned} \tag{2-7}$$

These expressions represent the summation of all L propagation paths arriving at the receiver, with the lth path having an amplitude a_l and phase ϕ_l uniformly distributed on $(0,2\pi)$. The Doppler shift w_l, associated with each ray results from the transmitter-receiver relative velocity:

$$w_l = \frac{2\pi v}{\lambda} \cos(\gamma_l) \tag{2-8}$$

where v is the relative velocity, λ the carrier wavelength and γ_l the arrival angle of the lth ray, uniformly distributed on $(0,2\pi]$. From equation (2-5), the envelope and phase of the received signal can be expressed as:

$$\begin{aligned} A(t) &= \sqrt{T_c^2(t) + T_s^2(t)} \\ \theta(t) &= \arctan\left[\frac{T_s(t)}{T_c(t)}\right] \end{aligned} \tag{2-9}$$

The probability distribution of the received signal is derived from equations (2-5) and (2-6) and is given by:

$$p(r) = \frac{r}{\sigma^2} \exp\left(-\frac{r^2}{2\sigma^2}\right) \tag{2-10}$$

Equation (2-10) is the well-known Rayleigh distribution function and is shown along with the Gaussian distribution in figure (2-4).

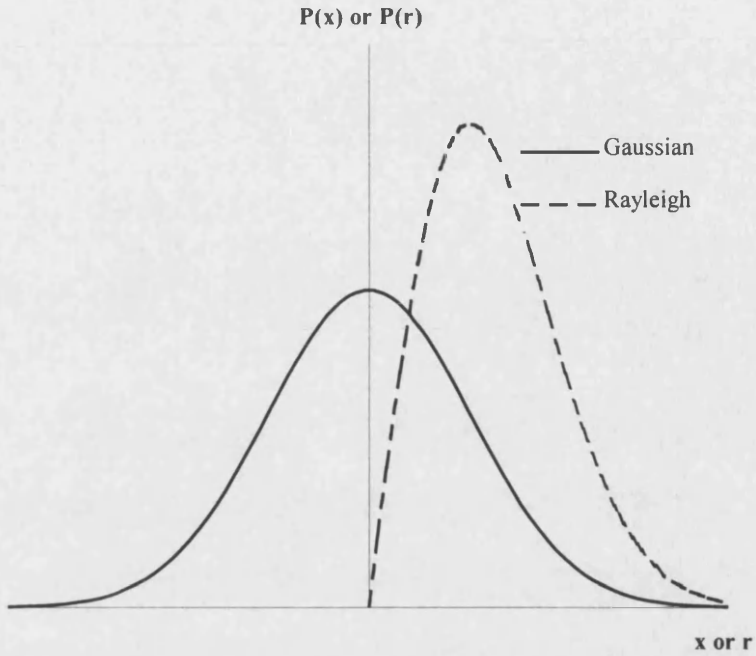

Figure 2-4. Gaussian and Rayleigh distribution functions

The Rayleigh or fast fading signal envelope *A(t)* exhibits deep fades of up to 40dB below the mean signal level, accompanied by rapid phase fluctuations of up to π radians. Tracking the signal phase under these conditions can be particularly difficult, especially for high fade rates in the order of microseconds or less.

The Rayleigh distribution assumes that no line-of-sight component is present, and if such a component does exist, it is no longer possible to assume that the variables $T_c(t)$ and $T_s(t)$ will have zero mean. The envelope now assumes a Ricean distribution, given by:

$$p(z) = \frac{1}{2\pi\sigma^2}\exp\left[\frac{z^2+m^2}{2\sigma^2}\right] I_o\left(\frac{mz}{\sigma^2}\right) \tag{2-11}$$

where $I_o(x)$ is the modified Bessel function of the first kind and zero order:

$$I_o(x) = \frac{1}{2\pi}\int_0^{2\pi}\exp(x\cos\theta)d\theta \tag{2-12}$$

The term $m^2/2\sigma^2$ in equation (2-11) is often called the *K-factor* and describes the ratio of the power in the LOS component to that in the scattered signal components. For high K factors, the received signal statistics are dominated by those of the LOS path, while for K=0 the Rayleigh distribution is obtained.

In general it is harder to achieve successful communications under Rayleigh fading conditions than Ricean, as the lack of line-of-sight path leads to deeper fades in the signal envelope. The LOS path is likely to be absent in the urban environment, where buildings obscure the basestation. Thus, Rayleigh fading statistics are assumed for this work which is primarily aimed at achieving successful communication in the urban mobile and fixed wireless access environment. A CDMA receiver which is tolerant of Rayleigh fading can be expected to offer further improved performance under less harsh Ricean conditions.

2.3 Slow fading

If the rapid time-varying fluctuations in signal strength experienced by a mobile receiver undergoing Rayleigh fading are removed from the signal by averaging long term variations in signal strength, an inherent slow fading signal will remain. In addition to the short-term statistics of the mobile radio channel, which lead to time- and frequency-selective fading, the presence of location dependent obstacles leads to long-term fading. These variations, which appear over tens of wavelengths, are termed shadowing and are caused by buildings and other structures in the mobile environment obscuring rays. Although shadowing results in a time-varying received signal, this fading phenomenon is unlike time-selective fading as vehicle speed is not a factor in determining the fading statistics. Instead, the nature of the terrain, surrounding the base and mobile antennas, as well as the respective antenna heights with respect to the terrain determines the extent of shadowing. Since obstacles in the propagation path between the base and the mobile or fixed antenna lead to shadowing, frequently simply moving the location will change the effects of shadowing.

Shadowing may be modelled as a multiplicative, slowly time-varying log-normal random process. Slow fading therefore arises through the changing average of rays, rather than the fast changing phasor addition of the Rayleigh fading mechanism.

The shadowing random process is generally assumed to be log-normally distributed (i.e. the distribution function associated with the long-term fading process is a normal distribution when the values are measured in decibels). Suzuki [3] has shown by extensive measurement that, for most purposes, slow fading can be modelled by a log-normal distribution, with a standard deviation between 5 and 12dB.

The standard normal distribution is given by:

$$y = \frac{1}{\sqrt{2\pi}} \exp\left(-\frac{x^2}{2}\right) \qquad (2\text{-}13)$$

By defining $z = 10^{x/20}$, the log-normal distribution is then given by substitution of z into equation (2-13):

$$y2 = \frac{1}{\sqrt{2\pi}} \exp\left(-\frac{z^2}{2}\right) \tag{2-14}$$

The standard deviation σ and mean μ can be incorporated into the distribution by utilising the transformation:

$$x' = \frac{x - \mu}{\sigma} \tag{2-15}$$

Provided that all parameters are measured in decibels (as is customary in propagation measurements), the density function usually dealt with is the Gaussian density function. In this case the mean μ and standard deviation σ are measured in decibels.

2.4 Characterisation of the mobile radio channel

The mobile radio channel exhibits the short-term statistics of a doubly-spread Gaussian wide-sense stationary uncorrelated scattering (GWSSUS) model [4]. Doubly-spread channels are so called because they spread the time and frequency waveforms of a signal transmitted through the channel. Short-term fading over these channels is often such that the short-term fading statistics are approximately stationary over time. Hence it is convenient to define a subclass of the general fading channel model known as wide-sense stationary (WSS) channels. In addition, due to the specific environment in which a mobile radio operates, the mobile radio channel is often characterised by long-term statistics that are distributed on a log-normal basis. This was introduced earlier. In the following subsections, each of the foregoing properties of the mobile radio channel will be described further.

2.4.1 Time-selective fading

A doubly-spread GWSSUS channel model exhibits both time- and frequency-selective fading. The earliest studies of the mobile radio channel [7] indicated the presence of time-selective fading on both narrowband and wideband radio channels. The time-selective fading manifests itself as rapid variations of the received signal envelope as the mobile receiver moves through a field of local scatterers.

A time-selective fading channel may be characterised in terms of its Doppler power spectrum, correlation time etc. As Gans [9] has noted, the statistical characteristics of the received signal for a mobile radio channel are functions of the polarisation of the antenna with respect to the received signal. While this would lead to three separate characterisations of time-selective fading for the mobile radio channel, in the following, only one such characterisation (the "vertical monopole" case) is considered, with the other two cases of polarisation described in the literature [9,10]. From consideration of the angle of arrival and the polarisation of the antenna, the auto-correlation function of the signal received by a mobile radio receiver corresponding to a constant, unmodulated carrier transmitted signal is given by:

$$R(\tau) = I_o(2\pi f_d \tau) \tag{2-16}$$

where $I_o(\cdot)$ is the zero-order Bessel function of the first kind and f_d is the maximum Doppler frequency shift, given by:

$$f_d = \frac{v}{\lambda} = \frac{vf_o}{c} \tag{2-17}$$

in which v is the vehicle speed (in m/s), λ the wavelength of the transmitted signal, c the speed of light (= 3 x 10^8 m/s in a vacuum), and f_o the frequency of the transmitted signal (in Hertz). The Doppler spectrum is the Fourier transform of the auto-correlation function and is given by:

$$S(f) = \begin{cases} \dfrac{1}{\pi f_d} \cdot \dfrac{1}{\sqrt{1-(f/f_d)^2}} & |f| \le f_d \\ 0 & \text{elsewhere} \end{cases} \tag{2-18}$$

Equation (2-18) is valid only for vertical monopole antennas and scatterers uniformly distributed around the antenna. A plot of the Doppler spectrum for a mobile radio channel is shown in figure (2-5).

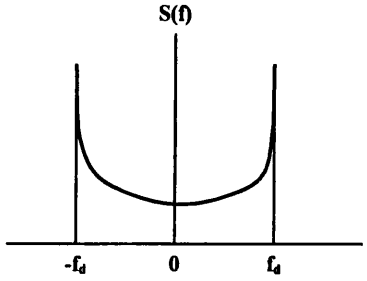

Figure 2-5. Plot of Doppler spectrum for a mobile radio channel

Note the abrupt frequency cut-off of the Doppler spectrum as a function of the maximum Doppler frequency f_d. The correlation (or coherence) time of this channel is usually assumed to be given by:

$$\tau_c = \frac{1}{2f_d} \tag{2-19}$$

In addition to the correlation time of the channel, in the digital communications literature, the term *normalized Doppler* appears. The normalised Doppler is defined to be the product of the maximum Doppler frequency and the symbol duration of the transmitted signal. As indicated above, the duration of a fade is a function of the vehicle speed and the mobile radio frequency. It can be shown [1, 6] that for a vertically polarized monopole in a Rayleigh fading mobile radio environment, the duration of a fade, defined to be the average duration of a fade below a given threshold A, is given by:

$$\bar{t} = \frac{\lambda}{\sqrt{2\pi}vR}\left(e^{R^2} - 1\right) \tag{2-20}$$

where,

$$R = \frac{A}{\sqrt{2\sigma^2}} \tag{2-21}$$

in which $2\sigma^2$ is the average power of the received signal.

2.4.2 Frequency-selective multipath fading

In addition to exhibiting time-selective fading, the mobile radio channel also exhibits frequency-selective fading. The fundamental difference between the narrow and wideband channel is that fading becomes frequency selective in nature through the multipath time dispersion of the received rays in the wideband channel. The *coherence bandwidth*, Δf, defined as the frequency separation over which two tones have a correlation greater than 0.9^2 describes the extent to which a channel is wideband or frequency selective. If techniques to mitigate multipath in systems with a bandwidth greater than the channel coherence bandwidth are not employed, the resulting inter-symbol interference introduces irreducible bit error rate floors.

The wideband behaviour of a channel is fully characterised by its power delay profile, which is a measure of received power versus excess time delay for a transmitted impulse. In a typical profile, multipath 'echoes' of a transmitted impulse are clearly visible, as seen in figure (2-6).

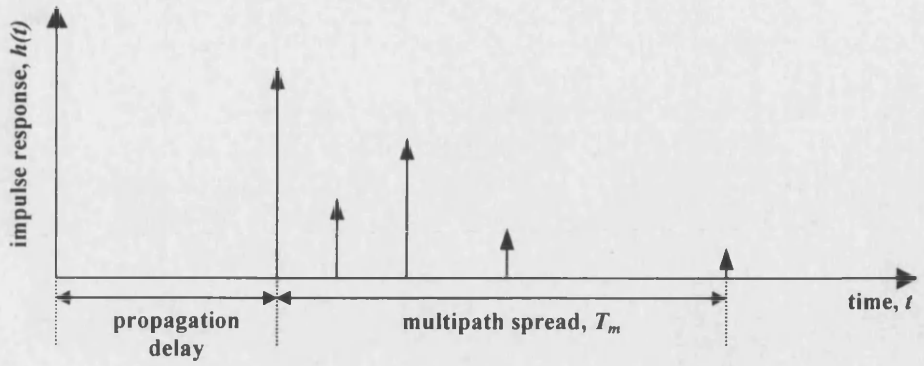

Figure 2-6. Typical wideband channel impulse response

The power delay profile of a channel describes completely the variation of received power with time, but it is often more convenient to simplify this to a single quantity, termed the *rms delay spread*, s_m, which is calculated as the temporal dispersion of the received power around the half power point of the delay profile. The terms are defined as follows.

Let $P_m(\tau_l)$ denote the average power delay profile, where τ_l is the propagation delay from the transmitter to the receiver. Then,

$$\text{mean excess delay} \equiv d_m = \frac{\sum \tau_l P_m(\tau_l)}{\sum P_m(\tau_l)} - \tau_A \qquad (2\text{-}22)$$

where τ_A is the first arrival delay. Similarly,

$$\text{rms delay spread} \equiv s_m = \left[\frac{\sum (\tau_l - d_m - \tau_A)^2 P_m(\tau_l)}{\sum P_m(\tau_l)} \right]^{1/2} \qquad (2\text{-}23)$$

and maximum excess delay = $T_m = \max(\tau_l - \tau_A)$.

The rms delay spread values are on the order of 1 to 3 μs for urban terrain, 0.1 to 1 μs for suburban terrain, and 6 to 7 μs for rural mountainous terrain, respectively. Care should be exercised when using rms delay spread to predict the deleterious effects of ISI, as the inclusion of low power multipaths at large excess time delays can unduly influence the value of s_m.

In addition to the various delay profile parameters noted above, in characterizing spread-spectrum systems operating over mobile radio channels it is often necessary to specify the

power delay profile of the channel. Because the power delay profile is location dependent, this is often a very difficult task. Nonetheless, in 1986, a scientific study group in Europe specified several "average" power delay profiles that modeled the mobile radio channel at 900 MHz quite well and were in fact used later in specifying the performance of the GSM digital cellular system. Figure (2-7) plots two of these profiles for the typical urban environment and for the hilly terrain environment. Although both of these average power delay profiles are decaying exponentials in delay, indicating a minimum phase channel characteristic (i.e., the channel impulse response decays as time increases), non-minimum-phase channels *can* exist in the mobile radio environment and must be taken into account in designing digital communication systems.

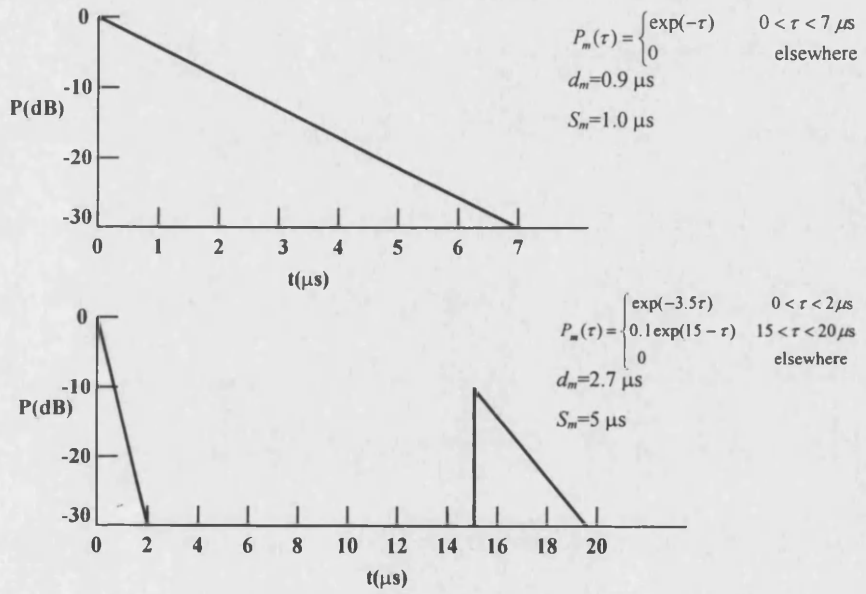

Figure 2-7. COST 207 average power delay profiles: (a) typical delay profile for suburban and urban areas; (b) typical "bad"-case delay profile for hilly terrain

2.4.3 Approximation of the delay power profiles by discrete taps

Hardware multi-tap simulators can only be set to discrete values in both amplitude and delay. Different types of fading simulators may differ in the parameters to be set, and therefore the approximation of the delay power profiles needs to be performed according to some specific rules [5]. A discrete approximation of the continuous power delay profiles, given in figure (2-7), requires the definition of certain parameters such as the delay spread, delay interval, total number of taps and the delay spacing. These are summarised as follows:

(i) The delay spread is defined as in equation (2-23), with a value (and tolerance) of 1.0μs ± 0.1μs for the typical urban profile and 5.0μs ± 0.2μs for the bad-case hilly terrain profile.

(ii) The delay interval defines the period within which 90% of the total received energy of a short pulse is detected. For discrete taps, this value usually does not exist and must therefore be linearly interpolated between the delays of the tap where a value is just below 90% of the energy and the next tap where the energy is just above 90%. These values lie within 2.3μs ± 0.6μs for typical urban profiles and 6.6μs ± 1.0μs for bad-case hilly terrain profiles.

(iii) The total number of taps should not be smaller than 3 for the rural (non-hilly) area, 4 for the typical urban profile and 6 for the bad urban and hilly terrain models

(iv) The delay spacing between the taps should be chosen to avoid a regular spacing as this will ensure that the frequency transfer function of the radio channel will not have large periodicities

The final parameters of a typical channel simulation for different power delay profiles is given below in tables (2-1)-(2-4). Note that the Doppler classifications Class, Rice, Gaus1 and Gaus2 refer to the type of Doppler spectra present on each particular path. For the purpose of simulations, we have chosen to use the worst case of the time variance of the radio channel by applying the classical Doppler spectra as defined by equation (2-18) to all taps.

Tap No	Delay (μs)	Power (dB)	Doppler Category	Delay Spread (μs)
1	0	0	Rice	0.1
2	0.1	-4	Class	
3	0.2	-8	Class	
4	0.3	-12	Class	
5	0.4	-16	Class	
6	0.5	-20	Class	

Table 2-1. Rural (non-hilly) area

Tap No	Delay (μs)	Power (dB)	Doppler Category	Delay Spread (μs)
1	0	-2	Class	1.1
2	0.2	0	Class	
3	0.6	-2	Gaus1	
4	1.5	-6	Gaus1	
5	2.4	-8	Gaus2	
6	5.0	-10	Gaus2	

Table 2-2. Typical urban (non-hilly) area

Tap No	Delay (μs)	Power (dB)	Doppler Category	Delay Spread (μs)
1	0	-3	Class	2.4
2	0.4	0	Class	
3	1.0	-3	Gaus1	
4	1.6	-5	Gaus1	
5	5.0	-2	Gaus2	
6	6.6	-4	Gaus2	

Table 2-3. Bad urban (hilly) area

Tap No	Delay (μs)	Power (dB)	Doppler Category	Delay Spread (μs)
1	0	0	Class	5.0
2	0.2	-2	Class	
3	0.4	-4	Class	
4	0.6	-7	Class	
5	15.0	-6	Gaus2	
6	17.2	-12	Gaus2	

Table 2-4. Hilly terrain

2.5 Equivalent baseband model of channel

The multipath phenomena ultimately provides a significant performance degradation to narrowband signals over mobile channels, causing severe ISI. This can be used to advantage if the bandwidth of the signal is selected to be as wide as possible, allowing the ISI to be resolved with the use of RAKE receivers. In this case the multipath is said to give *diversity* through different paths. Obtaining an equivalent baseband model of the channel with a discrete number of independent taps can therefore be accomplished in the following way.

We assume that there are L multipath components (diversity channels), carrying the same information-bearing signal. Each channel is assumed to be frequency-nonselective and slowly fading with Rayleigh distributed envelope statistics. The fading and noise processes among the L diversity channels are assumed to be mutually statistically independent. Thus, at baseband, this multipath mobile channel can be represented by its low-pass equivalent complex impulse response:

$$h(t) = \sum_{l=1}^{L} \alpha_l \exp(j\phi_l)\delta(t-\tau_l) \tag{2-24}$$

where α_l and ϕ_l are the magnitude and phase of the lth element in an impulse response with L samples and $\delta(t-\tau_l)$ is an impulse delayed by τ_l.

This equivalent low-pass channel model is frequently used in the analysis of mobile and fixed wireless digital communication systems.

2.6 A discrete-time model for a channel with ISI

In dealing with band-limited channels that result in ISI, it is convenient to develop an equivalent discrete-time model for the analog (continuous-time) system. It has been shown in [16] that the filter in the receiver matched to the channel impulse response $h(t)$ is given by the complex conjugate $h^*(-t)$. Since the transmitter sends discrete-time symbols at a rate $1/T_b$ symbols per second and the sampled output of the matched filter at the receiver is also a discrete-time signal with samples occuring at a rate $1/T_b$ per second, it follows that the cascade of the analog filter at the transmitter with impulse response $g(t)$, the channel with impulse response $c(t)$, the matched filter at the receiver with impulse response $h^*(-t)$ and the sampler can be represented by an equivalent discrete-time transversal filter having tap gain coefficients a_l. Its input is the sequence of information symbols s_k and its output is the discrete-time sequence y_k. The equivalent discrete-time model is shown in figure (2-8).

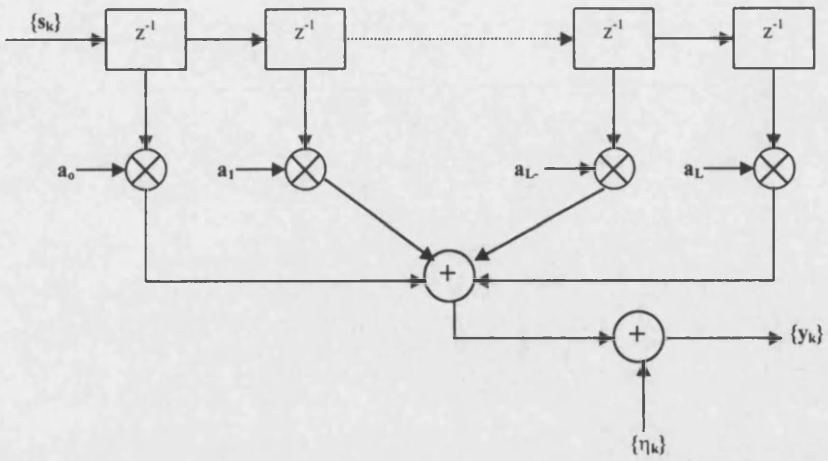

Figure 2-8. Equivalent discrete-time model of ISI channel with AWGN

The output sequence y_k can be expressed as:

$$y_k = \sum_{l=0}^{L} a_l s_{k-l} + \eta_k \tag{2-25}$$

where η_k is a white Gaussian noise sequence with zero mean and variance N_o, and a_l is a set of tap coefficients of an equivalent discrete-time transversal filter.

In summary, the cascade of the transmitting filter, the channel and the matched filter and sampling function can be represented as an equivalent discrete-time transversal filter having the set a_l as its tap coefficients.

The coefficients a_l will be complex time-varying fading signals with an average power attenuation given by tables (2-1)-(2-4). The time-varying fading can be classified as Doppler spectra, obtained from filtering two independent Gaussian distributed variables with the equivalent Doppler filter approximation. To simulate the Doppler spectra defined by equation (2-18) of the channel it is possible to approximate the frequency response by a simple two-stage cascaded Butterworth filter. The first stage provides a 'ringing' at frequency f_d and the second filter is a low-pass filter to reduce the transition bandwidth, therefore giving the response a sharper cut-off. The filter approximation in the s-plane is given by:

$$H(s) = \frac{1}{s^2 + s\sqrt{2} + 1} \cdot \frac{1}{s^2 + 0.02 \cdot s + 1} \tag{2-26}$$

Using the bilinear transform we can pre-warp the denominator poles and obtain the corresponding z-plane filter transfer functions. For a Doppler frequency f_d=300 Hz and sampling frequency f_s=8000 Hz we obtain:

$$G_1(z) = \frac{0.014\left(z^2 + 2z + 1\right)}{1.1814z^2 - 1.972z + 0.8466} \tag{2-27}$$

for the first stage, and

$$G_1(z) = \frac{0.014\left(z^2 + 2z + 1\right)}{1.01636z^2 - 1.972z + 1.01163} \tag{2-28}$$

for the second stage. This gives a successful approximation to the Doppler spectra; for different sampling frequencies and Doppler frequency settings the total power from the cascaded second order filters need to be weighted by an appropriate scaling factor to give unity power. The simulated Doppler frequency response can be seen in figure (2-9).

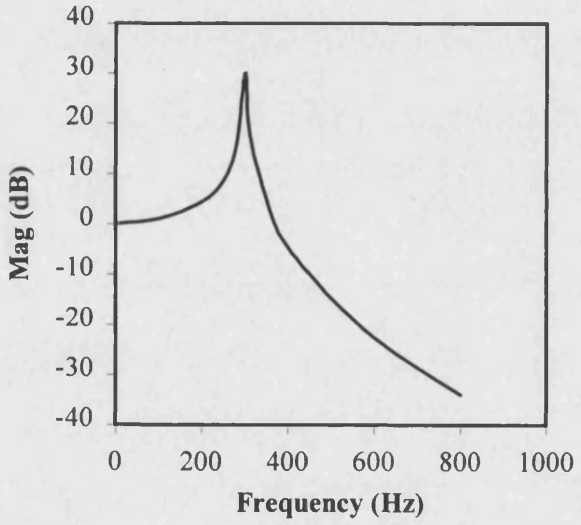

Figure 2-9. Simulated Doppler spectrum with f_s=8000 Hz, f_d=300 Hz

2.7 Summary

In section (2-1) the propagation mechanisms of the mobile channel were discussed and it was demonstrated that the combination of line-of-sight, diffracted, reflected and scattered rays at the receiver can give rise to a signal which may rapidly fade in and out by as much as -40 dB below the mean signal level over a distance of less than a wavelength. Fading is most severe when the line-of-sight path is obscured and under these conditions the signal envelope exhibits a Rayleigh distribution. The typical delay spread of a mobile radio environment is displayed graphically to show the harshness of the channel properties.

The main differences between fast and slow fading and diffraction shadowing have been outlined in conjunction with line-of-sight communication, using the Ricean distribution, and non line-of-sight communication using the Rayleigh distribution on the reflected multipath signals. These may include the effects of Doppler to represent the movement of the mobile transmitter and receiver. Of course, for FWA systems the effects of Doppler are minimal. The log-normal distribution has been introduced as a concept of classifying the severity of the shadowing effects in the channel, especially in time-selective faded channels.

In a wideband system, such as that considered in this work, the problems due to fading are exacerbated as multipaths give rise to signal echoes which can severely degrade system performance through the introduction of ISI. The multipath time dispersion of a channel can be characterised by the temporal dispersion of the received power around the half power point, known as the rms delay spread, s_m. A channel with significant multipath activity will be wideband in nature and give rise to fading which is frequency selective. The mechanisms described above are also compounded by the effects of thermal noise and propagation loss, prevalent in all wireless communication systems. Frequency-selective multipath channels are classified by their coherence bandwidth, delay spread and maximum excess delay.

The power delay profiles of the hilly terrain, bad urban, typical urban and rural areas have been outlined together with the appropriate approximations of the delay power profiles using discrete taps. The equivalent baseband model of the channel is an important feature for successful simulation of the channel over which the basestation and subscriber are communicating. The discrete-time model for a channel with ISI can be used to model the cascade of the transmitting filter, the channel and receiver's matched filter. By providing a time-varying signal on the complex tap coefficients of the equivalent discrete-time transversal filter we can simulate the time-varying properties such as Doppler on the channel. The two-stage cascaded 2^{nd} order

Butterworth filter has been shown to provide a good approximation for simulation of the Doppler spectrum.

2.8 References

[1] Lee, W C Y, "Mobile Communications Engineering", *McGraw Hill*, New York, 1982

[2] Rice, S O, "Mathematical analysis of random noise", *Bell Systems Technical Journal*, Vol. 24, pp.46-156, Jan 1945

[3] Suzuki, H, "A statistical model for urban radio propagation", IEEE Transactions on Communications, Vol. 25, pp.673-680, July 1977

[4] Elliot, D (ed.), "Handbook of Digital Signal Processing", San Diego, CA, *Academic Press*, Inc., 1987

[5] Failli, M, "Digital land mobile radio communications", *Tech. Report COST-207*, 1989

[6] Jakes, W C, "Microwave Mobile Communications", *Wiley*, New York, 1974

[7] Clarke, R H, "A statistical theory of mobile radio reception", *Bell Syst. Tech. Journal*, Vol. 47, pp. 957-1000, 1968

[8] Gilbert, E N, "Energy reception for mobile radio", *Bell Syst. Tech. Journal*, Vol. 44, pp.1779-1803, 1965

[9] Gans, M J, "A power spectral theory of propagation in the mobile radio environment", *IEEE Trans. Veh. Tech.*, Vol. VT-21, pp.27-38, 1972

[10] Martin, U, "Echo Estimation – Deriving Simulation Models for the Mobile Radio Channel", *IEEE Conference Proceedings*, pp. 231-235, 1995

[11] Schwartz, K, Martin, U and Schuessler, H W, "Devices for Propagation Measurements in Mobile Radio Channels", *IEEE Conf. Proc. PIMRC'93*, pp. 387-391, Yokohama, 1993

[12] Berthoumieux, D, and Pertoldi, J M, "Hardware propagation simulator of the frequency-selective fading channel at 900 MHz", *Proc. of the 2nd Nordic Seminar*, pp. 214-217, Stckholm 1986

[13] De Brito, G, et al, "An overview of the COST 207 Programmes in Support of GSM", *Proc. of the 3rd Nordic Seminar*, Copenhagen 1988

[14] Schuessler, H W, and Thielecke, J M, "A digital frequency fading simulator", *Proc. of the 2nd Nordic Seminar*, pp.331-336, Stockholm 1986

[15] Laurenson, D I, Cruickshank, D G M and Povey, G J R, "A Computationally Efficient Multipath Channel Simulator for the COST-207 Models", *IEEE Conference Proceedings*, 1994

[16] Proakis, J G, "Digital Communications" 3rd edition, *McGraw-Hill Series*, 1995

CHAPTER 3:

CELLULAR APPLICATIONS

3.1 Introduction

The previous two chapters have introduced some of the multiple-access strategies that may be used when communicating through channels of fading and noise. These designs can be used in a variety of applications, such as satellite-land-mobile radio communication, mobile cellular wireless applications and fixed wireless systems. All these systems profit from designs employing efficient multiple-access strategies to provide reliable communication over the particular channels in question.

This chapter deals with wireless mobile and fixed radio communication in cellular structures. In particular, we focus on the different cell shapes that are used to approximate the geometric coverage over a particular area and the effects this can have on the interference approximations of cellular structures. The method of interference rejection through directional antenna and cell sectorisation is also included in the analysis, with some novel investigations into the effects this has on the shadowing and correlation statistics on the uplink.

There has been significant interest in the use of DS-CDMA for a variety of mobile and fixed user applications, and many of the current designs which focus on particular aspects of cellular designs must be suitable for the environment they are used in. Mobile channels introduce the worst possible interference and fading effects, as detailed earlier in chapter 2, whereas fixed wireless access (FWA) systems offer the chance to provide high quality links with better error performance due to less severe channel environments. The next two sections will introduce some of the significant differences between mobile and fixed cellular structures.

3.2 Introduction to FWA systems

Local loop fixed access wireless (FWA) systems are currently being developed to offer high quality data channels directly to the fixed subscriber (e.g. home users) without the need for copper wire technology run from a local exchange. Deregulation of telecommunication services has focused attention on finding more economic methods of connecting customers which would allow new companies to enter the marketplace without the large investments needed to replicate this "access network". Fixed radio access - "wireless local loop" - is one very attractive technology for this application.

Fixed access wireless local loop systems offer a means of very rapid network deployment which avoid local access constraints and infra-structure problems. This is particularly important in a number of key markets where there is a large potential demand for telephony and high-rate data

applications capable of delivering ISDN services. This requirement for a high quality service has placed great emphasis on establishing a communication link which is both robust and spectrally efficient. Central to this work are the technological advances that are being made in modulation and coding schemes which provide an efficient use of frequency spectrum and the use of adaptive schemes, particularly with regard to flexible frequency planning, for applications in countries with different frequency allocations and different geographical environments.

A fixed system can take advantage of an external, directional antenna to optimise the performance of the radio link. This avoids several artifacts of mobile systems, including fast fading, excessive multipath delay spread, building attenuation, and severe shadowing, and of course the fixed system will not need hand-off. If a system is engineered for satisfactory fixed coverage, these factors will badly affect the quality of service for a "partially mobile" user. Conversely, if the system is engineered for the mobile user it will probably be grossly over-engineered for the fixed users. It is essential that the system should work properly in the user's premises (in the same way as a normal fixed telephone) and it is unlikely that a mobile system can provide good in-premises service quality without hand-off. Whilst mobile air-interfaces can be applied to providing fixed service, the quality and bandwidth requirements of fixed radio access, seen as an alternative to wired connections, imply that optimised technologies are preferred.

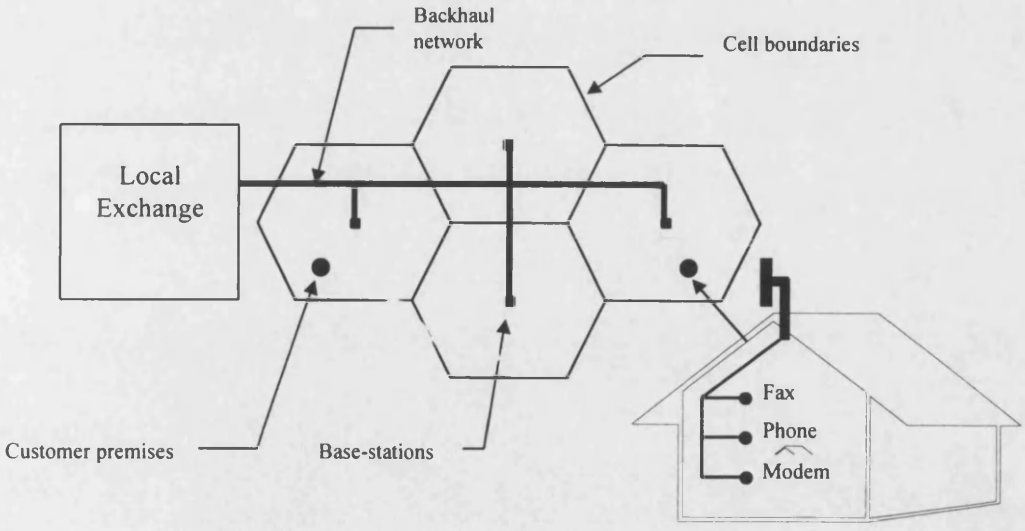

Figure 3-1. Outline radio access system

DS-CDMA techniques are being considered as likely contenders for the next generation cellular mobile radio schemes, and their application to the fixed wireless environment is also under consideration, largely on the promise of reasonable capacity and flexible use of contingent

bandwidth. There are various methods which may lead to improved performance efficiency, many of which form the basis of this thesis.

Subject to the differences in the channel environment outlined earlier, the capacity of both fixed access and mobile links are limited by statistical effects such as multipath fading, inter-cell interference and 'other-user' interference.

Fixed access wireless schemes have the advantage that the remote subscribers can make use of highly directional antennas, as opposed to omni-directional antennas found in mobile radio systems. These reduce the power requirements of both the base-station and the remote transmitter and give greater interference rejection both to inter-cell interference and intra-cell interference. They also reduce the outer-cell interference in a universal frequency re-use plan, and both these factors have a significant effect on capacity. The inter-cell degradation factor should, therefore, be as close to 1.0 as possible.

The basestation will receive all users power controlled to their own basestation with a margin of error, especially in strong fading environments. In addition, all users transmit through their own channel and are non-orthogonal to each other on the uplink. Therefore, the capacity of a DS-CDMA system is inherently smaller on the uplink than the downlink. The strongest interference will be seen from "other-user" noise in the same cell which can only be minimised through the use of perfectly time-aligned orthogonal sequences or multi-user interference cancellation. This places the requirements for a coherent link where the channel parameters can be estimated on a continuous basis. One approach to achieving a coherent uplink is to use a pilot tone transmitted from each user within the same bandwidth. Each pilot tone will require a minimum of energy from each user, however, and this will affect the capacity of the system.

A second approach which does not require a pilot tone is to use non-coherent modulation techniques, whereby the orthogonality between users is strictly reduced to quasi-orthogonality, since a knowledge of the phase and amplitude statistics is now more difficult to establish. This causes an inherent reduction in capacity, though, which may be significantly smaller than the loss in capacity through the use of pilot tones. Simulation results and theoretical studies are combined in this thesis to show fruitful capacity advantages on the uplink and downlink of these systems.

3.3 *Inter-cell interference analysis*

In DS-CDMA systems, the interference seen by a single basestation on the uplink comprises not only of other users in the wanted cell, but also all users in the surrounding cells. This is due to the fact that all users are operating on the same frequency in every cell (universal frequency re-use). The interference from other subscribers in surrounding cells communicating with their own local base-station can have significant interference effects on the uplink capacity of the wanted cell. There are many types of cell structures to be considered for future personal networks and depending on factors such as terrain features, data rates, etc., certain cell arrangements may be more advantageous than others. For the following CDMA cell structure, the interference effects from only 6 surrounding cells have been studied and further interference effects from other interfering cells have been neglected. These cells are assumed circular with overlapping boundaries, but other cellular structures, such as hexagonal cells and non-overlapping circular cells are investigated later in the report.

As the neighbouring subscribers will be power controlled to their own base-station, the interference effects will inevitably depend on the position of each subscriber within the particular neighbouring cell. A valid mathematical model can be constructed by assuming each base-station to have its subscribers uniformly distributed within the cell area.

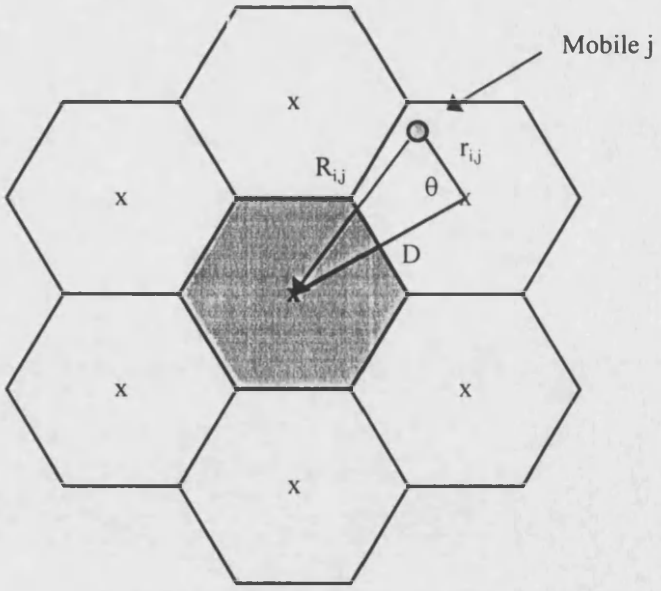

Figure 3-2. Outer cell interference for a 7 cell cluster on the uplink

Figure (3-2) shows the 1st tier of interfering cells to a central basestation in a DS-CDMA uplink scenario. The *j*th subscriber communicating to his own basestation, to which he is power controlled, is at a distance $r_{i,j}$ from his own basestation. The distance between all basestations is

assumed to be D and each mobile will interfere to the ith basestation from his own cell, j. θ is the corresponding angle between the direct line D and $r_{i,j,}$ and will have values ranging between $[0,2\pi]$.

At the outset it is assumed that the subscriber j in the ith cell is perfectly power controlled. To determine the transmitted power $P_{i,j}$ from each subscriber it is necessary to define this power relative to cell site i which is power controlled by basestation i:

$$P_{i,j} = \frac{P}{N_u} \cdot (r_{i,j})^{\alpha} \tag{3-1}$$

where P is the power received at the base-station from all subscribers, N_u is the number of simultaneous users in one cell and $r^{-\alpha}$ is the attenuation of the transmitted power at a distance r from the subscriber. For free space radiation from an isotropic source, α=2, but for a multipath fading channel α empirically takes on a value of 3 to 6. If a two-ray attenuation model is assumed, the value of α will take on a different value at different radii. The effective interference power seen at the base-station from a subscriber in a surrounding cell will decay proportionally to $R_{i,j}^{-\alpha}$:

$$Interference\ I_{i,j} = \left(\frac{P}{N_u}\right)\left(\frac{r_{i,j}}{R_{i,j}}\right)^{\alpha} \tag{3-2}$$

Let the area of a cell be approximated to a circular area of πr_d^2 where r_d is the radius of the cell and the received power P be normalised by the number of active users N_u. This enables the interference to be described per unit area:

$$\begin{aligned} \frac{dI}{dA} &= \frac{P}{\pi . r_d^{\,2}} \cdot \left(\frac{r_{i,j}}{R_{i,j}}\right)^{\alpha} \\ &= \frac{P}{\pi . r_d^{\,2}} \cdot \left(\frac{r_{i,j}}{\sqrt{D_i^{\,2} + r^2{}_{i,j} - 2D_i r_{i,j}\cos\theta}}\right)^{\alpha} \end{aligned} \tag{3-3}$$

since $R_{ij}^2 = D_i^2 + r_{ij}^2 - 2\, D_i r_{ij} \cos\theta$.

The unit area dA for a segment is related to the radius r_{ij} by:

$$dA = dr.r_{i,j}.d\theta \tag{3-4}$$

To obtain an expression for the total average interference from one surrounding cell it is necessary to integrate equation (3-3) over the complete area of a circle. Assuming an equal average loading of all cells the interference from one surrounding cell can then be extended to a total of N_c cells:

$$dI = \frac{P}{\pi.r_d^{\,2}} \cdot \frac{r_{i,j}^{\,\alpha}}{\left(D_i^{\,2} + r_{i,j}^{\,2} - 2D_i r_{i,j}\cos\theta\right)^{\frac{\alpha}{2}}} \cdot r_{i,j} \cdot dr \cdot d\theta$$

$$\therefore\ I_i = \frac{P}{\pi.r_d^{\,2}} \int_0^{2\pi} \int_0^{r_d} \frac{r^{\alpha+1}}{\left(D_i^{\,2} + r^2 - 2D_i r\cos\theta\right)^{\frac{\alpha}{2}}} \cdot dr \cdot d\theta \tag{3-5}$$

for all cells N_c,

$$I = \frac{P}{\pi.r_d^{\,2}} \sum_{i=1}^{N_c-1} \int_0^{2\pi} \int_0^{r_d} \frac{r^{\alpha+1}}{\left(D_i^{\,2} + r^2 - 2D_i r\cos\theta\right)^{\frac{\alpha}{2}}} \cdot dr \cdot d\theta$$

This expression can be analysed analytically to obtain a value for the interference power from all surrounding cells on the wanted base-station.

In order to gain an estimate of the influence of the outer cell interference on the number of simultaneous users it is necessary to calculate a scaling factor which can be substituted directly into the capacity equation for N_u. Assuming that all users in the wanted and interfering cells are uncorrelated, the signal-to-noise ratio at the input to the receiver of the basestation is given by:

$$SNR = \frac{P_1}{(N_u - 1)P_1 + I + N_o} \tag{3-6}$$

where P_1 is the power received from any one subscriber and N_o is the noise power spectral density due to thermal noise at the front end of the receiver. The denominator consists of the three main terms of interference: (i) the first term represents the intra-cell interference, (ii) the second term is the inter-cell interference, and the last term (iii) represents the thermal noise effects. If the spreading ratio is given by W/R_b, where W is the bandwidth occupied by the spread signal and R_b is the total data-rate to be transmitted, and the noise power N_o is assumed to be much smaller than the other-cell interference, I, equation (3-6) can be re-written as:

$$N_u \approx \frac{W / R_b}{E_b / N_o} - \frac{I}{P_1} \tag{3-7}$$

where E_b/N_o is the signal-to-noise ratio at the output of the receiver. The reduction in the number of simultaneous users in one cell due to the inter-cell interference can be described by the inter-cell degradation factor, F_m, given by the ratio of the number of users in a multi-cell environment to the number of users in a single cell environment. Therefore:

$$\begin{aligned} F_m &= N_u \cdot \frac{E_b / N_o}{W / R_b} \\ &= \frac{N_u}{N_u + I/P_1} \\ &= \frac{1}{1 + I/P} \end{aligned} \tag{3-8}$$

where P is the total power received from all subscribers within a cell, and,

$$I = \frac{P}{\pi . r_d^{\,2}} \sum_{i=1}^{N_c - 1} \int_0^{2\pi} \int_0^{r_d} \frac{r^{\alpha+1}}{\left(D_i^{\,2} + r^2 - 2 D_i r \cos\theta\right)^{\frac{\alpha}{2}}} \cdot dr \cdot d\theta \tag{3-9}$$

Figure (3-3) shows the variation of interference level with respect to P for a 7 cell cluster for different values of decay index α. The interference level increases for low values of α since the interfering signals in surrounding cells need a longer distance to decay and hence the average interference power as seen by the central basestation increases.

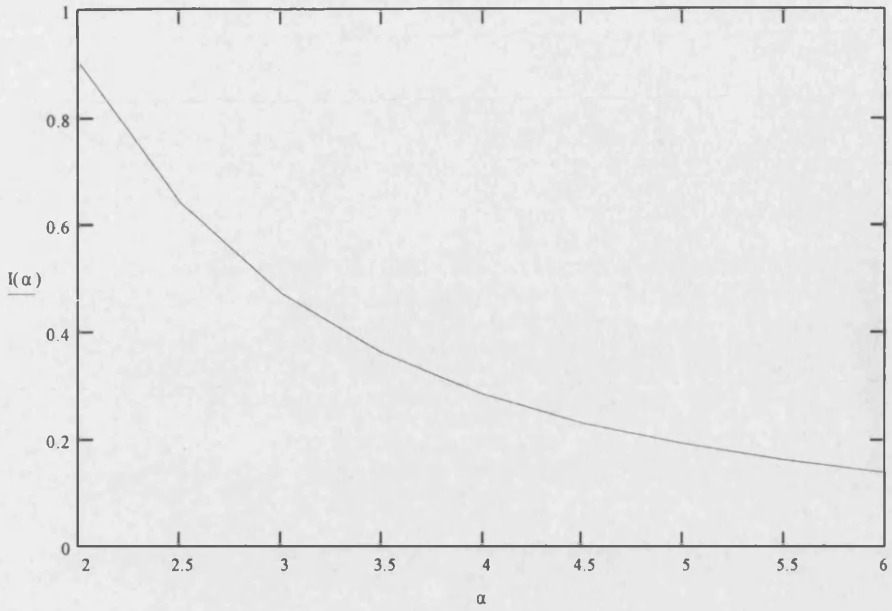

Figure 3-3. Graph displaying the inter-cell interference level for a 7 cell cluster for different decay index values

3.4 *FWA interference statistics*

The mobile radio channel statistics are very severe at high frequencies, being dominated by strong Rayleigh fading with multipath interference and diffraction shadowing effects. In a fixed access system, the use of stationary subscribers with highly directional antenna reduces the severity of the interference statistics in the channel medium. The temporal change in channel statistics for a fixed access system is much slower than that for the mobile channel, hence the phase and amplitude information acquired through the possible use of a pilot channel does not change as rapidly as for a mobile communication system. For this reason it may not be profitable to sacrifice spectrum for a pilot channel on the uplink to achieve coherency. Nevertheless, the interference statistics of the fixed access wireless system play an important role in the estimation of the subscriber capacity per bandwidth allocation per unit area.

3.4.1 Interference Rejection through Directional Antenna

The use of directional antennas and multiple element combining arrays in the receiver introduces spatial interference rejection. An ideal antenna pattern would produce a radiation pattern that is highly uniform in the horizontal plane, as shown in figure (3-4).

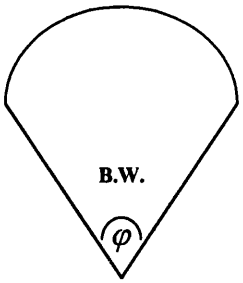

$$Gain = \begin{cases} 1 & -\frac{B.W}{2} < \varphi < \frac{B.W.}{2} \\ 0 & \text{elsewhere} \end{cases}$$

Figure 3-4. Ideal antenna pattern

If a wireless link carries one call continuously for one hour it is said to carry one Erlang of traffic. The Erlang, named after the Danish pioneer of teletraffic theory, A. K. Erlang [33], is expressed in mathematical terms as:

$$Erl = \lambda/\mu \tag{3-10}$$

where Erl = traffic in Erlangs, λ = mean call arrival rate (=calls per unit time) and $1/\mu$ = mean call holding time measured in the same time units as λ. The Erlang capacity is therefore the same for each sector of the antenna pattern. Hence, if the beamwidth $B.W=2\pi/3$, the capacity is theoretically tripled. In real life, though, the antenna radiation patterns are not ideal and lead to overlapping patterns. This reduces the effective gain through tri-sectorisation by an amount directly related to the directivity of the antenna pattern. First, the antenna gain G_A must be defined:

$$G_A = \frac{\text{amplitude in wanted direction}}{\text{average pattern amplitude over } 2\pi} \tag{3-11}$$

If the beamwidth $B.W=2\pi/j$, where there are j antennas and $j \leq N_{out}$ outputs, the capacity of one sector is given by:

$$\text{Capacity of sector} = \text{Capacity} \times \frac{G_A}{N_{out}} \tag{3-12}$$

Therefore, the difference in path loss between two base stations can be expressed as:

$$L_{dB} = -\alpha \cdot 10\log(r_1/r_2) - 10\log(G_A) \tag{3-13}$$

where r_1 is the distance of the interfering subscriber to its own base station and r_2 is the distance from the interfering subscriber to the wanted base station, as shown in figure (3-5).

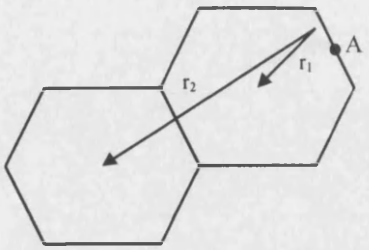

Figure 3-5. Distance of interfering subscriber to wanted basestation

It will become apparent that, for cell areas of equal size and perfect power control, the worst position is the farthest point from the neighboring cell (point A in figure 3-5). For any general re-use pattern m the following difference in path losses are reported in table (3-1).

Re-use pattern (m)	Difference in path loss (L/α dB)
1	-10·log(1/3)
3	-10·log(1/4)
4	-10·log(1/5)
7	-10·log(1/6)

Table 3-1

At any one particular time there could be $6N_u$ interfering subscribers located at the worst site. For a cluster size of m=1 and W/R_b=32 the worst value of C/I will therefore be:

$$C/I = -10\cdot\log(1/3) - 10\cdot\log(32) - 10\cdot\log(6) \quad (3\text{-}14)$$
$$= -8.5 \text{ dB}$$

Similarly, for m=3, the worst value of C/I is:

$$C/I = -10\cdot\log(1/4) - 10\cdot\log(32) - 10\cdot\log(6) \quad (3\text{-}15)$$
$$= -5 \text{ dB}$$

In general, it is possible to show that the reduction of interference with respect to the worst case becomes greater with the increase in the cluster size. This could be explained by looking at figure (3-6), where we consider the cases m=1 and m=4. In this figure we see that the user's antenna radiates toward the interfered cell with different angles, even though placed at the same site for both interfering cell. In particular, a greater cluster size leads to a larger radiation pattern angle, producing as a consequence a lower amount of interference, not only due to better path loss. Such a fact leads to the following consideration: A very strong frequency re-use (m=1)

must be accomplished by a very good user's antenna in order to reduce as much as possible the interference from adjacent cells. On the other hand, a higher cluster size leads to more negligible interference, path loss reduction increases with m as well known, but, in addition, the interference from adjacent cells reduces because of the larger radiation angle path.

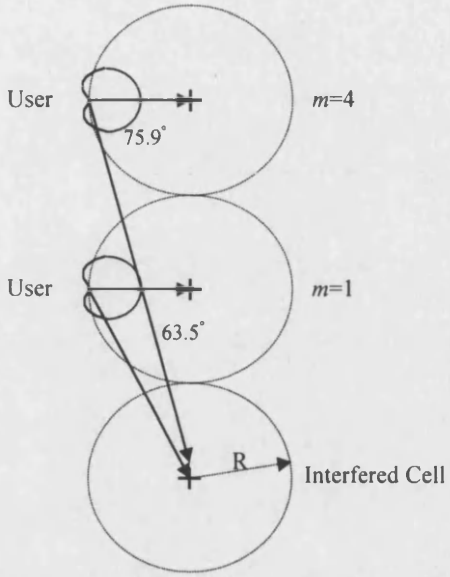

Figure 3-6. Radiation angle path for user's antenna (m=1, m=4)

3.4.2 Inter-Cell Interference Analysis including shadowing

The propagation loss is generally modeled as the product of the αth power of distance and a log-normal component representing shadowing losses. This model represents slowly varying signals, even for users in motion, and applies to both the uplink and downlink. For FWA applications this represents a valid model of the fading characteristics. Thus, for any subscriber at a distance r from the basestation, attenuation is proportional to:

$$attenuation \propto r^{\alpha} \cdot 10^{\phi/10} \tag{3-16}$$

where ϕ is the decibel attenuation due to shadowing, with zero mean and standard deviation σ, which is typically 8dB for the case of an omni-directional antenna [34,35]. Note that in this case the shadowing term refers to power attenuation and therefore yields a value of 10 in the denominator of the power term. The received power, P_r, at the subscriber or base-station site can then be directly related to the transmitted power, P_t, by the relation:

$$P_r \propto P_t \left(\frac{10^{\frac{\phi}{10}}}{r^{\alpha}} \right) \tag{3-17}$$

where α is the decay index and ϕ is the Gaussian randomly distributed variable with mean μ=0 and standard deviation σ. For values of ϕ which give a value greater than one the mobile experiences a handover to the nearest base-stations. Since the fixed access link rarely has greater than 2 independent paths, the influence of multipath fading has been neglected in the study of the channel statistics.

Consider a cellular structure where each interfering fixed user in neighbouring cells is power-controlled to its own base-station in order to counter the effects of shadowing (which is assumed to have Gaussian statistics ϕ_0 with regard to its own cell and Gaussian statistics ϕ_1 on the uplink to the base-station it is interfering with). Each variable ϕ_i is distributed with a variance of σ^2, hence the overall shadowing effects, ϕ, are described by a Gaussian distribution with a variance of $2\sigma^2$ and mean of zero. Each individual shadowing component of ϕ_i is made of two separate shadowing components:

$$\phi_i = a\xi + b\xi_i \tag{3-18}$$

were $a^2 + b^2 = 1$ and ξ is the shadowing component common to all base-stations. The terms a and b represent the weighting between ξ and ξ_i. These can be of equal value in mobile applications, but for FWA systems it is shown later that these values may differ. Considering the interference statistics of two basestations in a cellular structure, the overall shadowing component is related by:

$$\begin{aligned} \phi &= \phi_0 - \phi_1 \\ &= b(\xi_0 - \xi_1). \end{aligned} \tag{3-19}$$

It is important to note that in mobile communications, where omni-directional antenna are used, the constants a and b can be considered independent variables of equal amplitude, hence $a^2 = b^2 = 1/2$. Therefore, the variables ξ_0 and ξ_1 are also considered to be independent random variables with a mean of zero and standard deviation 8dB. The overall standard deviation of the interference effects due to two base-stations is then given as:

$$
\begin{aligned}
s.d &= 10\log\left(2\sigma^2\right)^{1/2} \\
&= 5\log\left(2\cdot 10^{\frac{8\times 2}{10}}\right) \\
&= 9.5\text{dB}
\end{aligned}
\tag{3-20}
$$

Conventional designs employ closed-loop power control to adjust the transmitting power of the fixed subscriber. As a consequence, shadowing on the uplink of the outer cells (within the line-of-sight of the base-station of the wanted cell) causes the interference power at the wanted cell's base-station to be modulated. The highly directional structure of the antenna from the interfering subscriber, positioned on the line-of-sight path as shown in figure (3-7), will inevitably experience shadowing on the same path as the power-control uplink to its own base-station. Therefore, some degree of correlation between the two shadowing components *a* and *b* will be seen, hence *a* and *b* are now no longer of equal value, since the channel through which the mobile is power controlled is shared also by the interference from the subscriber to the base-station experiencing outer-cell interference.

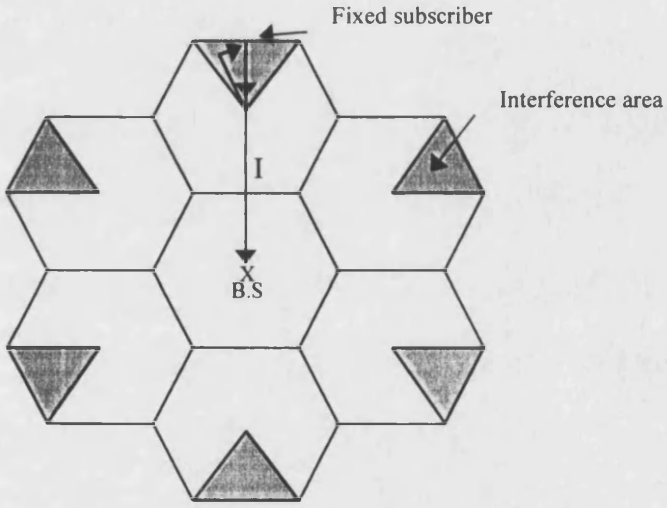

Figure 3-7. Directional antenna interference analysis

To show how the typical values of *a* and *b* may vary, figure (3-8) considers the different simple scenarios of a lorry parked at different positions in the line-of-sight of the propagation paths.

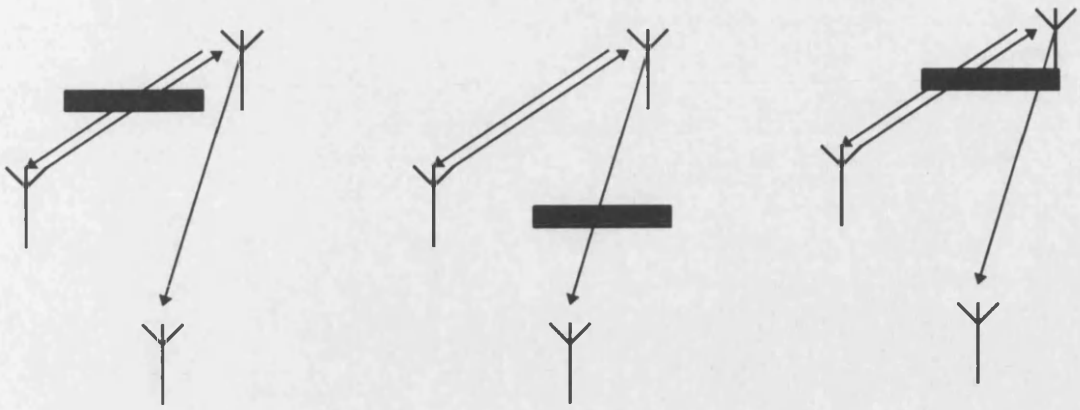

Figure 3-8. Variation of correlation statistics *a* and *b*

Using equation (3-9), it is possible to modify the outer-cell interference statistics in section 3.4.2 from a circular cell design to a hexagonal cell structure, taking into account the interference levels due to the highly directional antenna used. The major differences in the calculation can be seen in figure (3-9), where the interfering arc from the circle is related to a triangle as a function of R_I and θ.

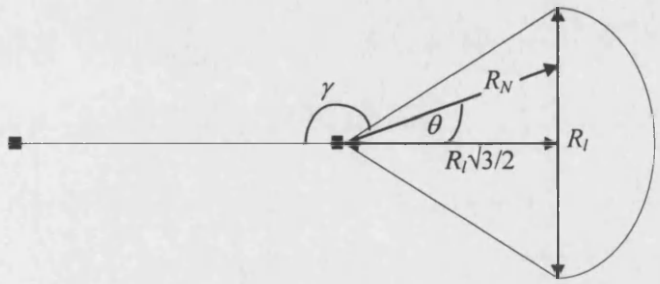

Figure 3-9. Sector analysis

Now, the value of R_N can be found as:

$$R_N = \frac{R_I\sqrt{3}}{2\cos(\theta)} \tag{3-21}$$

As discussed earlier, the area of an arc can be formulated as:

$$Area\big|_{arc} = \int_{-\pi/6}^{\pi/6} \int_{0}^{radius} r.dr.d\theta \tag{3-22}$$

Using the same equation, the area of the triangle can be given by the relation:

$$Area|_{\Delta} = \int_{-\pi/6}^{\pi/6} \int_{0}^{\frac{R_l\sqrt{3}}{2\cos(\theta)}} r.dr.d\theta \tag{3-23}$$

The user density for the hexagonal cell is given by:

$$N_{density} = \frac{2N_u}{3\sqrt{3}R_l^2} \tag{3-24}$$

and the angle θ can be related as:

$$\theta + \gamma = \pi \tag{3-25}$$

For the hexagonal cell structure, assuming that each subscriber is perfectly power-controlled in its own cell, the total interference seen by the central base-station can be now given as:

$$I = \frac{12P_t}{3\sqrt{3}R_l^2} \int_{\frac{5\pi}{6}}^{\frac{7\pi}{6}} \int_{0}^{\frac{\sqrt{3}R_l}{2\cos(\gamma-\pi)}} \frac{(r)^{\alpha+1}}{((\sqrt{3}R_l)^2 + r^2 - 2(\sqrt{3}R_l)r\cos\gamma)^{\frac{\alpha}{2}}} \cdot dr \cdot d\gamma \tag{3-26}$$

where,

P_t = Transmit power of subscriber in interfering cell

R_l = Radius of cells

r = Distance of interfering subscriber from its own base-station

γ = Angle over which integral is valid (integral bound over 360^0 for omni-directional subscriber antenna, 60^0 for directional antenna of beamwidth $\pm 20^0$)

The total outer-cell interference, I_s, including the effects of shadowing is related to equation (3-26) by:

$$I_s = I \cdot \mathrm{E}\left[\frac{10^{\phi_2/10}}{10^{\phi_1/10}}\right] \tag{3-27}$$

Next, the expected value of equation (3-27) must be found. This is obtained from:

$$
\begin{aligned}
E\left[10^{\frac{(\phi_0-\phi_1)}{10}}\right] &= E\left[\exp\left(\frac{\ln 10(\phi_0-\phi_1)}{10}\right)\right] \\
&= E\left[\exp(B(\phi_0-\phi_1))\right] \\
&= E\left[\exp(Bbx)\right] \\
&= \int_{-\infty}^{\infty} \exp(Bbx)\frac{\exp\left(-x^2/4\sigma^2\right)}{\sigma\sqrt{4\pi}}dx \\
&= \exp(b^2(B\sigma)^2)
\end{aligned}
\qquad (3\text{-}28)
$$

where $B=(ln10)/10$ and $x=\xi_0-\xi_1$

Using equation (3-27) and equation (3-28) the interference level due to outer cells can be determined and the inter-cell degradation factor (i.e. the frequency re-use efficiency) including the effects of shadowing, F, defined as:

$$F = \frac{1}{1+\frac{I_s}{P}} \qquad (3\text{-}29)$$

Figure (3-10) shows the variation of F in a hexagonal cell structure using a directional antenna of beamwidth 25^0 for different correlation statistics. For high correlation between the two links, a low value of b will give a nearly optimum value for the inter-cell degradation factor. These results are also plotted for different propagation decay factors α.

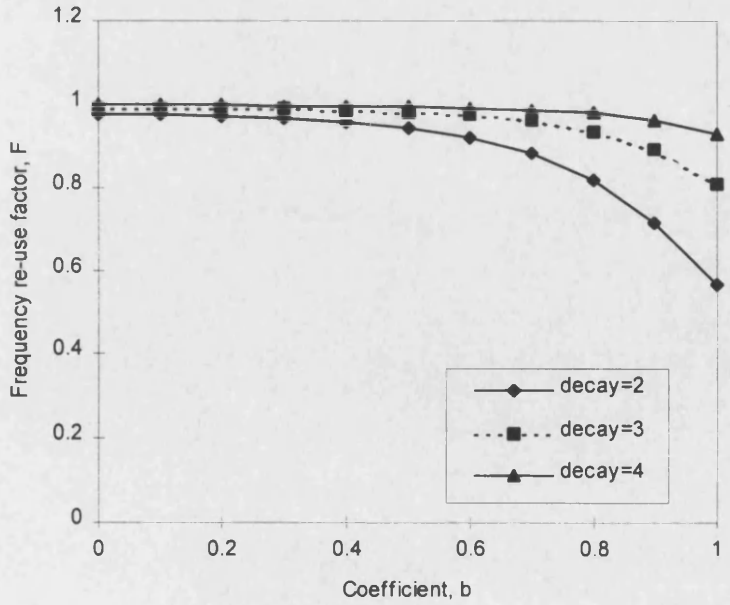

Figure 3-10. Directional antenna, B.W. = 25^0, hexagonal cells

The variation in F for a hexagonal cell structure with a larger beamwidth of 40^0 can be seen in figure (3-11). At higher values of b a slight performance degradation in the inter-cell degradation factor F can be seen.

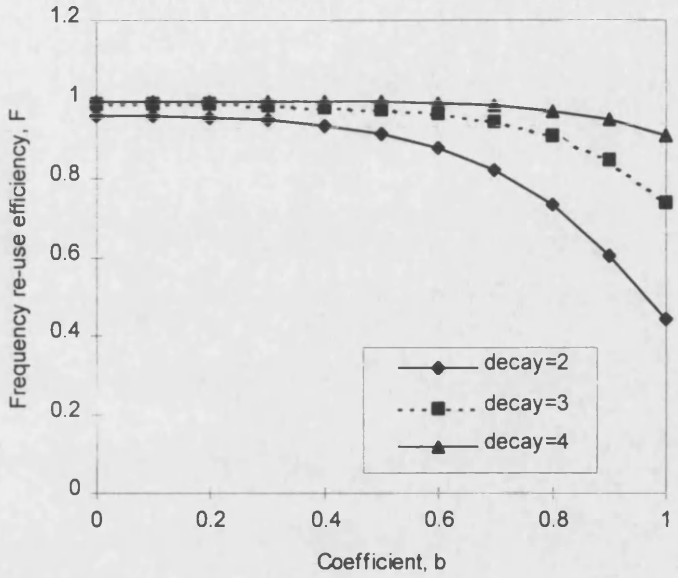

Figure 3-11. Directional antenna, B.W. = 40°, hexagonal cells

Figure (3-12) shows a comparison using directional antenna with the same previous beamwidth of 40^0, but circular cells with overlapping boundaries inside a hexagonal cell layout. Since the total area covered by the interfering users is considerably lower in this case, it can be clearly seen that this cellular layout assumption for FWA systems with directional antenna gives a considerable potential improvement in the inter-cell degradation factor.

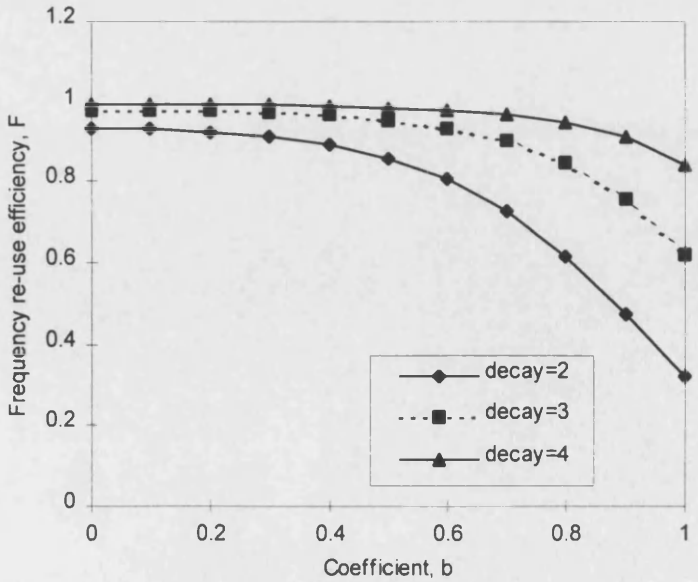

Figure 3-12. Directional antenna, B.W.=40^0, overlapping circular cells

These curves show that as the correlation between fades in the wanted cell and outer cell (within the bore-sight of the directional antenna) is increased (i.e. coefficient $b \rightarrow 0$), the frequency re-use efficiency approaches 100%. For typical mobile radio cellular structures the correlation between a and b is assumed equal, hence $b^2=1/2$ (i.e. $b=0.707$). As expected, if the decay index is increased, the path loss between the outer cell and the wanted cell is increased and the inter-cell interference is reduced, again resulting in a higher frequency re-use efficiency.

3.5 Cellular mobile systems

In this section a specific example of the general fading channel model, the mobile radio channel, will be characterised in terms of its statistical properties due to the omni-directionality of the antenna. Due to the specific environment in which a mobile radio operates, the mobile radio channel is also characterised by long-term statistics that are distributed on a log-normal basis. This long-term statistic is caused by shadowing by various obstacles in the direct path of the mobile radio wave. Because the presence or absence of these obstacles varies from location to location, the ability to communicate with any given mobile radio station may be statistically characterised in terms of a coverage reliability parameter. This section will present a modification to the analysis of the earlier section to take into account the mobile subscribers in a hexagonal cell structure.

The inherent design of cellular mobile applications in spread-spectrum designs introduces higher interference levels on the uplink due to omni-directional antenna from active mobile users. The calculations must now be extended to include all interfering users within the total area of the hexagon.

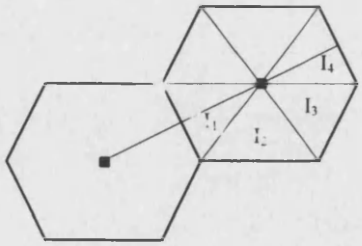

Figure 3-13. Hexagonal cell interference analysis

The total outer-cell interference from one cell in the first tier of interfering cells is given by:

$$I_{total} = 2(I_1 + I_2 + I_3 + I_4) \tag{3-30}$$

where,

$$I_1 = \frac{12P_t}{3\sqrt{3}R_t^2}\int_0^{\frac{\pi}{6}}\int_0^{\frac{\sqrt{3}R_t}{2\cos(\gamma)}} \frac{(r)^{\alpha+1}}{((\sqrt{3}R_t)^2 + r^2 - 2(\sqrt{3}R_t)r\cos\gamma)^{\frac{\alpha}{2}}} \cdot dr \cdot d\gamma$$

$$I_2 = \frac{12P_t}{3\sqrt{3}R_t^2}\int_{\frac{\pi}{6}}^{\frac{\pi}{2}}\int_0^{\frac{\sqrt{3}R_t}{2\cos(\gamma-\pi/3)}} \frac{(r)^{\alpha+1}}{((\sqrt{3}R_t)^2 + r^2 - 2(\sqrt{3}R_t)r\cos\gamma)^{\frac{\alpha}{2}}} \cdot dr \cdot d\gamma$$

$$I_3 = \frac{12P_t}{3\sqrt{3}R_t^2}\int_{\frac{\pi}{2}}^{\frac{5\pi}{6}}\int_0^{\frac{\sqrt{3}R_t}{2\cos(\gamma-2\pi/3)}} \frac{(r)^{\alpha+1}}{((\sqrt{3}R_t)^2 + r^2 - 2(\sqrt{3}R_t)r\cos\gamma)^{\frac{\alpha}{2}}} \cdot dr \cdot d\gamma$$

$$I_4 = \frac{12P_t}{3\sqrt{3}R_t^2}\int_{\frac{5\pi}{6}}^{\pi}\int_0^{\frac{\sqrt{3}R_t}{2\cos(\gamma-\pi)}} \frac{(r)^{\alpha+1}}{((\sqrt{3}R_t)^2 + r^2 - 2(\sqrt{3}R_t)r\cos\gamma)^{\frac{\alpha}{2}}} \cdot dr \cdot d\gamma \qquad (3\text{-}31)$$

This yields new values for the total interference I_s, which can be related to the frequency re-use efficiency, F, seen in figure (3-14) for the case of omni-directional antennas. Comparing figure (3-14) with figure (3-10) clearly shows the reduction in frequency re-use efficiency through the use of omni-directional antennas in hexagonal cell structures.

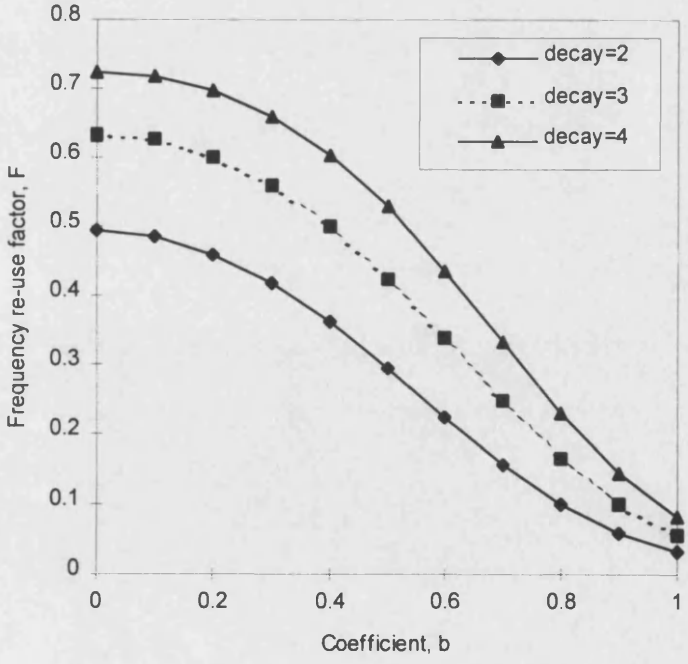

Figure 3-14. Hexagonal cell structure using omni-directional antenna

Figure (3-15) shows the inter-cell interference degradation factor for omni-directional antenna in a circular cell layout with the sides of all circles touching, rather than overlapping. This obviously leads to potential blackspots in the cellular coverage. A significant improvement in the inter-cell degradation factor, nevertheless, can be found.

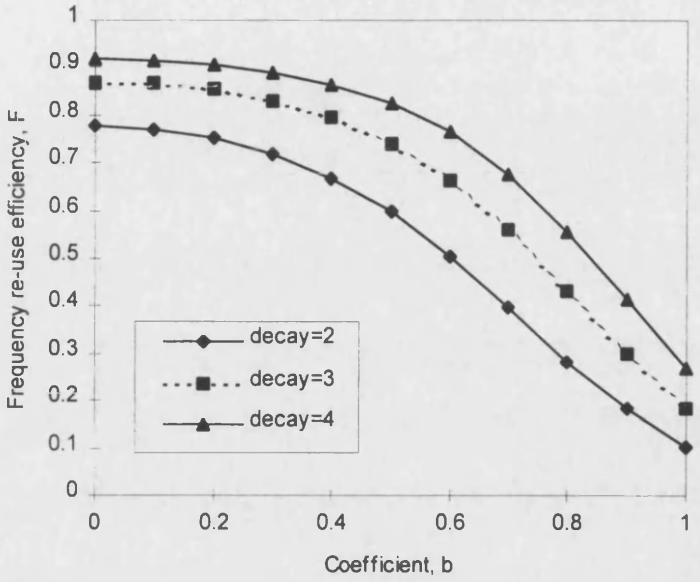

Figure 3-15. Circular cell structure (touching cells) using omni-directional antenna

Considering circular cells with overlapping edges, as shown in figure (3-16), will invariably increase the inter-cell degradation factor but reduce the area of 'blackspots' in the coverage

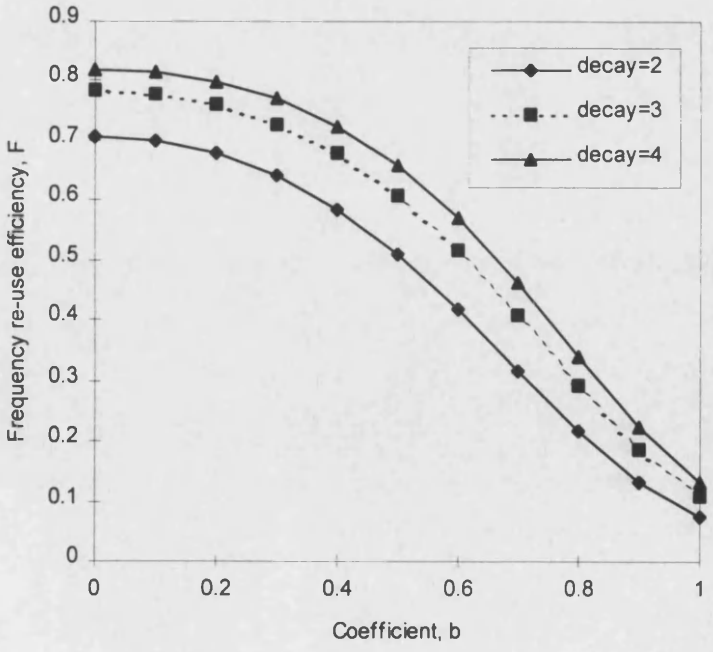

Figure 3-16. Circular cell structure (overlapping cells) using omni-directional antenna

area. Of course, the potential number of interferers to the wanted basestation will increase, therefore reducing the value of F.

3.6 Summary

DS-CDMA techniques provide a spectrally efficient technique of multiplexing a large user base to a central basestation for fixed and mobile wireless access systems. Whilst mobile air-interfaces can be applied to providing a fixed service, the quality and bandwidth requirements of fixed radio access imply that optimised technologies are preferred. Since DS-CDMA systems are inherently interference limited, it is of great importance to estimate the worst level of interference from other users in the surrounding tier of cells.

It has been shown how the assumptions about the type of cells used in the interference estimation can have a dramatic effect on the degradation in performance. With overlapping edges on circular cells the area of 'blackspots' is reduced at the expense of an increased level of inter-cell degradation factors.

For FWA systems, the interference levels are dominated by the effects of shadowing, which are directly related to the correlation between signals on the up- and downlink. This correlation between signals on the uplink of the interfering subscriber to his own basestation and the signal from the interfering subscriber to the unwanted basestation is higher than in mobile systems. This is due to the relative line-of-sight path that both links share, therefore giving, on average, a stronger weighting on correlated signals than an evenly distributed correlation. This result has been included in the interference analysis and has been shown to give dramatic interference reductions.

The use of highly directional antenna, on the other hand, reduces the interference from other users but is limited by the scattering effects and lack of direct line-of-sight paths. It can be seen that the use of highly directional antenna of beamwidth 40 degrees in a hexagonal cellular structure and assuming a decay factor of 3 will give a frequency re-use factor of nearly 0.9. This assumes that the correlation coefficient $b^2=1/2$. For overlapping circular cells, the frequency re-use factor F will not deviate much from its original value of 0.9.

An antenna beamwidth of less than 40 degrees will most likely be inappropriate for realistic FWA designs in urban hilly environments and the use of omni-directional antenna can be considered realistic for mobile applications. Indeed, the value of F for omni-directional antenna

and the same parameters as before using a hexagonal cell structure will give a value of 0.3 for the frequency re-use factor. A circular cell structure with touching cells will increase the level of F to 0.55.

In summary, we have shown that the correlation statistics for FWA applications are not the same as in mobile applications and lead to an increase in the frequency re-use efficiency. The use of directional antenna, in particular, leads to increased interference rejection and provides substantial capacity improvements. For these systems, the frequency re-use factor F is not as dependent on the type of cellular structure (i.e. hexagonal, circular overlapping or circular touching cells) as for mobile systems employing omni-directional antenna.

The overall effects on the total system capacity of FWA systems using the theory presented here can be seen in chapter 10.

3.7 References

[1] Gilhousen, K S, et al, "On the Capacity of a Cellular CDMA System", *IEEE Transactions on Vehicular Technology*, Vol. 40, No.2, pp.303-312, May 1991

[2] Ananasso, F, and Priscoli, F D, "Technology challenges in TDMA approach to 3rd generation personal communication services", pp. 702- 706, *IEEE Conf. Proceedings*, 1994

[3] Priscoli, F D, "Procedures for a fully integrated system including a cellular network and a GEO satellite system", *European Transactions on Telecommunications*, ETT, 1994

[4] Goodman, D J, "Efficiency of Packet Reservation Multiple Access", *IEEE Trans. on Veh. Techn.*, Vol. 40, No. 1, Feb 1991

[5] Newson, P and Heath, M R, "The Capacity of a Spread spectrum CDMA System for Mobile Radio with consideration of system imperfections", *IEEE JSAC*, Vol.12, No.4, May 1994

[6] Sklar, B, "Digital Communications - Fundamentals and Applications", *Prentice Hall* 1988

[7] Edwards, K R: Internal Technical Working Paper, NORTEL, Issue 1.1, NT/IP1/134/KRE/371, August 1995

[8] Monogioudis P, Edmonds R, Tafazolli R and Evans BG, "Multirate 3rd generation CDMA systems", *IEEE Int. Conf. On Comm.*, pp. 151-155

[9] Maxey, J J, and Ormondroyd, R F, "A study of wideband DS-CDMA systems for future generation fixed wireless access schemes", *Internal Report to NORTEL*, 27.1.97

[10] Maxey, J J, and Ormondroyd, R F, "A DS-CDMA design for fixed wireless schemes", *Internal Report to NORTEL*, 10.6.96

[11] Maxey, J J, and Ormondroyd, R F, "Evaluation of a fixed wireless access DS-CDMA system employing low-rate orthogonal convolutional codes", pp. 277-282, *Fifth European Conference on Fixed Radio Systems and Networks (ECRR'96)*, Bologna, Italy, May 1996

[12] Benedetto, V, and Scarabosio, L, "DS-CDMA systems for point-to-multipoint fixed radio in the access network", pp. 27-32, *Fifth European Conference on Fixed Radio Systems and Networks (ECRR'96)*, Bologna, Italy, May 1996

[13] Hewitt, T, Parente, P and Vepsalainen, P, "Future fixed service spectrum requirements – An operators' perspective", pp. 19-24, *Fifth European Conference on Fixed Radio Systems and Networks (ECRR'96)*, Bologna, Italy, May 1996

[14] Bollmann, A, *et al*, " Link-capacity and cellular planning aspects for a point to multipoint fixed radio access sytem", pp. 87-93, *Fifth European Conference on Fixed Radio Systems and Networks (ECRR'96)*, Bologna, Italy, May 1996

[15] Ericsson, "A comparison of CDMA and TDMA systems", CIRR TG 8/1, Washington, May 1991

[16] Monogioudis, P, Edmonds, R, Tafazolli, R and Evans, B G, "Multirate 3rd generation CDMA systems", *IEEE International Conference on Communications*, ICC'93, pp. 151-155, 1993

[17] Burr, A G, "Capacity improvement of CDMA systems using M-ary code shift keying", *IEE Conference Publication*, No. 351, pp. 63-67, 1991

[18] Ulloa, J A, Taylor, D P and Poehlman, W F S, "An Expert System Approach for Cellular CDMA", *IEEE Transactions on Vehicular Technology*, Vol. 44, No.1, pp.146-154, 1995

[19] Gass, J H, Noneaker, D L and Pursely, M, "Spectral Efficiency of a Power-Controlled CDMA Mobile Personal Communication System", *IEEE Journal on Selected Areas in Comms.*, Vol. 14, No. 3, April 1996, pp. 559-569

[20] Kudoh, E and Matsumoto, T, "Effect of Transmitter Power Control Imperfections on Capacity in DS-CDMA Cellular Mobile Radios", *Proc. of ICC'92*, Chicago, IL, pp.237-242, June 1992

[21] Viterbi, A J *et al*, "Performance of Power Controlled Wideband Terrestrial Digital Communication", *IEEE Transactions on Communications*, 41(4), pp.559-569, 1993

[22] Zou, J *et al*, "Reverse link analysis and performance evaluation for DS-CDMA cellular systems", *Proc. of IEEE PIMRC'94*, Sept. 1994

[23] Bhargava, V, "High Rate Data Transmission in Mobile and Personal Communications", *PIMRC'94*, pp. 1106-1113

[24] Lee, W C Y, "Increasing System Capacity in PCS", *IEEE Conf. Proceedings of PIMRC'94*, pp. 38-49, 1994

[25] Lee, W C Y, "Smaller cell for greater performance", *IEEE Communication Magazine*, pp. 19-23, Nov 1991

[26] Turkmani, A D *et al*, "Measurement and modelling of wideband mobile radio channels at 900 MHz", *IEE Proceedings*, Vol. 138, No.5, pp.447-457, October 1991

[27] Le Boudec, J Y, "The Asynchronous Transfer Mode: a tutorial", *Computer Networks and ISDN Systems*, No. 24, pp. 279-309, 1992

[28] Walrand, J, "Communication Networks: A first course", Aksen Associates, 1991

[29] Mueller, A J *et al*, "Code Rate Optimisation for Coded Packet CDMA Cellular Networks", *ICUPC'94*, Sept. 1994

[30] Mowbray, R S *et al*; "Increased CDMA system capacity through adaptive cochannel interference regeneration and cancellation", *IEE Proceedings-I*, Vol. 139, No.5, October 1992

[31] Yoo, Y C, Kohno, R and Imai, H, "A Spread-Spectrum Multiaccess System with Cochannel Interference Cancellation for Multipath Fading Channels", *IEEE J. on Selected Areas in Communications*, Vol. 11, No.7, pp. 1067-1075, Sept. 1993

[32] Kerr, R, Wang, Q, and Bhargava, V, "Capacity Analysis of Cellular CDMA", *Proc. ISSSTA'92*, pp. 235-238, March 1992

[33] Brockmeyer, B, Halstron, H L and Jensen, A, "The life and Works of A. K. Erlang", *Copenhagen Telephone Company*, 1943

[34] Jakes, W C, "Microwave mobile communications", *J Wiley & Sons*, New York

[35] Lee, W C Y, "Mobile Cellular Telecommunications Systems", *McGraw-Hill*, New York

CHAPTER 4:

DIRECT-SEQUENCE SPREAD-SPECTRUM

4.1 Introduction

This chapter describes the concept of direct-sequence spread-spectrum (DS-SS) modulation and how it forms the heart of a code-division multiple access scheme (DS-CDMA). The benefits of DS-SS in providing diversity in the mobile channel, through the use of a RAKE receiver, is discussed. In particular, the chapter describes different types of coding strategy that can be used in conjunction with DS-SS to enhance the performance of the DS-CDMA system. The use of orthogonal spreading sequences in combination with coding is described and a new spread-spectrum system that combines orthogonal coding and spreading is introduced. Finally the chapter describes a new high-performance orthogonal spreading/coding system. The performance of these new systems is presented in chapter 6.

DS-SS techniques are currently receiving considerable attention as likely contenders for the next generation cellular digital personal communications network (PCN). In particular, the use of DS-CDMA systems is at present looking very promising, compared to the conventional advanced Time Division Multiplex Access (TDMA) systems, and are only now implementable due to the availability of increased signal processing power. The ultimate goal is to maximise the potential number of simultaneous users sharing the same bandwidth within any specific cell boundary per unit area.

Some of the claimed CDMA advantages [1] are:

- High spectrum efficiency (high traffic capacity)
- No frequency planning required
- Soft hand-off and macrodiversity
- Graceful degradation (soft capacity)
- Low power consumption
- Flexible data rates, suitable for packet data

Conventional spread-spectrum systems rely on an internally generated PN sequence to spread the data in the receiver by means of modulo-2 addition. This causes the original data to be spread in bandwidth by a factor dependant on the PN sequence chip rate. If the PN sequence is of repetition length N, and one data period lasts for the whole repetition length, as is often the case, then the data will experience a spread in bandwidth proportional to N, as seen in figure (4-1). The factor N, by which the data is increased in bandwidth, can be termed the spreading ratio

of the base-station transmitter, and from this spreading ratio may be obtained a process gain representing the ratio that additive noise from the channel is reduced prior to data demodulation.

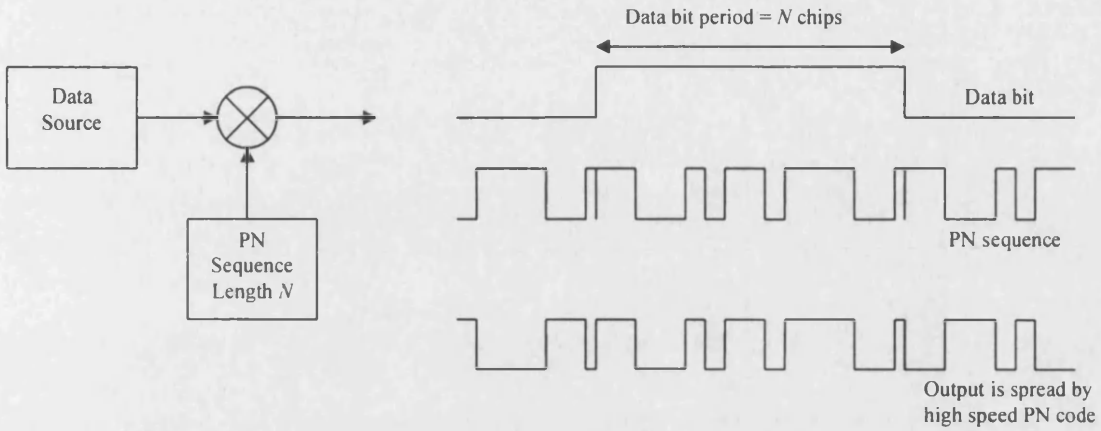

Figure 4-1. A simple spread-spectrum system design principle

In the receiver, the wideband spread signal is multiplied by the same synchronised PN sequence to obtain the original data information, and through a demodulator such as matched filters or integrate-and-dump systems (used for rectangular signals) followed by threshold detection can be successfully detected. The matched filter for any signal has an impulse response that is the shifted time reverse of the signal (conjugate time reverse for a complex signal). The typical layout of a spread-spectrum modem is shown in figure (4-2).

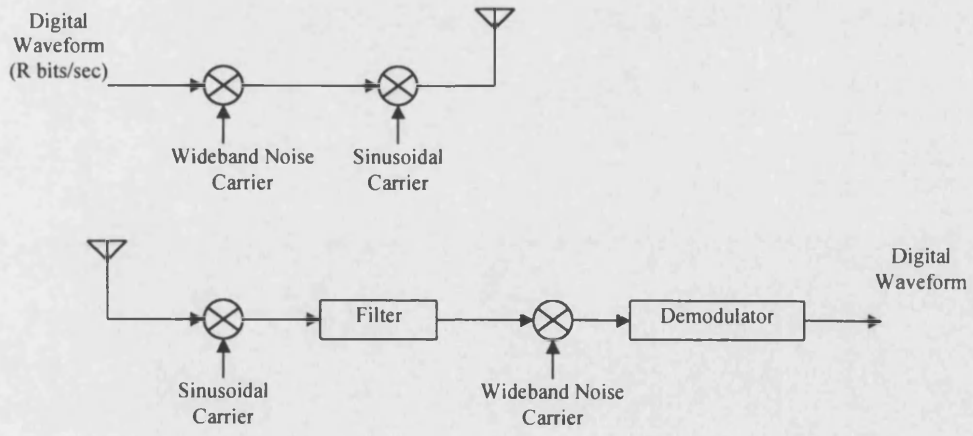

Figure 4-2. Spread-spectrum modem

This is not the only way of spreading the bandwidth of the data in the transmitter base-station, however. Figure (4-3) shows how a convolutional encoder of rate $1/N$ also introduces a redundancy of N symbols and hence also provides bandwidth spreading. If the PN sequence

spreading process is now replaced by an equivalently low-rate convolutional code, the complete spread-spectrum implementation could be re-configured to incorporate spreading and coding within the same unit. It is this type of spreading that is analysed in this chapter.

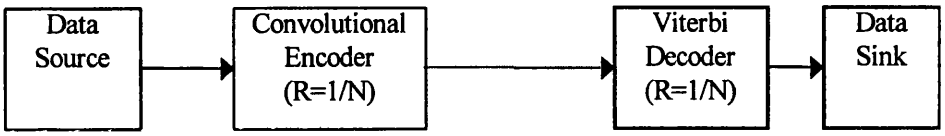

Figure 4-3. Spread-spectrum using convolutional coding

4.2 *Signature Waveform Generation*

In a multi-user system, the data for all N_u users in the system is spread using a unique signature code or waveform for each user. One seeks codes that exhibit high auto-correlation values and consistently low periodic cross-correlation statistics, such as the well-known Gold codes [2]. These codes are therefore particularly well suited to DS-CDMA applications.

The basis for using pseudo-random noise generators is contained within their auto-correlation properties, in other words, the result of multiplying the code by a delayed version of itself, and then adding linearly a predetermined number of successive resulting binary digits should be very small for all delays other than zero. Here we need to consider delays only in terms of whole numbers of code bits or clock periods (for a DS-CDMA system these are termed *chips*). There are many ways in which such a sequence can be generated.

It is important to note that because of the auto-correlation properties of the code, it is vital to ensure perfect synchronisation between transmitter and receiver, otherwise the correlation of these codes would significantly degrade the performance. Since any PN sequence has the property of having numbers of 0s and 1s differing by one, there is great advantage for clock synchronisation since no long periods of zeros or ones will be present in the signal. For maximal length sequences (*m*-sequences), the length of a run is a maximum of *m* code symbols.

Because of its excellent auto-correlation function and good cross-correlation characteristics, the *m*-sequence is probably the most useful PN sequence for many DS-CDMA applications. The usual way of generating a maximal length sequence is with a linear feedback shift register circuit. The typical auto-correlation function of a maximal-length sequence is illustrated in figure (4-4).

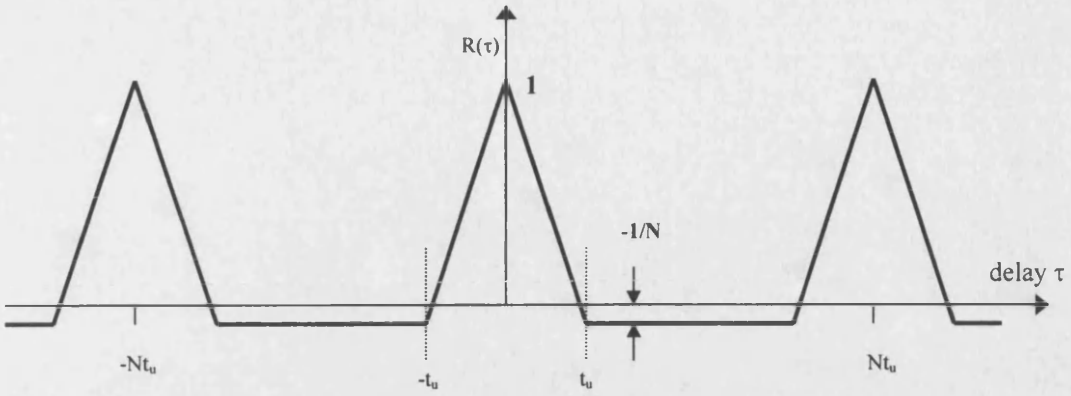

Figure 4-4. Auto-correlation function of an m-sequence

Note, that on a normalised basis, figure (4-4) has a maximum value of one that repeats itself every period, but between the peaks, the level is of constant value $-1/N$. If N is a very large number, the auto-correlation function will be very small in this region. It is thus possible to obtain a set of codes that are almost mutually orthogonal by simply employing delayed versions of the same sequence. This is one way of generating codes for users in a DS-CDMA system. It is this property which produces excellent user isolation within a DS-CDMA system, and is therefore also called code division multiple access (CDMA), since direct-sequence spread-spectrum transmissions can co-exist in the same bandwidth. Most CDMA systems rely on spreading codes that give low cross-correlation between users and a high auto-correlation peak for delays directly proportional to the sequence length.

An alternative method of generating orthogonal codes for users in a DS-CDMA system can be accomplished by cascading 2 *m*-sequence generators as shown in figure 4-5. For different users thus enables each user to cause little interference to the others. Of course, in realistic channel models where multipath fading dominates, the orthogonality between users is significantly degraded, or even completely destroyed.

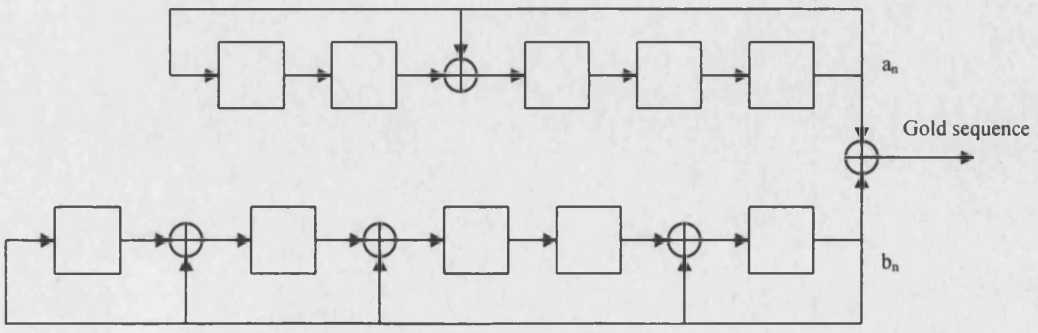

Figure 4-5. Generation of a Gold code

Gold codes are another important class of PN sequence and generated by the modulo two addition of a preferred pair of *m*-sequences, say $\mathbf{a} = [a_1, a_2, ..., a_n]$ and $\mathbf{b} = [b_1, b_2, ..., b_n]$. The characteristics of preferred pairs of *m*-sequences are defined later in this section. Figure (4-5) shows how each *m*-sequence is generated from a chip-spaced cyclic shift register with feedback connections corresponding to a preferred polynomial. In figure (4-5), two 6th order sequences are used with taps corresponding to the polynomials:

$$a_n = n^5 \oplus n^2 \oplus 1$$
$$b_n = n^5 \oplus n^4 \oplus n^2 \oplus n \oplus 1 \qquad (4\text{-}1)$$

For this simulation preferred polynomial pairs have been taken from the tables produced by Peterson and Weldon [3].

A full set of Gold codes is constructed by modulo 2 addition of **a** with cyclically shifted versions of **b** or vice versa. Thus, for m^{th} order *m*-sequences, 2^m-1 Gold codes can be generated. Since **a** and **b** also constitute members themselves, there are a total of 2^m+1 Gold sequences in the set. This is the upper limit on the number of users in a DS-CDMA system before sequence re-use has to be considered. However, other factors such as the bit-error rate dictate the maximum number of users.

It is desirable to find reasonably large sets of spreading sequences that have small auto-correlation sidelobes in the time intervals during which delayed signals with significant power are expected. This will minimise the self-interference due to multipath. The spreading sequences must have small cross-correlation sidelobes over all delays because the uplink transmissions are asynchronous. A subset of the Gold sequences can be constructed having these desirable correlation properties. Gold [4] showed that the cross-correlation function between any pair of sequences from the set of 2^m+1 Gold codes and the off-peak auto correlation functions take one of the three possible values –1, -*t*(*m*), *t*(*m*)-2 where,

$$t(m) = \begin{cases} 2^{(m+1)/2} + 1 & \text{m odd} \\ 2^{(m+2)/2} + 1 & \text{m even} \end{cases} \qquad (4\text{-}2)$$

These are known as preferred pairs of *m*-sequences. Of these $2^m + 1$ sequences, $2^{m-n+1} + 1$ of them will have their first auto-correlation [*t*(*m*)-2 or –*t*(*m*)] at least *n* chip durations from the main lobe. Consequently, this subset of sequences will introduce negligible self-interference if used on a channel having *n* or fewer significant paths.Throughout this dissertation Gold codes are set equal in length to the system symbol period. A length 31 chip code will therefore have a

processing gain or bandwidth spreading factor equivalent to its length; a system with chip rate of 1 MHz and 14.9dB (10log 31) of processing gain will have a symbol rate of 32.26 kbaud.

An alternative approach to the generation of orthogonal signature waveforms is to employ Walsh-Hadamard sequences. These sequences provide orthogonal code set isolation between individual users, but exhibit bad auto-correlation properties. In a fully synchronous downlink mobile radio communication channel we can use Hadamard Walsh codes as an optimum orthogonal set, because we do not have to pay attention to the auto-correlation characteristics of the spreading code. Applications requiring a good auto-correlation function, however, need to employ additional PN randomising strategies. These methods are covered in the next sections.

4.3 Modulation Schemes

The simulations described in this thesis employ binary phase-shift keying (BPSK) modulation, whereby the carrier is modulated according to:

$$\begin{aligned} r(t) &= d(t)\cos(w_0 t) \\ &= \pm\cos(w_0 t) \end{aligned} \tag{4-3}$$

where $d(t)$ is the bipolar data to be transmitted at time t. Most receiver carrier recovery techniques have a phase ambiguity of $\pm\pi$ radians, which clearly presents a problem for BPSK demodulation. To circumvent the problem of phase ambiguity, differential binary phase shift keying (DPSK) is used. The data stream for transmission is differentially encoded by modulo-2 addition of each bit with the previously encoded bit, as shown in figure (4-6).

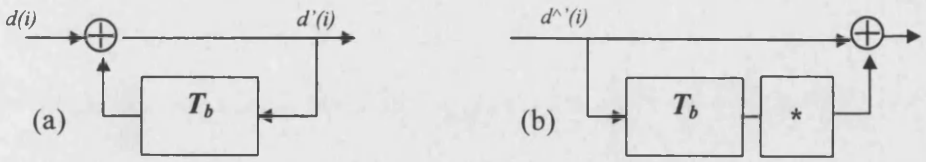

Figure 4-6. Differential encoding, (a), and decoding, (b)

The differentially encoded data stream $d'(i)$ is given by:

$$d'(i) = d'(i\text{-}T_b) \oplus d(i) \tag{4-4}$$

The result is that $d(i) = 1$ now gives rise to a π change of phase of the carrier and $d(i) = 0$ to no change in carrier phase. Thus, the DPSK output corresponds to:

$$r(t) = d'(t)\cos(w_0 t) = \pm\cos(w_0 t) \tag{4-5}$$

To differentially decode the signal at baseband, the received signal is modulo-2 added with a delayed version of the complex conjugate of itself, resulting in the decoded signal:

$$\hat{d}(i) = \hat{d}'(i) \oplus \hat{d}^{*'}(i - T_b) \tag{4-6}$$

As decoding of a bit is carried out by comparison with the bit in the previous time interval, bit errors always occur in pairs in DPSK. A mistake in decoding a bit leads to the succeeding bit being compared with the bit in error and it too will be falsely decoded. Using differential phase-shift keying incurs a penalty of about 0.5 dB in E_b/N_o at a bit-error rate of 10^{-5} over standard PSK, but it is commonly employed because of the phase ambiguity problem alluded to above. DPSK modulation schemes are also in great favor for non-coherent transmission schemes, since no channel characteristics need be known at the receiver – demodulation and detection relies on a relatively constant phase and amplitude variation of the channel from one bit to the next.

Although only BPSK modulation is implemented in the simulations presented here, more complex modulation schemes such as *M*-ary QAM or *M*-ary PSK could be employed. These schemes are of particular high interest in bandwidth-limited and power-limited channels, respectively.

4.4 Forward Error Correction Coding

The structure of a convolutional code is fundamentally different from the processing of data in a PN encoded CDMA system. Specifically, information sequences are not encoded by simply using one data bit at a time to provide the encoded output sequence but rather a continuous sequence of information bits is mapped into a continuous sequence of encoder output symbols. To achieve this, the data sequence is fed into a linear shift register system consisting of K shift registers. The value of K is often referred to as the constraint length of the convolutional code. This mapping is highly structured, enabling a decoding method considerably different from the despreading process in a spread-spectrum system to be used. It can be argued that convolutional coding can achieve larger coding gain than a PN sequence encoded system of the same complexity. This is the prime reason for yielding such a large interest in the field of spread-spectrum communications, especially due to the fact that real-time decoding strategies can be

formulated for forward error correction. Specifically, the encoder maps sequences of source code outputs into sequences of code symbols for transmission over the discrete memoryless channel (DMC). The purpose of this mapping is to improve communication efficiency by enabling the system to correct transmission errors. Convolutionally coded systems process lengthy sequences of information symbols to generate code sequences which are correspondingly lengthy.

4.4.1 Convolutional Codes

The elegant structure of convolutional codes enables processing (i.e. coding and decoding) of these lengthy sequences a few symbols at a time, both in the encoder and decoder. The codeword sequences are generated in a manner that ensures that codeword sequences due to different information sequences are separated from one another in Hamming distance. This separation allows several transmission errors to be corrected by the decoder. The more symbols that are used to represent one data bit, the higher the probability of obtaining no errors on decoding the data. This is therefore reflected in the code rate R of the system, since a low code-rate implies a low probability of bit-errors in the decision process.

The optimum decoding rule for convolutional codes used in a spread-spectrum system is the same as for PN codes; the decoder will estimate the transmitted code sequence to be the sequence which was most likely to have been transmitted given the known code structure, channel characteristics and received sequence. An efficient algorithm such as the Viterbi algorithm is often used to decode blocks of convolutionally encoded data.

To understand the mathematical concept behind convolutional coding, consider an encoder of constraint length 3 and code rate 1/2. The information sequence $Y = (y_0, y_1, y_2, y_3, \ldots)$ enters the encoder one bit at a time. The two encoder output sequences X_1 and X_2 can be obtained as the convolution of the input sequence Y_1 with the two encoder "impulse responses". The impulse responses of the encoder can be found by using an input sequence of {1 , 0 , 0 , ...} and observing the two output sequences. Since the encoder has K shift register stages, the impulse response will last for a maximum of m time units, and is written as $g1=(g1_0, g1_1, g1_2, \ldots, g1_{K-1})$ and $g2=(g2_0, g2_1, g2_2, \ldots, g2_{K-1})$.

For this particular encoder, not surprisingly, the impulse responses yield a "one" for each tap:

$$g1=\{1,1,1\} = 1+D+D^2$$
$$g2=\{1,0,1\} = 1+D^2 \quad (4\text{-}7)$$

These are termed the generator sequences of the code.
The encoding equations can now be written as:

$$X_1 = Y * g1$$
$$X_2 = Y * g2 \quad (4\text{-}8)$$

Where * denotes discrete convolution and all operations are modulo-2 (i.e.-OR). Hence, this type of operation is the origin of terming this type of coding as convolutional.

It can be shown that this type of encoding operates in the same linear way as a spread-spectrum system does. To illustrate this, consider two different message signals which may be labelled as $Y_1(D)$ and $Y_2(D)$. These two code sequences are defined by the products of:

$$X1_j(D) = Y_1(D)g_j(D)$$
$$X2_j(D) = Y_2(D)g_j(D) \quad (4\text{-}9)$$

where $j = 1,2$ since the encoder is of rate $R=1/2$.

The modulo-2 sum of these two sequences is represented by:

$$X1_j(D) + X2_j(D) = Y_1(D)g_j(D) + Y_2(D)g_j(D)$$
$$= g_j(D)[\,Y_1(D) + Y_2(D)\,] \quad (4\text{-}10)$$

Since the modulo-2 sum of any two message sequences is a another message sequence, and the product of a message sequence and $g_j(D)$ yields a code sequence, the sum of two code sequences is another code sequence. Thus, the principle requirement for linearity has been fulfilled. This principle of linearity is extremely important if convolutional coding is to imitate a PN sequence in a spread-spectrum system.

The relation between constraint length and code rate of a convolutional encoder provides the boundaries for provisional implementation of such a design into a spread-spectrum system. As described earlier, a convolutional coding strategy is linear. Thus, such a design can be implemented into a spread-spectrum system if the codes are orthogonal. At present there are few

codes that provide good orthogonality (except Walsh codes) and the main problem lies in providing an optimum arrangement for tap specification for the encoder.

The free distance of a convolutional code depends strongly on the constraint length and set-up of the encoder. Assume that the "all-zero" path is the correct path. If at any stage of the decoding process one wrong path is chosen (in this case a data input of '1'), the path will merge with the correct all-zero path after a few states through the trellis. The number of corresponding bits associated with each branch on the wrong path which are different from the all-zero branch metrics is called the free distance.

Different constraint length encoders and decoders have variations in their bit-error performance curves. As the constraint length of an encoder is increased, the number of possible states in the Markov state model grows exponentially, and therefore the free distance will also increase. An increase in free distance can be interpreted as making the convolutional code more efficient in low bit-error environments. Viterbi [5] has shown, that the BER performance of a Viterbi algorithm, operating under AWGN, and using hard decision limiting is given by:

$$BER < \sum_{z=dfree}^{\infty} c_z P_z \tag{4-11}$$

$$\text{where } P_z = \begin{cases} \sum_{e=(z+1)/2}^{z} \binom{z}{e} p^e (1-p)^{z-e} & \text{z odd} \\ \frac{1}{2}\binom{z}{z/2} p^{z/2}(1-p)^{z/2} + \sum_{e=z/2+1}^{z} \binom{z}{e} p^e (1-p)^{z-e} & \text{z even} \end{cases} \tag{4-12}$$

It can thus be seen that an increase in free distance will inevitably reduce the value for P_z. The probability of any bit-errors on the received signal will be related directly to the Q-function of the signal-to-noise ratio (SNR). If the value of z increases, the probability p will be involved in a polynomial function whose degree depends on z (see 4-12). Therefore, the BER versus SNR will involve a polynomial whose degree increases as the free distance increases. It must be mentioned that the coefficients c_z, which are determined from the generating function of the convolutional encoder, will increase in value as z increases. This has the further effect of shaping the BER performance for different noise levels; hence giving a CDMA system, operating in AWGN, a large coding gain at low noise levels and a worse performance than the conventional DS-CDMA implementation at high noise levels.

The resulting effect of varying the constraint length K of the encoder can be viewed in figure (4-7). The theoretical graph displays a rate R=1/2 convolutional encoder operating in an additive white Gaussian noise (AWGN) environment with hard limiting. As expected, with an increase in K overhead, the BER performance improves at low bit-error rates at the cost of reduced efficiency at high bit-error rates. Note also, that the 'gradient' of each graph can be seen to increase as the constraint length increases, the reason having been explained earlier.

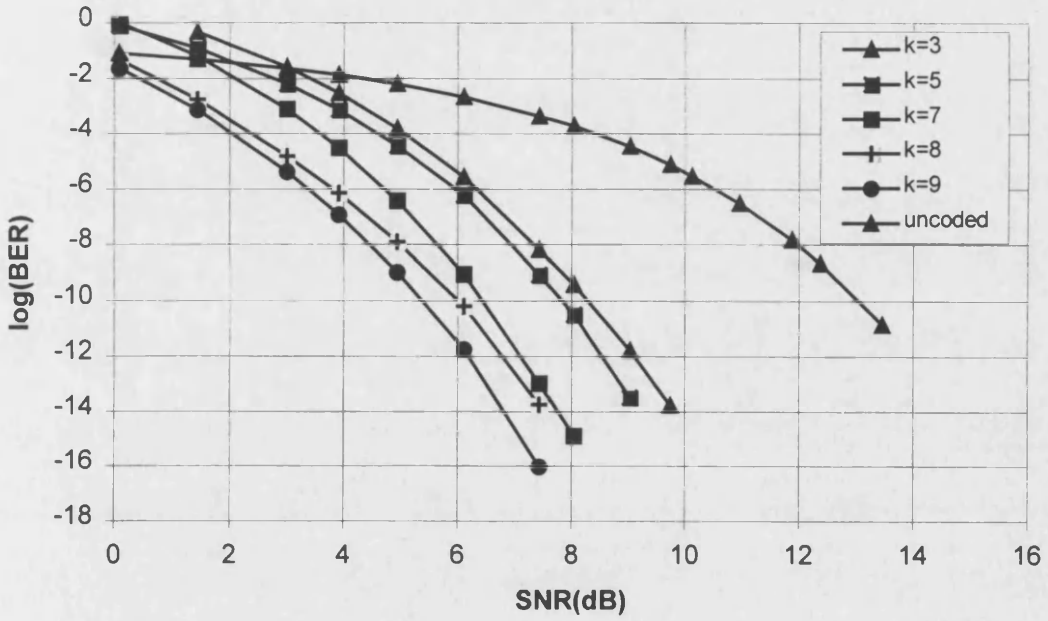

Figure 4-7. BER performance of R=1/2 convolutional codes

At present, coding techniques have been well established to approach the Shannon limit of -1.6dB as closely as possible. As the coding techniques become more advanced, large coding gains are available to the system. With the increase in coding gain available, it is possible to effectively increase the number of users in a CDMA system through the use of more complex coding schemes and hardware.

The advantage gained by employing a convolutional encoder directly onto the data input is extracted from the coding gain of the convolutional coding technique. This can be explained by the simple example of a theoretical spread-spectrum CDMA system, described below.

Assuming that an ordinary direct sequence spread-spectrum system employs a PN sequence of length 128, each data bit will be effectively represented by 128 bits. Thus, an increase of 128 times the original bandwidth will be encountered. This will therefore reduce the necessary SNR required to achieve a given BER by 21.07dB (10log 128), the trade-off being an increase in necessary bandwidth of 128 times the original bandwidth of the data input signal. In practical

CDMA systems, an encoder of rate R=1/2 and constraint length K=7 will yield a coding gain of about 6dB, at the cost of an effective 3dB loss due to a bandwidth expansion of factor 2 (i.e. 1/Code Rate). Therefore, an additional 3dB will be gained by the system and if the performance under AWGN was the same as for multi-user interference, the number of users could theoretically be doubled. In realistic applications, nevertheless, the multi-user interference presents different interference and noise statistics and the gains achievable are thus much lower.

4.4.2 Low-Rate Orthogonal Convolutional Codes

If the present-day PN sequence generation method is now replaced by the convolutional encoder, operating at a rate R=1/16, each data bit will have a redundancy of 16. There will be an effective increase in bandwidth of factor 16. In the receiver, the maximum-likelihood decoding algorithm will achieve a coding gain governed by the construction of the convolutional code. The advantage such a system has over the conventional DS-CDMA design is due to the fact that any additional coding gain which may be present will be available to the system user at no cost of increased bandwidth! Because the convolutional encoder spreads the data signal there is no need to modulo-2 add the PN sequence to the data bit.

The need for orthogonality between different simultaneously transmitting users in the shared bandwidth of a DS-CDMA system has placed great emphasis on the design of PN spreading sequences which produce the least amount of self interference by other users within a cellular boundary.

It is widely known that there are 3 major possibilities of spreading the data bits (Figure (4-8)-figure (4-10)). In figure (4-8) code spreading is accomplished by multiplying the data signal of each user by a unique PN sequence with a period much larger than the data bit duration T_b. DS-CDMA systems suffer from the disadvantage that the cross interference produced by the multiple users cannot be easily controlled and optimised by proper code selection. This is due to the fact that the cross interference is determined by the more or less random cross-correlation of spreading code segments with the symbol length T_b which is only a small portion of the full PN sequence. On the other hand, code selection and management is simplified considerably.

Another method which forms the basis for the system in this featured low-rate convolutional DS-CDMA implementation is illustrated in figure (4-9). Here each user has its data bits uniquely mapped onto a set of orthogonal code sequences with a duration equal to T_b. Each code

sequence which is present simultaneously with the code sequences generated by other users must all be orthogonal to each other.

The major advantage of orthogonal symbol-by-symbol code spreading lies in the fact that the orthogonality and the cross-correlation functions (and hence the cross interference) of the spreading code sequences can be directly controlled by careful selection of the code sets. If synchronous symbol transmission and reception on the downlink can be achieved within a cell this will enable considerable capacity improvement.

The last implementation is displayed in figure (4-10), where DS-CDMA is combined with orthogonal symbol-by-symbol code spreading. The PN sequence is continuously multiplied by a Walsh function with period T_b, which is uniquely assigned to each of the subscribers. By applying a complete set of orthogonal Walsh functions to a single fixed PN sequence a finite set of long-period DS spreading functions can be defined with guaranteed orthogonality between each bit-length correlation. This type of implementation is used by the current Qualcomm CDMA system.

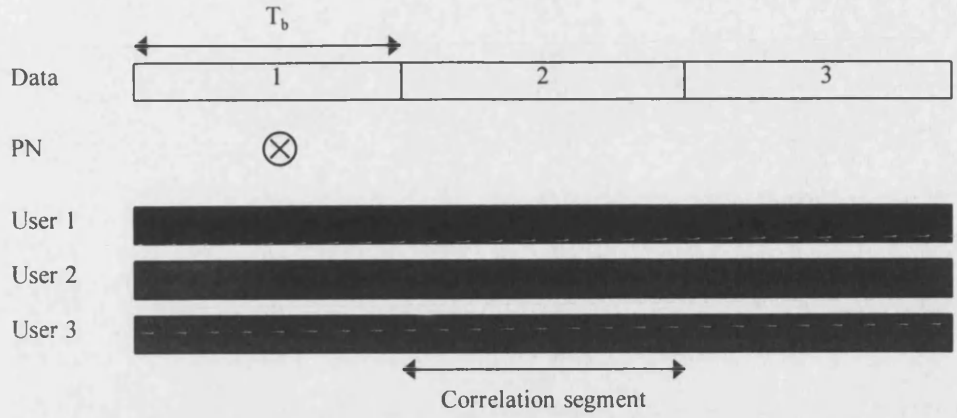

Figure 4-8. Direct sequence code spreading

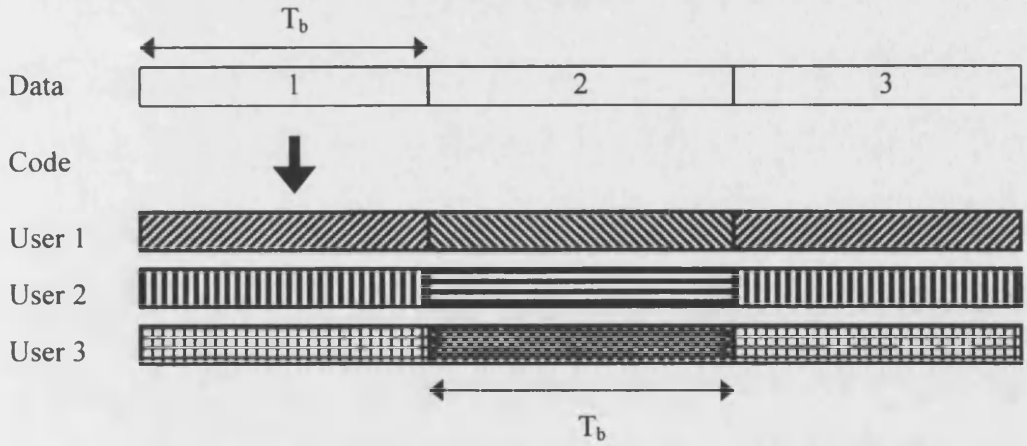

Figure 4-9. Orthogonal symbol-by-symbol code spreading

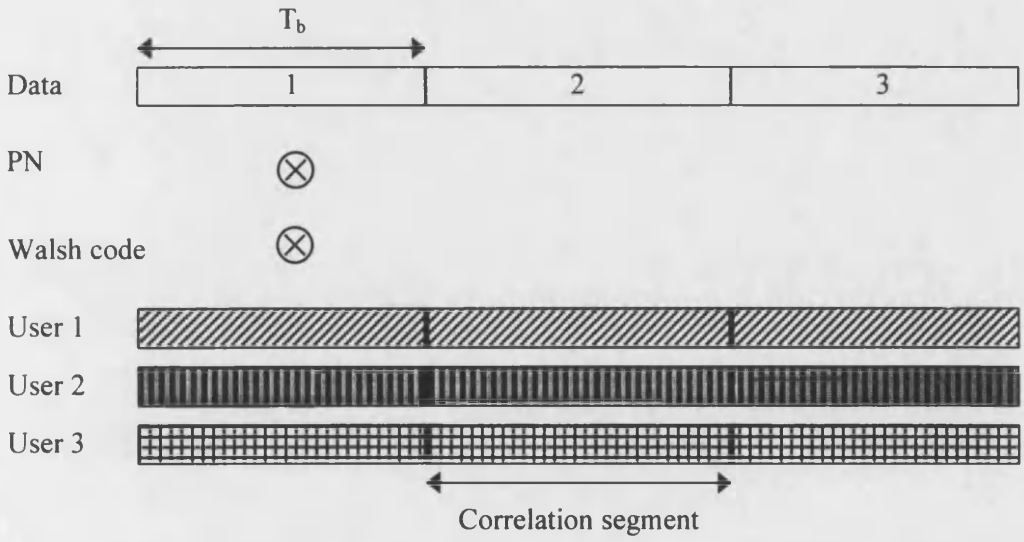

Figure 4-10. Combined DS and Orthogonal symbol-by-symbol code spreading

The orthogonality of ordinary convolutional codes is very poor, and this would lead to a small number of simultaneous users. If low-rate convolutional codes are to be implemented into a DS-CDMA system then the output bit sequence corresponding to a particular shift register state must be orthogonal to all other output sequences generated by other users. One way of providing orthogonal convolutional codes is through cascading a convolutional encoder with a Hadamard block encoder [8,9]. A Hadamard block encoder, as shown in figure (4-11), works by selecting one of the rows of a $2^K \times 2^K$ Hadamard matrix, the state of the convolutional shift register system dictating which row is selected. If all users have different tap configurations linking the convolutional encoder to the Hadamard encoder then the users can be said to be operating with mutually orthogonal codes which all follow a different trellis. Since the encoder comprises of K shift registers, the number of possible states it can have is 2^K. It is therefore necessary to provide 2^K different rows in the Hadamard matrix. A code array of size $2^K \times 2^K$, where K is the constraint length of the code, which is given by the matrix relation:

$$H_k = \begin{bmatrix} H_{k-1} & H_{k-1} \\ H_{k-1} & \overline{H}_{k-1} \end{bmatrix} \quad k = 1,2,.....K \tag{4-13}$$

where H_0=0 and $\overline{H}_k$ is the complement to H_k, will produce 2^K rows which are all completely orthogonal to one another. If the block encoder chooses one row consisting of 2^K symbols, the effective code rate will be 2^{-K} bits per code symbol. If the Hadamard block encoder maps a convolutional shift register system of constraint length K=4 into one row of data there will be 16 possible states corresponding to 16 rows of the Hadamard block encoder. The spreading ratio (i.e. processing gain) of such a design will be equal to 16.

For this implementation, the following 16×16 Hadamard matrix is produced:

$$H_4 = \left|\begin{array}{cccccccccccccccc}
0&0&0&0&0&0&0&0&0&0&0&0&0&0&0&0\\
0&1&0&1&0&1&0&1&0&1&0&1&0&1&0&1\\
0&0&1&1&0&0&1&1&0&0&1&1&0&0&1&1\\
0&1&1&0&0&1&1&0&0&1&1&0&0&1&1&0\\
0&0&0&0&1&1&1&1&0&0&0&0&1&1&1&1\\
0&1&0&1&1&0&1&0&0&1&0&1&1&0&1&0\\
0&0&1&1&1&1&0&0&0&0&1&1&1&1&0&0\\
0&1&1&0&1&0&0&1&0&1&1&0&1&0&0&1\\
0&0&0&0&0&0&0&0&1&1&1&1&1&1&1&1\\
0&1&0&1&0&1&0&1&1&0&1&0&1&0&1&0\\
0&0&1&1&0&0&1&1&1&1&0&0&1&1&0&0\\
0&1&1&0&0&1&1&0&1&0&0&1&1&0&0&1\\
0&0&0&0&1&1&1&1&1&1&1&1&0&0&0&0\\
0&1&0&1&1&0&1&0&1&0&1&0&0&1&0&1\\
0&0&1&1&1&1&0&0&1&1&0&0&0&0&1&1\\
0&1&1&0&1&0&0&1&1&0&0&1&0&1&1&0
\end{array}\right|$$

The way in which each row is generated is simple: On each data transition of time period T_b the shift register system takes on a new state. For this state an output sequence of 2^K bits is generated by clocking the switches and lower shift registers 2^K times faster than the upper shift registers. This implies that the Hadamard block encoder must operate at a speed of $\frac{T_b}{2^K}$. The switching matrix comprises of a simple mapping of shift registers to the Hadamard block encoder inputs and can be varied for every user.

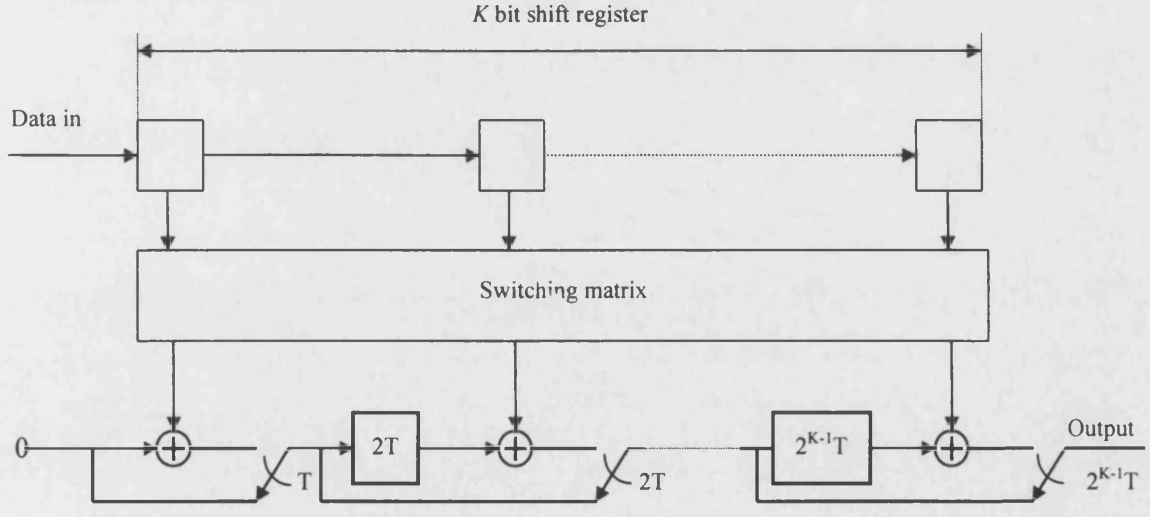

Figure 4-11. A low-rate orthogonal convolutional encoder

In order to provide reliable communication in a burst noise environment, this data is also interleaved, and it has been shown [10] that the interleaving depth of this low rate convolutional design can be lower than current digital DS-CDMA systems.

When observing the 16 output symbols of each row, it can be seen that the anticipated auto-correlation function of the output signal is very poor; i.e. there are 'spikes' in the auto-correlation function at values other than the zero delay. The typical output power spectrum of four encoded data bits from a Hadamard encoder of constraint length K=4 can be viewed in figure (4-12). It can be seen that the spectrum does not yield a smooth response at low frequencies but instead gives power spectra concentrated into particular frequencies, especially at the low frequency band.

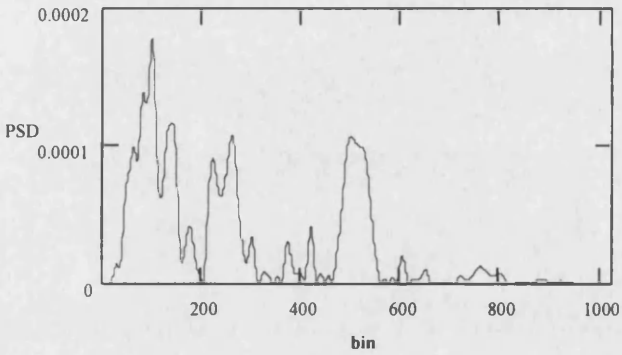

Figure 4-12. Power spectrum of Hadamard encoded data via FFT of 1024 points

Since the cross-correlation property of the orthogonal codes is also very poor, an additional stage of randomisation is provided after the orthogonal encoder, effectively providing a smoother spectrum. For DS-CDMA systems it is desirable to have the smoothest possible spectrum for the shared bandwidth between all users.

Another mathematical approach is to define the auto-correlation function of the encoded output signal before and after randomisation to gain insight into the typical spectral density distribution.

First, the auto-correlation function of a typical orthogonal signal is studied. Since the output signal has a distinct pattern within each data bit period (see 16x16 Hadamard matrix), the output spectrum will be very different from that of a random signal. Assuming one form of orthogonal periodic signal to be as illustrated in figure (4-13), the mean square value is given by A^2. The auto-correlation function for such a signal can therefore be deduced as:

$$R(\tau) = \begin{cases} A^2\left(1 - \dfrac{\tau}{xt_u}\right) & (x-1)t_u < \tau < xt_u \\ A^2\left(\dfrac{\tau}{xt_u} - 1\right) & xt_u < \tau < (x+1)t_u \end{cases} \qquad (4\text{-}14)$$

where x = 1 , 3 , 5 .....

Using the auto-correlation points at intervals of $2t_u$ will result in a frequency response with many different frequency components, thus giving a very uneven spectrum over the bandwidth concerned:

$$S(w) = A^2 + 2A^2\cos(wT_s) + 2A^2\cos(2wT_s) + 2A^2\cos(3wT_s) .... \qquad (4\text{-}15)$$

This type of frequency response is non-optimal for a DS-CDMA system and hence it is necessary to improve the frequency spectrum.

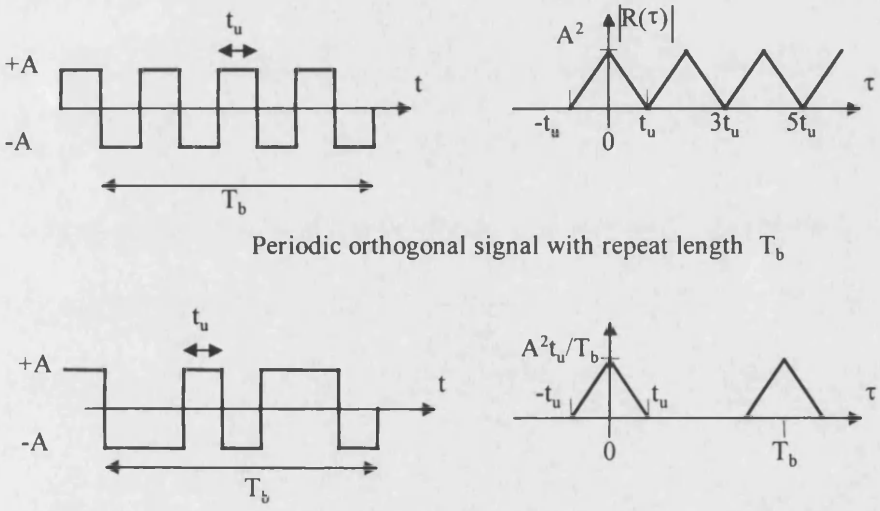

Figure 4-13

The mean square value of a pseudo-random periodic sequence, however, is given as A^2t_u/T_b, and hence the auto-correlation function is related by:

$$R(\tau) = \frac{A^2}{T_b}\left(t_u - \tau\right) \qquad \text{for} \qquad -t_u < \tau < t_u \qquad (4\text{-}16)$$

To determine the spectral density characteristic *S(w)* of the random signal a simplified approach can be used. Taking the limiting value of $R(\tau)$ as $t_u \to 0$ describes $R(\tau)$ in terms of a unit impulse response and hence a flat spectrum in the frequency domain:

$$\lim_{t_u \to 0} R(\tau) = \frac{A^2 t_u^2}{T_b} \delta(t) \qquad (4\text{-}17)$$

Since the frequency response of the unit impulse yields a constant spectrum, it can thus be seen that the frequency response will be constant over the bandwidth in operation with a value of $A^2t_u^2/T_b$.

Randomisation is easily achieved by means of employing a PN sequence generator of the same length as the spreading ratio. The resulting power spectrum after randomisation can be viewed in figure (4-14). It can be seen that the power is spread out more evenly over the low frequency band, thus providing a smoother output spectrum. This is of great importance to the system designer since it minimises the interference levels produced by "other-user" noise, which are encountered at the output of the correlator in the receiver.

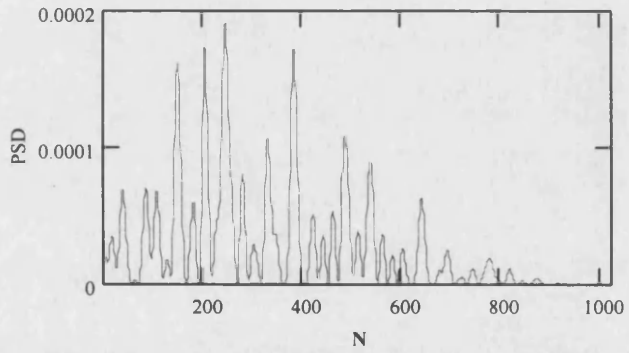

Figure 4-14. Output power spectrum of Randomiser via FFT of 1024 points

It has therefore been shown that the use of randomisation on the orthogonally encoded signal from each user will give significant spectral improvements and optimise the performance in "other-user" noise.

4.4.3 Hyper-Orthogonal Codes and State Diagrams

The usual method of representing convolutional encoders is by generating a state diagram of all possible states for the shift register memory. On each transition, caused by a binary input of zero or one, the output symbols are compared with the all zero path to determine the Hamming distance, *w*, between branches of the Trellis. In the same way, this method also applies to low-rate convolutional codes.

We start with a simple low constraint length low-rate orthogonal code. The state diagram for a K=4 low-rate orthogonal convolutional code is shown in figure (4-15).

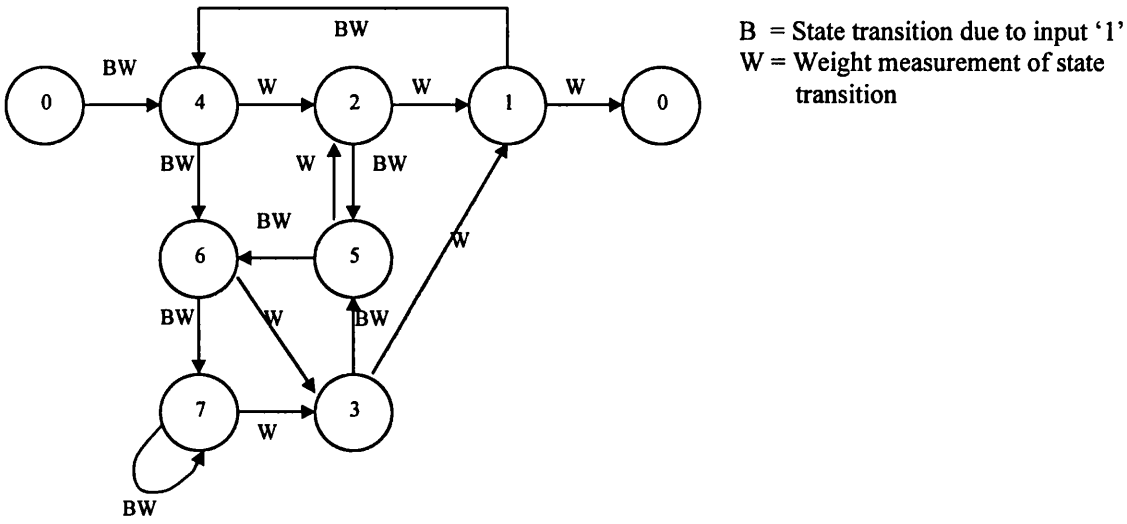

Figure 4-15. State diagram for a K=4 LROC code

Observing the state transitions above, it can be seen that this state diagram may be simplified in terms of the Hamming distance required to enter the all zero state. For example, if the current state transition 4 to 6 due to an input of one is proceeded by three zero inputs, the Hamming distance required to enter state 0 is equivalent to proceeding along the 4,2,1,0 path. Since this holds for all other state transitions with a loop back into state 4, the state diagram of figure (4-15) can thus be simplified by inspection to give a state diagram for an arbitrary constraint lengths K:

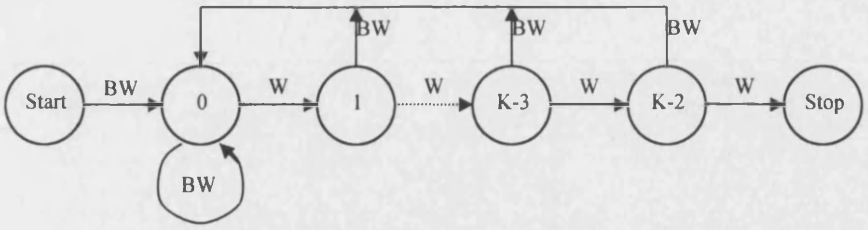

Figure 4-16. Simplified state diagram for any length LROCC

The state transition diagram is used to determine the transfer function by considering the through path from the START to STOP state and all the neighboring loops in this path. Hence the generating transfer function can be bound as:

$$T(W,B) = \frac{BW^K}{1 - BW - BW^2 - BW^3 - \ldots - BW^{K-1}} = \frac{BW^K}{1 - B\left(W + W^2 + \ldots + W^{K-1}\right)} \tag{4-18}$$

We then factorise the denominator of this function through the polynomial series, giving:

$$T(W,B) = \frac{BW^K}{1 - BW\left(\frac{1 - W^{K-1}}{1 - W}\right)} = \frac{BW^K(1-W)}{1 - W\left[1 + B\left(1 - W^{K-1}\right)\right]} \tag{4-19}$$

The super-orthogonal encoder design can be viewed in figure (4-17). This encoder enables the output of the Hadamard block encoder to additionally output the bi-orthogonal code set. In this way, the user may achieve greater Hamming distance on some state transitions. It turns out that these are only generated on the initial entry to the Trellis structure and on the last output transition.

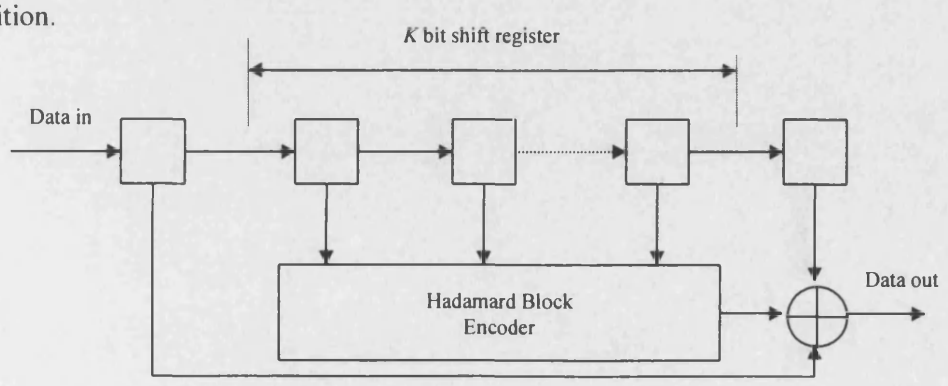

Figure 4-17. Super-orthogonal encoder design

Nevertheless, this will ultimately provide some improvement to the performance and coding gain. Similarly to figure (4-15), the state diagram for a super-orthogonal encoder will give an increased euclidean distance on the initial starting state transition and the final last stage state transition. The new state diagram is then configured as shown in figure (4-18).

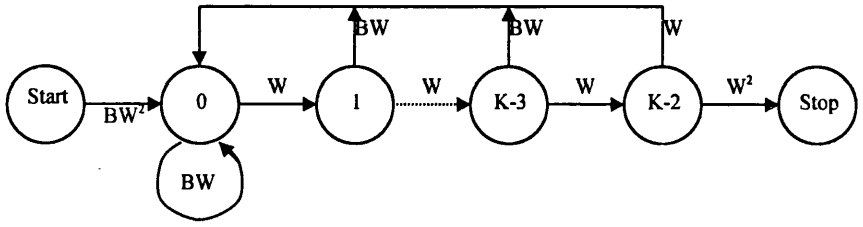

Figure 4-18. Simplified state diagram for any length super-orthogonal low-rate convolutional encoder

In a similar process to the previous evaluation of equations (4-19) and (4-20), the new generating transfer function may be found as:

$$T(W,B)=\frac{BW^{K+2}(1-W)}{1-W\left[1+B\left(1+W^{K-3}-2W^{K-2}\right)\right]} \tag{4-20}$$

This encoder design does not therefore utilise the full potential of the bi-orthogonal code set, since we could also introduce additional state transitions within the main part of the trellis to enhance the coding gain. This analysis can be extended further to a new novel concept of encoding the signal using a low-rate orthogonal encoder. This novel technique draws upon aspects of low-rate orthogonal coding and super-orthogonal coding structures in combination to provide a coding strategy which is superior in performance to either of these techniques. This method uses increased hardware complexity by allowing the constraint length of the encoder to be a variable quantity, but at the same time keeps the output symbols orthogonal and of the same rate (i.e. constant bandwidth expansion factor).

A diagrammatic representation of the proposed encoder can be seen in figure (4-19).

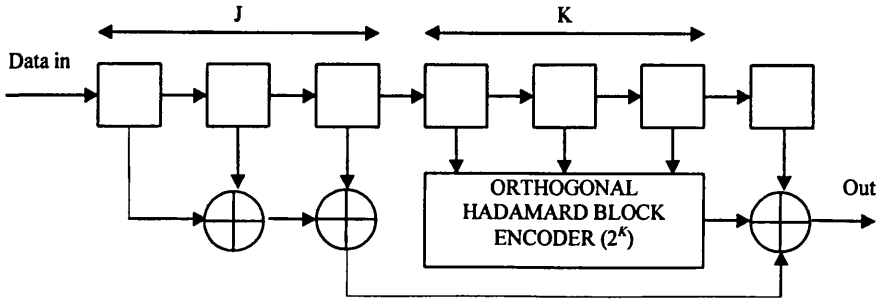

Figure 4-19. Hyper-orthogonal encoder

This design uses the conventional low-rate orthogonal convolutional encoder, based on Hadamard matrices of size $2^K \times 2^K$, and produces a biorthogonal symbol set of length 2^K and depth 2^{K+1}. This has the added advantage of introducing increased numbers of rows in the orthogonal matrix, therefore creating improved isolation between interfering users. For a typical K=2, J=1 constraint length encoder the output symbol set is defined as:

$$H_{K=2} = \begin{vmatrix} + & + & + & + \\ + & - & + & - \\ + & + & - & - \\ + & - & - & + \\ - & - & - & - \\ - & + & - & + \\ - & - & + & + \\ - & + & + & - \end{vmatrix} \tag{4-21}$$

Therefore, an increase in the free distance between the wanted and unwanted path will be inherent in the trellis code structure of the encoder. Depending on the size of J and K, the number of states in the trellis for this encoder will be given by:

$$States = 2^{K+J} = 2^{K_T} \tag{4-22}$$

This obviously increases the hardware complexity of both the encoder and decoder, but depending on the severity of the channel conditions, the number of states in the trellis can be increased or reduced. This allows the coding scheme to be adaptive and at the same time keeps the bandwidth of transmission constant, no matter how deep the trellis gets.

For example, a K=2 and J=2 hyper-orthogonal encoder will have a set of 16 possible states and yield a state diagram as shown in figure (4-20).

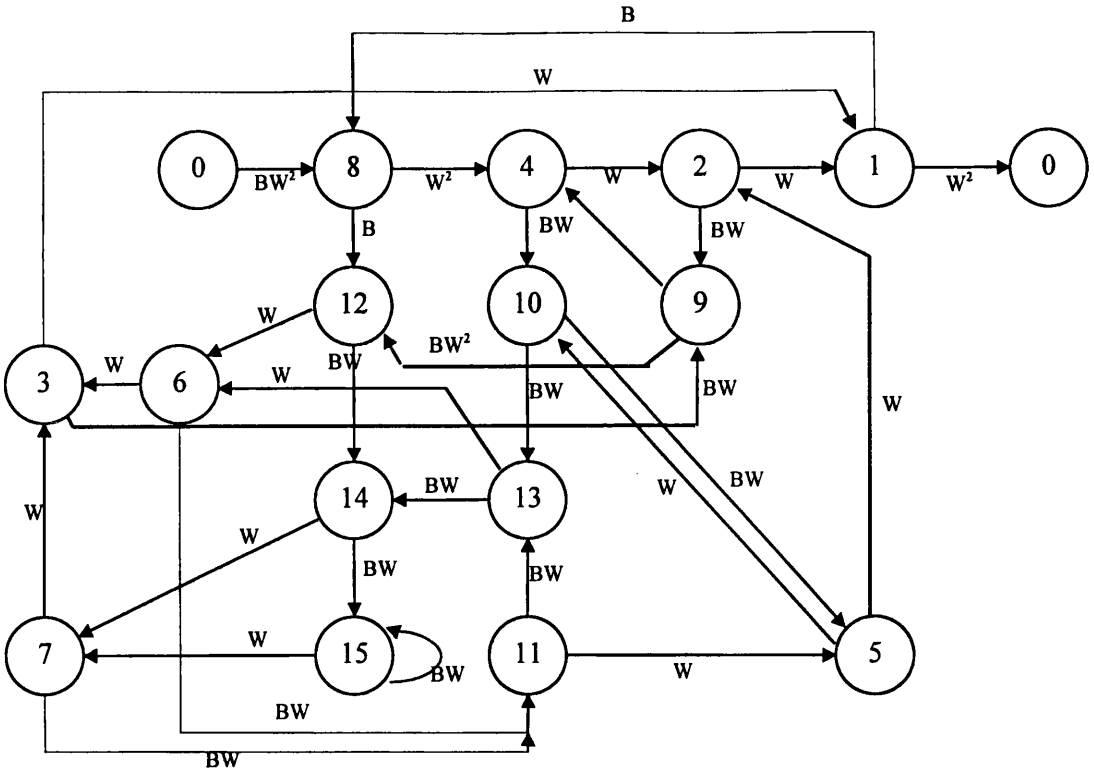

Figure 4-20. State diagram for hyper-orthogonal encoder

To evaluate the transfer function of this state diagram would be much too complicated, but nevertheless, a general expression for the *free distance* of the code can be determined for any variable constraint length hyper-orthogonal code. For the J=2, K=2 code featured above, the free distance yields:

$$\begin{aligned} d_{free} &= 2w + 6w \\ &= 2\left(\frac{2^{K_T-2}}{2}\right) + 3\left(2^{K_T-2}\right) \\ &= 4\left(2^{K_T-2}\right) \\ &= 16 \end{aligned} \tag{4-23}$$

For any other constraint length code, the free distance can be found as:

$$\begin{aligned} d_{free} &= (J+1)\left(2^{K_T-2}\right) + \frac{K}{2}\left(2^{K_T-2}\right) \\ &= 2^{K_T-2}\left(J + \frac{K}{2} + 1\right) \end{aligned} \tag{4-24}$$

Therefore, for a conventional K=6 (64-ary) low-rate orthogonal convolutional code, employing this hyper-orthogonal technique, with J=2, gives a new free distance of 384.

The free distance of any ordinary low-rate convolutional code is given by,

$$d_{free} = 2^{K-1}(K+1) \tag{4-25}$$

For the equivalent K=6 low-rate code, the free distance yields a value of 224. With the new hyper-orthogonal code configuration, setting J=2 gives an improvement of 72% in the free distance of the code at the expense of increased decoder complexity, without further increase in bandwidth. This can be compared to the design of QAM schemes, where enhanced coding gain is achieved at the expense of decoder complexity and *not* increased bandwidth. The upper bound for any convolutional code is generally given by [11]:

$$gain \leq 10\log(Rd_{free}) \tag{4-26}$$

where the gain is in decibels and R is the code rate. The upper bound for low-rate orthogonal convolutional codes and low-rate hyper-orthogonal convolutional codes, J=2, employing equal bandwidths can be seen in table (4-1).

Code Rate (R)	K	LROCC		LRHOCC (J=2)	
		d_{free}	gain(dB)	d_{free}	gain(dB)
1/16	4	30	2.73	80	6.99
1/32	5	96	4.77	176	7.40
1/64	6	224	5.44	384	7.78
1/128	7	512	6.02	832	8.13
1/256	8	1152	6.53	1792	8.45
1/512	9	2560	6.99	3840	8.75

Table 4-1. Coding gain comparisons of LROCC and LRHOCC

These results might be somewhat optimistic and accurate simulation results might be needed to validate the figures. Nevertheless, it can be seen that for equal bandwidth some significant coding gains can be expected through using hyper-orthogonal coding schemes. As J increases, the gain will also increase.

4.5 Demodulation and Decoding

4.5.1 Diversity RAKE Receivers

Provided that the inverse of the spreading code chip duration, T_c, of a system is significantly greater than the coherence bandwidth, Δf, of the mobile channel, spread-spectrum techniques are capable of resolving the individual echoes or multipaths from which the received signal is composed. As these paths generally undergo independent fading and have different near-far ratios they provide a level of internal diversity in the receiver. The ability to exploit multipath is central to the success of CDMA and is a considerable advantage as multipath imposes a severe limitation on other multiple access techniques. The number of multipaths resolvable is given by [12,13]:

$$L \leq \frac{1}{T_c \Delta f} + 1 \leq \frac{T_m}{T_c} + 1 \tag{4-27}$$

Path diversity is ordinarily exploited with a RAKE [14] receiver as shown in figure (4-21). The term RAKE refers to the fashion in which the receiver "rakes" out the multipath echoes from the received signal.

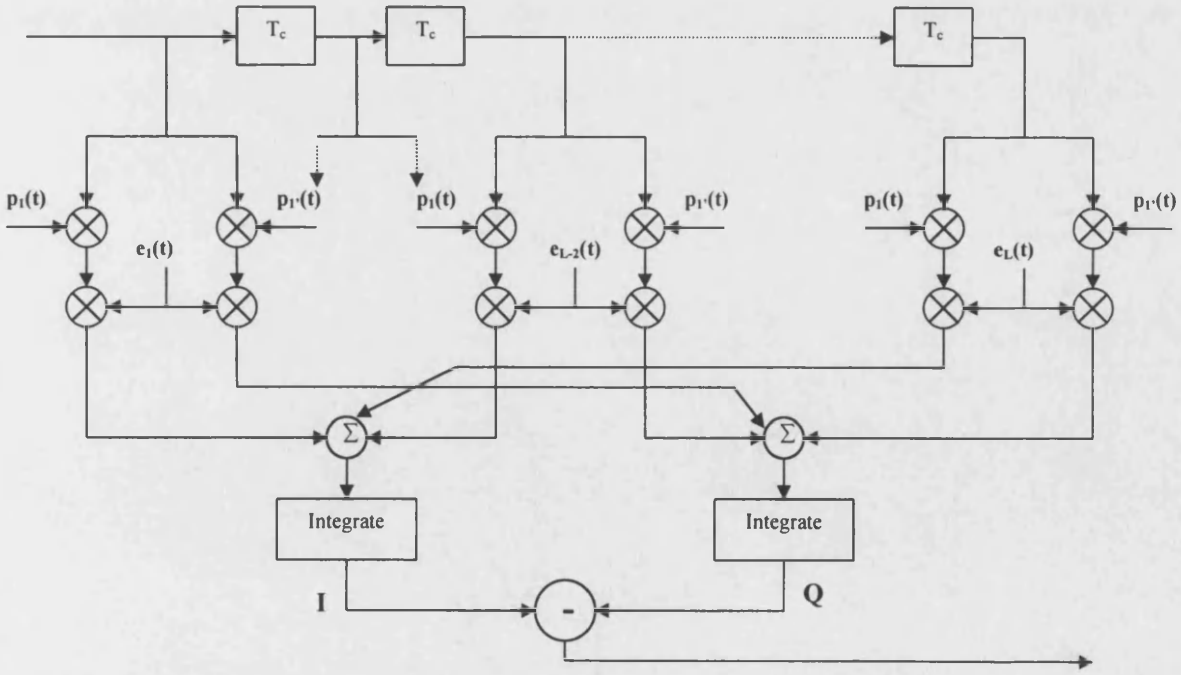

Figure 4-21. Spread-spectrum RAKE receiver for binary signalling

The receiver attempts to coherently combine the signal energy from all received paths that fall within the span of the delay-line. Delayed versions of the received signal are matched filtered with the user's signature waveform $p_l(t)$, prior to being weighted by an estimate of the strength of the signal path, e_l. All outputs are then summed and integrated over the symbol period to provide the decision statistic.

Proakis [15] has shown that the bit-error probability for a RAKE receiver that estimates e_l perfectly (i.e. maximal ratio combining) and for SNRs much greater than 1, can be approximated by:

$$P_e \approx C_L^{2L-1} \prod_{l=1}^{L} \frac{1}{\left[2\gamma_l(1-p)\right]} \tag{4-28}$$

where γ_l is the average SNR for the lth path and p=-1 for antipodal signals (i.e. BPSK) and p=0 for orthogonal signals (e.g. QPSK). The average SNR is defined as:

$$\gamma_l = \frac{E_b}{N_0} \mathrm{E}(\alpha_l) \tag{4-29}$$

where $\alpha_l = |c_l|$. For the case of differential binary phase shift keying the BER expression has been shown to be [15]:

$$P_e = \frac{1}{2^{2L-1}} \sum_{z=0}^{L-1} z! b_z \sum_{l=1}^{L} \frac{\pi_l}{\gamma_l} \left(\frac{\gamma_l}{1+\gamma_l} \right)^{z+1} \tag{4-30}$$

where:

$$b_z = \frac{1}{z!} \sum_{n=0}^{L-1-z} C_n^{2L-1} \tag{4-31}$$

and:

$$\pi_l = \prod_{i=1, i \neq l}^{L} \frac{\gamma_l}{\gamma_l - \gamma_i} \tag{4-32}$$

Equations (4-28) and (4-30) represent lower bounds on the error rate of the RAKE receiver. These are valid for a channel with non-equal SNRs in each path. For channels with an equal SNR distribution along each path, the bit-error rate is given as [15]:

$$P_e = \left(\frac{1-\mu}{2}\right)^L \sum_{l=0}^{L-1} C_l^{L-1+l} \left(\frac{1+\mu}{2}\right)^l \tag{4-33}$$

where,

$$\mu = \sqrt{\frac{\gamma_l}{1+\gamma_l}} \quad BPSK \tag{4-34}$$

$$\mu = \frac{\gamma_l}{1+\gamma_l} \quad DPSK \tag{4-35}$$

In practice, the non-stationary mobile channel makes precise estimation of the RAKE receiver tap weights difficult and the contribution of taps which do not contain significant received signal path energy will induce self-noise, degrading performance.

In the urban situation there is invariably gross multipath activity due to the number of scattering and reflecting objects in the environment (rms delay spread values of between 1 and 10 μs are typical) and large diversity advantages are available. In rural areas, multipath activity is reduced and there is likely to be a line-of-sight path to the basestation, resulting in Ricean fading statistics and consequently less benefit from large diversity receivers. Nevertheless, a frequency selective Rayleigh faded channel with Doppler spread will invariably introduce an irreducible bit-error rate in the receiver. Figure (4-22) shows the performance of a DPSK spread-spectrum system employing Gold codes of length 31, with an aggregate data rate of 248 kb/s and a Doppler spread of 300Hz in the channel using a 4-path RAKE receiver matched to the number of multipath components. At low *Eb/No* the Monte-Carlo simulation can be seen to follow the theoretical bound very closely and at high *Eb/No* the irreducible bit-error rate becomes visible due to the effects of Doppler in the channel model.

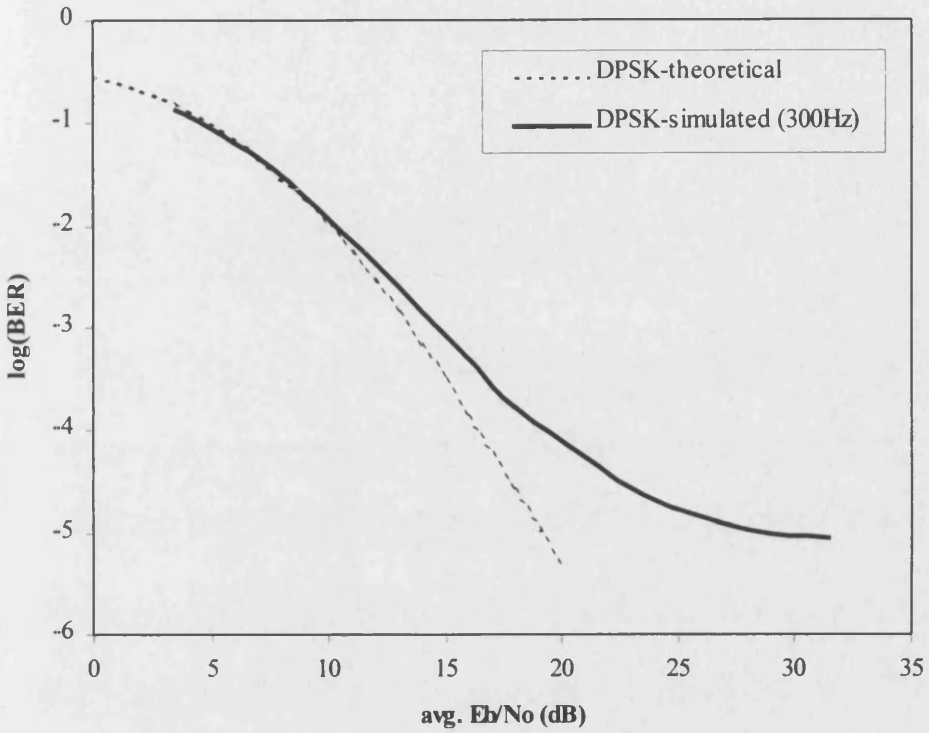

Figure 4-22. Performance of a spread-spectrum RAKE using DPSK in a 4-path Rayleigh faded channel

4.5.2 The Viterbi Algorithm

At the receiver, the reverse operation is performed. After demodulation and multiplication by the appropriate PN randomising sequence, the received 2^K codes are mapped into their most likely K bit symbols representing one state in the Viterbi decoder. The Viterbi decoder must have knowledge of the state mappings from the orthogonal convolutional encoder and consequently through the method of maximum likelihood detection the most likely path through the trellis is determined and the decoded output data sequence is obtained. The function of the Viterbi algorithm for this particular application is very similar to the conventional implementation of the algorithm, except a few minor configurations and conceptual modifications to the state metric calculations. Figure (4-23) shows how the new algorithm is configured to evaluate the euclidean distance for each possible state transition by correlating the received signal sequence with the 2^K rows of the Hadamard matrix. The Viterbi algorithm then calls upon the relevant value stored in the 2^K deep memory.

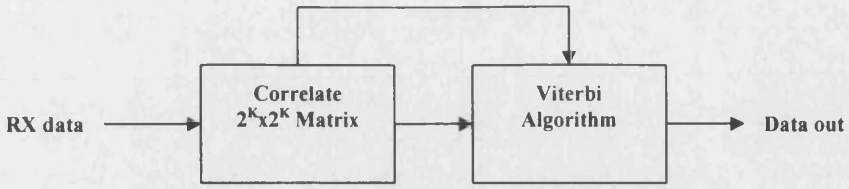

Figure 4-23. Modified Viterbi algorithm

The equivalent operation for a pure soft decision Viterbi algorithm is then formed by evaluating the effective euclidean distance between the received sequence and expected sequence in a one-dimensional space, where the decision for each state is based on:

$$v_{i,0} + metric_{depth\ (i-1),0} < v_{i,1} + metric_{depth(i-1),1} \tag{4-36}$$

where the metric increments $v_{i,0}$ and $v_{i,1}$ are obtained from the correlation values stored in the matrix at the input to the receiver. The equivalent trellis operation can be viewed in figure (4-24).

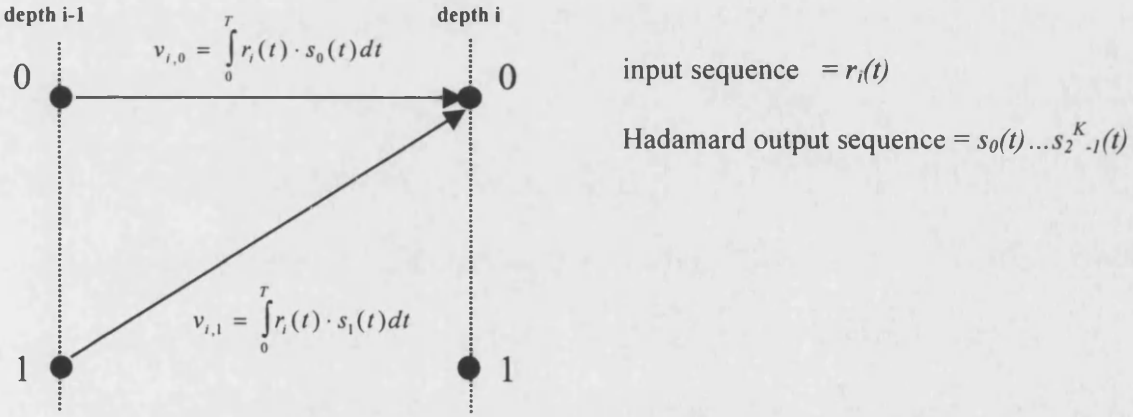

Figure 4-24. Section of trellis diagram in V.A.

The Viterbi algorithm has *a priori* knowledge of the state transitions for each user. This nevertheless requires an evaluation of the state diagram to determine the performance of this coding strategy, particularly for the more complex coding structures introduced here.

4.6 Summary

The ability of DS-CDMA to support a number of users in a common bandwidth arises through the use of a unique bandwidth spreading code for each user, hence the term Code Division Multiple Access, used to describe such a system. The spreading code, or signature waveform, may control spreading of the information bandwidth by direct sequence, frequency hopping or

time hopping modulation techniques. It is the increase in transmission bandwidth above the required information bandwidth that provides resistance to interference and facilitates multiple use within a common spectrum.

This chapter has introduced the concept of forward error correction coding for spread-spectrum systems, in particular the use of convolutional coding. To facilitate a good bit-error performance, the concept of low-rate orthogonal, super-orthogonal and novel hyper-orthogonal convolutional codes have been introduced. If these schemes are cascaded with randomising sequences to randomise the orthogonal sequences it can be seen that these coding strategies will yield improvements in the theoretical bit-error performance compared with high-rate convolutional codes. The potential improvements in performance through using LRHOCC has been shown to give coding gains of more than 8 dB in AWGN and nearly 7dB for LROCC codes.

The concept of BPSK coherent modulation gives superior performance than DPSK modulation techniques, but also presents problems in the carrier phase recovery at the receiver. This can be eliminated through the use of DPSK techniques at the cost of approximately 2dB in signal-to-noise ratio. DPSK demodulation techniques are also very popular because they don't need knowledge of the channel characteristics and the detection relies on a constant phase and amplitude variation of the channel from one bit to the next.

In multipath channels, the use of RAKE receivers to combat the frequency selectivity of the channel is vital in order to maximise the signal-to-noise ratio at the input to the receiver. It has been shown that the effective order of time-diversity in the receiver depends heavily on the number of fingers employed at the input, and hence the RAKE receiver must include a sufficient numbers of taps. If the channel is dominated by Ricean fading, the benefits of diversity diminish quickly and the use of large tap RAKE receivers becomes questionable.

4.7 References

[1] "A comparison of CDMA and TDMA systems", *Internal Report CIRR TG 8/1 Washington, Ericsson,* May 1991

[2] Gold, R, "Optimal binary sequences for spread spectrum multiplexing", in *IEEE Transactions on Information Theory*, Vol. 13, pp. 619-621, October 1967

[3] Peterson, W and Weldon, E J, "Error Correcting Codes", pp.472-492, *MIT Press*, second ed., 1972

[4] Kasami, T, "Weight distribution formula for some class of cyclic codes", *Tech. Report*, R-285, University of Illinois, Coordinated Science Laboratory, January 1966

[5] Gold, R, "Maximal recursive sequences with 3-valued recursive cross-correlation functions", *IEEE Transactions on Information Theory*, Vol. 14, pp.154-156, January 1968

[6] Viterbi, A J, "Convolutional Codes and Their Performance in Communication Systems", *IEEE Transactions on Comm. Technology*, COM-19, No.5, October 1971

[7] Jacobs, I, "Practical Applications of Coding", *IEEE Trans. Inf. Theory*, Vol. IT20, May 1974, pp.305-310

[8] Viterbi, A J, "Very Low-Rate Convolutional Codes for Maximum Theoretical Performance of Spread-Spectrum Multiple-Access Channels", *IEEE Journal on Selected Areas in Communications*, Vol. 8, No. 4, May 1990

[9] Green, R R, "A serial orthogonal decoder", *JPL Space Programs Summary*, Vol. 37-39, pp. 247-253, Jet Propulsion Lab., Pasadena, CA 1966

[10] Viterbi, A J, "CDMA-Principles of Spread Spectrum Communication", *Addison Wesley*, 1995

[11] Sklar, B, "Digital Communications – Fundamentals and Applications", *Prentice Hall*, Englewood Cliffs, New Jersey, 1988

[12] Allpress, S A, "Optimising Signal Rate and Internal Diversity Order for Mobile Cellular DS-CDMA Systems", *PhD thesis*, University of Bristol, 1993

[13] Allpress, S A, *et al*, "Diversity signal processing requirements of direct sequence CDMA networks in cellular & microcellular environments", *6th IEE Mobile Radio and Personal Communications Conference*, 1993

[14] Price, R, and Green, P E, "A communications technique for multipath channels", *Proc. IRE*, Vol. 46, pp. 555-570, March 1958

[15] Proakis, J G, "Digital Communications", *McGraw-Hill*, 3rd edition, 1993

[16] Couture, M A and Linnartz, J-P, "Improved Channel Modelling for Performance Analysis of a DS-CDMA Link", *PIMRC'94*, pp. 705-710

[17] Wu, K T and Tsaur, S A, "Error performance for diversity DS-SSMA communications in fading channels", *IEE Proc. Commun.*, Vol. 141, No. 5, pp. 357-363, Oct. 1994

[18] Wu, K T and Tsaur, S A, "Error performance for diversity DS-SSMA communications in fading channels", *IEE Proc. Commun.*, Vol. 141, No. 5, pp. 357-363, Oct. 1994

[19] Nilsson, P and Maseng, T, "RAKE Receiver CDMA Performance", *PIMRC'94*, pp. 696-669

[20] Chau, Y A, and Laih, A S, "Diversity for noncoherent DPSK direct-sequence CDMA over a shadowed Rician-fading satellite channel", pp. 386-392, *IEE Proc. Commun.*, Vol. 142, No. 6, Dec 1995

[21] Salama, I M, and Al-Hussaini, E K, "CDMA Rake receiver for cellular mobile radio in Nakagami fading frequency selective channels", pp. 720-724, *IEEE Proc. of PIRMC'94*

[22] Gass, J H, Noneaker, D L and Pursley, M B, "Spectral efficiency of a Power-Controlled CDMA Mobile Personal Communication System", *IEEE Jornal on Select. Areas in Comms.*, pp. 559-569, Vol. 14, No. 3, April 1996

[23] Forney, G D, "Convolutional Codes I: Algebraic Structure", *IEEE Trans. Information Theory*, IT-16, pp. 720-738, 1970

[24] Forney, G D, "Coding and Its Application in Space Communications", *IEEE Spectrum* 7, pp. 47-58, 1970

[25] Zehavi, E, and Viterbi, AJ, "On new classes of orthogonal convolutional codes", Bilkent International Conference in New Trends in Communication, Control and Signal Processing, Ankara, Turkey, 1990

[26] Ziemer, R E, and Peterson, R L, "Introduction to Digital Communication", *Maxwell Macmillan International Editions*, 1992

[27] Kempf, P, and Khunjush, J, "A generalised concatenated coding scheme for CDMA digital radio communication systems", pp. 543-547, *IEEE Proc. of PIMRC'94*

[28] Forney, G D, "The Viterbi Algorithm", *Proc. of the IEEE*, pp. 268-278, Vol. 61, No. 3, March 1973

[29] Heller, J A, and Jacobs, I M, "Viterbi Decoding for Satellite and Space Communication", pp. 835-848, *IEEE Trans. on Communication Technology*, Vol. COM-19, No. 5, Oct 1971

[30] Porath, J E, and Aulin, T, "Algorithmic Construction of Trellis Codes", pp. 649-654, *IEEE Trans. on Comms.*, Vol. 41, No. 5, May 1993

[31] Seshadri, N, and Sundberg, C E W, "List Viterbi Decoding Algorithms with Applications", pp. 313-323, *IEEE Trans. on Comms.*, Vol. 42, No. 2/3/4, Feb/march/April 1994

CHAPTER 5:

MULTI-USER DS-CDMA SYSTEMS

5.1 Introduction

We have so far seen how spread-spectrum modulation may be used in DS-CDMA techniques to combat multipath channel fading and provide reliable communication using convolutional coding and orthogonal spreading. This chapter deals with a multi-user scenario and introduces a theoretical analysis of a synchronous and asynchronous uplink. The downlink scenario presents fewer problems in a multiple-access environment as the users can be added orthogonally in the basestation, therefore reducing the effects of "other-user" noise. In a multipath environment, however, the orthogonality between users is considerably destroyed and degrades the bit-error performance.

The first part of this chapter is devoted to a detailed uplink analysis using BPSK and DPSK demodulation in conjunction with a matched filter for every user. The Gaussian approximation for a large number of active users is introduced together with more complex calculations assuming perfect detection of a single user. The performance of multi-user systems in Rayleigh and Ricean faded multipath channels is also shown. The second part of the chapter presents a typical multi-user downlink with a RAKE receiver and introduces some of the concepts of achieving diversity in multipath faded channels. A number of techniques to combat the near-far problem are then given at the end of this chapter.

5.2 DS-CDMA Uplink Analysis

The use of linear multi-user receivers is vital for successful communication in DS-CDMA systems that use a unique code for each user through PN sequences with low cross-correlation. Since linear multi-user detectors require that the waveforms assigned to the users be linearly independent, the number of users is constrained to be less than or equal to the number of dimensions, which is determined by the total bandwidth, the per-user bit rate, the error control coding redundancy and the number of bits per modulation symbol of each user. This last parameter can be arbitrarily high by using multi-level modulation, but problems such as amplifier non-linearities and fading channels limit the number of levels that may be employed in the modulation scheme for cellular systems. In practice, BPSK or QPSK is almost always employed.

A conventional N_u user DS-CDMA uplink scenario is depicted in figure (5-1). Each user transmits a data sequence $d_i(t)$ of rectangular pulses from the set ± 1 with a period of T_s. Every

user is assigned an independent signature waveform (a spreading or code sequence) $p_i(t)$ of chip period T_c which is then used to modulate the data $d_i(t)$. For all system configurations considered in this work, the duration of the signature waveform is assumed to match the system symbol period, T_s, i.e. $T_s=NT_c$ where N is the number of chips in the signature waveform. DS-CDMA systems where this requirement is not satisfied exist but their inclusion is outside the scope of this work.

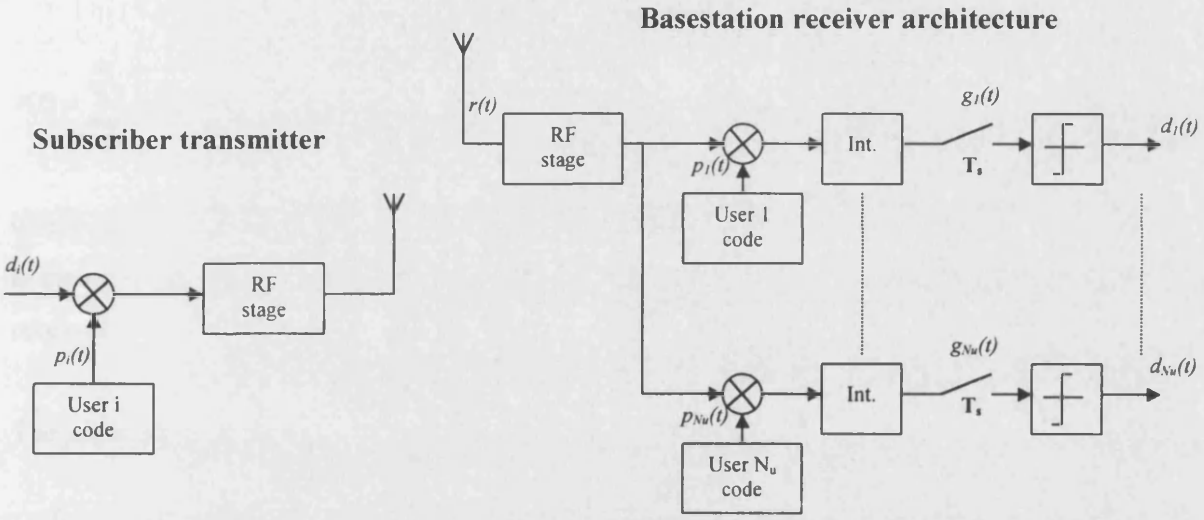

Figure 5-1. Conventional multi-user DS-CDMA uplink system operation

The choice of spreading code depends on a number of factors, including system capacity, bandwidth, data rate as well as the properties of the chosen code set such as the cross-correlation and auto-correlation between set members. The selection of a suitable code set is crucial to the performance of a CDMA system. As described earlier, Gold codes of differing lengths have uniformly low cross-correlation between set members and high auto-correlation, and are therefore chosen for a large part of the system simulations in this work. Nevertheless, the use of low-rate orthogonal codes with randomising sequences presents another viable solution to the coding strategy employed in a DS-CDMA system.

The conventional multi-user detector (equivalent to the basestation in a cellular system) comprises a bank of correlators, each of which is matched to a user's waveform. The output of each correlator is integrated, sampled at the symbol rate and passed to a threshold device, which, in its most simple form hard-limits the output to determine the data sequence. The combination of correlator, integrator and sampler constitutes a matched filter.

The transmitted signal of the ith user can be described by:

$$s_i(t) = \sqrt{2P_i}\, d_i(t) p_i(t) \cos(w_0 + \theta_i) \tag{5-1}$$

where P_i is the transmitted power, w_0 is the carrier frequency and θ_i is the random phase of the ith carrier, uniformly distributed on $(0,2\pi)$.

The signal received by the basestation depicted in figure (5-1) is the summation of the received signals from all active users in the system:

$$r(t) = \sum_{i=1}^{N_u} A_i d_i(t-\tau_i) p_i(t-\tau_i) \cos(w_0 t + \theta_i) + n(t) \tag{5-2}$$

where τ_i is the transmission delay associated with the ith user, uniformly distributed on $(0,T_s]$, A_i is the received signal amplitude and $n(t)$ is additive white Gaussian noise at the front end of the receiver.

The jth matched filter multiplies $r(t)$ by the function

$$\frac{2}{T_s} \int_0^{T_s} p_j(t) \cos(w_0 t) dt \tag{5-3}$$

and from equations (5-2) and (5-3) the matched filter output is then given by:

$$g_j(t) = A_j + \frac{1}{T} \sum_{i=1, i\neq j}^{N_u} A_i \int_0^T d_i(t-\tau_i) p_i(t-\tau_i) p_j(t) \cos(\theta_i) dt + \frac{2}{T} \int_0^T n(t) p_j(t) \cos(w_0 t) dt \tag{5-4}$$

It is apparent from equation (5-4) that the matched filter output comprises three distinct terms:

1. The first term, A_j, is the required output on which a hard decision is made and arises through the auto correlation of the signature waveform with the matched filter.

2. The second term is the cross-correlation interference between each of the $p_i(t-\tau_i)$ signature waveforms and $p_j(t)$. This is usually termed multiple access interference (MAI) in DS-CDMA systems.

3. The third term represents interference arising through correlation of $p_j(t)$ with the AWGN of the channel.

Both the second and third terms of equation (5-4) represent unwanted interference. When the third term dominates, the receiver is noise limited and the conventional detector has been shown by Verdu [1] to be optimal under such conditions. In CDMA however, it is invariably the second term which has the greater magnitude due to the summation of the cross-correlation interference contribution of all users (i.e. CDMA is other-user interference limited rather than noise limited) and interference cancelling receivers all attempt to reduce the impact of this term.

The despread signal represented by equation (5-4) is useful as it allows the origin of system interference to be demonstrated, but in practice it is an over-simplification. The received signal is in fact the summation of a number of time-delayed replicas which arise as the transmitted wave is reflected and scattered by obstacles. At baseband this multipath mobile channel can be represented by its lowpass equivalent complex impulse response:

$$h(t) = \sum_{l=1}^{L} \alpha_l \exp(j\phi_l)\delta(t-\tau_l) \tag{5-5}$$

where α_l and ϕ_l are the magnitude and phase of the lth element in an impulse response with L samples and $\delta(t-\tau_l)$ is an impulse delayed by τ_l. The received signal $r(t)$ is then formed from the convolution of $s(t)$ and $h(t)$ and an additive Gaussian noise term:

$$\begin{aligned} r(t) &= s(t) * h(t) + n(t) \\ &= \sum_{i=1}^{N_u} \sqrt{2P_i} \left\{ \sum_{l=1}^{L} \alpha_l d_i(t-\tau_i-\tau_l) p(t-\tau_l-\tau_i) \times \cos\left[w_0(t-\tau_l-\tau_i) + \theta_i + \phi_l \right] \right\} + n(t) \end{aligned} \tag{5-6}$$

This invariably has the effect of introducing a fourth term into equation (5-4), thus representing the self-interference of the desired signal due to the rest of the multipath echoes.

DS-CDMA systems can be distinguished by whether they are asynchronous or synchronous in operation. In a synchronous system, transmission is arranged such that the relative delay $\tau_i = 0$ for all users, the spreading codes of all users are aligned in time and are almost near-orthogonal, maximising system capacity. This calls upon reservation of extra bandwidth for the synchronisation channel.

5.2.1 DS-CDMA bit-error rate calculations

Most analyses of communication system error rates assume that the limit on performance is determined by the receiver front end noise. In CDMA, thermal noise influences performance but it is invariably multiple access interference (MAI) from users in the same and adjacent cells which sets the limit on achievable bit error rate. Bit error rate is one of the most useful measures

of communications system performance and in this section the upper bound on coherent synchronous DS-CDMA bit error rate is shown based on the Chernoff bound [2]. Details of the Chernoff bound can be found in Appendix B.

For channels where the predominant interference is additive white Gaussian noise and the level of MAI is negligible, the DS-CDMA bit error rate for coherent binary phase-shift keying (BPSK) is lower bounded by [3]:

$$P_e = Q\left(\sqrt{2E_b / N_o}\right) \tag{5-7}$$

where E_b is the energy per bit N_0 is the noise power spectral density and $Q(x)$ the Gaussian integral function

$$Q(x) = \frac{1}{\sqrt{2\pi}} \int_x^{\infty} e^{-t^2/2} . dt \tag{5-8}$$

With differentially coherent detection, [3] gives the lower bound on the bit error probability as:

$$P_e = \frac{1}{2} e^{-E_b/N_o} \tag{5-9}$$

Equations (5-7) and (5-9) in fact describe the bit error rate of the optimum single user detector and represent the limit of performance when MAI can be completely cancelled from the

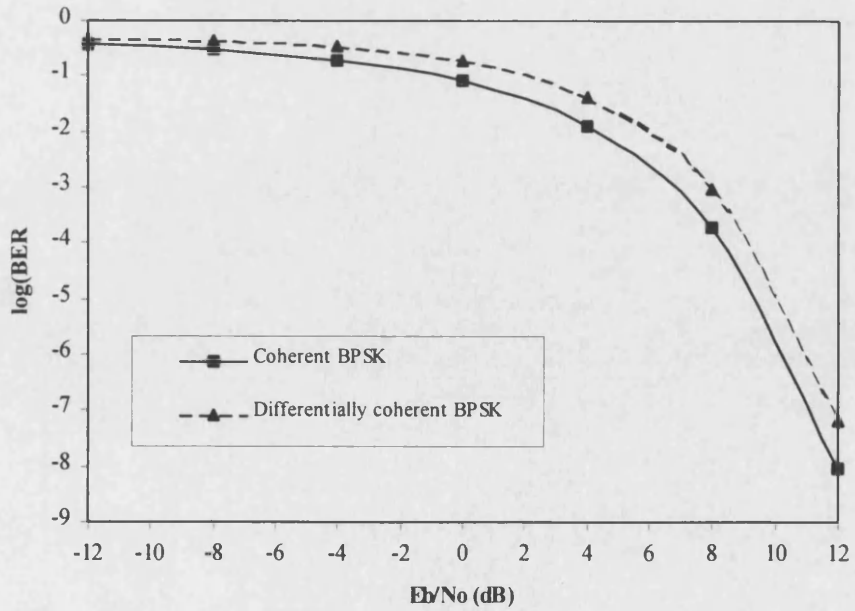

Figure 5-2. Optimum single user detector using coherent BPSK and differentially coherent BPSK

received signal in a multiple user environment. Figure (5-2) shows that at usable error rates ($<10^{-3}$) the difference between differentially coherent and coherent reception predicted by these equations is less than 2 dB.

The equations are useful as they define a lower bound on the achievable performance of a near-far resistant receiver and can also be used to evaluate metrics which describe the near-far performance of a receiver. They are equally applicable to synchronous and asynchronous communications as they describe the performance of the single user or situations where MAI has been completely removed from the received signal.

In a practical DS-CDMA system the interference from other system users means that Equations (5-7) and (5-9) no longer hold and it is necessary to include the effect of multiple access interference in BER expressions. In general, the theoretical calculation of closed form expressions for synchronous DS-CDMA bit error rate can be achieved with reasonable confidence, but most methods are computationally intensive with the computational requirement growing linearly (e.g. the BER approximation method of Geraniotis *et al* [4]) or exponentially (e.g. the method of upper and lower bounds of Pursley *et al* [5]) with the number of users.

Omura [2] has derived an expression using the Chernoff bound for the bit error rate of a synchronous DS-CDMA system undergoing interference from adjacent cells. The treatment can be modified to obtain an expression for the BER of an asynchronous CDMA system arising from inter- and intra-cell interference. Assuming coherent BPSK modulation and no interference due to other users, the output of a user's matched filter will be A if the data bit sent was a '1' and $-A$ if the bit sent was a '0'. In the presence of multiple access interference of magnitude I the bit error probability will be given by:

$$P_{BER} = prob\{-A + I \geq 0\} \tag{5-10}$$

The BER is now dependent on the pdf of the interference term I. If the number of bits sent is large, it can be assumed that I is a random variable with zero mean, but it is generally difficult to obtain an expression for I without resorting to evaluating it directly, which is too computationally intensive for most practical purposes. One method is to derive a bound on the error, which if sufficiently tight, will give a good estimate on the BER and circumvent the requirement to calculate the distribution of I. The Chernoff bound can be applied to obtain an upper bound on the BER:

$$\begin{aligned}\Pr\{-A+I\geq 0\} &= \mathrm{E}\{U(-A+I)\} \leq \mathrm{E}\left\{e^{\rho(-A+I)}\right\} \\ &= e^{-\rho A}\mathrm{E}\left[e^{\rho I}\right]\end{aligned} \tag{5-11}$$

For a synchronous system with N_u users the interference contribution to the jth user from all other users is given by:

$$I = \sum_{i=1,i\neq j}^{N_u} d_{i,n}C_{i,j}\cos\theta_i \tag{5-12}$$

where $d_{i,n}$ is the nth random data bit of the ith user, $C_{i,j}$ the cross-correlation between the signature waveforms of the desired (jth) user and the ith user and θ_i is the carrier phase. The data and phase are assumed to be random variables with uniform probability density. The interference term can then be substituted into the Chernoff bound:

$$\begin{aligned}E\{e^{\rho I}\} &= E\left\{e^{\rho\sum_{i=1,i\neq j}^{N_u} d_{i,n}C_{i,j}\cos\theta_i}\right\} \\ &= \prod_{i=1,i\neq j}^{N_u} E\left\{e^{\rho d_{i,n}C_{i,j}\cos\theta_i}\right\} \\ &= \prod_{i=1,i\neq j}^{N_u} I_0\left(\rho C_{i,j}\right)\end{aligned} \tag{5-13}$$

where I_0 is the modified Bessel function of zero order defined as:

$$\begin{aligned}I_0(x) &= \frac{1}{2\pi}\int_0^{2\pi} e^{x\cos\theta}.d\theta \\ &= \sum_{n=0}^{\infty}\frac{(x/2)^{2n}}{(n!)^2}\end{aligned} \tag{5-14}$$

Since $n!>1$, the simple bound

$$I_0 \leq \sum_{n=0}^{\infty}\frac{(x/2)^{2n}}{(n!)^2} = e^{(x/2)^2} \tag{5-15}$$

can be applied to equation (5-13) to obtain:

$$e^{\rho I} = e^{\frac{\rho^2 J_0}{4}} \tag{5-16}$$

where J_0 is defined as the sum of the square of all the interfering cross-correlation terms (whether they be inter- or intra-cell in origin):

$$J_0 = \sum_{i=1, i\neq j}^{N_u} C_{j,i}^2 \tag{5-17}$$

From equation (5-11) the BER is bounded by:

$$P_{BER} \leq \frac{1}{2} e^{-\rho A} e^{\frac{\rho^2 J_0}{4}} \tag{5-18}$$

This equation is minimised with a value of $\rho = 2A/J_0$ which upon substitution gives the final form of the upper bound:

$$P_{BER} \leq \frac{1}{2} e^{-A^2/J_0} \tag{5-19}$$

As $A^2T=E_b$, the bit energy, this Chernoff bound is equivalent to the single user error rate of equation (5-9) with the noise power spectral density N_0 replaced by the sum of cross-correlation powers, J_0. A^2/J_0 is therefore the equivalent measure to E_b/N_0 for a MAI limited channel. Equation (5-19) gives the upper bound for differentially coherent reception and the BER for a coherent system should be within 2dB of this level, as predicted in figure (5-2).

The spreading sequences are usually deterministic and periodic. Nevertheless, the analysis of DS-CDMA systems is often simplified by assuming that the spreading sequences are completely random. With this approach, the MAI at the front end of the receiver matched to the desired signal is modelled as additional broadband Gaussian noise [7-11]. The presence or absence of chip and phase alignment of the co-users can be accounted for by scaling the processing gain [11]. The effect of using deterministic rather than random spreading sequences can also be accounted for by scaling the processing gain, but in a more complicated fashion [7]. The results in [8-10] tend to suggest that a Gaussian approximation is quite accurate.

In [12] it has been shown that the multi-user interference is approximately Gaussian for $N_u>1$ with signal-to-noise ratio:

$$SNR \approx \left[\frac{(N_u - 1)}{3N} + \frac{N_o}{2E_b} \right]^{-1} \tag{5-20}$$

We recall that a DPSK receiver operating solely in the presence of AWGN has probability of error:

$$P_{BER} = \frac{1}{2} e^{-E_b/N_o} \tag{5-21}$$

The exponent in (5-21) corresponds to *SNR*/2 when N_u=1. By extension, because of the assumption that the effect of the inter-user interference is equivalent to adding more Gaussian channel noise, we have for N_u>1:

$$P_{BER} = \frac{1}{2} \exp\left[-\frac{1}{2} \left(\frac{N_u - 1}{3N} + \frac{N_o}{2E_b} \right)^{-1} \right] \tag{5-22}$$

The approximation in equation (5-22) is good as long as N is sufficiently large, and the upper bound for 31 chip Gold code sequences can be seen in figure (5-3).

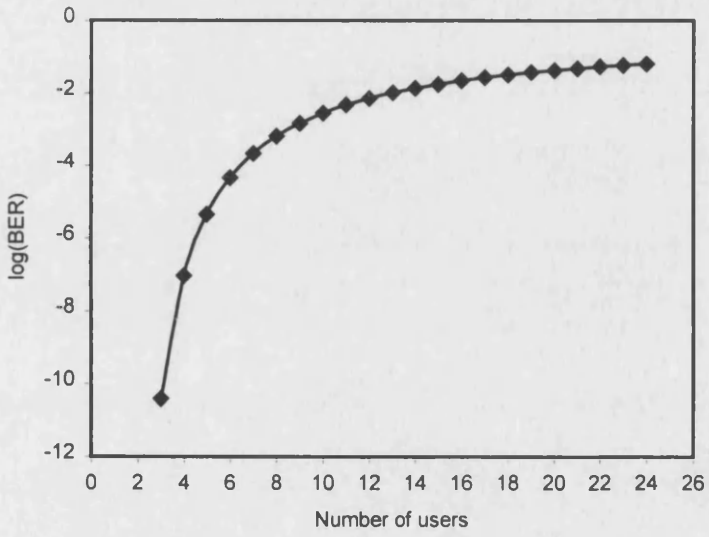

Figure 5-3. Gaussian approximation of 31 chip Gold codes in a multi-user environment with no AWGN

5.2.2 Bit-error probability in faded multi-user channels

The low-pass equivalent impulse response of the passband fading channel for the link between the *i*th users' transmitter and its receiver is:

$$h_i(t) = \sum_{l=1}^{L} \alpha_{l,i} \delta\left(t - \tau_{l,i}\right) e^{j\phi_{l,i}} \tag{5-23}$$

where $\delta(\cdot)$ is the Dirac impulse while $\alpha_{l,i}$, $\tau_{l,i}$ and $\phi_{l,i}$ are, respectively, the *l*th path gain, time delay and phase of the *i*th user.

The channel output $y_i(t)$ is further corrupted by MAI and thermal noise $n(t)$, which is modelled as AWGN with two-sided spectral density $N_o/2$. The received signal is as shown earlier:

$$r(t) = \sum_{i=1}^{N_u} \sum_{l=1}^{L} \sqrt{2P}\alpha_{l,i} d_i\left(t - \tau_{l,i}\right) p_i\left(t - \tau_{l,i}\right) \cos\left(w_o t + \phi_{l,i}\right) + n(t) \tag{5-24}$$

Let us assume that the reference receiver 1 can ideally lock onto the first path. With no loss in generality let us assume that $\phi_{1,1} = 0$ and $\tau_{1,1} = 0$. If the received signal $r(t)$ is the input to the correlation receiver1 matched to $s_1(t)$, then the output is:

$$Z_{1,1} = \int_0^{T_b} r(t) p_1(t) \cos(w_o t).dt \tag{5-25}$$

$Z_{1,1}$ represents the decision statistic of the receiver 1 when locked onto the first path. Substituting equation (5-24) into equation (5-25) one obtains:

$$Z_{1,1} = \sqrt{P/2}\alpha_{1,1} d_1^0 T_b + \sqrt{P/2} \sum_{i=2}^{N_u} \alpha_{1,i} W_{1,i} \cos\left(\phi_{1,i}\right) + \sqrt{P/2} \sum_{i=1}^{N_u} \sum_{l=2}^{L} \alpha_{l,i} W_{l,i} \cos(\phi_{l,i}) + \eta \tag{5-26}$$

where,

$$W_{l,i} = \left[d_i^{-1} R_{1,i}(\tau_{l,i}) + d_i^0 \hat{R}_{1,i}(\tau_{l,i})\right] \tag{5-27}$$

and d_i^{-1} and d_i^0 represent a pair of consecutive data bits of the ith signal; $R_{1,i}(\tau_{l,i})$ and $R'_{1,i}(\tau_{l,i})$ are the continuous time partial cross-correlation functions of the ith and 1st spectral waveforms as defined in [12].

Assuming that data bits are equiprobable, the bit error probability is:

$$P_b = prob\left(Z_{1,1} < 0 \middle| d_1^0 = 1\right) \tag{5-28}$$

The Gaussian assumption is to treat all the interference in equation (5-26) as Gaussian noise. To compute the probability of bit-error we first find the probability of bit-error conditioned on $\alpha_{1,1}$. The first term of equation (5-26) is the signal term, and for fixed $\alpha_{1,1}$ it has an average power of $P_{sig} = P(T_b\alpha_{1,1})^2/2$. The last term is a Gaussian random variable having zero mean and power $P_{noise} = N_o T_b/4$. The second and third terms of equation (5-26) represents the MAI. Since all

terms of the summation are independent, then the mean of the MAI reduces to zero, and the average power, which is also equal to the variance, is given by the sum of the variances of the second and third terms. The variances of the second and third terms are given by:

$$\begin{aligned}\sigma_{\text{int}2}^2 &= \sum_{i=2}^{N_u} E\left\{\left[\sqrt{P/2}\alpha_{1,i}W_{1,i}\cos\phi_{1,i}\right]^2\right\} \\ &= \frac{P}{2}\sum_{i=2}^{N_u} E\left[\left(W_{1,i}\right)^2\right]E\left[\left(\alpha_{1,i}\cos\phi_{1,i}\right)^2\right] \\ \sigma_{\text{int}3}^2 &= \sum_{l=2}^{L}\sum_{i=1}^{N_u} E\left\{\left[\sqrt{P/2}\alpha_{l,i}W_{l,i}\cos\phi_{l,i}\right]^2\right\} \\ &= \frac{P}{2}\sum_{l=2}^{L}\sum_{i=2}^{N_u} E\left[\left(W_{l,i}\right)^2\right]E\left[\left(\alpha_{l,i}\cos\phi_{l,i}\right)^2\right]\end{aligned} \tag{5-29}$$

For Gold codes with sequence length N, Pursley [12] has shown that:

$$E\left[\left(W_{l,i}\right)^2\right] = \frac{2T_b^2}{3N} \tag{5-30}$$

Since $\alpha_{l,i}$ is Rician, then $E\{[\alpha_{l,i}\cos\phi_{l,i}]^2\} = \sigma_{l,i}^2 + c_i^2/2$. Similarly, $\alpha_{l,i}$ is Rayleigh for $l \neq 1$, and is given as $E\{[\alpha_{l,i}\cos\phi_{l,i}]^2\} = \sigma_{l,i}^2$. We assume that all c_i and $\sigma_{l,i}^2$ are equal for all i users over l paths in the channel. Substituting these results into equations (5-29) and (5-30), one obtains:

$$\begin{aligned}SNR &= \frac{P_{sig}}{P_{noise} + \sigma_{\text{int}2}^2 + \sigma_{\text{int}3}^2} \\ &= \frac{\alpha_{1,1}^2}{\frac{N_o}{2E_b} + \frac{(N_u - 1)}{3N}\left(c^2 + 2\sigma_1^2\right) + \frac{N_u(L-1)}{3N}2\sigma_1^2}\end{aligned} \tag{5-31}$$

where $E_b = PT_b$ is the energy per bit. The conditional probability of bit-error is:

$$P_b(\alpha_{1,1}) = Q\left[\sqrt{SNR}\right] \tag{5-32}$$

To obtain the probability of bit-error when $\alpha_{l,1}$ is random, we must integrate $P_b(\alpha_{l,1})$ over the pdf of $\alpha_{l,1}$, which can be found in Chapter 2 for the case of Ricean and Rayleigh statistically distributed variables. This means that we must evaluate the integral:

$$P_b = \int_0^{\infty} P_b(\alpha_{1,1})p(\alpha_{1,1})d\alpha \tag{5-33}$$

The theoretical BER performance of an asynchronous DS-CDMA system in an L=4 paths Rayleigh faded channel (c_i=0) and L=1 Ricean channel is shown in figure (5-4). It can be seen that in 4-path Rayleigh faded channels the other-user noise quickly degrades the performance of the DS-CDMA system and bit-error rates less than 10^{-2} cannot be reached. In Ricean channels where the power ratio of the direct-to-scattered component is 10dB adequate performance can be achieved. Nevertheless, such favourable environments are not always achievable and alternative methods need to be sought to improve matters.

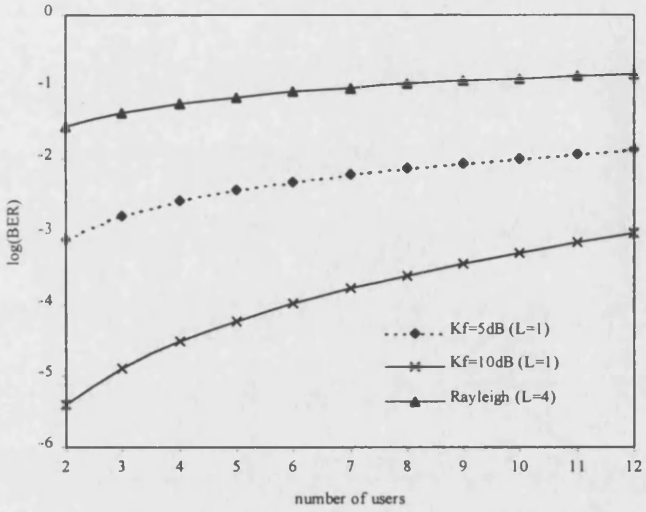

Figure 5-4. BER performance of asynchronous DS-CDMA multi-user system with PN code length of 31 in Ricean and Rayleigh faded channels

5.2.3 The Near-Far Problem

The principle limitation of DS-CDMA is the near-far effect. Since it is not possible to make all user codes completely orthogonal for all possible user delays, a degree of cross-correlation noise or multiple access interference exists between users. In situations where users' signals are received at differing power levels, the magnitude of cross-correlation noise is enhanced giving rise to the near-far effect and an associated increase in bit error rate. Under these conditions, the interference contribution from users with a high signal level swamps the desired signal. In terms of the DS-CDMA theoretical model developed in section 5-1 the near-far effect arises when the A_i of equation (5-4) are dissimilar. Such variations in received signal power may occur through:

- Users transmitting at differing power levels.

- The spatial distribution of users resulting in differing propagation losses between transmitter and receiver.

- Fading of mobile paths relative to each other; even if one transmitter is nearer to the receiver than another it may be received more weakly due to a fade in the mobile channel. Both slow and fast fading can generate the near-far effect in this manner.

In a practical system, near-far effect problems will arise through a combination of all of the above mechanisms. As the number of users increases, the cross-correlation noise, or multiple access interference increases and the system becomes increasingly susceptible to the near-far effect. Near-far problems are also more significant on the uplink than the downlink as the propagation path varies for all users. Near-far problems can only arise on the downlink when a mobile receives signals at differing power levels from two or more basestations, such as occurs at a cell boundary.

5.2.4 Asymptotic multi-user efficiency

The near-far resistance of a receiver may be quantified by its multi-user asymptotic efficiency ξ_b as defined by Verdu [6]. This quantity measures the performance of a multi-user detector in an asynchronous multiple access channel and is defined as the ratio of the SNR required to achieve the same uncoded bit error rate in the absence of interfering users to the SNR required with N_u asynchronous users sharing the channel. For the ith user the value of ξ is thus defined as:

$$\xi_i = \lim_{\eta \to 0} \frac{SNR_{eff}}{SNR_i} \tag{5-34}$$

where η is the thermal noise power. As asymptotic efficiency measures performance loss due to the existence of other active users in the channel, it is a powerful metric for the comparison of near-far resistant receivers. In the presence of other users, the conventional single-user receiver (a matched filter followed by a threshold comparison) has a nonzero probability of error as $\eta \to 0$ and, as a consequence of this irreducible error floor, the asymptotic efficiency is equal to zero. A receiver which is optimally near-far resistant will have an asymptotic efficiency of unity. The zero efficiency of the conventional receiver and impracticality of optimal receivers is the motivation for seeking realizable receiver designs with nonzero asymptotic efficiency.

In tangible systems and their computer simulations it is impractical to measure bit error rate at zero noise levels, and the low-noise system error rate suffices as an approximation for the

calculation of ξ_i. The asymptotic efficiency can then be obtained by evaluating the effective SNR with equation (5-7) for coherent reception or equation (5-9) for differentially coherent reception.

Turin [13] has estimated that for an asynchronous DS-CDMA system in which all users' signals are single path non-fading and received at the same power, K_{Max}, the maximum number of users that can be supported by the system is 10-20% of N for bit error rates of 10^{-3} to 10^{-5}. With a 63 chip signature waveform this corresponds to just 6 to 12 users. For a fading channel, K_{Max} falls to just 1-5% of N, less than 4 users for a 63 chip code. DS-CDMA is therefore rendered unusable in the mobile environment without employing an effective means of countering the near-far problem.

5.3 DS-CDMA Downlink Analysis

The downlink of a cellular DS-CDMA system presents fewer problems than the uplink scenario, mainly because all users can be added orthogonally in the basestation and only one channel needs to be estimated in the subscriber receiver. This can be achieved directly through the pilot-tone transmitted continously by the basestation for synchronisation, power control and channel estimation. Nevertheless, the multipath faded channel will inevitably introduce distortions to the received signal and consequently destroy the orthogonality between users. This calls for more sophisticated receivers employing RAKE receivers and 'other-user' interference elimination.

In a conventional DS-CDMA system, several problems arise on the downlink:

- **Multi-user Interference** – As the number of active users increases, the performance of the DS-CDMA system decreases rapidly, since the capacity of a DS-CDMA system is limited by the other-user interference

- **Complexity** – In order to exploit all the multipath diversity it is necessary to apply a matched filter in the form of a RAKE receiver structure with a sufficient number of arms. The maximum number of arms is governed by the maximum number of discrete multipath components. In addition, the receiver has to be matched to the time-variant channel impulse response. Thus, proper channel estimation is necessary. This leads to additional receiver complexity, adaptive receiver filters and considerable signaling overhead.

- **Single/Multi-Tone Interference** – Furthermore, for the case of single-tone or multi-tone interference, the conventional DS-CDMA receiver spreads the interference signal over the whole transmission bandwidth whereas the desired signal path is despread. If this interference suppression is not sufficient, additional operations have to be applied at the receiver, such as notch filtering in the time domain (based on the least mean square algorithm) or in the frequency domain (based on the Fast Fourier Transform) to partly decrease the level of interference [20,21]. However, this extra processing leads to additional receiver complexity.

Figure (5-5) shows a typical downlink scenario of a multi-user single-cell system.

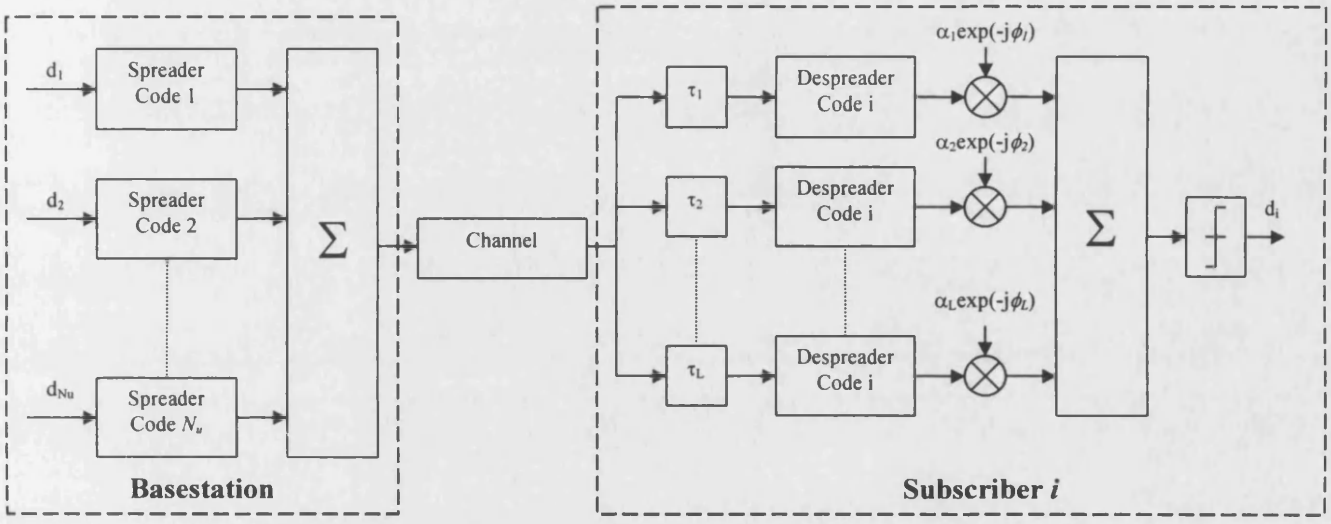

Figure 5-5. DS-CDMA downlink scheme with a RAKE receiver

Here, the matched filter resolves nearly all the multipath in the channel by using a RAKE receiver. The maximum number of arms in the RAKE receiver is limited due to hardware complexity. In each arm of the time-domain received signal, the signal is delayed by τ_l, where $l = 1,2\ldots L$, and despread with the same user specific code, i. Before being summed over all paths, the despread signal is further weighted by the complex conjugate of the instantaneous value of the time-varying complex channel coefficient of the assigned echo. This effectively implements maximum ratio combining (MRC); a combining method which seeks to combine the maximum signal-to-noise ratio of each echo. Alternatively, the RAKE receiver could employ equal gain combining (EGC) to bring the phases of each path to a common point. This method does not perform as well as MRC, but can be simpler to implement. Finally, the RAKE receiver adds the results obtained from each arm and makes a decision on the ith users transmitted data bit.

5.3.1 AWGN Channel Performance

We consider a synchronous downlink and assume that the other-user interference can be taken into account using the Gaussian approximation outlined earlier. Due to the central limit theorem this assumption is sufficiently good, especially for large number of users (more than 20% of the spreading length). The resulting error probability can be approximated by [22]:

$$P_e = \frac{1}{2} erfc\left(\sqrt{\frac{\gamma}{1+\gamma \cdot I}}\right) \tag{5-35}$$

where $\gamma = E_b/N_o$ is the SNR per bit and the total other-user interference I is given by equation (5-12). For random codes, $I = (N_u\text{-}1)/N$, and for preferentially phased Gold codes, introduced in chapter 4, this interference term is given as $I = (N_u\text{-}1)/N^2$ [22,23].

If we select Walsh-Hadamard orthogonal sequence spreading codes, the error probability expression is given by the single-user case:

$$P_e = \frac{1}{2} erfc\left(\sqrt{\gamma}\right) \tag{5-36}$$

5.3.2 Frequency Selective Fading Channel

We now investigate the implementation of a matched filter using a RAKE receiver with a given number of arms in a frequency selective Rayleigh faded channel. The number of RAKE "fingers" is assumed to be matched to the number of resolved multipath components in the channel. Therefore we can derive an expression for the BER of a RAKE receiver with a given diversity using the Gaussian assumption.

For the single-user case, the bit-error probability P_e for a DS-CDMA system using a RAKE receiver of diversity L can be written in the closed form [24]:

$$P_e = \left(\frac{1-\mu}{2}\right)^L \sum_{j=0}^{L-1} \binom{D-1+j}{j} \left(\frac{1+\mu}{2}\right)^j \tag{5-37}$$

where μ is defined as:

$$\mu = \sqrt{\frac{\gamma}{L+\gamma}} \tag{5-38}$$

It is assumed that the average signal-to-noise ratio per path is equal for all paths so that the SNR γ per data bit is:

$$\gamma = L\,\gamma_l \tag{5-39}$$

where γ_l is the SNR per path. To handle the other-user interference, we consider the Gaussian assumption, as detailed earlier in equation (5-20). The bit-error rate for a RAKE receiver in the multi-user case can therefore be approximated by substituting (5-20) into (5-37) and (5-38):

$$P_{BER} \approx \left(\frac{1}{2} - \frac{1}{2} \sqrt{\frac{\gamma}{L + \gamma + L\gamma \dfrac{2(N_u - 1)}{3L}}} \right)^{L} \sum_{j=0}^{L-1} \binom{L-1+j}{j} \left(\frac{1}{2} + \frac{1}{2} \sqrt{\frac{\gamma}{L + \gamma + L\gamma \dfrac{2(N_u - 1)}{3L}}} \right)^{j} \tag{5-40}$$

We now consider a downlink RAKE receiver using coherent BPSK with preferentially phased Gold codes of length N=31 in a multipath channel, where each path has an equal average SNR. It can be seen in figure (5-6) that the BER performance degrades significantly in an L=4 multipath channel as the number of users is increased. For only 4 active users, an irreducible BER of 10^{-3} is already the limiting factor on performance.

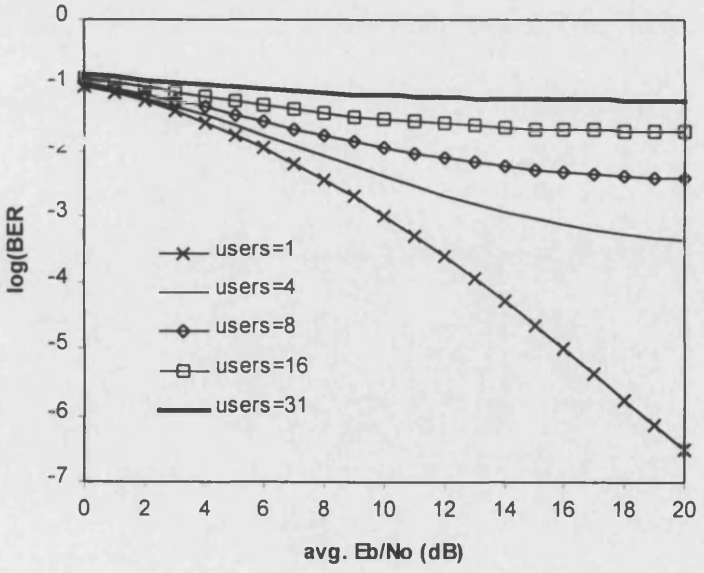

Figure 5-6. DS-CDMA RAKE receiver performance for a diversity of L=4 paths

Considering a fixed number of 4 simultaneous active users, it is shown in figure (5-7) that increasing the level of diversity from a single path up to 32 paths can reduce the irreducible BER by a considerable amount; from 10^{-3} to 10^{-6}, a reduction factor of 3 orders. Hence, at the cost of receiver complexity, diversity can provide considerable performance gains in multipath faded channels.

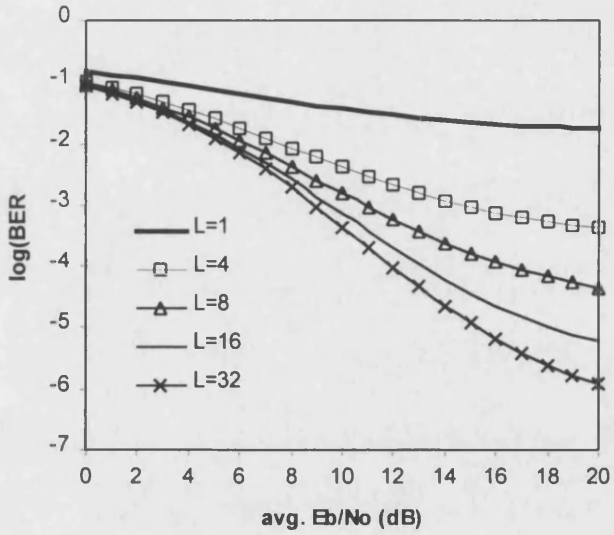

Figure 5-7. Increasing the level of diversity for a DS-CDMA downlink RAKE receiver with 4 active users

5.4 Techniques to combat multi-user interference

In the preceding section it was stated that mobile DS-CDMA is effectively unusable without some means to counter the near-far effect and MAI. Techniques which have been proposed for this purpose and which are used to varying extent in current systems are described below.

5.4.1 Power control

This is the most commonly employed technique to counter near-far effects and maximise capacity and has been adopted by Qualcomm Inc. in the United States for the IS-95 CDMA standard. Power control works by adjusting the transmitted power of the mobile handset to ensure that the received power from all users is the same at the basestation. In this way the

interference contribution to the desired user is minimised and the severity of near-far is reduced. Where the cellular system employs a pilot signal for synchronisation the pilot can be used to sound the forward link and adjust for propagation loss and slow fading on the reverse link.

For full duplex systems having differing transmit and receive frequencies the signal will undergo independent fading on the up- and downlinks as the transmit-receive channel separation will exceed the channel coherence bandwidth. This dictates the need for closed loop power control where a dedicated power control channel adjusts the handset transmit power to compensate for the fading channel. The control algorithm must be capable of tracking the fast fading variations and have a low loop latency and an update rate of around 1 kHz is normal.

Incorporating power control increases system complexity, and although the near-far effect is reduced, it does not remove the root cause: multiple access interference. It is, however, always desirable to retain some form of crude, low-rate power control to compensate for slow fading and enable transmission at minimum power levels to reduce the interference contribution from other users and maximise battery life, even when using a joint-detection receiver or MAI cancellation.

5.4.2 Diversity

Provided the inverse of the spreading code chip duration, T_c, of a system is significantly less than the coherence bandwidth Δf of the mobile channel, DS-CDMA is capable of resolving the individual echoes or multipaths from which a received signal is comprised. As these paths generally undergo independent fading and have different near-far ratios, they provide a level of internal diversity in the receiver. Path diversity is ordinarily exploited with a RAKE receiver as described in chapter 4.

5.4.3 Adaptive antennas

Interference from other users can be reduced with the aid of an adaptive antenna at the basestation. Two different approaches are applicable, dependent on the cell size. In larger cells the multipaths associated with a particular user tend to arrive from roughly the same azimuth angle and the interference from other users can be nulled by steering a beam towards the desired user. In smaller cells, the arrival angles of the desired paths are more uniformly distributed and

the antenna pattern is adaptively tuned to steer nulls towards significant interference sources and select strong desired paths.

5.4.4 Interference cancellation

Interference cancellation techniques for CDMA wireless systems is a topic of intense research. One major motivation to their study is to achieve further improvements in the capacity of cellular CDMA systems. These techniques can be classified into two basic categories. The first class of techniques is nonlinear in nature, termed parallel interference cancellation, and uses the principle of decision feedback. There are several variants of this principle [25-27]. Depending on the number of iterative stages of decision feedback, whether hard or soft decisions are made, error control coding is used etc. Broadly speaking, in such a reciever, in order to demodulate a user, a tentative decision is made of the bits of interferers to this user. These interferers are then subtracted out and it is possible this in an iterative or multistage fashion [26,27].

In a coded system, it is not desirable to make decisions at the code symbol level because the symbol SNR is too low, both due to the rate of the code and because the symbol energy is a fraction of the bit energy. Hence the second technique of interference cancellation employs successive decoding. In [25], a design approach is presented in which the users employ very low-rate orthogonal convolutional codes, as presented in chapter 4, and are allocated powers in a geometric progression. The strongest user is decoded first and then re-encoded, re-modulated and subtracted out from the received signal. Demodulation and decoding proceeds to the next strongest user. It is shown that this method can asymptotically achieve the Shannon capacity of the band-limited AWGN channel.

In either case, the use of decision feedback techniques requires accurate knowledge (or estimates) of amplitude, phase and delay of all users and hence is suitable mainly in AWGN channels without impairments such as fading, multipath, shadowing, frequency and phase variations etc. Cellular channels suffer from all these degradations and hence nonlinear interference cancellers are not practical in such channels. The IS-95 CDMA system has been specifically designed to be robust to these impairments. It is possible to use decision feedback based interference cancellation along with the IS-95 system, but for the aforementioned reasons, performance is likely to be good only in AWGN channels.

Attention is focused in this thesis on DS-CDMA techniques employing a unique dimension to each user which uses PN sequences that have a period of one bit or code symbol for each user.

In this case the sequences assigned to different users are designed to have low cross-correlations and multi-user receivers are employed to combat the mutual interference among these users. The concept of assigning a unique dimension to each user is very similar to the concept of FDMA or TDMA, and in AWGN channels the capacities are virtually the same. In these schemes, the dimensional separation of users is exploited in order to reduce the interference. Redundancy due to error control codes reduces the effective dimensionality available for user-separation though it also reduces the SNR necessary to achieve a given BER. Hence, the combination of error control coding and interference cancellation is a topic of interesting research.

5.5 Summary

This chapter has introduced the concept of multiple-access direct-sequence spread spectrum communications for mobile applications on the up- and downlink with particular emphasis on synchronous and asynchronous multi-user applications.

Deterministic DS-CDMA systems that use a user defined sub-space of PN codes with low cross-correlation have been treated in an analysis of both synchronous and asynchronous DS-CDMA. It was shown that the output of a filter matched to the desired user's signature waveform comprises two distinct interference sources, namely, correlation with channel AWGN and cross-correlation between the desired user's waveform and those of all other users. In DS-CDMA, the cross-correlation term invariably has the greater magnitude resulting in a system that is interference rather than noise-limited. The selection of a suitable code set is crucial to the performance of a CDMA system and an analysis of an interference limited rather than noise limited system has been given. Optimal interference canceling receivers have been analysed, and a 2dB difference in performance between coherent BPSK and coherent DPSK is assumed valid if the MAI is cancelled completely. This holds for synchronous as well as for asynchronous operation. In situations where users' signals are received at differing power levels, the magnitude of cross-correlation noise is enhanced, giving rise to the near-far effect.

In a practical DS-CDMA system the interference from other users is also included in the BER expressions. The Gaussian approximation is quite accurate for a large number of active users and has consequently been applied the BER expressions, showing the inherent soft-capacity degradation of DS-CDMA. It is this feature that makes CDMA an attractive technique for cellular applications.

In faded channels the performance of many users is quickly degraded through ISI self-interference and other users. In fact, the maximum number of users that may be supported by an asynchronous faded DS-CDMA system is around 10-20% of the signature sequence length N. Without line-of-sight paths the BER quickly degrades and no adequate throughput is achieved. This calls for more sophisticated receiver implementations to reduce the level of interference from the other users to reduce the near-far effect. Near-far represents the principle limitation of DS-CDMA and without an effective means to counter it, such as accurate power control, frequency-domain or time-domain diversity, adaptive antennas, interference cancellation techniques or (quasi-) coherent orthogonal user detection, DS-CDMA is rendered useless in the mobile and fixed wireless access environment. Of course, there are also imminent problems with the inter-cell interference from the surrounding cells, causing unnecessary interference that is difficult to reduce using some of the methods introduced earlier.

A downlink model in a fading multipath environment has shown to provide some performance gains compared to uplink strategies. Broadly speaking, the downlink requires less complex receiver architectures and can separate the users more easily if orthogonal codes are used, but nevertheless, may use interference cancellation techniques as well as the uplink. This is due to the inherent orthogonality destroying traits of multipath fading. In this case, more complicated receivers are needed. Channel estimation may be incorporated into the pilot tone or midambles inserted between successive data bits. This reduces the spectral efficiency and calls for more sophisticated channel estimation strategies.

We have shown that the performance of a DS-CDMA RAKE receiver in a multipath Rayleigh faded channel depends heavily on the level of diversity employed in the receiver. The use of preferentially phased Gold codes of length N=31 in a multipath channel of length L=4 on the downlink has shown to give irreducible bit-error rates of 10^{-3} for 4 active users. This can be reduced to 10^{-6} by increasing the level of diversity. It has been shown that, of course, the improvement in performance is greater as the order of diversity increases up to about L=16, and little improvement is expected when the order of diversity is increased even further. For the aforementioned reason we suggest alternative diversity schemes in subsequent chapters that may give additional diversity at a relatively reduced cost in receiver complexity compared with DS-CDMA RAKE receivers.

In summary, we have seen that multi-user DS-CDMA techniques do not necessarily give direct capacity advantages over conventional access strategies, but some of the inherent features, such as soft degradation with increased numbers of active users and some of the cellular concepts involved may give DS-CDMA the rising 'edge' for future third generation applications. We

have shown that a DS-CDMA multi-user cellular system is capacity limited on the uplink rather than the downlink, and the near-far effect is a problem that requires more sophisticated receiver implementations to be introduced.

The thesis deals with some of the near-far effect reducing concepts that may be used in techniques such as multi-carrier designs rather than the conventional single-carrier spread-spectrum schemes introduced so far. In this way, we can potentially merge some of the fundamental advantages of DS-CDMA with more complex transmitters and receivers to give additional gains in capacity, ease of cellular implementation, variable bit-rates, higher resistance to frequency-selective fading and reduced interleaving requirements. As is well known, many of these issues provide a fundamental limit on the data-rate throughput that may be achieved on mobile and fixed wireless access channels.

5.6 References

[1] Verdu, S, "Minimum probability of error for asynchronous Gaussian multiple-access channels", *IEEE Trans. on Information Theory*, Vol. 32, No. 1, pp.85-96, January 1986

[2] Omura, J K, "Spread spectrum radios for personal communications services", *IEEE 2nd International Symposium on Spread Spectrum Techniques and Applications (ISSSTA'92)*, Yokohama, Japan, December 1992

[3] Simon, M K, Omura, J K, Scholtz, R A, and Levitt, B K: Spread Spectrum Communications, Vol. I-III, *Computer Science Press*, Inc., 1985

[4] Geraniotis, E A, and Pursley, M B, "Error probability for direct-sequence spread-spectrum multiple-access communications – Part II: Approximations", *IEEE Trans. on Communications*, Vol. 30, No. 5, pp. 985-995, May 1982

[5] Pursley, M B, Sarwate, DV and Stark, W E, "Error probability for direct-sequence spread-spectrum multiple-access communications —Part I: Upper and lower bounds", *IEEE Trans. on Communications*, Vol. 30, No. 5, pp.975-984, May 1982

[6] Verdu, S, "Optimum multiuser asymptotic efficiency", *IEEE Transactions on Communications*, Vol. 34, No. 9, pp.890-897, Sep 1986

[7] Weber, C L, Huth, G K and Batson, B H, "Performance considerations of code division multiple-access systems", *IEEE Trans. on Vehicular Tech.*, Vol. VT-30, pp.3-9, Feb. 1981

[8] Geraniotis, E A, and Pursely, M B, "Performance of coherent direct-sequence spread-spectrum communications over specular multipath fading channels", *IEEE Trans. on Commun.*, Vol. COM-33, pp.502-508, June 1985

[9] Geraniotis, E A and Pursely, M B, "Performance of noncoherent direct-sequence spread-spectrum communications over specular multipath fading channels", *IEEE Trans. on Commun.*, Vol. COM-34, pp.219-226, March 1986

[10] Geraniotis, E A, "Direct-sequence spread-spectrum multiple-access communications over nonselective and frequency selective Rician fading channels", *IEEE Trans. on Commun.*, Vol. COM-34, pp.756-764, Aug. 1986

[11] Morrow, R K, and Lehnert, J S, "Bit-to-bit error dependence in slotted DS/SSMA packet systems with random signature sequences", *IEEE Trans. on Commun.*, Vol. 37, pp.1052-1061, Oct. 1989

[12] Pursley, M B, "Performance evaluation for phase coded spread spectrum multiple-access communication. Part I: system analysis; Part II: code sequence analysis", *IEEE Trans. on Commun.*, Vol. COM-25, pp. 795-803, August 1977

[13] Turin, G A, "The effects of multipath and fading on the performance of direct-sequence CDMA systems", *IEEE Journal on Selected Areas in Communications*, Vol. 34, No. 9, pp. 890-897, September 1986

[14] Stüber, G L, and Kchao, C, "Analysis of a multiple-cell direct-sequence CDMA cellular mobile radio system", *IEEE Journal of Select. Areas in Comms.*, Vol. 10, No. 4, May 1992

[15] Trabelsi, C, and Yongacoglu, A, "Bit-error rare performance for asynchronous DS-CDMA over mmultipath fading channels", *IEE Proc. Commun.*, Vol. 142, No.5, Oct 1995

[16] Lataief, K B, Chuang, C I and Murch, R D, "Multicode High-Speed Transmission for Wireless Mobile Communications", *IEEE Proc. of VTC'95*, pp. 1835-1839, 1995

[17] Lataief, K B and Hamdi, M, "Efficient Simulation of CDMA Systems in Wireless Mobile Communications", *IEEE Proc. of VTC'95*, pp. 1799-1803, 1995

[18] Wu, K T, and Tsaur, S A, "Error performance for diversity DS-SSMA communications in fading channels", *IEE Proc. Commun.*, pp. 357-363, Vol. 141, No. 5, October 1994

[19] Mowbray, R S, Pringle, R D, and Grant, P M, "Increased CDMA system capacity through adaptive interference regeneration and cancellation", *IEE Proceedings-I*, pp. 515-524, Vol. 139, No. 5, Oct 1992

[20] Milstein, L, "Interference rejection techniques in spread-spectrum communications", IEEE Proceedings, Vol. 75, pp. 211-222, 1988

[21] Ketchum, J, and Proakis, J, "Adaptive algorithms for estimating and suppressing narrow-band interference in PN spread-spectrum systems", IEEE Trans. on Communications, Vol. 30, pp. 913-924, 1982

[22] Geraniotis, E, and Ghaffari, B, "Performance of binary and quaternary direct sequence spread-spectrum multiple-access systems with random signature sequences", IEEE Trans. on Comms., Vol. 39, pp. 713-724, 1991

[23] Massey, J, and Mittelholzer, T, "Technical assistance for the CDMA communications system analysis", Tech. Report 8696/89/NL/US, ESTEC Contract, 1991

[24] Proakis, J G, "Digital Communications", *McGraw-Hill*, 3rd edition, 1993

[25] Viterbi, A J, "Very low-rate convolutional codes for maximum theoretical performance of spread-spectrum multiple access channels", IEEE Jorunal on Selected Areas in Communications, May 1990, pp. 641-649

[26] Divalsar, D, and Simon, M K, "Improved CDMA Performance Uding Parallel Interference cancellation" JPL Publications 95-21, Pasadena, CA, Oct. 1995

[27] Varanasi, M K, and Aazhang, B, "Multistage Detection in Asynchronous Code-Division Multiple Access Systems", IEEE Trans. on Comm., pp. 509-519, April 1990

CHAPTER 6

LOW-RATE ORTHOGONAL CONVOLUTIONAL CODES

6.1 Introduction

Low-rate orthogonal convolutional codes (LROCC) were introduced in Chapter 4 as an alternative coding and spreading scheme for DS-CDMA applications. We have introduced the method of generating orthogonal codes by selecting a row from the corresponding Hadamard matrix. We have also shown the spectra of such codes and the problem this can cause on the uplink in DS-CDMA applications by containing large signal powers within certain parts of the total bandwidth. This has led to the concept of using randomising sequences to improve the spectral power profile of these orthogonal sequences and randomise the signal.

To analyse the performance of convolutional codes we introduced the concept of transfer functions to describe the state diagram of the Markov state model. In this chapter, we take this process one step further and obtain an estimate of the theoretical upper bound on the performance of low-rate orthogonal, super-orthogonal and hyper-orthogonal codes in AWGN and Rayleigh faded multipath channels. For AWGN channels we introduce the Gaussian approximation for a large user base and compare the theoretical and simulated results. The modulation in faded channels in the analysis is based on non-coherent detection using non-coherent combining on the real and imaginary part of the received signal whereas the simulations were carried out using coherent BPSK. Nevertheless, we use these results to obtain an upper bound on the performance.

An LROCC encoder can be used to form an extension to simple low-rate convolutional codes by using orthogonal code sequence sets rather than random binary sequences following a particular trellis. It was shown that through cascading a convolutional encoder with a Hadamard block encoder, a set of orthogonal code sequences can be selected from the Walsh-Hadamard matrix and be used to represent the transmitted data symbol. The mapping of the data symbol to the code sequence set is determined by the state of the convolutional shift register stages, as seen in figure (6-1).

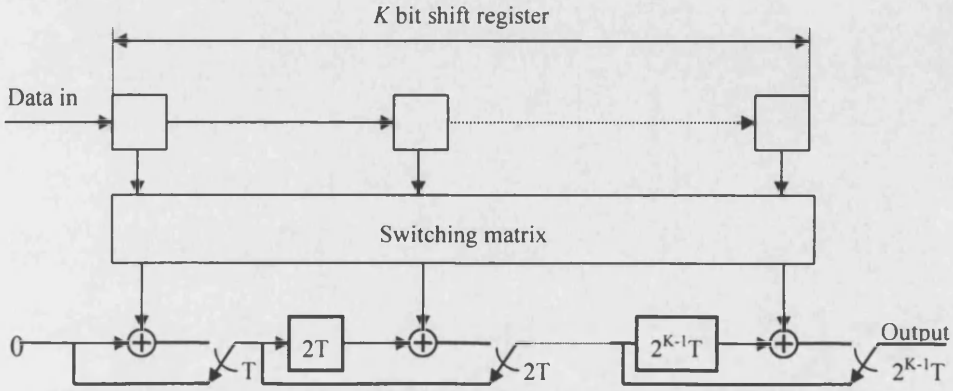

Figure 6-1. A low-rate orthogonal Hadamard convolutional encoder

A constraint length K orthogonal convolutional code may be used in two ways:

1. 2^K symbols are clocked out for every K data bits in the shift registers, equivalent to an M-ary modulation format at a code rate of $R=K/2^K$, or,
2. A set of 2^K symbols are output for every single data bit clocked into the shift register, giving a code rate of $R=1/2^K$, similar to the spreading process in a DS-CDMA system

The first method serves in the similar way to M-ary orthogonal coding, and is not considered in this work. The alternative method of mapping 2^K symbols to each data bit provides an equivalent spreading ratio of 2^K for DS-CDMA applications. This method is investigated in more detail in the following sections.

6.2 Theoretical basis

6.2.1 AWGN channels

It has been shown earlier that a low-rate convolutional Hadamard encoder provides an encoded sequence of 2^K output symbols for each consecutive input data bit. There are 2^K different sequence sets, each of length 2^K symbols and orthogonal to any other sequence. The inherent orthogonal properties of the Hadamard codes are based on the fact that any two sequences of length 2^K differ in 2^{K-1} symbol positions, thus giving a 64 symbol length Hadamard code 32 different symbol combinations.

The received signal can be decoded with a maximum likelihood detection scheme such as the Viterbi algorithm. To decode the received signal sequence with a Viterbi decoder it is necessary to find the most likely path through the trellis state diagram. Since each user may have a different unique mapping of state outputs in the shift register to the Hadamard block encoder, the trellis for each user will be considerably different. This therefore enables all simultaneous users to be detected individually.

In order to establish a theoretical prediction of how such a decoder performs in a hostile noise environment it is important to understand the structure of the Hadamard orthogonal codes and to have a knowledge of the free distance of the code, which plays an important part in the performance under AWGN.

It is well known [1] that the bit-error rate (BER) performance of a Viterbi decoder is directly related to the free distance of the convolutional code. The BER probability in continuous additive white Gaussian noise channels is given as:

$$P_{BER} < \sum_{z=dfree}^{\infty} C_z P_z \tag{6-1}$$

where,

$$P_z = Q\left(\sqrt{\frac{2zRE_b}{N_o}}\right) \tag{6-2}$$

and R is the rate of the code, E_b/N_o is the required SNR at the output of the decoder and C_z is determined by the code structure of the convolutional encoder.

The Hamming distance between any two symbol sequences is known to be 2^{K-1} and for a constraint length K=6 code will yield a value of 32 symbols. Without any loss of generality, it is reasonable to assume the all zero path as the correct path for all bit-error calculations. To determine the free distance of any convolutional code it is necessary to count the number of paths (and hence the number of symbols) which will take the decision path back to the all zero path after one erroneous data bit decision. This, of course, is related directly to the constraint length K, and the minimum number of paths which will take the decoder decision to the all zero state is K+1. The free distance of the K=6 Hadamard convolutional code is therefore $2^{K-1}(K+1)$=224. This is the theoretical optimum free distance any convolutional code could have and is the basis for giving the orthogonal codes a superb performance in noisy channels.

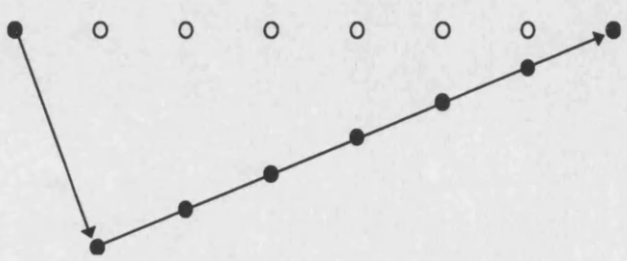

Figure 6-2. Determining the free distance of a K=6 convolutional code

The values for C_z have to be obtained through an exhaustive search of the trellis structure. This was carried out in this work and for a K=6 Hadamard code, neglecting the higher order terms, yields a bound on the bit-error probability of:

$$P_{BER} < P(224) + 2P(256) + 6P(288) + 16P(320) + 35P(352) + 60P(388) \ldots \quad (6\text{-}3)$$

This gives an upper bound on the performance of the LROCC implementation in a DS-CDMA system with predominantly additive white Gaussian noise on the channel. In figure (6-3) the theoretical performance of the LROCC design implementation using soft decisions is compared with a conventional rate R=1/2, K=6 convolutionally encoded system. It can be seen that for high signal-to-noise ratios the performance of both systems is very similar, whereas for low signal-to-noise ratios the LROCC design performs much better than the rate ½ encoded data. Improvements of up to 1.5dB can be found at very low signal-to-noise ratios. It is particularly noticeable that the level of E_b/N_o where the coded and uncoded curves cross is much lower for the LROCC system than for the R=1/2, K=6 system.

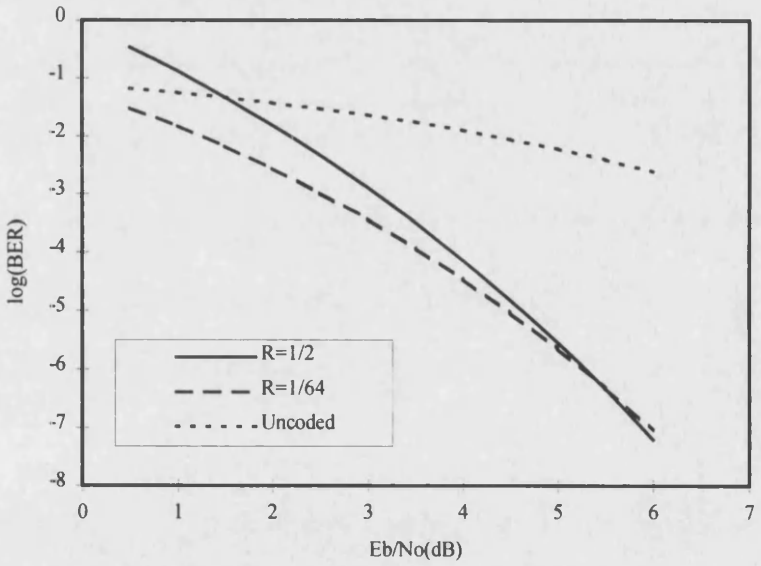

Figure 6-3. A comparison of conventional convolutional encoding and the new LROCC design in AWGN

The theoretical upper bound on the BER performance may be determined from the generating transfer function given by equation (4-19) in chapter 4:

$$T(W,B) = \frac{BW^K(1-W)}{1-W\left[1+B\left(1-W^{K-1}\right)\right]} \quad (6\text{-}4)$$

where B denotes a transition in the trellis diagram caused by a data input of '1', W is a weight measurement for each branch metric and relates the average energy-per-bit to the noise density ratio per distance weight. For coherent AWGN channels, it can also be shown (Appendix B):

$$W = Z^{\frac{1}{2R}} \tag{6-5}$$

where R is the code rate and $Z = \exp(-E_b/N_0)$. For other channels (such as the Rayleigh faded channel), W follows a different statistic, as will be seen later.

In the receiver, to determine the upper bound for the bit-error rate of the LROC code for any general class of channel, equation (6-4) must be differentiated with respect to B, and B then set to 1:

$$\left.\frac{dT(W,B)}{dB}\right|_{B=1} = \frac{W^K(1-W)^2}{\left(1-2W+W^K\right)^2} \tag{6-6}$$

Figure (6-4) below shows the BER performance obtained from equation (6-6) for different values of K.

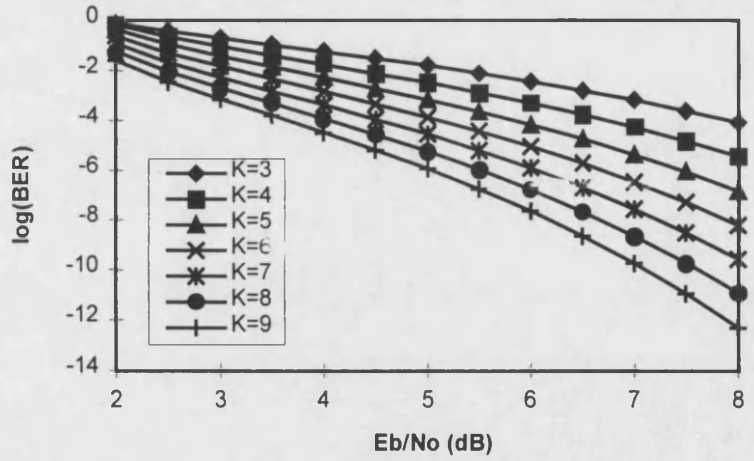

Figure 6-4. Theoretical *BER* v. E_b/N_o for an LROCC system in AWGN

6.2.2 LROCC performance in *L*-path Rayleigh fading

In the receiver, it is assumed that the received signal is represented as I and Q signals, and a maximum ratio combining technique of equal length to the number of L multipath components is employed. Maximum ratio combining is assumed since this combining method weights each faded path by the complex conjugate attenuation factor and provides the simplest way of calculating the upper bound on performance. The branch metric of the typical demodulated input variables Y_I and Y_Q is determined from the input variable $Z = Y_I^2 + Y_Q^2$. It is assumed that the received signal comprises of L components from L independent Rayleigh faded paths. The amplitude, λ, of each independent Rayleigh faded signal is related by the probability function, $p(\lambda)$:

$$p(\lambda) = \frac{\lambda}{\sigma^2} e^{\left(-\lambda^2/2\sigma^2\right)} \tag{6-7}$$

where the chip energy E_c is multiplied by λ^2 and σ^2 is the variance of the fading process. The average chip energy, E_{avg}, for each path is derived from the chi-squared probability density function in the usual way [2], from which it is found that:

$$E_{avg} = \sigma^2 E_c \tag{6-8}$$

Thus the average mean-squared signal power is given by $M^2 = J^2 E_{avg}$, where J is the number of symbols per input data bit in the shift registers of the Hadamard encoder. From [2] it can be seen that the probability of a correct signal, $P_C(z)$, and the incorrect signal probability, $P_I(z)$, is given by:

$$P_C(z) = \frac{z^{L-1} e^{-\left(\frac{z}{1+J E_s/N_0}\right)}}{(L-1)!\left(1+J E_s/N_0\right)^L}$$

$$P_I(z) = \frac{z^{L-1} e^{-(z)}}{(L-1)!} \tag{6-9}$$

where E_s is the average symbol energy per path. Therefore,

$$E_s = E_b / LJ \tag{6-10}$$

where E_b is the total bit-energy received from all L paths.

The performance of any convolutional code in the maximum-likelihood decoding algorithm is determined through evaluation of the branch metrics on the correct and incorrect paths through the trellis state diagram. Letting the correct branch metrics be denoted as (y_1, y_2, ... y_d) and the incorrect branch metrics as (x_1, x_2, ... x_d), the probability of a wrong decision being made at the point of path remerging is:

$$P_d = \text{Prob.}\left(\sum_{i=1}^{d} x_i > \sum_{i=1}^{d} y_i\right) \tag{6-11}$$

Since the branch metrics can be treated as random variables due to the independence imposed on successive symbol set transmissions, the Chernoff bound can be applied to equation (6-11). Hence,

$$P_d < E\left[\exp\left(p\sum_{i=1}^{d} x_i - y_i\right)\right] = \left\{E[\exp(p(x-y))]\right\}^d \tag{6-12}$$

where p is a variable from the exponential function of the Chernoff bound. To obtain the upper-bound on the bit-error performance it is necessary to determine the minimum value of the expected value of equation (6-12). It can be shown [2] that:

$$\begin{aligned} E[\exp(p(x-y))] &= \int_0^\infty e^{px} P_I(x).dx \int_0^\infty e^{-py} P_C(y).dy \qquad p>0 \\ &= \frac{1}{(1-p)^L} \frac{1}{[1+p(1+U)]^L} \end{aligned} \tag{6-13}$$

where $U = (E_b/N_0)/L$ and the minimum value can be seen at $p = (U/2)/(1+U)$. Hence,

$$P_d < \left\{ \frac{1}{\left(1-(U/2)/(1+U)\right)^L} \frac{1}{\left(1+\frac{(U/2)/(1+U)}{1+U}\right)^L} \right\}^d \qquad (6\text{-}14)$$

$$= \left[\frac{1+U}{(1+(U/2))^2} \right]^{Ld}$$

Therefore,

$$P_d < W^d \qquad (6\text{-}15)$$

where,

$$W = \left(\frac{1+U}{(1+(U/2))^2} \right)^L .$$

This value for W is substituted directly into equation (6-15) to give the performance of the LROCC design for a specific constraint length, K, in L-path Rayleigh faded channels. The performance for L=4 (i.e. a 4 path model) is shown in figure (6-5).

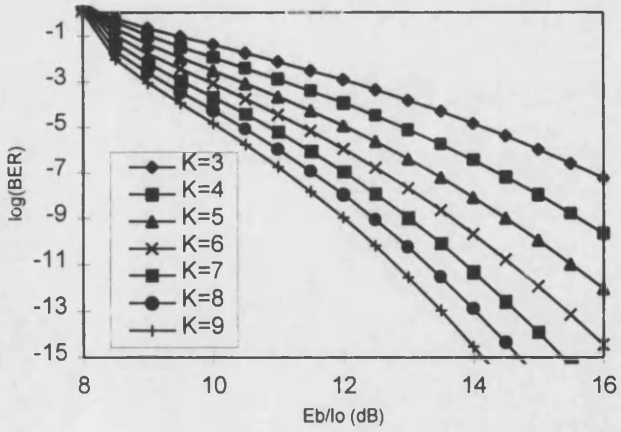

Figure 6-5. Theoretical *BER* v. E_b/N_o for the LROCC System AWGN and *L*-path Rayleigh fading channels

It is clear from this graph that there is a degradation in the bit error rate performance of the LROCC system in Rayleigh fading (compared with the non-faded system) which is dependent on the prevailing E_b/N_o. Typically, there is at least a 6dB degradation in performance.

Next, we seek to obtain a relation between the excess E_b/N_o required for the faded system performance compared to the AWGN channel, for a given value of signal-to-noise ratio per path L. This ratio is obtained as:

$$\text{Excess } E_b/N_o = \frac{2\exp\left(\frac{E_b}{2LN_o}\right) - 2 + \frac{1}{2}\sqrt{16}\sqrt{\exp\left(\frac{E_b}{2LN_o}\right)}\sqrt{\exp\left(\frac{E_b}{2LN_o}\right) - 1}}{E_b/LN_o} \tag{6-16}$$

The results of equation (6-16) are displayed graphically in figure (6-6).

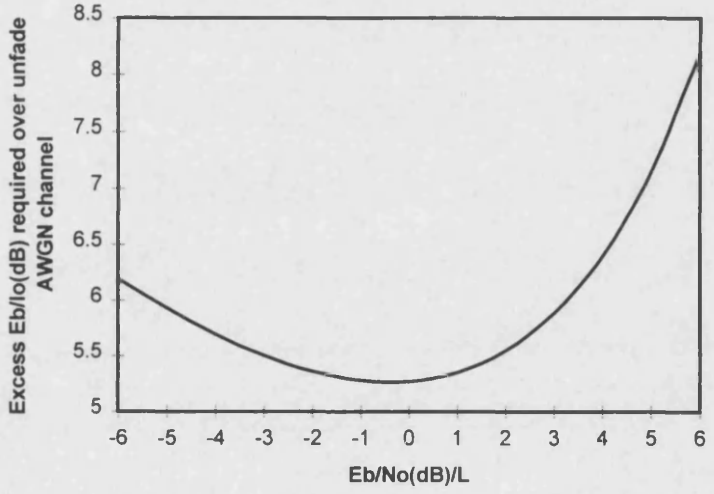

Figure 6-6. Excess E_b/N_o required for non-coherent Rayleigh fading employing LROCC

From these results one can obtain an estimate of the total required E_b/N_o for different values of diversity L. Note that values of excessive diversity cause increased performance degradation due to the non-coherent combining losses in the receiver.

6.3 Simulation results

6.3.1 AWGN performance

Computer simulations were carried out at baseband with BPSK modulation. Figure (6-7) shows the results of computer simulations of the LROCC encoder (K=6, R=1/64) in AWGN, where E_b/N_o is the signal-to-noise ratio at the output of the correlator/decoder. The low-rate of the code effectively implements bandwidth spreading that needs to be taken into account to determine the E_b/N_o at the receiver. This concept is equivalent to normalising to the processing gain in a DS-

CDMA system to make a fair comparison of the BER performance for a given SNR in the same bandwidth. Before decoding the received signal in the Viterbi decoder, the received samples may be quantised into 2,3 or more levels. Because of the elegant structure of the codes and the Viterbi algorithm, convolutional decoders can and do make use of channel reliability information. This reliability information is generated by allowing the discrete memoryless channel to have a larger number of outputs than inputs. In the limit, the channel output is allowed to be a continuum of values. To create a hard decision channel, the matched filter output space (the real number line) is partitioned into two regions. When reliability information is output from the channel, the channel is called a soft decision channel. The Viterbi algorithm can be used to find the correct path through the trellis for hard or soft decisions, but considering a quantisation of 3 or more levels is regarded as approaching the same performance limit reached through pure soft decision channels. Consequently, all simulations carried out in this thesis for pure soft decision channels would hold equally as accurate as for received signals with 3 bit quantisation.

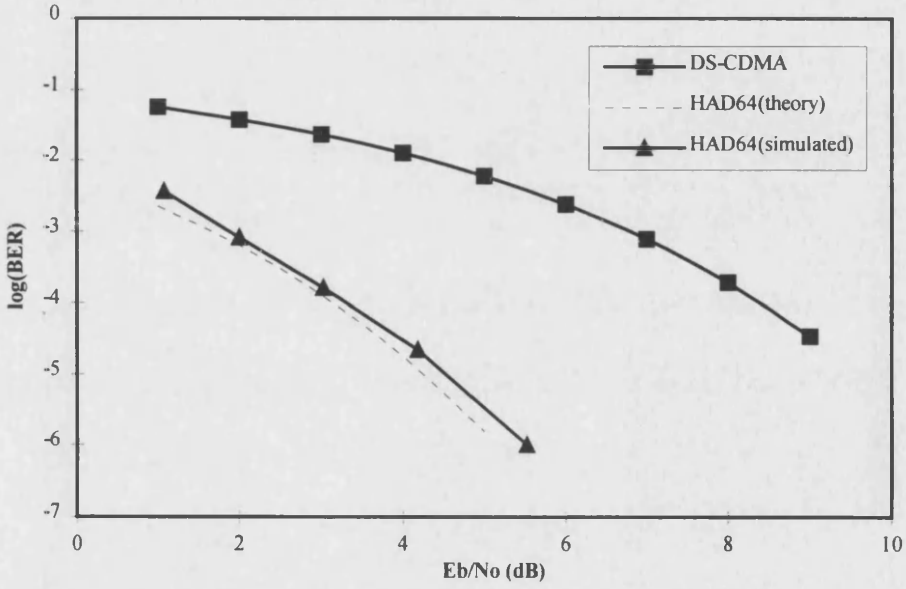

Figure 6-7. Performance of LROCC encoded and uncoded DS-CDMA in AWGN

The performance of the LROCC design implementation in AWGN can be seen to give a significant improvement over the uncoded DS-CDMA system. At a bit-error rate of 10^{-4}, coding gains of 5dB can easily be achieved. Under low noise environments this improvement in performance increases considerably. Because the free distance of these orthogonal codes is at an optimum high level, the improvement is larger than the conventional high-rate (i.e. R=1/2,1/3..) coded DS-CDMA system occupying the same equivalent bandwidth for a given data rate.

6.3.2 Super- and Hyper-Orthogonal Convolutional Codes

The performance of super- and hyper-orthogonal codes has also been simulated in AWGN channels. Super-orthogonal codes are formed from an extension of LROCC codes by extending the convolutional shift register system. This has the effect of including the bi-orthogonal code set in addition to the conventional orthogonal Walsh-Hadamard code set, therefore extending the possible range of codes that may be transmitted. The probability of selecting a wrong path in the trellis can depend quite heavily on the initial first and last trellis branches. Therefore, the main difference in performance gains is achieved by further increasing the Hamming distance between code words on the initial starting states of the trellis and the final truncation stages. Figure (6-8) shows the encoder configuration for a super-orthogonal coding scheme.

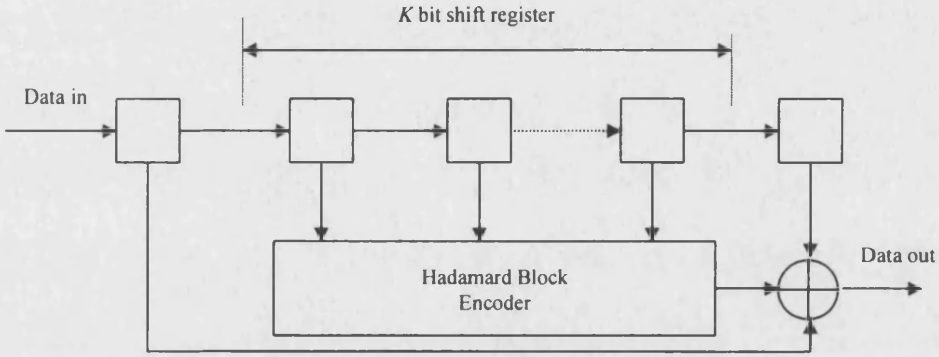

Figure 6-8. Super-orthogonal encoder structure

If we wish to further extend the Hamming distance between individual branches in the main core of the trellis structure by employing sequences from the bi-orthogonal code set we can add additional shift register stages to the front end of the encoder. This obviously increases the complexity of the encoder and decoder, but at the same time keeps the bandwidth of the transmitted signal constant and provides additional coding gain. This novel encoder implementation is termed a hyper-orthogonal convolutional coding scheme and is under patent pending [35] by the author. A diagrammatic representation of such an encoder scheme can be seen in figure (6-9).

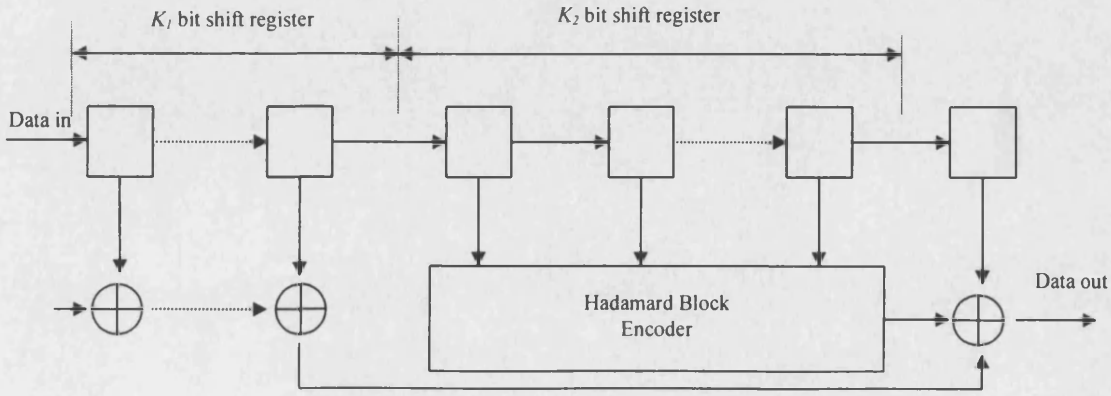

Figure 6-9. Hyper-orthogonal encoder structure

Table (6-1) below shows some of the different encoder structures that have been tested:

Name	K_1	K_2	R
LROCC	0	5	1/32
LRHOCC1	2	2	1/4
LRHOCC1b	3	2	1/4
LRHOCC2	2	3	1/8
LRHOCC3	2	6	1/64

Table 6-1. Different encoder structures for FEC in DS-CDMA

The performance for an adaptive constraint length hyper-orthogonal code with a constant spreading ratio of rate R=1/4 can be seen in figure (6-10) for increased levels in the constraint length K_1. As expected, the performance gets better as K_1 is increased. A gain of nearly 1dB can be achieved for the same bandwidth expansion factor, but at the cost of increased decoder complexity. A remarkable result is obtained from this graph: LRHOCC1b consists of 32 states in the trellis with 4 comparisons per branch compared to the LROCC encoder with 32 states and 32 comparisons per branch, and still out-performs the LROCC encoder at high E_b/N_0. This shows that for a relatively similar decoder depth and reduced decoder complexity by a factor of 8 the use of hyper-orthogonal codes can give an improved performance. For DS-CDMA systems employing multi-carrier techniques, a large bandwidth expansion factor is often required and hence it is important to strike the right balance between decoder complexity and efficient bandwidth utilisation. For FWA applications, in particular, where the channel is virtually time-invariant, this coding technique will have excellent applications.

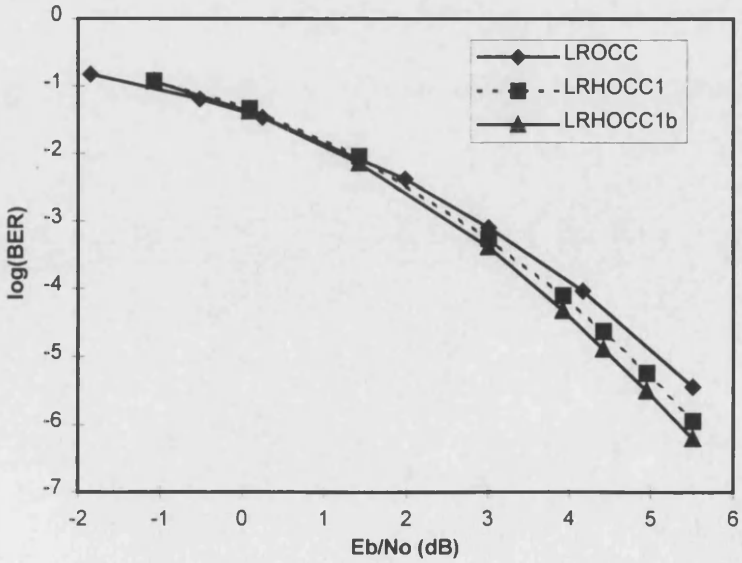

Figure 6-10. Hyper-orthogonal encoder in AWGN

For a full comparison of the different encoder designs featured in the table above, figure (6-11) shows the different performance improvements that can be obtained through the use of hyper-orthogonal coding strategies.

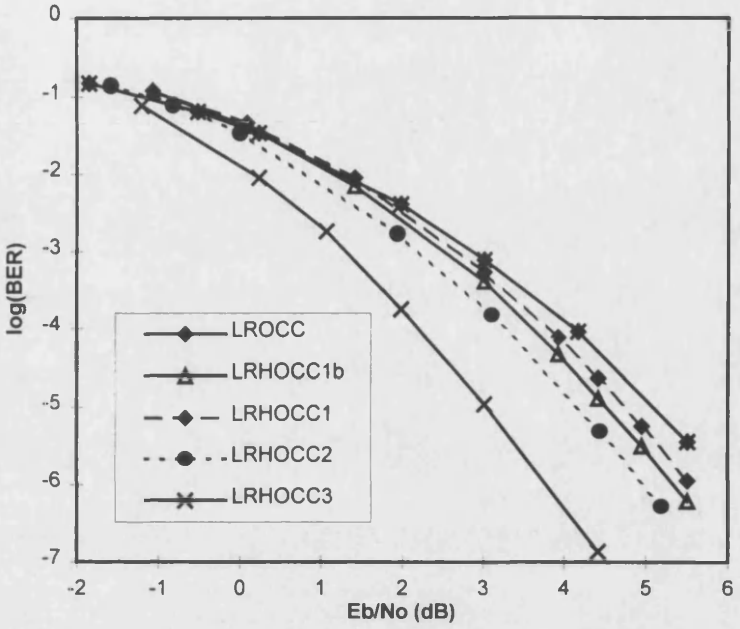

Figure 6-11. Hyper-orthogonal encoders in AWGN

A powerful code with a large trellis structure such as LRHOCC3 can be seen to give an improvement of more than 2dB compared to LROCC codes in AWGN channels. Such an encoder would give a feasible implementation in very noisy channels, especially in designs where processing power and complexity are of no concern.

6.3.3 Multi-user environment

The implementation of low-rate orthogonal convolutional codes has been simulated through computer simulations of a synchronously operated downlink physical channel with other-user noise present. Two cases have been tested: The use of a PN randomiser for each user and the performance without the use of the randomiser. The PN randomising sequences are Gold codes that have been generated through two different maximal-length sequences of equal period. The use of shorter PN sequences has also been tested. The DS-CDMA system analysed here assumes that the downlink from the basestation to the subscriber is synchronous and uses a pilot tone to synchronise all users to the basestation. Hence, the base station has an exact knowledge of how many users are present in the particular cell it is communicating to. This pilot tone can

also be used to enable each subscriber station to adjust its transmitter power by measuring the strength of the received pilot tone in order to eliminate neighboring subscribers shadowing one another through excessive transmitter powers.

Figure (6-12) shows the schematic of a DS-CDMA basestation transmitter for a cellular radio system, based on the use of low-rate convolutional codes rather than the more usual PN spreading sequences. The orthogonality of ordinary convolutional codes, however, is very poor, and due to high levels of co-channel interference this would lead to a small number of simultaneous users being accommodated within a cell. This can be improved significantly by using LROC codes which directly code and spread the data signal. This system provides an encoded bit sequence of length *1/R* on each data bit input from the data source, and in effect provides complete spreading of the bandwidth.

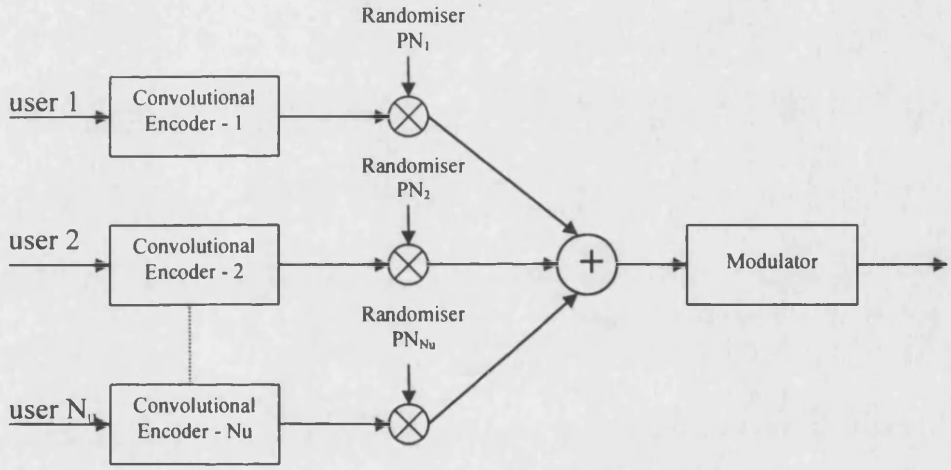

Figure 6-12. Simplified diagram of the proposed BS transmitter

It was shown in chapter 4, that orthogonal functions, such as these considered here, do not have good auto-correlation properties. Therefore, the direct use of orthogonal functions can lead to poor transmission spectral characteristics (e.g. non-uniform spreading) which lead to very high spectral powers at certain frequencies. With a high number of simultaneous users sharing the same bandwidth it is desirable to have a smooth, uniform bandwidth for each user to prevent potentially large interference signals appearing at the output of the correlator. To reduce this problem, an additional stage of randomisation is added to the LROCC encoded data symbols to improve the auto-correlation property of the resulting transmitted signal. This does not provide additional spreading of the signal but serves as a direct multiplication of two equal rate signals. A more detailed analysis of the auto-correlation properties has been given in chapter 4.

The receiver structure performs the inverse operation by first demodulating the received signal, then decoding the convolutionally encoded signal and providing an estimate of the most likely

transmitted data bit. Since this system is coherent for the downlink to the subscriber station, the receiver has an exact knowledge of the timing information of the signal. The decoding method employed is based on the modified Viterbi algorithm as detailed in chapter 4.

The DS-CDMA systems simulated here use a spreading ratio of 64, hence limiting the capacity improvement compared to the maximum possible coding gain achievable with higher constraint length codes. This system is described to simply point out the fact that a significant advantage can be found over the conventional spread-spectrum implementation by using LROCC based systems. The multi-user system was simulated for one cell with all users received under equal power conditions. Figure (6-13) shows how a soft decision low-rate orthogonal convolutional decoder performs under "other-user" noise and can be seen to closely follow the theoretical curve given by equation (6-3).

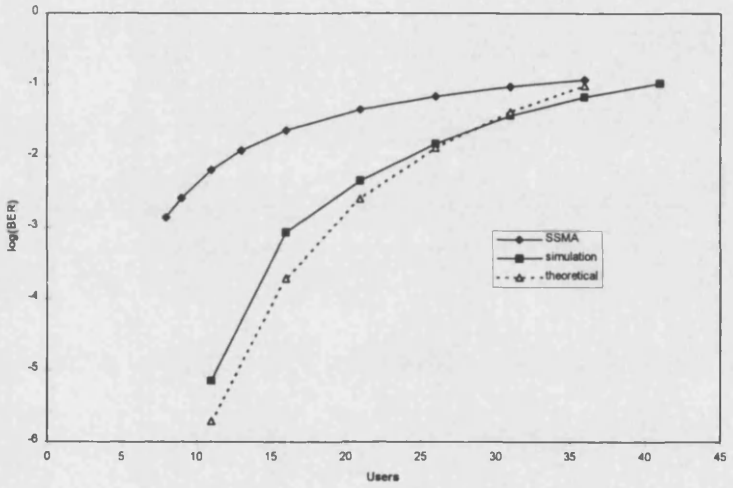

Figure 6-13. Theoretical and simulated performance of LROCC in other user noise

It can be seen that the use of low-rate convolutional codes offers a significant advantage when the number of simultaneous users remains below 40. To achieve a BER=10^{-3} a maximum number of 7 users could be employed in a conventional DS-CDMA system, but the use of low-rate convolutional coding can lead to an increase of nearly 130%, giving a new maximum number of 16 users. This gain in capacity is entirely due to the coding gain given by convolutional codes and the orthogonal properties of the codes. All results shown here have been found through computer simulations with a low constraint length encoder of length K=6. Employing a higher constraint length encoder for practical situations will yield a much higher coding gain at low bit-error rates and provide a higher processing gain, thus substantially improving the implementation.

The use of PN sequences to randomise the output of the low-rate convolutional encoder was mentioned earlier as a method to improve the spectral characteristics of the orthogonal codes and provide better isolation between users without causing any further spreading of the encoded signal. The resulting improvement can be seen in figure (6-14). It has been shown that the use of a PN sequence to randomise the encoded symbols yields a significant advantage approaching a value of at least 2dB. It must be mentioned that no significant degradation is encountered through halving the rate of the PN sequence.

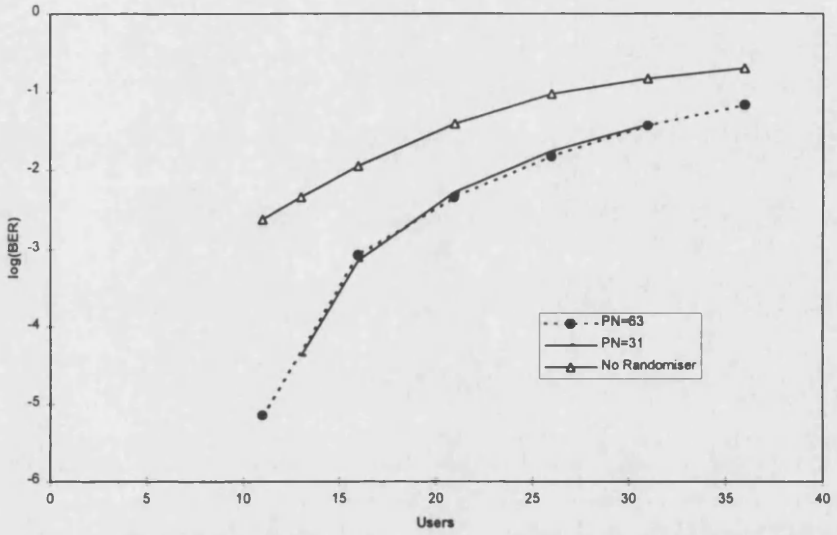

Figure 6-14. Performance improvement through PN randomisers

6.3.4 Multipath Rayleigh faded channels

The multipath fading characteristics in the downlink (base-to-subscriber) channel can ultimately destroy all orthogonality between users, resulting in significant processing gain loss. This degradation is explored through LROC codes by randomising all the users data with powerful codes that exhibit a low cross-correlation and give each user a unique identity in the channel without unnecessarily high interference levels.

The simulated system comprises of a single user link over a Rayleigh faded channel with 4 equal strength multipath components and a spreading ratio of 32 for the K=5, R=1/32 LROCC code. The receiver comprises of an equal number of rake fingers to combine the maximum signal to noise ratio of each path, similar to the RAKE structure detailed in chapter 4, using maximum ratio combining (MRC). The modulation format is coherent BPSK since the channel characteristics are assumed to be perfectly known at the receiver. The channel model consists of 4 equal strength multipath components spaced at equal time intervals equivalent to the inverse of the aggregate total data rate. The fading on each path is Rayleigh with a Doppler of 300Hz.

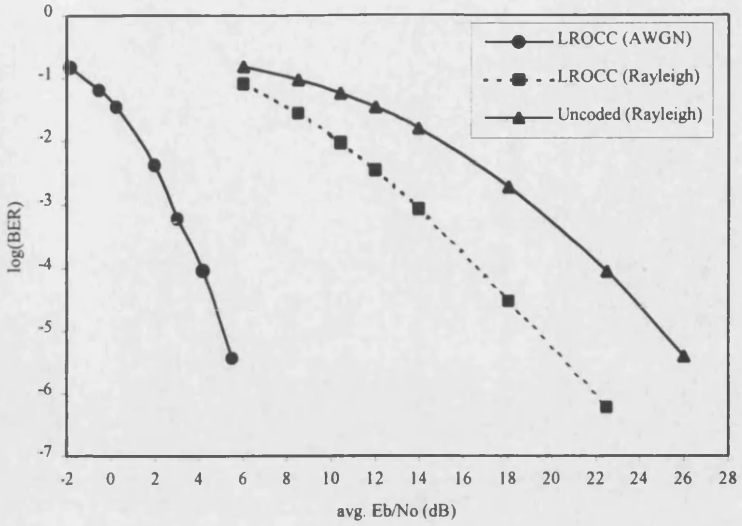

Figure 6-15. LROCC coherent BPSK performance in 4-tap Rayleigh faded channel

Figure (6-15) shows the performance improvements achieved through LROCC coding in a Rayleigh faded channel with coherent detection. The overall improvement over the uncoded case is about 6 dB, with higher gains achievable at low BER. The performance of an LROCC RAKE receiver in Rayleigh fading is degraded by 14dB in comparison to an ordinary LROCC receiver operating in AWGN.

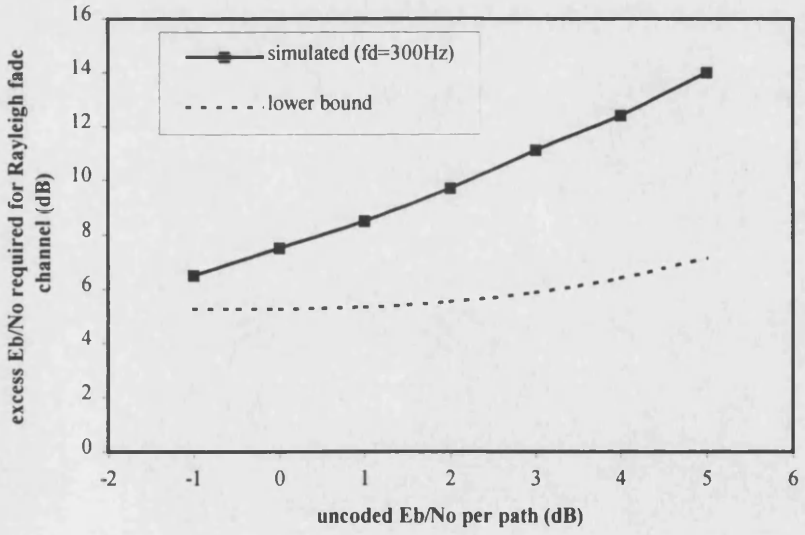

Figure 6-16. Required excess Eb/No for coherent Rayleigh fading with LROCC codes

The excess E_b/N_o required in order to obtain the same performance as the unfaded AWGN channel performance of LROCC codes can be seen in figure (6-16). The additional excess E_b/N_o required for the simulated results compared with the lower bound is due to the 300Hz Doppler. In this sense the simulated results are far more realistic and serve to show that considerable E_b/N_o adjustments must be made in strong fading environments to maintain acceptable E_b/N_o. With less extreme Doppler, the SNR requirements for a given BER are obviously reduced and require less interleaving due to a reduction in the time-selectivity of the channel.

Figure (6-17) illustrates the performance of hyper-orthogonal convolutional codes in a 4-path Rayleigh faded channel with high Doppler. It can be seen that the use of hyper-orthogonal convolutional codes gives a further significant improvement in performance, with more than a 4dB gain at signal-to-noise ratios greater than 15dB.

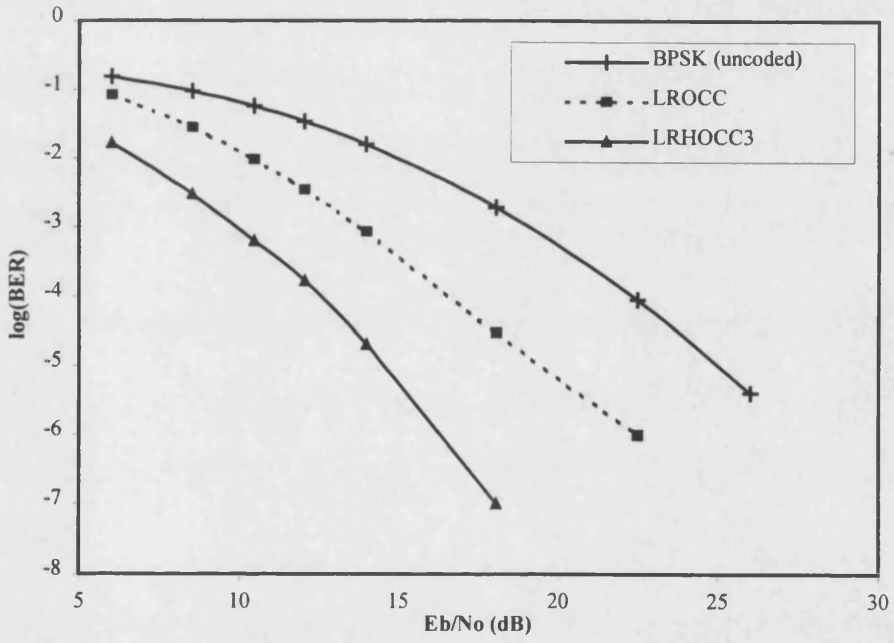

Figure 6-17. Hyper-orthogonal coder and low-rate orthogonal coder in a Rayleigh fading channel of 4 equal gain multipaths

6.4 Summary

LROCC codes using a bandwidth expansion factor of 2^K have been studied in AWGN, Rayleigh faded and multi-user channels. The theoretical performance curves have shown to closely follow the simulated results, and the upper bounds derived from state diagrams of the Markov model have shown to give tight bounds on the simulated results. Nevertheless, a discrepancy between the simulated and theoretical results stems from the assumptions made. The theoretical results assume independent fading and perfect interleaving for a non-coherent square law combing technique whereas the simulations were carried out for coherent BPSK. In this case, the theoretical curves still serve the purpose of providing us with an upper bound on the bit-error performance. To achieve a BER=10^{-3} in a multiple-access environment using K=6, R=1/64 LROCC codes gives an improvement of nearly twice the maximum numbers of users, yielding a capacity of 15 simultaneous users as compared to 7 users in an uncoded system.

The use of randomising codes such as Gold sequences has shown to give an improvement of 2dB in a multi-user environment. For the single user case, of course, randomisation is not necessary, as the spectral shape of the transmitted signal does not matter. Gold codes are only of odd length whereas orthogonal codes have even lengths, and therefore Gold codes can be extended by an arbitrary bit to increase their length.

LROCC codes have been simulated using the RAKE receiver structure introduced in chapter 4 for DS-CDMA applications. There are slight modifications, however, that need to be carried out when used in conjunction with such designs. With LROCC coding we "rake" the signal over the specific number of multipath components in the channel and adjust each path by a weighting factor of the estimated channel response. Compared to conventional DS-CDMA applications, we do not correlate the received signal with the wanted user sequence but rather de-randomise the signal in each path and then feed the soft signal estimate into the Viterbi algorithm. In this way, we do not make a decision on the original data bit until the output of the Viterbi algorithm. This method has shown to give extremely good results in the faded channel environment and consequently makes this type of coding strategy an attractive alternative solution to conventional high-rate convolutional coding with spreading sequences.

A novel implementation of LROCC has been studied. Hyper-orthogonal codes, proposed in chapter 4, have been studied for various combinations of constraint length configurations. It has been found that equal constraint length but lower-rate codes do not perform as well as the

higher-rate code of lower complexity. This is an extremely positive result, indicating that hyper-orthogonal codes may be able to combine both the advantages of LROCC and conventional higher-rate convolutional coding strategies to give optimum results. The use of novel hyper-orthogonal codes has also shown to give improvements in performance of more than 2 dB at high signal-to-noise rations at the cost of increased receiver complexity but constant bandwidth. This improvement becomes highly visible in Rayleigh faded channels with high Doppler, where an increase in 4dB in the maximum coding gain has been obtained at E_b/N_o greater than 15dB.

6.5 References

[1] Viterbi, A J, "Convolutional Codes and Their Performance in Communication Systems", *IEEE Transactions on Comm. Technology*, COM-19, No.5, October 1971

[2] Viterbi, A J, "CDMA-Principles of Spread Spectrum Communication", *Addison Wesley*, 1995

[3] Forney, G D, "Convolutional Codes I: Algebraic Structure", *IEEE Trans. Information Theory*, IT-16, pp. 720-738, 1970

[4] Forney, G D, "Coding and Its Application in Space Communications", *IEEE Spectrum* 7, pp. 47-58, 1970

[5] Zehavi, E, and Viterbi, AJ, "On new classes of orthogonal convolutional codes", *Bilkent International Conference in New Trends in Communication, Control and Signal Processing*, Ankara, Turkey, 1990

[6] Ziemer, R E, and Peterson, R L, "Introduction to Digital Communication", *Maxwell Macmillan International Editions*, 1992

[7] Kempf, P, and Khunjush, J, "A generalised concatenated coding scheme for CDMA digital radio communication systems", pp. 543-547, *IEEE Proc. of PIMRC'94*

[8] Forney, G D, "The Viterbi Algorithm.", *Proc. of the IEEE*, pp. 268-278, Vol. 61, No. 3, March 1973

[9] Seshadri, N, and Sundberg, C E W, "List Viterbi Decoding Algorithms with Applications", pp. 313-323, *IEEE Trans. on Comms.*, Vol. 42, No. 2/3/4, Feb/March/April 1994

[10] Porath, J E, and Aulin, T, "Algorithmic Construction of Trellis Codes", pp. 649-654, *IEEE Trans. on Comms.*, Vol. 41, No. 5, May 1993

[11] Heller, J A, and Jacobs, I M, "Viterbi Decoding for Satellite and Space Communication", pp. 835-848, *IEEE Trans. on Communication Technology*, Vol. COM-19, No. 5, Oct 1971

[12] Lin, S, and Costello, D J, "Error Control Coding: Fundamentals and Applications", *Englewood Cliffs, NJ, Prentice Hall*, 1983

[13] Viterbi, A J, "Error Bounds for Convolutional Codes and an Asymptotically Optimum Decoding Algorithm", *IEEE Trans. on Information Theory*, Vol. IT-13, pp. 260-269, April 1967

[14] Odenwalder, J P, "Error Control", Data Communications, Networks, and Systems, Thomas Bartee (ed), Indianapolis: *Howard W. Sams*, 1985

[15] Forney, G D, "Convolutional Codes II: Maximum Likelihood Decoding", *Information and control*, Vol. 25, pp. 222-226, July 1974

[16] Clark, G C, and Cain, J B, "Error-Correction Coding for Digital Communications", New York, *Plenum*, 1981

[17] Wozencraft, J M, and Jacobs, I M, "Principles of Communication Engineering", *John Wiley*, New York, 1965

[18] Viterbi, A J, and Omura, J K, "Principles of Digital Communication and Coding", *McGraw-Hill*, New York, 1979

[19] Heller, J A, and Jacobs, I M, "Viterbi Decoding for Satellite and Space Communications", *IEEE Transactions on Communication Technology*, Oct. 1971

[20] Odenwalder, J P, "Optimal Decoding of Convolutional Codes", *PhD Dissertation*, University of California, Los Angeles, 1970

[21] Larsen, K J, "Short convolutional codes with maximum free distance for rates 1/2, 1/3 and 1/4", *IEEE Trans. on Information theory*, Vol. IT-19, pp. 371-372, May 1973

[22] Massey, J L, "Threshold decoding", *MIT Press*, Cambridge, MA, 1963

[23] Cain, J B, and Geist, J M, "Modulation, Coding and Interleaving Tradeoffs for Spread-Spectrum systems", *IEEE National Telecommunications Conference*, pp. 37.2.1-37.2.6, 1981

[24] Forney, G D, "Burst-Correcting Codes for the Classic Bursty Channel", *IEEE Trans. on Communication Technology*, Vol. COM-19, pp.772-781, Oct. 1971

[25] Yuen, J H, "Deep Space Telecommunications Systems Engineering", *Plenum*, New York, 1983

[26] Forney, G D, "Concatenated Codes", *MIT Press*, Combridge, MA, 1967

[27] Gallager, R G, "Information Theory and Reliable Communication", *JohnWiley & Sons*, New York, 1968

[28] Fano, R M, "A Heuristic Discussion of Probabilistic Decoding", *IRE Trans. on Information Theory*, Vol. IT9, No. 2, pp. 64-74, 1963

[29] Omura, J K, "On the Viterbi Decoding Algorithm", *IEEE Trans. Inf. Theory*, Vol IT15, pp. 177-179, Jan 1969

[30] Jacobs, I M, "Practical Applications of Coding", *IEEE Trans. on Inf. Theory*, Vol. IT-20, pp. 305-310, May 1974

[31] Ramsey, J L, "Realisation of Optimum Interleavers", *IEEE Trans. on Inf. Theory*, Vol. IT-16, No. 3, pp. 338-345, May 1970

[32] Steele, R, (ed) "Mobile Radio Communications", *Pentech Press*, London, 1992

[33] Ziemer, R E, and Peterson, R L, "Introduction to Digital Communication", *Maxwell Macmillan*, 1992

[34] Martin, J, "Signals & Processes: A Foundation Course", *Pitman Publishing*, 1991

[35] Maxey, JJ, "An adaptive constraint length hyper-orthogonal convolutional coding scheme", *Patent Pending*, Maguire Boss Patent Attorneys, Cambridge, filed P.5855, November 1997

CHAPTER 7:

ORTHOGONAL FREQUENCY DIVISION MULTIPLEX

7.1 Introduction

So far our treatment of mobile and fixed wireless communications has concentrated on single carrier systems that may be used in narrowband or wideband applications. These systems have been shown to suffer particularly in multipath faded channels when the data rate is high. This calls for powerful coding schemes and RAKE receivers with accurate channel knowledge to be implemented in spread-spectrum applications. This may lead to relatively complex systems that require large overheads and consequently reduce the spectral efficiency of the system. Alternatively, the user data rate may be reduced in the channel to combat the effects of fading and introduce equalisers to attempt to restore the original waveform and reduce the inter-symbol interference. Another method of reducing the effective data rate is to split the original high rate data bit stream into many low-rate data signals. This is termed as *multi-carrier* modulation.

Digital multi-carrier (MC) transmission schemes are an alternative approach to single carrier modulation formats, employing the same fundamental concepts as ordinary transmission schemes, but with a few alternative approaches to providing an optimum system solution. One of the earliest systems, described by Doeltz *et al* [1] and called Kineplex, was used for digital transmission in the HF band. Other early work on multi-carrier system design has been reported in the papers by Chang [2] and Saltzberg [3]. The use of DFT for modulation and demodulation of multi-carrier systems was proposed by Weinstein and Ebert [7]. The breakthrough for MC communications happened in the 1990s as OFDM was the modulation chosen for the European digital audio broadcasting (DAB) standard [4]. Further prominent applications include its selection in 1995 as the modulation for the European digital terrestrial television broadcasting (DTTB) system [5].

In broad terms, multi-carrier modulation (MCM) techniques sub-divide the available bandwidth or spectrum into many narrow-band sub-carriers. Hence, such methods are termed parallel transmission schemes. In a conventional serial data stream, the symbols are transmitted sequentially, with the frequency spectrum of each data symbol allowed to occupy the entire available bandwidth. A parallel data transmission system is one in which several sequential streams of data are transmitted simultaneously, so that at any instant many data elements are being transmitted. In such a system, the spectrum of an individual data element normally occupies only a small part of the available bandwidth, which may of course vary in time.

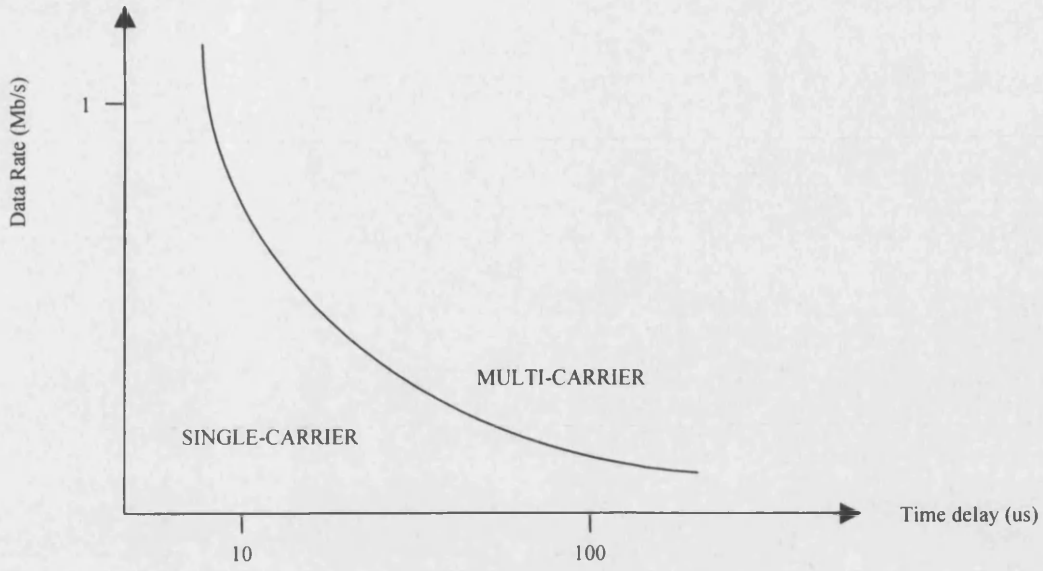

Figure 7-1. Boundary conditions for single-carrier and multi-carrier modulation techniques

Figure (7-1) shows the boundary where the use of multi-carrier modulation methods is more favourable than single-carrier modulation techniques. For channels with a relatively low delay spread, single-carrier modulation techniques can tolerate higher data rates than in channels with a high delay spread. The use of multi-carrier modulation techniques, however, is invaluable in channels with high delay spread values, especially for high data rates.

A parallel approach has the advantage of spreading out a frequency selective fade over many symbols. By using a large number of sub-carriers, a high immunity against multipath dispersion can be provided. The symbol duration T_s of each sub-stream will be much longer than the channel time dispersion, hence the effects of inter-symbol interference (ISI) can be minimized. This long symbol duration allows signal fades or impulse interference to be averaged out in the detector, so that, instead of several adjacent symbols being completely destroyed, many symbols are slightly distorted. This allows successful reconstruction of a majority of symbols even without forward error correction (FEC). Since each sub-carrier covers only a small fraction of the original bandwidth, equalisation is potentially simpler than in a serial system. A simple equalisation algorithm can minimise the mean-square error distortion on each sub-carrier, and the implementation of differential encoding can provide an alternative solution to avoid equalisation completely.

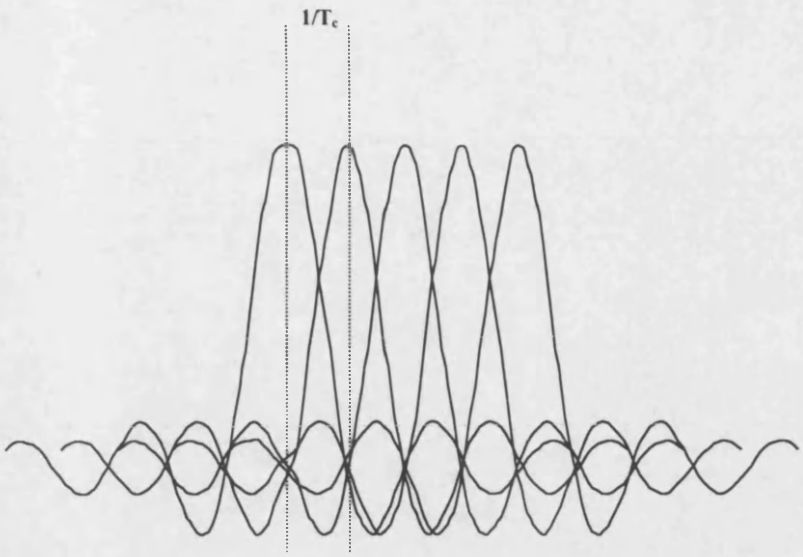

Figure 7-2. OFDM Spectrum

When the period of a data bit symbol, which is being transmitted over a mobile radio channel, is of the same order as the channel impulse response, there is a high probability of data errors due to inter-symbol interference caused by the effects of multipath propagation. As the symbol period is increased, the effect of fast deep fades is reduced using relatively simple averaging receiver structures. This approach nevertheless reduces the maximum allowable data rate over the channel. An alternative approach is to use channel coding and interleaving to reduce the effects of burst errors, which may annihilate several consecutive bits, so that they are more equivalent to random errors. In coded orthogonal frequency division multiplexing (COFDM), this process is taken one stage further.

In an OFDM or COFDM system, the symbol rate of the serial data is reduced by a factor N through multiplexing the original symbol stream into N parallel paths which are then modulated onto N sub-carriers. By increasing the period of each symbol so that it is many times longer than the channel impulse response, the symbol error rate due to multipath propagation effects can be significantly reduced [6]. Although serial to parallel conversion effectively provides an interleaving distance of N original symbol periods, additional performance benefits can be achieved by further interleaving and by the use of error correcting codes. A number of different coding strategies can be used, including block codes, convolutional codes, Reed-Solomon codes and Turbo codes. Considering the use of convolutional codes as being typical, the original data stream is convolutionally encoded prior to serial to parallel conversion. Depending on the modulation scheme used, such as DPSK or QAM, the data bits are then mapped into symbols. The encoded data symbols are then transmitted on N carriers, where they are subjected to random errors and fading. However, for most of the time, not all N data symbols will be corrupted simultaneously and the data on the degraded carriers can be corrected in a Viterbi

receiver (for example) aided by non corrupted data symbols on the other channels. Where extreme resilience of fading is required, block codes can be combined with convolutional codes. The optimum coding strategy depends critically on the application to which COFDM is being put, and this forms a major part of the current work.

OFDM, having densely spaced sub-carriers with overlapping spectra, abandons the use of steep band-pass filters to detect each sub-carrier, as used in frequency division multiple access schemes. Therefore, OFDM offers a high spectral efficiency since we can now accommodate more sub-carriers in a confined bandwidth. The key to the spectral efficiency of OFDM lies in the way each symbol is modulated onto the N carriers. Normally, it would be necessary to separate the frequency spacing of each carrier by more than the bandwidth of the modulated data to prevent upper and lower sidebands of adjacent carriers from overlapping and producing aliasing. This is a wasteful use of spectrum. In OFDM/COFDM the carriers are all chosen to be orthogonal and using appropriate modulation schemes such as QPSK, DPSK or QAM it is possible for upper and lower sidebands to fully overlap, yet be demodulated correctly. Since the number of filters and oscillators is considerable for large numbers of sub-carriers, an efficient digital implementation such as the Fourier Transform method [7] has been proposed. Depending on the value of N, either the DFT or the FFT can be used, however there are obvious benefits of reduced computational overhead if the FFT is used. Figure (7-3) illustrates a typical COFDM system based on the IFFT/FFT transform pair.

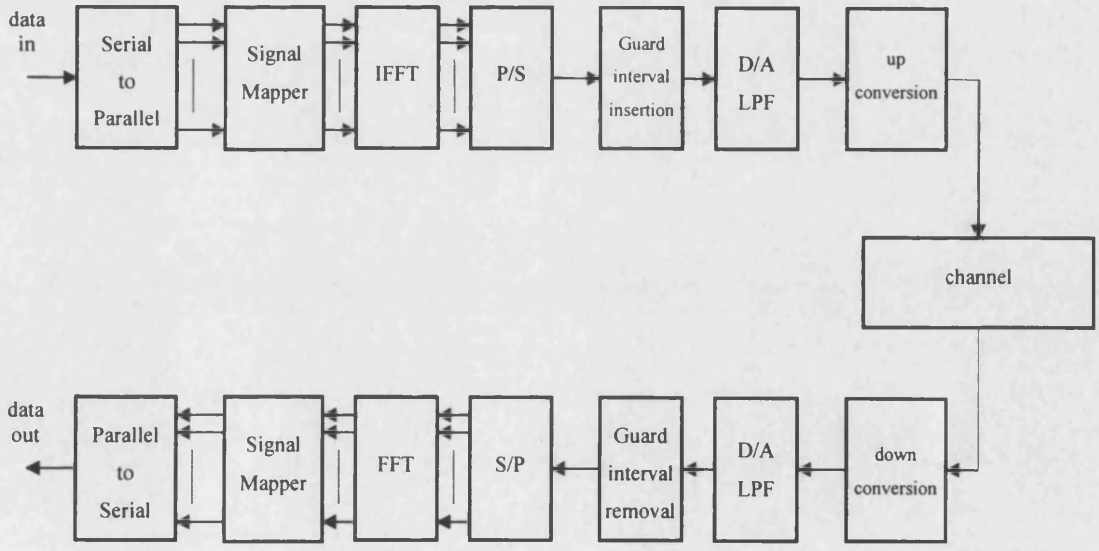

Figure 7-3. Typical COFDM system based on the IFFT/FFT transforms

Although frequency guard bands are not required, it has been suggested in a number of papers that a time guard band is required, which may be as large as 25% of the symbol duration to

suppress ISI and to maintain orthogonality between adjacent OFDM blocks. This guard period, or cyclic extension, can be used to obtain correct timing to mark the start of each transformation and helps to solve the problem of excessively long propagation delays (echoes) that may cause ISI. The cyclic extension does mean, however, that the efficiency of data transmission is significantly degraded.

In the receiver, the signal is down-converted to baseband and after digital sampling and guard-band removal fed into the FFT. This behaves like a multi-carrier matched filter and detects all sub-carriers. In this block, the sub-carriers may also be equalised to remove the effects of fading on the channel. The signal is then mapped into the original code symbol and converted from parallel to serial. If coding is employed, the code symbol is fed into a detection algorithm such as a maximum likelihood detector to give improved detection on the wanted data bit.

7.2 Theoretical Analysis

In serial transmission, sequences of data are transmitted as a train of serial pulses. However, in parallel transmission schemes each bit of a sequence of N bits modulates a carrier. In the multi-carrier technique the transmission is parallel. The block diagram of this technique is shown in figure (7-4). In the modulator the input data with rate R is divided into N parallel information sequences with rate R/N. Each sequence modulates a sub-carrier.

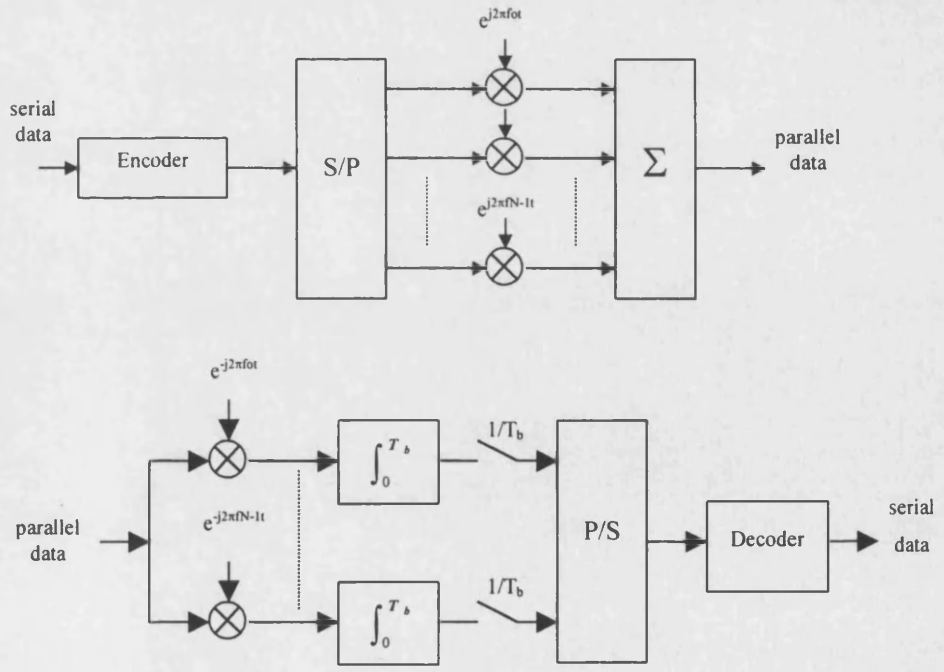

Figure 7-4. Block diagram of a multicarrier system: (a) modulator and (b) demodulator

The frequency of the nth carrier, f_n, is given as:

$$f_n = f_o + n/T_b \qquad n = 0,1 \,..\, N\text{-}1 \tag{7-1}$$

where f_o is the lowest frequency of the carriers and T_b is the effective OFDM block duration (i.e. $T_b=NT_s$, where T_s is the period of each symbol prior to blocking-up). The multi-carrier transmitted signal is written as:

$$s(t) = \sum_{n=0}^{N-1} \sum_{i=-\infty}^{\infty} d_{n,i} e^{j2\pi f_n (t-iT_b)} p(t - iT_b) \tag{7-2}$$

where $d_{n,i}$ is the symbol of the nth sub-carrier at time interval iT_b. For BPSK and QPSK modulation, $d_{n,i}$ is ± 1 and $\pm 1 \pm j$ respectively. $p(t)$ is the response of the transmitter filter for which a rectangular pulse with duration T_b and amplitude 1 is assumed. The spectra of the multicarrier signal can be obtained by considering the power spectra of a sequence of identically independent distributed rectangular pulses having a period of T_b. This results in a power spectrum of shape $T_b sinc^2 fT_b$. Using the shift property, the Fourier transform of the multicarrier signal, $s(t)$, becomes:

$$S(f) = \sum_{n=0}^{N-1} T_b \sin c^2 (f - f_n) T_b \tag{7-3}$$

This spectrum can be seen in figure (7-5). From this figure, it is clear that adjacent overlapping spectra create a small ripple on the power spectrum in the wanted bandwidth.

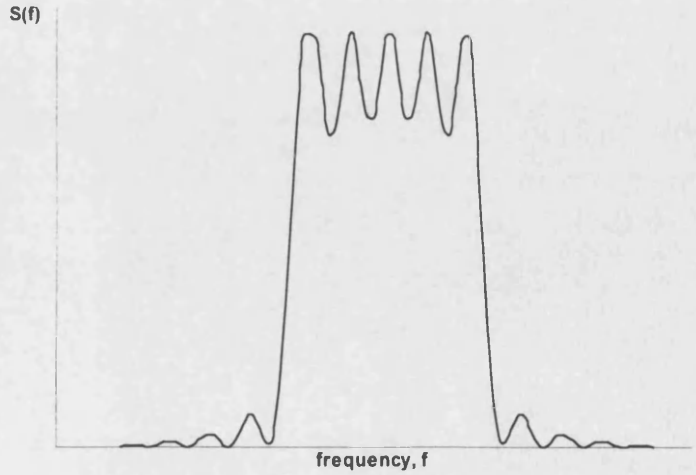

Figure 7-5. Power spectrum S(f) of an OFDM signal

The bandwidth of the baseband multicarrier signal is given by:

$$B_{MC} = f_o + \frac{N}{T_b} - \left(f_o - \frac{1}{T_b}\right) = \frac{N+1}{T_b}$$
$$\approx \frac{N}{T_b} = \frac{1}{T_s} \tag{7-4}$$

where T_s is the time duration of the original signal. With this technique we can take a number of tones (sub-carriers) and subsequently increase the symbol duration without increasing the bandwidth. When the number of carrier becomes large, the OFDM power spectrum tends to a perfect rectangular spectrum with a cut-off frequency of $1/T_s$. Of course, one cannot increase the number of sub-carriers arbitrarily as the effects of Doppler quickly become visible in the performance. Referring to equation (7-1) it is seen that the sub-carrier frequencies are separated by multiples of $1/T_b$. For a multi-carrier system it will be seen from equation (7-7) that the sub-carriers are orthogonal, i.e.,

$$\frac{1}{T_b}\int_0^{T_b} e^{j2\pi f_{n1}t} e^{-j2\pi f_{n2}t}.dt = \begin{cases} 1 & \text{if } n_1 = n_2 \\ 0 & \text{otherwise} \end{cases} \tag{7-5}$$

Therefore, considering ideal transmission, and in spite of overlapping of the spectra, detection of the signal in one sub-carrier gives no output for any other sub-carrier. In non-ideal transmission channels, this may be achieved optimally by using equalisers and time guard-band intervals.

7.3 Spectral Efficiency

If we consider M-ary modulation and a symbol rate of $R=1/T_s$, the bit-rate of an M-ary system is $R\log_2 M$. Since in multi-carrier transmission each sub-carrier has a longer time duration, each sub-carrier rate is $(R/N)\log_2 M$. Referring to figure (7-2) and the bandwidth of the multi-carrier signal in equation (7-4), the spectral efficiency of a multi-carrier system is defined as the bit-rate per unit bandwidth, given by [10]:

$$\text{spectral efficiency} = \frac{R\log_2 M}{B_{MC}} = \frac{R\log_2 M}{N + 1/T_b} \tag{7-6}$$
$$= \frac{\log_2 M}{1 + 1/N}$$

Accordingly, the M-ary digital modulation scheme using OFDM can achieve a spectral efficiency of about log_2M bit/s/Hz when a large number of N sub-carriers are used.

7.4 Orthogonal Basis Functions

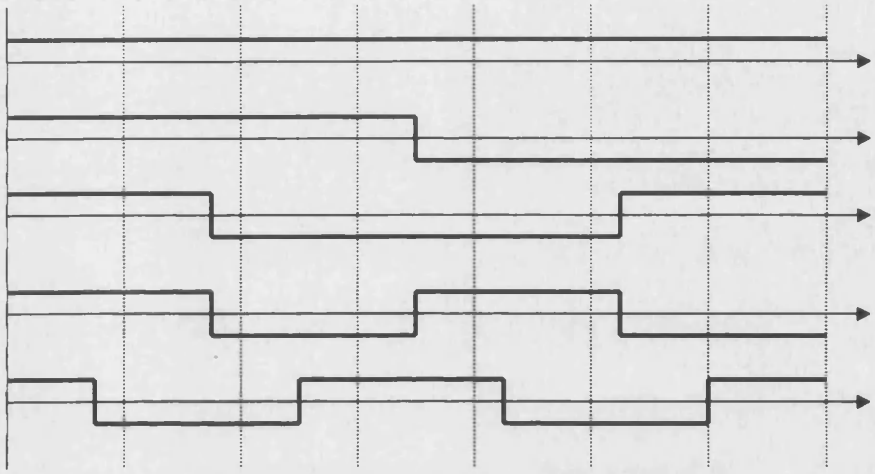

Figure 7-6. Sequency ordered Walsh functions

Just as the FFT is based on a set of harmonically related cosine and sine waveforms, so the discrete Walsh transform (DWT) is based on a set of harmonically related rectangular waveforms, such as Walsh functions. However, frequency is not defined for rectangular waveforms and so the analogous term sequency is used. Sequency is half the average number of zero crossings per unit time. Figure (7-6) shows the set of Walsh functions up to the order five drawn in order of increasing sequency. They are said to be sequency, or Walsh, ordered. Inspection of figure (7-6) shows that there are equal numbers of even and odd Walsh functions, just as there are corresponding cosinusoidal and sinusoidal Fourier series components. The beauty of using cosinusoidal and sinusoidal Fourier series components is that they produce a time-varying signal that is easily modulated for typical wireless applications. Nevertheless, the signal is strongly fluctuating in amplitude and can consequently create problems due to the requirement of highly linear power amplifiers in the transmitter.

The cosinusoidal and sinusoidal Fourier series components provide an alternative method of multiplexing the data onto orthogonal sub-carriers, formed from the cosine and sine basis functions. The generation of the N orthogonal sub-carriers and the multiplexing of the N parallel low-rate data channels onto these sub-carriers is assumed to be carried out via the inverse fast

Fourier transform (IFFT). This technique has its origins through the use of orthogonal basis functions, given by:

$$\varphi_n(t) = \begin{cases} e^{j2\pi f_n t} & 0 \le t \le T_b \\ 0 & \text{otherwise} \end{cases} \tag{7-7}$$

The time-domain OFDM signal at the output of the IFFT is thus given by:

$$s(t) = \sum_{i=-\infty}^{\infty} \sum_{n=0}^{N-1} d_{i,n} \varphi_n(t - iT_b) \tag{7-8}$$

where $d_{i,n}$ is the data sequence being transmitted on the n^{th} sub-carrier in the i^{th} block.

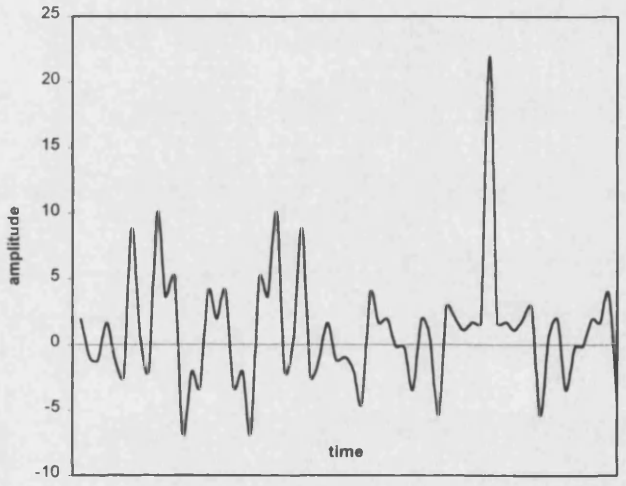

Figure 7-7. Time-domain multi-carrier OFDM signal with N=32 sub-carriers

The typical time-domain output signal from a multi-carrier OFDM system using the Fourier transform can be seen in figure (7-7). Note that the signal is extremely random with large fluctuations in amplitude.

7.5 Discrete Fourier Transform

The multicarrier modulator and demodulator can be effectively constructed by using Fast Fourier Transform (FFT) methods. Referring to equation (7-8), the transmitted multicarrier signal within a time interval of iT_b is written as:

$$s(t) = \sum_{n=0}^{N-1} d_n e^{j2\pi f_n t} \tag{7-9}$$

By assuming $t=mT_s$ and using equation (7-9) we obtain:

$$s_m = \sum_{n=0}^{N-1} d_n e^{j\frac{2\pi}{N}nm} \qquad 0 \le m \le N\text{-}1 \tag{7-10}$$

where $s_m \cong s(mT_s)$. Therefore, the sequence s_m is the inverse discrete Fourier transform (IDFT) of input data d_n. In fact, multicarrier modulation is performed by grouping a block of N consecutive input symbols and computing the IDFT of these blocks. In the same way, demodulation can be performed using DFT techniques. These properties, in association with the FFT are used in Digital Signal Processing (DSP) for full digital implementation of a multicarrier modulator and demodulator. The block diagram of the multicarrier system using DFT's is shown in figure (7-8).

Figure 7-8. Block diagram of multicarrier OFDM using the DFT

According to equation (7-10), the amplitude of the multi-carrier signal is the summation of N phasors that vary in time. This makes OFDM signals very sensitive to non-linearities of the power amplifier. Indeed, the requirement for highly linear transmitters capable of handling high peak-to-average ratios is one of the main drawbacks of the multi-carrier technique [11]. This problem is important when the multi-carrier system is used for broadcasting over wide areas. Due to lower power level requirements in indoor wireless systems, for example, this limitation may be less of a problem here. This shortcoming of multi-carrier systems may be alleviated by amplifying the signal of each sub-carrier and then summing the outputs.

7.6 Linear Channel Analysis

In this section we study the behaviour of the MC signal when it is transmitted through the linear channel. We consider here a linear channel with transfer function $H(f)$. At sub-carrier frequency f_n this is written as:

$$H(f) = H_n e^{j\phi_n} \tag{7-11}$$

where $H_n = |H(f_n)|$ and $\phi_n = \tan^{-1}\{\text{Im } H(f_n)/Re\ H(f_n)\}$. If $1/T_b < B_{MC}$, we can assume that $H(f)$ does not change too much over all sub-carriers. Therefore, in a first approximation, the output of the channel $r(t)$ can be written as:

$$r(t) = \sum_{n=0}^{N-1} d_n H_n e^{j(2\pi f_n t + \phi_n)} \qquad 0 \le t \le T_b \tag{7-12}$$

According to the block diagram of the MC system shown in figure (7-8), samples of the signal $r(t)$ are applied to the DFT. Therefore, the output of the DFT is:

$$\begin{aligned} z_i &= \sum_{m=0}^{N-1} r_m e^{-j\frac{2\pi}{N}mi} \\ &= \sum_{m=0}^{N-1}\left(\sum_{n=0}^{N-1} d_n H_n e^{j\phi_n} e^{j\frac{2\pi}{N}nm}\right) e^{-j\frac{2\pi}{N}mi} \\ &= \sum_{m=0}^{N-1}\sum_{n=0}^{N-1} d_n H_n e^{j\phi_n} e^{j\frac{2\pi}{N}m(n-i)} \end{aligned} \tag{7-13}$$

where $r_m = r(mT_s)$. The output of the DFT, z_i, may therefore be expressed as:

$$z_i = \begin{cases} d_i H_i N e^{j\phi_i} & \text{if } m = i \\ 0 & \text{otherwise} \end{cases} \tag{7-14}$$

Therefore, the estimate of the data at the receiver is obtained by [7]:

$$\hat{d}_i = \frac{1}{N}\frac{z_i}{H_i} e^{-j\phi_i} \tag{7-15}$$

From equation (7-15), the influence of the amplitude and the phase of the channel on the detected bit is clear. It can be seen, that the received data bit is weighted by the total number of sub-carriers N and the attenuation and argument of the discrete-time channel transfer function at sub-carrier i. Another approximation of the channel is a linear frequency dependence on the magnitude and phase of the channel around frequency f_n. In this case, the transfer function of the channel is approximated by [7]:

$$H(f) = \left[H_n + \alpha(f - f_n)\right] e^{j\left[\phi_n + 2\pi t_{g_n}(f - f_n)\right]} \tag{7-16}$$

where $H_n = |H(f_n)|$, $\phi_n = \angle H(f_n)$ and α_n is the slope of the magnitude of the transfer function of the channel at frequency f_n,

$$\alpha_n = \left.\frac{d|H(f)|}{df}\right|_{f=f_n} \tag{7-17}$$

and t_{gn} is the group delay of the channel at frequency f_n,

$$t_{g_n} = \frac{1}{2\pi}\left.\frac{d\angle H(f)}{df}\right|_{f=f_n} \tag{7-18}$$

Considering the pulse $p(t)$ with unit amplitude in the interval $(0,T_b)$ and by convolution of the multicarrier signal of $d_n e^{j2\pi f_n t} p(t)$ with the impulse response of the channel (i.e. the inverse Fourier transform of equation (7-16)), it is shown in [7] that the resultant signal is:

$$\begin{aligned} y(t) &= \mathrm{Re}\left[d_n e^{j2\pi f_n t}\, p(t) * h(t)\right] \\ &= d_n H_n \cos(2\pi f_n t + \phi_n)\, p\left(t - t_{g_n}\right) + \frac{\alpha_n}{2\pi}\sin(2\pi f_n t + \phi_n)\frac{d}{dt}\, p\left(t - t_{g_n}\right) \end{aligned} \tag{7-19}$$

It is seen that due to the effect of the channel, the nth carrier is modified by the amplitude and phase of the channel as well as the group delay, t_{gn}. The second term in equation (7-19) shows the distortion which is due to variations of $H(f)$ and is a potential source of inter-channel interference. In [7] it is shown that if T_b is large enough, depending on T_s and the maximum range value of t_{gn}, there exists a time T_g such that for the time interval $-T_g \le t \le T_b$:

$$\frac{d}{dt}\, p\left(t - t_{g_n}\right) = 0 \tag{7-20}$$

and the effect of inter-channel interference can be suppressed. This is similar to the guard interval in the fading channel which is discussed in the next section.

7.7 Guard-Band Interval Analysis

The use of guard intervals maintains the orthogonality between OFDM symbols, preventing interference between successive blocks and this allows the channel fading on each sub-carrier to

be viewed as independent. The addition of the guard interval is normally performed in the time-domain, as shown in figure (7-9).

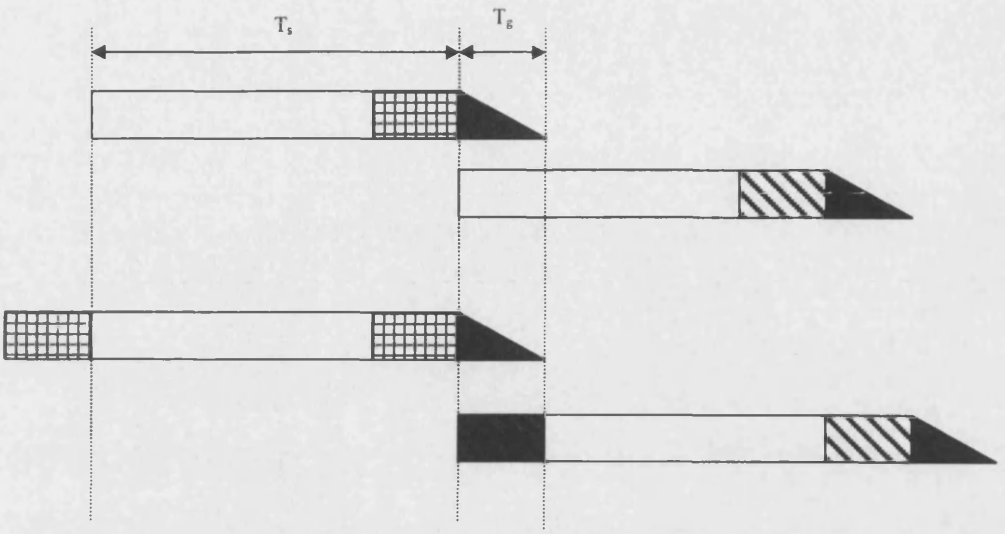

Figure 7-9. Guard-band (cyclic extension) insertion

It can be seen that the cyclic extension is an identical copy of Δ symbols, where $T_g=\Delta T_s$, from the end (or front) of the OFDM block symbol, of length N, and is inserted at the front (or end, respectively) between successive blocks. This ensures that the orthogonality between successive OFDM symbols remains, and hence suppresses the degradation caused by ISI. Nevertheless, multipath distortion in the channel will inevitably introduce interference between individual sub-carriers, and therefore inter-carrier interference (ICI) still remains a problem.

The use of a time guard-interval will only reduce ISI if the guard-interval is longer than the maximum delay spread of the channel. If the time-guard band is shorter than the maximum delay spread, the orthogonality conditions between the sub-carriers do not hold anymore. This introduces two main interfering terms: one is produced through the echo of the preceding block and the second is due to the loss of orthogonality in the remaining part of the integration interval. The second interfering term is still present even in systems with a guard-interval longer than the maximum delay spread since the multipath fading will still affect individual sub-carriers. This causes distortion within the same sub-carrier (ICI). If the channel impulse response is perfectly known the level of ICI can be reduced by using efficient equalising techniques. In practice, the insertion of known period sequences enables the receiver to track slowly fading channel variations produced by the vehicle movement to estimate the channel coefficients. In the following, the analysis of the effect of multipath fading on the performance of an OFDM system with time guard-interval by Viterbo and Fazel [12] is applied to the case where the system also has high-rate convolutional and low-rate orthogonal convolutional coding in an OFDM system.

The addition of a guard-interval, T_g, gives a new total block duration of:

$$T_b' = T_b + T_g \tag{7-21}$$

The generation of the N orthogonal sub-carriers and the multiplexing of the N parallel low-rate data channels onto these carriers is assumed to be carried out *via* the inverse Fast Fourier Transform (IFFT). The orthogonal basis functions now apply over the new total block duration:

$$\phi_n(t) = \begin{cases} e^{j2\pi f_n t} & -T_g \le t \le T_b \\ 0 & \text{otherwise} \end{cases} \tag{7-22}$$

The time-domain transmitted OFDM signal at the IFFT output is thus given by:

$$s(t) = \sum_{i=-\infty}^{\infty} \sum_{n=0}^{N-1} d_{i,n} \phi_n (t - iT_b') \tag{7-23}$$

where $d_{i,n}$ is the data sequence being transmitted on the n-th sub-carrier in the i-th block.

At the receiver, the FFT is performed on the samples of the received signal to demultiplex it. This is performed over the block duration T_b for each sub-carrier n = 0,1 ... N-1, on the i-th block by neglecting the first T_g seconds of the received block:

$$\begin{aligned} d_{i,n} &= \frac{1}{T_b} \int_0^{T_b} x(t) \phi_n^{*} (t - iT_b').dt \\ &= \frac{1}{T_b} \int_0^{T_b} x(t) e^{-j2\pi f_n (t - iT_b')}.dt \end{aligned} \tag{7-24}$$

The interference environment of a typical mobile multipath fading channel can often lead to severe degradation of the bit-error rate performance. If we consider a simple two path fading model as:

$$y(t) = x(t) + Ae^{j(\theta + 2\pi f_D t)} x(t - \tau) \tag{7-25}$$

where τ is the delay, f_D the Doppler frequency, θ the phase rotation and A the attenuation, then the output of the n-th sub-carrier for the i-th block can be written as two terms:

$$z_{i,n} = v_{i,n} + w_{i,n} \tag{7-26}$$

where $v_{i,n}$ is the term due to the direct path and the term $w_{i,n}$ represents the interfering term due to the echoes of the preceding blocks. Depending on the length of the guard-interval, this interfering term may be minimised to yield only the reflected echoes of the channel:

$$w_{i,n} = Ae^{j(\theta+2\pi f_D iT_b')}e^{-j2\pi f_n \tau}v_{i,n} \tag{7-27}$$

In this case, the orthogonality conditions are satisfied and the subsequent attenuation and phase effects on the wanted symbols $v_{i,n}$ may be cancelled out through efficient equalisation strategies. If the guard time-interval is less than the maximum delay spread on the channel, further distortion effects take place in the interfering term:

$$w_{i,n} = Ae^{j(\theta+2\pi f_D iT_b')}\left[\sum_{k=0}^{N-1} w_{i-1,k}\lambda_{k,n}(\tau) + \sum_{k=0}^{N-1} v_{i,k}\mu_{k,n}(\tau)\right] \tag{7-28}$$

where $\lambda_{k,n}$ and $\mu_{k,n}$ determine the level of dependence between the sub-channel fading effects on the N carriers. These have been found to be given as [12]:

$$\lambda_{k,n}(\tau) = \begin{cases} \left(\dfrac{\tau - T_g}{T_b}\right)e^{j2\pi i(T_b'-\tau)/T_b} & \text{for k = n} \\ e^{j\pi\left[2k(T_b'-\tau)/T_b + (k-n)(\tau-T_g)/T_b\right]}\dfrac{\sin\left[\pi(k-n)(\tau-T_g)/T_b\right]}{\pi(k-n)} & \end{cases} \tag{7-29}$$

and,

$$\mu_{k,n}(\tau) = \begin{cases} \left(\dfrac{T_b - \tau + T_g}{T_b}\right)e^{-j2\pi n\tau/T_b} & \text{for k = n} \\ -e^{j\pi\left[-2k\tau/T_b + (k-n)(\tau-T_g)/T_b\right]}\dfrac{\sin\left[\pi(k-n)(\tau-T_g)/T_b\right]}{\pi(k-n)} & \end{cases} \tag{7-30}$$

For the multipath channel model considered here, the received signal is given as:

$$z_{i,n} = \frac{\mu_{n,n}}{\sqrt{L}}v_{i,n} + \sum_{k=0,k\neq n}^{N-1}\frac{\mu_{k,n}}{\sqrt{L}}v_{i,k} + \sum_{k=0}^{N-1}\frac{\lambda_{k,n}}{\sqrt{L}}v_{i-1,k} \quad \text{for } n=0\ldots N\text{-}1 \tag{7-31}$$

where,

$$\lambda_{k,n} = \sum_{\tau \in \{\tau_l > T_g\}} H_l \lambda_{k,n}(\tau) \quad \text{for } k \neq n$$

$$\mu_{k,n} = \sum_{\tau \in \{\tau_l > T_g\}} H_l \mu_{k,n}(\tau) \quad \text{for } k \neq n$$

$$\mu_{n,n} = \sum_{\tau \in \{\tau_l \leq T_g\}} H_l e^{j2\pi f_n \tau} + \sum_{\tau \in \{\tau_l > T_g\}} H_l \mu_{n,n}(\tau) \tag{7-32}$$

and the channel coefficients for each reflected path are given by $H_l = e^{j(\theta_l + 2\pi f_{D_l} i T_b')}$.

If the channel is assumed to be slowly varying, H_l will also be slowly varying from one block integration interval to the next. Since the guard time interval does not sufficiently eliminate the effects of inter-block interference the information symbols can no longer be easily extracted from $z_{i,n}$. This interference results in both ICI and ISI. Finally, we can obtain the ratio of the signal power to interference power at the output of each sub-channel as:

$$\left(\frac{C}{I}\right)_n = \frac{\left|\mu_{n,n}\right|^2}{\sum_{k=0,k\neq n}^{N-1} \left|\mu_{k,n}\right|^2 + \sum_{k=0}^{N-1} \left|\lambda_{k,n}\right|^2} \quad n = 0 \ldots N\text{-}1 \tag{7-33}$$

Figure (7-10) shows the relationship between the *C/I* ratio of each sub-carrier and the length of the guard-band relative to the total block length. As expected, as the guard-band approaches the maximum delay spread, the *C/I* ratio increases towards infinity.

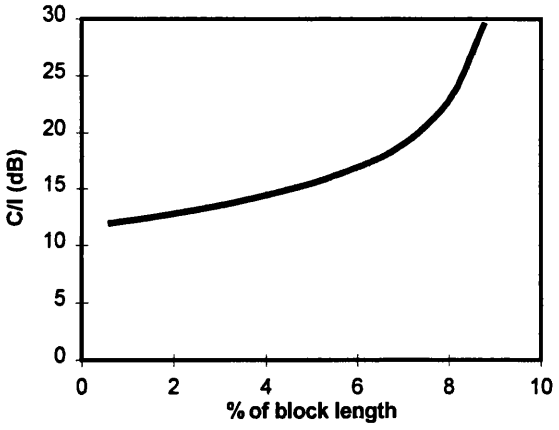

Figure 7-10. *C/I* ratio improvement for increase in time-guard band length

The total bit-error rate (BER) is the average of the BER in each channel. The BER using QPSK modulation can be expressed as:

$$BER \approx \frac{1}{N}\sum_{n=0}^{N-1} Q\left[\left(\sqrt{\frac{C}{I}}\right)_n\right] \tag{7-34}$$

Equation (7-34) gives a final estimate of the OFDM performance in the noiseless fading channel by effectively averaging out the BER in each sub-channel from the carrier-to-interference levels for each carrier.

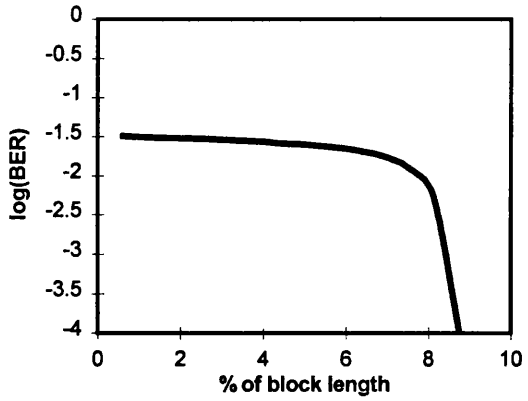

Figure 7-11. Effect of time-guard length on irreducible BER

Figure (7-11) shows the variation in irreducible BER for different time-guard intervals of an OFDM design operating at a carrier frequency of 1.6 GHz, 32 sub-carriers, a block length of 160μs. The channel model is a 3-path fading model with one direct path (line-of-sight) and two reflected paths, one at a delay of 1μs and the second at 15μs. Note, how the residual BER drops extremely rapidly as the time-guard band approaches a level of 10% increase in bandwidth - the length of the maximum delay spread component.

7.7.1 Convolutional Coding Techniques

We now compare the performance of an OFDM system using conventional high-rate (R=1/2, K=5) convolutional coding and LROCC of rate R=1/32 and constraint length K=5. In chapter 4 we showed that ordinary rate R=1/2 convolutional codes can be upper-bounded on the bit-error probability through use of their generating function to weight error events by the number of bit-errors. This can be generalised as:

$$BER_k < \sum_{j=d_{free}}^{\infty} c_j P_j \tag{7-35}$$

where P_j is the calculated bit-error probability (dependent on the channel) for a particular E_b/N_o and c_j are the coefficients determined through the generating function of particular code in question.

The performance improvements of the OFDM system through the use of the convolutional coding featured earlier can be seen in figure (7-12). It is clear that coding will give a substantial resilience to guard intervals of shorter length than an uncoded system design. Of course, for relatively small lengths of guard interval, the fading effects will dominate the performance degradation and the coding gain will not be as large. As the length of the guard interval approaches its optimum value, a more significant coding gain can be seen.

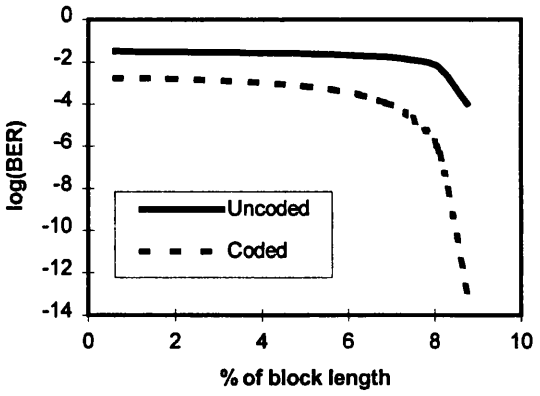

Figure 7-12. Improvement on irreducible BER through the use of convolutional coding

For LROCC codes the upper-bound is given in terms of constraint length K codes and has been found to be:

$$BER_n < \frac{W_n^K (1-W_n)^2}{(1-2W_n+W_n^K)^2} \tag{7-36}$$

where,

$$W_n = Q\left[\left(\sqrt{\frac{C}{I}}\right)_n\right] \tag{7-37}$$

A noise power of variance σ_n^2 gives an additional AWGN term in the *C/I* ratio for all sub-carriers, and therefore is used to determine the performance of convolutional codes in multipath fading for different noise levels. We obtain the average BER for all N sub-carriers, for a specific E_b/N_o, by averaging the bit-error probability over all sub-carriers:

$$BER < \frac{1}{N}\sum_{n=0}^{N-1} BER_n \tag{7-38}$$

Figure (7-13) shows the performance of the OFDM system using conventional high-rate convolutional codes in the multipath fading environment detailed earlier with different guard-band interval lengths. It can be seen that the convolutional code has little performance benefits when the guard-band interval is short, but nevertheless, yields good performance bounds for high guard-band intervals. As expected [30-32], the use of LROC codes gives a slightly improved performance bound at low rates, hence the performance in figure (7-14) gives a better overall result.

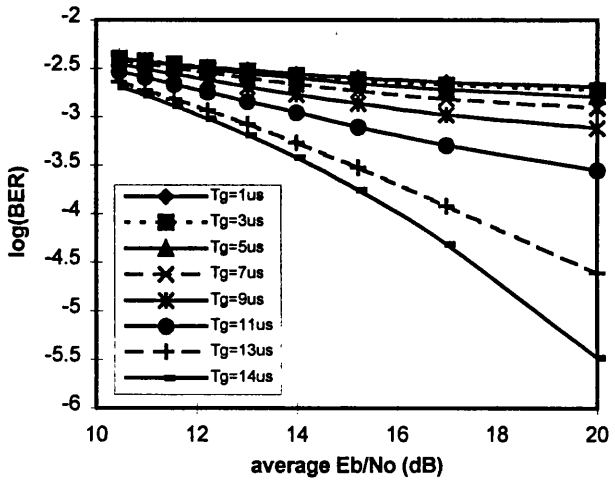

Figure 7-13. Performance of R=1/2 convolutional codes with different guard band lengths

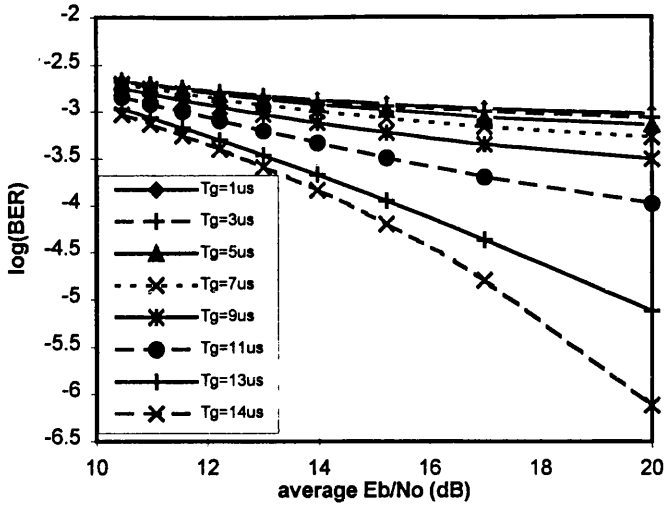

Figure 7-14. Performance of R=1/32 LROC codes with different guard band lengths

7.8 Asynchronous OFDM in a Fading Channel

In this section we study the behaviour of an asynchronous multi-carrier OFDM system when it is transmitted through a general multipath faded channel. In chapter 2 a model of the typical mobile communication channel was introduced in detail. Employing multicarrier modulation techniques for channels with impulse response $h(t)$ gives the received signal $r(t)$ as:

$$r(t) = s(t) * h(t) + n(t) \tag{7-39}$$

where $n(t)$ is AWGN with a spectral density height of $N_o/2$. The first term of equation (7-39) is written as:

$$s(t)*h(t) = \sum_{l=0}^{L-1}\sum_{n=0}^{N-1}\sum_{i=-\infty}^{\infty} a_l d_n(i) e^{j\left[2\pi f_n\left(t-\tau_l-iT_b\right)+\theta_l\right]} p\left(t-iT_b-\tau_l\right) \tag{7-40}$$

where a_l, τ_l and θ_l are the amplitude, time of arrival and phase of the multipath components, respectively, and L is the number of multipath components of the impulse response of the channel. In the receiver, the recovery of the data associated with the carrier f_k is performed by taking the decision variable z_k as:

$$z_k = \int_0^{T_b} r(t)p(t)e^{-j2\pi f_k t}.dt \tag{7-41}$$

which can be written as:

$$z_k = \sum_{l=0}^{L-1}\sum_{n=0}^{N-1}\sum_{i=-\infty}^{\infty} a_l d_n(i) e^{-j\left[2\pi f_n(iT_b+\tau_l)-\theta_l\right]} \int_0^{T_b} e^{j\frac{2\pi}{T_b}(n-k)t} p(t-iT_b-\tau_l)p(t).dt + \int_0^{T_b} n(t)p(t)e^{-j\frac{2\pi k}{T_b}}.dt \quad (7\text{-}42)$$

For BPSK signaling it becomes,

$$z_k = \sum_{l=0}^{L-1}\sum_{n=0}^{N-1} a_l \left\{ d_n(-1)\int_0^{\tau_l} \cos\left[2\pi(f_n-f_k)t-\phi_{n,l}\right].dt + d_n(0)\int_{\tau_l}^{T_b} \cos\left[2\pi(f_n-f_k)t-\phi_{n,l}\right].dt \right\} + \int_0^{T_b} n(t)\cos(2\pi f_k t).dt \quad (7\text{-}43)$$

where $\phi_{n,l} = 2\pi f_n \tau_l - \theta_l$. Equation (7-43) can be written as:

$$\begin{aligned} z_k &= \sum_{l=0}^{L-1} a_l \left\{ d_k(-1)\int_0^{\tau_l} \cos\phi_{n,l}.dt + d_k(0)\int_{\tau_l}^{T_b} \cos\phi_{n,l}.dt \right\} \\ &+ \sum_{n=0,n\neq k}^{N-1}\sum_{l=0}^{L-1} a_l \left\{ d_n(-1)\int_0^{\tau_l} \cos\left[2\pi(f_n-f_k)t-\phi_{n,l}\right].dt + d_n(0)\int_{\tau_l}^{T_b} \cos\left[2\pi(f_n-f_k)t-\phi_{n,l}\right].dt \right\} \\ &+ \int_0^{T_b} n(t)\cos 2\pi f_k t.dt \end{aligned} \quad (7\text{-}44)$$

Without loss of generality, we can assume that the receiver is matched to the first path of the multipath component, i.e. we assume τ_o=0 and θ_o=0. Therefore,

$$\begin{aligned} z_k^{(0)} &= a_0 d_k(0) T_b + \sum_{l=1}^{L-1} a_l \left\{ d_k(-1)\int_0^{\tau_l} \cos\phi_{n,l}.dt + d_k(0)\int_{\tau_l}^{T_b} \cos\phi_{n,l}.dt \right\} \\ &+ \sum_{l=0}^{L-1}\sum_{n=0,n\neq k}^{N-1} a_l \left\{ d_n(-1)\int_0^{\tau_l} \cos\left[2\pi(f_n-f_k)t-\phi_{n,l}\right].dt + d_n(0)\int_{\tau_l}^{T_b} \cos\left[2\pi(f_n-f_k)t-\phi_{n,l}\right].dt \right\} \\ &+ \int_0^{T_b} n(t)\cos 2\pi f_k t.dt \end{aligned} \quad (7\text{-}45)$$

where $d_n(-1)$ and $d_n(0)$ indicate the previous and current symbols respectively, which are transmitted at the carrier f_n. Equation (7-45) can be written as the following:

$$z_k^{(0)} = a_0 d_k(0) T_b + \sum_{l=1}^{L-1} a_l \left\{ d_k(-1) X_{k,k}^l + d_k(0) \hat{X}_{k,k}^l \right\} + \sum_{l=0}^{L-1} \sum_{n=0, n\neq k}^{N-1} a_l \left\{ d_n(-1) \left[X_{n,k}^l + Y_{n,k}^l \right] + d_n(0) \left[\hat{X}_{n,k}^l + \hat{Y}_{n,k}^l \right] \right\} + \eta_k \tag{7-46}$$

where,

$$\eta_k = \int_0^{T_b} n(t) \cos\left(\frac{2\pi k}{T_b} t \right) . dt \tag{7-47}$$

and,

$$\begin{aligned} X_{k,k}^l &= \cos\phi_{k,l} R_{k,k}(\tau_l) & \hat{X}_{k,k}^l &= \cos\phi_{k,l} \hat{R}_{k,k}(\tau_l) \\ X_{n,k}^l &= \cos\phi_{n,l} R_{n,k}(\tau_l) & \hat{X}_{n,k}^l &= \cos\phi_{n,l} \hat{R}_{n,k}(\tau_l) \\ Y_{n,k}^l &= \sin\phi_{n,l} R'_{n,k}(\tau_l) & \hat{Y}_{n,k}^l &= \sin\phi_{n,k} \hat{R}'_{n,k}(\tau_l) \end{aligned} \tag{7-48}$$

and the partial cross correlations are given by [13]:

$$\begin{aligned} R_{k,k}(\tau) &= \int_0^{\tau} dt = \tau \\ \hat{R}_{k,k}(\tau) &= \int_{\tau}^{T_b} dt = T_b - \tau \\ R_{n,k}(\tau) &= \int_0^{\tau} \cos\frac{2\pi(n-k)}{T_b} dt = T_b \frac{\sin\left[2\pi(n-k)\tau/T_b\right]}{2\pi(n-k)} && n \neq k \\ R'_{n,k}(\tau) &= \int_0^{\tau} \sin\frac{2\pi(n-k)}{T_b} dt = T_b \frac{1-\cos\left[2\pi(n-k)\tau/T_b\right]}{2\pi(n-k)} && n \neq k \\ \hat{R}_{n,k}(\tau) &= \int_{\tau}^{T_b} \cos\frac{2\pi(n-k)}{T_b} dt = -T_b \frac{\sin\left[2\pi(n-k)\tau/T_b\right]}{2\pi(n-k)} && n \neq k \\ \hat{R}'_{n,k}(\tau) &= \int_{\tau}^{T_b} \sin\frac{2\pi(n-k)}{T_b} dt = -T_b \frac{1-\cos\left[2\pi(n-k)\tau/T_b\right]}{2\pi(n-k)} && n \neq k \end{aligned} \tag{7-49}$$

From equation (7-46) it can be seen that the second term is due to intersymbol interference (ISI) caused by the multipath channel. The third term relates to the loss of orthogonality between subcarriers also due to multipath fading of the channel, which is termed the intercarrier or inter-

channel interference (ICI). The last term is due to noise. Accordingly, equation (7-46) can be written as:

$$z_k^{(0)} = \text{desired signal} + \text{ISI} + \text{ICI} + \text{noise} \tag{7-50}$$

where,

$$ISI = \sum_{l=1}^{L-1} a_l \left[d_k(-1) X_{k,k}^l + d_k(0) \hat{X}_{k,k}^l \right] \tag{7-51}$$

and,

$$ICI = \sum_{l=0}^{L-1} \sum_{n=0, n\neq k}^{N-1} a_l \left\{ d_n(-1) \left[X_{n,k}^l + Y_{n,k}^l \right] + d_n(0) \left[\hat{X}_{n,k}^l + \hat{Y}_{n,k}^l \right] \right\} \tag{7-52}$$

One of the features of the multicarrier technique is to cope with the frequency selectivity of the channel. This is achieved by consideration of the guard interval. In this case the impulse response of the receiving filter will have a rectangular shape but with duration of T_b'-T_g and the distance between carriers (i.e. $\Delta f = f_{n+1} - f_n$) will be $1/T_b'$. By considering the guard period greater than the minimum excess delay of the propagation channel, the effect of ISI can be suppressed. However, by applying a guard period, due to the different durations for the transmitting and receiving filters, an optimal matched filter condition is not completely fulfilled, and a fraction of the transmitter power is sacrificed in order to avoid ISI. Besides, this reduces the bandwidth efficiency by a factor of $10log(1+Tg/T_b')$ dB.

7.9 Error Probability

The error probability is calculated as the probability of the sampled signal being less than zero assuming a one has been transmitted, or,

$$P_b = prob\left(z_k^{(0)} < 0 \middle| d_k = 1 \right) \tag{7-53}$$

Referring to equations (7-51) and (7-52) and by considering interference terms that comprise random path amplitudes, time of arrivals and phases of the multipath channel, and considering a large number of components, the decision variable can be approximated as a Gaussian random variable. With this assumption, the error probability is calculated as:

$$P_b = Q\left(\sqrt{\frac{(a_0 T_b)^2}{\mathrm{var}(z_k^0)}}\right) \tag{7-54}$$

Referring to equation (7-50), the variance of $z_k^{(0)}$ contains the variance of the ISI, ICI and noise terms. The variance of the ISI is calculated as (see Appendix C):

$$\sigma_{ISI}^2 = \sum_{l=0}^{L-1} \sigma_{a_l}^2 \left[\overline{\tau_l^2} - T_b \overline{\tau_l} + \frac{T_b^2}{2}\right] \tag{7-55}$$

where σ_{al}^2 is the expected value of a_l^2. The variance of the ICI, as shown in Appendix D, is given as:

$$\sigma_{ICI}^2 = \frac{T_b^2}{2\pi^2} \sum_{l=0}^{L-1} \sigma_{a_l}^2 \sum_{i=-k, i\neq 0}^{N-k-1} \frac{1}{i^2} \tag{7-56}$$

The variance of the noise term is given as $N_0T_b/4$. If we assume OFDM communication using N=512 carriers with a total channel data throughput of 1.028 Mb/s, an equal gain and tap delay channel profile with L=4 paths and an average power of unity for all paths, the term in equation (7-55) has been found to reduces to a value of $4.92158\text{x}10^{-7}$. Considering independent interference terms, the total variance of the interference is therefore calculated as:

$$Var(z_0^0) = 4.92158\times 10^{-7} \cdot \sum_{l=1}^{L-1} \sigma_{a_l}^2 + \frac{T_b^2}{2\pi^2} \sum_{l=0}^{L-1} \sigma_{a_l}^2 \sum_{i=1}^{N-1} \frac{1}{i^2} + \frac{N_0 T_b}{4} \tag{7-57}$$

The bit-error probability as given by equation (7-54) is then averaged over the probability density function of the path amplitude a_0. The performance of a multi-carrier OFDM system with N=512 carriers operating in a multipath Rayleigh faded channel and no time guard-band is shown in figure (7-15). At higher E_b/N_o, the curve very soon reaches the irreducible BER which can only be reduced further through guard-time intervals, equalisation and coding strategies.

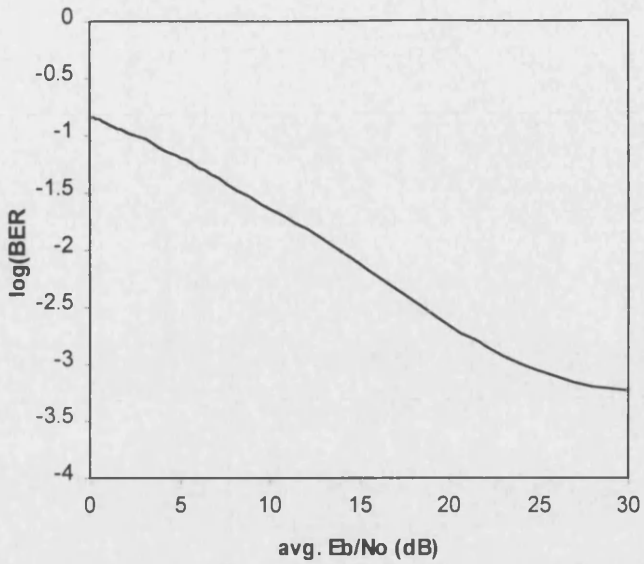

Figure 7-15. Performance of asynchronous OFDM with N=512 sub-carriers

7.10 OFDM Channel Estimation

A number of recent publications [14-19] have focused on possible channel estimation strategies for multi-carrier DS-CDMA designs, with a large interest devoted to efficient pilot tone estimation strategies. Particularly for multi-carrier systems, it is vital to provide a good estimate of the channel characteristics, with heavy emphasis on determining the optimum number of sub-carriers, pilot tones and their spacing patterns.

Pilot-based approaches are widely used to estimate the channel properties and to correct the received signal. Some methods have been developed under the assumption of a slow fading channel, where the channel transfer function for the previous OFDM data block is used as the transfer function for the present data block.

In practice, a wideband radio channel is time-variant, frequency-selective and noisy. The estimation of its transfer function becomes rather difficult. First, the slow fading assumption does not always hold. Thus the transfer function might have significant changes even over adjacent OFDM data blocks. Therefore, it is preferable to estimate the channel based on the pilot signals in each OFDM data block. Secondly, the pilot signals are also corrupted by ICI, due to the fast variation of the mobile channel. In addition, AWGN always exists. ICI and AWGN components in the received pilot signals strongly affect the accuracy of the estimation.

The method employed in this work is based on estimating the channel characteristics through the insertion of known pilot symbols at the input to the IFFT in the transmitter, periodically

spaced over the entire bandwidth. A comb-type sub-carrier arrangement is adopted. The different types of pilot-tone spacing that may be employed are shown in figure (7-16):

1. Pattern (a) measures all sub-carriers at the same time in stepped time intervals, as in broad-band single carrier systems, and interpolates the estimated values on successive time-intervals by comparing the results with the previous channel measurement
2. Pattern (b) is a comb-type method which measures the sub-carriers in increasing order, one at a time.
3. Pattern (c) measures every 4^{th} sub-carrier and makes an estimate of the channel through interpolation. This method measures the assigned pilot tones at the same time.
4. Pattern (d) measures the channel in a two-dimensional comb-type pattern, with equidistant spacings in the time and frequency domain. This is one of the most efficient methods, and requires 2-D Wiener filtering to estimate the channel transfer function.
5. Pattern (e) uses pilot symbol locations that are shifted one step in frequency at each pilot interval and interpolates the estimates between values in frequency and time.
6. Pattern (f) has a constant channel estimation in time at one particular sub-carrier and probes the adjacent sub-carriers in increasing order at every time interval. It therefore enables the system to measure the fading on each consecutive sub-carrier relative to the base pilot tone and interpolates between values.

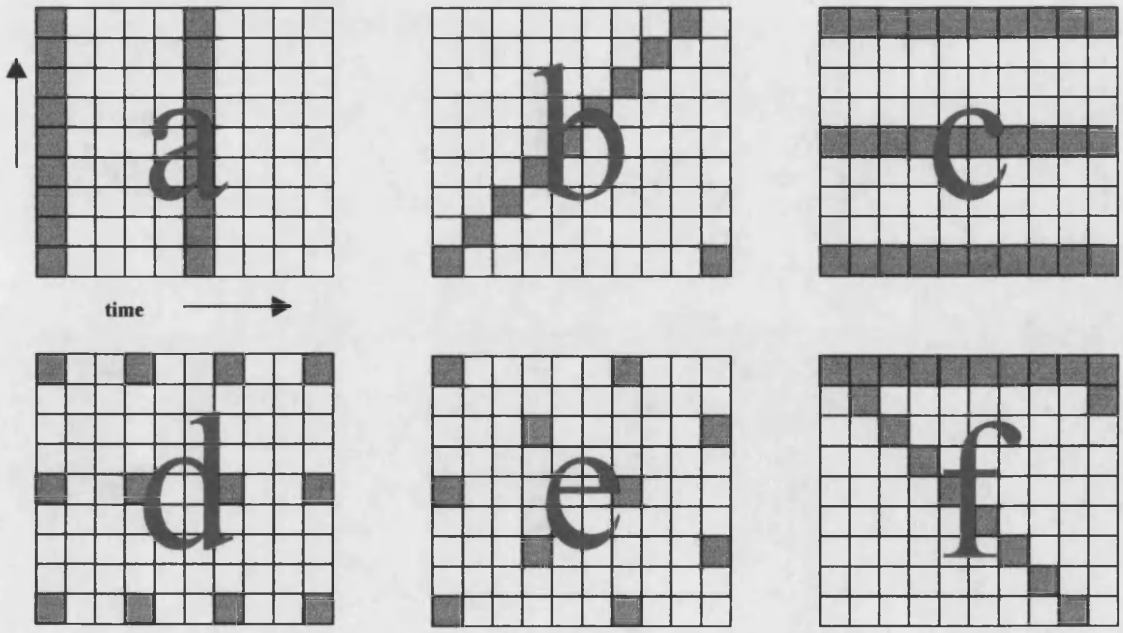

Figure 7-16. Examples of possible pilot patterns for OFDM channel estimation

The channel estimation technique employed in this thesis is based on pattern (c), since the channel is fast time-varying and requires accurate channel estimates in the frequency domain.

Interpolating between 4 sub-carriers has been shown to give adequate performance in fast fading channels. The key points to this channel parameter estimation technique are as follows:

1. The ICI and AWGN in the pilot sub-carriers are reduced by lowpass filtering in a transform domain.
2. The passband of the filter is determined dynamically from the received pilot signals
3. The channel transfer function for all the sub-carriers is obtained by the high-resolution interpolation realised by zero padding and DFT/IDFT

This method is applicable to all linear modulation OFDM systems.

The total N sub-carriers of the OFDM system are arranged as follows. Adjacent T ($T<<N$) sub-carriers are grouped together, without overlapping between adjacent groups. In each group, the first sub-carrier is used to transmit the pilot signal and thus is called the pilot sub-carrier. The rest of the sub-carriers bear information data and thus are called information sub-carriers. Therefore, there are total $M=N/T$ pilot sub-carriers and T-M information sub-carriers. The variable n = [0,1,...,N-1] denotes the index in the discrete time domain and k = [0,1,...,N-1] denotes the index in the discrete frequency domain. k is further expressed as $k=mT+l$ with integers l = [0,1,...,T-1] and m = [0,1,...,M-1]. Assuming that all the pilot signals have an equal complex value c, the OFDM signal modulated on the kth sub-carrier can be expressed as:

$$X(k) = X(mT + l) = \begin{cases} c & l = 0 \\ \text{data} & l = 1,\ldots,T-1 \end{cases} \tag{7-58}$$

The corresponding time-domain signal is the obtained via the IFFT.

The effects of the channel on the transmitted sequence s_k may be expressed as the convolution of the channel impulse response, that is:

$$y_k = h_k * s_k \tag{7-59}$$

This convolution process may be regarded as an equivalent frequency domain multiplication of the transmitted signal spectrum with the channel frequency response via the Fourier domain equivalence. Denoting $H(k)$ as the FFT of the baseband low-pass equivalent channel transfer function h_k, the received frequency-domain OFDM signal at the output of the FFT in the receiver can then be expressed as:

$$Y(k)=X(k)H(k) + I(k) + W(k) \tag{7-60}$$

where $H(k)$ is the channel transfer function at the kth subcarrier, $I(k)$ is the ICI component in the received signal and $W(k)$ represents the Fourier transform of the AWGN component. The channel estimation method based on pilot signals and transform-domain processing is depicted in figure (7-17).

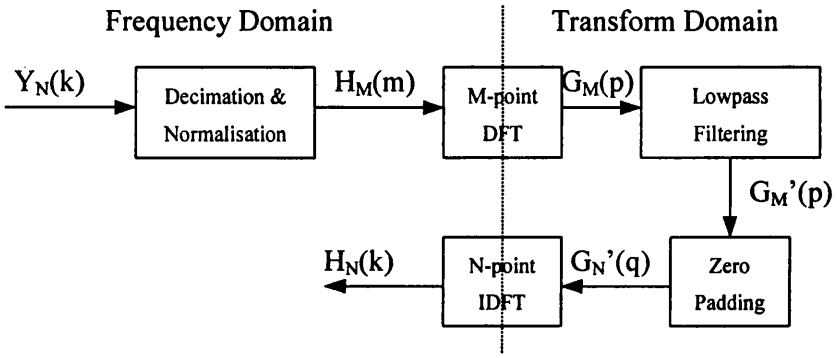

Figure 7-17. Channel estimation approach

By down-sampling T:1 the received sequence the samples at pilot subcarriers are picked up and a sequence of length M is obtained. Normalising this sequence to the pilot signal value c gives the noisy channel transfer function $H_M(m)$ which is identical to the rough estimate $H_N(m)$, that is:

$$H_M(m) = H_M(m) + [I_M(m) + W_M(m)]/c \tag{7-61}$$

Since the ICI and AWGN in time-domain are zero mean random processes, it can be derived [14] that the noise component $[I_M(m)+W_M(m)]/c$ is a random process with zero mean and Gaussian distribution.

The variation of the actual transfer function $H_M(m)$ is very slow with respect to the pilot subcarrier index m, while the noise component changes very fast. Therefore they are separable. The key is to use a relevant strategy.

Considering that the channel parameters are unknown and changing from time to time, it is difficult to reduce the noise component in the frequency domain by normal curve-fitting algorithms based on fixed low-order polynomial assumptions. On the contrary, a low-pass filtering strategy in a transform domain is straightforward and feasible. We define the transform domain so that any sequence in this domain is the DFT of its counterpart in the frequency domain. Therefore, a sequence in the transform domain is the 'spectral sequence' of its

counterpart in the frequency domain. The argument p in the transform domain can be viewed as the 'frequency' which reflects the variation speed of a frequency domain function.

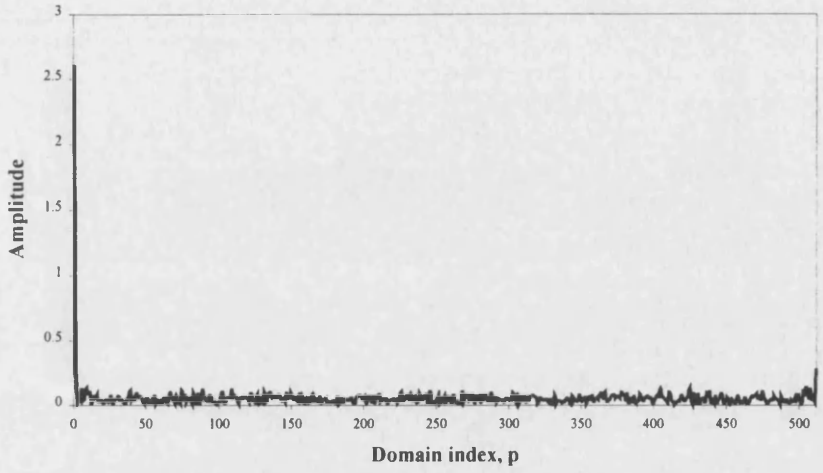

Figure 7-18. Transform domain representation of $G_M(p)$

The transform domain representation of $H_M(m)$ is then:

$$G_M(p) = \sum_{m=0}^{M-1} H_M(m) \exp\left(-j\frac{2\pi}{M}mp\right) \tag{7-62}$$

where p is the transform-domain index and $p = [0,1,\ldots,M\text{-}1]$. As expected, the signal component in $G_M(p)$ is located at the lower 'frequency' while the noise component is spread over the whole 'frequency' region, as shown in figure (7-18). The low-pass filtering can be realised simply by setting the samples in the 'high frequency' region to zero, that is:

$$G_M'(p) = \begin{cases} G_M(p), & 0 \le p \le p_c \\ 0 & \text{otherwise} \end{cases} \tag{7-63}$$

where p_c is the 'cut-off frequency' of the filter in the transform domain. This cut-off frequency is determined by selecting the first 95% of the signals' energy in the transform domain. Since the channel is slowly varying, its transfer function can be viewed as the sum of several sinusoidal functions with respect to k. However, the number and the 'frequencies' of the sinusoids vary due to the changes in the mobile radio channel. To avoid the model mismatch problem, we do not transform $G_M'(p)$ back to the frequency domain and then perform interpolation. Instead, a high-resolution interpolation approach based on zero-padding and DFT/IDFT is used [17].

First, the M-sample transform domain sequence $G_M'(p)$ is extended to an N-sample sequence $G_N'(q)$ by padding with N-M zero samples at the 'high frequency' region, giving:

$$G_N'(q) = \begin{cases} G_M'(q) & 0 \le q \le p_c \\ 0 & p_c < q < N - p_c \end{cases} \tag{7-64}$$

This N-sample sequence is the Fourier transform of the desired estimate of the channel transfer function. By performing an N-point IDFT, the estimated transfer function, with its lower noise levels is obtained.

This approach provides an accurate estimate because no assumption of the signal variation speed is made, thus there is no model mismatch problem; and all the desired 'frequency' components in the transform domain are reserved and transformed to the frequency domain.

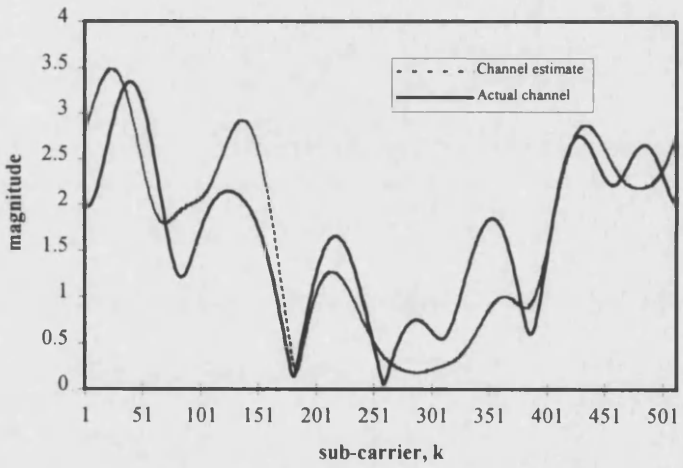

Figure 7-19. Performance of noisy channel estimation at *Eb/No*=10dB and cut-off at p_c=10 (interpolation between 4 sub-carriers)

The performance of this technique in a frequency selective bad urban COST-207 channel model with Doppler of 300Hz can be seen in figure (7-19). Here the signal-to-noise ratio was set to 10 dB and the cut-off point was at p_c=10. The OFDM signal comprised of 512 carriers, with 25% used for channel estimation and linear interpolation between 4 sub-carriers. The performance of a typical multi-user basestation downlink using OFDM and CDMA with noisy channel estimation and perfect channel estimation is compared in figure (7-20).

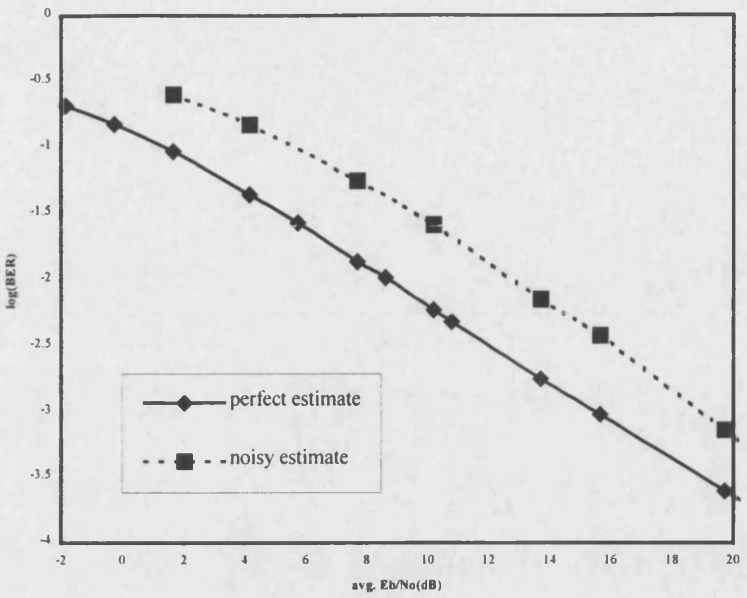

Figure 7-20. Performance degradation of a MC-CDMA system due to noisy channel estimation

It can be seen that the degradation in performance is typically about 4dB if the channel parameters are estimated under the influence of Gaussian noise. A more enhanced description of the simulation results is given in chapter 9, where the system is compared with different equaliser structures and multi-user interference cancellation techniques.

7.11 Summary

OFDM techniques offer a considerable resistance to channels dominated by frequency selective fading by effectively spreading the fading over many symbols, very much like a spread-spectrum system. In fact, OFDM techniques are comparable to spread-spectrum systems in many ways. If the channel has a high delay spread and the user requires high data rates, it becomes preferable to use multi-carrier instead of single-carrier techniques. Using densely spaced overlapping sub-carriers also eliminates the requirement for steep bandpass filters as in FDMA systems.

Using densely spaced sub-carriers with overlapping spectra in OFDM systems abandons the use of steep band-pass filters to detect each sub-carrier as used in FDMA schemes. Increasing the number of sub-carriers provides greater resilience to multipath fading in the frequency-domain and effectively randomises burst errors caused by fading or impulse interference. Instead of

several adjacent symbols being completely destroyed, many symbols are now slightly distorted. There is a fundamental limit, however, to the number of sub-carriers that may be employed.

As the number of sub-carriers is increased, the spacing between each sub-carrier is decreased and consequently the Doppler spread of the channel effects the performance. The maximum number of sub-carriers is therefore dependent on the time-selectivity of the channel, but this degradation can be reduced through more sophisticated coding, equalisation, combining and interleaving strategies. The use of time-guard bands to maintain orthogonality between OFDM symbols is, of course, indispensable for multi-carrier systems.

A theoretical treatment has shown the importance of using guard-bands and the level of irreducible BER and *C/I* ratio with different guard-interval lengths. Even with adequate coding, the performance degradation is still severe in frequency-selective faded channels. The bit-error rate performance for an asynchronous OFDM system has been analysed in a multipath channel with 4 paths. It has been shown that uncoded multi-carrier schemes are not as sensitive to increases in the number of paths as single-carrier systems. This, again, is due to the inherent frequency diversity of multi-carrier systems, giving a more robust feature in multipath channels.

To maintain a coherent link for modulation techniques such as BPSK or QPSK requires accurate knowledge of the phase and amplitude statistics of the channel. This can only be achieved by employing a small overhead of known sequences for channel sounding. A more advanced and sophisticated method has been introduced in this chapter.

The basic principle of pilot-symbol-aided channel estimation is to multiplex training symbols known to the receiver into the data stream. Hence the receiver is able to estimate the channel at any time, given the observations at the pilot locations, assuming the sampling time is sufficient with respect to the channel bandwidth. A good 1-D channel parameter estimation procedure has been introduced and has shown to give a reasonably good estimate of the true channel transfer function. When the channel is probed simultaneously in both time and frequency domains, the overhead of pilot symbols can be reduced significantly. Presently, state of the art is filtering with two cascaded orthogonal 1-D filters, referred to as 2 x 1-D filtering [18]. With higher order estimation procedures such as 2-D Wiener filtering the 25% pilot tone overhead can be reduced by a factor greater than 4 through time-domain and frequency-domain interpolation, rather than frequency-domain interpolation alone.

7.12 References

[1] Doeltz, M L, Heald, E T and Martin, D L, "Binary Data Transmission Techniques for Linear Systems", *Proc. IRE*, Vol. 45, pp. 656-661, May 1957

[2] Chang, R W, "Synthesis of Band-Limited Orthogonal Signals for Multichannel Data Transmission", *Bell Syst. Techn. Journal*, pp. 1775-1796, Vol. 45, Dec 1966

[3] Saltzberg, B R, "Performance of an efficient Parallel Data Transmission System", IEEE *Trans. on Comms.*, Vol. COM-15, pp. 805-811, Dec 1967

[4] *ETSI*, ETS 300 401, "Radio Broadcast Systems: Digital Audio Broadcasting (DAB) to mobile, portable and fixed receivers"

[5] *ETSI*, pr ETS 300 744, "Radio broadcast system for television, sound and data services; Framing structure, channel coding and modulation for digital terrestrial television"

[6] Casas, E F, and Leung, C, "OFDM for data communication over mobile radio FM channels – part 1", *IEEE Transactions on Communications*, Vol. 39, pp. 783-793, 1991

[7] Weinstein, SB and Ebert, PM, "Data transmission by frequency division multiplexing using the discrete Fourier transform", pp. 73-83, *IEEE Transactions on Communication Technology*, Vol. COM 19, Oct. 1971

[8] Vahlin, A and Holte, N, "Use of guard interval in OFDM on multipath channels", *Electronics Letters*, Vol. 30, No. 24, pp. 2015-2016, Nov. 1994

[9] Alard, M and Lassalle, R, "Principles of modulation and channel coding for digital broadcasting for mobile receivers", *EBU Review*, No. 224, August 1987, pp. 168-190

[10] Pollet, T, Bladal, M, and Moeneclaey, M, "The effect of carrier frequency offset and phase noise on the BER performance of OFDM signals", *Proceedings of the IEEE 1st Symposium on Comms. and Vehicular Tech.*, pp. 4.2-1 – 4.2-4, Oct. 1993, Delft, Netherlands

[11] Petrovic, R, Roehr, W and Cameron, D W, "Multicarrier modulation for narrowband PCS", *IEEE Trans. on Veh. Techn.*, Vol. 43, No. 4, pp. 856-862, Nov. 1994

[12] Viterbo, E and Fazel, K, "How to combat long echoes in OFDM transmission schemes: Sub-channel equalisation or more powerful channel coding", *IEEE Conference Proceedings*, pp. 2069-2074, 1995

[13] Vandendorpe, L, "Multitone transmission in a multipath Rician fading channel", IEEE *Conference Proc. of 1st Symposium on Comm.* Veh. Techn., Benelux, pp. 2.1.1-2.1.6, Delft, Netherlands, Oct. 1993

[14] Beek, J J, *et al*, "On channel estimation in OFDM systems", pp. 815-819, *IEEE 45th Vehicular Technology Conference*, Chicago, IL, USA, July 1995

[15] Edfors, O, *et al*, "OFDM channel estimation by singular value decomposition", pp. 923-927, *Proc. IEEE 46th Vehicular Technology Conference*, Atlanta, GA, USA, April 1996

[16] Mignone, V, and Morello, A, "CD3-OFDM: A novel demodulation scheme for fixed and mobile receivers", *IEEE Transactions on Communications*, Vol. 44, pp. 1144-1151, Sept. 1996

[17] Zhao, Y, and Huang, A, "A novel channel estimation method for OFDM mobile communication systems based on pilot signals and transform-domain processing", pp. 2089-2093, *IEEE 47th Vehicular Technology Conference*, Phoenix, Arizona, AZ, USA, May 1997

[18] Hoeher, P, Kaiser, S, and Robertson, P, "Pilot-Symbol-Aided Channel Estimation in Time and Frequency", *Multi-Carrier Spread Spectrum (Kluwer Academic Publishers)*, p. 169-178, 1997, Printed in Netherlands

[19] Steiner, B, "Time Domain Uplink Channel Estimation in Multicarrier-CDMA Mobile Radio System Concepts", *Multi-Carrier Spread Spectrum (Kluwer Academic Publishers)*, p. 153-160, 1997, Printed in Netherlands

[20] Vandendorpe, L, "Multitone Spread Spectrum Multiple Access Communications System in a Multipath Rician Fading Channel", *IEEE Transactions on Vehicular Technology*, pp. 327-337, Vol. 44, No. 2, May 1995

[21] Sourour, E and Nakagawa, M, "Performance of orthogonal Multicarrier CDMA in a Multipath Fading Channel", *IEEE Transactions on Communications*, pp. 356-367, Vol. 44, No. 3, March 1996

[22] Kondo, S and Milstein, L, "Performance of Multicarrier DS-CDMA Systems", *IEEE Transactions on Communications*, pp. 238-246, Vol. 44, No. 2, February 1996

[23] Yee, N, Linnartz, JP and Fettweis, G, "Multi-Carrier CDMA in Indoor Wireless Radio Networks", *IEICE Transactions on Communications*, pp. 900-904, Vol. E77-B, No.7, July 1994

[24] DaSilva, V and Sousa, E, "Multicarrier Orthogonal CDMA Signals for Quasi-Synchronous Communication Systems", *IEEE Journal on Selected Areas in Communications*, pp. 842-852, Vol. 12, No. 5, June 1994

[25] Prasad, R and Hara, S, "An Overview of Multi-Carrier CDMA", pp. 107-114, *IEEE Proceedings of ISSSTA'96*, Mainz, Germany, September 1996

[26] Cimini, LJ, "Analysis and simulation of a digital mobile channel using orthogonal frequency division multiplexing", *IEEE Transactions on Communications*, Vol. COM-33, No.7, pp. 665-675, July 1986

[27] Nikookar, H, and Prasad, R, "OFDM performance evaluation over measured indoor radio propagation channels", *ICUPC'95*, Tokyo, Japan, Nov. 1995

[28] Chow, J S, Tu, J C and Cioffi, J M, "A Discrete Multitone Transceiver System for HDSL Applications", *IEEE JSAC*, Vol.9, pp.895-908, 1991

[29] Fazel, K, *et al* "A Concept of Digital Terrestrial Television Broadcasting", *Wireless Personal Communications*, Vol. 2, No 1&2, pp.9-27, 1995

[30] Ormondroyd, R F, and Maxey, JJ, "Comparison of time guard-band and coding strategies for OFDM digital cellular radio in multipath fading", *IEEE Proc. of Veh. Techn.*, pp. 850-854, Phoenix, Arizona, May 1997

[31] Maxey, J J and Ormondroyd, R F, "Optimisation of orthogonal low-rate convolutional codes in a DS-CDMA system", *IEEE/URSI Conference Proceedings of ISSSE'95*, Vol. 95TH8047, pp. 493-496, 1995

[32] Maxey, J J and Ormondroyd, R F, "Low-Rate Orthogonal Convolutional Coded DS-CDMA using Non-Coherent Multi-Carrier Modulation over the AWGN and Rayleigh Faded Channel", *IEEE Conference Proceedings of ISSSTA '96*, Vol. 2, pp.575-579, 1996

CHAPTER 8:

MULTI-CARRIER CDMA SYSTEMS

8.1 Introduction

To operate future-generation multimedia communications systems, high data rate transmission needs to be guaranteed with a high quality of service. For instance, the third generation cellular mobile systems should offer a high data rate up to 2 Mbit/s for video, audio, speech and data transmission [1]. In addition, the important challenge for these cellular systems will be the choice of an appropriate multiple access scheme. These trends motivated many researchers to look for multiple access systems that offer a high spectral efficiency.

Spread spectrum techniques originating from military applications may partly fulfill the above requirements. DS-CDMA relies on spreading the data stream using an assigned spreading code for each user in the time domain. The capability of minimising multiple access interference (MAI) is given by the cross-correlation properties of the spreading codes. It is known that without coding or diversity the performance of DS-CDMA degrades rapidly when the number of users increases. In the multipath propagation environment, the capability of distinguishing one multipath component from others in the composite received signal is offered by the correlation properties of the spreading codes [2]. Therefore the RAKE receiver may contain multiple correlators, each matched to a different resolvable path in the received composite signal [1]. The performance of a DS-CDMA system will depend strongly on the number of active users, the channel characteristics and on the number of arms employed in the RAKE, as shown earlier. A RAKE receiver can be utilised to achieve path diversity, but it must, however, continuously estimate the relative delay of each path and, if maximal-ratio combining is used, the gain of each path must also be estimated. Significant signal processing is needed, especially with the existence of other users' multipath interference.

Self- and multiple access interference (MAI), which results from the imperfect auto- and cross-correlation properties of the spreading codes, limit the system capacity. Therefore, it is often very difficult for a DS-CDMA receiver to make full use of the received signal energy scattered in the time domain and hence handle a full load [2].

Another problem occurs in high data rate applications where the channel delay spread exceeds the symbol duration. DS-CDMA signals have a wide bandwidth and may be subject to frequency selective multipath fading. In this case, the conventional DS-CDMA system is subject to severe intersymbol interference (ISI) and is practically not usable. However, in DS-CDMA, even if the data rate is low and ISI is negligible, multipath fading causes severe degradation due to inter-chip-interference. A technique of reducing the symbol rate is essential in this case.

On the other hand, multi-carrier transmission techniques have recently been receiving wide interest for high data rate applications. Multi-carrier systems help to reduce the effect of ISI and adapt to channel conditions. In addition, these systems provide a robust link over frequency selective fading channels and have the additional capability of narrow-band interference rejection. The use of multi-carrier modulation techniques transforms the equalisation problem into the frequency domain and considerably reduces the complexity of the signal processing stages in the receiver.

The advantages and success of multi-carrier (MC) modulation and spread spectrum (SS) techniques have motivated many researchers to investigate the suitability of the combination of MCM with SS, known as multi-carrier spread-spectrum (MC-SS) for cellular systems. This combination, introduced in 1993 as a multiple access scheme, will allow the benefits of both schemes to be combined: higher flexibility, higher spectral efficiency, simpler detection techniques, narrow band interference rejection capability, etc. Different multiple access concepts based on the combination of MC modulation with DS-CDMA for mobile and wireless indoor communications have been introduced during late 1993 [9-16]. The main differences between them are in the spreading, frequency mapping and the detection strategy. It is expected that by proper choice of modulation parameters, such as the number of chips, number of carriers, the sequence structure, etc. MC-SS systems can combine the advantages of both techniques.

8.2 Current System Proposals

A number of multi-carrier DS-CDMA (MC-CDMA) systems have been proposed [9-21]. The most prominent MC-CDMA systems to have been put forward are based on the designs of Kondo and Milstein[14], Sourour and Nakagawa[10], Sousa[13], Fazel[11] and Vandendorpe[15]. In the following, the three different multi-carrier CDMA concepts introduced in 1993 will be examined. A detailed description covering these and further concepts is given in [18], which are summarised below.

The very first multi-carrier DS-CDMA concepts were based on providing a spreading sequence or code before multiplexing the combined signal onto N sub-carriers. This concept is known as MC-CDMA, and is based on a serial concatenation of DS spreading with MC modulation [9,11,12,16]. The high-rate DS spread data stream is MC modulated in such a way that the chips of a spread data symbol are transmitted in parallel on each sub-carrier, as seen in figure (8-1).

Here, the data $d_i(t)$ of the ith user is spread by the sequence $c_i(t)$ and consequently modulated by orthogonal basis functions at frequencies $f_0, f_1, \ldots f_{N-1}$. As for DS-CDMA, a user occupies the total bandwidth for the transmission of a single data symbol. The separation of the user's signals is performed in the code domain. The two main concepts are either to employ one data bit, multiplexed over all sub-carriers (termed frequency-domain spreading MC-CDMA, or Concept I), or spread the individual data bit over each sub-carrier using the same spreading code for each sub-channel (termed time-domain spreading MC-DS-CDMA, treated later in Concept II). In both schemes, when setting the number of sub-carriers to be one, they become equivalent to a normal single-carrier DS-CDMA scheme. In Concept I, the receiver uses all the received signal energy scattered in the frequency domain. Hence this approach has an additional degree of freedom compared to DS-CDMA systems because the mapping onto the frequency domain allows simple methods of signal detection in the frequency domain to be used. This concept was proposed in conjunction with OFDM for optimum use of the available bandwidth. However, through a frequency selective fading channel, the sub-carriers may have different amplitude levels and different phase shifts, and this results in the loss of orthogonality between users. It is therefore crucial for such multi-carrier designs to be used in conditions of frequency non-selective fading over each sub-carrier. The realisation of this concept also implies a guard time between adjacent OFDM symbols to prevent ISI [11,12], or to assume that the symbol duration is significantly larger than the time dispersion of the channel [9]. Thus the number of sub-carriers, N, has to be chosen sufficiently large to guarantee frequency non-selective fading on each sub-carrier. The application of orthogonal codes, such as Walsh-Hadamard codes for a synchronous system, e.g. the downlink of a cellular system, guarantees the absence of multiple access interference (MAI) in an ideal channel and minimum MAI in a fading channel [11,12]. The detection techniques that have been investigated with this system are based on equal-gain combining, zero forcing equalisation, maximum ratio combining, minimum mean square error equalisation, iterative detection, maximum likelihood detection and interference cancellation.

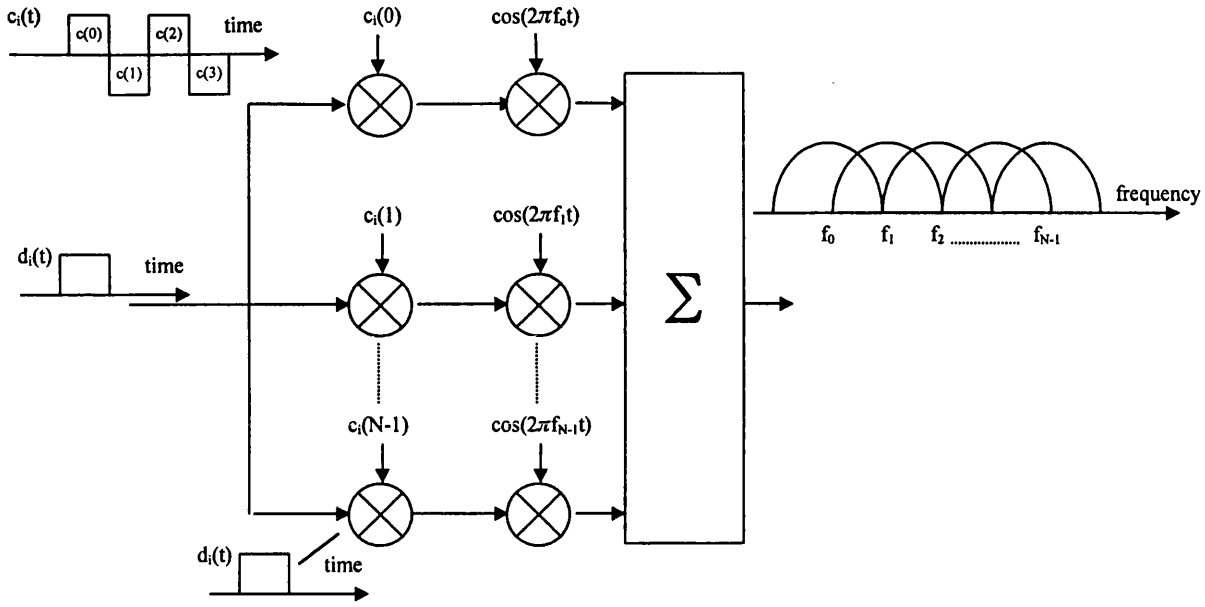

Figure 8-1. MC-CDMA transmitter design and the output frequency spectrum

Alternatively, if the original symbol rate is high enough to become subject to frequency selective fading, the signal needs to be converted into parallel sub-channels before spreading over the frequency domain. This forms the basis of Concept II and Concept III of the combination of MCM with SS, and is based on first converting the data stream into parallel low rate sub-streams before applying DS spreading on each sub-stream, in the time domain, and then consequently modulating onto each sub-carrier [13-15].

Concept II, known as MC-DS-CDMA, modulates the sub-streams on sub-carriers with a carrier spacing proportional to the inverse of the chip rate and can be seen in figure (8-2). This will guarantee the orthogonality between the spectrums of the sub-streams [13,14]. If the spreading code length is smaller or equal to the number of sub-carriers N, a single data symbol is not spread in the frequency domain but in the time domain. Spread spectrum is obtained by modulating N data symbols spread in time on parallel sub-carriers. This concept of using large numbers of sub-carriers benefits from time diversity. However, due to the frequency non-selective fading per sub-channel achieved through MC modulation, frequency diversity could only be exploited if channel coding with interleaving or sub-carrier hopping is employed, or if the same information is transmitted parallel on several sub-carriers. Indeed, copying the resulting spread sequence on each sub-stream may efficiently exploit the frequency diversity of the MC system. However, this approach is equivalent to a repetition coding that reduces the data rate by a factor N. Furthermore, the sub-carrier spacing might be chosen to be larger than the inverse chip rate to give higher frequency diversity to the system [14]. This concept was investigated for an asynchronous uplink scenario. For data detection, N coherent (non-RAKE) receivers might be used.

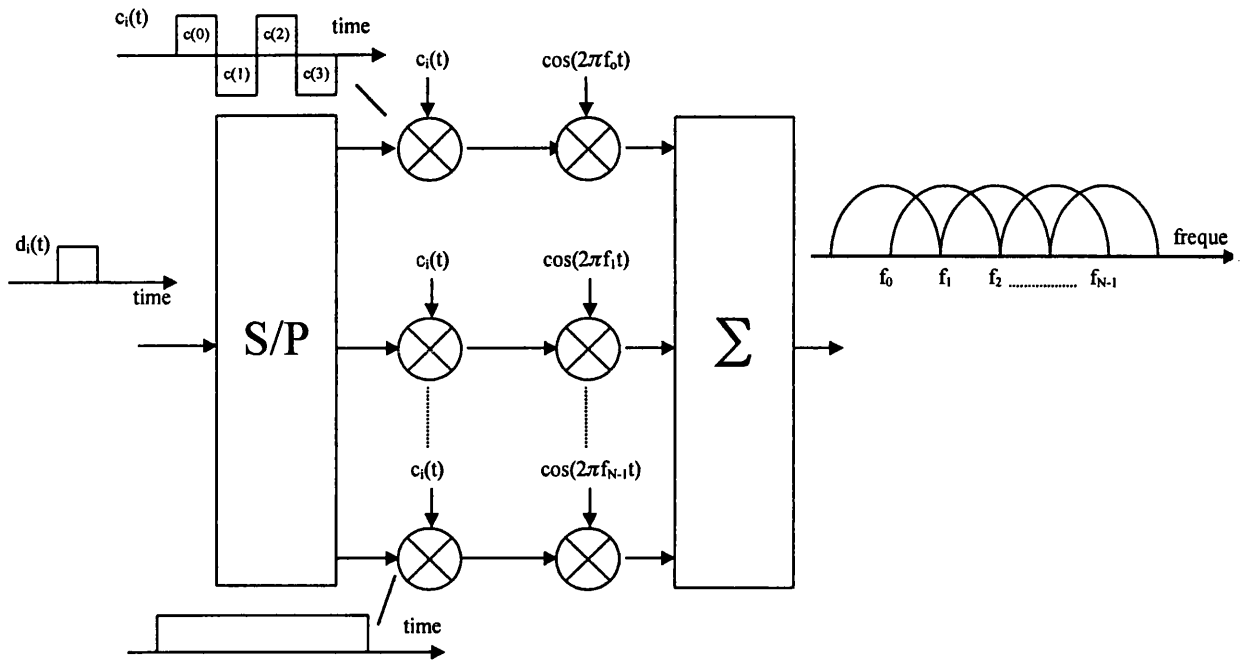

Figure 8-2. MC-DS-CDMA transmitter design and the output frequency spectrum

The MC-DS-CDMA concept based on the system proposed by Sourour et al [10] utilises a small number of carriers to solve both the ISI and inter-carrier interference (ICI) problems. Here, the initial data stream is serial to parallel converted to a number of lower rate streams and each stream feeds a number of parallel streams with the same rate. On each of the latter streams, bits are interleaved and spread by a PN code of a suitable chip rate. Then, these streams modulate orthogonal carriers with successively overlapping bandwidths. Consequently the processing gain is increased and frequency/time diversity is achieved through independent sub-carriers. The disadvantages of this design is the inherent need to provide sufficient interleaving and the need for a large number of carriers to resolve the multipath in the channel. With sufficient number of carriers, the condition of single path fading for each carrier can be achieved. Of course, the signals whose spectra overlap will be subject to correlated fading.

The system proposed by Sousa et al [13] considers an orthogonal MC-SS system with an optimal sequence set based on the Sylvester-type Hadamard matrices (Walsh functions) to provide an improvement over Hadamard orthogonal sequences. This design also introduces the idea of non-rectangular pulse shaping in the transmitter to minimise the cross-interference and multiple-access interference in the case of quasi-synchronous operation. It has been shown to give better performance than raised cosine pulses at the cost of higher excess bandwidths. Nevertheless, such schemes can provide an alternative solution to asynchronous designs using sophisticated interference cancellation techniques.

Concept III, shown in figure (8-3), is known as multi-tone-CDMA (MT-CDMA) and applies the same data mapping and spreading as concept II. However, its sub-carrier spacing is by a factor N smaller than the inverse of the chip rate [15]. Thus, the N parallel converted data symbols before DS-spreading fulfill the orthogonality requirements. However, after DS spreading per sub-carrier the orthogonality condition is not kept up, hence it results in ICI. On the other hand, the tight sub-carrier spacing enables the use of spreading codes that are approximately N times longer than the spreading code of a DS-CDMA system. The disadvantage of the multi-tone based approach is that it suffers ICI, while the capability to use longer spreading codes results in the reduction of the self-interference and multiple access interference. In a channel where this improvement is dominant, the multi-tone based approach can outperform the DS-CDMA scheme and therefore, at the expense of higher ICI, can supply more users than a single carrier spread-spectrum system [15]. Since each sub-channel might be affected by frequency selective fading, RAKE receivers or more complex multi-user detectors are required [15]. This concept was also investigated for the asynchronous uplink case.

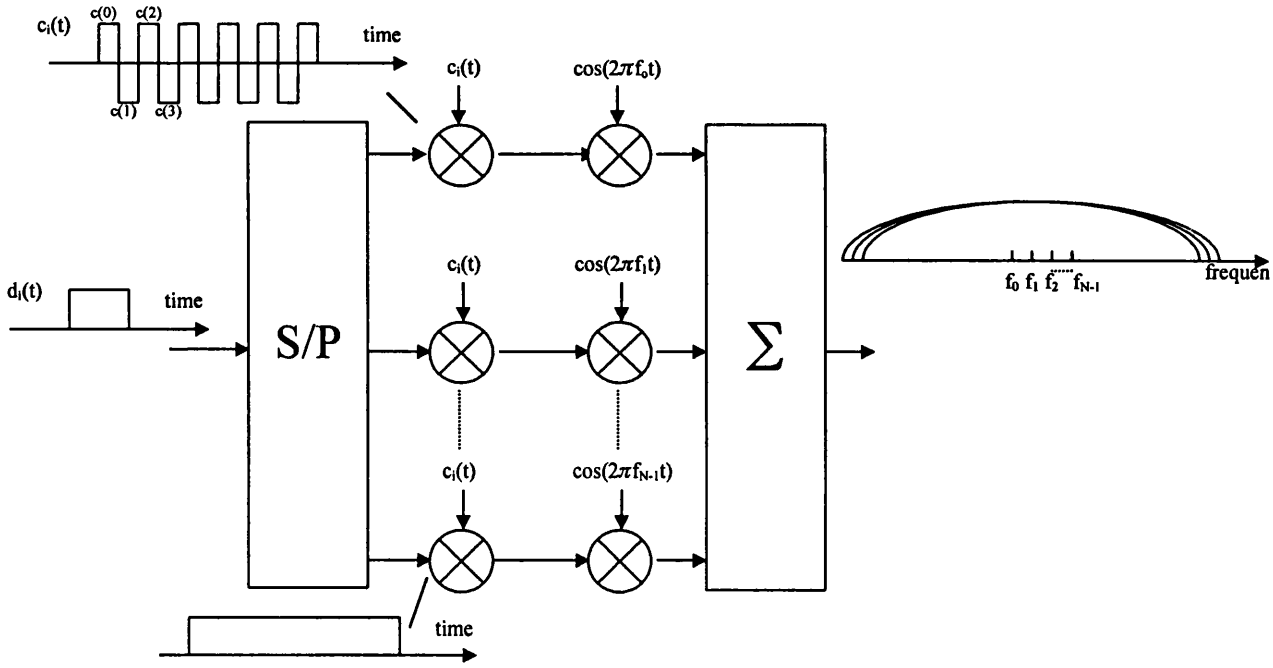

Figure 8-3. MT-CDMA transmitter design and the output frequency spectrum

Since 1993, the above main three concepts have been deeply studied, and new alternative solutions have been proposed. An overview of the research activity in this new field shows that a multitude of activities was addressed to develop these three concepts and to derive appropriate detection strategies [17,18]. A performance comparison between these concepts through software simulations is given in [18].

However, there is still a lot room for answering open questions and implementing novel solutions in this new research topic. In particular, investigations on the implementation of MC-SS systems for cellular mobile communications or other real applications have not been yet carried out sufficiently. These open questions cover the problem for the design of a suitable MC-SS scheme on both the up- and downlink. Some of the research so far has focused on simple coding and joint detection strategies, the design of powerful channel estimation and synchronisation techniques (especially for the uplink), cellular concepts (i.e. the design of hierarchical cells such as macro, micro and pico cells), problems of non-linearities and low cost receiver design.

This thesis will attempt to cover some of the issues relating to multi-carrier DS-CDMA designs, with particular attention being paid to coding, detection strategies and channel estimation techniques. The first part of this chapter is devoted to coherent BPSK MC-CDMA with the second part focusing on non-coherent DPSK MC-CDMA aspects. This chapter covers only single-user strategies, whereas chapter 9 pays more attention to multi-access detection strategies on the up- and downlink of a cellular system. Both systems, nevertheless, are based on the first concept, termed MC-CDMA.

8.3 Coherent BPSK design

The MC-CDMA transmitter using coherent BPSK was shown in figure (8-1) and represents a system where the N carriers are spaced in frequency by $1/T_b$, where T_b is the original data bit duration. Each branch of the parallel data stream is then multiplied by a chip from the spreading code of equal length N. Following the spreading function, the output is then modulated onto the N carriers via a series of orthogonal basis functions such as the Fourier series.

To reduce the complexity of the transmitter and receiver, the bank of mixers can be replaced by sampling the signal and using the inverse fast Fourier transform (IFFT) and the fast Fourier transform (FFT), respectively. This effectively implements a discrete inverse Fourier and discrete Fourier transform. The digital transmitter configuration can be viewed in figure (8-4).

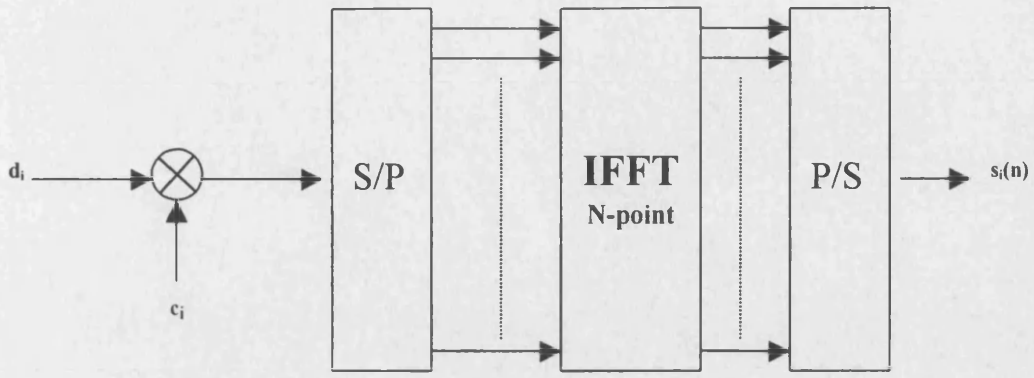

Figure 8-4. MC-CDMA transmitter using the IFFT

At the receiver, the MC-CDMA signal is sampled and serial to parallel converted before input to an N-point FFT. The output of the FFT is then multiplied by the equaliser coefficients $g_i(n)$ and user specific spreading code c_i before being summed over the N parallel branches. The equaliser coefficients can be estimated from the channel impulse response, which may be measured using the channel estimation methods discussed in chapter 7. An estimate of the data bit is then formed by threshold detection on the final stage of the receiver architecture.

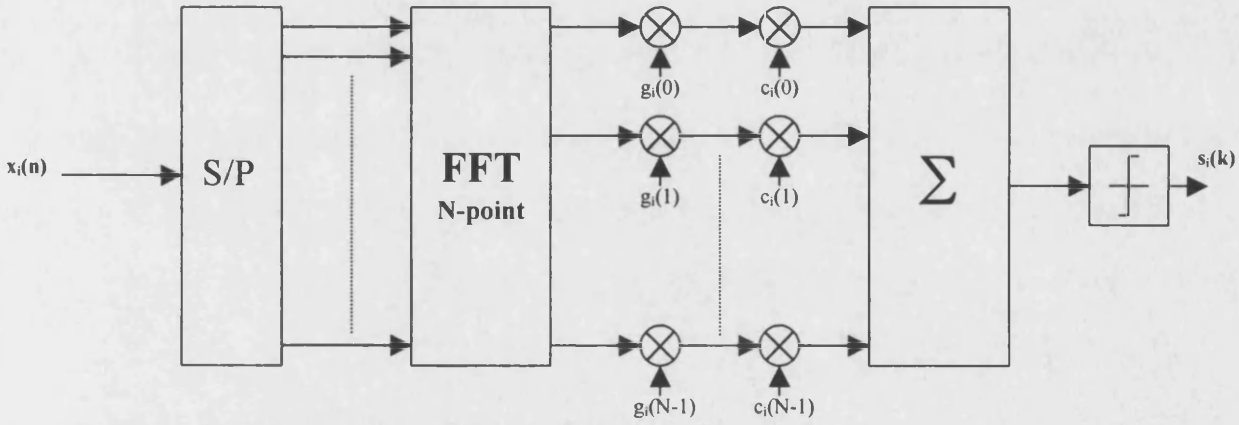

Figure 8-5. MC-CDMA receiver using the FFT

The coherent BPSK transmitter and receiver designs also incorporate coding and interleaving to achieve additional diversity and coding gain. The coding methods investigated in this thesis are restricted to conventional convolutional coding and low-rate orthogonal convolutional coding techniques.

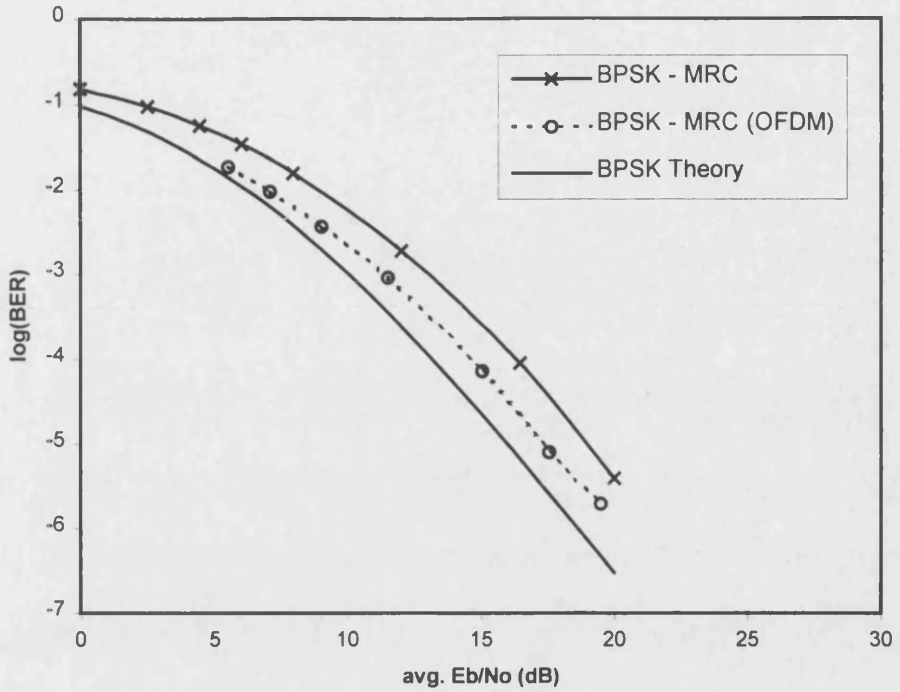

Figure 8-6. BER performance in L=4 path Rayleigh fading

The performance of the system featured above using MRC in a frequency selective Rayleigh faded channel as in chapter 2 is shown in figure (8-6). It can be seen that the MC-CDMA BPSK receiver approaches the lower bound of a conventional DS-CDMA RAKE receiver more closely than the simulated performance of a DS-CDMA receiver in the same channel. The inherent frequency selectivity of the channel clearly has a more degrading effect on DS-CDMA systems than MC-CDMA systems, with a performance improvement of at least 2 dB over DS-CDMA systems.

The coherent BPSK design featured here forms the basis of the proposed system in chapter 9, where this design is incorporated into the uplink design of a multi-user system employing different detection strategies and interference cancellation. For the remainder of this chapter we will concentrate on non-coherent DPSK designs using multi-carrier modulation and spread-spectrum techniques.

8.4 Non-Coherent DPSK design

The use of non-coherent DPSK modulation techniques alleviates the need for channel estimation techniques in the receiver and is therefore another potentially attractive proposal for

future MC-CDMA designs. This method with convolutional coding techniques to spread and code the data is proposed in the following section.

The system proposed in this chapter uses non-coherent combining where the individual sub-carriers are equalised. This gives improved performance in multipath channels where the delay spread is large (i.e. small coherence bandwidth), and hence provides additional frequency diversity. This type of system is therefore only attractive to single-user channels where multipath fading is the dominant performance limitation. In multi-user channels it would be more attractive to use coherent methods or non-coherent DPSK over each data bit, but the overall performance for a single-user system using the latter method in multipath channels will be degraded [28]. For the foregoing reason, we are devoting the analysis in this chapter to non-coherent DPSK employing differential encoding/decoding on each sub-carrier.

In the methods proposed to date, each user's data is spread by a unique PN sequence, in the usual way to DS-CDMA. The chips are then mapped into complex valued symbols prior to being serial/parallel converted into a vector of N complex values. Interleaving of the chips can also be used with this type of system. In the base station, each user's N value vector is summed at this point. The resulting vector is then orthogonally modulated onto the carrier.

The LROCC coding method effectively expands the data by a factor 2^K, where K is the constraint length of the convolutional encoder, before being modulated on $N=2^K$ orthogonal parallel carriers. With perfect synchronisation and no multipath, this enables several simultaneous users in the cellular structure to be isolated from one another in the time domain and through the use of orthogonally spaced carriers provides isolated data streams in the frequency domain. With OFDM, it is possible to separate each low bit-rate modulated carrier by as little as $1/T_s$, where T_s is the period of the symbols, and still have no inter-symbol interference. Figures (8-7) and (8-8) show a more detailed outline of the proposed transmitter and receiver structure.

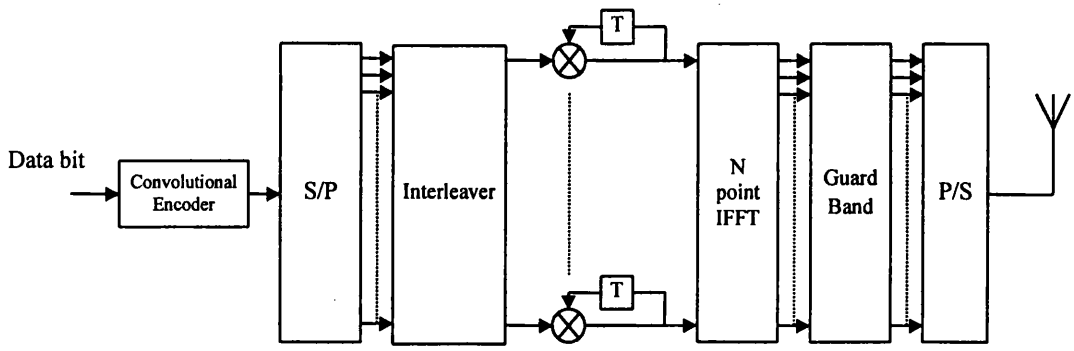

Figure 8-7. Transmitter design using LROCC coding, differential encoding, interleaving and OFDM modulation

As the presence of multipath fading introduces amplitude and phase distortions on the signal, it is difficult to track the phase information without the use of a pilot tone. Therefore, a non-coherent modulation technique such as differential PSK is introduced, where the phase information in the demodulator is derived from the previous symbol. As long as the phase distortion factor due to multipath is nearly constant or at least slowly varying over the symbol duration T_s, a square law detector may be used for non-coherent demodulation.

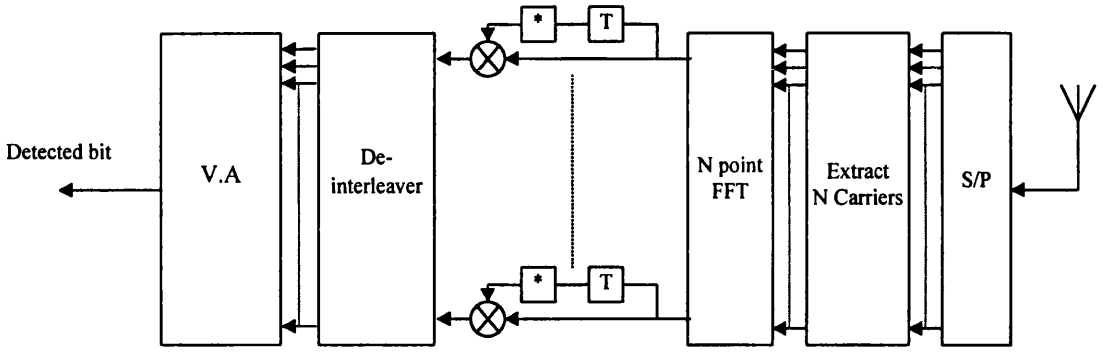

Figure 8-8. Receiver design employing DPSK demodulation on each FFT output

The theoretical performance of LROCC in Rayleigh faded channels has been analysed [23,24]. As this process involves a maximum likelihood detection scheme, such as the Viterbi algorithm, it is possible to use conventional theoretical performance evaluation techniques for high-rate convolutional codes to obtain an estimate for the upper-bound in Rayleigh faded channels.

Each data bit of duration T_b is first encoded in the LROCC coder where it is replaced with a corresponding chip sequence of length N, each chip having a duration T_c. The rate of the code is therefore $R=1/N$, where $N=2^K$ and K is the constraint length of the convolutional encoder. The chip sequence $y(n)$ is then converted into a parallel block of N chips and differentially encoded on each arm of the modulator. The input to the interleaver is then given as:

$$y(n) = y(n) \cdot y(n-N) \qquad n>N \tag{8-1}$$

Note that the delay term N represents the delay introduced through the serial-to-parallel conversion in the transmitter block.

This sequence is then interleaved and after the IFFT is given as:

$$x(k) = \frac{1}{N}\sum_{n=0}^{N-1} y(n)e^{j2\pi nk/N} \qquad k=0,1, \ldots N-1 \qquad (8\text{-}2)$$
$$= \frac{1}{N}\sum_{n=0}^{N-1} y(n)e^{j2\pi f_n t_k}$$

where Δt is an arbitrarily chosen interval and,

$$f_n = \frac{n}{N\Delta t} \text{ and } t_k = k\Delta t \qquad (8\text{-}3)$$

This parallel sequence, including a time guard band, is then converted into serial form and transmitted over the channel. It is assumed that the guard band is sufficiently larger than the channel impulse response to maintain independence of the OFDM blocks. The multipath nature of the fading channel will induce a phase and amplitude distortion on the original sequence. Thermal noise origins in the receiver will further produce AWGN. The DFT of the channel impulse response can be given as a complex channel fading sequence:

$$h(n) = p(n)e^{j\phi(n)} \qquad (8\text{-}4)$$

where $p(n)$ is the Rayleigh distributed attenuation coefficient and $\phi(n)$ represents the uniformly distributed phase distortion.

The received signal will contain the frequency selective faded wanted signal and an additional AWGN term due to thermal noise. The N chips per block are extracted after the time guard band removal and then fed into the FFT algorithm, giving:

$$g(n) = \frac{1}{N}\sum_{k=0}^{N-1} H(k)Y(k)e^{j2\pi f_n t_k} + \mu(n) \qquad (8\text{-}5)$$
$$= h(n)y(n) + \mu(n)$$

where $\mu(n)$ is the complex Gaussian distributed noise term at the output of the FFT.

The sequence $g'(n)$ at the output of the DPSK demodulator is given as:

$$g'(n) = g(n) \cdot g^*(n-1)$$
$$= [h(n)y(n)+\mu(n)] \cdot [h^*(n-1)y^*(n-1)+)+\mu^*(n-1)] \qquad (8\text{-}6)$$

but,

$$h(n) = p(n)e^{j\phi(n)}$$
$$h^*(n-1) = p^*(n-1)e^{-j\phi(n-1)} \quad (8\text{-}7)$$

Therefore,

$$\begin{aligned} g'(n) = {} & p(n)e^{j\phi(n)}\, p^*(n-1)e^{-j\phi(n-1)}y(n)y^*(n-1) + \\ & \mu(n)p^*(n-1)e^{-j\phi(n)}y^*(n-1) + \\ & \mu^*(n-1)p(n)e^{j\phi(n)}y(n) + \\ & \mu(n)\mu^*(n-1) \end{aligned} \quad (8\text{-}8)$$

For the ideal noiseless case $\mu(n)=\mu(n-1)=0$ and,

$$\begin{aligned} g'(n) &= p(n)p^*(n-1)e^{j[\phi(n)-\phi(n-1)]}y(n)y^*(n-1) \\ &= h(n)h^*(n-1)y(n)y^*(n-1) \end{aligned} \quad (8\text{-}9)$$

where $\phi(n)-\phi(n-1)$ is the phase difference. From equation (8-9), the mean value of $g'(n)$ is independent of the carrier phase and the output sequence can be detected correctly. Of course, for non-zero values of $\mu(n)$ the reliability of detection becomes worse as the background noise level increases.

8.5 Simulation Approach

The primary objective is to demonstrate whether MC-CDMA techniques can provide significant improvements in performance in multipath channels and to what degree convolutional coding techniques can help. The performance of low-rate orthogonal convolutional codes in AWGN and Rayleigh faded channels is well documented [23-26], and the work here is set to investigate if the fading on each sub-channel for multi-carrier systems can be regarded as independent, therefore yielding potential results that may closely approach the theoretical upper bounds of chapter 6. It was shown in chapter 2 that the response of the mobile channel model can be attributed to several different mechanisms, including fast and slow fading, multipath and thermal noise. In CDMA communication systems the scenario is further complicated by the presence of multiple access interference (MAI). Therefore, the different systems investigated here have been studied in different channel models, with heavy emphasis on the effects of MAI and the performance of interference cancellation schemes in multipath faded channels.

8.6 System and Channel Configuration

The software has been written with a view to allowing simulation of a wide range of DS-CDMA systems. Table (8-1) shows the parameters of the uplink simulation employing multi-carrier modulation schemes on a non-coherent spread-spectrum design.

System Parameters	
modulation	DPSK
carrier frequency	1.6 GHz
timing mode	synchronous
coding	LROCC (R=1/32, k=5)
randomising sequence	Gold (31 chip + 1 chip)
data-rate	8 kb/s
number of sub-carriers	32
FFT length	32
guard interval length	4

Table 8-1. System parameters

Channel Model	
model type	tapped delay line (equal strength & delay)
time resolution	>0.5 us
number of multipath	4,7
Doppler frequency	300 Hz

Table 8-2. Channel model

8.7 Performance Results

The system design shown in figure (8-7) and (8-8) was simulated for a single user over a flat-band and frequency selective Rayleigh faded channel using LROC coding with and without an interleaver. The interleaver was chosen to be large enough to make successive block transmissions independent in the prevailing fading environment, therefore enhancing the decoder performance in high interference and fading levels. In practice, interleaving of depth 160 symbols was found to provide independent fading for each symbol and for the MC design it effectively provides interleaving in the frequency domain.

Figure (8-9) shows that the use of interleaving also plays a major part in frequency non-selective (flat-band) Rayleigh fading. Interleaving can improve the performance by more than an order in magnitude in BER, and hence is of vital importance if the fading is the limiting factor in performance. Even though the channel is frequency non-selective, the use of coding

still requires considerable interleaving in the time-domain to enable burst errors to appear independent over time in groups of successive code symbols. In frequency selective faded channels it is required to interleave the code symbols in the frequency domain. This method is engaged in the following simulations.

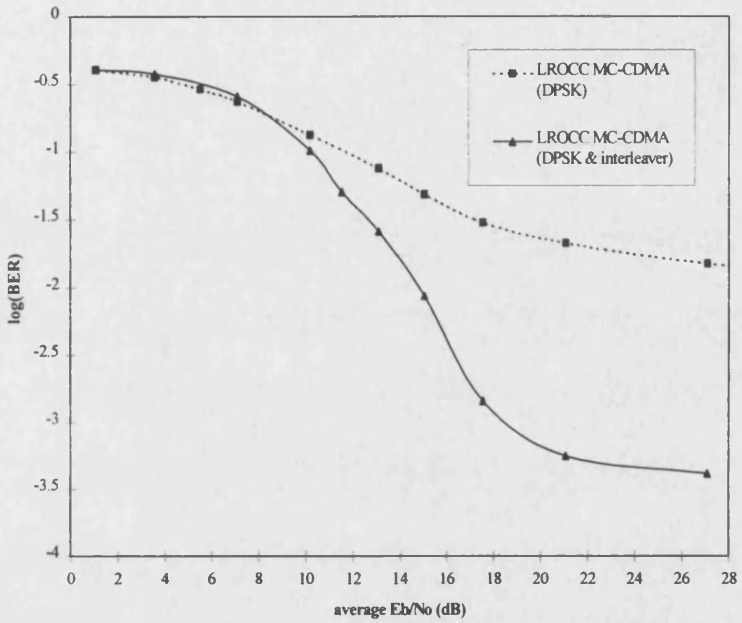

Figure 8-9. LROCC MC-CDMA single user case in flat-band Rayleigh fading with and without interleaver

The total bandwidth expansion (spreading factor) was set to 32 for all simulations of the system (including code rate and PN sequence length, where each PN sequence was increased in length by a single chip inserted on the end of the sequence). The Rayleigh fading component on each multipath signal in the frequency selective channel model was statistically independent for each path of the channel with a total mean signal power of unity. The number of distinct Rayleigh faded paths, L, at the receiver was set to 4 and 7 paths with a Doppler frequency of f_d=300Hz, corresponding to a vehicle speed of 203km/h at a carrier frequency of 1.6GHz. Figure (8-10) shows the performance for the uncoded and LROCC coded MC-CDMA design. Increasing the number of multipath components in the channel from L=4 to L=7 can be seen to have little effect on the BER performance in a frequency selective Rayleigh faded channel, as the effective order of diversity for the multi-carrier design is very high (≈32). Since the non-coherent differential equalisation and demodulation procedure is effectively carried out in the frequency domain, the number of paths that can be resolved in the receiver is of a relatively high order, compared with a conventional DS-CDMA RAKE receiver, as seen later.

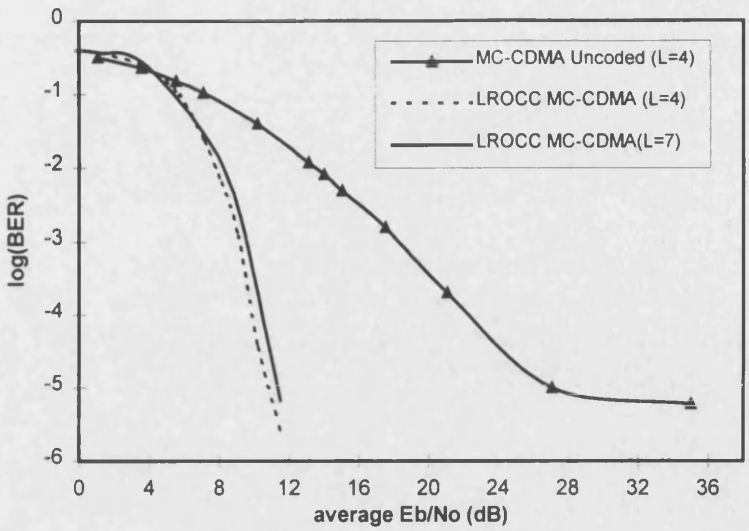

Figure 8-10. Uncoded MC-CDMA with 1 user using Gold codes v. LROCC MC-CDMA in L-path frequency selective Rayleigh fading

Next, a comparison is drawn between conventional single carrier DS-CDMA designs using convolutional coding and RAKE receivers. The DS-CDMA RAKE design uses conventional convolutional coding of rate R=1/2, K=5 to encode the data bits together with Gold codes of length 15 to provide additional spreading in the transmitter.

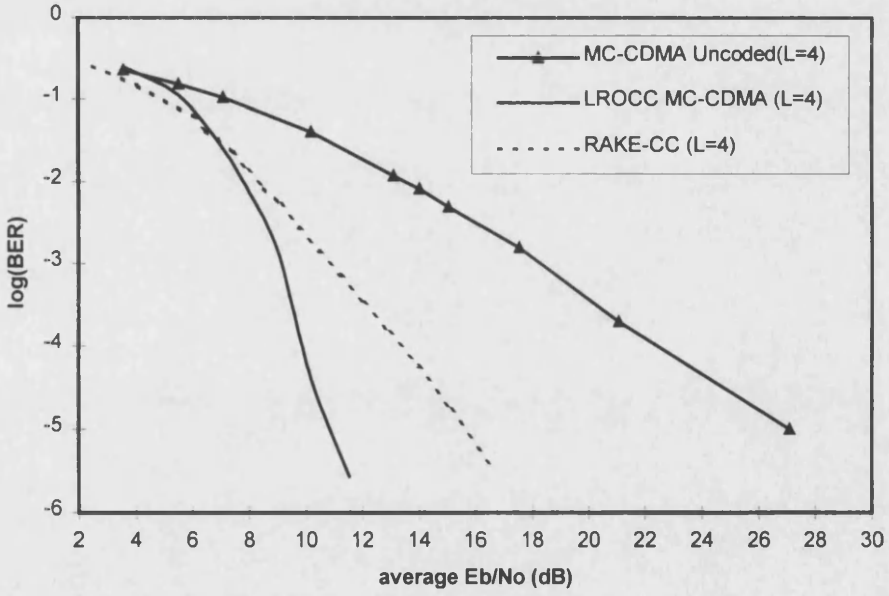

Figure 8-11. LROCC MC-CDMA v. single carrier DS-CDMA RAKE receiver for 1 user employing rate R=1/2 convolutional coding and Gold codes

It can be seen that the MC-CDMA LROCC implementation shows considerable performance improvements at high signal-to-noise ratios (figure 8-11 and 8-12). Note, that an increase in the

number of multipath components in the channel has a much more dramatic effect on the BER performance of a DS-CDMA RAKE receiver than for MC-CDMA coded designs.

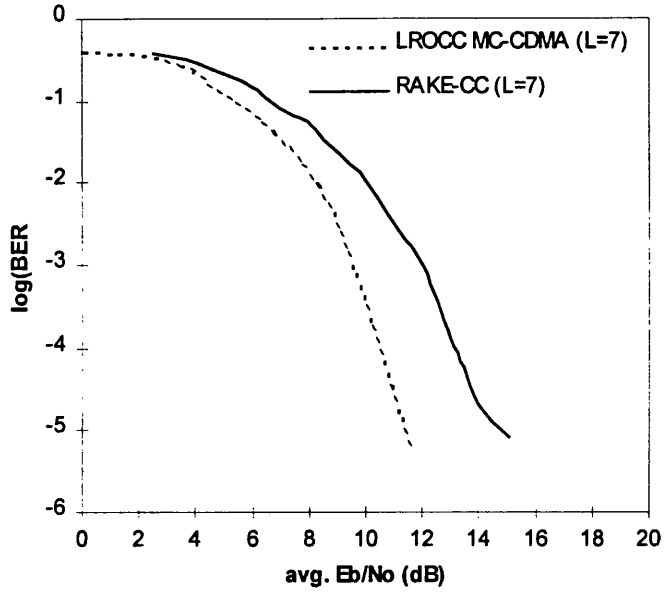

Figure 8-12. Uncoded and coded MC-CDMA compared with conventional coded RAKE design in 4-path fading for 1 user using Gold codes

This is due to the fact that the non-coherent equalisation for the RAKE receiver is now performed in the time-domain, where the effects of Doppler and the high number of multipath components are much more difficult to resolve.

8.8 Summary

This chapter has proposed the use of multi-carrier modulation for conventional DS-CDMA applications with coding and interleaving in a multipath faded channel.

The three main concepts of multiplexing spread-spectrum systems with multi-carrier schemes have been introduced with an outline of the relative advantages and disadvantages. The MC-CDMA system that has been investigated in this chapter uses a relatively small set of sub-carriers that are spaced in frequency by the inverse of the bit duration. Hence, the sub-carriers are allowed to overlap and the received amplitudes and phases of adjacent sub-carriers are correlated. Through adequate coding and equalisation this effect can be reduced, and a fair comparison could be drawn between an equivalent single carrier DS-CDMA system and a multi-carrier scheme using the same bandwidth.

A coherent BPSK MC-CDMA system was introduced with a performance comparison between the former system and a conventional DS-CDMA RAKE receiver using coherent detection and MRC. It could be seen that the MC-CDMA design approaches the lower bound on the BER performance much more closely than the DS-CDMA RAKE receiver. Coherent detection strategies, nevertheless, require knowledge about the channel statistics and are therefore not always the best choice for spectrally efficient systems. This calls upon the concept of non-coherent detection strategies, such as DPSK, which have been analysed in more detail for MC-CDMA designs using coding and interleaving.

The use of LROCC coding in conjunction with DPSK MC-CDMA without interleaving has shown to perform relatively badly in a flat-band Rayleigh faded environment. If interleaving is used, the coded system will improve in BER by an order of magnitude. This might not be so obvious at first, since we are dealing with a fading signal that is constant in magnitude over the whole spectrum. Nevertheless, we require adequate interleaving over a number of consecutive data bits (i.e. a large number of chip sets of length N) to randomise the effects of the fading signal. This is particularly important for coded systems where we seek to achieve random symbol errors. The effects of introducing interleaving are therefore to provide time diversity rather than frequency diversity in channels with high Doppler.

The use of LROCC strategies in MC-CDMA has shown to provide an extremely positive result in the overall coding gain achieved in multipath faded channels. A total coding gain of up to 12dB has been achieved for BER=10^{-5}, with little degradation in reduced levels of multipath.

It has also been shown that MC-CDMA techniques offer considerable improvement in performance over conventional time-domain RAKE receivers and in addition to higher-rate convolutional coding, LROCC coding with MC-CDMA can provide significant BER improvements. In a typical 7-path Rayleigh fading environment with Doppler of 300 Hz the performance improvement using LROCC MC-CDMA rather than rate 1/2 convolutionally coded DS-CDMA can be up to 3dB.

MC-CDMA techniques are far more resistant to increased number of multipath components compared with conventional time-domain RAKE receivers. Increasing the number of reflected paths from L=4 to L=7 has shown little degradation in BER performance.

To conclude, this chapter has shown the potential improvements that may be achieved through convolutional coding techniques and interleaving functions in MC-CDMA systems. We can see that the inherent frequency diversity of such a design is sufficiently large enough to provide

sufficient resilience to time-varying multipath channels with high Doppler. Nevertheless, adequate performance degradations would be anticipated in multi-user links, and for this reason the investigations in chapter 9 are more appropriate for multi-access communications.

8.9 References

[1] Baier, A *et al*, "Design study for a CDMA-based third generation mobile radio system", *IEEE JSAC*, Vol.12, pp.733-734, May 1994

[2] Prasad, R, "CDMA for Wireless Personal Communications", *Artech House*, Boston, London, 1996

[3] Weinstein, S B and Ebert, P M, "Data transmission by frequency division multiplexing using the discrete Fourier transform", *IEEE Trans. on Comm. Tech.* Vol. COM-19, pp.628-634, Oct.1971

[4] Alard, M and Lassalle, R, "Principles of modulation and channel coding for digital broadcasting for mobile receivers", *EBU Review*, Technical No.224, pp.47-69, Aug. 1987

[5] Chow, J S, Tu, J C and Cioffi, J M, "A Discrete Multitone Transceiver System for HDSL Applications", *IEEE JSAC*, Vol.9, pp.895-908, 1991

[6] *ETSI*, ETS 300 401, "Radio Broadcast Systems: Digital Audio Broadcasting (DAB) to mobile, portable and fixed receivers"

[7] Fazel, K, *et al* "A Concept of Digital Terrestrial Television Broadcasting", *Wireless Personal Communications*, Vol. 2, No 1&2, pp.9-27, 1995.

[8] *ETSI*, pr ETS 300 744, "Radio broadcast system for television, sound and data services; Framing structure, channel coding and modulation for digital terrestrial television"

[9] N. Yee, J.-P. Linnartz and G. Fettweis, "Multi-carrier CDMA for indoor wireless radio networks," Proc. IEEE-PIMRC'93, Yokohama, Japan, pp.103-113, Sept.1993.

[10] Sourour, E A and Nakagawa, M, "Performance of Orthogonal Multicarrier CDMA in a Multipath Fading Channel", IEEE Trans. on Comms., Vol. 44, No. 3, March 1996, pp. 356-367

[11] K. Fazel, "Performance of CDMA/OFDM for mobile communications system", Proc. IEEE-ICUPC'93, Ottawa, Canada, pp.975-979, Oct.1993

[12] K. Fazel, L. Papke, "On the performance of convolutionally coded CDMA-OFDM for mobile communications system", Proc. IEEE-PIMRC' 93, Yokohama, Japan, pp.468-472. Sept.1993

[13] V. DaSilva and E.S. Sousa, "Performance of orthogonal CDMA codes for quasi-synchronous communications systems," IEEE-ICUPC' 93, Ottawa, Canada, pp.995-999, Oct.1993

[14] S. Kondo and L.B. Mistein, "On the use of multicarrier direct sequence spread spectrum systems", *IEEE-MILCOM'93*, Boston, USA, *pp.52-56,* Oct.1993

[15] L. Vandendorpe, "Multitone direct sequence CDMA system in an indoor wireless environment," *Proc. IEEE-First Symposium of Communications and Vehicular Technology*, Delft, The Netherlands, pp.4.1.1-4.1.8, Oct.1993

[16] A. Chouly, A. Brajal, S. Jourdan, "Orthogonal multi-carrier techniques applied to direct sequence spread spectrum CDMA system", *Proc. IEEE Globecom'93*, Houston, USA, pp.1723-1728, Nov/Dec. 1993

[17] S. Kaiser, "Multi-Carrier CDMA Mobile Radio Systems", *Manuscript (PhD Thesis)*, to appear end 1997

[18] R. Prasad and S. Hara, "An Overview of Multi-Carrier CDMA", *Proc. IEEE ISSSTA'96*, Mainz, Germany, pp.107-114, Sept.1996

[19] Y. Yukitoshi and M. Nakagawa, "A Multiuser Interference Cancellation Technique Utilizing Convolutional Codes and Orthogonal Multicarrier Modulation for Wireless Indoor Communications", *IEEE Journal on Selected Areas in Communications*, Vol. 14, No.8, October 1996

[20] K. Fazel, S. Kaiser and M. Schnell, "A Flexible and High Performance Cellular Mobile Communications System Based on Orthogonal Multi-Carrier SSMA", *Wireless Personal Communications*, Kluwer Academic Publishers, pp.121-144, 1995

[21] T. Mueller *et al,* "Comparison of different Detection Algorithms for OFDM/CDMA in Broadband Rayleigh Fading", *IEEE Conference Publication*, pp. 835-838, 1995

[22] S. Kaiser, "OFDM-CDMA versus DS-CDMA: Performance evaluation for fading channels", *Proc. IEEE International Conference on Communications* (ICC'95), pp.1722-1726, June 1995

[23] Maxey, J J and Ormondroyd, R F, "Optimisation of orthogonal low-rate convolutional codes in a DS-CDMA system", *IEEE/URSI Conference Proceedings of ISSSE'95*, Vol. 95TH8047, pp. 493-496, 1995

[24] Maxey, J J and Ormondroyd, R F, "Low-Rate Orthogonal Convolutional Coded DS-CDMA using Non-Coherent Multi-Carrier Modulation over the AWGN and Rayleigh Faded Channel", *IEEE Conference Proceedings of ISSSTA'96*, Vol. 2, pp.575-579, 1996

[25] Viterbi, A J, "Very Low-Rate Convolutional Codes for Maximum Theoretical Performance of Spread-Spectrum Multiple-Access Channels", *IEEE Journal on Selected Areas in Communications*, Vol. 8, No. 4, May 1990

[26] Viterbi, A J, "CDMA-Principles of Spread Spectrum Communication", *Addison Wesley*, 1995

[27] COST 207: *Digital land mobile radio communications*, Final Report, Commission of the European Communities, Luxembourg 1989

[28] Stirling-Gallacher, R A and Povey, G J R, "Comparison of MC-CDMA with DS-CDMA Using Frequency Domain and Time Domain RAKE Receivers", *Wireless Personal Communications*, pp. 105-119, Kluwer Publications, 1995

CHAPTER 9:

MULTI-USER MC-CDMA SYSTEMS

9.1 Introduction

The system investigated here is similar to the design in chapter 8, except that we now employ a much higher number of N overlapping sub-carriers on the downlink, each with a low data-rate. The up- and downlink schemes are regarded as fully coherent in a multi-access environment, with an uplink strategy similar to the non-coherent design featured in the previous chapter. Here, the number of sub-carriers for every user is relatively small compared to the downlink OFDM modulator. This allows a direct mapping of the LROCC spreading to the number of orthogonal sub-carriers in the IFFT. By allowing the sub-carriers to overlap, we obtain a much higher spectral efficiency than through non-overlapping carrier separation. Chapter 8 has shown that the MC-CDMA design can outperform a conventional DS-CDMA RAKE receiver in a single-user multipath environment. We now extend our work to include a multi-access strategy with interference from other active users in the channel. This requires more sophisticated detection strategies such as interference cancellation and channel estimation strategies to be used.

In addition to the MC-CDMA system introduced previously in chapter 8, the OFDM modulator here uses more than one data bit for each OFDM symbol per user. This has the added advantage of providing an increase in the total number of sub-carriers, therefore lowering the data rate on each sub-carrier. This system, of course, is based purely on a coherent design, and is therefore of particular interest to the downlink of a mobile or fixed wireless access communication system. To maintain orthogonality between the individual sub-carriers and prevent ISI, an extended guard interval is introduced into the system. This guard interval must be longer than the maximum delay spread of the multipath channel. The relative advantages and disadvantages of using such a system are discussed in the following sections.

9.2 Independent Fading Channel

In an OFDM system, a blockwise transmission of blocklength $N+\Delta$, where Δ is the length of the guard interval (cyclic extension), is assumed to eliminate the inter-block interference if the cyclic extension is greater than or equal to the length of the channel impulse response. It can be shown that in OFDM systems, if in addition to the cyclic expansion the transmission function is (nearly) constant during one block, then the different sub-channels are de-coupled. Hence, the inverse Fourier transform in the transmitter and the Fourier transform in the receiver transform a frequency selective channel into N parallel flatband faded channels.

The simplified model of a basic MC-CDMA system is depicted in figure (9-1).

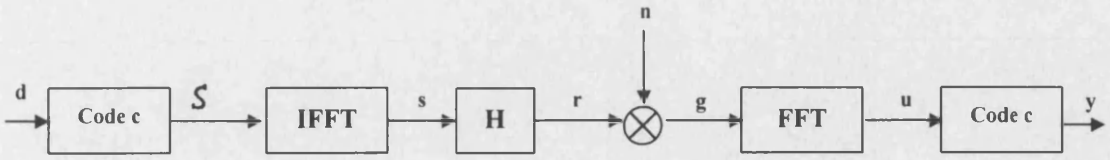

Figure 9-1. Simplified MC-CDMA system model

In this model, the transmitted sequence ***S*** (after coded by code ***c*** of length N) is applied to the inverse FFT, then passed through the channel with the discrete transfer function ***H*** and received with AWGN vector ***n***. In the receiver, the signal is then passed through the FFT to obtain an estimate of the transmitted data. The variables, $h_{l,l}$, representing the fading of the sub-carriers, are correlated variables with Rayleigh statistics and can be assumed uncorrelated when the carriers are separated further than the coherence bandwidth. Hence, the matrices ***H*** and ***G*** are diagonal matrices with non-zero values at $h_{l,l}$ and $g_{l,l}$, l=1,2...N, respectively. The discrete-time channel transfer function is derived from the channel impulse response via the FFT, and hence the complete system can be modeled as a simple 'straight-wire' model with independent fading on each sub-carrier. The equivalent discrete-time model is shown in figure (9-2).

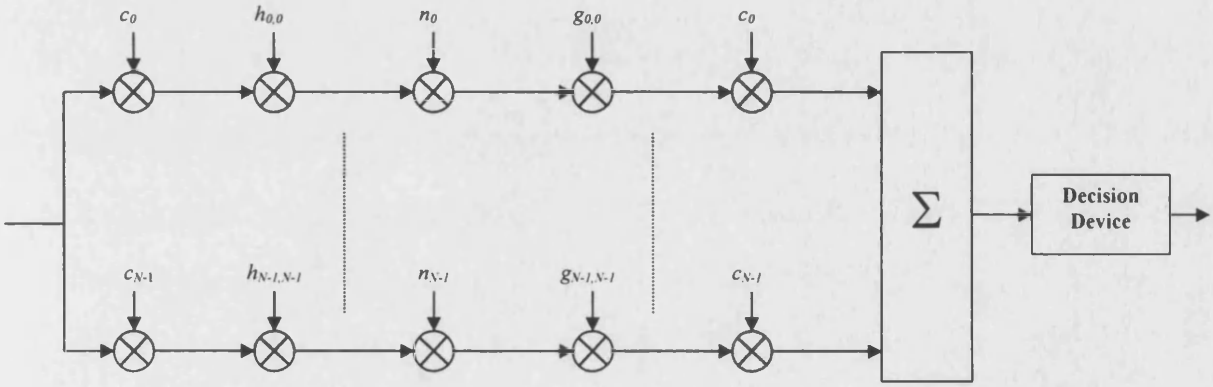

Figure 9-2. Simplified frequency-domain independent sub-channel faded MC-CDMA system model

The complex time-domain signal, $s(t)$, at the output of the OFDM modulator can be given by:

$$s(t) = \sum_{l=0}^{N-1} d_l c_l e^{j2\pi f_l t} \qquad t \in [0, T_b] \tag{9-1}$$

where f_l is the assigned sub-carrier frequency, given by:

$$f_l = f_o + \frac{l}{T_s} \tag{9-2}$$

with f_o as the lowest sub-carrier frequency at a distance of $1/T_s$, where T_s is the symbol duration. The NxN matrix $\boldsymbol{H}$ describes the complex channel fading on the sub-carriers assigned to the transmitted vector $\boldsymbol{s}$ and the corresponding complex equalisation matrix is given by $\boldsymbol{G}$. After equalisation by the complex NxN matrix $\boldsymbol{G}$ the output of the FFT demodulator, $\boldsymbol{u}$, can be expressed as a complex vector of length N (assuming Δ has been chosen greater than the multipath spread of the channel):

$$\mathbf{u} = \mathbf{d} \cdot \mathbf{c} \cdot \mathbf{G} \cdot \mathbf{H} + \mathbf{G} \cdot \mathbf{n} \tag{9-3}$$

It can therefore be shown that a valid simplification to the transmitter, fading channel model and receiver can be made. Assuming that a guard-band greater than the maximum delay spread of the channel is used to eliminate ISI, we can approximate our analysis with the independent fading channel model over all sub-carriers of the MC-CDMA system.

9.3 Multi-User MC-CDMA System

The work in this thesis forms an extension of the system proposed in [1]. Here, the transmitted data bits of the individual users in the system are spread by the user specific orthogonal code (such as Walsh-Hadamard codes) and then summed over all users. In this way, all users remain orthogonal in the basestation and can consequently be interleaved and modulated as a composite signal onto the N orthogonal sub-carriers in the OFDM modulator. An overhead for the pilot symbols must be taken into consideration since coherent detection is assumed. The MC-CDMA system proposed in [1] can be seen in figure (9-3).

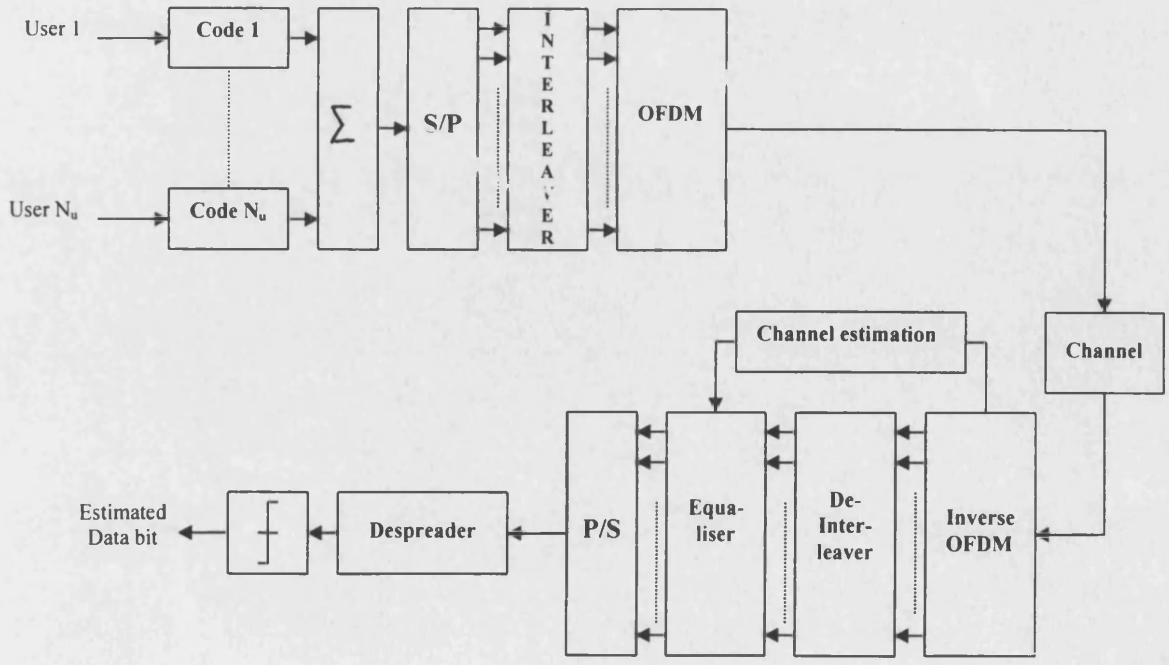

Figure 9-3. MC-CDMA downlink system

In the receiver, the OFDM demodulator attempts to restore the orthogonality of the received sequence by removing the guard-band interval and equalising over all N sub-carriers. To detect the received signal at the output of the OFDM demodulator, the channel statistics must be known or estimated. A variety of equalisation strategies may be used:

1. Zero-forcing (ZF)
2. Equal Gain Combining (EGC) (Phase-only equalisation)
3. Maximum Ratio Combining (MRC)
4. Controlled Equalisation (CE)
5. Minimum Mean Square Error (MMSE)
6. Maximum Likelihood Detection (MLD)

The use of MLD places strict requirements on the processing power available and is therefore only feasible for small spreading sequences, on the order of M=10 or less, since 2^M sequences must be evaluated in the receiver. The frequency diversity achievable with such a system is therefore limited, but makes the use of MLD detection schemes more realistic. It has been shown [2] that the order of frequency diversity, nevertheless, does not need to exceed values of more than 10 for considerable improvements in performance. The use of low spreading ratios will inevitably give a small number of sub-carriers in the OFDM modulator, which may present a problem in channels with a large coherence bandwidth.

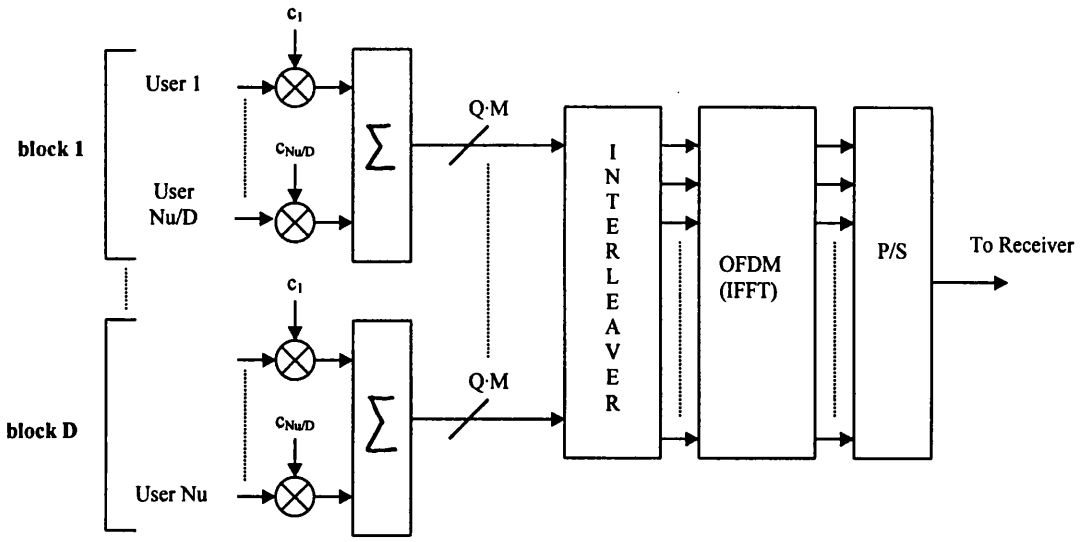

Figure 9-4. MC-CDMA downlink basestation transmitter

To combat this problem a slightly modified version of figure (9-4) has been proposed [2] that enables smaller spreading sequences to be employed and still uses a relatively large number of

sub-carriers. Here, the user's in the basestation are grouped into D blocks of 8 users, typically, with spreading codes of equal length M=8 and orthogonal over all 8 users. This gives a maximum frequency diversity of 8. The same codes are used for all blocks and each block collects the output of Q=8 successive data bits to give a total of 64 chips per 8 user block for each OFDM symbol. This enables the sub-carriers to be separated in the frequency domain through the interleaver by at least 64 sub-carriers. A total of 64 users can therefore be accommodated on N=512 carriers and achieve MLD upon evaluation of 256 sequences.

The performance of different equaliser structures have been studied in [2] and are featured in more detail in the next section.

9.4 Equalisation and Detection

A variety of different detection techniques have been discussed in the literature [3-10] and the purpose of this section is to familiarize the reader with the different algorithms available. Some are more complex than others and provide a better bit-error rate performance depending on the type of channel knowledge required at the receiver. Hence, a complexity comparison can not always be justified as being the most accurate method of system comparison.

9.4.1 Equal Gain Combining (EGC)

This method is also commonly referred to as *phase only* equalisation since it brings all phases to a common point and combines them. It is based on correcting the phase shift of each sub-channel but not the attenuation of the channel fading. The equaliser coefficients for all sub-carriers using EGC are given by:

$$g_{l,l} = \frac{h_{l,l}^{*}}{|h_{l,l}|} \tag{9-4}$$

where $h_{l,l}$ and $g_{l,l}$ are the diagonal matrix elements of $\boldsymbol{H}$ and $\boldsymbol{G}$, respectively. The method of EGC is a suitable approach for an AWGN channel, where the function $g_{l,l}$=1 for all sub-carriers, but fading channels with different amplitudes $g_{l,l}$ will cause interference between the information symbols, hence the orthogonality between the Walsh-Hadamard codes is violated. EGC is interference-limited and has a large error floor, as can be seen later in figure (9-5).

9.4.2 Zero-Forcing (ZF)

An ideal zero-forcing equaliser is simply an inverse filter which has a frequency response that is the inverse of the frequency response of the transmitter and channel cascaded and folded about the sampling frequency, $1/T_s$. The simplest way to equalise the channel would be to multiply all sub-carriers by the inverse of the discrete-time channel transform in attempt to restore the orthogonality of the spreading sequences. The term *zero-forcing* originates from the concept of nulling out and forcing zeros at the sampling instants either side of the main pulse response. Therefore, the interfering symbols can be nulled or forced to zero, hence eliminating ICI. The equaliser coefficient $g_{l,l}$ is given by:

$$g_{l,l} = \frac{1}{h_{l,l}} \tag{9-5}$$

The zero-forcing equaliser does not account for the effects of noise, and in addition, the traditional finite-length transversal filter equaliser in the time-domain excessively enhances the channel noise at frequencies where the folded channel frequency response has high attenuation. For this reason zero-forcing equalisation schemes are noise limited rather than interference-limited when $h_{l,l}$ is small, since it is an orthogonality-restoring correlation function. In a rapid fast-fading environment, nevertheless, this can quickly become a problem, and it is therefore more applicable to suggest a combined equaliser structure that only applies zero-forcing when the fading signal on each sub-carrier is greater than a given threshold.

9.4.3 Controlled Equalisation (CE)

This equalisation function reduces the noise introduced by amplification of weak sub-carriers through the use of a pre-determined threshold value, p_{thres}. If the channel attenuation $|h_{l,l}|$ is below the threshold, only phase equalisation is applied to prevent noise amplification, and if the channel attenuation is above the threshold, zero-forcing equalisation is applied. The assigned equalisation co-efficient is given by:

$$g_{l,l} = \begin{cases} \dfrac{1}{h_{l,l}} & |h_{l,l}| \geq p_{thres} \\ \dfrac{h_{l,l}^*}{|h_{l,l}|} & |h_{l,l}| < p_{thres} \end{cases} \tag{9-6}$$

The BER depends on the noise level and on the interference due to sub-carriers that fade below the threshold. As the level of p_{thres} rises, the bit-error rate is dominated by the loss of orthogonality when $h_{l,l}$ is small. This phenomenon is particularly prominent at low signal to noise ratios. At high E_b/N_o, we still incur an irreducible BER due to the loss of orthogonality through the application of EGC when the attenuation on the sub-carriers is high.

9.4.4 Maximum Ratio Combining (MRC)

The term *maximum ratio* refers to maximising the signal-to-noise ratio, whereby this combining technique attempts to combine the maximum SNR of each multipath component. This technique is a very popular choice in the design of time-domain RAKE receivers for conventional DS-CDMA applications. Viewed in the frequency domain, maximum ratio combining (MRC) can be viewed as correcting the phase shift and weighting the received signal with the attenuation of the channel fading. This technique does not suffer in the same way as zero-forcing equalisation when $h_{l,l}$ is small. The assigned equalisation co-efficient is given simply as the complex conjugate of the channel co-efficient, i.e,

$$g_{l,l} = h_{l,l}^{*} \tag{9-7}$$

A performance comparison of an OFDM-CDMA downlink design based on figure (9-3) with different equalisation and combining techniques can be seen in figure (9-5).

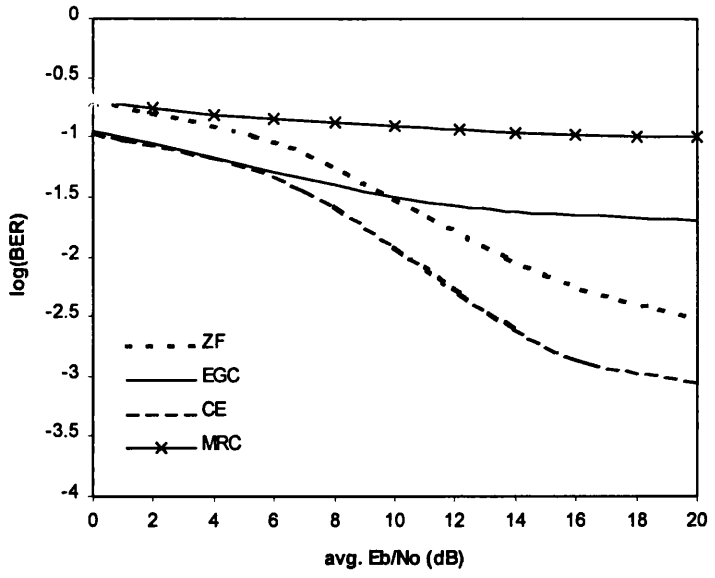

Figure 9-5. BER performance of a MC-CDMA downlink at N_u= 64 users

Here, the basestation is loaded to half its maximum capacity and communicating with each mobile over the Bad Urban channel (COST 207) at a Doppler frequency of 200 Hz. Each user communicates at a data rate of 19 kb/s and is spread by orthogonal Walsh-Hadamard sequences of length 64. The number of data bits per user per OFDM symbol is set to 8, therefore giving a total number of 512 sub-carriers.

It can be seen that controlled equalisation performs better than zero-forcing equalisation and equal gain combining (phase only) at high E_b/N_o, as expected, but there is, in general, only a marginal discrepancy in performance between EGC and MRC.

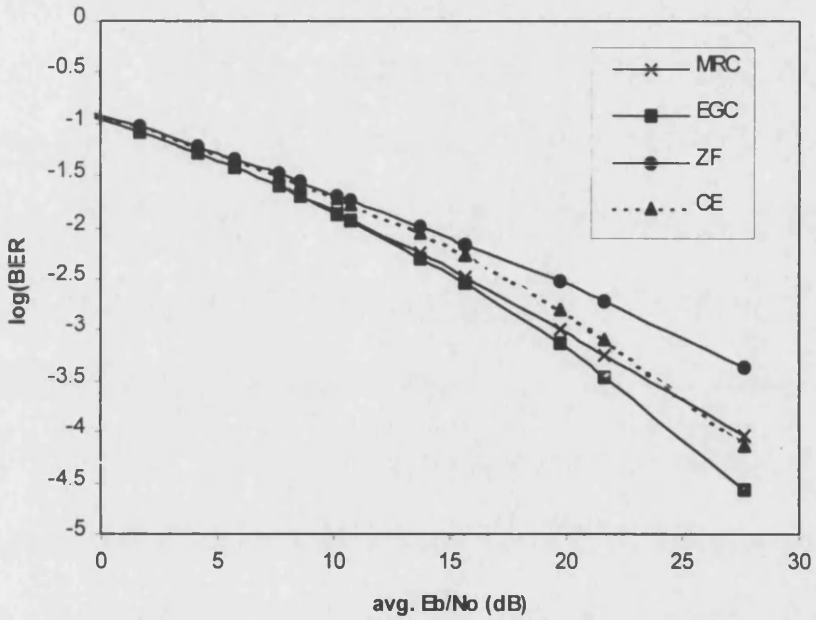

Figure 9-6. Comparison of different equalisation schemes at N_u=16 users in a Bad Urban channel

At N_u=16 active users only a small discrepancy in performance between the different equalisers can be found. This is shown in figure (9-6). The small variation in performance is due to the fact that the loss of orthogonality between users due to inadequate equalisation has less implication on the overall performance than at a higher number of active users.

To improve the performance at high numbers of active users we need to use more sophisticated equalisation structures. These require a little more information about the channel, such as the number of active users or SNR, and are presented in the next sub-sections.

9.4.5 Minimum Mean-Square Error (MMSE) Detection

The MMSE equalisation structure requires knowledge about the channel signal-to-noise ratio and the number of active users, N_u, and attempts to correct the phase shift and attenuation of the channel fading by minimising the mean-square error which consists of the sum of the squares of all the ISI terms plus the noise power at the equaliser output. The MMSE equaliser therefore maximises the signal-to-distortion ratio at its output within the constraints of the equaliser length and delay. The MMSE criteria is given by Proakis [15]:

$$g_l = \frac{h_l^*}{|h_l|^2 + \frac{\sigma_n^2}{\sigma_a^2}} \tag{9-8}$$

where σ_n^2 is the variance of the additive noise and σ_a^2 is the variance of the transmitted data symbol. For data of amplitude {+1,-1} with equal probability the variance is $\sigma_a^2=1$, since the probability of transmitting +1 or −1 is equally likely, i.e. p(-1) = p(+1) = ½. In a multi-user environment, the variance of the additive noise per carrier is given as:

$$\sigma_a^2 = N_u$$
$$\sigma_n^2 = M\frac{N_o}{2E_b} \tag{9-9}$$

where $2E_b/N_o$ is the SNR per data bit. Therefore, for multi-user MC-CDMA applications this results in an equalisation co-efficient given as:

$$g_{l,l} = \frac{h_{l,l}^*}{|h_{l,l}|^2 + \frac{MN_o}{2N_uE_b}} \tag{9-10}$$

where N_u is the number of active users, E_b/N_o denotes the average signal-to-noise ratio and M is the spreading ratio. The additional complexity needed to obtain information about the number of active users and the average SNR can be avoided by employing a sub-optimal MMSE equalisation method. This fixes the value of N_u to be set at the full maximum user capacity and E_b/N_o to be the maximum allowable SNR. In [3] it has been shown that the optimal and sub-optimal solution have a similar performance for E_b/N_o in the range of 10dB up to 16dB. At higher signal-to-noise ratios (e.g. 20dB) the sub-optimal solution performs up to 2dB worse. For E_b/N_o much smaller than 10dB both solutions fail.

9.4.6 Maximum Likelihood Detection (MLD)

Instead of despreading the received sequence using a simple PN sequence multiplication, the receiver is modified by inserting a MLD to detect the most likely sequence sent. This requires knowledge of the number of users and the channel statistics, and hence its complexity grows exponentially when the number of active users increases. The MLD evaluates the Euclidean distance, δ_i^2, between the received and all possible transmitted sequences, $\boldsymbol{p}_i$. The sequence that minimises the function

$$\delta_i^2 = \min\left\|\mathbf{g} - \mathbf{G}\mathbf{p}_i\right\|^2 \tag{9-11}$$

is chosen as the survivor, $\boldsymbol{p}$. In this technique the sequences $\boldsymbol{p}_i$ are therefore weighted with the channel fading $\boldsymbol{H}$ to give a resulting equalisation co-efficient:

$$g_{l,l} = h_{l,l} \tag{9-12}$$

The sequence $\boldsymbol{p}$ that minimises (9-11) is then despread by the spreading code $\boldsymbol{c}$ in the conventional way.

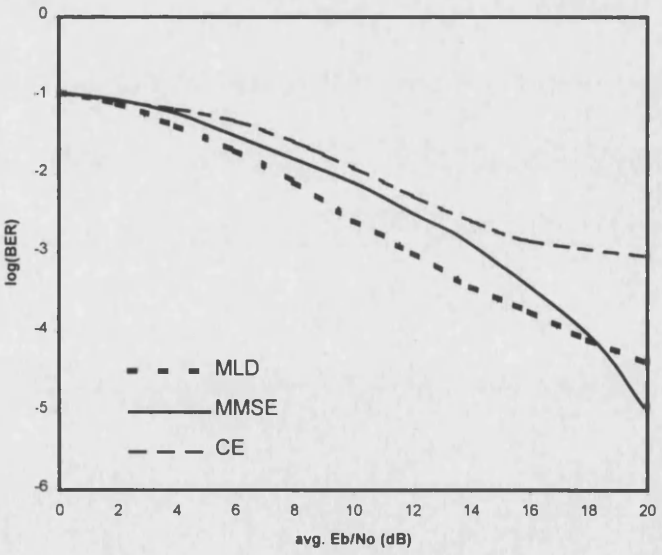

Figure 9-7. Comparison of MLD, CE & MMSE equalisation schemes at full user capacity N_u=64 in a Bad Urban channel

It has been shown by Verdu [16] that MLD will ultimately give the best performance and, although it offers the best performance, the MLD function is not as robust as the MMSE criterion. This can be seen in figure (9-7), where the MLD scheme approaches an irreducible

BER of 10^{-5} and the MMSE algorithm still drops further in BER at high SNR. At relatively low SNR, the MLD scheme outperforms the MMSE algorithm by about 2dB.

9.5 Successive Interference Cancellation

For a single-cell multiple access system, assuming unfaded transmission for each user over a common additive white Gaussian noise channel, information theory can be used to demonstrate that interference from same-cell users can be completely eliminated by a process of successive cancellation of interfering users [17,18]. The resulting capacity of the multiple user channel is given by the classical AWGN formula [19], with rate referring to the sum of the rates of all users and signal power being the sum of the received powers (at the basestation) from all users. Though the proof of this result is constructive, meaning that the method for achieving the result is specified, there are several aspects of the technique that will render it impractical:

1. an arbirarily long and powerful FEC code is required
2. arbitrarily long processing delays are involved
3. reception is unfaded, or fading is very slow compared to a frame duration
4. all received users must be processed together to recover any one user

All four of these conditions can be relaxed, with some compromise in performance, to achieve a reasonable level of complexity and delay. However, the resulting performance will most likely be worse than can be achieved by applying other simple, more robust techniques. Nevertheless, the use of multi-carrier DS-CDMA systems can attempt to transform the frequency-selective fading channel into a slow-fading non-selective channel, making interference cancellation techniques a likely contender; especially for fixed wireless access (FWA) systems. The need to employ convolutional coding techniques has been assumed as established and provides the necessary requirements for successfully implementing interference cancellation schemes.

There are two main types of interference cancellation proposed to date: (a) successive (or serial) interference cancellation, and (b) parallel interference cancellation.

The technique of successive interference cancellation (IC) relies on locally regenerating an interference replica within the receiver, which can then be subtracted from the compound signal to increase the signal-to-interference ratio of the residual. Successive interference cancellation schemes rely on knowledge of the strongest user's received signal on the uplink and consequently delete the interference effects on the next successive strongest interferer. This

technique can therefore provide the best performance if all users are received at different power levels (such as a geometric power distribution) rather than power-controlled to their own basestation. One or more cancellation stages may be employed in order to reduce interference to the requisite level. Subsequent stages then cancel interference from other users in order of received power level.

Clearly, effective cancellation relies on a number of factors including accurate knowledge of the received signal levels, cross-correlation and user timing. Figure (9-8) depicts an interference canceller for the *k*th user, which is typical of those proposed in the literature. Two interference cancellation stages follow the initial detection, with estimates of the data available at each stage. The most accurate estimate of the received symbol is available at the output of the final stage.

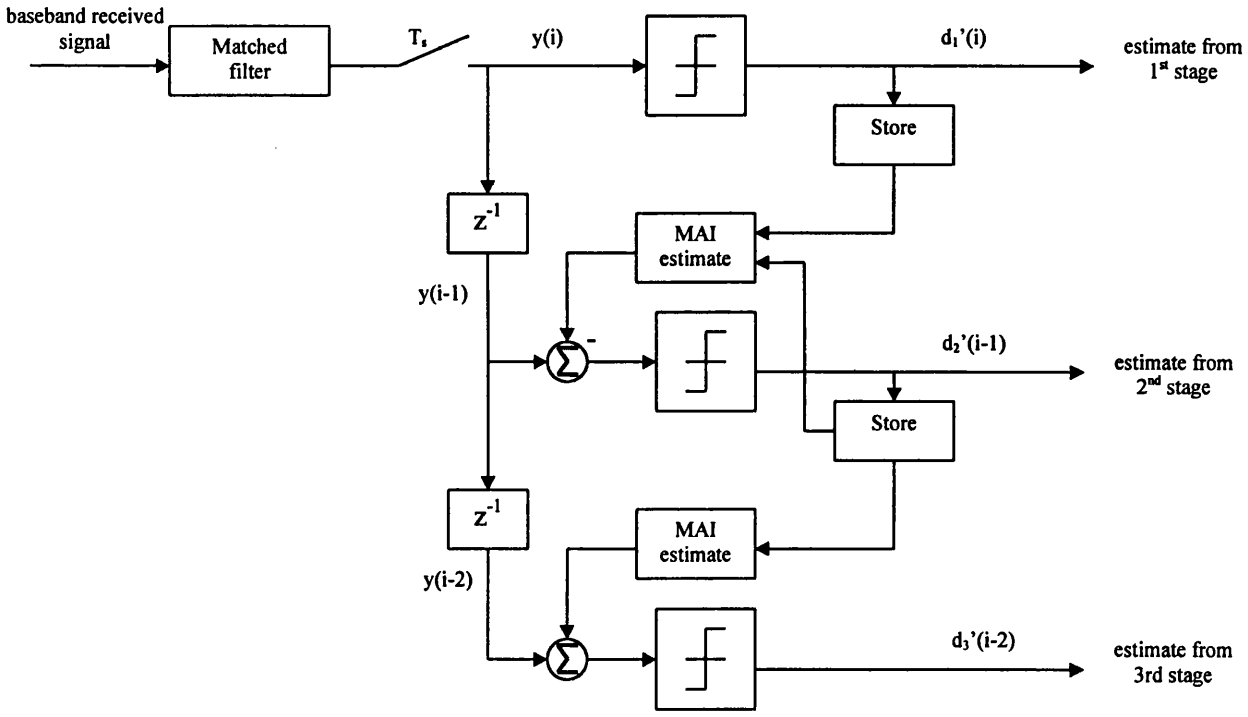

Figure 9-8. Successive interference canceller for the *k*th user of a multi-user system

The application of successive interference cancellation techniques to multi-user detectors for DS-CDMA has been considered by Varanasi [20] and several other authors [21-24]. These receivers are effective under ideal conditions but all tend to suffer from the following shortfalls in a realistic environment which prohibit complete mitigation of the near-far effect:

- **Time delay**

  Interference cancellation can introduce a significant time delay penalty, particularly when a number of stages are employed. For the example shown in figure (9-8) the most reliable estimate of the received data is delayed by two symbol periods. This time delay may be intolerable in certain systems.

- **Complexity**

  For a multi-user receiver employing several cancellation stages for each user the hardware requirement rapidly becomes burdensome, particularly as hardware is also required for accurate signal level measurement and timing recovery.

- **Poor performance under equal-power conditions**

  In the Rayleigh fading channel near-far conditions prevail for the majority of the time and IC schemes will perform well as a reliable decision can be made on the strongest signal, but as the channel is non-stationary, users will at times have equal powers and outages could occur as a result of poor IC performance under such conditions. When equal-power conditions arise, some schemes revert to conventional detection. More generally, the non-stationarity of the channel means that the optimum number of cancellation stages varies and fixed architectures will perform badly under equal-power conditions.

- **Susceptibility to errors in channel and timing parameter estimation**

  Little work currently exists on the performance of interference cancellers under conditions of imperfect timing recovery and signal level estimation, but nevertheless successful interference cancellation is strongly dependent on the estimates of these parameters.

- **Susceptibility to 'unknown' interference sources**

  Interference regeneration can only be performed for known sources. For multi-user cellular solutions this means that only intra-cell interferers may be cancelled (as their signature waveforms and timing are known to the basestation receiver) inter-cell interference may therefore still set limits on performance improvements available from interference cancellation. Other unforeseen sources might include the 'open' failure of a handset or cochannel interference from conventional narrowband systems.

9.6 Parallel Interference Cancellation

The use of parallel interference cancellation suffers from many of the same tradeoffs as successive interference cancellation schemes outlined earlier. Unlike successive schemes, parallel interference cancellation structures require the received power of every user to be the same. In this way, all users are demodulated, decoded and detected simultaneously and subtracted from the composite original received signal at the same time. This process can be then repeated in an iterative fashion, but it has been found that the first initial iteration gives the highest gain, with only a marginal improvement in subsequent stages [3]. The problem of time-delay quickly becomes a limiting factor on the number of iterations if coding techniques and more complicated demodulation schemes are used. For the aforementioned reasons we only concern ourselves with one stage of cancellation, therefore reducing the problems of time-delay in the receiver.

9.6.1 Downlink Model

The base station to mobile downlink offers a number of options for the most efficient detection process of the wanted-user. Orthogonal CDMA codes give the most robust distance separation in the code domain and will inherently give the best performance for time-aligned users in the basestation transmitter. The introduction of convolutional coding can significantly improve the BER, depending on the operating E_b/N_o. This improvement is at the cost of bandwidth but, generally, the coding gain is larger than the bandwidth penalty. In AWGN channels, orthogonal codes give an optimum performance and no further improvements in BER can be gained through MAI cancellation techniques. However, in frequency selective faded channels, the performance of the system can be enhanced through parallel interference cancellation, which uses a two-stage detection process. This is the situation assumed in this thesis.

9.6.1.1 Basestation Transmitter

The downlink design is based closely on the system proposed by Fazel [2], shown in figure (9-9). In this system, the base station communicates with N_u users simultaneously. Walsh-Hadamard orthogonal codes are assumed for the CDMA spreading sequence and all data bits and spreading chips are assumed to be time-aligned. In order to shorten the length of the orthogonal spreading sequence of each user, and to allow more complex detection algorithms

such as MLD to be employed, this transmitter architecture groups the N_u simultaneous users into D transmission blocks. Each of these blocks can be viewed as a 'mini CDMA' base station of only N_u/D users, rather than N_u users. Within this block, each user, i=1,2...N_u/D, transmits a data sequence, $d_i \in (-1,+1)$, clocked at a rate, $1/T_b$, and this is encoded using a convolutional encoder of rate R to produce a sequence of encoded symbols, e_i, each of duration $T_{cod}=RT_b$. The encoded symbols are then multiplied by the individual, user-specific, orthogonal spreading code, $c_i=[c_i(1),c_i(2)...c_i(N_u/D)]^T \in (-1,+1)$, where $[.]^T$ is the transposed matrix. Note that each block of N_u/D users employs the same set of orthogonal codes as the other (D-1) blocks. The overall spreading ratio for each data bit is therefore given as, $M=N_u(D.R)^{-1}$. Because orthogonal spreading codes have zero cross- correlation, the maximum capacity of the base station for all D blocks is $N_B=N_u$. The coded and spread data is summed bit- and chip-synchronously with the other-users of the block and then buffered. In the analysis below we ignore the time index and consider the processing of a single block of data bits.

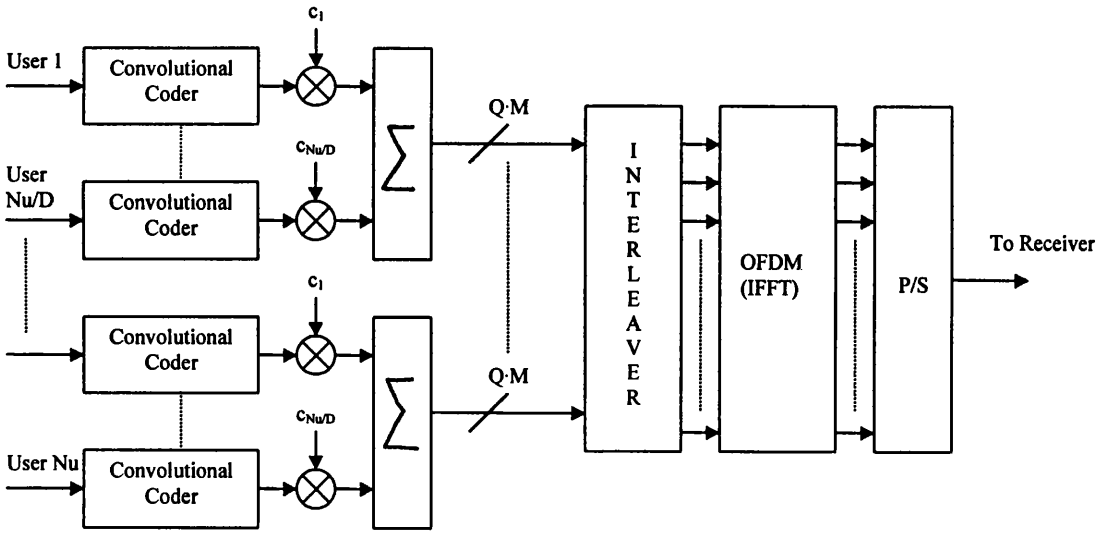

Figure 9-9. Convolutional coded multi-user MC-CDMA downlink basestation transmitter design

Consequently, the transmission vector, S_d, of the spread signals in the buffer of the d^{th} transmission block prior to interleaving and OFDM modulation is given by:

$$S_d = \sum_{i=M(d-1)+1}^{Md} e_i c_i \tag{9-13}$$

To give some freedom to the number of sub-carriers that can be generated per data bit, each user can transmit Q data bits per OFDM symbol. Each of these are spread by the factor, M. Consequently, the size of each summing buffer is $Q.M$ and the total number of parallel inputs to

the interleaver (and hence the size of the IFFT which performs the OFDM modulation) for all D blocks is thus $D.Q.M$.

After interleaving and OFDM modulation the output sequence may be represented by the complex vector sequence $\mathbf{V} = [v_1, v_2 \ldots v_{D \cdot Q \cdot M+\Delta}]$ where Δ is the guard interval length. This vector contains Δ additional terms representing the guard interval that is inserted between adjacent OFDM frames. The guard interval forms a cyclic extension to the vector sequence $\mathbf{V}$, whereby the first Δ elements of $\mathbf{V}$ are duplicated as the last Δ elements of $\mathbf{V}$. This reduces the effects of ISI due to the multipath spread in the fading channel, and if the guard interval length is greater than the multipath spread length of the channel, the OFDM blocks are orthogonal. The output of the OFDM modulator may be expressed as:

$$x(t) = \sum_{q=0}^{Q-1} \sum_{d=0}^{D-1} \sum_{l=0}^{M-1} s_{q,d,l} \cdot e^{j2\pi f_{qDM+dM+l} t} \quad \text{for } -\Delta < t < T_b \tag{9-14}$$

where $s_{q,d,l}$ is the l^{th} component of S_d of the q^{th} data bit and the orthogonal sub-carrier frequency, $f_{qDM+dM+l}$ is given by:

$$f_{qDM+dM+l} = f_o + \frac{qDM + dM + l}{T_s} \tag{9-15}$$

where f_o is the lowest sub-carrier frequency and T_s is the symbol duration.

The output vector to be transmitted over the channel is represented by complex coefficients on the output of the IFFT in the modulator. Although all the users are orthogonally coded, because of the effect of the multipath channel, the wanted-user is corrupted by the other users. In this case, the channel has the same effect on the other-user interference as the wanted-user and so effective equalisation plays an important part in regaining orthogonality between the users in the received signal at any remote receiver. The amplitude and phase characteristics of the channel may be described by a complex matrix, H_d, of size $M \times M$ for the d^{th} transmission block. Since a perfect guard-interval length is assumed, the channel matrix H_d is a diagonal matrix with diagonal components $h_{l,l}$.

9.6.1.2 Remote Receiver

In the remote receiver of the wanted-user, shown in figure (9-10), the multi-user OFDM signal is demodulated in the usual way using the FFT. As is often the case, we assume that the delay spread of the channel is less than the guard interval and that the channel statistics can be

considered stationary over the OFDM block duration, T_b (i.e. $T_b << 1/f_{dop}$ where f_{dop} is the Doppler frequency offset). The received signal is given by:

$$y(t) = \sum_{q=0}^{Q-1} \sum_{d=0}^{D-1} \sum_{l=0}^{M-1} h_{q,d,l} s_{q,d,l} \cdot e^{j2\pi f_{qDM+dM+l}} + n(t) \tag{9-16}$$

where $h_{q,d,l} = \rho_{q,d,l} e^{j\phi_{q,d,l}}$ is the complex channel fading characteristic with attenuation $\rho_{q,d,l}$ and phase shift $\phi_{q,d,l}$ at sub-carrier frequency $f_{q,d,l}$ and $n(t)$ is the additive noise.

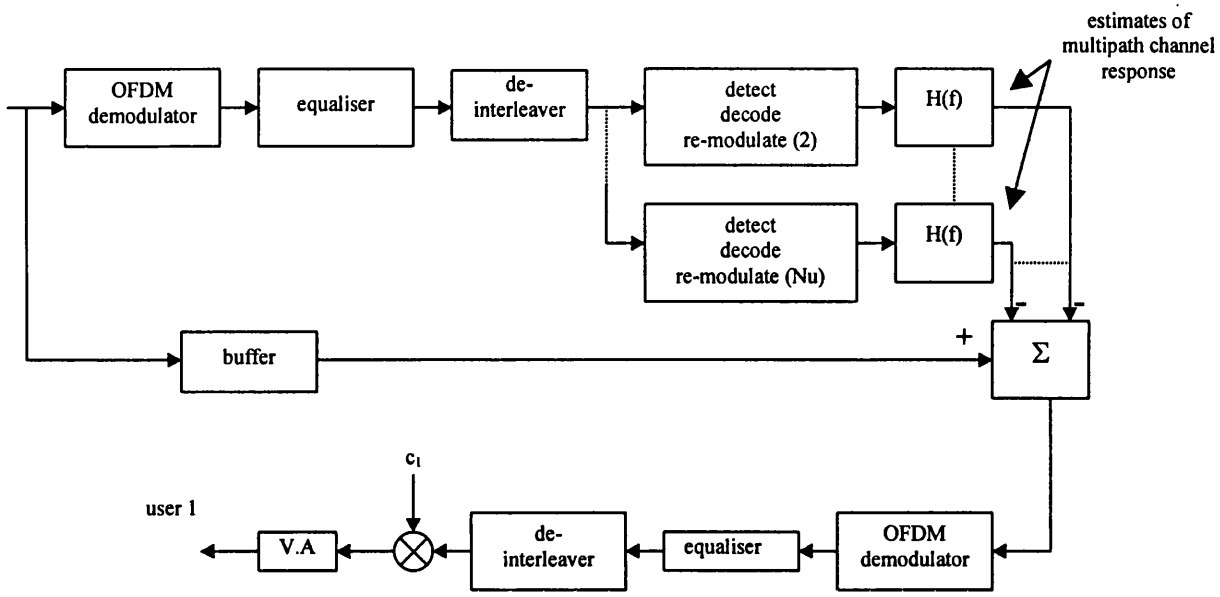

Figure 9-10. Subscriber receiver architecture for user 1

The received complex signal vector $\boldsymbol{R}_d$ of the d^{th} transmission block after OFDM demodulation and can be written as:

$$\boldsymbol{R}_d = \boldsymbol{H}_d \boldsymbol{S}_d + \boldsymbol{N}_d \tag{9-17}$$

where $\boldsymbol{H}_d$ is the diagonal matrix representing the Rayleigh fading on the sub-carriers assigned to block d, assuming a perfect guard-interval length and no ISI. $\boldsymbol{N}_d$ represents the complex noise vector at the receiver.

Using an estimate of the channel frequency response, frequency domain equalisation is then carried out on all N_u sub-carriers to reduce the effect of multipath distortion and the symbols on the sub-carriers are then de-interleaved. After equalisation and de-interleaving, using the matrix of the first-stage equaliser, $\boldsymbol{G}_d(1)$, the signal before detection is given by:

$$\boldsymbol{R'}_d = \boldsymbol{G}_d(1)(\boldsymbol{H}_d \boldsymbol{S}_d + \boldsymbol{N}_d)$$

$$= \boldsymbol{G_d(1)H_dS_d} + \boldsymbol{G_d(1)N_d} \tag{9-18}$$

This signal is decoded and demodulated using a maximum likelihood detector such as the Viterbi algorithm to provide an estimate of the transmitted data bit d'_i. The estimated data bit is then re-encoded and re-modulated to form an estimate of the interference from the i^{th} user. This process is carried out for all (N_u-1) interfering users. Assuming that the wanted user is user 1 and the interfering users are given as N_u-1 users, the estimated interference is given as:

$$y'(t) = \sum_{q=0}^{Q-1}\sum_{d=0}^{D-1}\sum_{l=0}^{M-1} s'_{q,d,l} \cdot e^{j2\pi f_{qDM+dM+l}t} \qquad \text{for } -\Delta<t<T_b \tag{9-19}$$

where $s'_{q,d,l}$ is the l^{th} component of $\boldsymbol{S'_d}$ of the q^{th} data bit, and,

$$\boldsymbol{S'_d} = \sum_{\substack{i=M(d-1)+1 \\ i\neq 1}}^{Md} e'_i c_i \tag{9-20}$$

where $\mathbf{e'_i}$ is the estimated encoded output sequence of $\mathbf{d'_i}$.

Therefore the wanted signal after MAI cancellation is now given by:

$$y(t) = y(t) - y'(t) \tag{9-21}$$

This signal is then demodulated and decoded for the wanted-user using the second stage complex equalisation matrix $\boldsymbol{G_d(2)}$, where we now use a <u>different</u> equalisation algorithm to detect our wanted-user. This can be simplified to:

$$y'(t) = \sum_{q=0}^{Q-1}\sum_{d=0}^{D-1}\sum_{l=0}^{M-1} (s_{q,d,l} - s'_{q,d,l}) \cdot e^{j2\pi f_{qDM+dM+l}t} \qquad \text{for } -\Delta<t<T_b \tag{9-22}$$

The received signal after OFDM demodulation and MAI cancellation is now given by:

$$\boldsymbol{R_d} = \boldsymbol{G_d(2)}[\boldsymbol{H_d}(\boldsymbol{S_d}-\boldsymbol{S'_d})+\boldsymbol{N_d}] \tag{9-23}$$

This is then decoded with wanted-user's orthogonal sequence and detected using the Viterbi algorithm. Depending on the level of error in the estimation of the interfering user's data sequences, the bit-error performance of the wanted-user can vary drastically. In a channel of

high other-user noise levels the BER performance will degrade quickly unless sophisticated interference cancellation techniques are employed.

9.6.1.3 Downlink Simulation Results

The bit error rate performance of the downlink was obtained using a discrete-time computer simulation written in C. The user data rate was set at 19 kb/s and the convolutional code was of rate R=1/2 and constraint length K=5. The encoded signals were spread using orthogonal Walsh-Hadamard sequences of length 16, giving a total bandwidth expansion factor of 32 and a maximum user capacity of 16 users per block. The total number of blocks was set to D=8 and Q=2 data bits of each user were transmitted per OFDM block. The number of sub-carriers is therefore $D.Q.M$ = 512, which results in a total bandwidth of 1.216 MHz and a sub-carrier spacing of 2.375kHz. The corresponding base station capacity is 16 x 8 =128 and these were represented in the simulation by randomly generated data bits.

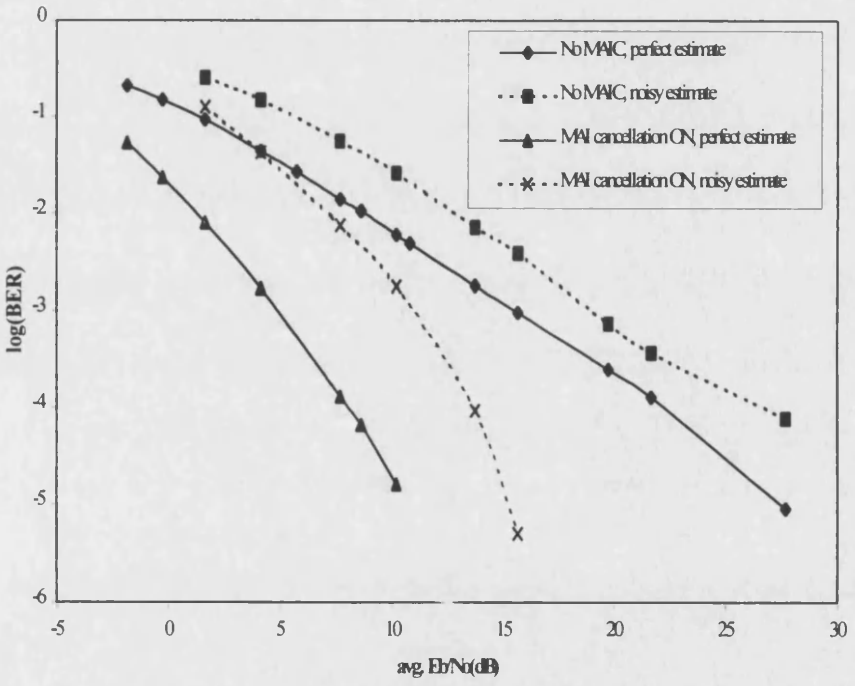

Figure 9-11. Performance using zero-forcing equalisation on the first iteration and MRC on the second detection (perfect channel estimates & noisy channel estimates)

The simulated channel is based on the COST 207 frequency selective Rayleigh faded bad urban (BU) channel model [28]. The Doppler frequency was set to 200Hz and perfect power control was assumed. For many of the results described in this section, perfect channel estimation is assumed, i.e. the effect of the AWGN on the channel estimate is not included. This ensures that those results are 'best-case'. However, in some of the results, 25% of the sub-carriers were used as pilot tones for the purpose of channel sounding. In this case, the effect of the AWGN in the channel is included in the channel estimates. The channel transfer function coefficients of the non-sounded sub-carriers were obtained by interpolation of adjacent sounded sub-carrier coefficients.

As described in section 9.6.1.2, the first stage of the MAI cancelling receiver used either frequency domain zero-forcing or controlled equalisation, whereas the second stage of the receiver used MRC. The bit error rate performance for the wanted-user in the presence of AWGN and the interference of 127 equal-power other-users for a system using zero-forcing equalisation for the first stage and MRC for the second stage is shown in figure (9-11). In this graph, the solid curves represent the situation where perfect channel estimates have been made for systems where MAI cancellation is available or not, respectively. The dashed curves correspond to the case where imperfect estimates of the channel have been made, as described earlier. Considering the case of perfect channel estimates, it is seen that MAI cancellation yields significant performance improvements for a wide range of values of E_b/N_o. The degradation that results from having imperfect channel estimates is clearly seen.

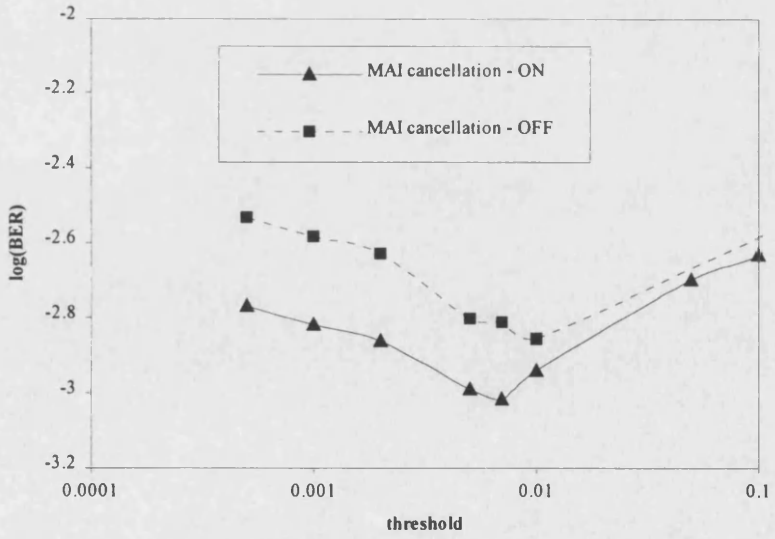

Figure 9-12. Optimum threshold value for controlled equalisation techniques on the downlink using MAI cancellation and no MAI cancellation

The main disadvantage of the zero-forcing technique is that unwanted noise is amplified in deep fades. It has been found that for conventional non-MAI cancellation receivers, controlled equalisation schemes can provide a considerable improvement in performance [8] in conditions where deep fades are prevalent. Since MAI cancellation techniques rely on good estimates of the interfering user's data, it is important to optimise the equalisation technique in the first stage.

Consequently, it is likely that controlled equalisation will provide improved performance for the case where MAI cancellation is applied. To estimate the threshold level at which the optimum performance is achieved, simulations using MAI cancellation and no MAI cancellation in the receiver were carried out at an SNR of 15.6dB. Figure (9-12) shows that the optimum value for the threshold level for this downlink system is at 0.07, regardless of whether MAI cancellation is implemented or not.

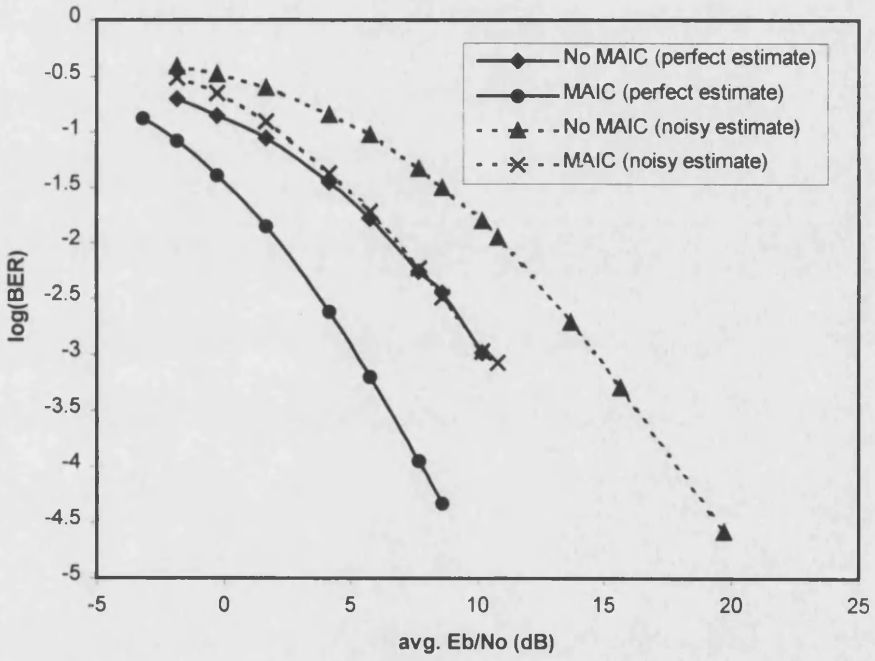

Figure 9-13. Performance using controlled equalisation on the first iteration and MRC on the second iteration

Using this optimum threshold, the BER performance of the downlink was obtained with and without MAI cancellation, as shown in figure (9-13). This graph shows that there is typically a 4dB improvement in E_b/N_o by using MAI cancellation and controlled equalisation for the first stage together with MRC equalisation on the second stage. This is much smaller than for the case of zero forcing equalisation. The reason for this can be seen by a comparison of figures (9-11) and (9-13). It is clear that when there is no MAI cancellation, controlled equalisation outperforms the zero-forcing algorithm quite considerably, but when MAI cancellation is used

the performance improvement obtained through controlled equalisation is relatively small. This figure also shows the effect of imperfect channel estimation for the case of controlled equalisation with and without MAI cancellation, and it can be clearly seen that the effect of noise on the channel estimates will reduce the *Eb/No* improvement by up to 5dB, countering any potential improvements thus gained by MAI cancellation. Clearly, a similar degradation in performance would be expected if MAI cancellation had not been used.

9.6.2 Uplink Model

Alternatively, the basestation can perform closed-loop power control in attempt to eliminate the near-far effect, and consequently cancel the interference effects of all other users that are simultaneously demodulated in the basestation. Our premise is that each basestation processes all users it controls, but none of those controlled by other basestations.

The uplink design proposed here is somewhat different to the downlink system and is based on OFDM modulation and low-rate orthogonal convolutional coding (LROCC) [18,26-27] to provide the necessary spreading and coding rather than a high rate convolutional coder and orthogonal spreading sequences. It is assumed that a small overhead is needed to provide the base station with an estimate of the channel transfer function of each user, possibly through the use of small training sequences (midambles) inserted between the data or *via* pilot tones.

Steiner [11,12] in particular has investigated methods of achieving time-domain channel estimation for a synchronous multi-user system. These are based on selecting channel estimation sequences that are delayed for every user, such that the receiver may select the frequency-domain channel coefficients, then obtain the appropriate selection of time-domain channel coefficients and transform the selected coefficients back to the frequency-domain. Rather than transmitting a known pilot tone sequence of ones, for example, the transmitter will now transmit a different exponential function for every user on the pilot-tone sub-channels. This consequently gives a time-delayed version of the pilot-tones for every user and enables the channel estimates of the active users to be separated at the basestation receiver.

The data bit, d_i, of the ith user is first encoded by the LROCC encoder, then randomised by a user specific Gold code c_i and modulated onto N subcarriers in the OFDM modulator. In the uplink, each user transmits over a different multipath channel H_i. In the receiver, this signal is then corrupted with Gaussian noise, n. The receiver assumes that the wanted user is user 1, and

the interference effects of users 2 to N_u (where N_u is the total number of simultaneous users) are partially removed through interference cancellation.

9.6.2.1 Remote Transmitter

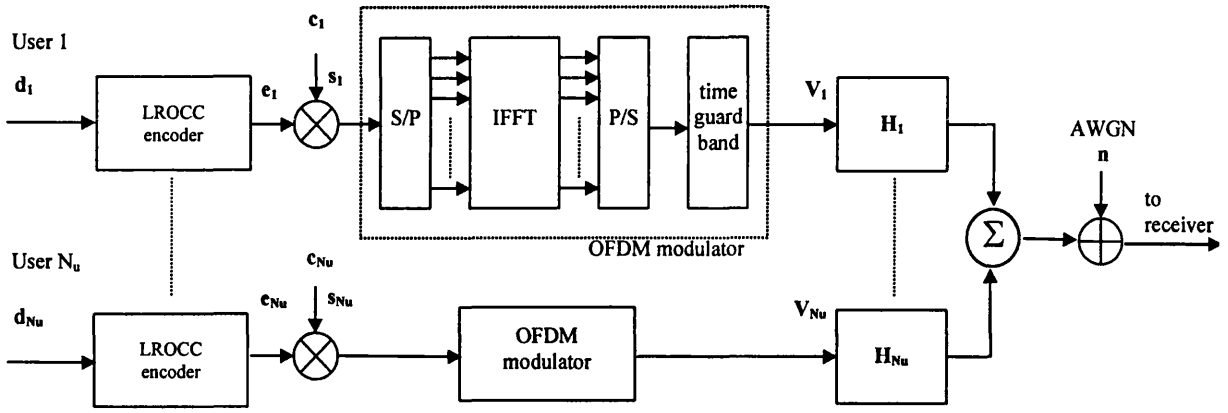

Figure 9-14. Simulation model of transmitter design for all uplink users and the channel model

Each user transmits a data sequence d_i, where i = 1,2 ... N_u. Each data bit is of duration T_b seconds and is consequently coded in a convolutional encoder of rate $R=K/M$. The input sequence d_i of K data bits produces an output sequence e_i of length n = [1 ... M], where each subsequent output symbol $e_i(n)$ is of duration $T_c=RT_b$. For LROCC codes the code rate is given as $R=1/M$, where M defines the spreading ratio of the user specific output sequence and is given as $M=2^K$. In this particular design this equates to the bandwidth expansion factor. The encoded sequence consisting of orthogonal Walsh-Hadamard codes is further multiplied by a randomising sequence of equal length M, given as $c_i=[c_i(1), c_i(2) \ldots c_i(M)]^T$, where $[.]^T$ denotes the transposition of the matrix. The data is modulated as a block, hence for each block the input to the interleaver and OFDM modulator is given as:

$$s_i(n) = e_i(n)c_i(n) \tag{9-24}$$

Note that no further spreading is achieved through use of the randomising sequence, c_i.

After OFDM modulation and interleaving the output sequence may be represented by the vector sequence $\mathbf{V_i} = [v_i(1), v_i(2) \ldots v_i(M+\Delta)]$ where Δ is the guard interval length, as described earlier. The output vector to be transmitted over the channel is represented by complex coefficients on the output of the IFFT in the modulator.

9.6.2.2 Basestation Receiver

The basestation receiver design can be seen in figure (9-15).

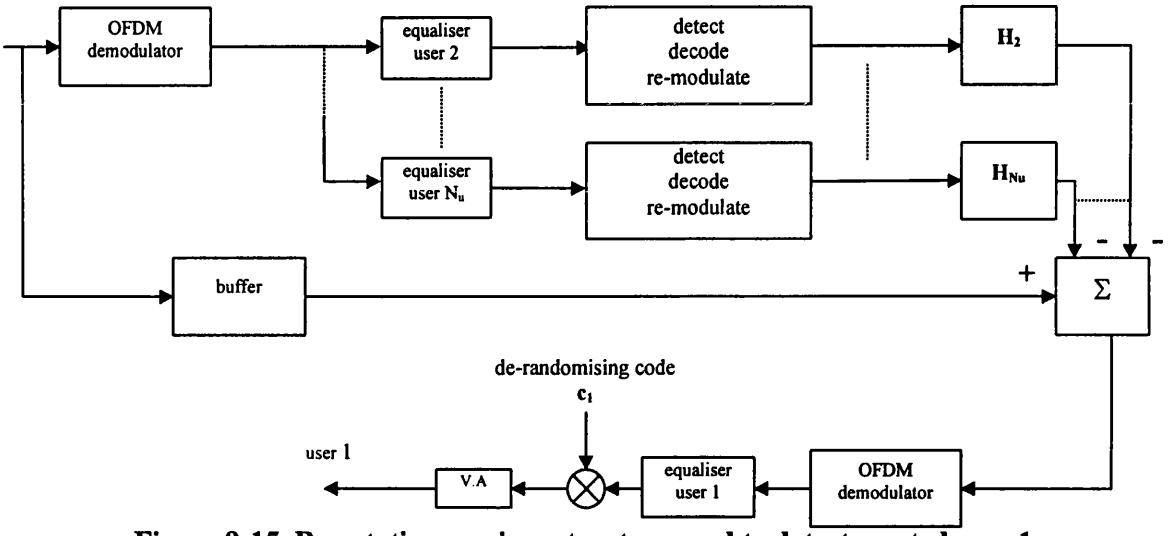

Figure 9-15. Basestation receiver structure used to detect wanted user 1

Since each user communicating to the basestation experiences different independent fading statistics, the channel coefficents are different for each user. The channel may be described by a complex matrix H_i (in the frequency domain) of size $M \times M$ for each user, effecting the subcarriers V_i assigned to the transmitted sequence on the transmitter for user i. Since a perfect guard-interval length is assumed, the channel matrix H_i is a diagonal matrix with diagonal components $h_{n,n}$. The vector N represents the complex AWGN in the channel. Therefore, the received sequence at the output of the OFDM demodulator, assuming perfect interleaving and guard-band insertion, is given by:

$$R = \sum_{i}^{N_u} e_i \cdot c_i \cdot H_i + N \tag{9-25}$$

The basestation receiver obtains information on the complex channel coefficients through the midambles inserted between symbol sequences. For this analysis we assume that the channel estimation is perfect. Using the complex channel estimates for each user we equalise the demodulated sequence for each user separately and obtain an estimate of the interference from other users. This is achieved through de-randomising the equalised signal by the user specific code c_i and performing maximum likelihood detection using the Viterbi algorithm. The estimated data sequences of all interfering users are re-modulated and re-encoded with the appropriate channel estimates and subsequently subtracted from the original received sequence.

Depending on the level of error in the estimation of the interfering user's data sequences the bit-error performance of the wanted user can vary drastically. In a channel of high other user noise levels the BER performance will degrade quickly unless sophisticated interference cancellation techniques are employed. The equalisation strategies that have been used are similar to those used for the downlink case. The first stage equalisers use either zero-forcing or controlled equalisation, whereas the second stage equaliser uses MRC.

9.6.2.3 Uplink Simulation Results

The simulated uplink channel assumes a service provision of a 32 kb/s data stream for each user. A constraint length of K=5 provides a spreading ratio of 32 in the LROCC encoder and is then randomised through the user-specific Gold code c_i of the same rate. This code provides no further additional spreading, but merely serves as a randomising sequence for the LROCC orthogonal code sets [29]. The number of sub-carriers is N=32 in a bandwidth of 1.028 MHz, and therefore the OFDM block period is 31.25μs. As for the downlink case, the channel is based on the COST 207 frequency selective Rayleigh faded bad urban (BU) channel model. The Doppler frequency was set to 200Hz and perfect power control is assumed.

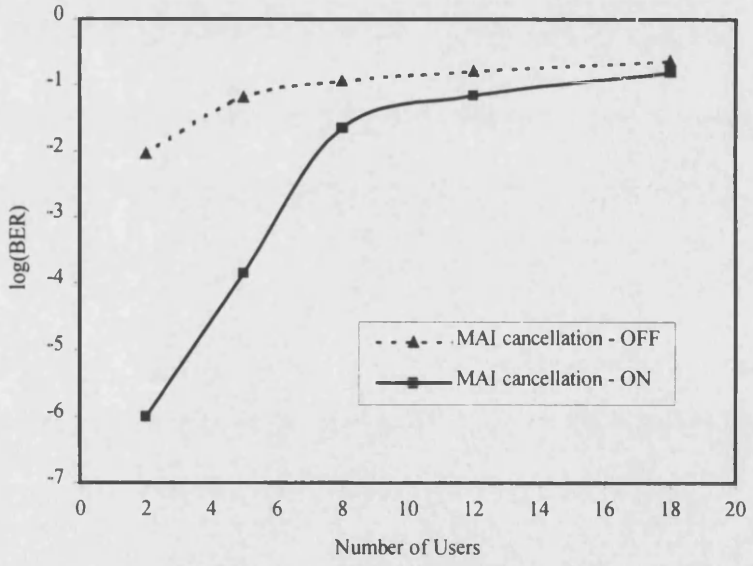

Figure 9-16. Uplink capacity comparison using zero-forcing equalisation on the first iteration and MRC on the second detection stage

Figure (9-16) shows the bit-error rate performance for different number of simultaneous users communicating with the base-station. The performance without interference cancellation can be seen to quickly degrade significantly when more than 5 users are present. The use of interference cancellation increases this to at least 10 users, and this is a significant gain in

performance. Conversely, at low user numbers, the BER for 32 kb/s per user is substantially improved by MAI cancellation. Without MAI cancellation it is not possible to achieve an acceptable BER for any user numbers.

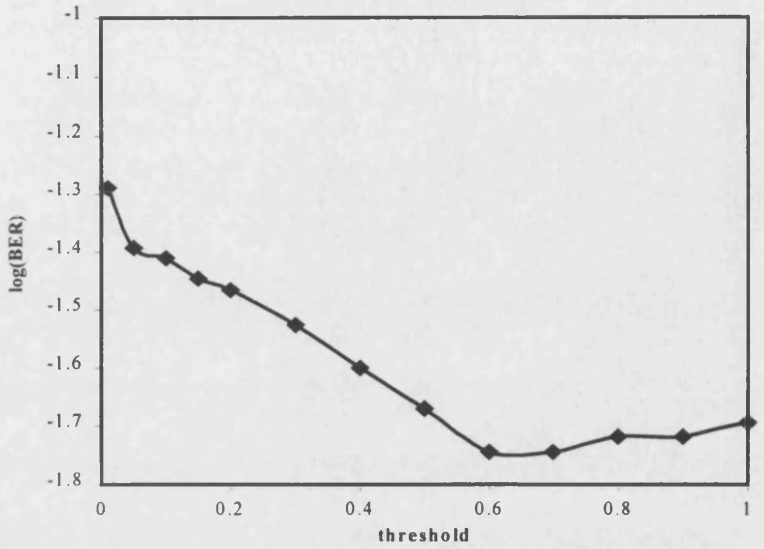

Figure 9-17. Optimum threshold value for controlled equalisation on initial detection

A more efficient equalisation scheme is based on controlled threshold equalisation. The threshold level displayed in figure (9-17) was estimated for the initial threshold detection strategy using no MAI cancellation and 8 simultaneous users in the channel. Figure (9-17) suggests an optimum threshold value of about 0.6 that was subsequently used for the equalisation structure employed in the Monte-Carlo simulations shown in figure (9-18).

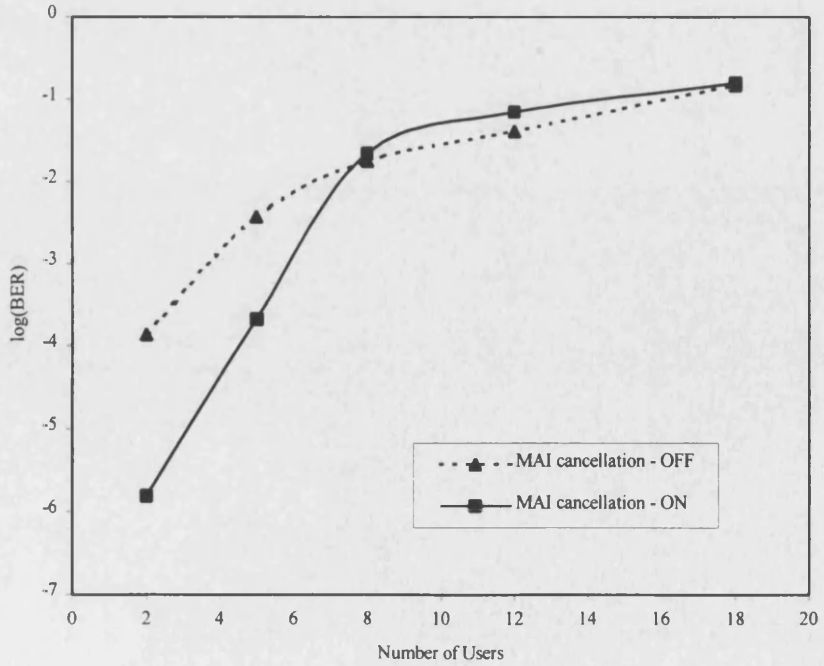

Figure 9-18. Uplink capacity comparison using controlled equalisation on the first iteration and MRC on the second detection stage

This technique shows a significant performance improvement for detection using no MAI cancellation in other-user noise environments but a smaller performance improvement using MAI cancellation compared to the zero-forcing strategy on the initial iteration, as shown earlier. At high user capacities (above 8 users typically) the performance gets worse compared to simple one stage detection schemes. When the uplink channel is saturated with other-user noise, the initial estimates on the first stage of MAI cancellation become very unstable. This causes the interference estimates of all other interfering users to give errors that propagate and actually harm the bit-error rate performance.

The LROCC coding scheme relies primarily on independent errors to yield good results and it is therefore important to provide initial good estimates on the first iteration of interference estimation in the receiver and to use strong interleaving in heavily faded channels. The use of OFDM in frequency selective channels helps to further combat the fading effects and effectively provides independent fading on each sub-channel. Combining this modulation strategy with LROCC coding provides an ultimately robust transmission design for such channels.

9.7 Summary

An equivalent frequency domain model can be used to approximate the standard OFDM system consisting of the IFFT modulator, guard-band insertion, channel response, guard-band removal, FFT demodulation and equalisation. This frequency-domain approximation is only valid, nevertheless, if the guard-band is longer than the maximum delay spread of the channel to maintain orthogonality between successive symbols. The independent fading channel model can be successfully implemented to simulate the effects of the frequency-selective fading channel without using large FFT's in the transmitter and receiver model.

A number of different frequency domain equalisation schemes have been summarised. It has been shown that the optimum method without knowledge of the input SNR and number of active users in the system is controlled equalisation, which uses zero-forcing equalisation on sub-carriers with no deep fade and phase-only recovery on strongly attenuated sub-channels.

The two main types of interference cancellation designs that may be used in a multi-user access system in context to MC-CDMA schemes on the up- and downlink have been introduced. In particular, the use of parallel interference cancellation methods has been shown for this type of system. Successive interference cancellation is only useful in systems where all the users are received at different power levels. This stems from the principle in which the users are detected.

Successive interference cancellation schemes detect the strongest user first, then remove its signal and proceed to the next strongest user. This process is repeated until all users have been demodulated. Of course, this type of system needs to have knowledge of the relative powers of all different users communicating to the basestation.

The multi-user MC-CDMA system simulated in this thesis presents an interesting concept of implementing interference cancellation on the downlink as well as the uplink. Orthogonal coding for all users in AWGN channels on the downlink would give no additional improvement using interference cancellation schemes, but in multipath channels considerable improvements can be accomplished. As the orthogonality between all users is severely distorted in multipath channels, it becomes necessary to attempt to restore the orthogonality between the users through appropriate equalisation methods on the first stage and then combine the maximum SNR on all sub-carriers for the wanted user. This can only be achieved by introducing different equalisers on the initial detection and final equalisation/combining stages. In this way, the use of orthogonality restoring equalisers such as zero-forcing or controlled equalisers are implemented on the first stage of detection and an optimum and simple combining method such as MRC on the final stage. At the last stage of detection it assumed that the unwanted users have been removed from the composite signal and the use of MRC is therefore in favour of orthogonality restoring equalisers.

Channel estimation of all the users on the downlink presents little problem, since the composite signal of all orthogonally coded users experiences the same fading. On the uplink, on the other hand, we must estimate the channel of every user separately. This can be considerably more difficult, and calls for more sophisticated channel estimation strategies. For the simulations presented here we have assumed that the channel is perfectly known.

This model has been introduced in the simulation of the up- and downlink of a multi-user MC-CDMA system using 512 sub-carriers and various equalisation and detection methods. It has been shown that controlled equalisation is in favour of MRC, EGC and zero-forcing strategies without requiring information about the channel SNR or the number of active users. If interference cancellation techniques are to be used, it has been shown that the use of zero-forcing or controlled equalisers is not as important and gives virtually the same results. In this case, it is more important to have more accurate knowledge of the channel statistics than to use threshold levels for controlled equalisation. Nevertheless, the use of MAI cancellation techniques has shown to introduce little deviation of the optimum threshold level for implementing controlled equalisation.

In summary, we can conclude that the use of orthogonal coding and multi-carrier modulation techniques with interleaving provides a robust and spectrally efficient design for the downlink of a cellular multi-user system. In the subscriber receiver, the use of interference cancellation techniques has shown to give good performance improvements in multipath channels. For the uplink, low-rate orthogonal convolutional codes have been proposed with parallel interference cancellation. It has been shown that these methods on an uplink strategy with a relatively lower number of sub-carriers in the OFDM modulator can provide good bit-error rates as long as the channel statistics can be accurately determined. It has been suggested that a time-alignment procedure between users could potentially allow all users' channels to be estimated separately. This is potentially attractive for FWA applications, where the channel is frequency-selective but also slowly time-varying. It has been shown that the performance in channels of high Doppler is still adequate, but the accuracy of the channel estimation strategies would become questionable. This applies especially to high data-rate applications.

9.8 References

[1] Fazel, K, "Performance of CDMA/OFDM for mobile communication systems", *IEEE 2nd International Conference on Universal Personal Communications (ICUPC) Proc.*, October 1993

[2] K. Fazel, S. Kaiser and M. Schnell, "A Flexible and High Performance Cellular Mobile Communications System Based on Orthogonal Multi-Carrier SSMA", *Wireless Personal Communications*, Kluwer Academic Publishers, pp.121-144, 1995

[3] Kaiser, S, "Analytical Performance Evaluation of OFDM-CDMA Mobile Radio Systems", *Proc. 1st European personal and Mobile Communications Conference (EPMCC'95)*, Bologna, Italy, November 1995, pp. 215-220

[4] Qureshi, S, "Adaptive Equalisation", *IEEE Communication Magazine*, Vol. 20, pp. 9-16, March 1982

[5] Proakis, J G, "Digital Communications", *McGraw-Hill Book Company*, New York, 1983

[6] Korn, I, "Digital Communications", *Van Nostrand Reinhold Company, Inc.*, New York, 1985

[7] Wu, W W, "Elements of Digital Satellite Communication", *Computer Science Press, Inc.*, Rockville, Md., 1984

[8] T. Mueller *et al*, "Comparison of different Detection Algorithms for OFDM-CDMA in Broadband Rayleigh Fading", *IEEE Conference Publication*, pp. 835-838, 1995

[9] Wiel, O and Vandendorpe, L, "Adaptive Equalisation for Multitone CDMA Systems", *IEEE Proc. PIMRC'94*, pp. 253-257

[10] Cimini, L J, "Analysis and Simulation of a Digital Mobile Channel Using Orthogonal Frequency Division Multiplexing", IEEE Trans. on Communications, Vol. COM-33, No. 7, July 1985, pp. 665-675

[11] Steiner, B, "Uplink Performance of a Multicarrier-CDMA Mobile Radio System Concept", pp. 1902-1906, *IEEE Transactions on Vehicular Technology*, Phoenix, Arizona, May 1997

[12] Steiner, B, "Ein Beitrag zur Mobilfunk-Kanalschätzung unter besonderer Berücksichtigung synchroner CDMA-Mobilfunksysteme mit Joint Detection (in German)", *PhD Thesis, VDI Fortschritt-Berichte*, Reihe 10, Nr. 337, Düsseldorf 1995

[13] Rohling, H, *et al*, "Comparison of multiple access schemes for an OFDM downlink system", *Proc. First International Workshop on Multi-Carrier Spread-Spectrum*, DLR Oberpfaffenhofen, Germany, April 1997

[14] Kondo, S and Milstein, L, "Performance of Multicarrier DS-CDMA Systems", *IEEE Transactions on Communications*, pp. 238-246, Vol. 44, No. 2, February 1996

[15] Proakis, J G, "Digital Communications", *McGraw-Hill*, 3rd edition, 1993

[16] Verdu, S, "Minimum probability of error for asynchronous Gaussian multiple-access channels", *IEEE Transactions on Information Theory*, Vol. 32, No. 1, pp. 85-96, Jan 1986

[17] Wyner, A D, "Recent results in the Shannon Theory", *IEEE Trans. on Information Theory*, IT-20, pp. 2-10, 1974

[18] Viterbi, A J, "Very low-rate convolutional codes for maximum theoretical performance of spread-spectrum multiple-access channels", *IEEE Journal on Select. Areas in Comms.*, pp. 641-649, May 1990

[19] Shannon, C E, "Communication in the presence of noise", *Proc. IRE*, pp. 10-21, 1949

[20] Varansi, M K, and Aazhang, B, "Multistage detection in asynchronous code division multiple-access communications", *IEEE Trans. on Communications*, Vol. 38, No. 4, pp. 509-519, April 1990

[21] Kubota, S, Kato, S, and Feher, K, "Inter-channel interference cancellation techniques for CDMA mobile/personal communication systems", *IEEE Third Intern. Symp. on Personal, Indoor and Mobile Radio Communications (PIMRC'92)*, pp. 112-117, Oct 1992

[22] Li, Y, and Steele, R, "Serial interference cancellation method for CDMA", *Electronics Letters*, Vol. 30, No. 19, pp. 1581-1583, IEE, Sept. 1994

[23] Giallorenzi, T R, and Wilson, S G, "Decision feedback multiuser receivers for asynchronous CDMA systems", *IEEE GLOBECOM'93*, Houston, Texas, pp. 1677-1682, Nov 1993

[24] Kawabe, M, *et al*, "Advanced CDMA scheme based on interference cancellation", *IEEE Vehicular Technology Conference*, pp. 448-451, 1993

[25] Vandendorpe, L, "Multitone Spread Spectrum Multiple Access Communications System in a Multipath Rician Fading Channel", *IEEE Transactions on Vehicular Technology*, pp. 327-337, Vol. 44, No. 2, May 1995

[26] Maxey, J J and Ormondroyd, R F, "Optimisation of orthogonal low-rate convolutional codes in a DS-CDMA system", *IEEE/URSI Conference Proceedings of ISSSE'95*, Vol. 95TH8047, pp. 493-496, 1995

[27] Maxey, J J and Ormondroyd, R F, "Low-Rate Orthogonal Convolutional Coded DS-CDMA using Non-Coherent Multi-Carrier Modulation over the AWGN and Rayleigh Faded Channel", *IEEE Conference Proceedings of ISSSTA'96*, Vol. 2, pp.575-579, 1996

[28] COST 207: *Digital land mobile radio communications*, Final Report, Commission of the European Communities, Luxembourg 1989

[29] Ormondroyd, R F, and Maxey, J J, "Performance of Low-Rate orthogonal Convolutional Codes in DS-CDMA Applications", *IEEE Trans. on Vehicular Technology*, pp. 320-328, Vol. 46, No. 2, May 1997

[30] Schilling, D L, *et al*, "Spread-spectrum for commercial communications", *IEEE Communications Magazine*, pp. 66-79, April 1991

[31] Bingham, J A, "Multicarrier modulation for data transmission: An idea whose time has come", *IEEE Communications Magazine*, pp. 5-14, May 1990

[32] Hoeher, P, "TCM on frequency-selective land-mobile fading channels", *Proc. Tirrenia International Workshop on Digital Communications*, Sept. 1991

[33] Chouly, A, Brajal, A and Jourdan, S, "Orthogonal multicarrier techniques applied to direct sequence spread-spectrum CDMA systems", *Proc. IEEE Global Telecommunications Conference (GLOBECOM'93)*, pp. 1723-1728, November 1993

[34] Jung, P, Baier, P W, and Steil, A, "Advantages of CDMA and spread spectrum techniques over FDMA and TDMA in cellular mobile radio applications", *IEEE Trans. on Vehc. Technology*, Vol. 42, pp. 357-364, August 1993

[35] Schnell, M, and Werner, M, "Comparison between different transmission schemes for mobile radio channels", *IEEE Proc. of ISSSE'92*, pp. 705-708, 1992

[36] Fazel, K, "Narrow-band interference rejection in orthogonal multi-carrier spread-spectrum communications", *IEEE 3rd International Conference on Universal Personal Communications (ICUPC)*, pp. 46-50, 1994

[37] Milstein, L, "Interference rejection techniques in spread-spectrum communications", IEEE Proceedings, Vol. 75, pp. 211-222, 1988

CHAPTER 10:

CAPACITY CALCULATIONS

10.1 Overview

The analysis of mobile and FWA systems gives rise to a number of questions that can be resolved if the capacity of such systems is analysed. The thesis so far has simulated and predicted the performance of single- and multi-carrier techniques in a variety of channels. Some of the mobile channels may not be directly applicable to FWA systems, and vice versa, but nevertheless the mobile channel will give an upper bound on the FWA performance. As is well known, FWA channels do not exhibit large Doppler, and although the frequency selective faded channel model still applies, it is considered virtually time-invariant over a block of data bits.

This chapter deals with a comparison of the typical capacities that may be achieved using adaptive TDMA (ATDMA) and MC-CDMA techniques in a cellular environment. Attention is paid, in particular, to the FWA cellular environment and the Erlang statistics that are used in determining the theoretical total number of subscribers that may be accommodated in a FWA system. We introduce some of the basic techniques involved in ATDMA systems and continue with some performance measures of both ATDMA and MC-CDMA.

The capacity comparisons do not include the effects of synchronisation and power control errors, nor do they include pilot tone and guard band overheads, unequal cell loading and imperfect channel estimation. The use of channel estimation strategies, synchronisation and guard band overheads is important for ATDMA as well as MC-CDMA systems, and play a major role in the overall performance of these multiple-access strategies. Their effect on ATDMA systems can vary from system to system, and a number of international companies are reluctant to publish the results of the performance degradation experienced by their own commercially available products. The results of the previous chapters of this thesis have been able to cover some of the degradations encountered by MC-CDMA systems through imperfect channel estimation, insufficient guard-band lengths, the use of MAI cancellation with convolutional coding and equalisation techniques. For the capacity results in this chapter we consequently assume that all these parameters have been perfectly matched to the requirements of the system. This enables a fair and valid comparison of the two multiple-access strategies, as can be seen later.

10.1.1 Adaptive Time Divison Multiple Access (ATDMA)

For TDMA systems, the need to reduce the effects of inter-symbol-interference (ISI) is usually achieved by time-domain equalisation. There are a number of approaches that can be taken. One would be to assume very little knowledge of the channel and to perform an adaptive 'blind equalisation'. In this approach, it is usual to send some known training sequence over the channel and through the equaliser and to adapt the parameters of the equaliser until there is a minimum mean square error (MMSE) in the detected data. An alternative approach is to use the time that would have been spent sending the training sequence to perform a channel sounding. This yields the channel impulse response, *h(t)* from which an approximation to the inverse of the channel response, representing the equaliser response, can be obtained. When the channel statistics are stationary, as for the case of FWA, either approach is relatively straightforward. Consequently, it is accepted practice to separate the process of channel estimation and data detection and the data structure of TDMA systems typically consist of sections carrying data and sections containing training sequences (or channel soundings). An advantageous structure is obtained by placing the training sequences into the centre of the data timeslot, which are termed *midambles*, and to locate one data section before and after the midamble. This data structure guarantees that the channel estimate, which is actually only valid for the time of arrival of the midamble, is approximately valid for the two data sections of the timeslot.

Concerning the length of the midamble, the maximum delay of the radio channel has to be taken into account. As a rule of thumb, the length of the midamble should be at least twice the duration of the channel impulse response. Consequently, in mountainous regions with large-area cells where the impulse response is long, longer midambles are needed than in small urban cells. The transmission time dedicated to the midamble is not available for data transmission. Therefore, the midambles should be chosen to be as short as possible, and the total timeslot length as large as possible in order to reduce the midamble overhead. Unfortunately, when long timeslots are used, the channel impulse responses estimated from the midambles become less relevant towards the ends of the timeslots because of the time variation of the channel parameters. For this reason, the burst duration has to be limited to values well below the coherence time of the radio channel. Burst lengths are also restricted by requirements on the maximum tolerable latency time, which is larger in the case of data transmission than in the case of voice transmission.

The TDMA scheme has several advantages for FWA schemes:-

(i) By using either channel sounders or midambles, relatively simple equaliser structures can be used and this reduces the overall receiver complexity. Also, because of the orthogonality of the TDMA signals, good separation of the various user signals at the receiver is possible, especially if guard intervals are provided between successive bursts. Due to this robust disjointness, the demands on power control can also be kept to moderate levels of complexity.

(ii) The concept of burst transmission separated by bursts of other user signals fits nicely together with interleaving, which in combination with forward error correction coding helps to combat the fading effects of the radio channel.

(iii) By allotting larger or smaller numbers of time slots to individual users, the data rate can be flexibly adjusted on demand. The maximum data rate for a given user can be obtained by assigning all the time slots and frequency bands of a cell to a single user.

The advantages of TDMA are accompanied by some disadvantages:-

(i) The time slot scheme requires mutual synchronisation of the different users of a cell, and variable data rates, in combination with good total system capacity, can only be realised by carefully organising the distribution of the time slots in the sense of dynamic channel allocation. In this respect, also the exploitation of voice activity monitoring is not trivial in TDMA systems.

(ii) A further disadvantage of TDMA results from the fact that the average transmitted power of each user signal is concentrated within time slots separated by pauses. This type of pulsed transmitter operation from the subscriber has a high peak-power to mean power ratio and this places severe linearity constraints on the transmitter RF amplifier.

Adaptive TDMA (ATDMA) systems allow an increased user capacity by taking advantage of the statistics of voice data. In this type of system, the capacity is enhanced by adapting the power and rate of the error-correcting code to the co-channel interference conditions of the channel. Nevertheless, the interference must be monitored in the channel to determine the rate of the code. If the channel interference is high, a low-rate code will be employed, and vice versa for low channel interference values. For high interference conditions a low-rate code will consequently use more time slots per user. However, to keep interference levels in adjacent cells constant, the time slot usage must be kept stable.

To effectively implement adaptive TDMA, each channel is split into time slots rather than fixed assigned channels. Efficient time-slot management is implemented through a *packet reservation multiple access* (PRMA) protocol [2,3]. This allows the data to be treated as packets, where the fixed channels are reserved for streams of such packets for the duration of the stream. The length of each time-slot is determined by the occupancy required at the maximum code rate of the system. As the interference level decreases, the code rate increases, leaving spare time-slots available. Figure (10-17) shows how these spare time-slots may then be filled by time-slots from other subscribers. The advantage of PRMA, therefore, is to allow naturally occurring gaps in speech, for example, to be re-used by other users in the system and hence give increased (overall) capacity in a multi-user access environment. This offers the possibility of achieving 100% base-station availability since the code-rate may be as low as possible at the expense of increased bandwidth.

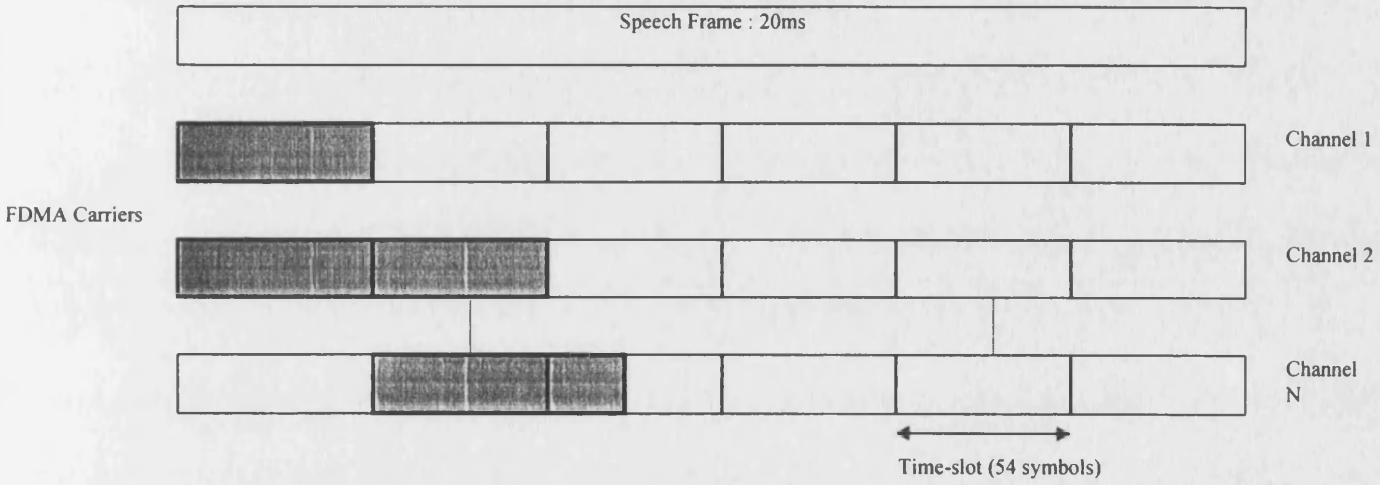

Figure 10-1. Time-slot assignment in TDMA systems

ATDMA techniques based on PRMA provide a number of disadvantages to the system designer. First, the channel needs to be monitored while transmission occurs and it is capacity limited by the access method to the channel. An inherent loss in throughput can lead to some delays in the transmission of individual packets, and in the worst case this can lead to a loss of packets during system adaptation. To rectify this potential problem, a buffer may be implemented to store and re-transmit packets, where the maximum number of packets stored is related to the packet length and the allowed delay budget.

In the typical channel environment of a fixed wireless access system, described earlier, the observation of a few time-invariant multi-path components make the channel environment frequency selective on both the up-link and down-link. Under these conditions, the efficiency of PRMA techniques suffer significant degradation unless sophisticated multipath countermeasures

are employed. Ongoing research will hopefully provide the necessary results on the effectiveness of PRMA protocols in more realistic (i.e. fading) environments. In ordinary AWGN channels, the efficiency gain for the PRMA protocol has been given as ε = 1.5 - 1.6. The capacity equations that follow, which are based on the AWGN channel will therefore lead to over-optimistic results and should be treated with care.

10.1.2 Capacity of an Adaptive TDMA FWA System

For fixed wireless access systems using hexagonal cellular structures with a directional base-station antenna of beamwidth 40°, the relationship between the re-use distance ratio, k, and the re-use pattern m is somewhat different than for conventional mobile cellular structures. The main differences in the results can be seen in Table (10-1). These results were obtained from [35].

Re-use pattern (m)	1	3	4	7	9
k (directional)	3	4	5	6	7
k (omni)	1	2	2.65	3.61	4.36

Table 10-1

Next, consider all the interference to come from other users in neighbouring cells, with one interfering user per re-use cell. With perfect power control, we can determine the re-use distance ratio k as follows:

$$k = \left(\frac{S}{I}\sigma_{i,r}\right)^{\frac{1}{\alpha}} \tag{10-1}$$

where,

S/I = Signal-to-noise ratio at the front end of the receiver

α = Propagation exponent (typically 3 - 4)

$\sigma_{i,r}$ = Sum of the possible first tier interfering active paths (0...6)

For a given value of BER, the signal-to-noise ratio at the front end of the receiver is determined for different coding strategies using QPSK modulation, say. This is then used to find the equivalent value of k which can achieve this value of S/I. From this, the re-use factor of the

cellular structure can be determined for use in the calculation of capacity and spectral efficiency.

The impact of different convolutional coding schemes [6] to achieve a particular level of frequency re-use pattern at a bit-error rate of 10^{-9} and a power decay exponent of α=3 is shown in Table (10-2).

Coding level	Uncoded	R=1/2 K=8	R=1/3 K=8	R=2/3 K=8	R=3/4 K=9
E_b/N_o (dB)	12.5	6.0	5.5	6.3	7.2
S/I (dB)	15.5	6.0	3.7	7.5	8.9
k	5.9	2.8	2.4	3.2	3.6
m	7	1	1	3	3

Table 10-2

To make a fair comparison with the CDMA system, we assume that a universal frequency re-use (m=1) is required for the TDMA system. This means that a strong coding scheme, such as R=1/2 or R=1/3, is required for the uplink design of the FWA system. Consequently, a TDMA design using a bandwidth allocation of 15 MHz, transmitting data at a bit-rate of R_b=64kb/s and using R=1/3 convolutional codes is considered for the uplink of a FWA system. Using QPSK modulation and a root-raised cosine filter with a roll-off factor of 0.4, the channel separation can be as low as 134.4 kHz. This can be achieved with a frequency re-use pattern of m=1, and the number of available high quality channels is therefore given as:

$$\begin{aligned} N &= \frac{\text{Bandwidth allocation}}{\text{Channel spacing} \times \text{m}} \\ &= \frac{15}{0.1344 \times 1} \\ &= 111 \text{ channels} \end{aligned} \qquad (10\text{-}2)$$

In a realistic scenario, the system designer would provide a range of services, ranging from voice data (32 kb/s), FAX/Modem (64 kb/s) to ISDN services (144 kb/s). For the calculations given in this report, a packet reservation multiple access (PRMA) protocol is assumed to be effective mainly on voice band channels. From the earlier discussion, current research has shown an overall efficiency gain, relative to conventional TDMA, of ε =1.5 - 1.6 can be obtained through the use of PRMA techniques [4]. Using this result, the theoretical number of voice channels in an ATDMA system could be as high as:

$N = 111 \times 1.6 = 177$ channels (10-3)

To make a fair comparison with CDMA systems in frequency-selective fading channels we now consider the capacity of a ATDMA system in the same fading environment as the simulated MC-CDMA systems in this thesis. The physical channel allotment and capacity obtained from equation (10-3) still remain the same, but the frequency re-use pattern, m, could very well be higher than one for faded channels.

Considering the same data rate requirement of 64 kb/s with QPSK modulation and rate 1/2 convolutional coding, we may use the results of chapter 9, figure (9-11) to obtain an E_b/N_o value of about 12dB for a BER=10^{-6}. Therefore, the value of the re-use distance ratio k can be given as:

$$k = \left(10^{12/10} \cdot 6\right)^{\frac{1}{3}} = 4.56 \tag{10-4}$$

Clearly, this requires a cellular frequency re-use of m=7, therefore giving a capacity of:

$N = 177/7 = 25$ channels/sector (10-5)

With tri-sectorisation of the base-station antenna, it is possible to provide a further increase in the user capacity of a single cell. Assuming that the standard Erlang requirements for one subscriber are given by 60 mE (i.e. each subscriber is active for 3.6 minutes, on average, in one hour), Table (10-3) gives an approximate value for the number of subscribers that can be supported theoretically in an ATDMA system. The probability that a new subscriber is refused a call is given by the Erlang B formula:

$$P_b = \frac{\frac{\left(\frac{\lambda}{\mu}\right)^N}{N!}}{\sum_{j=0}^{N} \frac{\left(\frac{\lambda}{\mu}\right)^j}{j!}} \tag{10-6}$$

where,

P_b = Probability of a blocked call

N = Number of available traffic channels

λ/μ = Erlang statistics (e.g. 60 mE per subscriber)

The Erlang B statistic is a frequently used model to determine the occupancy distribution and probability of lost calls, where it is assumed that if a new user attempts to enter the network when all slots are occupied, it departs and re-enters later after a random interval. This is often referred to as the "lost call cleared" (LCC) model. Another distribution is based on the "lost call held" (LCH) model, which is introduced at a later stage of this chapter.

For FWA systems, a blocking probability of 0.1% will be required to offer the necessary quality of service in becoming a transparent link when compared to ordinary copper wire PSTN networks. The results for the number of subscribers per basestation in table (10-3) were obtained by dividing the Erlang B capacity by the Erlang statistics per user (i.e. 60mE per user).

	Omni-directional BS	Tri-sectored BS
No. of channels	25	75
Erlang B capacity	13E	53.5E
Subscribers per BS	216 subscribers	891 subscribers

Table 10-3

This large subscriber base is highly optimistic. However, it should be noted that these figures are based on the provision of 64 kb/s channels. In a more realistic scenario, each user would need access to at least an ISDN link. With these requirements in mind, the total data bit-rate required by the user would be on the order of 144 kb/s, which, using the same modulation and coding schemes introduced earlier, would use a bandwidth of 303 kHz. The number of multi-service channels is now given as:

$$\begin{aligned} N &= \frac{\text{Bandwidth allocation}}{\text{Channel spacing} \times \text{m}} \\ &= \frac{15}{0.303 \times 1} \\ &= 49 \text{ channels/sector} \end{aligned} \qquad (10\text{-}7)$$

Each channel on this service effectively provides a 144 kb/s stream. Considering PRMA techniques to be effective on the voice data only, the number of possible channels will increase by a factor of:

$$N = 49 \times \left(1 + \frac{32}{144}(0.6)\right) \quad (10\text{-}8)$$
$$= 55 \text{ channels}$$

For Rayleigh faded channels, where the cellular frequency re-use factor is given as m=7, the number of channels is now given as:

$$N = 55/7 = 8 \text{ channels/sector} \quad (10\text{-}9)$$

Table (10-3) can now be modified to:

	Omni-directional BS	Tri-sectored BS
No. of channels	8	24
Erlang B capacity	2.05E	12.2E
Subscribers per BS	34 subscribers	203 subscribers

Table 10-4

10.1.3 Capacity of a DS-CDMA FWA System

The majority of this study will focus on the implementation of DS-CDMA for FWA designs. The use of DS-CDMA in FWA systems will inevitably focus on the uplink and downlink of a multi-point to point link in a cellular universal frequency re-use structure.

Much work has been performed in evaluating the capacity of cellular DS-CDMA systems. The effects of diversity and power control on system capacity have been investigated from different points of view [19-22].

For high speed and high quality traffic the system performance with a small number of simultaneous subscribers is also very important, since only a small number of users may be supported by the system when the quality requirements are very high. In this case, the Gaussian approximation of the interference power may not be exact. To calculate the outage analysis, the key is to understand the nature of the multi-user, multi-cell interference. The validity of this approximation is examined in a multi-user, multi-cell interference power environment with log-normal shadowing on the reverse link of a DS-CDMA cellular system. For the forward link, the interference power is the sum of a small number of weighted random variables with correlation.

A fast and efficient way to evaluate the system performance has been developed through analysis and modelling. More details can be found in [22]. Here we evaluate an integrated voice and ISDN service.

The uplink from the subscriber to the base-station introduces an interference environment which is more limiting on capacity than the downlink. To achieve orthogonality between users is virtually impossible due to the number of different orthogonal code sets arriving from individual subscribers with different phase and amplitude statistics. The effects of scattering therefore require a coherent demodulation technique to give information on the channel state conditions or a non-coherent scheme at the expense of reduced capacity.

For a given bandwidth and signal-to-noise ratio E_b/N_o, the well known capacity equation can be used:

$$N_u = 1 + \frac{W/R_b}{E_b/N_o} \cdot F \cdot V \cdot T \qquad (10\text{-}10)$$

where,

W = Bandwidth allocation
R_b = Data bit-rate
E_b/N_o = Signal-to-noise ratio
F = Inter-cell degradation factor
V = Voice activity factor
T = Antenna diversity at the base-station

Referring to equation (10-4), the Erlang-B distribution for DS-CDMA resembles more the case for unslotted multiple access, and is often termed as the Erlang-C distribution of lost calls held (LCH). In this model, it is assumed that the unserved users repeat their attempts to place a call immediately, and thus remain in the system, though unserved with a successful connection. Equation (10-4) can be re-written as:

$$P_b = e^{-\frac{\lambda}{\mu}} \sum_{j=N_u}^{\infty} \frac{(\lambda/\mu)^j}{j!} \qquad (10\text{-}11)$$

10.1.3.1 Downlink Capacity

First, we consider a synchronous downlink scenario with a data-rate of 64 kb/s per user. This may be used for voice or fax data, but for the time being we assume that this data is purely used for voice data. The channel is similar to the COST 207 Bad Urban channel with a Doppler of 200 Hz. Of course, for FWA applications this is a very pessimistic approach, but nevertheless it gives a lower bound on the achievable capacity. Using the results from the MC-CDMA multi-user basestation-to-subscriber downlink with MAI cancellation and assuming perfect channel knowledge, we can achieve a BER of 10^{-6} at E_b/N_o=12 dB. If we assume that the inter-cell degradation factor is about 0.8 from the analysis for FWA cellular systems presented in chapter 4, the total number of channels that may be supported in a single cell is given as:

$$N = 1 + \frac{15MHz/64kb/s}{12dB} \cdot 0.8 \cdot \frac{8}{3} \qquad (10\text{-}12)$$
$$= 32 \text{ channels/sector}$$

It can be seen in Table (10-5) that this is a slightly higher result than the capacity given for an ATDMA system in (10-5). In addition, this evaluation is based on a universal frequency re-use of m=1, hence giving the cellular system more flexibility geographically in the deployment of cells.

	Omni-directional BS	Tri-sectored BS
No. of channels	32	96
Erlang C capacity	20E	74E
Subscribers per BS	333 subscribers	1233 subscribers

Table 10-5

10.1.3.2 Uplink Capacity

To accurately determine the capacity on the uplink of a MC-CDMA system in fading is more difficult to determine, but we will serve an approximate capacity analysis based on the results of some of the simulations carried out in this thesis. We will include the effects of voice detection and the method of tri-sectorisation for each basestation.

Figure (9-18) in chapter 9 has shown that only 2 users could be supported for a BER=10^{-6} at a bit-rate of 32 kb/s in a bandwidth of 1.216 MHz. Considering a bandwidth of 15 MHz and a data rate of 64 kb/s per user, the total number of theoretical users would be:

$$N = \frac{15MHz/64kb/s}{1.216MHz/32kb/s} \cdot 2 \cdot F \cdot V \qquad (10\text{-}13)$$
$$= 26 \text{ channels/sector}$$

This result is very close to the theoretical channel capacity of an ATDMA system outlined in (10-5). We can therefore conclude that even though the capacity of a MC-CDMA system is limited by the uplink, we still nevertheless achieve the same capacity as an ATDMA system on the uplink and an even higher capacity than ATDMA on the downlink. This makes MC-CDMA an attractive solution, especially for FWA systems with directional antenna.

	Omni-directional BS	Tri-sectored BS
No. of channels	26	78
Erlang C capacity	15E	58E
Subscribers per BS	250 subscribers	966 subscribers

Table 10-6

10.1.3.3 Higher Data Rate Systems

Considering now a data rate of R_b = 144kb/s in the same bandwidth of 15 MHz, the capacities for the uplink and downlink may now be determined. To obtain some measure of the anticipated capacity of such design, it is assumed that the bandwidth is allocated to voice and data/ISDN traffic proportionally to their data rate requirements. Therefore, the bandwidth of 15 MHz is split in the ratio of 32:144. Even though the allocated 144 kb/s would be used to carry voice data in realistic applications and would require a BER of 10^{-9}, this analysis assumes a BER requirement of 10^{-6} and draws attention to the data rate requirements separately to simplify the capacity calculations.

For data traffic at 144 kb/s operating in a bandwidth of 11.66 MHz the theoretical number of channels is given as:

$$N_u = 1 + \frac{11.666\,\text{MHz} / 144\,\text{kb/s}}{12dB} \cdot 0.8 \qquad (10\text{-}14)$$
$$= 5\,\text{channels}$$

and for voice traffic at 32 kb/s operating in a bandwidth of 3.33 MHz:

$$N_u = 1 + \frac{3.33\,\text{MHz} / 32\,\text{kb/s}}{12dB} \cdot 0.8 \cdot \frac{8}{3} \qquad (10\text{-}15)$$
$$= 15\text{channels}$$

Therefore, the total number of channels available to the one sector of the basestation is about 20 channels. Using these values, we obtain the following capacity results:

	Omni-directional BS	Tri-sectored BS
No. of channels	20	60
Erlang C capacity	10.97E	43.2E
Subscribers per BS	182 subscribers	720 subscribers

Table 10-7

10.2 Summary

This chapter has introduced the concepts involved in maximising the efficiency of TDMA systems through the use of PRMA techniques on voice data and has given a capacity comparison of both ATDMA and MC-CDMA cellular designs. The capacity calculations are based on service provision of voice and ISDN data at 32 kb/s and 144 kb/s, respectively, in a bandwidth of 15 MHz and a blocking probability of 0.1%. Each user is assumed to be active for an average of 3.6 minutes per hour, giving an Erlang requirement of 60mE per user. For a fair comparison between the two multiple access strategies, we have assumed a BER requirement of 10^{-6} for both voice and ISDN data, which of course is too low for voice and too high for ISDN. Nevertheless, it enables a somewhat easier capacity comparison to be made on the simulation results of this thesis.

The MC-CDMA strategy from chapter 9 has been assumed to be used on the uplink and downlink in a relatively high Doppler environment of 200 Hz and multipath fading according to the COST 207 Bad Urban channel. In a sense, this provides a realistic channel for mobile

situations and at the same time a pessimistic result on the capacity of FWA systems. The capacity comparisons, however, still present valid and fair results.

Whilst not much attention has been paid to alternative ATDMA techniques, one could argue that TDMA systems are superior on a number of different key issues. Even so, the concept of multi-carrier CDMA should not be disregarded as a likely contender for next generation wireless systems. From the results of the analysis shown here, it is clear that significant advantages in capacity can be found, especially on the downlink of a cellular system. For the foregoing reason, it is likely that hybrid systems using different multiple access strategies may be used in next generation systems. MC-CDMA designs clearly perform as well or even better in FWA applications than conventional DS-CDMA techniques because they provide good resilience to frequency-selective fading. For this reason it can be seen that MC-CDMA designs provide a viable alternative to conventional ATDMA designs introduced for future generation FWA systems.

We can conclude that whilst MC-CDMA will have at least the same or higher capacity than ATDMA systems, it can also yield additional advantages in the general behavior within a cellular system. The inherent soft capacity degradation of DS-CDMA with coding techniques was shown in chapters 5 and 9, and the use of multi-carrier techniques for this type of system has shown additional advantages in the flexibility of the system. MC-CDMA systems offer the potential to integrate or overlay services onto existing wireless communication systems. Due to the high number of sub-carriers employed, it is possible to adaptively integrate variable bit-rate requirements into MC-CDMA systems. The performance for different bit-rates in a multi-access environment using MC-CDMA has shown good performance with respect to the achievable BER. Even higher bit-rates of 32 kb/s for good quality audio/voice can quite easily be accommodated, and in conjunction with MAI cancellation and coding have shown that the uplink can support these services.

The capacity advantages of MC-CDMA become clear when compared with respect to the theoretical Erlang capacity that thus may be achieved. Whilst the occupancy distribution of LCH gives a lower capacity due to users remaining in the system, MC-CDMA still gives a higher number of potential subscribers than ATDMA. The potential number of users that may be served by a central basestation with tri-sectorisation can be as high as 1233 on the downlink of a MC-CDMA system compared with 891 using ATDMA. Since MC-CDMA cellular systems are ultimately uplink limited, this reduces to a level of 966 potential subscribers on the uplink. Nevertheless, the capacity is still higher than for ATDMA designs.

In AWGN channels, the SNR requirement to achieve a particular BER at the input to the receiver is much lower than for faded channels. For this reason, ATDMA systems can operate with universal frequency re-use using conventional high-rate convolutional codes. In channels with fading, the SNR requirements consequently increase and allow only a frequency re-use greater than 1 to be employed. This is the limiting factor on the capacity of ATDMA systems.

10.3 References

[1] Gilhousen, K S, et al, "On the Capacity of a Cellular CDMA System", *IEEE Transactions on Vehicular Technology*, Vol. 40, No.2, pp.303-312, May 1991

[2] Ananasso, F, and Priscoli, F D, "Technology challenges in TDMA approach to 3rd generation personal communication services", pp. 702- 706, *IEEE Conf. Proceedings*, 1994

[3] Priscoli, F D, "Procedures for a fully integrated system including a cellular network and a GEO satellite system", *European Transactions on Telecommunications*, ETT, 1994

[4] Goodman, D J, "Efficiency of Packet Reservation Multiple Access", *IEEE Trans. on Veh. Techn.*, Vol. 40, No. 1, Feb 1991

[5] Newson, P and Heath, M R, "The Capacity of a Spread spectrum CDMA System for Mobile Radio with consideration of system imperfections", *IEEE JSAC*, Vol.12, No.4, May 1994

[6] Sklar, B, "Digital Communications - Fundamentals and Applications", *Prentice Hall* 1988

[7] Edwards, K R: Internal Technical Working Paper, NORTEL, Issue 1.1, NT/IP1/134/KRE/371, August 1995

[8] Monogioudis P, Edmonds R, Tafazolli R and Evans BG, "Multirate 3rd generation CDMA systems", *IEEE Int. Conf. On Comm.*, pp. 151-155

[9] Maxey, J J, and Ormondroyd, R F, "A study of wideband DS-CDMA systems for future generation fixed wireless access schemes", *Internal Report to NORTEL*, 27.1.97

[10] Maxey, J J, and Ormondroyd, R F, "A DS-CDMA design for fixed wireless schemes", *Internal Report to NORTEL*, 10.6.96

[11] Maxey, J J, and Ormondroyd, R F, "Evaluation of a fixed wireless access DS-CDMA system employing low-rate orthogonal convolutional codes", pp. 277-282, *Fifth European Conference on Fixed Radio Systems and Networks (ECRR'96)*, Bologna, Italy, May 1996

[12] Hewitt, T, Parente, P and Vepsalainen, P, "Future fixed service spectrum requirements – An operators' perspective", pp. 19-24, *Fifth European Conference on Fixed Radio Systems and Networks (ECRR'96)*, Bologna, Italy, May 1996

[13] Bollmann, A, *et al*, " Link-capacity and cellular planning aspects for a point to multipoint fixed radio access sytem", pp. 87-93, *Fifth European Conference on Fixed Radio Systems and Networks (ECRR'96)*, Bologna, Italy, May 1996

[14] Ericsson, "A comparison of CDMA and TDMA systems", CIRR TG 8/1, Washington, May 1991

[15] Monogioudis, P, Edmonds, R, Tafazolli, R and Evans, B G, "Multirate 3rd generation CDMA systems", *IEEE International Conference on Communications*, ICC'93, pp. 151-155, 1993

[16] Burr, A G, "Capacity improvement of CDMA systems using M-ary code shift keying", *IEE Conference Publication*, No. 351, pp. 63-67, 1991

[17] Ulloa, J A, Taylor, D P and Poehlman, W F S, "An Expert System Approach for Cellular CDMA", *IEEE Transactions on Vehicular Technology*, Vol. 44, No.1, pp.146-154, 1995

[18] Gass, J H, Noneaker, D L and Pursely, M, "Spectral Efficiency of a Power-Controlled CDMA Mobile Personal Communication System", *IEEE Journal on Selected Areas in Comms.*, Vol. 14, No. 3, April 1996, pp. 559-569

[19] Kudoh, E and Matsumoto, T, "Effect of Transmitter Power Control Imperfections on Capacity in DS-CDMA Cellular Mobile Radios", *Proc. of ICC'92*, Chicago, IL, pp.237-242, June 1992

[20] Viterbi, A J *et al*, "Performance of Power Controlled Wideband Terrestrial Digital Communication", *IEEE Transactions on Communications*, 41(4), pp.559-569, 1993

[21] Zou, J *et al*, "Reverse link analysis and performance evaluation for DS-CDMA cellular systems", *Proc. of IEEE PIMRC'94*, Sept. 1994

[22] Bhargava, V, "High Rate Data Transmission in Mobile and Personal Communications", *PIMRC'94*, pp. 1106-1113

[23] Lee, W C Y, "Increasing System Capacity in PCS", *IEEE Conf. Proceedings of PIMRC'94*, pp. 38-49, 1994

[24] Lee, W C Y, "Smaller cell for greater performance", *IEEE Communication Magazine*, pp. 19-23, Nov 1991

[25] Turkmani, A D *et al*, "Measurement and modelling of wideband mobile radio channels at 900 MHz", *IEE Proceedings*, Vol. 138, No.5, pp.447-457, October 1991

[26] Walrand, J, "Communication Networks: A first course", Aksen Associates, 1991

[27] Mueller, A J *et al*, "Code Rate Optimisation for Coded Packet CDMA Cellular Networks", *ICUPC'94*, Sept. 1994

[28] Jakes, W C, "Microwave mobile communications", *J Wiley & Sons*, New York

[29] Mowbray, R S *et al*; "Increased CDMA system capacity through adaptive cochannel interference regeneration and cancellation", *IEE Proceedings-I*, Vol. 139, No.5, October 1992

[30] Yoo, Y C, Kohno, R and Imai, H, "A Spread-Spectrum Multiaccess System with Cochannel Interference Cancellation for Multipath Fading Channels", *IEEE J. on Selected Areas in Communications*, Vol. 11, No.7, pp. 1067-1075, Sept. 1993

[31] Kerr, R, Wang, Q, and Bhargava, V, "Capacity Analysis of Cellular CDMA", *Proc. ISSSTA'92*, pp. 235-238, March 1992

[32] Brockmeyer, B, Halstron, H L and Jensen, A, "The life and Works of A. K. Erlang", *Copenhagen Telephone Company*, 1943

[33] Lee, W C Y, "Mobile Cellular Telecommunications Systems", *McGraw-Hill*, New York

[34] Benedetto, V, and Scarabosio, L, "DS-CDMA systems for point-to-multipoint fixed radio in the access network", pp. 27-32, *Fifth European Conference on Fixed Radio Systems and Networks (ECRR'96)*, Bologna, Italy, May 1996

[35] Maxey, JJ, and Ormondroyd, R F, "A study of Wideband DS-CDMA Systems for Future Generation Fixed Wireless Access Schemes", *Internal Report to NORTEL*, February 1997.

CHAPTER 11:

CONCLUSIONS & FUTURE WORK

11.1 Conclusions

The technological challenge presented by third generation mobile communications is far from insignificant and one issue which has been, and which remains the subject of extensive debate is what multiple access technique the new systems will exploit. Time division (TDMA) and code division multiple access (CDMA) are both candidates. In the United States, several companies are supporting direct-sequence CDMA for future networks, citing a number of advantages over other multiple access techniques. These include a gradual degradation in link quality with increases in capacity, the ability to exploit multipath for diversity reception and the potential for accommodating more users in a given bandwidth than TDMA. These advantages do not all accrue without some disadvantages, the most significant of which is the vulnerability of DS-CDMA to the multi-user interference. On the uplink, in particular, the fading is independent for each user which enhances the near-far effect at the basestation receiver. It is estimated that for an asynchronous DS-CDMA mobile system the number of users that can be supported without countering the near-far effect in some way is just 1-5% of the signature waveform length; less than 4 users for a 63 chip length code.

This shortcoming has motivated the work presented in this thesis into more sophisticated receiver structures that employ the relevant coding techniques and channel equalisation to multi-carrier CDMA systems in multipath faded channels.

11.1.1 Low-Rate Hyper-Orthogonal Convolutional Coding: Rationale

An alternative method of coding and spreading the data in a spread-spectrum system has been proposed. Instead of cascading a convolutional code with a PN sequence multiplier one can employ a convolutional encoder of very low-rate to encode and spread the input signal simultaneously. If a form of history exists between consecutive data bits then these can be decoded using maximum-likelihood algorithms such as the Viterbi decoder.

The orthogonality of ordinary convolutional codes is very poor, however, and this would lead to a small number of simultaneous users in a multiple access strategy. If low-rate convolutional codes are to be implemented into a DS-CDMA system, then the output bit sequence corresponding to a particular shift register state must be orthogonal to all other output sequences generated by other users. One way of providing orthogonal convolutional codes has been shown through cascading a convolutional encoder with a Hadamard block encoder. In this way, one

can generate orthogonal sequences which follow a pre-determined trellis tree and at the same time use sequences with maximum free distance. This enables the coding gain to be exploited more efficiently.

To utilise the full bi-orthogonal code set, super-orthogonal coding schemes may be used that provide further increases to the coding gain by employing an extra shift register on the front and back end of the conventional Hadamard LROCC system. In this way, the bandwidth expansion factor remains the same and the potential code set is doubled to incorporate not only the orthogonal codes but also their bi-orthogonal sub-set.

To achieve an even higher coding gain, the number of shift registers may be increased arbitrarily (at the cost of hardware complexity, of course!) to achieve further coding gains for the same level of bandwidth expansion. This novel encoder is termed a low-rate hyper-orthogonal convolutional coding (LRHOCC) scheme. This thesis has shown that this process can lead to an increased free distance of the convolutional code by eliminating more paths with a Hamming distance of only half the spreading length and replacing them with paths having a Hamming distance of the full spreading length. This is particularly important at the initial starting paths and the final paths of the trellis.

11.1.2 Low-Rate Hyper-Orthogonal Convolutional Coding: Performance

The performance of LROCC and novel LRHOCC schemes have been studied in a single-user and multi-user AWGN environment and multipath Rayleigh faded channels. Considerable performance improvements have been found for both coding strategies compared to conventional rate ½ convolutional coding strategies.

Theoretical curves using the upper-bound on LROCC and higher rate convolutional codes have shown that LROCC codes can give potential coding gains that are about 1dB higher than rate ½ convolutional codes at low E_b/N_o values, but a similar performance at signal-to-noise ratios greater than 5dB. The theoretical excess E_b/N_o required for non-coherent Rayleigh faded channels is about 6dB more than the coherent unfaded case.

The simulated results have been shown to closely follow the theoretical curves, with an E_b/N_o level of 4.5dB required to achieve a BER of 10^{-5}. Using LRHOC codes of constraint length 6 and rate ¼ reduces the signal-to-noise ratio to 4dB and to a level of 3dB with a constraint length 8, rate 1/64 code.

The importance of using randomising sequences has been outlined in a multi-user environment. It has been shown that at least 2dB will be lost through not employing the correct randomising sequences to effectively make the interference from other users appear Gaussian in nature. To achieve a BER of 10^{-3} without coding and using Gold codes of length 63 can accommodate about 7 users, whereas LROC coding has shown to increase the potential capacity to about 15 users, hence providing nearly twice an increase in capacity.

The simulation of a rate 1/32, constraint length 5 LROCC scheme in a 4-path Rayleigh faded channel with a Doppler of 300Hz has shown to provide extremely good coding gains. Compared to uncoded faded channels, a coding gain in the order of 6dB was found for bit-error rates of 10^{-5} using LROCC structures with BPSK modulation. Using LRHOCC coding with a constraint length of 8 and rate 1/64 has shown to increase the coding gain to over 10dB at BER=10^{-6}. Of course, this is achieved at the expense of increased hardware complexity.

In summary, the use of LROCC coding can potentially achieve significant coding gains as high or even higher than conventional convolutional codes of high rate. Of course, in a multi-user environment these codes exploit coding and spreading without the bandwidth/code-rate penalty. The use of LRHOCC has shown to provide further increases in the coding gain in unfaded and faded channels. These codes are particularly attractive to adaptive systems that may wish to increase the complexity of the code when the channel conditions degrade without increasing the bandwidth of the code.

11.1.3 Multi-Carrier CDMA: Rationale

The orthogonality between all active users in a cellular environment plays an important part in the performance level and capacity that may be achieved. If all users are separated in the code-domain through deterministic PN code sequences, the unwanted interference in an AWGN channel may be eliminated if the interference from all active users is cancelled. In faded multipath channels, this is more burdensome, and only limited capacity advantages may be achievable. The level of orthogonality in the time-domain could therefore be replaced by an alternative modulation scheme using orthogonal multiple carriers in the frequency domain to achieve diversity and orthogonality between users. Due to the inherent low levels of Doppler in FWA systems this method becomes extremely attractive.

If the symbol or chip period of a spread-spectrum system is greater than the time-delay spread of the channel, the fading characteristics on the transmitted signal are frequency non-selective. This gives the receiver little or no diversity and hence presents a problem to successful reception. On the other hand, if the symbol length is less than the time-delay spread of the channel, the channel is frequency-selective and can provide diversity at the cost of increased problems with ISI. The implementation of RAKE receivers resolves this problem and can give time domain diversity. Alternatively, one can provide spreading in the frequency domain and modulate the spread signal over a number of sub-carriers, termed as MC-CDMA or MC-DS-CDMA.

The primary advantage of MC-CDMA is its ability to operate in a high user rate system that has only a limited system bandwidth available for spreading. Because MC-CDMA strategically tries to reduce the effects of multi-user interference through sub-carriers and guard intervals, MC-CDMA does not become less efficient in terms of bits/s/Hz when the spreading factor is reduced, as in DS-CDMA systems. Therefore, the goal of MC-CDMA is to address the area of weakness of the DS-CDMA system by supporting higher data-rates. Since a MC-CDMA system is able to adjust the number of sub-carriers per user signal, MC-CDMA is highly flexible with respect to variable rate traffic.

MC-CDMA is directly applicable to the downlink where the rigid requirement of synchronisation can more easily be met. Moreover, the downlink must provide a high capacity signaling method that uses inexpensive receivers for use in the mobile units.

To achieve bandwidth allocations for ever increasing bandwidth requirements, frequency allocation for PCS will involve frequency ranges higher than those currently in use. High carrier frequencies and high mobile speeds combined with the long symbol duration of an OFDM data block render the multipath fading channel highly time-varying. We wish to maintain a constant, time-invariant fading level over the duration of an OFDM block. This poses a challenge to the equalisation of such a channel.

A number of techniques to equalise the channel effectively have been introduced and shown to provide sufficient diversity to combat the frequency selectivity of the fading channel and provide multiple access. Relatively simple equalisation structures have been compared and shown to provide a good performance if incorporated together with interference cancellation structures, orthogonal coding and adequate interleaving.

11.1.4 Multi-Carrier CDMA: Performance

First, the performance of a MC-CDMA design using a relatively small number of overlapping sub-carriers has been introduced in context with coherent and non-coherent modulation formats. The system was modeled using 32 sub-carriers and a data-rate of 8 kb/s in a frequency selective Rayleigh fading channel with 4 and 7 paths.

The MC-CDMA frequency-domain RAKE receiver using coherent BPSK demodulation has shown to closely approach the lower theoretical bound of a DS-CDMA RAKE receiver. To achieve a BER=10^{-3} it can be seen that the MC-CDMA system requires about 11dB whereas the DS-CDMA RAKE receiver requires nearly 1dB more. To achieve a BER as low as 10^{-5} would require at least 17dB. This method, though, requires perfect knowledge of the channel amplitude and phase. It has therefore been suggested to investigate non-coherent DPSK modulation techniques.

The DPSK MC-CDMA frequency-domain RAKE receiver was implemented over the same channel with LROC coding, block interleaving and guard-bands. The channel model also includes Doppler fading of 200 Hz which corresponds to a vehicle speed of 135km/h at a carrier frequency of 1.6GHz. It was shown that this type of implementation is very resistant to increases in the number of multipaths in the channel. This is due to the inherent frequency diversity available through multi-carrier modulation and interleaving in the frequency-domain.

The use of LROCC strategies in MC-CDMA has also shown to provide an extremely positive result in the overall coding gain achieved in multipath faded channels. A total coding gain of up to 12dB has been achieved for BER=10^{-5}, with little degradation in reduced levels of multipath. Comparing these results with conventional DS-CDMA RAKE receivers using rate ½, constraint length 7 convolutional coding has shown that the difference in performance can be as high as 4dB for L=4 paths and 2dB for L=7 paths, therefore giving MC-CDMA LROCC schemes considerable performance advantages.

In multi-user environments it has been shown that the use of increased number of sub-carriers can reduce the interleaving depth requirements and provide independent frequency non-selective fading on each sub-channel as long as the guard-interval is longer than the maximum delay spread of the channel. This eliminates ISI but still introduces fading between neighboring sub-carriers. Therefore, the type of equalisation scheme to be implemented is extremely

important for the performance of the system. A number of different equalisers with dissimilar complexity have been introduced. MRC and EGC have been shown to be of no practical use for the downlink since they do not restore the orthogonality of the users in the receiver. The use of ZF equalisers can be seen to give improvements in performance by attempting to restore the orthogonality between users but still performs worse than EGC at low E_b/N_o due to noise amplifications in the equaliser. The concept of controlled equalisation is therefore an attractive alternative method to combine the advantages of EGC and ZF equalisation. The receiver, of course, must estimate the optimum threshold level. Nevertheless, with this method it is possible to achieve a BER of 10^{-3} at about 15dB, with an irreducible BER level of about 10^{-4} as the SNR approaches infinity.

More complex equalisers using channel statistics such as the number of active users and the received SNR have also been investigated. The use of MMSE equalisation has shown to reduce the E_b/N_o requirement at a BER of 10^{-3} to 14dB, and 20dB for a BER of 10^{-5}, a level which cannot be achieved using controlled equalisation. The use of MLD at maximum user capacity has shown to reduce the E_b/N_o requirement at a BER=10^{-3} to about 12dB at the cost of increased hardware complexity.

The multi-user MC-CDMA system simulated in this thesis presents an interesting concept of implementing interference cancellation on the downlink as well as the uplink. Orthogonal coding for all users in AWGN channels on the downlink would give no additional improvement using interference cancellation schemes, but in multipath channels considerable improvements can be accomplished. As the orthogonality between all users is severely distorted in multipath channels it becomes necessary to attempt to restore the orthogonality between the users through appropriate equalisation methods on the first stage and then combine the maximum SNR on all sub-carriers for the wanted user. This can only be achieved by introducing different equalisers on the initial detection and final equalisation/combining stages. In this way the use of orthogonality restoring equalisers such as zero-forcing or controlled equalisers are implemented on the first stage of detection and an optimum and simple combining method such as MRC on the final stage. At the last stage of detection it assumed that the unwanted users have been removed from the composite signal and the use of MRC is therefore in favour of orthogonality restoring equalisers.

This model has been introduced in the simulation of the up- and downlink of a MC-CDMA system using 512 sub-carriers and various equalisation and detection methods. These systems were simulated over the Bad Urban COST-207 channel with Doppler of 200Hz. It has been shown that controlled equalisation is in favor of MRC, EGC and zero-forcing strategies without

requiring information about the channel SNR or the number of active users. If interference cancellation techniques are to be used, it has been shown that the use of zero-forcing or controlled equalisers is not as important and gives virtually the same results. In this case, it is more important to have more accurate knowledge of the channel statistics than to use threshold levels for controlled equalisation. Nevertheless, the use of MAI cancellation techniques has shown to introduce little deviation of the optimum threshold level for implementing controlled equalisation. To achieve a BER of 10^{-3} the level of E_b/N_o required at the receiver can be reduced to 5dB and to 10dB for a BER of 10^{-5} using one iteration of interference cancellation. More realistic measurements with noisy channel estimates increase the E_b/N_o requirement by 5dB, giving an SNR requirement of 10dB for BER=10^{-3} and 15dB for BER=10^{-5}.

On the uplink, it has been found that controlled equalisation is in strong favour of zero-forcing equalisation and its application is particularly important when no interference cancellation is implemented. For a total spreading ratio of 32 it can be seen that already at 8 users the performance has been degraded sufficiently to render the system saturated. However, at low numbers of active users the use of interference cancellation can be seen to provide sufficient improvements in the reduction of BER. To achieve a BER=10^{-3}, only 3 users can be served using controlled equalisation, whereas interference cancellation allows twice as many users. Of course, at higher levels of active users the use of interference cancellation schemes becomes questionable. In fact, system performance is worse using interference cancellation than controlled equalisation alone. This is because at high levels of interference through multiple users the interference estimates become highly corrupted and only serve to degrade performance rather than improve it.

For this reason it can be concluded that interference cancellation schemes may only provide reasonable capacity gains on the uplink if the channel parameters can be estimated accurately and the level of interference from other users is relatively low. On the downlink, however, the use of interference cancellation presents little problem and serves to improve capacity at all levels of E_b/N_o and full user capacity.

11.2 Concluding Remarks

The significant advantages of the investigation into coherent and non-coherent transmitter and receiver designs for FWA and mobile cellular systems presented in this thesis can be summarised as:

- In FWA and mobile cellular systems it has been shown that the correlation statistics on the link level between the subscriber and basestation can have dramatic effects on the inter-cell interference. The use of highly directional antennas and stationary users has shown that the effects of shadowing depend heavily on the correlation of the fading signals on the uplink. The anticipated inter-cell frequency re-use factor for realistic values of decay index (2 to 4) unlikely will drop below 0.85. For mobile cellular applications it has been found that this value can be as low as 0.2, therefore having a significant effect on the overall cellular capacity.

- The use of tri-sectorisation at the basestation gives further opportunity for increases in user capacity through the improvement in the fading statistics, in addition to the obvious improvement in capacity through sectorisation of the cell area. For coherent systems, the use of pilot tones is necessary, giving a reduction in user capacity at the expense of spectrum for pilot tone occupancy. It is therefore of vital importance to treat the inherent advantages of coherent designs over non-coherent designs with great care.

- The use of LROOC coding has been shown to give extremely positive results, and with further enhancements to the original encoder design, the use of hyper-orthogonal convolutional coding schemes can give additional coding gain in AWGN and multipath Rayleigh faded channels.

- Orthogonal Hadamard sequences have particularly bad auto-correlation properties and to improve these, different PN randomising sequences have been tested and found to improve both the spectral properties of the transmitted signal, and the isolation between users.

- Using low-rate orthogonal convolutional codes in non-coherent DS-CDMA applications where the channel is impaired by L-path Rayleigh fading can yield improved performance as long as the data is interleaved at the bit level. The minimum signal-to-noise ratio per bit required to achieve the same performance as in an unfaded AWGN channel is seen to be at

about 6dB. Therefore, for equal system complexity, the losses encountered through non-coherent combining degrade any gain achieved through diversity, either achieved at the data bit level through K-fold interleaving or an increase in the number of path levels, L.

- The LROCC-OFDM technique has shown to provide considerable resilience to increases in the number of multipaths in the channel and through non-coherent differential modulation on each output of the FFT in the receiver it is possible to resolve some of the frequency selective fading components in the frequency domain.

- Considerable performance improvements have been found with LROCC strategies applied to multi-carrier OFDM designs with adequate interleaving to make the multipath fading effects independent on each channel.

- The implementation of LROCC in multi-carrier systems will give improved performance over other conventional coding techniques in partial band interference and fading, as the use of diversity is increased at an even coarser level. The independence between successive branches is one way of achieving this diversity. It has been shown that the anticipated performance degradation due to interference concentrated into selected sub-bands of the multi-carrier system will be most likely position independent, compared to previously suggested high-rate coded systems, where it can be found that partial band interference performances are dependant on the position within the total bandwidth occupied by the system.

- The use of LROCC and controlled equalisation with MAI cancellation in the uplink have been shown to provide a capacity gain of at least 25% at BER=10^{-3}, and likewise a 10dB gain in E_b/N_o in the downlink with rate R=1/2 convolutional codes. More realistic performance results with noisy channel estimates have been found to provide a degradation of at least 6dB on this result, yielding a potential improvement of 4dB.

- The use of zero-forcing equalisers would not lead to a good performance without MAI cancellation, but through the use of MAI cancellation it is possible to combine zero-forcing algorithms with MRC on the final detection stage to give good results. It has been shown, however, that controlled equalisation for the first detection stage, in combination with MRC on the second detection stage outperforms the zero-forcing equaliser. This improvement is particularly noticeable for the system when MAI cancellation is not used.

- A capacity comparison of ATDMA and MC-CDMA for FWA applications has shown that MC-CDMA designs have a potentially higher capacity, particularly on the downlink, compared to ATDMA designs with PRMA. The capacity advantages that may be achieved with MC-CDMA become clear when compared with the theoretical Erlang capacity. Whilst the occupancy distribution of LCH gives a lower capacity due to users remaining in the system, MC-CDMA still gives a higher number of potential subscribers than ATDMA. The potential number of users that may be served by a central basestation with tri-sectorisation can be as high as 1233 on the downlink of a MC-CDMA system compared with 891 using ATDMA. Since MC-CDMA cellular systems are ultimately uplink limited, this reduces to a level of 966 potential subscribers on the uplink. Nevertheless, the capacity is still higher than for ATDMA designs.

- Whilst MC-CDMA designs may have an improved capacity compared with ATDMA techniques, they also provide universal frequency re-use, a feature that makes CDMA techniques favourable in their own right.

11.3 Future Work

The work described in this thesis has highlighted a number of areas worthy of further investigation and these are listed within this section.

11.3.1 Synchronisation

The work in this thesis has not covered the aspects of synchronisation for coherent and non-coherent multi-carrier and single-carrier DS-CDMA systems. It is widely known that the use of non-coherent DPSK in both single-carrier and multi-carrier systems yields a much simplified approach with little need for accurate synchronisation as in coherent systems. Using spectrum shaping techniques [3] before the IFFT in the transmitter of a MC-CDMA system has shown considerable advantages in the synchronisation, but at the cost of increased self-interference within each block. This calls for more complex equalisation structures.

11.3.2 Reduction of the Crest Factor

Multi-carrier modulation techniques have a large peak to mean envelope ratio and therefore the power amplifier in the portable unit must be highly linear and have a high power efficiency. This requires operation in a non-linear region such as class B or class AB [4]. In this case the multi-carrier signal suffers from a high level of inter-modulation distortion, AM/AM and

AM/PM distortions. The crest factor used to describe the relative variation in amplitude level at the input to the power amplifier in the transmitter needs to be as low as possible, otherwise the large fluctuations in amplitude calls for highly linear amplifiers in the upper region of the response curve. As most amplifiers in the transmitter can only cope with relatively small fluctuations in amplitude, a number of research topics focus on the linearisation of power amplifiers and/or the reduction of the crest factor. Hence to minimize this distortion it is preferred that the signal be amplified using a constant envelope, like GMSK modulation, for example. The reduction of the crest factor leads to three main possibilities: (a) spectrum shaping of the signal before the IFFT and, (b) the use of alternative modulation methods or (c) replacing the IFFT with a wavelet based design, which is treated in the next section.

11.3.3 Wavelet Based Transmission

Wavelets are a pre-defined stored number of samples of a signal that constitute a small section of a continuous waveform. In this way, it is possible to form a composite signal from a number of sub-sections of compactly supported orthogonal wavelets. This has been shown to give a significantly higher bandwidth efficiency [1] than conventional MC-CDMA systems. Wavelet based designs posses almost the same desirable characteristics (e.g. frequency diversity and small ISI) as conventional FFT based multi-carrier systems, and in addition provide new dimensions for the anti-fading and interference immunity by the suitable choice of the wavelet functions and the wavelet frequency bands. Of course, wavelet based designs require more complex transmitter hardware, but for sophisticated multimedia applications they could provide an attractive alternative solution.

11.3.4 Decoding Strategies

It is possible to employ a soft output Viterbi algorithm by modifying the Viterbi decoder in the receiver. This has the advantage of not making a hard decision at the output and integrating the output estimate with sophisticated interference cancellation techniques to remove the other-user unwanted interference. This could lead to potential capacity improvements, especially on the uplink of a FWA system.

11.3.5 Channel Estimation

The pilot tone overhead of 25% used in the simulations of this thesis can be reduced to at least 6.25% by further interpolating in the time-domain rather than the frequency-domain solely. This

is achieved by Wiener filtering in 2-D rather than 1-D. The concept has been analyzed in [5], where it can be shown to yield considerable reduction in pilot-tone overheads without degrading the bit-error performance significantly. The slower the fading in the channel, of course, the better this method will work. An interesting filed of future research could be the investigation of other channel estimation algorithms.

11.4 References

[1] Chang, K H et al, "Performance Analysis of Wavelet-based MC-CDMA for FPLMTS/IMT-2000", pp. 1356-1360, *IEEE Proceedings of ISSSTA '96*, Mainz, Germany, September 1996

[2] Boccuzzi, J, "Performance evaluation of non-linear transmit power amplifiers for North-American digital cellular portables", *IEEE Trans. on Veh. Tech.*, Vol. 44, No. 2, pp. 220-228, May 1995

[3] Schneider, K, and Tranter, W, "Efficient simulation of multi-carrier digital communication systems in non-linear channel environments", *IEEE JSAC*, Vol. 11, No. 3, pp. 328-339, April 1993

[4] Sundstrom, L, et al, "Effect of reconstruction filters in digital pre-distortion linearizers for RF amplifiers", *IEEE Trans. on Veh. Tech.*, Vol. 44, No. 1, pp. 131-138, February 1995

[5] Hoeher, P, Kaiser, S, and Robertson, P, "Pilot-Symbol-Aided Channel Estimation in Time and Frequency", *Multi-Carrier Spread Spectrum (Kluwer Academic Publishers)*, p. 169-178, 1997, Printed in Netherlands

APPENDIX A

A.1 Spectrum of a Pulse Train

A signal of great interest in digital communications is an ideal periodic sequence of rectangular pulses, called a pulse train, illustrated in figure (A-1).

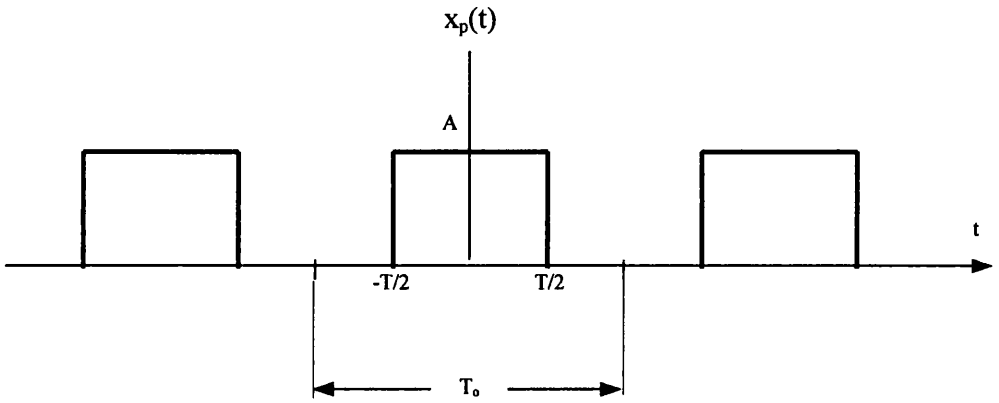

Figure A-1. Pulse train

For the pulse train, $x_p(t)$, with pulse amplitude A, pulse width T, and period T_0, the reader can verify, using the standard Fourier coefficient equations:

$$x(t) = \sum_{n=-\infty}^{\infty} c_n e^{j2\pi n f_o t} \tag{A-1}$$

where,

$$c_n = \frac{1}{T_o} \int_{-T_o/2}^{T_o/2} x(t) e^{-j2\pi n f_o t} . dt \tag{A-2}$$

that the Fourier series coefficients are given as:

$$c_n = \frac{AT}{T_o} \frac{\sin(n\pi T / T_o)}{n\pi T / T_o} = \frac{AT}{T_o} \sin c \frac{nT}{T_o} \tag{A-3}$$

where,

$$\sin c\, y = \frac{\sin(\pi y)}{\pi y} \tag{A-4}$$

The sinc function, as shown in figure (A-2), has a maximum value of unity at y=0 and approaches zero as y approaches infinity, oscillating through positive and negative values. It goes through zero at $y = \pm 1, \pm 2, \ldots$

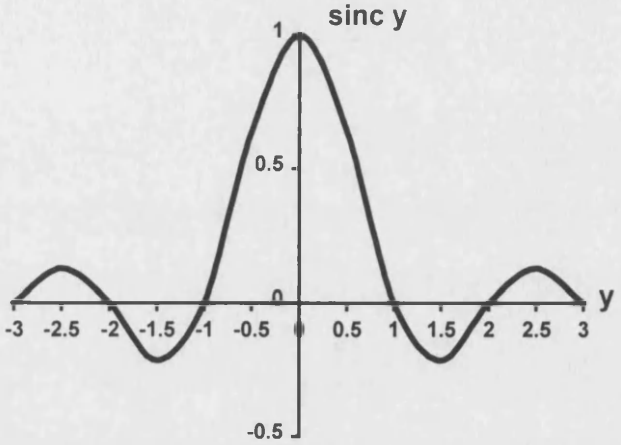

Figure A-2. Sinc function of pulse train

The pulse train magnitude spectrum, $|c_n|$ as a function of n/T_o is plotted in figure (A-3), and the phase spectrum, θ_n, is plotted in figure (A-4).

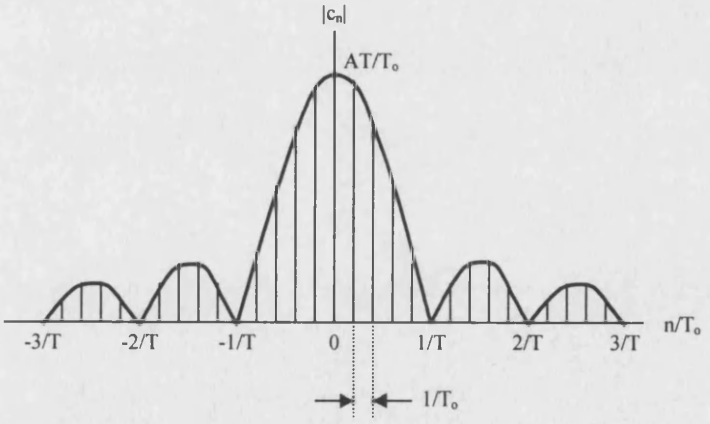

Figure A-3. Magnitude spectrum of pulse train

The positive and negative frequencies of the two-sided spectrum represent a useful way of expressing the spectrum mathematically; of course, only the positive frequencies can be reproduced in a laboratory.

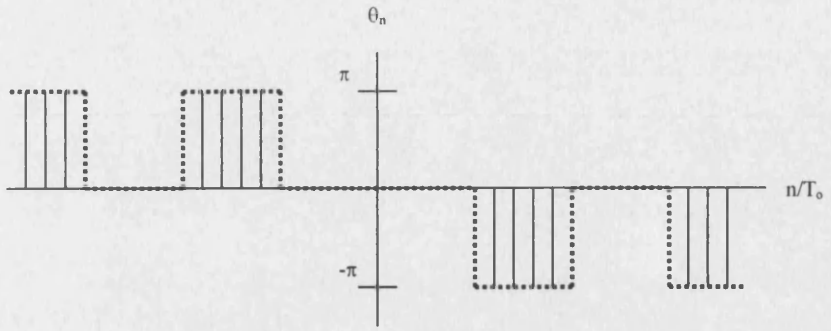

Figure A-4. Phase spectrum of pulse train

Synthesis is performed by substituting the coefficients of equation (A-3) into equation (A-1). The resulting series below yields the original ideal pulse train, $x_p(t)$, synthesised from its component parts.

$$x_p(t) = \frac{AT}{T_o} \sum_{n=-\infty}^{\infty} \sin c \frac{nT}{T_o} e^{j2\pi f_o t} \qquad \text{(A-5)}$$

The ideal periodic pulse train contains frequency components at all integer multiples of the fundamental. In communication systems the significant portion of a baseband signal's power or energy is often assumed to be contained within the frequencies from zero to the first null of the magnitude spectrum (see figure (A-3)). Therefore, $1/T$ is often used as a measure of signal bandwidth, in Hertz, for a pulse train with pulse width T. Note that the bandwidth is inversely proportional to pulse width; the narrower are the pulses, the wider the bandwidth associated with these pulses. Also, notice that the spacing between spectral lines $\Delta f = 1/T_o$ is inversely proportional to the pulse period; as the period increases, the lines move closer together.

APPENDIX B

B.1 Chernoff Bound

We seek to evaluate some well-known bounding techniques for constant amplitude and phase signals, coherently demodulated in additive Gaussian noise. We then proceed to show that same bounds hold in some cases when the actual multiple access interference distributions are used in place of the Gaussian approximation. These bounding techniques have applications in many statistical bit-error rate calculations for digital communication systems.

The Chernoff bound on a distribution is an extension of the older Chebyshev bound. It is obtained by upper-bounding the unit step function inherent in the following calculation. For the random variable x, we can express the complementary distribution function,

$$\Pr(x > X) = \int_{-\infty}^{\infty} u(x - X)dF(x) = \mathrm{E}[u(x - X)] \tag{B-1}$$

where $u(\cdot)$ is the unit step function,

$$u(\xi) = \begin{cases} 1 & \text{if } \xi \geq 0, \\ 0 & \text{otherwise} \end{cases} \tag{B-2}$$

and $F(x)$ is the distribution function.

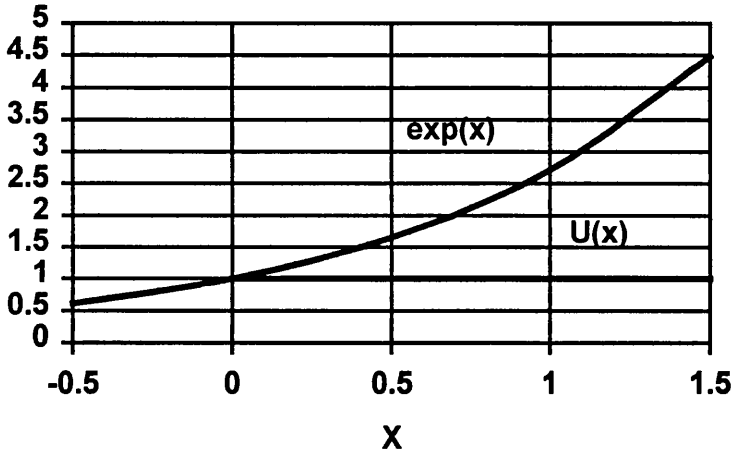

Figure B-1. Bound on exponential and unit step function

Then since,

$$u(\xi) \le \exp(\rho\xi) \qquad \rho>0 \tag{B-3}$$

with equality if and only if $\xi=0$, it follows that,

$$\begin{aligned} \Pr(x > X) &< \mathrm{E}\left\{\exp\left[\rho(x-X)\right]\right\} \\ &= \mathrm{e}^{-\rho X}\int_{-\infty}^{\infty} e^{\rho x}\,dF(x) \qquad \rho>0 \end{aligned} \tag{B-4}$$

Minimising with respect to ρ, we obtain,

$$\Pr(x > X) < \min_{\rho>0} e^{-\rho X}\mathrm{E}\left(e^{\rho x}\right) \tag{B-5}$$

which is the *Chernoff* bound.

B.2 Bhattacharyya bound

When the random variable represents a likelihood function and $X=0$ so that the probability (B-4) becomes an error probability, applying the Chernoff bound gives rise to another well known bound. Let y be the decision variable and let $p_0(y)$ and $p_1(y)$ be the respective probability density functions under the hypotheses that "0" or "1" was sent. Then, given that "0" was sent,

$$\begin{aligned} P_{E_0} &= \Pr\left(\ln\frac{p_1(y)}{p_0(y)} > 0 \,|\, \text{"0" sent}\right) < E\left[\exp\left\{\rho\ln\left[p_1(y)/p_0(y)\right]\right\}|\,\text{"0" sent}\right] \\ &= \int_{-\infty}^{\infty}\left[\frac{p_1(y)}{p_0(y)}\right]^{\rho} p_0(y)dy \\ &= \int_{-\infty}^{\infty} p_0^{1-\rho}(y)p_1^{\rho}(y)dy, \qquad \rho>0 \end{aligned} \tag{B-6}$$

The same applies to P_E with $p_0(y)$ and $p_1(y)$ interchanged. Choosing ρ = ½ leads to the particularly simple expression:

$$P_E \le \int_{-\infty}^{\infty} \sqrt{p_0(y)p_1(y)}.dy \tag{B-7}$$

known as the *Bhattacharyya* bound.

B.3 Bounds for Gaussian noise channels

As an example application of both the Chernoff bound consider coherent reception in Gaussian noise with energy-to-noise density E/I_0. Then the normalised demodulator output variable y is Gaussian, with variance $I_0/2$ and mean $\pm\sqrt{E}$. The sign depends on whether the transmitted symbol had a positive or negative sign corresponding to a "0" or "1", respectively. Then, since by symmetry $P_{E0}=P_{E1}=P_E$,

$$\begin{aligned} P_E = \Pr(y>0|-) &= \frac{1}{\sqrt{\pi I_0}} \int_0^{\infty} \exp\left[-\left(y+\sqrt{E}\right)^2 \Big/ I_0 \right].dy \\ &= \frac{1}{\sqrt{2\pi}} \int_{\sqrt{2E/I_0}}^{\infty} e^{-x^2/2}.dx \\ &= Q\left(\sqrt{2E/I_0}\right) \end{aligned} \tag{B-8}$$

The Chernoff bound to this probability is obtained using (B-5), where x has mean $-\sqrt{E}$ and variance $I_0/2$ and X=0. Thus,

$$\begin{aligned} E\left(e^{\rho x}\right) &= \frac{1}{\sqrt{\pi I_0}} \int_{-\infty}^{\infty} e^{\rho x} e^{-\left(x+\sqrt{E}\right)^2/I_0}.dx \\ &= \exp\left[\left(\rho I_0 - 2\sqrt{E}\right)^2 / 4I_0 \right] e^{-E/I_0} \quad , \quad \rho > 0 \end{aligned} \tag{B-9}$$

and

$$P_E < \underset{\rho>0}{Min}\, E\left(e^{\rho x}\right) \tag{B-10}$$

This expression is minimised by the choice $\rho=2\sqrt{E/I_0}$, for which

$$P_E < e^{-E/I_0} \tag{B-11}$$

The same result is obtained from the Bhattacharyya bound, as can be seen by applying (B-7) with:

$$p_0(y) = \frac{1}{\sqrt{\pi I_0}} \exp\left[-\left(y - \sqrt{E}\right)^2 / I_0\right]$$
$$p_1(y) = \frac{1}{\sqrt{\pi I_0}} \exp\left[-\left(y + \sqrt{E}\right)^2 / I_0\right] \quad \text{(B-12)}$$

Hence,

$$P_E < \int_{-\infty}^{\infty} \sqrt{p_0(y) p_1(y)}.dy = \frac{e^{-E/I_0}}{\sqrt{\pi I_0}} \int_{-\infty}^{\infty} e^{-y^2/I_0}.dy = e^{-E/I_0} \quad \text{(B-13)}$$

which gives an upper bound on the bit-error probability for Gaussian noise channels.

B.4 References

[1] Gallager, R G, *Information Theory and Reliable Communication*, Wiley, New York, 1968

[2] Viterbi, A J, CDMA – Principles of Spread Spectrum Communication, Addison-Wiley, 1995

APPENDIX C

C.1 Derivation of equation (7-55)

Referring to equation (7-55), the mean of the ISI term is:

$$E\{ISI\} = E\left\{\sum_{l=1}^{L-1} a_l\left[d_k(-1)X_{k,k}^{l} + d_k(0)\hat{X}_{k,k}^{l}\right]\right\}$$
$$= \sum_{l=1}^{L-1} E\left\{a_l\left[d_k(-1)X_{k,k}^{l} + d_k(0)\hat{X}_{k,k}^{l}\right]\right\} \qquad \text{(C-1)}$$

Due to independence of a_l with d_k and $X_{k,k}$ and $\hat{X}_{k,k}$, it becomes:

$$E\{ISI\} = \sum_{l=1}^{L-1} \overline{a_l}\left[\overline{d_k(-1)}\,\overline{X_{k,k}^{l}} + \overline{d_k(0)}\,\overline{\hat{X}_{k,k}^{l}}\right] \qquad \text{(C-2)}$$

Since $E\{d_k(-1)\}=E\{d_k(0)\}=0$, the mean of the ISI will be zero. Nevertheless, the variance is:

$$\sigma_{ISI}^2 = E\left\{\sum_{l_1=1}^{L-1}\sum_{l_2=0}^{L-1} a_{l_1}a_{l_2}\left[d_k(-1)X_{k,k}^{l_1} + d_k(0)\hat{X}_{k,k}^{l_1}\right]\cdot\left[d_k(-1)X_{k,k}^{l_2} + d_k(0)\hat{X}_{k,k}^{l_2}\right]\right\} \qquad \text{(C-3)}$$

Again, because a_l and d_k are independent of $X_{k,k}$ and $\hat{X}_{k,k}$, and due to the independence of data bits at different intervals, (C-3) can be written as:

$$\sigma_{ISI}^2 = \sum_{l_1=1}^{L-1}\sum_{l_2=0}^{L-1} \overline{a_{l_1}a_{l_2}}\left[\overline{d_k(-1)^2 X_{k,k}^{l_1}X_{k,k}^{l_2}} + \overline{d_k(0)^2\hat{X}_{k,k}^{l_1}\hat{X}_{k,k}^{l_2}}\right] \qquad \text{(C-4)}$$

which is,

$$\sigma_{ISI}^2 = \sum_{l_1=1}^{L-1}\sum_{l_2=0}^{L-1} \overline{a_{l_1}a_{l_2}}\left[\overline{X_{k,k}^{l_1}X_{k,k}^{l_2}} + \overline{\hat{X}_{k,k}^{l_1}\hat{X}_{k,k}^{l_2}}\right] \qquad \text{(C-5)}$$

Considering independent path components, that is $E\{a_{l_1}a_{l_2}\} = \sigma_{a_{l_1}}{}^2\delta(l_1 - l_2)$ becomes:

$$\sigma_{ISI}^2 = \sum_{l=1}^{L-1} \sigma_{a_l}{}^2 \left[\overline{\left(X_{k,k}^l\right)^2} + \overline{\left(\hat{X}_{k,k}^l\right)^2} \right] \tag{C-6}$$

Using equation (7-48), the first term in the bracket of (C-6) is calculated as:

$$\overline{\left(X_{k,k}^l\right)^2} = E\left[\cos^2 \phi_{k,l} R_{k,k}^2(\tau_l)\right] = E\left[\frac{\tau_l^2}{2}\right] + E\left[\frac{\tau_l^2}{2}\cos(4\pi f_k \tau_l - 2\theta_l)\right] \tag{C-7}$$

where $\phi_{k,l} = 2\pi f_k \tau_l - \theta_l$. By denoting

$$g(\tau_l, \theta_l) \equiv \tau_l^2 \cos(4\pi f_k \tau_l - 2\theta_l) \tag{C-8}$$

Equation (C-7) can be written as:

$$\overline{\left(X_{k,k}^l\right)^2} = \frac{\overline{\tau_l^2}}{2} + \frac{1}{2}E[g(\tau_l, \theta_l)] \tag{C-9}$$

The second term of (C-9) can be calculated as:

$$E[g(\tau_l, \theta_l)] = E_{\theta_l}\left\{E_{\tau_l}[g(\tau_l, \theta_l)|\theta_l]\right\} \tag{C-10}$$

Omitting the subscript l for the ease of notation,

$$\begin{aligned} E_\tau[g(\tau,\theta)|\theta] &= \int_\tau \tau^2 \cos(4\pi f_k \tau - 2\theta) f_{T_b}(\tau) d\tau \\ &= \cos 2\theta \underbrace{\int_\tau \tau^2 \cos(4\pi f_k \tau) f_{T_b}(\tau) d\tau}_{\alpha_1} + \sin 2\theta \underbrace{\int_\tau \tau^2 \sin(4\pi f_k \tau) f_{T_b}(\tau) d\tau}_{\alpha_2} \\ &= \alpha_1 \cos 2\theta + \alpha_2 \sin 2\theta \end{aligned} \tag{C-11}$$

where $f_{Tb}(\tau)$ is the probability density function of τ. By assuming a uniform $[0,2\pi)$ distribution for θ, equation (C-10) results in:

$$\begin{aligned} E\left[g(\tau,\theta)\right] &= E_\theta\left[\alpha_1 \cos 2\theta + \alpha_2 \sin 2\theta\right] \\ &= \alpha_1 E\left[\cos 2\theta\right] + \alpha_2 E\left[\sin 2\theta\right] = 0 \end{aligned} \tag{C-12}$$

Therefore, equation (C-9) yields:

$$\overline{\left(X_{k,k}^{I}\right)^2} = \frac{\overline{\tau_I^2}}{2} \tag{C-13}$$

In a same manner one can show that

$$\overline{\left(\hat{X}_{k,k}^{I}\right)^2} = \frac{T_b^{\,2}}{2} - T_b\,\overline{\tau_I} + \frac{\overline{\tau_I^2}}{2} \tag{C-14}$$

Substituting equation (C-13) and (C-14) in (C-6) finally gives the variance of the ISI as:

$$\sigma_{ISI}^2 = \sum \sigma_{a_I}^{\,2}\left[\overline{\tau_I^2} - T_b\,\overline{\tau_I} + \frac{T_b^{\,2}}{2}\right] \tag{C-15}$$

APPENDIX D

D.1 Derivation of equation (7-56)

Referring to equation (7-56), the ICI can be written as:

$$ICI = \sum_{l=0}^{L-1} \sum_{n=0, n\neq k}^{N-1} a_l \left\{ d_n(-1) U_{n,k,l} + d_n(0) V_{n,k,l} \right\} \tag{D-1}$$

where,

$$\begin{aligned} U_{n,k,l} &= X^l_{n,k} + Y^l_{n,k} \\ V_{n,k,l} &= \hat{X}^l_{n,k} + \hat{Y}^l_{n,k} \end{aligned} \tag{D-2}$$

Similar to what was carried out for the calculation of the mean of the ISI term, one can show that E{ICI}=0. The variance of the ICI can be calculated as:

$$\sigma^2_{ICI} = E \sum_{l_1=0}^{L-1} \sum_{n_1=0, n_1\neq k}^{N-1} \sum_{l_2=0}^{L-1} \sum_{n_2=0, n_2\neq k}^{N-1} a_{l_1} a_{l_2} \left[d_{n_1}(-1) U_{n_1,k,l_1} + d_{n_1}(0) V_{n_1,k,l_1} \right] \cdot \left[d_{n_2}(-1) U_{n_2,k,l_2} + d_{n_2}(0) V_{n_2,k,l_2} \right] \tag{D-3}$$

Using similar assumptions as Appendix C, equation (D-3) can be written as:

$$\sigma^2_{ICI} = E \sum_{l_1=0}^{L-1} \sum_{n_1=0, n_1\neq k}^{N-1} \sum_{l_2=0}^{L-1} \sum_{n_2=0, n_2\neq k}^{N-1} \overline{a_{l_1} a_{l_2}} \left[\overline{d_{n_1}(-1) d_{n_2}(-1)} \cdot \overline{U_{n_1,k,l_1} U_{n_2,k,l_2}} + \overline{d_{n_1}(0) d_{n_2}(0)} \cdot \overline{V_{n_1,k,l_1} V_{n_2,k,l_2}} \right] \tag{D-4}$$

or,

$$\sigma^2_{ICI} = E \sum_{l_1=0}^{L-1} \sum_{l_2=0}^{L-1} \sum_{n=0, n\neq k}^{N-1} \overline{a_{l_1} a_{l_2}} \left[\overline{U_{n,k,l_1} U_{n,k,l_2}} + \overline{V_{n,k,l_1} V_{n,k,l_2}} \right] \tag{D-5}$$

Using the independent path components it becomes:

$$\sigma^2_{ICI} = E \sum_{l=0}^{L-1} \sum_{n=0, n\neq k}^{N-1} \sigma^2_{a_l} \left[\overline{U^2_{n,k,l}} + \overline{V^2_{n,k,l}} \right] \tag{D-6}$$

and,

$$\overline{U_{n,k,l}^2} = \overline{\left(X_{n,k}^l\right)^2} + \overline{\left(Y_{n,k}^l\right)^2} + 2\overline{X_{n,k}^l Y_{n,k}^l}$$
$$\overline{V_{n,k,l}^2} = \overline{\left(\hat{X}_{n,k}^l\right)^2} + \overline{\left(\hat{Y}_{n,k}^l\right)^2} + 2\overline{\hat{X}_{n,k}^l \hat{Y}_{n,k}^l} \quad \text{(D-7)}$$

By the assumption of independent uniform distributions for τ and θ in the interval of $[0,T_b)$ and $[0, 2\pi)$ respectively, it can be shown that:

$$\overline{\left(X_{n,k}^l\right)^2} = \overline{\left(\hat{X}_{n,k}^l\right)^2} = \frac{T_b^2}{16\pi^2(n-k)^2}$$
$$\overline{\left(Y_{n,k}^l\right)^2} = \overline{\left(\hat{Y}_{n,k}^l\right)^2} = \frac{3T_b^2}{16\pi^2(n-k)^2} \quad \text{(D-8)}$$
$$\overline{X_{n,k}^l Y_{n,k}^l} = \overline{\hat{X}_{n,k}^l \hat{Y}_{n,k}^l} = 0$$

Therefore, the variance of the ICI term is:

$$\sigma_{ICI}^2 = \sum_{l=0}^{L-1} \sum_{n=0, n\neq k}^{N-1} \frac{1}{2}\sigma_{a_l}^2 \frac{T_b^2}{\pi^2(n-k)^2} \quad \text{(D-9)}$$

or

$$\sigma_{ICI}^2 = \frac{T_b^2}{2\pi^2} \sum_{l=0}^{L-1} \sigma_{a_l}^2 \sum_{i=-k, i\neq 0}^{N-k-1} \frac{1}{i^2} \quad \text{(D-10)}$$

Performance of Low-Rate Orthogonal Convolutional Codes in DS-CDMA Applications

R. F. Ormondroyd and J. J. Maxey

Abstract—**Low-rate orthogonal convolutional codes (LROCC), originally proposed by A. J. Viterbi, can be used in a direct-sequence code-division multiple access (DS-CDMA) system to achieve both spreading of the data and providing coding gain. The implementation of this type of multiplexing in a practical DS-CDMA system is presented, and the theoretical performance of the proposed system under "other-user" noise, additive white Gaussian noise (AWGN), intercell interference, and thermal noise is established using a computer simulation. The improvement in system performance, gained through the use of a nonspreading randomizing sequence on the encoded output symbols, is also studied. Performance curves for a rate 1/64 orthogonal convolutional code are shown, and the impact of code rate, quantization methods, and constraint length on the overall system performance are discussed.**

Index Terms—**Cellular radio convolutional codes, DS-CDMA, intercell interference, low-rate orthogonal convolutional coding.**

I. Introduction

DIRECT-SEQUENCE code-division multiple access (DS-CDMA) techniques are currently receiving considerable attention as likely contenders for the next-generation cellular digital personal communications network (PCN). DS-CDMA systems are, at present, looking very promising compared to the conventional advanced time division multiplex system (TDMA), with some of the claimed CDMA advantages [1] being:

1) high-spectrum efficiency (high-traffic capacity);
2) no requirement for frequency planning;
3) soft handoff and macrodiversity;
4) graceful degradation (soft capacity),
5) low power consumption;
6) flexible data rates, suitable for packet data.

Above all, the prospect of maximizing the potential number of simultaneous subscribers occupying a given bandwidth per unit area within any specific cell boundary is of greatest importance to the system designer. While conventional DS-CDMA spread-spectrum systems have been shown to offer some capacity benefits over TDMA systems, it is clear that further benefits in capacity can be achieved by using powerful coding strategies on the data prior to spreading with the pseudo-noise (PN) sequence. An alternative strategy, originally proposed by Viterbi [2], which forms the basis of this paper, is to use low-rate orthogonal convolutional codes (LROCC) to provide both spectrum spreading and a very powerful convolutional code.

Conventional DS-CDMA systems increase the symbol rate of the subscriber data by a modulo-2 addition of the data with an internally generated PN sequence. This spreads the bandwidth of the transmitted signal by a factor dependent on the PN-sequence chip rate. For example, if the PN sequence is of repetition length L chips and one data-bit period lasts for the whole repetition length, then the data will experience a spread in bandwidth by a factor L called the *spreading ratio*. PN spreading sequences are designed to not only spread the bandwidth of the data, but also to produce low levels of interference to other subscribers within the cellular boundary. Recovery of the subscriber data from this "other-user" interference in the receiver of such a system is by means of correlation or an equivalent operation, such as matched filtering.

This is not the only way of spreading the bandwidth of the data in the transmitter, however. A convolutional encoder of rate $1/L$, as shown in Fig. 1, also introduces a redundancy of L symbols, and this also provides bandwidth spreading as well as coding benefits.

Fig. 2 shows the schematic of a DS-CDMA basestation transmitter for a cellular communication system, which is based on the use of low-rate convolutional codes rather than the more usual PN spreading sequences. The orthogonality of ordinary convolutional codes, however, is very poor, and this would lead to only a small number of simultaneous subscribers being accommodated within a cell, due to high levels of cochannel self-interference, which is the normal limiting factor of the capacity of DS-CDMA systems. This can be improved significantly by using LROCC coding, which directly codes and spreads the data signal [2].

However, these low-rate orthogonal functions do not have good autocorrelation properties [2], and the spectrum of the transmitted coded signal can be very poor indeed (when compared with conventional direct-sequence spread-spectrum signals), with highly nonuniform spreading and potentially large interference signals. In a practical CDMA system, these large interference signals can significantly reduce the achievable capacity of the cell. To reduce this problem, a stage of randomization is added [2] to the LROCC encoded data symbols to improve the autocorrelation property of the resulting transmitted signal.

Unlike conventional DS-CDMA systems, in the LROCC system, the PN sequences are only used to randomize the output of the low-rate convolutional encoder to improve the spectral characteristics of the orthogonal codes and provide

Manuscript received September 20, 1995; revised February 19, 1996. This work was supported by EPSRC.

The authors are with the School of Electronic and Electrical Engineering, University of Bath, Claverton Down, Bath, BA2 7AY U.K.

Publisher Item Identifier S 0018-9545(97)03116-2.

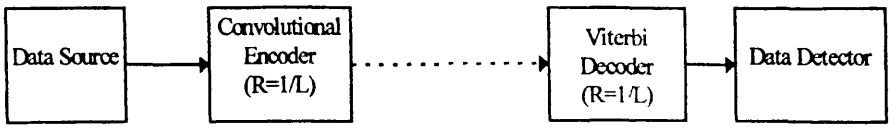

Fig. 1. Spectrum spreading using low-rate convolutional coding.

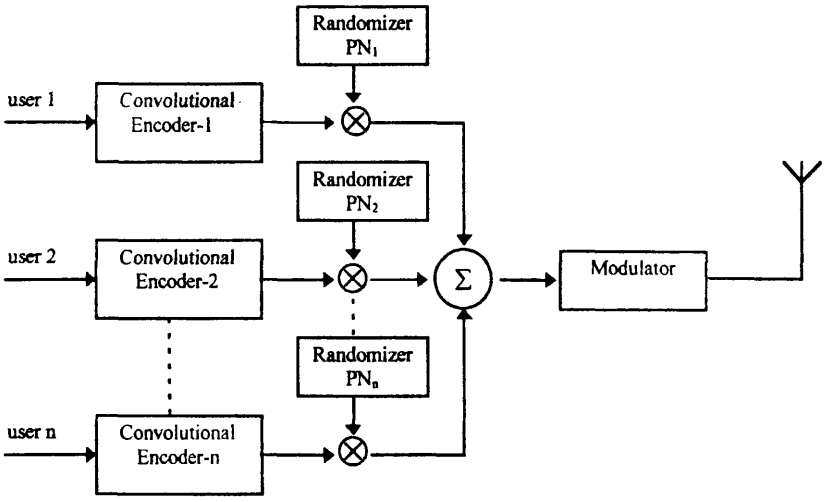

Fig. 2. Simplified diagram of basestation transmitter.

better isolation between subscribers without causing any further spreading of the encoded signal. This can be done by using a PN sequence of the same or lower rate than the orthogonal output sequence.

The receiver performs the inverse operation by first demodulating the received signal, then, derandomizing the signal before finally decoding the convolutionally encoded signal and providing an estimate of the most likely transmitted data bit. The decoding algorithm used by the receiver must use the maximum-likelihood decoding technique since the probability of any codeword being transmitted is equally likely. The Viterbi algorithm has been chosen as the most suitable method for decoding on the basis of its speed and simplicity.

II. LROCC Design

In the LROCC system, the data bits of each subscriber are uniquely mapped onto a set of orthogonal code sequences, with a duration equal to T. The code sequences generated by all the other subscribers must be orthogonal to each other to ensure recovery of individual user data. One way of providing orthogonal convolutional codes is through cascading a convolutional encoder with a Hadamard block encoder [3], such that each data bit is represented by 2^K b of the Hadamard sequence. The Hadamard block encoder, shown in Fig. 3, works by selecting one of the rows of a $2^K \times 2^K$ Hadamard matrix in which the state of the convolutional shift register system dictates which row is selected. To give each subscriber a unique trellis structure, different tap configurations linking the convolutional encoder to the Hadamard encoder are used.

If the block encoder chooses one row consisting of 2^K symbols, the effective code-symboling rate will be 2^K times as fast as the data rate. Thus, if the Hadamard block encoder maps a convolutional shift register system of constraint length, $K = 4$, for example, into one row of data, there will be 64 possible states corresponding to 64 rows of the Hadamard block encoder. The spreading ratio of such a design will be equal to 64. In a conventional DS-CDMA system, this spreading ratio would also equate to the process gain of the system, i.e., the ability of the system to recover the data from white noise.

The way in which each row is generated is simple: on each data transition of time period T, the shift register system takes on a new state. For this state, an output sequence of 2^K b is generated by clocking the switches and lower shift registers 2^K times faster than the upper shift registers. This requires that the Hadamard block encoder must operate with a clock period of $T/2^K$.

The major advantage of orthogonal symbol-by-symbol code spreading lies in the fact that the orthogonality and the autocorrelation functions of the spreading code sequences can be directly controlled by careful selection of the code sets. For synchronous symbol transmission and reception, considerable capacity improvements will be found. In order to provide reliable communication in a burst-noise environment, this data is also interleaved, and it has been shown [4] that the interleaving depth of this low-rate convolutional design can be lower than current digital DS-CDMA systems.

Unlike maximal-length PN sequences used in conventional DS-CDMA, the autocorrelation function of the encoded Hadamard output symbols is very poor; i.e., there are "spikes" in the autocorrelation function at values other than the zero time delay. The effect that this has on the output spectrum is shown in Fig. 4. In this figure, a typical output power spectrum of four encoded data bits from the Hadamard encoder of Fig. 3, with constraint length $K = 6$, is shown. It can

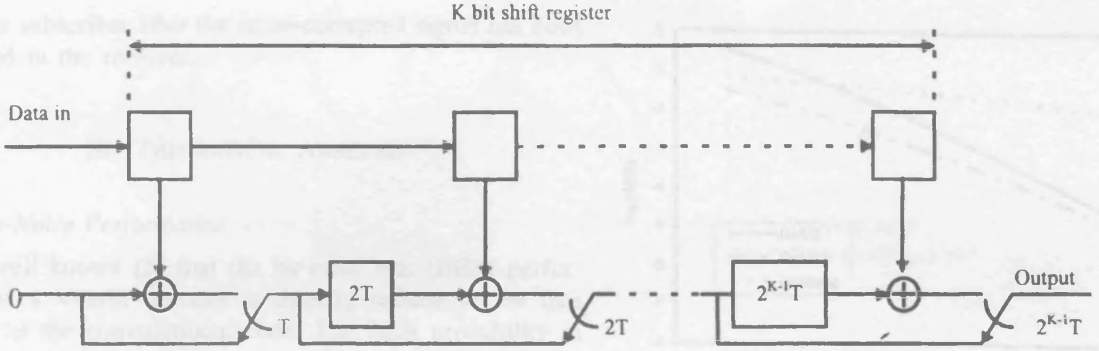

Fig. 3. A low-rate convolutional encoder.

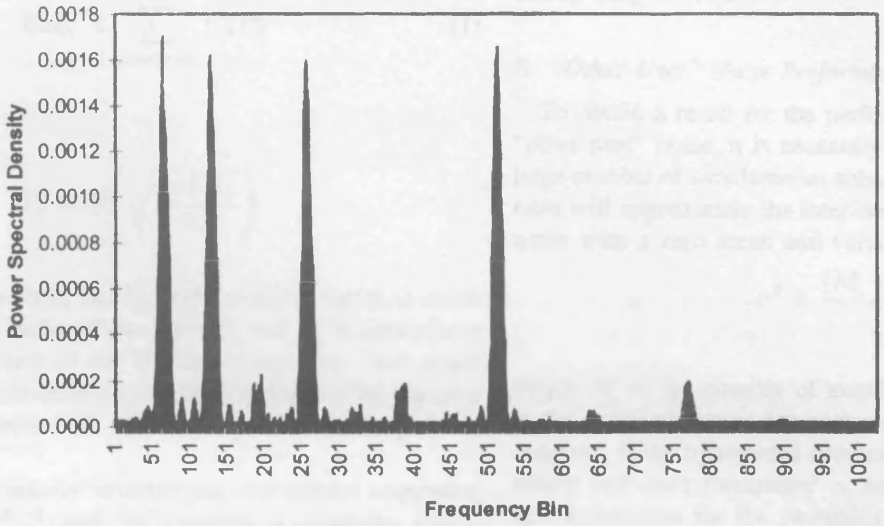

Fig. 4. Power spectrum of Hadamard encoded data via fast Fourier transform (FFT) of 1024 points.

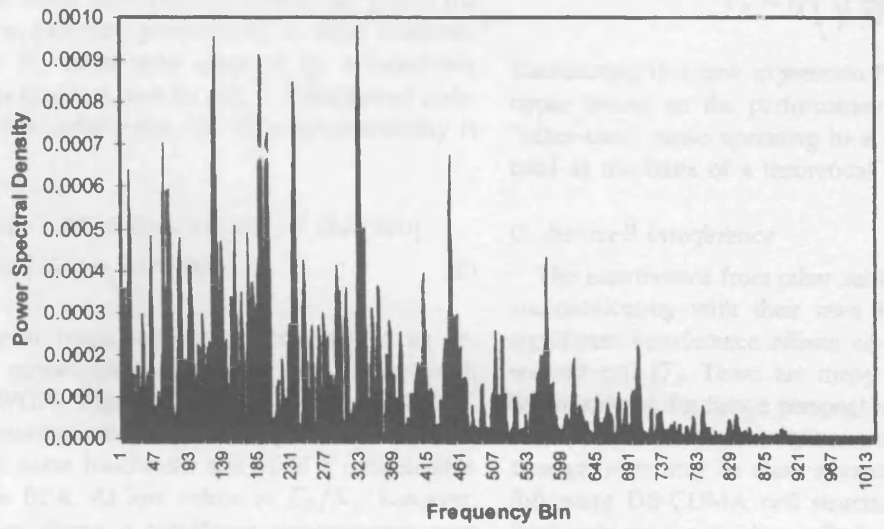

Fig. 5. Output power spectrum of randomize via FFT of 1024 points.

be seen that the spectrum of the encoded data sample is not uniformly spread over the main lobe of the Hadamard "spreading sequence," and, consequently, this would be a poor choice for a direct-sequence spreading code in some applications.

The resulting power spectrum after randomization with a PN sequence is shown in Fig. 5. It can be seen that the power density is much more uniformly spread over the main lobe.

This is of great importance to the system designer since it minimizes the interference levels encountered by any one

particular subscriber after the noise-corrupted signal has been correlated in the receiver.

III. Theoretical Analysis

A. White-Noise Performance

It is well known [5] that the bit-error rate (BER) performance of a Viterbi decoder is directly related to the free distance of the convolutional code. The BER probability in the continuous output additive white Gaussian noise (AWGN) channel is

$$\text{BER} < \sum_{x=dfree}^{\infty} C_x P_x \qquad (1)$$

where

$$P_x = Q\left(\sqrt{\frac{2xRE_b}{N_o}}\right).$$

R is the rate of the code, E_b/N_o is the required signal-to-noise ratio (SNR) at the output of the decoder, and C_x is determined by the code structure of the Hadamard encoder. This result holds for a pure soft-decision decoding strategy. The use of a hard-decision decoder will reduce the performance by about 2 dB [6].

The Hamming distance between any two symbol sequences is known to be 2^{K-1}, and, for example, a constraint length $K = 6$ code will yield a value of 32 symbols. This is the theoretical optimum Hamming distance that any rate 1/64 convolutional code could have and is the basis for giving the orthogonal codes an excellent performance in noisy channels.

The values for C_x have been obtained by exhaustively searching the trellis structure, and for a $K = 6$ Hadamard code, neglecting the higher order terms, the bit-error probability is given by

$$\text{BER} < P(224) + 2P(256) + 6P(288) + 16P(320) + 35P(352) + 60P(388)\cdots. \qquad (2)$$

This yields an upper bound on the performance of an orthogonally coded spread-spectrum system in a channel with predominantly AWGN. Fig. 6 compares the new LROCC design with conventional rate $R = \frac{1}{2}$ coding. Both implementations occupy the same bandwidth and yield a considerable coding gain at low BER. At low values of E_b/N_o, however, the LROCC design shows a significant improvement over the high-rate code, which is purely due to the fact that the construction of LROCC codes is much better.

An interesting artifact of Fig. 6 is the crossover point at E_b/N_o of 5.3 dB. This is due to truncating the number of terms in (2). In the limit of a large number of terms, the curves of $R = \frac{1}{64}$ and $R = \frac{1}{2}$ merge at high E_b/N_o. For real applications, this upper bound will still outperform the results of a rate 1/2 coded system.

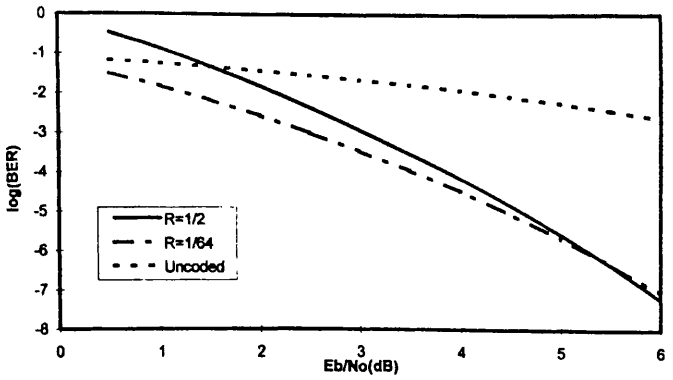

Fig. 6. A comparison of conventional convolutional encoding and the new LROCC design in AWGN.

B. "Other-User" Noise Performance

To obtain a result for the performance of such a system in "other-user" noise, it is necessary to assume that a relatively large number of simultaneous subscribers and a high-spreading ratio will approximate the interference as normally distributed noise with a zero mean and variance of

$$\sigma^2 = \frac{(M-1)P}{\frac{1}{R}} \qquad (3)$$

where M is the number of simultaneous subscribers and P is the received power for each user. This result only holds, however, if the transmitted symbol sequences are of a random nature and each transmitter is perfetly power controlled. A new expression for the probability P_x of choosing a wrong path in the trellis now yields

$$P_x = Q\left(\sqrt{\frac{2x}{M-1}}\right). \qquad (4)$$

Substituting this new expression for P_x into (1) will give an upper bound on the performance of the LROCC design in "other-user" noise operating in a single cell, and this can be used as the basis of a theoretical analysis.

C. Intercell Interference

The interference from other subscribers in surrounding cells communicating with their own local basestation can have significant interference effects on the uplink capacity of the wanted cell [7]. There are many types of cell structures to be considered for future personal networks, and depending on factors, such as terrain features, data rates, etc., certain cell arrangements may be more advantageous than others. For the following DS-CDMA cell structure, the interference effects from only six surrounding cells have been studied, and further interference effects from the next layer of surrounding cells have been neglected.

As the neighboring subscribers will be power-controlled to their own basestation, the interference effects will inevitably depend on the position of each subscriber within the particular neighboring cell. A valid mathematical model can be constructed by assuming each basestation to have its subscribers uniformly distributed within the cell area, as shown in Fig. 7.

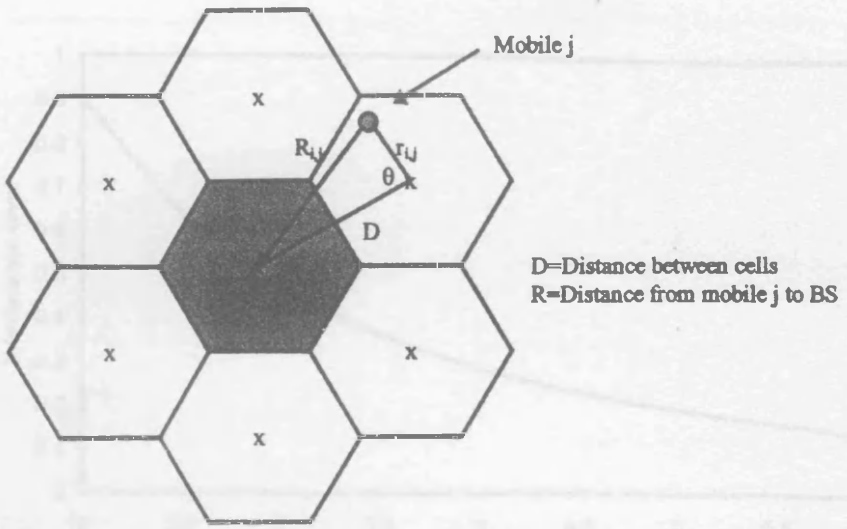

Fig. 7. Outer-cell interference for a seven-cell cluster on uplink.

To determine the transmitted power $P_{i,j}$ from each subscriber, it is necessary to define this power relative to cell site i, which is power-controlled by basestation i:

$$P_{i,j} = \frac{P}{M} \cdot (r_{i,j})^{\alpha} \tag{5}$$

where P is the power received at the basestation from any subscriber j, M is the number of simultaneous subscribers in one cell, and α is the decay index. The effective interference power seen at the basestation from a subscriber in a surrounding cell will decay proportionally to $R_{i,j}^{-\alpha}$:

$$\text{Interference } I_{i,j} = \left(\frac{P}{M}\right)\left(\frac{r_{i,j}}{R_{i,j}}\right)^{\alpha}. \tag{6}$$

Let the area of a cell be approximated to a circular area of $\pi.r_d^2$, where r_d is the radius of the cell. This enables the interference to be described per unit area:

$$\frac{dI}{dA} = \frac{P}{\pi.r_d^2} \cdot \left(\frac{r_{i,j}}{R_{i,j}}\right)^{\alpha} = \frac{P}{\pi.r_d^2} \cdot \left(\frac{r_{i,j}}{\sqrt{D_i^2 + r_{i,j} - 2D_i r_{i,j} \cos\theta}}\right)^{\alpha} \tag{7}$$

since $R_{i,j}^2 = D_i^2 + r_{i,j}^2 - 2D_i r_{i,j} \cos\theta$.

The unit area dA for a segment is related to the radius $r_{i,j}$ by

$$dA = dr.r_{i,j}.d\theta. \tag{8}$$

To obtain an expression for the total average interference from one surrounding cell, it is necessary to integrate (7) over the complete area of the circle:

$$dI = \frac{P}{\pi.r_d^2} \cdot \frac{r_{i,j}^{\alpha}}{(D_i^2 + r_{i,j}^2 - 2D_i r_{i,j} \cos\theta)^{\alpha/2}} \cdot r_{i,j} \cdot dr \cdot d\theta$$

$$\therefore I_i = \frac{P}{\pi.r_d^2} \int_0^{2\pi} \int_0^{r_d} \frac{r^{\alpha+1}}{(D_i^2 + r^2 - 2D_i r \cos\theta)^{\alpha/2}} \cdot dr \cdot d\theta$$

for all cells N_c,

$$I = \frac{P}{\pi.r_d^2} \sum_{i=1}^{N_c - 1} \int_0^{2\pi} \int_0^{r_d} \frac{r^{\alpha+1}}{(D_i^2 + r^2 - 2D_i r \cos\theta)^{\alpha/2}} \cdot dr \cdot d\theta. \tag{9}$$

This expression can be analyzed analytically to obtain a value for the interference power from all surrounding cells on the wanted basestation.

In order to gain an estimate of the influence of the outer-cell interference on the number of simultaneous subscribers, it is necessary to calculate the scaling factor F, which can be substituted directly into the capacity equation for M. The SNR seen at the input to the receiver for one subscriber is

$$\text{SNR} = \frac{P_1}{(M-1)P_1 + I + N_o} \tag{10}$$

where

P_1 power received from one subscriber;
N_o thermal noise power within the receiver.

By assuming that I is considerably larger than N_o

$$M \approx \frac{\frac{W}{R}}{\frac{E_b}{N_o}} - \frac{I}{P_1}. \tag{11}$$

This reduction in the number of simultaneous subscribers in one cell can be described as the factor F, given by the ratio of the number of subscribers in a multiple-cell environment to the number of subscribers in a single-cell environment. Therefore

$$F = M \cdot \frac{\frac{E_b}{N_o}}{\frac{W}{R}} = \frac{M}{M + \frac{I}{P_1}} = \frac{1}{1 + \frac{I}{P}} \tag{12}$$

where P = total power received from all subscribers within the cell and

$$I = \frac{P}{\pi.r_d^2} \sum_{i=1}^{N_c - 1} \int_0^{2\pi} \int_0^{r_d} \frac{r^{\alpha+1}}{(D_i^2 + r^2 - 2D_i r \cos\theta)^{\alpha/2}} \cdot dr \cdot d\theta. \tag{13}$$

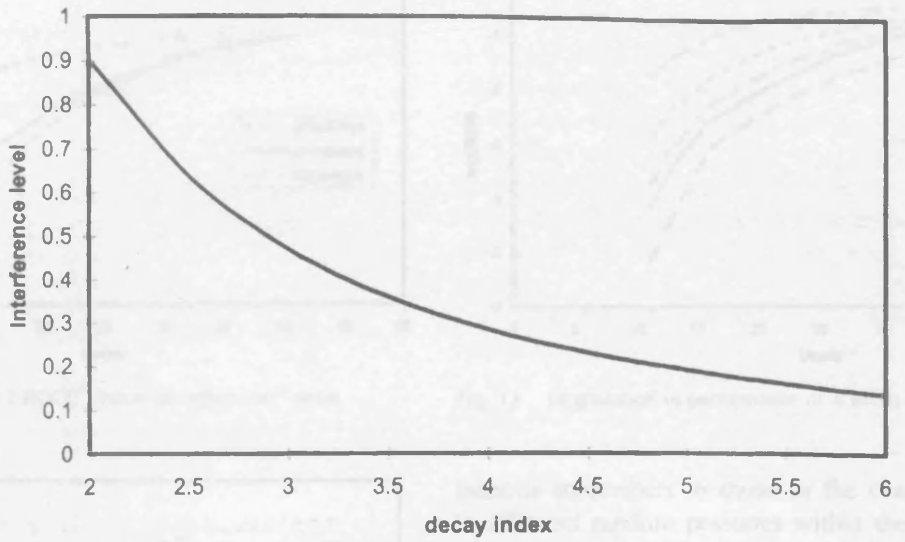

Fig. 8. Graph displaying the interference level for a seven-cell cluster with differing decay index α.

Fig. 8 shows the variation of interference level with respect to P for a seven-cell cluster, each cell having a radius of 2 km. As expected, the level of interference in the wanted cell is greatest for low values of α, corresponding to free-space or near free-space propagation. Where multipath fading losses are high, the interference effect on the wanted cell is lower.

IV. Computer Simulation Results

In this section, the theoretical and computer-simulated performances of the LROCC system are compared with a conventional DS-CDMA system which uses no coding on the data. In both cases, the spreading ratio is limited to 64. This means that the capacity of either system is not as large as could be obtained by using larger spreading ratios (i.e., larger constraint length K for the case of the LROCC system), but this value of spreading ratio still allows a fair comparison between the two types of systems. A Monte Carlo computer simulation of the LROCC system was carried out at baseband with data bits sampled on each transition. Further improvements in performance might be expected with different modulation schemes [8].

The system simulated in this paper has been assumed to have perfect synchronization. Since the design is based on a low-rate Hadamard encoder, the users will be detected noncoherently, as the orthogonal codes precede a further stage of randomization. This has the effect of reducing the other-user noise in the receiver for the wanted signal. Consequently, a loss in synchronization is reflected as an increase in the self-noise from the own code of the system. The term *orthogonality* in this design is based on all users sharing the same bandwidth, with maximum Hamming distance in the code sets. The stage of randomization destroys most of the orthogonality between users in the channel, but nevertheless an improved performance is found due to the robust coding and interleaving techniques employed on the data. It is therefore important to address the fact that any loss in synchronization will have

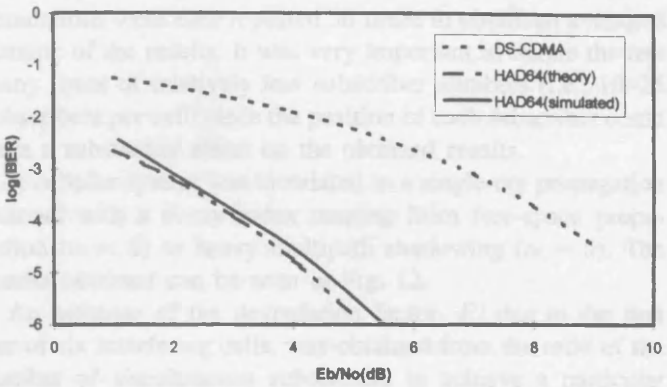

Fig. 9. Performance of the LROCC system in AWGN.

the same impact on the BER performance as in conventional DS-CDMA detectors.

Fig. 9 compares the BER performance of the computer-simulated LROCC system in AWGN, with the conventional DS-CDMA system, and the theoretical performance predicted by application of (1)–(4) as a function of E_b/N_o at the output of the correlator/decoder. The E_b/N_o values are therefore normalized to the processing gain of the DS-CDMA system, and a fair comparison of performance per bandwidth can be made for both types of system.

The results of the LROCC simulation are obtained for a pure soft-decision Viterbi decoder. In practice, one might use 3-b quantization and expect to suffer a small BER penalty.

The performance of the LROCC design implementation in AWGN can be seen to give a significant improvement over the uncoded DS-CDMA system. At a BER of 10^{-4}, coding gains of 5 dB can easily be achieved. Under low-noise environments, this gain in performance increases considerably. Because the free distance of these orthogonal codes is at an optimum high level, the improvement is larger than the conventional high-rate (i.e., $R = \frac{1}{2}, \frac{1}{3} \cdots$) coded DS-CDMA system occupying the same equivalent bandwidth for a given data rate.

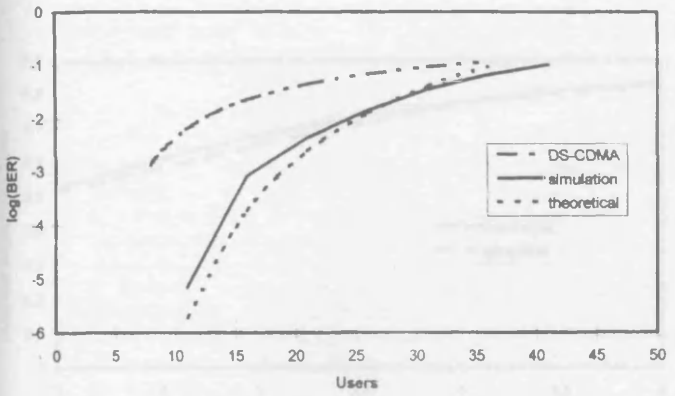

Fig. 10. Performance of the LROCC system in "other-user" noise.

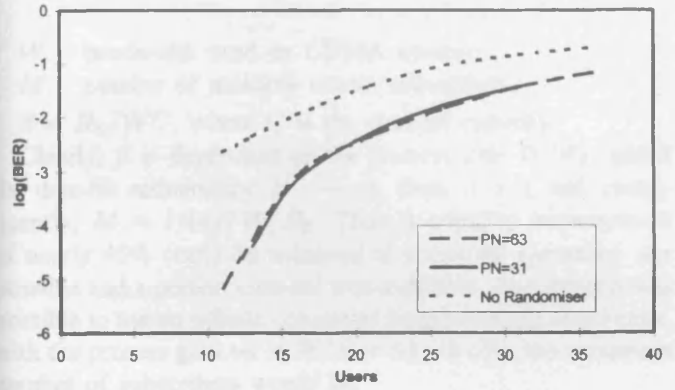

Fig. 11. Comparison of different PN randomizing sequences.

Fig. 10 shows a soft-decision receiver operating under multiple-access conditions, where there are high levels of "other-user" noise. It can be seen that the use of low-rate convolutional codes yields significant improvements in BER when the number of simultaneous subscribers is lower than about 40 (for a spreading ratio of 64). To achieve a BER $= 10^{-3}$, a maximum number of seven subscribers could be employed in a conventional DS-CDMA system, but the use of low-rate convolutional coding can lead to an increase of nearly 130%, giving a new maximum number of 16 subscribers.

This gain in capacity is entirely due to the coding gain given by convolutional codes and the orthogonal properties of the codes. The use of higher constraint length codes would further improve the performance.

The use of PN sequences to randomize the output of the low-rate convolutional encoder has two effects. First, it improves the spectral characteristics of the orthogonal codes, and second, it provides better isolation between subscribers without causing any further spreading of the encoded signal. The resulting improvement can be viewed in Fig. 11. This figure shows that the use of a PN sequence to randomize the encoded symbols yields a significant advantage approaching a value of at least 2 dB. It was also found that no significant degradation is encountered when the rate of the PN sequence is halved.

In order to simulate the interference generated from subscribers operating in outer cells, an equal number of simultaneous subscribers to those in the central cell were placed in different random positions within their cell boundary, and the effect of these on the BER of a single power-controlled subscriber in the central cell was obtained. Each of the users in the outer cells was assumed to be perfectly power-controlled with respect to their own basestations. These Monte Carlo simulations were then repeated 50 times to obtain an averaged statistic of the results. It was very important to iterate the test many times at relatively low subscriber numbers (i.e., 10–25 subscribers per cell) since the position of each subscriber could have a substantial effect on the obtained results.

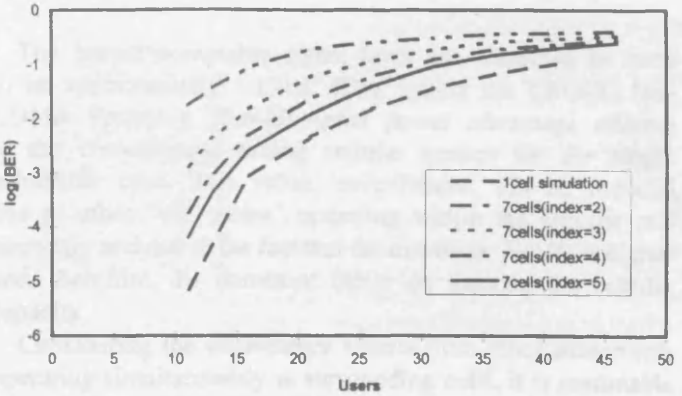

Fig. 12. Degradation in performance of a seven-cell cluster.

A cellular system was simulated in a single-ray propagation channel with a decay index ranging from free-space propagation ($\alpha = 2$) to heavy multipath shadowing ($\alpha = 5$). The results obtained can be seen in Fig. 12.

An estimate of the degradation factor, F, due to the first tier of six interfering cells, was obtained from the ratio of the number of simultaneous subscribers to achieve a particular BER in a single cell and was compared with the equivalent number of subscribers for the same BER performance in a multicell environment. The value of the BER used in the comparison plays an insignificant role in the value of F, and, subsequently, little difference in F has been found between calculations based on a BER $= 10^{-1}$ and BER $= 10^{-4}$.

A comparison between the simulated results for F, which have been averaged between a BER $= 10^{-1}$ to a BER $= 10^{-3}$, and the theoretical predicted values are shown in Fig. 13. It can be seen that both curves are very close.

V. Evaluation of Results

Since the convolutional code will yield an additional coding gain depending on the constraint length, a higher constraint length encoder than the one described will provide an even higher improvement over the conventional DS-CDMA system. Viterbi [2] has shown that the maximum bandwidth efficiency achievable is given by

$$\eta = \frac{R_T}{W} = \frac{MR_k}{W} = \frac{\beta}{\ln 2} \tag{14}$$

where

R_T total combined data rate of all subscribers;

R_k data rate of kth subscriber;

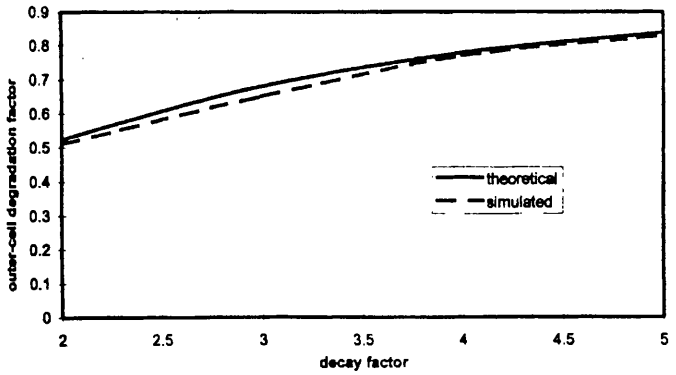

Fig. 13. Comparison of simulated and theoretical results for F.

W bandwidth used by CDMA system;
M number of multiple access subscribers.
$\beta = R_k/WC$, where C is the channel capacity.

Clearly, β is dependent on the process gain W/R_k, and if the data-bit redundancy $2^K \rightarrow \infty$, then, $\beta = 1$ and, consequently, $M = 1.4427\,W/R_k$. Thus, a capacity improvement of nearly 45% could be achieved if unlimited spreading was possible and a perfect channel was available. Assuming it was possible to use an infinite constraint length convolutional code, with the process gain set at $W/R = 64$ (18 dB), the maximum number of subscribers would be

$$M = 1.44\frac{W}{R} = 92. \tag{15}$$

Having obtained different performance results for the new LROCC design implementation in DS-CDMA applications, it is of importance to evaluate the performance improvement within current cellular systems [9].

The existing analog mobile radio network, as specified by the Federal Communications Commission (FCC), has given a value for the received signal power on the boundary of a cellular system as -93 dBm for a dipole antenna matched to a 50-Ω load at 850 MHz. For the proposed third-generation DS-CDMA system, it is necessary to determine the lowest acceptable signal level for which adequate performance may be obtained.

Third-generation personal communication will use speech coded at very low rates approaching 8 kb/s to which a bandwidth of 1.024 MHz would give a process gain of 128. For an infinite constraint length code, (15) would give a maximum number of 184 simultaneous subscribers. Adequate performance for speech quality can be obtained with a BER $< 10^{-3}$, thus giving $E_b/N_o > 4.5$ dB (i.e., $C/I = -16.57$ dB) for the LROCC design on the uplink.

The thermal noise is therefore

$$\text{kTB} = 1.3728 \times 10^{-20} \times 290 \times 1.024 \times 10^6 = -114 \text{ dBm}. \tag{16}$$

Given that the front-end noise of an average quality receiver is about 9 dB, the total noise power, N, is

$$N = -114 + 9 = -105 \text{ dBm}. \tag{17}$$

The lowest acceptable signal level can therefore be seen to be approximately -121.6 dBm, giving the LROCC DS-CDMA system a 28.6-dB-signal power advantage relative to the conventional analog cellular system for the single subscriber case. This value, nevertheless, will be reduced due to other "user noise" operating within the specific cell boundary and due to the fact that the downlink E_b/N_o is higher and, therefore, the dominant factor on limiting the cellular capacity.

Considering the interference effects from other subscribers operating simultaneously in surrounding cells, it is reasonable to have a value of $F = 0.7$ for the outer-cell degradation factor at a decay index of $\alpha = 4$. It has been found that the voice duty cycle will yield a typical value of $d = \frac{3}{8}$, and the power-control errors approach a 2-dB (i.e., $Q = 0.5$) loss in performance [10].

Assuming a cell sectorization of $G = 3$ is used and the PCN system is to employ speech transmission with digital vocoders down to $R = 8$ kb/s, the number of subscribers M can be found by multiplying all factors together as

$$M = \frac{\frac{W}{R}}{\frac{E_b}{N_0}} \cdot F \cdot G \cdot \frac{1}{d} \cdot Q = \frac{358}{\frac{E_b}{N_o}}. \tag{18}$$

For an SNR of 4.5 dB, this would yield a maximum number of 127 subscribers in a cell of size 2 km. This can be compared with the theoretical maximum of 184 subscribers for a perfect channel and infinite constraint length LROCC design.

Such results must be treated with care, but nevertheless show a considerable improvement in performance over the conventional DS-CDMA system [10].

VI. Conclusions

A cellular CDMA system employing low-rate convolutional codes instead of PN sequences to spread the data bandwidth has been simulated under conditions of AWGN and "other-user" noise. The soft-decision implementation of the LROCC system has shown considerable improvement in performance under both AWGN and "other-user" noise over the uncoded DS-CDMA system, giving a coding gain of up to 5 dB at a BER of 10^{-4}, which yields an improvement in the number of subscribers per cell of 130%.

Orthogonal Hadamard sequences do not have good autocorrelation properties, and to improve these, different PN randomizing sequences have been tested and found to improve both the spectral properties of the transmitted signal and the isolation between subscribers.

The use of high-rate PN spreading sequences will give improved performance over noisy channels with a tradeoff in increased bandwidth. However, the coding gain of a particular coding strategy does not give a tradeoff in bandwidth, and it is therefore of direct use for the process gain in DS-CDMA applications. Using optimized convolutional codes (i.e., high-constraint lengths, low-coding rates, etc.) will give significant BER improvements without any tradeoff in bandwidth. It is for this reason that LROCC's give a considerable performance

improvement over ordinary DS-CDMA systems or high-rate convolutional encoded DS-CDMA systems.

REFERENCES

[1] Ericsson, "A comparison of CDMA and TDMA systems," presented at the CIRR TG 8/1 Conf., Washington, DC, May 1991.

[2] A. J. Viterbi, "Very low-rate convolutional codes for maximum theoretical performance of spread-spectrum multiple-access channels," *IEEE J. Select. Areas Commun.*, vol. 8, pp. 641–649, 1990.

[3] R. R. Green, "A serial orthogonal decoder," in *JPL Space Programs Summary Conf.*, 1966, pp. 247–253.

[4] P. Monogioudis, R. Edmonds, R. Tafazolli, and B. G. Evans, "Multirate 3rd generation CDMA systems," in *IEEE Int. Conf. Comm., ICC '93*, pp. 151–155.

[5] A. J. Viterbi, "Convolutional codes and their performance in communication systems," *IEEE Trans. Commun. Technol.*, vol. COMM-19, pp. 751–771, 1971.

[6] D. R. Anderson and P. A. Wintz, "Analysis of a spread-spectrum multiple-access system with a hard limiter," *IEEE Trans. Commun. Technol.*, vol. COMM-17, pp. 285–290, Apr. 1969.

[7] P. Newson and M. R. Heath, "The capacity of a spread spectrum CDMA system for cellular mobile radio with consideration of system imperfections," *IEEE J. Select. Areas Commun.*, vol. 12, pp. 673–684, 1994.

[8] A. G. Burr, "Capacity improvement of CDMA systems using M-ary code shift keying," in *Proc. Inst. Elect. Eng.*, vol. 351, pp. 63–67, 1991.

[9] J. A. Ulloa, D. P. Taylor, and W. F. S. Poehlman, "An expert system approach for cellular CDMA," *IEEE Trans. Veh. Technol.*, vol. 44, no. 1, pp. 146–154, 1995.

[10] K. S. Gilhousen *et al.*, "On the capacity of a cellular CDMA system," *IEEE Trans. Veh. Technol.*, vol. 40, pp. 303–312, May 1991.

R. F. Ormondroyd received the B.Eng. and Ph.D. degrees from the University of Sheffield, U.K., in 1971 and 1975, respectively. His Ph.D. research was in the area of amorphous chalcogenide threshold switches.

He was appointed a Lecturer in the School of Electronic and Electrical Engineering at the University of Bath, U.K., in 1975, where his research has been mostly concerned with spread-spectrum techniques and integrated optics components for optical communication systems. He is now a Reader at Bath University. His current research includes spectrally efficient modulations schemes for mobile and fixed wireless access radio and also novel architectures for PN code synchronization.

J. J. Maxey (S'96) was born in San Francisco, CA, in 1973. He received the B.Eng. degree in electronics and communication engineering from the University of Bath, U.K., in 1994, where he was sponsored by BTRL and worked on cellular spread-spectrum systems and lo-orbital satellite receiver designs. He is currently working toward the Ph.D. degree in the area of spread-spectrum communications and fixed wireless-access communications.

2. OFDM Fachgespraech
Braunschweig, Germany,
September 1997

A DOWNLINK AND UPLINK PERFORMANCE COMPARISON OF MULTI-CARRIER DS-CDMA SYSTEMS USING CODING AND INTERFERENCE CANCELLATION

J J Maxey and R F Ormondroyd

School of Electrical Engineering
The University of Bath
Claverton Down
Bath, BA2 7AY
Tel. (+44) 1225 826393 : Fax. (+44) 1225 826305
e-mail: eepjjm@bath.ac.uk and eesrfo@bath.ac.uk

ABSTRACT – OFDM DS-CDMA systems using convolutional coding techniques and multi-access interference (MAI) cancellation can be implemented effectively on both the downlink and uplink of a mobile radio channel as long as the interference statistics are known at the receiver. In this paper it is shown that it is extremely important to choose the right equalisation technique in order to maximise the SNR at the input to the detector. In particular, the use of maximum ratio combining (MRC) after MAI cancellation is found to give optimal results. In this work, the performance of zero-forcing equalisers used in conjunction with MAI cancellation and MRC techniques are compared with the use of controlled equalisation paired with MRC. Considerable performance improvements have been found when controlled equalisation techniques are used on the initial estimate of the interfering user's data.

INTRODUCTION

Multi-user OFDM techniques are increasingly gaining a wide interest in the field of mobile and fixed wireless communication systems using techniques such as DS-CDMA multiplexing. A number of recent papers have proposed the use of OFDM DS-CDMA for the downlink and uplink [1-3] in heavy frequency selective faded channels with high interference. OFDM can provide great resilience to frequency selective faded channels by transforming high bit-rate data on a single carrier to low-rate data streams on multiple orthogonal carriers, therefore reducing the problem of multipath. The use of DS-CDMA techniques with OFDM gives added frequency diversity to each data bit and protects the system from deep fades in the frequency response of the channel. In the limit, this has the advantage of enabling the received data streams to appear as flat faded data streams on each sub-carrier, and subsequently enables the equaliser at the receiver to demodulate the data more effectively. A number of techniques, such as (i) frequency- or time-domain interleaving, (ii) convolutional coding, (iii) guard-time insertion, (iv) frequency-domain equalisation and (v) MAI cancellation techniques (successive or parallel) have been proposed to combat these fading effects.

If the time-delay spread of the channel is large compared with the bit period, it becomes necessary to make use of guard-intervals to reduce the effects of ISI and ICI. No ISI will occur as long as the guard-time is greater than the maximum delay spread of the channel impulse response. Using DS-CDMA to spread the original bandwidth of the data enables the delay spread of the channel to be resolved more efficiently. Therefore DS-CDMA OFDM techniques can provide a robust multiple access scheme when many other users are transmitting over the same bandwidth in a faded channel with different user specific codes.

A number of techniques using equalisation structures of different complexity have been investigated [e.g. 3,4]. The use of OFDM modulation enables the equalisation to be performed in the frequency domain at the output of the FFT using a simple one tap equalisation structure, with its channel knowledge derived from the FFT of the channel impulse response. This can be measured using pilot channels or midambles inserted between the data. A relatively simple and effective equalisation structure that attempts to restore the orthogonality of the sub-channels [3] is controlled equalisation whereby the receiver has no knowledge of the received SNR nor the number of users using the channel. For more sophisticated receiver structures, the MMSE algorithm can provide considerable performance improvements compared with conventional equalisers. Sub-optimal ' MMSE algorithms can be employed by using a fixed value for the estimated number of users in the channel. This presents about 1dB loss in performance for the downlink channel.

One method of countering the effects of the interference of the other co-channel users is to use maximum likelihood detection (MLD). These schemes can only be used if the spreading sequences of all users are relatively short. However, the complexity increases exponentially with the sequence length. The use of coding, nevertheless, provides considerable performance benefits in memoryless and non-memoryless channels. In Rayleigh faded channels, the coding gain can be further enhanced through strong interleaving in the time- or frequency domain. A variety of sub-optimal interference cancellation schemes can be used to remove this interference as long as the spreading codes of all active users are known at the receiver. Power control methods are invariably used on the uplink of a cellular structure to reduce the interference effects from one cell to another and to reduce the near-far effect in the wanted cell. With this in mind, it is convenient to use parallel interference cancellation methods rather than successive

interference cancellation, since this requires geometrically distributed powers of different users in the cell, causing unnecessary inter-cell interference.

The work presented in this paper focuses on a novel MAI cancellation technique for the downlink and uplink of a mobile radio channel. Performance comparisons are shown for zero-forcing equalisation, controlled equalisation and maximum ratio combing (MRC) techniques.

UPLINK MODEM DESIGN

In this paper, the uplink design is based on OFDM modulation and LROCC coding [5,6] to provide the necessary spreading and coding. It is assumed that a small overhead is needed to provide the basestation with an estimate of the channel transfer function of each user, possibly through the use of small training sequences (midambles) inserted between the data. This allows the basestation to equalise each user's data sequence more effectively. A diagram of the proposed transmitter and receiver design is shown in figures 1 and 2. The data bit, d_i, of the ith user is first encoded by the LROCC encoder, then randomised by a user specific Gold code c_i and modulated onto N subcarriers in the OFDM modulator. In the uplink, each user transmits over a different multipath channel H_i. In the receiver, this signal is then corrupted with Gaussian noise, n. The receiver assumes that the wanted user is user 1, and the interference effects of users 2 to L (where L is the total number of simultaneous users) are partially removed through interference cancellation.

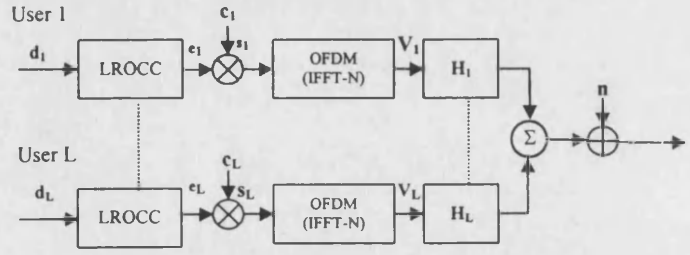

Figure 1. Simulation model of transmitter design for all uplink users and the channel model

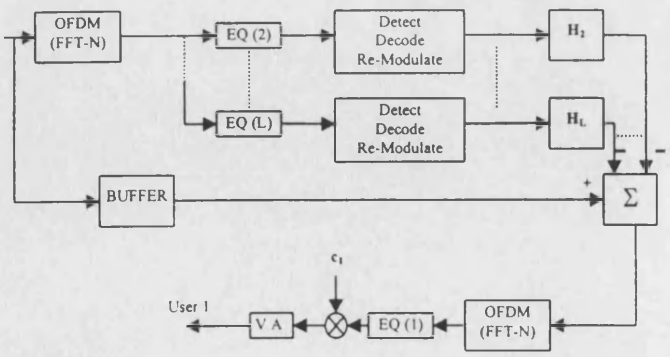

Figure 2. Basestation receiver structure to detect user 1

The first stage of detection uses either zero forcing or controlled equalisation methods, as discussed in [2,3,4]. Controlled equalisers perform phase-only equalisation if the signal magnitude drops below a certain threshold value and zero-forcing equalisation if the signal magnitude remains above that threshold. These equaliser structures attempt to restore the orthogonality and shape of the signals. If controlled equalisation is used in the receiver, a rapid deep fade in the channel transfer function below the set threshold value will cause the receiver to switch to phase-only equalisation on that particular carrier. These equalisers enable the receiver to obtain an initial estimate of the interfering user's data sequences. MRC provides a signal estimate by combining the maximum SNR of each faded sub-carrier and performs best with "clean" signals. This method is therefore used on the second iteration only and provides an optimal equalisation strategy since the "cleaned" signals are assumed to be relatively free of other-user interference. This signal is then de-randomised with the user specific sequence c_i and decoded using the Viterbi algorithm.

SIMULATION RESULTS

The simulated uplink channel assumes a service provision of a 32 kb/s data stream for each user. A constraint length of K=5 provides a spreading ratio of 32 in the LROCC encoder and this is then randomised through the user-specific Gold code of the same rate. This code provides no further additional spreading, but merely serves as a randomising sequence for the LROCC orthogonal code sets [5,6]. The number of sub-carriers is N=32 in a bandwidth of 1.028 MHz, and therefore each sub-carrier has a duration of 31.25μs. The simulated channel is based on the COST 207 frequency selective Rayleigh faded bad urban (BU) channel model [7]. The Doppler frequency was set to 200Hz and perfect power control is assumed.

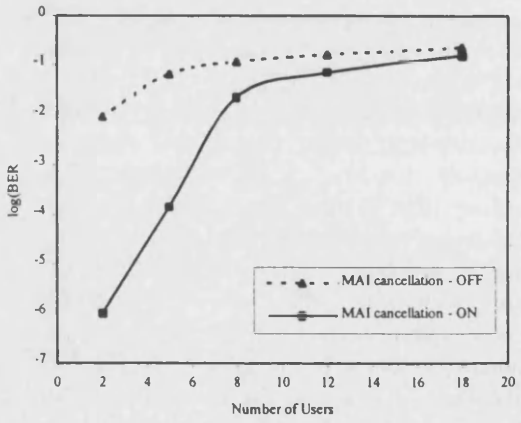

Figure 3. Uplink capacity comparison using controlled equalisation on the first iteration and MRC on the second detection stage

Figure 3 shows the bit-error rate performance for different numbers of simultaneous users communicating with the base-station. The performance without interference cancellation can be seen to degrade significantly when more than 5 users are present. The use of interference cancellation increases this to at least 10 users, which is a

significant gain in performance. Conversely, at low user numbers, the BER for 32 kb/s per user is substantially improved by MAI cancellation. Without MAI cancellation it is not possible to achieve an acceptable BER for any user numbers.

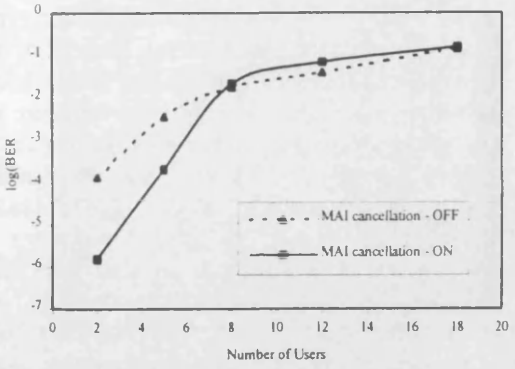

Figure 4. Uplink capacity comparison using zero forcing equalisation on the first iteration and MRC on the second detection stage

A threshold value of about 0.6 was found to be optimum from extensive simulation trials. This was subsequently used for the controlled equalisation structure employed in the Monte-Carlo simulations shown in figure 4. This technique shows a significant performance improvement for detection using no MAI cancellation in other-user noise environments but a smaller performance improvement using MAI cancellation compared to the zero-forcing strategy on the initial iteration shown earlier. At high user capacities (above 8 users typically) the performance is worse compared with simple one stage detection schemes. When the uplink channel is saturated with other user noise, the initial estimates on the first iteration become very unstable. This causes the interference estimates of all other interfering users to give errors that propagate and actually harm the bit-error rate performance.

The LROCC coding scheme relies primarily on independent errors to yield good results and it is important to provide initial good estimates on the first iteration of interference estimation in the receiver and to use strong interleaving in heavily faded channels. The use of OFDM in frequency selective channels helps to further combat the fading effects and effectively provides independent fading on each sub-channel. Combing this modulation strategy with LROCC coding provides a robust transmission design for such channels.

DOWNLINK MODEM DESIGN

The basestation-to-mobile downlink can present a variety of options for the most efficient detection process of the wanted user. Orthogonal codes give the most robust distance separation in the code domain and will inherently give the best performance for time-aligned users in the basestation transmitter.

The introduction of convolutional coding can improve matters, at the cost of bandwidth but with dramatic improvements in performance, yielding a coding gain larger than the bandwidth penalty. This coding gain may be further enhanced through MAI cancellation to reduce the effects of "other-user" noise. Orthogonal codes give an optimum performance in AWGN channels and no further improvements can be gained through MAI cancellation techniques. However, in frequency selective non-memoryless faded channels the performance can be enhanced through parallel interference cancellation.

The downlink design featured in this paper is based closely on the system proposed by Fazel [2]. This type of transmitter architecture groups L/D simultaneous users into D blocks. This shortens the orthogonal spreading code length of each user and enables more complex detection algorithms, such as MLD to be employed. An additional convolutional encoder of rate R=1/2 and constraint length K=5 is introduced before orthogonal spreading and further interference cancellation schemes are introduced into the receiver architecture. The channel statistics are assumed to be perfectly known through an additional pilot tone overhead from the basestation. The proposed transmitter and receiver is shown in figures 5 and 6.

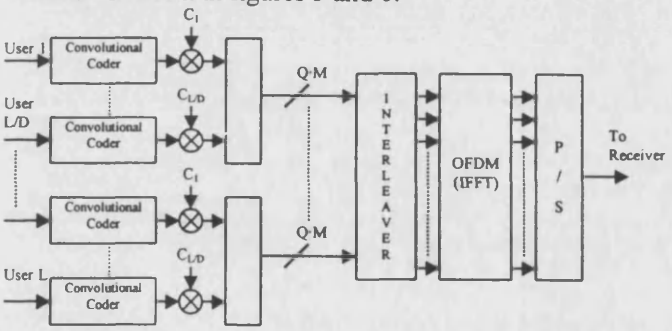

Figure 5. Convolutional coded OFDM-CDMA downlink basestation transmitter design

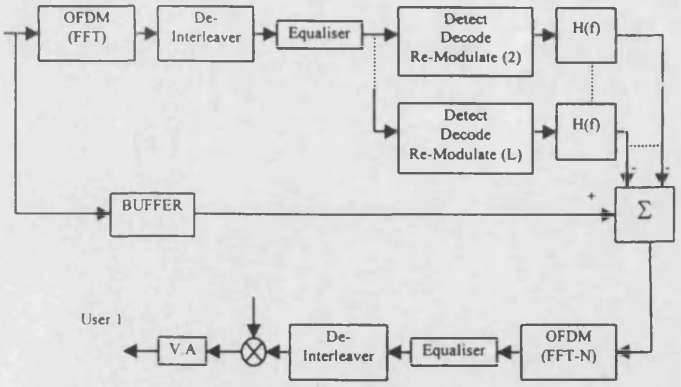

Figure 6. Subscriber receiver architecture for user 1

SIMULATION RESULTS

The simulated basestation downlink uses convolutional coding of rate R=1/2 and constraint length K=5 on the 19 kb/s data to be transmitted. This encoded signal is then further spread using orthogonal Walsh-Hadamard sequences of length 16, giving a total bandwidth expansion factor of 32 and a maximum user capacity of 16 users per block. The total number of blocks is set to D=8 and Q=2

data bits of each user are transmitted per block. The number of sub-carriers is therefore set to 512, providing a sub-carrier spacing of approximately 2kHz. The number of simultaneous users was set to 128 (full capacity).

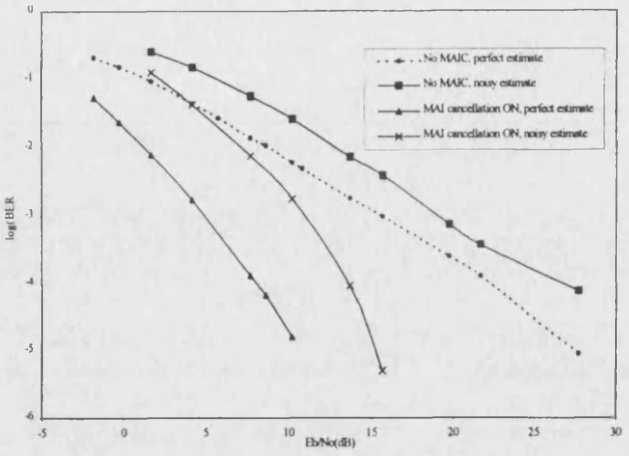

Figure 7. Performance using zero forcing equalisation on the first iteration and MRC on the second detection

The performance using zero-forcing equalisation on the initial data estimates of all interfering users and MRC on the wanted user's data estimate is shown in figure 7. Significant performance improvements of up to 10dB can be realised using such a technique assuming perfect channel estimation. The graph also shows the degradation which results from having imperfect channel estimates due to noise. The main disadvantage of the zero-forcing technique is that unwanted noise is amplified in deep fades. Since MAI cancellation techniques rely on good estimates of the interfering user's data, it is important to optimise the equalisation technique on the first iteration. Nevertheless, if no MAI cancellation is used, controlled equalisation schemes can provide a considerable improvement in performance. To estimate the threshold level at which the optimum performance is reached, simulations using MAI cancellation and no MAI cancellation in the receiver were obtained at an SNR of 15.6dB.

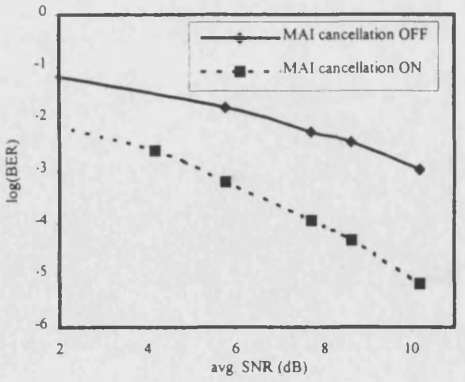

Figure 8. Performance using controlled equalisation on the first iteration and MRC on the second iteration

Next, the optimum threshold value was used to determine the performance of the convolutionally coded downlink using MAI cancellation. When no MAI cancellation is used, figure 8 shows that the controlled equalisation scheme outperforms the zero-forcing algorithm quite considerably, as would be expected, but with MAI cancellation and MRC used on the second stage of detection the performance is improved by a factor of 4dB.

CONCLUSIONS

Uplink and downlink receiver designs have been proposed for a mobile communication system in a channel of heavy frequency selective Rayleigh fading. The use of LROCC and controlled equalisation with MAI cancellation in the uplink have been shown to provide a capacity gain of at least 25% at BER=10^{-3}, and likewise a 10dB gain in the downlink with rate 1/2 convolutional codes. More realistic performance results with noisy channel estimates have shown to provide a degradation of at least 6dB on this result, yielding a potential improvement of 4dB. It has been further established that the use of zero forcing equalisers would not lead to a good performance without MAI cancellation, but through the use of MAI cancellation it is possible to combine zero-forcing algorithms with MRC on the final detection stage to give good results.

REFERENCES

[1] Y. Yukitoshi and M. Nakagawa, "A Multiuser Interference Cancellation Technique Utilizing Convolutional Codes and Orthogonal Multicarrier Modulation for Wireless Indoor Communications", *IEEE Journal on Selected Areas in Communications*, Vol. 14, No.8, October 1996

[2] K. Fazel, S. Kaiser and M. Schnell, "A Flexible and High Performance Cellular Mobile Communications System Based on Orthogonal Multi-Carrier SSMA", *Wireless Personal Communications*, Kluwer Academic Publishers, pp.121-144, 1995

[3] T. Mueller *et al*, "Comparison of different Detection Algorithms for OFDM-CDMA in Broadband Rayleigh Fading", *IEEE Conference Publication*, pp. 835-838, 1995.

[4] S. Kaiser, "OFDM-CDMA versus DS-CDMA: Performance evaluation for fading channels", *Proc. IEEE International Conference on Communications* (ICC'95), pp.1722-1726, June 1995.

[5] Maxey, J J and Ormondroyd, R F, "Optimisation of orthogonal low-rate convolutional codes in a DS-CDMA system", *IEEE/URSI Conference Proceedings of ISSSE'95*, Vol. 95TH8047, pp. 493-496, 1995

[6] Maxey, J J and Ormondroyd, R F, "Low-Rate Orthogonal Convolutional Coded DS-CDMA using Non-Coherent Multi-Carrier Modulation over the AWGN and Rayleigh Faded Channel", *IEEE Conference Proceedings of ISSSTA'96*, Vol. 2, pp.575-579, 1996

[7] COST 207: *Digital land mobile radio communications*, Final Report, Commission of the European Communities, Luxembourg 1989

5th European Conference on Fixed Radio Systems
and Networks, Bologna, Italy, May 1996

EVALUATION OF A FIXED WIRELESS ACCESS DS-CDMA SYSTEM EMPLOYING LOW-RATE ORTHOGONAL CONVOLUTIONAL CODES

J. J. Maxey, R. F. Ormondroyd and K. R. Edwards*
School of Electronic and Electrical Engineering
The University of Bath
Claverton Down, Bath, BA2 7AY, U.K.
Tel. (+44) 1225 826826
Fax. (+44) 1225 826305
e-mail: eepjjm@bath.ac.uk ; eesrfo@bath.ac.uk

ABSTRACT - The performance of a novel orthogonal DS-CDMA strategy based on low-rate orthogonal convolutional codes is examined. The scheme is applied to the problem of a fixed wireless access scheme capable of delivering speech and data with the same quality as conventional wire PSTN systems. The theoretical and simulated performance of a rate 1/64 convolutional orthogonal code operated in "other-user" noise are obtained. The effect on the inter-cell interference of using highly directional subscriber antennas, as well as sectored base-station antennas, is examined. Particular attention is paid to the effects of shadowing in a theoretical study of the interference statistics of this design.

1. INTRODUCTION

Fixed access wireless local loop systems offer a means of very rapid network deployment which avoid local access constraints and infra-structure problems. This is particularly important in a number key markets where there is a large potential demand for telephony and high-rate data applications capable of delivering ISDN services. This requirement for a high quality service has placed great emphasis on establishing a communication link which is both robust and spectrally efficient. Central to this work are the technological advances that are being made in modulation and coding schemes which provide an efficient use of frequency spectrum and the use of adaptive schemes, particularly with regard to flexible frequency planning, for applications in countries with different frequency allocations and different geographical environments.

The wireless link between fixed subscribers and a central base-station introduces a channel environment similar to that of a cellular mobile radio system, except that rapid deep fades are rare occurrences, Doppler effects are negligible and call hand-off is not a problem. In addition, synchronisation of remote subscribers on the network can be achieved on initial installation of the equipment and consequently the problems of rapid code synchronisation at the start of a call are no longer a problem. However, these benefits must be offset against the much higher required link performance of the fixed access link compared with the mobile link.

Direct-sequence code division multiple access (DS-CDMA) techniques are being considered as likely contenders for the next generation cellular mobile radio schemes, and their application to the fixed wireless environment is also under consideration, largely on the promise of reasonable capacity and flexible use of contingent bandwidth. There are various methods which may lead to improved performance efficiency, many of which form the basis of this paper. The most commonly employed techniques include:

- Frequency re-use which makes use of geographical separation to increase distance between interfering users
- Orthogonality of different users to minimise self-interference effects
- Convolutional coding strategies to minimise the required signal-to-noise ratio by each user
- Cell sectorisation to minimise interference effects
- Closed- or open-loop power control to eliminate the near-far effect, which plays a major part in limiting the ultimate capacity of DS-CDMA systems.

Subject to the differences in the channel environment outlined earlier, the capacity of both fixed access and mobile links are limited by statistical effects such as multipath fading, inter-cell interference and 'other-user' interference. In conventional DS-CDMA cellular mobile systems, emphasis is placed on the benefits achieved through the use of voice activity detection. This underlines a fundamental difference between the two systems. In the fixed wireless access system, it is assumed that data transmission forms an integral part of service provision, where voice activity detection is considered to be inappropriate, and hence we do not include this feature in our model.

* K. R. Edwards, Radio Infrastructure, NORTEL,
Brixham Road, Paignton, PT4 7BE, Devon, U.K.

It has been established [1-5] that the use of orthogonal coding techniques for DS-CDMA in digital cellular mobile radio promises capacity advantages. Whilst it is straightforward to achieve orthogonality on the down-link, it is difficult to obtain fully synchronous and orthogonal operation on the up-link from the mobile subscribers. For fixed access wireless systems, however, with the appropriate protocol and a pilot tone synchronisation strategy obtained from the base-station, it is feasible to achieve orthogonal operation of the system on both the down-link and the up-link using delay management techniques similar to those currently being used for digital mobile cellular schemes. The penalty of employing the pilot tone synchronisation strategy, of course, is the cost, either in terms of power or the number of users. In this paper, a worst-case analysis is considered where it is assumed that the up-link be non-orthogonal. Consequently, the capacity of the cell is limited by the non-orthogonal up-link rather than the orthogonal down-link due to the effects of incompletely cancelled "other-user" interference, channel noise and inter-cell interference.

Fixed access wireless schemes have the advantage that the remote subscribers can make use of highly directional antennas, as opposed to omni-directional antennas found in mobile radio systems. These reduce the power requirements of both the base-station and the remote transmitter and give greater interference rejection both to inter-cell interference and intra-cell interference. They also reduce the outer-cell interference in a universal frequency re-use plan, and both these factors have a significant effect on capacity. A more detailed analysis will be given in section 2. The inter-cell degradation factor should, therefore, be as close to 1.0 as possible.

Low-rate orthogonal convolutional codes (LROCC) have recently been proposed as a better alternative to conventional pseudo-noise (PN) codes normally used in DS-CDMA systems [1-5]. The coding strategy replaces both the forward error correcting code that might normally be used on the data bits and the high speed PN spreading sequence by a single orthogonal code which provides extremely powerful forward error correction coding and power density spreading in a single encoder. The performance of this LROC coding strategy provides the orthogonal convolutional codes with maximum free distance, hence giving optimum performance in AWGN and "other-user" noise environments. The result is that the orthogonal LROCC system outperforms the corresponding uncoded DS-CDMA system.

A study of the down- and uplink capacity will show that more attention must be paid to the design implementation of the uplink. The strongest interference will be seen from "other-user" noise in the same cell which can only be minimised through the use of perfectly time-aligned orthogonal sequences. This places the requirements for a coherent link where the channel parameters can be estimated on a continuous basis. One approach to achieving an orthogonal uplink is to use a pilot tone transmitted from each user within the same bandwidth, therefore enabling orthogonality to be maintained, since the low level of multipath is assumed to cause negligible degradation in orthogonality. Each pilot tone will require a minimum of energy from each user and therefore affect the capacity.

A second approach which does not require a pilot tone is to use non-coherent modulation techniques whereby the orthogonality between users is strictly reduced to quasi-orthogonality, since a knowledge of the phase and amplitude statistics is now more difficult to establish. This causes an inherent reduction in capacity, though, which may be significantly smaller than the loss in capacity through the use of pilot tones. Simulation results and theoretical studies into the capacity on the uplink may show fruitful capacity advantages.

2. INTERFERENCE STATISTICS

The mobile radio channel statistics are very severe at high frequencies, being dominated by strong Rayleigh fading with multipath interference and diffraction shadowing effects. In a fixed access system, the use of stationary subscribers with highly directional antenna reduces the severity of the interference statistics in the channel medium. The temporal change in channel statistics for a fixed access system is much slower than that for the mobile channel, hence the phase and amplitude information acquired through the possible use of a pilot channel does not change as rapidly as for a mobile communication system. For this reason it may not be profitable to sacrifice spectrum for a pilot channel on the uplink to achieve coherency. Nevertheless, the interference statistics of the fixed access wireless system play an important role in the estimation of the subscriber capacity per bandwidth allocation per unit area.

The received power P_r at the subscriber or base-station site can be directly related to the transmitted power P_t by the relation:

$$P_r \propto P_t \left(\frac{10^{\frac{\phi}{10}}}{r^{\alpha}} \right) \qquad (1)$$

where α is the decay index and ϕ is a Gaussian randomly distributed variable with mean $\mu = 0$ and standard

deviation, σ, which is typically 8dB for the case of an omni-directional antenna [6]. For values of ϕ which give a value greater than one the mobile experiences a handover to the nearest base-stations. Since the fixed access link rarely has greater than 2 independent paths, the influence of multipath fading has been neglected in the study of the channel statistics.

Consider a cellular structure where each interfering fixed user in neighbouring cells is power-controlled to its own base-station in order to counter the effects of shadowing (which is assumed to have Gaussian statistics ϕ_0 with regard to its own cell and Gaussian statistics ϕ_1 on the uplink to the base-station it is interfering with). Each variable ϕ_i is distributed with a variance of σ, hence the overall shadowing effects, ϕ, are described by a Gaussian distribution with a variance of $2\sigma^2$ and mean of zero. Each individual shadowing component of ϕ_i is made of two separate shadowing components:

$$\phi_i = a\xi + b\xi_i \qquad (2)$$

were $a^2 + b^2 = 1$ and ξ is the shadowing component common to all base-stations. Considering the interference statistics of two base-stations in a cellular structure, the overall shadowing component is related by:

$$\phi = \phi_0 - \phi_1 = b(\xi_0 - \xi_1). \qquad (3)$$

It is important to note that in mobile communications, were omni directional antenna are used, the constants a and b can be considered independent variables of equal amplitude, hence $a^2 = b^2 = 1/2$. Therefore, the variables ξ_0 and ξ_1 are also considered to be independent variables with a mean of zero and standard deviation 8dB. The overall standard deviation of the interference effects due to two base-stations is then given as 11.3 dB.

Conventional designs employ closed-loop power control to adjust the transmitting power of the fixed subscriber. As a consequence, shadowing on the uplinks of the outer cells (within the line-of-sight of the base-station of the wanted cell) causes the interference power at the wanted cell's base-station to be modulated. The highly directional structure of the antenna from the interfering subscriber, positioned on the line-of-sight path as shown in figure 1, will inevitably experience shadowing on the same path as the power-control uplink to its own base-station. Therefore, some degree of correlation between the two shadowing components a and b will be seen, hence a and b are now no longer of equal value, since the channel through which the mobile is power controlled is shared also by the interference from the subscriber to the base-station experiencing outer-cell interference.

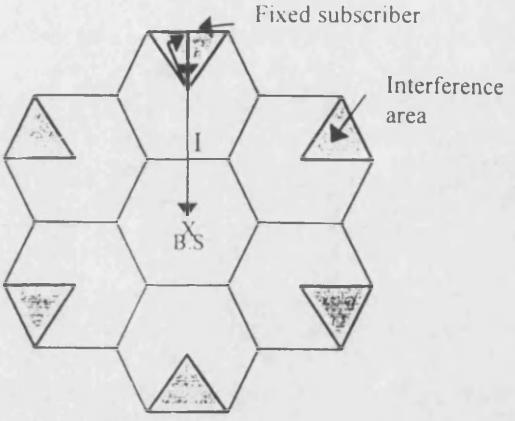

Figure 1

For a hexagonal cell structure, assuming that each subscriber is perfectly power-controlled in its own cell, the total interference seen by the central base-station can be given as:

$$I = \frac{12P_t}{3\sqrt{3}R^2} \int_{\frac{5\pi}{6}}^{\frac{7\pi}{6}} \int_{0}^{2\sqrt{3}R\cos(\gamma-\pi)} \frac{(r)^{a+1}}{((\sqrt{3}R)^2 + r^2 - 2(\sqrt{3}R)r\cos\gamma)^{\frac{a}{2}}} \cdot dr \cdot d\gamma \qquad (4)$$

where,

P_t = Transmit power of subscriber in interfering cell
R = Radius of cells
r = Distance of interfering subscriber from its own base-station
γ = Angle over which integral is valid (integral bound over 360^0 for omni-directional subscriber antenna, 60^0 for directional antenna of beamwidth $\pm 20^0$)

The total outer-cell interference, I_s , including the effects of shadowing is related to equation 4 by:

$$I_s = I \cdot \mathrm{E}\left[\frac{10^{\phi_0/10}}{10^{\phi_1/10}}\right] \qquad (5)$$

Next, the expected value of equation 5 must be found:

$$E\left[10^{\frac{(\phi_0-\phi_1)}{10}}\right] = E\left[\exp\left(\frac{\ln 10(\phi_0-\phi_1)}{10}\right)\right]$$
$$= E\left[\exp(B(\phi_0-\phi_1))\right]$$
$$= E\left[\exp(Bbx)\right]$$
$$= \int_{-\infty}^{\infty} \exp(Bbx)\frac{\exp\left(-x^2/4\sigma^2\right)}{\sigma\sqrt{4\pi}}dx$$
$$= \exp(b^2(B\sigma)^2) \qquad (6)$$

where $B=(ln10)/10$ and $x=\xi_0-\xi_1$

Using equation 4 and equation 5 the interference level due to outer cells can be determined and the inter-cell degradation factor (i.e. the frequency re-use efficiency), F, defined as:

$$F = \frac{1}{1+\frac{I_s}{P_t}} \qquad (7)$$

Figure 2 shows the variation of F for different correlation statistics. For high correlation between the two links, a low value of b will give a nearly optimum value for the inter-cell degradation factor. These results are also plotted for different propagation decay factors α.

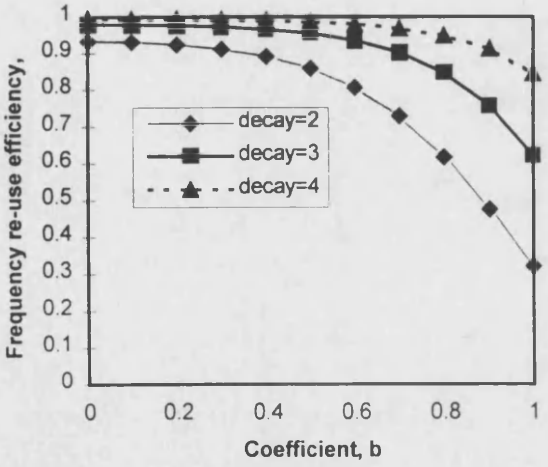

Figure 2

These curves show that as the correlation between fades in the wanted cell and outer cell (within the bore-sight of the directional antenna) is increased (i.e. coefficient $b\rightarrow 0$), the frequency re-use efficiency approaches 100%. For typical mobile radio cellular structures the correlation between a and b is assumed equal, hence $b^2=1/2$ (i.e. $b=0.707$). As expected, if the decay index is increased, this increases the path loss between the outer cell and the wanted cell and the inter-cell interference is reduced, again resulting in a higher frequency re-use efficiency. Figure 3 shows the case for omni-directional antennas. Comparing figure 2 with figure 3 clearly shows the reduction in frequency re-use efficiency through the use of omni-directional antennas.

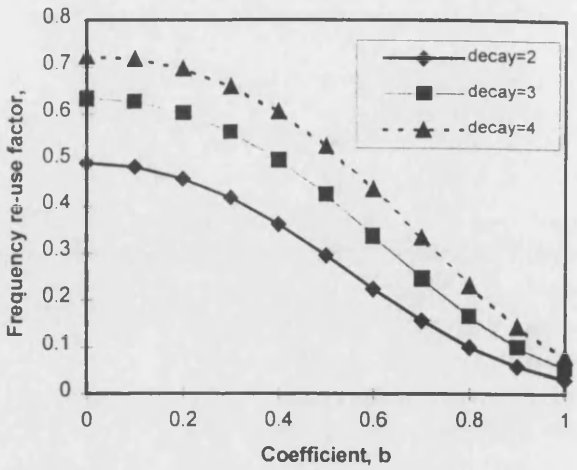

Figure 3

3. LOW-RATE ORTHOGONAL CONVOLUTIONAL CODING

Conventional DS-CDMA systems rely on an internally generated PN sequence, such as maximal length sequences or Gold codes, to spread the data in the transmitter by means of modulo-2 addition. This causes the original data to be spread in bandwidth by a factor dependant on the PN sequence chip rate. If the PN data is of repetition length L, and one data period lasts for the whole repetition length, then the data will experience a spread in bandwidth proportional to L. The factor L, by which the data is increased in bandwidth can be termed the *spreading ratio* of the base-station transmitter.

This is not the only way of spreading the bandwidth of the data in the transmitter base-station, however. Using a convolutional encoder of rate 1/L, as shown in figure 4, also introduces a redundancy of L symbols, hence this also provides bandwidth spreading.

Figure 4

The orthogonality of ordinary convolutional codes is very poor, and this would lead to a small number of simultaneous users when used in a CDMA system. This can be improved significantly by using low-rate

orthogonal codes [1-5] which directly code and spread the data signal. This system provides an encoded bit sequence of length L on each bit transition from the data source and in effect provides complete spreading of bandwidth.

The receiver structure performs the inverse operation by demodulating the received signal, then decoding the convolutionally encoded signal and providing an estimate of the most likely transmitted data bit. The decoding algorithm used by the receiver must use the maximum-likelihood decoding technique since the probability of any codeword being transmitted is equally likely. There are various decoding algorithms such as the Viterbi algorithm, sequential decoding (which is nearly maximum-likelihood) or concatenated coding schemes. One particular feature which is important to the decoding algorithm is its speed, especially if it is to be used for low rate codes in a DS-CDMA system where the throughput (i.e. the speed at which each data bit is processed) must be high. It is apparent that a low rate code will inevitably slow down the speed of operation in the decoder since a large number of symbol comparisons per data bit will be made.

The level of improvement that a convolutional code will give compared to an uncoded system is given by the *coding gain*. The Viterbi algorithm offers the advantage of providing a high coding gain at low bit-error rates, which can have an upper bound coding gain as high as 7.3dB for a rate 1/3, constraint length 8 soft decision code [7].

3.1 SIMULATION OF THE LROCC SYSTEM

Computer simulations of conventional DS-CDMA systems and the low-rate orthogonal code system were set up with identical basic parameters of code rate and spreading bandwidth for the two systems. In this way a fair comparison of bits/s/Hz/cell between the two systems can be established, hence it was possible to obtain a direct comparison of the number of simultaneous users between the two systems for a given bit-error rate (BER). For the case of the low-rate convolutional Hadamard encoder, shown in figure 5, the simulation provides an encoded sequence of 2^K output symbols for each consecutive input data bit. There are 2^K different sequence sets, each of length 2^K symbols and orthogonal to any other sequence. The inherent orthogonal properties of the Hadamard codes are based on the fact that any two sequences of length 2^K differ in 2^{K-1} bit positions, thus a 64 symbol code will vary in 32 symbol combinations and have 32 identical symbol combinations.

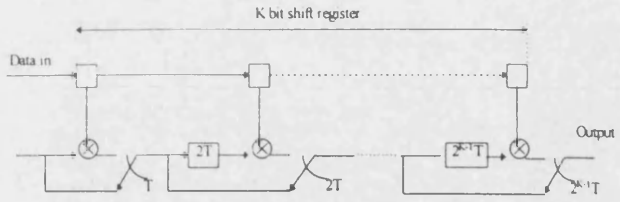

Figure 5

To decode the received signal sequence with a Viterbi decoder it is necessary to find the most likely path through the trellis state diagram. Since each user has a different unique mapping of state outputs in the shift register system to the inputs of the Hadamard block encoder, the trellis for each user will be considerably different, hence allowing all simultaneous users to be isolated from one another.

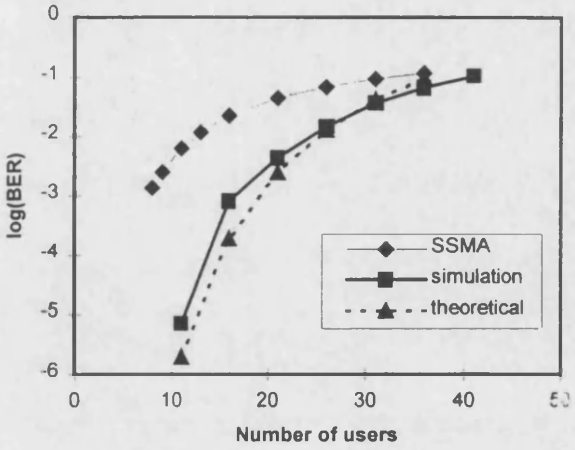

Figure 6

The performance of LROCC encoded signals in "other-user" noise is shown in figure 6. In this figure, only one cell is considered, the spreading ratio of the LROC code is 64, "other-user" noise is the dominant interference and perfect power-control is assumed. It can be seen that the theoretical and simulated results match closely. There is a significant improvement in the system capacity when compared with a conventional uncoded DS-SSMA design operating under similar conditions.

4. CAPACITY CALCULATIONS

The capacity of a fixed wireless access design is based on the provision of high quality channels (i.e. high data rates, typically 64 kb/s at BER<10^{-9}), and this should be contrasted with the case of a typical mobile link where the bit error rates are generally much higher. Neglecting the use of tri-sectorisation and power-control errors in the cellular structure of a non-coherent DS-CDMA system, the commonly used uplink capacity equation is found to be:

$$N = 1 + \frac{W/R}{E_b/N_0} \cdot F \cdot \frac{1}{d} \qquad (11)$$

where,

N = Number of simultaneous users (at 64kb/s)
W = Channel bandwidth
R = Input data rate
F = Inter-cell degradation factor
d = Voice activity factor

Low-rate convolutional coding at rate 1/64 will give a signal-to-noise ratio requirement of E_b/N_0 = 7dB at a BER<10^{-9}. From figure 2, the inter-cell degradation factor F, at a decay index α=3 and correlation factor b=0.3 is found to be 0.973, hence the number of channels per 4.096 MHz bandwidth allocation can be found as:

$$N = \left(1 + \frac{4.096/0.064}{5.012}\right) \cdot 0.973 \approx 13 \text{ channels} \qquad (12)$$

In comparison with a conventional mobile communication system, using omni-directional antennas, for equal system parameters, the number of high quality channels would be reduced to a value of 7 (i.e. reduction of about 60%). The use of tri-sectorisation in the LROCC encoded system will give a new capacity of 39 ultra-high quality channels per bandwidth allocation.

5. CONCLUSION

The use of highly directional antennas and stationary users has been found to have a significant impact on the interference statistics used to model the fixed wireless access (FWA) channel. An evaluation of the interference statistics in FWA systems has shown that the effects of shadowing depend heavily upon the correlation of fading signals on the uplink path to the central base-station. Even though a reduction in capacity of one cell will have a "knock-on" effect on the other cells which are not included in the interference model, a high correlation will still give little inter-cell degradation. The anticipated inter-cell degradation factor for realistic values of decay index (α=2 to 4) will unlikely drop below 0.85. Therefore, the use of universal frequency re-use in cellular FWA DS-CDMA systems will present little problem in the interference from surrounding cells.

The use of efficient coding techniques such as low-rate orthogonal convolutional codes (LROCC) has shown considerable improvements over uncoded DS-CDMA systems in the number of simultaneous users that can be supported, giving an improvement of up to 130%.

The use of tri-sectorisation at the base-station gives further opportunity for increases in user capacity through the improvement in the fading statistics, in addition to the obvious improvement in capacity through sectorisation of the cell area. For coherent systems, the use of pilot tones is necessary, giving a reduction in user capacity at the expense of spectrum for pilot tone occupancy. It is therefore of vital importance to treat the inherent advantages of coherent designs over non-coherent designs with great care.

ACKNOWLEDGEMENTS

The authors would like to thank Dr. J Lin and Mr. D. Hargreaves of NORTEL for their invaluable help and suggestions in the preparation of this paper. The support of EPSRC through Contract GR/K27902 and NORTEL is also gratefully acknowledged.

REFERENCES

[1] Viterbi, AJ: "Very low-rate convolutional codes for maximum theoretical performance of spread-spectrum multiple-access channels"; IEEE JSAC, Vol. 8, No.4, May 1990.

[2] Maxey, JJ and Ormondroyd, RF: "Optimisation of Orthogonal Low-Rate Convolutional Codes in a DS-CDMA System"; URSI/IEEE Conference Proceedings of ISSSE'95, San Francisco, Vol. 95TH8047, pp. 493-496, 1995.

[3] Ormondroyd, RF and Maxey, JJ: "A High Performance Cellular Radio System based on Low-Rate Convolutional Coding"; IEE Int. Conf. On Radio Receivers, No. 415, pp.17-21.

[4] Ormondroyd, RF and Maxey, JJ: "Performance of low-rate orthogonal convolutional codes in DS-CDMA applications", accepted for publication in IEEE Trans. on Vehicular Technology.

[5] Maxey, JJ and Ormondroyd, RF: "Low-rate orthogonal convolutional coded DS-CDMA using non-coherent multi-carrier modulation over the AWGN and Rayleigh faded channel", Submitted to ISSSTA'96.

[6] Newson, P and Heath, MR:"The Capacity of a Spread spectrum CDMA System for Mobile Radio with consideration of system imperfections", IEEE JSAC, Vol.12, No.4, May 1994.

[7] Sklar, B: "Digital Communications - Fundamentals and Applications", Prentice Hall 1988.

[8] Edwards, KR: Internal Technical Working Paper, NORTEL, Issue 1.1, NT/IP1/134/KRE/371, August 1995

[9] Monogioudis P, Edmonds R, Tafazolli R and Evans BG: "Multirate 3rd generation CDMA systems", IEEE Int. Conf. On Comm., pp. 151-155.

VTC'97, Phoenix, Arizona, May 1997

COMPARISON OF TIME GUARD-BAND AND CODING STRATEGIES FOR OFDM DIGITAL CELLULAR RADIO IN MULTIPATH FADING

R F Ormondroyd and J J Maxey

School of Electronic and Electrical Engineering
The University of Bath, Bath, BA2 7AY, UK
e-mail: eesrfo@bath.ac.uk; eepjjm@bath.ac.uk

Abstract - This paper focuses on the combined use of convolutional coding and orthogonal frequency division multiplexing (OFDM) in a multipath channel. The use of time guard-intervals to reduce CCI and ICI is vital for good performance in such channels, but is wasteful of bandwidth. The paper examines the degradation in performance due to the use of sub-optimal time guard-intervals for uncoded and coded OFDM designs. In particular, a comparison is made between the use of low-rate orthogonal convolutional codes (LROCC) and conventional high-rate convolutional codes for different time guard-intervals. It is found that LROCC codes outperform high-rate convolutional codes, particularly when the time guard-interval period approaches its optimum value.

I. INTRODUCTION

Orthogonal frequency division multiplexing (OFDM) has been found to be very effective in combating the signal distortion and inter-symbol interference due to multipath propagation. To improve the detection of the wanted signal the OFDM system offers a range of techniques, such as:

- Frequency and time interleaving
- Robust coding strategies
- Time or frequency domain equalisation
- Time guard-bands (cyclic extension)
- Frequency or time interleaving

Many of these techniques have been extensively studied [1-4] and considerable research is currently being carried out to determine the optimum implementation for a range of applications, especially for mobile and satellite personal communications.

In an OFDM system, the data symbols are blocked into groups of N and transmitted in parallel at a reduced rate on N orthogonal carriers. As N is increased, the data rate on each of the sub-channels is reduced to a value where the fading can be considered to be non-frequency-selective and this provides a measure of frequency diversity between the sub-channels which can be exploited by a suitable coding and interleaving strategy. Normally, Doppler spread sets the limit on the closeness to which the sub-carriers can be spaced, and this places an upper limit on N.

Multipath propagation broadens the channel impulse response. This results in inter-channel interference (ICI). One method of reducing ICI when using OFDM in broadcast applications, such as DAB and terrestrial HDTV, is to precede the (reduced-rate) symbol with a time guard-interval, which has a duration longer than the channel impulse response. In a multiple access system this is very wasteful of bandwidth, and hence capacity. An alternative strategy which attempts to recover the lost bandwidth, replaces the guard-interval by an equaliser, such as a simple zero-forcing equaliser, to counteract the channel impulse response [2,3]. However, in this paper we consider the benefits of using a convolutional coding strategy in conjunction with OFDM modulation to reduce the impact of the guard-interval.

II. EFFECTS OF THE TIME GUARD BAND FOR THE OFDM SYSTEM

OFDM techniques are particularly well suited to trans-mission over frequency selective fading channels. The use of a time guard-interval of length, T_g, before each block of N symbols maintains the orthogonality between the blocks and removes the necessity for further inter-channel interference (ICI) equalisation, but only if the guard-interval is longer than the maximum delay spread of the channel. If the guard- interval is shorter than the maximum delay spread, the orthogonality conditions between the sub-channels do not hold anymore. This introduces two main interfering terms: one is produced through the echo of the preceding block and the second is due to the loss of orthogonality in the remaining part of the integration interval. The second interfering term is still present even in systems with a guard-interval longer than the maximum delay spread. It causes distortion within the same sub-channel and is described as co-channel interference (CCI). This level of interference may be cancelled out through the use of efficient equalisers if the channel impulse response is perfectly known. In practice, the insertion of known period sequences enables the receiver to track slowly fading channel variations produced by the Doppler frequencies to estimate the channel coefficients. In the following, the analysis of the effect of multipath fading on the performance of an OFDM system with a time guard-interval by Viterbo and Fazel [5] is applied to the case where the system also has convolutional

coding and the concept of using low-rate orthogonal convolutional coding (LROCC) in conjunction with OFDM is introduced.

A. AWGN channel performance

Consider the transmission of an OFDM signal which uses N sub-carrier frequencies. Each sub-carrier frequency, f_k , is given as:

$$f_k = f_c + k/T_b \text{ for } k = 0,1 \ldots N\text{-}1 \quad (1)$$

where f_c is the carrier frequency and T_b is the effective OFDM block duration (i.e. $T_b = NT_S$, where T_S is the period of each symbol prior to blocking-up). The addition of a guard-interval, T_g, gives a new total block duration of:

$$T_b' = T_b + T_g \quad (2)$$

The generation of the N orthogonal sub-carriers and the multiplexing of the N parallel low-rate data channels onto these sub-carriers is assumed to be carried out *via* the inverse fast Fourier transform (IFFT). This technique has its origins through the use of orthogonal basis functions, given by:

$$\phi_k(t) = \begin{cases} e^{j2\pi f_k t} & -T_g \le t \le T_b \\ 0 & \text{otherwise} \end{cases} \quad (3)$$

The time-domain OFDM signal at the output of the IFFT is thus given by:

$$x(t) = \sum_{n=-\infty}^{\infty} \sum_{k=0}^{N-1} X_{n,k} \phi_k (t - nT_b') \quad (4)$$

where $X_{n,k}$ is the data sequence being transmitted on the k^{th} sub-channel in the n^{th} block.

At the receiver, the optimal decoding strategy for an AWGN channel with no fading effects is through the use of a bank of digital matched filters operating at each of the sub-carrier frequencies. However, a more efficient implementation uses the FFT on the samples of the received signal to demultiplex the received signal. This is performed over the block duration T_b for each sub-channel k = 0,1 … N-1, on the n^{th} block by neglecting the first T_g seconds of the received block:

$$X_{n,k} = \frac{1}{T_b} \int_0^{T_b} x(t) \phi_k^* (t - nT_b').dt = \frac{1}{T_b} \int_0^{T_b} x(t) e^{-j2\pi f_k (t - nT_b')}.dt \quad (5)$$

B. Multipath fading channel

The typical mobile radio channel is one suffering from severe multipath fading and this leads to severe degradation of the bit-error rate (BER) performance. For the example considered below, a simple two path faded channel is assumed. In general, the impulse response of a multipath channel is given by [6]:

$$h(t) = \frac{1}{\sqrt{L}} \sum_{m=1}^{L} e^{j(\theta_m + 2\pi f_{D_m} t)} \delta(t - \tau_m) \quad (6)$$

where L is the number of reflected multipaths, τ_m is the delay, θ_m represents the phase rotation and f_{Dm} is the Doppler frequency offset of the mth path. If L is large, and the Doppler frequency offsets are small compared to $1/T_b'$, the effect of the Doppler frequency shift can be replaced by a constant phase rotation in the n^{th} block integration.

If we consider a simple two path fading model as:

$$y(t) = x(t) + Ae^{j(\theta + 2\pi f_D t)} x(t - \tau) \quad (7)$$

where τ is the delay, f_D is the Doppler frequency, θ is the phase rotation and A the attenuation of the delayed signal component, then the output of the k^{th} sub-channel for the n^{th} block can be written as two terms:

$$Y_{n,k} = X_{n,k} + I_{n,k} \quad (8)$$

where $X_{n,k}$ is the term due to the direct path and the term $I_{n,k}$ represents the interfering term due to the echoes of the preceding blocks. Depending on the length of the guard-interval, this interfering term may be minimised to yield only the reflected echoes of the channel:

$$I_{n,k} = Ae^{j(\theta + 2\pi f_D n T_b')} e^{-j2\pi f_k \tau} X_{n,k} \quad (9)$$

In this case, the orthogonality conditions are satisfied and the subsequent attenuation and phase effects on the wanted symbols $X_{n,k}$ may be cancelled out through the use of an efficient equalisation strategy. If the guard-interval time is less than the maximum delay spread on the channel, further distortion effects take place in the interfering term:

$$I_{n,k} = Ae^{j(\theta + 2\pi f_D n T_b')} \left[\sum_{l=0}^{N-1} X_{n-1,l} \lambda_{l,k}(\tau) + \sum_{l=0}^{N-1} X_{n,l} \mu_{l,k}(\tau) \right] \quad (10)$$

where $\lambda_{l,k}$ and $\mu_{l,k}$ determine the level of dependence between the sub-channel fading effects on the N carriers. These have been found to be given as [5]:

$$\lambda_{l,k}(\tau) = \begin{cases} \left(\frac{\tau - T_g}{T_b} \right) e^{j2\pi k (T_b' - \tau)/T_b} & \text{for } l = k \\ e^{j\pi \left[2l(T_b' - \tau)/T_b + (l-k)(\tau - T_g)/T_b \right]} \frac{\sin\left[\pi (l-k)(\tau - T_g)/T_b \right]}{\pi (l-k)} & \text{otherwise} \end{cases} \quad (11)$$

and,

$$\mu_{l,k}(\tau) = \begin{cases} \left(\frac{T_b - \tau + T_g}{T_b} \right) e^{-j2\pi k \tau / T_b} & \text{for } l = k \\ -e^{j\pi \left[-2l\tau/T_b + (l-k)(\tau - T_g)/T_b \right]} \frac{\sin\left[\pi (l-k)(\tau - T_g)/T_b \right]}{\pi (l-k)} & \text{otherwise} \end{cases} \quad (12)$$

For the multipath channel model considered here, the received signal is given as:

$$Y_{n,k} = \frac{\mu_{k,k}}{\sqrt{L}} X_{n,k} + \sum_{l=0, l\neq k}^{N-1} \frac{\mu_{l,k}}{\sqrt{L}} X_{n,l} + \sum \frac{\lambda_{l,k}}{\sqrt{L}} X_{n-1,l} \quad \text{for } k=0\ldots N\text{-}1 \tag{13}$$

where,

$$\lambda_{l,k} = \sum_{\tau \in \{\tau_m > T_g\}} H_m \lambda_{l,k}(\tau) \qquad \text{for } l \neq k \tag{14}$$

$$\mu_{l,k} = \sum_{\tau \in \{\tau_m > T_g\}} H_m \mu_{l,k}(\tau) \qquad \text{for } l \neq k \tag{15}$$

$$\mu_{k,k} = \sum_{\tau \in \{\tau_m \leq T_g\}} H_m e^{j2\pi f_k \tau} + \sum_{\tau \in \{\tau_m > T_g\}} H_m \mu_{k,k}(\tau) \tag{16}$$

and the channel coefficients for each reflected path are given by $H_m = e^{j(\theta_m + 2\pi f_{D_m} n T_b')}$.

If the channel is assumed to be slowly varying, H_m will also be slowly varying from one block integration interval to the next. Since the guard-interval does not totally eliminate the effects of inter-block interference, the information symbols can no longer be easily extracted from $Y_{n,k}$. This interference results in both ICI and CCI. Finally, the ratio of the signal power to interference power at the output of each sub-channel can be obtained as:

$$\left(\frac{C}{I}\right)_k = \frac{|\mu_{k,k}|^2}{\sum_{l=0, l\neq k}^{N-1} |\mu_{l,k}|^2 + \sum_{l=0}^{N-1} |\lambda_{l,k}|^2} \qquad k = 0 \ldots N\text{-}1 \tag{17}$$

Fig. 1 shows the effect of the length of the guard-interval, T_g, (expressed as a percentage of the block length) on the C/I of an OFDM system arising from both CCI and ICI effects.

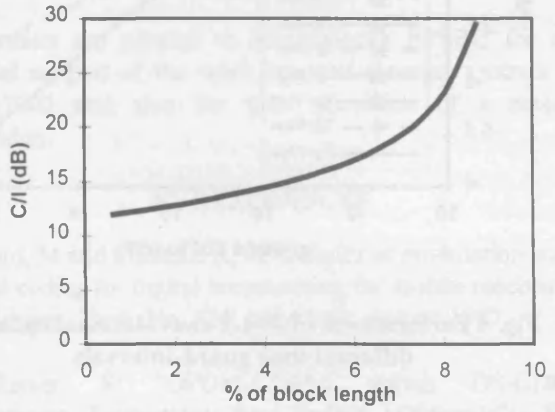

Fig. 1 *C/I* ratio improvement with increasing time guard-interval

The main operating parameters of the system modelled are: carrier frequency of 1.6GHz, with N=32 sub-channel carriers, QPSK modulation, a block length of 160μs in 3-path fading with one direct path and two reflected paths, one at a delay of 1μs and the second at 15μs. All reflected paths are assumed to have equal power ratios and a Doppler frequency of 200Hz. The total bit-error rate (BER) is the average of the BER in each channel. Neglecting the terms in $Q^2(\cdot)$, the BER for QPSK modulation can be expressed as:

$$BER \approx \frac{1}{N} \sum_{k=0}^{N-1} Q\left[\left(\sqrt{\frac{C}{I}}\right)_k\right] \tag{18}$$

Equation (18) gives an estimate of the OFDM performance in the noiseless fading channel by effectively averaging out the BER in each sub-channel from the carrier-to-interference levels for each carrier.

An average of the appropriate probability of error expression over all possible received powers can be obtained by evaluating the average *C/I* level over all k sub-carriers. The average *C/I*, defined as $\bar{\gamma}$, is given by:

$$\bar{\gamma} = \frac{1}{N} \sum_{k=0}^{N-1} \left(\frac{C}{I}\right)_k \tag{19}$$

and using [7], the probability of a bit error is:

$$P_b = \int_0^\infty Q\left(\sqrt{\gamma_k}\right) p(\gamma_k) d\gamma_k = \frac{1}{2}\left[1 - \sqrt{\frac{\bar{\gamma}}{1+\bar{\gamma}}}\right] \tag{20}$$

where $\gamma_k = (C/I)_k$ in sub-channel k.

Fig. 2 shows the variation in BER performance for different guard-intervals.

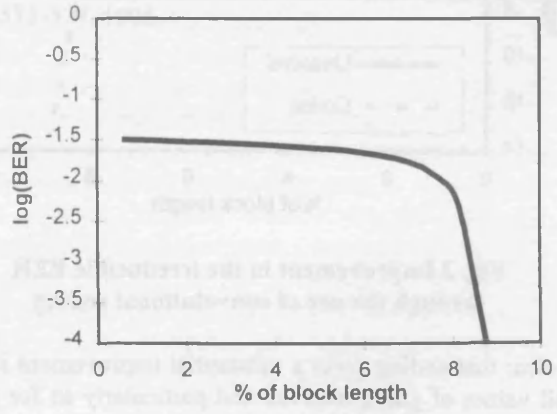

Fig. 2 Effect of time-guard interval on irreducible BER

Note how the residual BER drops extremely rapidly as the guard-interval time approaches a value equivalent to a 10%

increase in block length, which corresponds to the maximum delay-spread component of the signal.

C. Convolutional coding techniques

Forward error correction (FEC) coding can be integrated into the OFDM design to further optimise the performance improvements in multipath fading channels. One popular FEC coding strategy is convolutional coding. With this technique it is possible to add diversity to the system design in order to combat the fading effects on the individual sub-carriers. In this paper, we compare the performance of conventional high-rate (R=1/2, K=5) convolutional coding and low-rate orthogonal convolutional coding of rate R=1/32 and constraint length K=5. Ordinary R=1/2 convolutional codes can be upper-bound on the bit-error probability through use of their generating function to weight error events by the number of bit-errors. This can be generalised as [8]:

$$BER_k < \sum_{j=d_{free}}^{\infty} c_j P_{j,k} \tag{21}$$

where, d_{free} is the free distance of the convolutional code, $P_{j,k}$ is the calculated bit-error probability of the kth sub-channel (dependent on the channel) for a particular E_b/N_O, c_j are the coefficients determined through the generating function of the particular code in question.

The performance improvements for the case of the R=1/2, K=5 convolutional code are shown in Fig. 3.

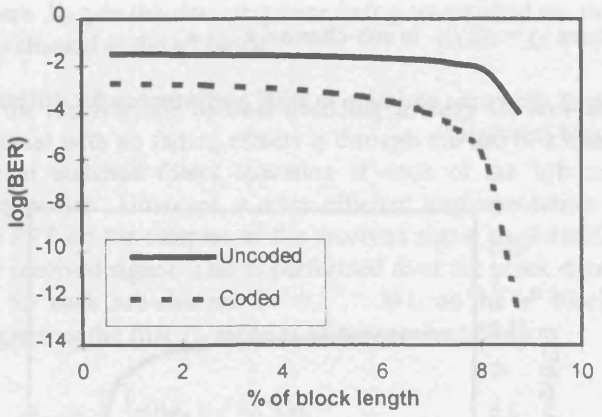

Fig. 3 Improvement in the irreducible BER through the use of convolutional coding

It is clear that coding gives a substantial improvement in BER for all values of guard-interval, and particularly so for guard-intervals close to the maximum value of delay-spread. For relatively small guard-intervals, fading dominates the degradation in performance and the coding gain is not as large.

For LROCC codes, an equivalent upper-bound can be obtained more generally for different constraint length codes through a simplified state diagram. This upper-bound on the BER for the k^{th} sub-carrier is given in terms of constraint length K codes and has been found to be [8]:

$$BER_k < \frac{W_k^K (1-W_k)^2}{(1-2W_k+W_k^K)^2} \tag{22}$$

where,

$$W_k = Q\left[\left(\sqrt{\frac{C}{I}}\right)_k\right] \tag{23}$$

A noise power of variance σ_k^2 gives an additional AWGN term in the C/I ratio for each of the sub-carriers, and is therefore used to determine the performance of convolutional codes in multipath fading for different noise levels. The average BER for all N sub-carriers can be obtained for a specific E_b/N_O, by averaging the bit-error probability over all sub-carriers:

$$BER < \frac{1}{N}\sum_{k=0}^{N-1} BER_k \tag{24}$$

Fig. 4 shows the BER performance of the R=1/2, K=5 convolutional codes for the multipath fading environment detailed earlier as a function of different guard-intervals. It can be seen, that there is little improvement in performance when the guard-interval is short, but the graph shows an improvement in the performance bounds as the guard-interval approaches the longest path delay.

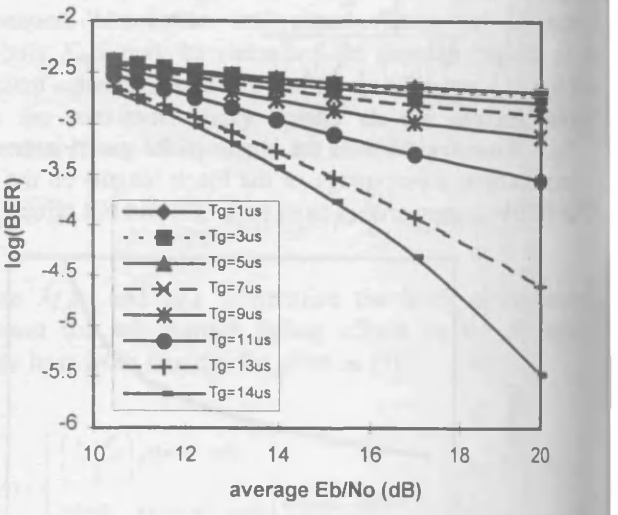

Fig. 4 Performance of R=1/2 convolutional codes for different time guard-intervals

As expected [8-11], Fig. 5 shows that the use of LROC codes together with the OFDM modulation scheme gives an improved performance bound for short guard-intervals relative to the high rate convolutional code, and this improvement is matched for the entire range of guard-intervals.

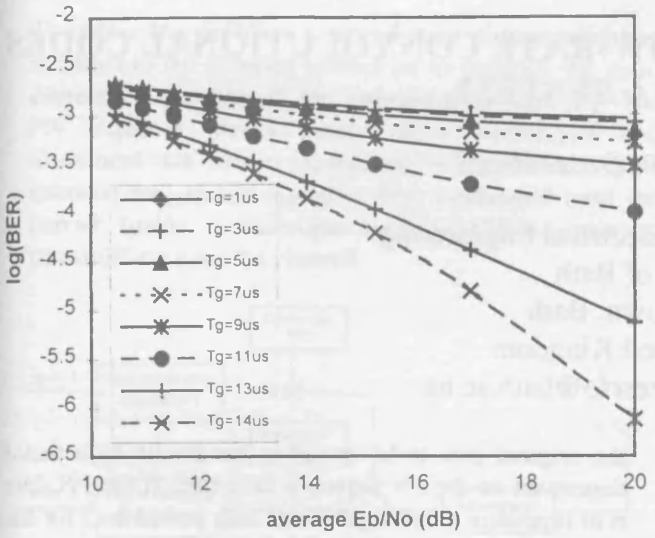

Fig. 5 Performance of R=1/32 LROC codes for different time guard-intervals

III. CONCLUSION

This paper has analysed the effect of the time guard-interval on the bit error rate performance of an OFDM modulation scheme used over a channel suffering from multipath fading. In particular, the paper has examined the improvement in performance made possible through the use of convolutional coding of the data. It is found that the BER is improved for all values of time guard-interval, but particularly so when the guard-interval is close to the maximum delay-spread of the channel. The use of LROC coding is found to offer further improvements in performance.

IV. ACKNOWLEDGEMENTS

The authors are pleased to acknowledge EPSRC for their financial support of the work reported through contract No. GR/K27902 and also for their provision of a research studentship.

V. REFERENCES

[1] Alard, M and Lassalle, R; "Principles of modulation and channel coding for digital broadcasting for mobile receivers"; EBU Review, Tech. No. 224, pp. 47-69, August 1987.

[2] Kaiser, S; "OFDM-CDMA versus DS-CDMA: Performance Evaluation for Fading Channels"; IEEE International Conference on Communications (ICC'95), pp. 1722-1726, June 1995.

[3] Vahlin, A and Holte, N; "Use of guard intervals in OFDM on multipath channels"; Electronics Letters, Vol.30, No.24, pp.2015-2016, 24th Nov. 1994.

[4] Sourour, E A and Nakagawa, M; "Performance of Orthogonal Multicarrier CDMA in a Multipath Fading Channel"; IEEE Transactions on Communications, Vol. 44, No.3, pp. 356-367, March 1996.

[5] Viterbo, E and Fazel, K; "How to combat long echoes in OFDM transmission schemes: Sub-channel equalisation or more powerful channel coding"; IEEE Conference Proceedings, pp. 2069-2074, 1995.

[6] Hoeher, P; "A statistical discrete time model for the WSSUS multipath channel"; IEEE Transactions on Vehicular Technology, Vol. 41, pp.461-468, No.4, February 1992.

[7] Proakis, J G; "Digital Communications"; McGraw-Hill, 1995.

[8] Viterbi, A J; "CDMA - Principles of Spread Spectrum Communication"; Addison-Wesley Wireless Communications Series, 1995.

[9] Maxey, J J and Ormondroyd, R F; "Optimisation of orthogonal low-rate convolutional codes in a DS-CDMA system"; IEEE/URSI Conference Proceedings of ISSSE'95, Vol. 95TH8047, pp. 493-496, 1995.

[10] Ormondroyd, R F and Maxey, J J; "A high performance CDMA cellular radio system based on orthogonal low-rate convolutional coding"; IEE International Conference on Radio Receivers and Associated Systems, Conference Proc. Vol.414, pp.17-21, 1995.

[11] Maxey, J J and Ormondroyd, R F; "Low-Rate Orthogonal Convolutional Coded DS-CDMA using Non-Coherent Multi-Carrier Modulation over the AWGN and Rayleigh Faded Channel"; IEEE Conference Proceedings of ISSSTA'96, Vol. 2, pp.575-579, 1996.

ISSSE'95, San Francisco, California, November 1995

OPTIMISATION OF ORTHOGONAL LOW-RATE CONVOLUTIONAL CODES IN A DS-CDMA SYSTEM

J.J. Maxey and R.F. Ormondroyd

School of Electronic & Electrical Engineering
University of Bath
Claverton Down, Bath
BA2 7AY, United Kingdom
eepjjm@bath.ac.uk, eesrfo@bath.ac.uk

ABSTRACT

The paper describes a novel approach to the use of direct-sequence spread-spectrum modulation for code division multiple access (DS-CDMA) applications by replacing the normal PN spreading code with an orthogonal low-rate convolutional code. This achieves both the spreading in bandwidth of the data and a powerful coding strategy within the output state of the convolutional shift register system, which maximises the number of simultaneous CDMA channels. In order to achieve orthogonality, Hadamard codes are incorporated within the convolutional coding strategy. The effects of using such a design within a DS-CDMA system are studied and the results show a direct increase in the capacity of the cellular system compared with a DS-CDMA using maximal length sequences. The importance of randomising the output symbols from the Hadamard encoder is also considered with respect to the spectral characteristics of the transmitted signal and the isolation between different simultaneously transmitting users.

1. INTRODUCTION

The field of spread spectrum multiple access is currently receiving considerable attention as a contender for the next generation mobile telephone system. DS-CDMA systems are at present looking very promising compared to advanced time division multiplex systems (TDMA) [1], as these systems offer increased flexibility in the frequency management of the cellular network, the prospect of temporary capacity overload and improved handover flexibility. The ultimate goal is to maximise the potential number of simultaneous users within a specific cell boundary.

Conventional DS-CDMA systems rely on an internally generated PN sequence, such as maximal length sequences or Gold codes, to spread the data in the transmitter by means of modulo-2 addition. This causes the original data to be spread in bandwidth by a factor dependant on the PN sequence chip rate. If the PN data is of repetition length L, and one data period lasts for the whole repetition length, then the data will experience a spread in bandwidth proportional to L. The factor L, by which the data is increased in bandwidth can be termed the *spreading ratio* of the base-station transmitter.

This is not the only way of spreading the bandwidth of the data in the transmitter base-station, however. Using a convolutional encoder of rate 1/L, as shown in figure 1, also introduces a redundancy of L symbols, hence this also provides bandwidth spreading.

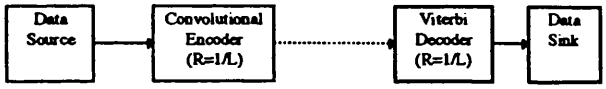

Figure 1 Spread-spectrum system using convolutional coding for signal spreading

Figure 2 shows the schematic of a CDMA base-station transmitter which is based on the use of low-rate convolutional codes rather than the more usual PN spreading sequences. The orthogonality of ordinary convolutional codes is very poor, and this would lead to a small number of simultaneous users when used in a CDMA system. This can be improved significantly by using low-rate orthogonal codes [2] which directly code and spread the data signal. This system provides an encoded bit sequence of length L on each bit transition from the data source and in effect provides complete spreading of bandwidth.

It is well known that orthogonal functions do not have good auto-correlation properties and therefore the direct use of orthogonal functions can lead to poor transmission spectral characteristics (e.g. non-uniform spreading) and large interference signals.

0-7803-2516-8/95 $4.00 © 1995 IEEE

To reduce this problem, a second stage of randomisation is added to the encoded symbol set to improve the auto-correlation property of the orthogonal signals [2]. The PN sequence serves purely as a randomiser and introduces no further spreading of bandwidth. This encoded and spread signal is then modulated onto the carrier (using a technique such as QPSK) prior to transmission over the channel.

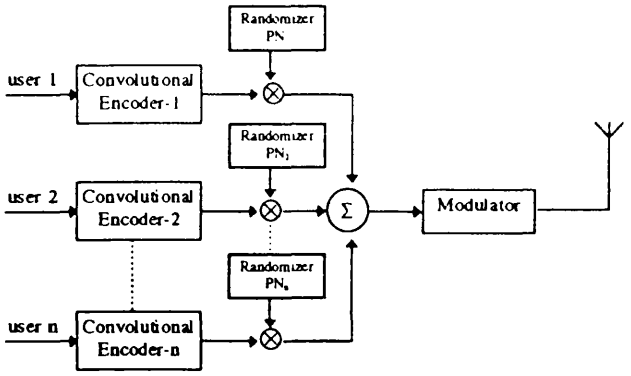

Figure 2 Simplified diagram of the proposed BS transmitter

The receiver structure performs the inverse operation by demodulating the received signal, then decoding the convolutionally encoded signal and providing an estimate of the most likely transmitted data bit. The decoding algorithm used by the receiver must use the maximum-likelihood decoding technique since the probability of any codeword being transmitted is equally likely. There are various decoding algorithms such as the Viterbi algorithm, sequential decoding (which is nearly maximum-likelihood) or concatenated coding schemes. One particular feature which is important to the decoding algorithm is its speed, especially if it is to be used for low rate codes in a DS-CDMA system where the throughput (i.e. the speed at which each data bit is processed) must be high. It will become apparent that a low rate code will inevitably slow down the speed of operation in the decoder since a large number of symbol comparisons per data bit will be made.

The Viterbi algorithm is a fast and efficient way of decoding convolutionally encoded data. It works by comparing the received sequence of encoded bits with the possible combinations of most likely transmitted bits and makes its decision after it has reached a decision on the most likely path through the trellis of the convolutional code. Thus it can be seen that this technique will yield an improvement over the simple correlating process in a conventional CDMA since a decoding decision is based not only on the complete set of L redundant symbols but also takes into account the previous data bits which had been present in the shift register system. Hence, improved error detection is provided where the level of improvement depends on the constraint length K of the code (i.e. number of shift registers used). As K is increased, the decoding method becomes more historic since the number of possible states in the trellis diagram will increase exponentially. The higher the number of possible states in the trellis, the better the bit-error performance. The drawback, of course, is that the decoding procedure will slow down as the number of states in the trellis increases, as the decoder has to compare many more possible data bit transitions.

The level of improvement that a convolutional code will give compared to an uncoded system is given by the *coding gain*. The Viterbi algorithm offers the advantage of providing a high coding gain at low bit-error rates, which can range from 1.5 dB to 4 dB at a BER of 10^{-5} using hard decision limiting with constraint lengths 3 and 8 respectively.

2. DS-CDMA SIMULATIONS

Computer simulations of conventional DS-CDMA systems and the low-rate orthogonal code system were set up with identical basic parameters of code rate and spreading bandwidth for the two systems. In this way a fair comparison of bits/s/Hz/cell between the two systems can be established, hence it was possible to obtain a direct comparison of the number of simultaneous users between the two systems for a given bit-error rate (BER). For the case of the low-rate convolutional Hadamard encoder, shown in figure 3, the simulation provides an encoded sequence of 2^K output symbols for each consecutive input data bit. There are 2^K different sequence sets, each of length 2^K symbols and orthogonal to any other sequence. The inherent orthogonal properties of the Hadamard codes are based on the fact that any two sequences of length 2^K differ in 2^{K-1} bit positions, thus giving a 64 symbol length Hadamard code 32 different symbol combinations.

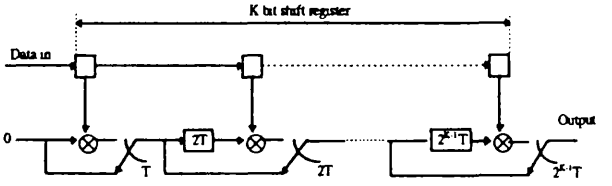

Figure 3 A low-rate convolutional encoder

To decode the received signal sequence with a Viterbi decoder it is necessary to find the most likely path

through the trellis state diagram. Since each user has a different unique mapping of state outputs in the shift register system to the inputs of the Hadamard block encoder, the trellis for each user will be considerably different, hence allowing all simultaneous users to be isolated from one another.

It is well known [3] that the BER performance of a Viterbi decoder is directly related to the free distance of the convolutional code, consequently the BER probability in the continuous additive white Gaussian noise channel is given as:

$$BER < \sum_{x=dfree}^{\infty} C_x P_x \qquad (1)$$

where $P_x = Q\left(\sqrt{\frac{2xRE_b}{N_o}}\right)$, R is the rate of the code, Eb/No is the required SNR at the output of the decoder and C_x is determined by the code structure of the Hadamard encoder. Equation (1) is the key to determining the structure of the most effective code performance for the continuous output additive white Gaussian noise channel. In order to use the same bandwidth in the most efficient way it is desirable to use a coding strategy which yields the highest free distance, ultimately governed by the code rate and constraint length of the encoder. The new code design featured in this paper will inevitably give a superior performance to a simple rate 1/2 encoder of same constraint length operating in a very noisy environment (i.e. high number of simultaneous users). At low user numbers the performance of both systems would yield an equal BER.

To obtain a result for the performance of such a system in "other-user" noise it is necessary to assume that a relatively large number of simultaneous users and a high spreading ratio will approximate the interference as normally distributed with a mean of zero and variance of

$$\sigma^2 = \frac{M-1}{1/R} \qquad (2)$$

where M is the number of simultaneous users. This will lead to a new expression for P_x:

$$P_x = Q\left(\sqrt{\frac{2x}{M-1}}\right) \qquad (3)$$

The free distance of the K=6 Hadamard convolutional code is governed by the total Hamming distance with respect to the "all-zero" path in the trellis and the number of paths which will take the decoder decision to the all-zero state, given as K+1. For the Hadamard convolutional encoder used in this simulation the free distance is 7×32=224. The values for C_x have been obtained using a full search of the trellis structure and for a K=6 Hadamard code, neglecting the higher order terms, yield a bit-error probability of:

$$BER < P(224) + 2P(256) + 6P(288) + 16P(320) + 35P(352) + 60P(388) \ldots \qquad (4)$$

The results of equations 3 and 4 are displayed graphically in figure 4. It must be noted that BER values of greater than 1 serve only on a theoretical basis. A comparison between the uncoded conventional DS-CDMA system and the new Hadamard encoded system shows considerable improvements with the new implementation at a low number of simultaneous users. These results are also compared to the conventional rate R=1/2 coded DS-CDMA implementation and show that the Hadamard rate R=1/64 implementation performs better at a relative high number of users.

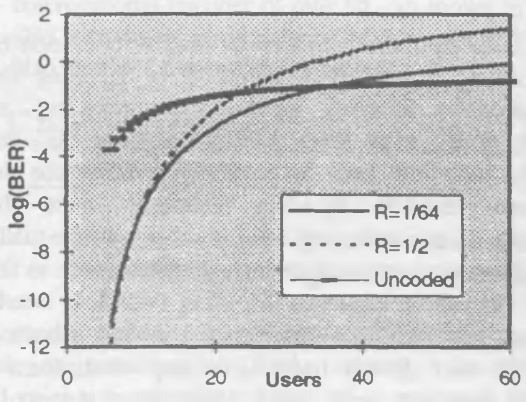

Figure 4 Theoretical performance of different coding schemes in other user noise

The resulting theoretical and simulated bit-error rate curves in "other-user" noise can be seen in figure 5. It is apparent that the theoretical prediction of the code matches the simulated results very closely, and a significant advantage in performance can be found when the number of simultaneous users is low.

To achieve a BER=10^{-3} a maximum number of 7 users could be employed in a conventional DS-CDMA system but the use of low-rate convolutional coding can lead to an increase of nearly 130%, giving a new maximum number of users of 16.

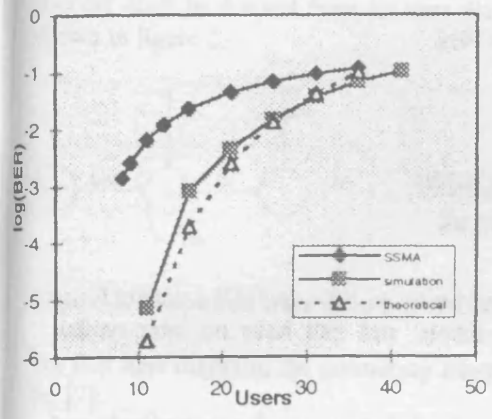

Figure 5 Performance of low-rate convolutional codes in other user noise

The use of PN sequences to randomise the output of the low-rate convolutional encoder is to improve the spectral characteristics of the orthogonal codes and provide better isolation between users without causing any further spreading of the encoded signal. This is done by using a PN sequence of the same rate as the orthogonal output sequence.

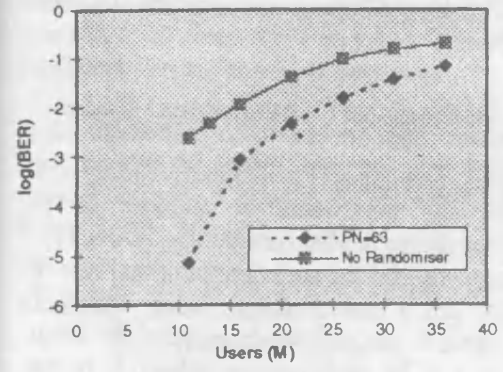

Figure 6 Graph displaying the advantages of using a randomiser

If $\delta \rightarrow 0$, where δ is the duration of one output symbol from the Hadamard encoder, the spectral density of a pseudo-random signal can be seen [2] to approach a constant value of E_s/T, where E_s is the symbol energy and T is the period of repeat of the pseudo-random noise sequence. It can therefore be seen that such a signal will give an almost uniform spectrum, which is desired in a DS-CDMA implementation. The sequence of output symbols from a low-rate orthogonal convolutional Hadamard encoder, however, have a periodic nature for each sequence set of length 2^K. Thus the auto-correlation properties of orthogonal sequences is extremely poor and yields a spectrum with large variations in amplitude, which has the direct effect of degrading the performance of the decoder to other user noise since the signal sets are not independent random processes. To eliminate this problem a PN sequence of same rate can be used to smooth out the spectrum and randomise the interference created by other users as seen in figure 6.

It is clearly evident that the second stage of randomisation improves the performance of the cellular DS-CDMA system by at least 60%, giving an equivalent improvement in BER performance of about 2dB.

3. CONCLUSIONS

This paper has shown the feasibility of using low-rate orthogonal convolutional coding for DS-CDMA applications. It has been found that the number of simultaneous users per cell is increased by at least 70% and there is an additional improvement of 60% when a randomiser is used, giving a total improvement of 130%.

4. ACKNOWLEDGEMENTS

The authors would like to thank EPSRC for their financial support of this research project through the provision of research contract N°- GR/K27902 and also a research studentship.

5. REFERENCES

[1] "A comparison of CDMA and TDMA systems"; CIRR TG 8/1 Washington; Ericsson May 1991.

[2] A.J Viterbi; "Very Low Rate Convolutional Codes for Maximum Theoretical Performance of Spread-Spectrum Multiple-Access Channels"; IEEE Journal on Selected Areas in Communications, Vol 8, No.4, May 1990.

[3] A.J. Viterbi; "Convolutional Codes and Their Performance in Communication Systems"; IEEE Transactions on Communications Technology, COM-19, No.5, Oct 1971.

Low-Rate Orthogonal Convolutional Coded DS-CDMA using Non-Coherent Multi-Carrier Modulation over the AWGN and Rayleigh Faded Channel

J J Maxey and R F Ormondroyd
School of Electronic and Electrical Engineering
University of Bath
Claverton Down, Bath
BA2 7AY, UK.
Tel. (+44) 1225 826615 : Fax. (+44) 1225 826305
E-mail. eepjjm@bath.ac.uk : eesrfo@bath.ac.uk

Abstract

An analysis of the performance of low-rate orthogonal convolutional codes is presented in multiple-access systems operating under Rayleigh fading and AWGN. These results are used to obtain the performance of a non-coherent orthogonal frequency division multiplexing (OFDM) design employing LROCC coding in a Rayleigh fading environment with interference from "other-user" noise and AWGN. Considerable improvement in the spectrum efficiency of this new implementation over coherent DS-CDMA is found.

1. Introduction

The use of direct-sequence code division multiple access (DS-CDMA) techniques for mobile communications is attracting considerable interest in fixed and mobile cellular systems. DS-CDMA techniques appear to be especially attractive in digital mobile cellular schemes due to their performance in fading channels and their flexible use of bandwidth. Given the difficult multipath channel environments for mobile communications and the limitations this imposes on obtaining higher data rates, it is important to design a system which is both robust and reliable.

One spread-spectrum multiplexing technique that is currently receiving attention is orthogonal frequency division multiplexing (OFDM), which uses multiple overlapping orthogonal carriers to transmit the data. This technique has been found to give better performance over single carrier systems in the mobile radio environment. In this paper, a new coding and modulation scheme is examined for multiple access applications which can be applied to OFDM to provide a signal which is orthogonal in both the frequency and time domain and which is extremely robust in fading conditions. The method adopted is to apply low-rate orthogonal convolutional coding, which effectively expands the data by a factor 2^K, where K is the constraint length of the convolutional encoder, and to add OFDM so that N data symbols are transmitted in parallel on N orthogonal carriers. This enables several simultaneous users in the cellular structure to be isolated from one another in the time domain and through the use of orthogonally spaced carriers provides isolated data streams in the frequency domain. With OFDM, it is possible to separate each low bit-rate modulated carrier by as little as $1/2T_s$, where T_s is the period of the symbols, and still have no inter-symbol interference.

As the presence of multipath fading introduces amplitude and phase distortion on the signal it is difficult to track the phase information without the use of a pilot tone. Therefore, a non-coherent modulation technique such as differential PSK is introduced, where the phase information in the demodulator is derived from the previous symbol. As long as the phase distortion factor due to multipath is nearly constant or at least slowly varying over the symbol duration T_s, a square law detector may be used in the non-coherent demodulation technique.

In the following sections the benefits of applying low-rate orthogonal convolutional codes (LROCC) to orthogonal multiple carriers in a multi-access environment will be considered.

2. Low-Rate Orthogonal Convolutional Codes

The use of low-rate orthogonal convolutional codes as a direct replacement for DS-CDMA in multiple access applications has been shown to offer considerable benefits [1-5]. In this section we consider the performance of this type of encoder in AWGN and L-path Rayleigh fading. Figure 1 shows a typical LROCC encoder which encodes the serial data bit stream in a K bit shift register, where K is the constraint length of the encoder, by providing a set of 2^K orthogonal Hadamard sequences for each data bit.

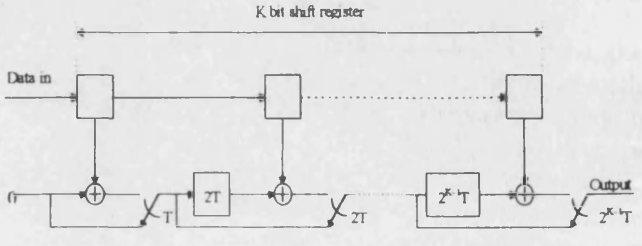

Figure 1. A low-rate orthogonal convolutional encoder

To achieve independent successive symbol set transmissions from each user, the data input to the block encoder is interleaved. In the next section, the performance of this encoder will be examined.

2.1 LROCC performance in AWGN

To analyse the performance statistics of the low-rate decoder in the receiver, the generating function of the encoder must be derived from its state diagram, which is shown in figure 2.

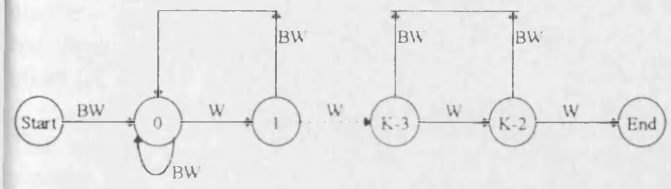

Figure 2. Simplified state diagram of LROCC design

For this state diagram, the generating function is found to be [7]:

$$T(W,B) = \frac{BW^K(1-W)}{1-W\left[1+B\left(1-W^{K-1}\right)\right]} \qquad (1)$$

where B denotes a transition in the trellis diagram caused by a data input of '1', W is a weight measurement for each branch metric and relates the average energy-per-bit to the noise density ratio per distance weight. Also, for the coherent AWGN channel:

$$W = Z^{\frac{1}{2r}} \qquad (2)$$

where r is the code rate and $Z = \exp(-E_b/I_0)$. For other channels (such as the Rayleigh fading channel), W follows a different statistic, as will be seen later.

In the receiver, to determine the upper bound for the bit-error rate of the LROC code for any general class of channel, equation 1 must be differentiated with respect to B, and B then set to 1:

$$\left.\frac{dT(W,B)}{dB}\right|_{B=1} = \frac{W^K(1-W)^2}{\left(1-2W+W^K\right)^2} \qquad (3)$$

Figure 3, below, shows the BER performance obtained from equation 3 for different values of K.

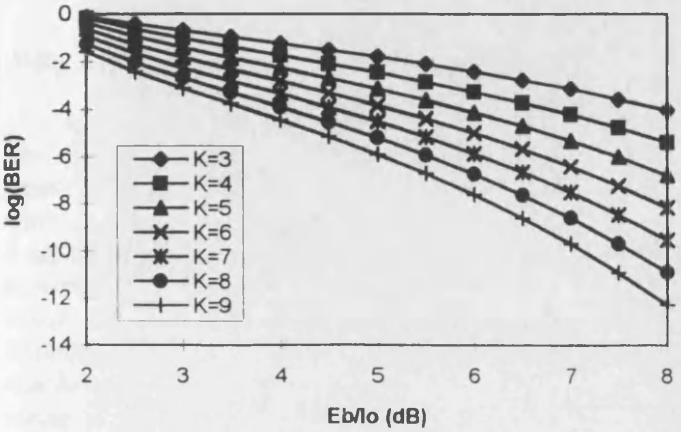

Figure 3. Theoretical *BER* v. E_b/I_o for an LROCC system in AWGN

2.2 LROCC performance in L-path Rayleigh fading

In the receiver, it is assumed that the received signal is represented as I and Q signals, and a maximum ratio combining technique of equal length as the number of L multipath components is employed. The branch metric of the typical de-modulated input variables Y_I and Y_Q is determined from the input variable $Z = Y_I^2 + Y_Q^2$. It is assumed that the received signal comprises of L components from L independent Rayleigh faded paths. The amplitude, λ, of each independent Rayleigh faded signal is related by the probability function, $p(\lambda)$:

$$p(\lambda) = \frac{2\lambda}{\sigma^2} e^{\left(-\lambda^2/\sigma^2\right)} \qquad (4)$$

where the chip energy E_c is multiplied by λ^2 and σ^2 is the variance of the fading process. The average chip energy, E_{avg}, for each path is derived from the chi-squared probability density function in the usual way [6], from which it is found that:

$$E_{avg} = \sigma^2 E_c \qquad (5)$$

Thus the average mean-squared signal power is given by $M^2 = J^2 E_{avg}$, where J is the number of symbols per input data bit in the shift registers of the Hadamard encoder. From [7] it can be seen that the probability of a correct signal, $P_C(z)$, and the incorrect signal probability, $P_I(z)$, is given by:

$$P_C(z) = \frac{z^{L-1} e^{-\left(\frac{z}{1+J E_s/I_0}\right)}}{(L-1)!\left(1+J\frac{E_s}{I_0}\right)^L}$$

$$P_I(z) = \frac{z^{L-1}e^{-(z)}}{(L-1)!} \qquad (6)$$

where E_s is the average symbol energy per path. Therefore,

$$E_s = E_b / LJ \qquad (7)$$

where E_b is the total bit-energy received from all L paths.

The performance of any convolutional code in the maximum-likelihood decoding algorithm is determined through evaluation of the branch metrics on the correct and incorrect paths through the trellis state diagram. Letting the correct branch metrics be denoted as (y_1, y_2, ... y_d) and the incorrect branch metrics as (x_1, x_2, ... x_d), the probability of a wrong decision being made at the point of path remerging is:

$$P_d = \text{Prob.}\left(\sum_{i=1}^{d} x_i > \sum_{i=1}^{d} y_i\right) \qquad (8)$$

Since the branch metrics can be treated as random variables due to the independence imposed on successive symbol set transmissions, the Chernoff bound can be applied to equation 8. Hence,

$$P_d < E\left[\exp\left(p\sum_{i=1}^{d} x_i - y_i\right)\right] = \left\{E\left[\exp(p(x-y))\right]\right\}^d \qquad (9)$$

where p is a variable from the exponential function of the Chernoff bound. To obtain the upper-bound on the bit-error performance it is necessary to determine the minimum value of the expected value of equation 9. It can be shown [7] that:

$$E\left[\exp(p(x-y))\right] = \int_0^\infty e^{px} P_I(x).dx \int_0^\infty e^{-py} P_Q(y).dy \qquad p>0 \qquad (10)$$

$$= \frac{1}{(1-p)^L}\frac{1}{\left[1+p(1+U)\right]^L}$$

where $U = (E_b/I_o)/L$ and the minimum value can be seen at $p = (U/2)/(1+U)$. Hence,

$$P_d < \left\{\frac{1}{\left(1-(U/2)/(1+U)\right)^L}\frac{1}{\left(1+\frac{(U/2)/(1+U)}{1+U}\right)^L}\right\}^d \qquad (11)$$

$$= \left[\frac{1+U}{\left(1+(U/2)\right)^2}\right]^{L.d}$$

Therefore,

$$P_d < W^d \qquad (12)$$

where $W = \left(\frac{1+U}{\left(1+(U/2)\right)^2}\right)^L$.

This value for W is substituted directly into equation 3 to give the performance of the LROCC design for a specific constraint length, K, in L-path Rayleigh faded channels. The performance for L=4 (i.e. a 4 path model) is shown in figure 4.

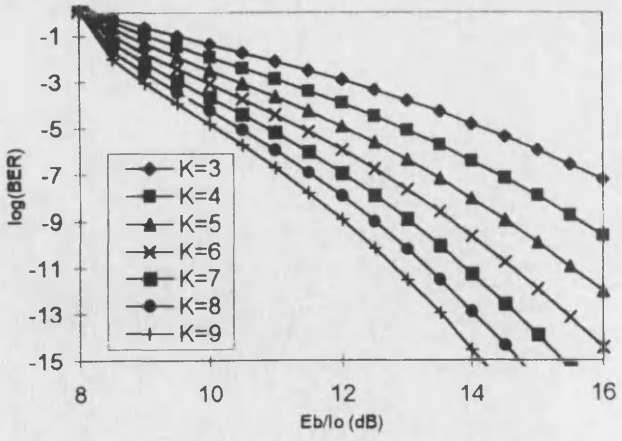

Figure 4. Theoretical *BER* v. E_b/I_o for the LROCC System AWGN and L-path Rayleigh fading channels

It is clear from this graph that there is a degradation in the bit error rate performance of the LROCC system in Rayleigh fading (compared with the non-faded system) which is dependent on the prevailing E_b/I_o. Typically, there is at least a 6dB degradation in performance.

Next, we seek to obtain a relation between the excess E_b/I_o required for the faded system performance compared to the AWGN channel, for a given value of signal-to-noise ratio per path L. This ratio is obtained as:

$$\text{Excess } E_b/I_o = \frac{2\exp\left(\frac{E_b}{2LI_o}\right) - 2 + \frac{1}{2}\sqrt{16}\sqrt{\exp\left(\frac{E_b}{2LI_o}\right)}\sqrt{\exp\left(\frac{E_b}{2LI_o}\right)-1}}{E_b/LI_o} \qquad (13)$$

The results of equation 13 are displayed graphically in figure 5.

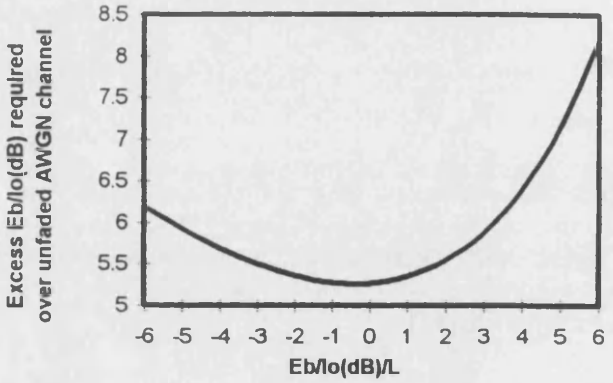

Figure 5. Excess E_b/I_o required for non-coherent Rayleigh fading employing LROCC

From these results one can obtain an estimate of the total required E_b/I_o for different values of diversity L. Note that values of excessive diversity cause increased performance degradation due to the non-coherent combining losses in the receiver.

3. OFDM-LROCC Implementation

A non-coherent multi-carrier orthogonal frequency division multiplexed system employing orthogonal low-rate orthogonal convolutional coding with DPSK modulation is shown in figure 6.

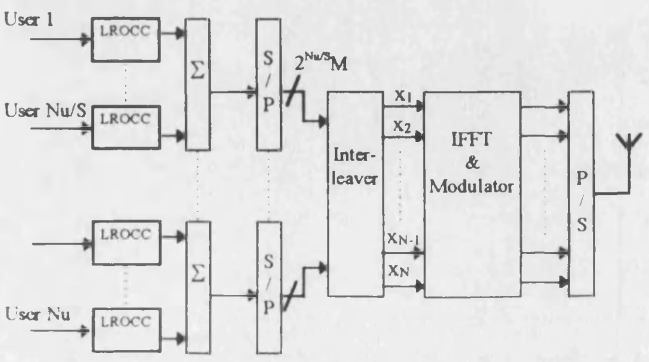

Figure 6. Multi-carrier transmitter implementation

From previous work [8] it has been found that the equivalent order of diversity L' in an OFDM modulated system is related to the spreading ratio in the time domain of the symbols before the IFFT, in the modulator. This has the direct effect of achieving diversity in the frequency domain, hence with a spreading ratio of 4 we can achieve a diversity of $L'=4$. Note also that in this paper the system employs neither frequency nor time guard-band intervals, but the inherent overhead due to guard-band intervals is taken into account in the capacity analysis.

The transmitter depicted in figure 6 groups the data signals of the N_u users into S blocks, with each block holding a maximum of N_u/S users. The data bits from each user are spread by a factor of $2^{Nu/S}$, which results in a diversity of $L'= 2^{Nu/S}$ in the receiver. Each block can transmit $M>1$ data bits per OFDM symbol, hence the input to the interleaver consists of $2^{Nu/S}M$ chips per block. Therefore, the total number of sub-carriers in the OFDM system will be equal to $2^{Nu/S}MS$.

3.1 System Performance

The OFDM system in figure 6 is analysed for a typical DS-CDMA application in the mobile environment. We assume a bandwidth of 1.25 MHz , which provides a chip duration of T_c=0.8μs. The system is in a fading channel with a multipath spread of T_m=10μs, and we wish to communicate with a $BER<10^{-3}$. Since we are using LROC codes, the system can support diversity factors of $L' = 4$, 8 , 16 , 32 , 64 ..., and for a maximum of N_u=64 users and 8 data bits per user per OFDM symbol we need 512 sub-carriers. The resulting sub-carrier spacing is therefore 2.441 kHz, hence the chip duration on each sub-carrier is T_s=409.6μs. In order to combat the effects of multipath spread, a guard interval of 16μs is considered sufficient. At maximum user capacity the bandwidth efficiency is then given by:

$$\eta = \frac{512}{1.25 \times 425.6} = 0.9624 \text{ b/s/Hz} \qquad (14)$$

In the presence of "other-user" noise we consider the Gaussian approximation for the asynchronous case, which gives a signal-to-noise ratio per data bit of:

$$SNR_{int} = \left(\frac{2(N_u - 1)}{3 \cdot 2^K} + \frac{I_o}{E_b} \right)^{-1} \qquad (15)$$

The minimum E_b/I_o for different values of constraint length K are obtained from figure 3, and then compared with SNR_{int} , therefore giving the necessary increase in required E_b/I_o to achieve a BER$<10^{-3}$. The channel is assumed to be at full capacity, N_u=64, and in addition, an excess E_b/I_o will be required to combat the effects of Rayleigh fading, which is displayed in figure 5. Since the equivalent diversity of the system is given by L', different values of constraint length K will give variations in the required signal-to-noise ratio for the AWGN channel, which also leads to a variation in the excess E_b/I_o required for the faded channel. The total E_b/I_o required for different values of constraint length K can be seen in figure 7.

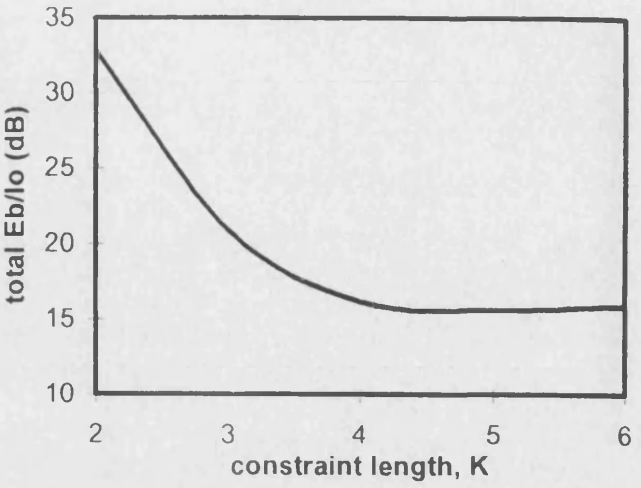

Figure 7. Total E_b/I_o required for LROCC-OFDM system operating in Rayleigh faded channel

Note, how the optimum performance is achieved for constraint length K=5 and values higher than this provide a further degradation in performance. This effect is due to the losses in non-coherent combining, since too much diversity can have a degrading effect on the performance of the system.

To compare the performance of this new OFDM implementation with a conventional DS-CDMA/ RAKE receiver of equal diversity L=16, we consider a coherent DS-CDMA system with 15% overhead for synchronisation and channel sounding. Both systems operate in a bandwidth allocation of 1.25MHz. The DS-CDMA/RAKE receiver yields a maximum achievable spectral efficiency of about 0.22 as $L' \to \infty$, hence not more than 20 users can be supported with adequate link quality. The LROCC-OFDM design has worse performance for low E_b/I_o but outperforms the RAKE receiver by a considerable amount at high values beyond E_b/I_o > 13dB.

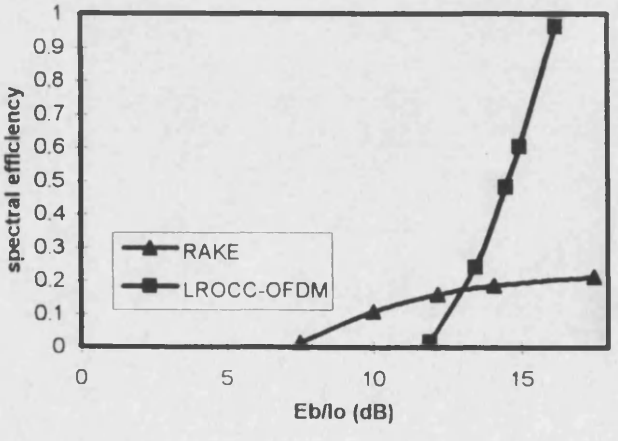

Figure 8. Comparison of spectral efficiency of DS-CDMA/RAKE v. LROCC-OFDM design for L'=16

4. Conclusions

The use of low-rate orthogonal convolutional codes in AWGN can yield considerable performance improvement over conventional coding strategies through the design and structure of the code. This has been verified theoretically and in simulated results, as shown in references [1-5].

Using low-rate orthogonal convolutional codes in non-coherent DS-CDMA applications where the channel is impaired by L-path Rayleigh fading can yield improved performance as long as the data is interleaved at the bit level. The minimum signal-to-noise ratio per bit required to achieve the same performance as in an unfaded AWGN channel is seen to be at about 6dB. Therefore, for equal system complexity, the losses encountered through non-coherent combining degrade any gain achieved through diversity, either achieved at the data bit level through K-fold interleaving or an increase in the number of path levels, L.

The implementation of LROCC in multi-carrier systems will give improved performance over other conventional coding techniques in partial band interference and fading, as the use of diversity is increased at an even coarser level. The independence between successive branches is one way of achieving this diversity. It has been shown that the performance of a non-coherent LROCC-OFDM system achieves much higher spectral efficiency than coherent DS-CDMA implementations using maximum ratio combining.

5. Acknowledgements

The authors are pleased to acknowledge EPSRC for their financial support of the work reported through Contract No. GR/K27902 and also for their provision of a research studentship.

6. References

[1] Maxey, J J and Ormondroyd, R F; "*Optimisation of orthogonal low-rate convolutional codes in a DS-CDMA system*"; IEEE/URSI Conference Proceedings of ISSSE'95, Vol. 95TH8047, pp. 493-496, 1995.

[2] Maxey, J J, Ormondroyd, R F and Edwards, K; "*Evaluation of a fixed wireless access DS-CDMA system employing low-rate orthogonal convolutional codes*"; Accepted for 5th European Conference on Fixed Radio Systems and Networks, Bologna, Italy, 14-17th May, 1996.

[3] Ormondroyd, R F and Maxey, J J; "*A high performance CDMA cellular radio system based on orthogonal low-rate convolutional coding*"; IEE International Conference on Radio Receivers and Associated Systems, Conference Proc. Vol.414, pp.17-21, 1995.

[4] Viterbi, A J; "*Very low-rate convolutional codes for maximum theoretical performance of spread-spectrum multiple-access channels*"; IEEE Journal on SAC, Vol.8, No.4, 1990.

[5] Monogioudis, P, Edmonds, R, Tafazolli, R and Evans, B G; "*Multirate 3rd generation CDMA systems*"; IEEE International Conference on Communications, ICC'93, pp. 151-155, 1993.

[6] Proakis, J G; *"Digital Communications"*; McGraw-Hill,1995.

[7] Viterbi, A J; *"CDMA - Principles of Spread Spectrum Communication"*; Addison-Wesley Wireless Communications Series, 1995.

[8] Kaiser, S; *"OFDM-CDMA versus DS-CDMA: Performance Evaluation for Fading Channels"*; IEEE International Conference on Communications (ICC'95), pp. 1722-1726, June 1995.

[9] Rowitch, D N and Milstein, L B; "*Convolutional Coding for Direct Sequence Multicarrier CDMA*"; IEEE Milcom'95, San Diego, 5-8th Nov, Vol. 1, pp.55-59, 1995.

IEE Colloquium, London, May 1996

COFDM - AN ALTERNATIVE STRATEGY FOR FUTURE-GENERATION MOBILE COMMUNICATIONS?

R F Ormondroyd, J J Maxey and E Alsusa

Introduction

Future generations of mobile radio systems, such as the mobile broadband system (MBS), will be required to provide data rates of 2Mb/s and above and it is the dispersive characteristics of the mobile radio channel that will play a key role in determining the most suitable, cost-effective, radio interface solution. The purpose of this paper is to consider the potential of multi-carrier multiple-access techniques as a means of providing a versatile high data rate radio interface for both terrestrial and satellite mobile PCS. After describing the two main forms of multiple-access multi-carrier systems that have been proposed very recently, the paper will describe a new variant of multi-access multi-carrier system called LROCC-OFDM.

There is considerable debate concerning the relative merits of TDMA and CDMA as the most appropriate choice of multiple access method for future generations of digital mobile cellular radio. Direct-sequence CDMA seems to provide a higher spectral efficiency in comparison to other conventional multiplexing methods[1-3], although this may be attributable more to the noise-limited cellular structure of these systems rather than to any inherent efficiency of the basic direct-sequence spread-spectrum modulation method. However, DS-CDMA systems are also often attributed with systems' benefits which may be potentially greater than pure spectral efficiency. These include:

- robustness against fading
- low density power spectrum - potential for bandsharing
- interference and jamming rejection
- code re-use rather than frequency re-use - improved frequency planning
- soft capacity
- soft hand-off

Certainly, these benefits are achieved individually but once the process gain has been used to achieve a high user capacity it cannot be re-used for jamming rejection etc., so these benefits cannot be achieved collectively. At high data rates over a severely fading channel, other factors may be of greater significance.

If a traditional TDMA approach is adopted at the high data rates anticipated for MBS, complex time domain equalisers based on either a non-recursive linear equaliser or decision feedback equaliser would have to be used to combat the intersymbol interference (ISI) resulting from the effect of multipath delays in the mobile channel. In addition, interleaving and coding would also have to be used to augment the resilience of the system to the burst errors in the fading environment. The problem is no less severe if a CDMA approach is taken because the transmission bandwidth must be extremely large to provide adequate process gain to achieve the required cell capacity. In this case, the bandwidth of the signal will be considerably wider than the coherence bandwidth of the mobile radio channel and so channel fading is likely to be highly frequency selective. Equivalently, this is represented by a channel impulse response with a broad time delay spread due to multipath propagation and the effects of Doppler spread. Consequently, when the channel impulse response is much longer than the symbol duration, significant intersymbol interference (ISI) occurs and the performance of the system is seriously degraded[4].

One of the advantages of the DS-CDMA system is that it can efficiently implement a RAKE receiver[5-6] which acts as a matched filter for multipath combining and effectively provides path diversity. The RAKE receiver must continuously estimate the relative delay of each path and there is considerable current research on the benefits of maximum ratio combining (MRC) and equal gain combining (EGC). These methods require considerable signal processing within the receiver, particularly if other users' multipath interference has to be

School of Electronic and Electrical Engineering, University of Bath, Bath, BA2 7AY

rejected. Also, the technique does not handle significant Doppler spread which may be a major problem for satellite systems.

To combat these effects in two high data rate broadcasting applications which are also subject to severe multipath fading, digital audio broadcasting[7] and terrestrial HDTV[8], coded orthogonal frequency division multiplexing (COFDM) has been proposed.

OFDM/COFDM Techniques

The broad aim of OFDM or COFDM is to sub-divide the available (non-ideal) channel bandwidth into a number of narrowband sub-channels such that the performance of each sub-channel is almost ideal. By making the bandwidth of each sub-channel sufficiently narrow, the effects of ISI become negligible and equalisation is unnecessary[6]. In OFDM systems, the symbol rate of the serial data is reduced by a factor N by multiplexing it into N parallel paths which are then modulated onto N carriers. The key to the spectral efficiency of OFDM lies in the way in which the symbols are modulated onto the N carriers. Normally, it would be necessary to separate the frequency spacing of each carrier with a frequency guard band to prevent upper and lower sidebands of adjacent carriers from overlapping and producing aliasing. In OFDM/COFDM the carriers are all chosen to be orthogonal so that with an appropriate modulation scheme such as QPSK or QAM it is possible for upper and lower 'sidebands' to fully overlap yet still be correctly demodulated. The common method of achieving a large number of orthogonal carriers is to use the Fourier transform method[9]. Figure 1 illustrates a typical OFDM system based on the IFFT/FFT transform pair.

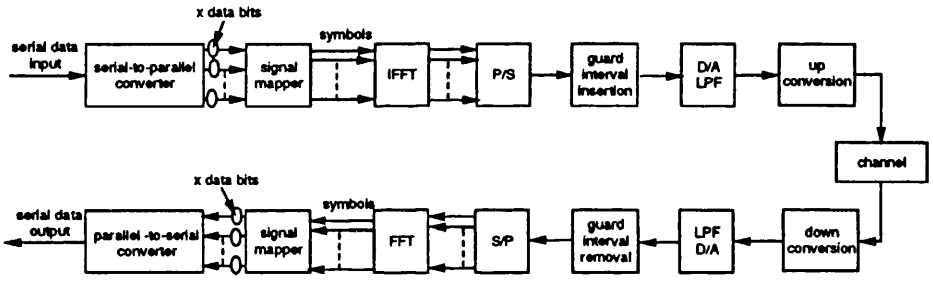

Figure 1 Typical OFDM system based on the IFFT/FFT transforms

Frames of M serial (encoded) data are first converted into $N' = M/x$ parallel groups of x data bits which are mapped into N complex value symbols, X_k, in the modulator corresponding to the signal constellation of the corresponding sub-carrier. Performing the inverse DFT on these N complex values results in N complex valued Fourier coefficients:

$$y_n = \frac{1}{\sqrt{N}} \sum_{k=0}^{N-1} X_k e^{j2\pi nk/N}, \quad n = 0,1,....N\text{-}1$$

where $1/\sqrt{N}$ is used for normalisation. These coefficients are then parallel to serial converted into a time sequence of N complex coefficients (or two real value time series representing real and imaginary parts of the complex Fourier coefficients) and these are clocked at the original symbol rate T_S such that the discrete time series $\{y_k\}$ represents samples of $y(t)$ at intervals of $t = nT_S/N$, where $n = 0,1...N\text{-}1$, i.e:

$$y(t) = \frac{1}{\sqrt{N}} \sum_{k=0}^{N-1} X_k e^{j2\pi kt/T_s}, \quad 0 \le t \le T_S$$

this signal is then used to modulate the carrier. From this it can be seen that the sub-carrier frequencies are:

$$f_k = k/T_S, \; k = 0,1,.....N$$

Furthermore, the baseband sub-carriers are all orthogonal in that:

$$\int_0^{T_s} \cos(2\pi f_i t + \theta_i) \cdot \cos(2\pi f_j t + \theta_j) dt = 0, \quad \text{for } i \neq j$$

It is also obvious from the above that the discrete DFT can be used in the receiver to recover the samples, X_k. By increasing the period of each frame of data, i.e. the period at which the IDFT is carried out, so that it is many times longer than the channel impulse response, it has been argued that the effects of ISI due to multipath propagation effects can be significantly reduced This can be achieved by increasing the size of the IDFT at the cost of computation complexity and the delay through the system is also increased. However, as the size of the DFT is increased, the sensitivity of the receiver to timing errors and phase jitter increases. Normally[10] Doppler spread sets the limit on the closeness to which the sub-carriers are spaced and this effectively places an upper limit on N and there may still be some ISI due to long echoes. To counter this, it has been suggested in a number of papers[10] that a time guard band is required at the end of each IDFT conversion, which may be as large as 25% of the symbol duration. This guard period, or cyclic extension is represented by a zero padding of the Fourier coefficients which lasts for T_g seconds beyond the normal frame period. Although this adds little complexity to the receiver, it means that the efficiency of data transmission is significantly degraded, however this period can also be used to obtain correct timing to mark the start of each Fourier transformation, which is very critical in maximising the system performance.

Viewed in the frequency domain, because the channel exhibits frequency selective fading not all N data symbols being transmitted in parallel will be corrupted simultaneously and the data on the degraded carriers can be corrected relatively easily with appropriate use of error correcting codes and interleaving. A number of different coding strategies have been considered, including: block codes, convolutional codes, Reed-Solomon codes and Turbo codes.

Clearly, to gain significant benefits from the use of COFDM, frequency selective fading is required. In fact, Sari *et al*[11] have pointed out, that except for PSK signals, OFDM does not solve the channel equalisation problem but simply shifts it from the time domain to the frequency domain. It has been argued, however, that this is a much easier problem to solve using the time guard band and a simple LMS algorithm one-tap equaliser after the DFT to provide frequency equalisation against co-channel interference. Most OFDM implementations use this structure, despite the obvious loss in capacity, but more complex multi-tap equaliser structures have been proposed recently[12-14] to reduce or remove the guard period and hence recover the capacity. However, these multi-tap equaliser systems can be optimised by the use of combining to form a RAKE structure[15] where it will be seen immediately that the use of a RAKE system after the DFT in the OFDM receiver will be very robust against Doppler spread. If Doppler spread is a problem, as it may be for satellite based broadband systems, the OFDM/COFDM approach is very powerful.

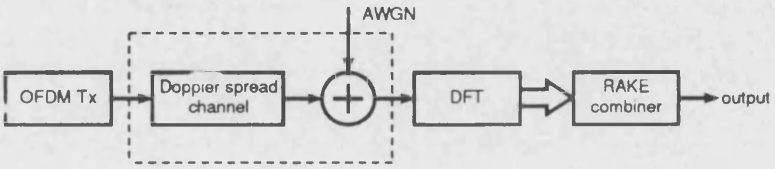

Figure 2 Simplified schematic showing how a RAKE combiner can be used with an OFDM receiver to combat multipath[15]

Multiple Access Systems Based on Multi-Carrier Techniques

Because of the success of COFDM in providing a high bit rate service in severe frequency selective fading and following the paper of Cimini[16], who proposed this form of signalling for digital mobile radio, there have been a number of recent proposals[17,18] for this and broadly similar multi-carrier [19,20](MC) techniques to be applied to multiple-access radio schemes.

In the systems proposed to date, multiple access capability is gained using conventional CDMA techniques and each user is given a unique PN code in the usual way. However, transmission of the users' data is achieved in one of two ways.

CDMA-OFDM In the first method, the data modulated spreading sequence is serial-to-parallel converted and each chip modulates a different carrier frequency via the IDFT routine. This implies that the number of carriers is equal to the processing gain and each carrier conveys a relatively narrowband waveform

rather than a direct-sequence waveform. Effectively, the FFT has given the resulting signal a PN coded structure in the frequency domain. This technique is referred to as CDMA-OFDM, or similar. A typical CDMA-OFDM base-station system is shown in figure 3. Other variants are possible.

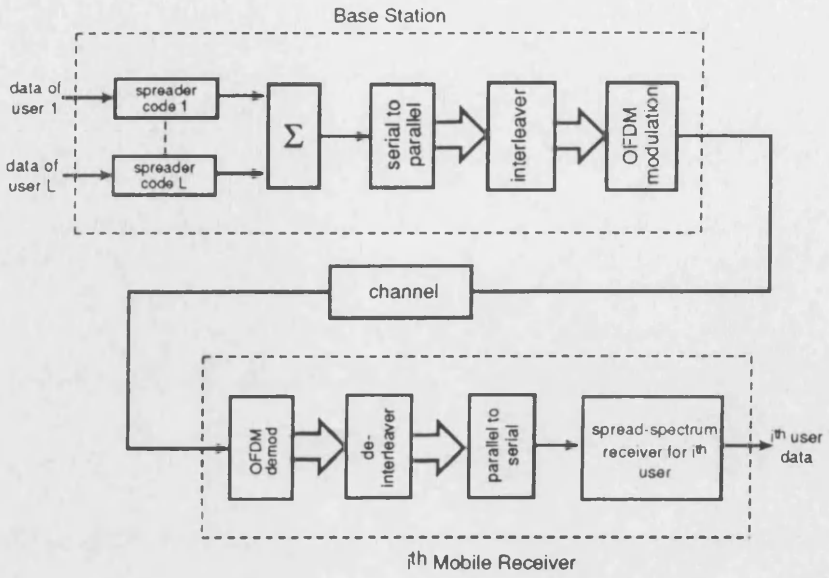

Figure 3 Simplified structure of the down-link of a CDMA-OFDM multiple access scheme

Here, each user's data is spread, in the usual way and the data modulated chips from each user are arithmetically summed (chip synchronously). The resulting non binary values are serial to parallel converted and interleaved before being transformed by the IDFT and modulated onto the carrier in the usual way. In the receiver, OFDM demodulation is accomplished by the DFT. The output of the parallel to serial converter is represented as a composite multi-user spread-spectrum signal from which any particular user can be demodulated in the usual way using a correlator, digital matched filter or maximum likelihood detector. In the above, steps to add and remove time guard bands, or the use of a RAKE receiver to reduce ISI and Doppler is assumed. As with other orthogonal systems, synchronisation of the symbols is essential and implicit on both the down-link (which is straightforward to arrange) and also on the up-link (which is not so straightforward!).

Multicarrier DS-CDMA In the other method, the total available frequency spectrum of the CDMA system is divided into M equi-width frequency bands, where M is the number of carriers, typically much less than the process gain and each frequency band is used to transmit a 'narrowband' DS-CDMA signal[20]. The response to frequency selective fading is similar in both cases, but it is claimed that this method is easier to implement. Figure 4 shows a typical implementation of a multi-carrier DS-CDMA system[20].

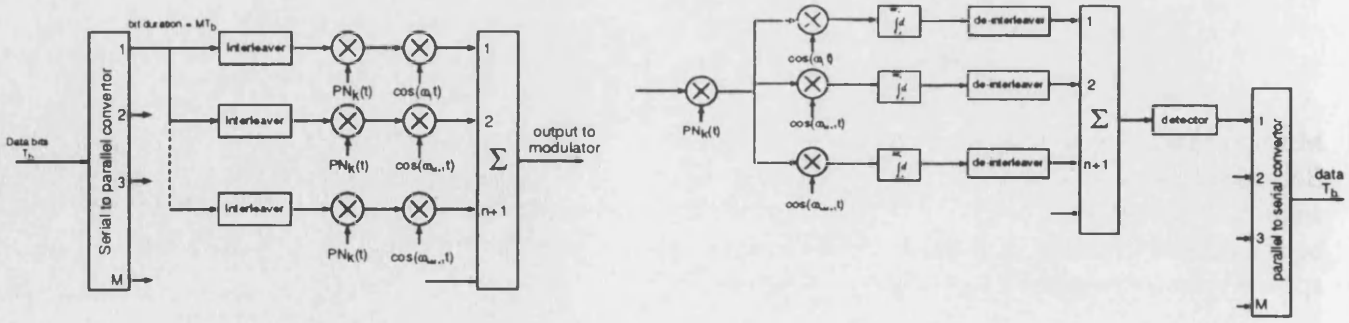

(a) Transmitter (b) Receiver

Figure 4 Simplified schematic of a multicarrier DS-CDMA system

In this system, the data is split into M parallel streams. Each of these streams is split S ways and spread by the same PN sequence and modulated onto S orthogonal carriers, i.e. the same data bit is transmitted on S carriers. The total number of carriers in this arrangement is thus M x S.

LROCC-OFDM

A new method of providing multi-access operation of an OFDM system which promises to have higher ultimate capacity than the CDMA-OFDM method is to use LROCC-OFDM. The technique replaces the conventional pseudo-noise spreading sequences of the CDMA part of the system by low-rate orthogonal convolutional codes (LROCC)[21]. The LROCC system combines the spreading function with powerful coding by the use of a low rate convolutiona code of rate 1/N, which is used to spread the data by N times. By using orthogonal codes based on the Hadamard matrix[22,23], large numbers of convolutional codes can be obtained, and isolation of users in a multi-access CDMA scenario is obtained, particularly if additional non-spreading PN randomisation is used[24]. The LROCC-OFDM transmitter, shown in figure 5, is similar to the CDMA-OFDM system of figure 2. A feature of the system is that since the convolutional codes are based on radix 2, rather than 2^n - 1 of the PN spreading codes, the DFT can be performed using the FFT .

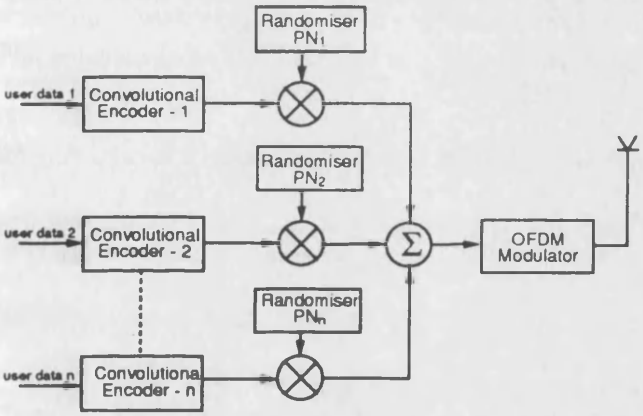

Figure 5a LROCC-OFDM Transmitter

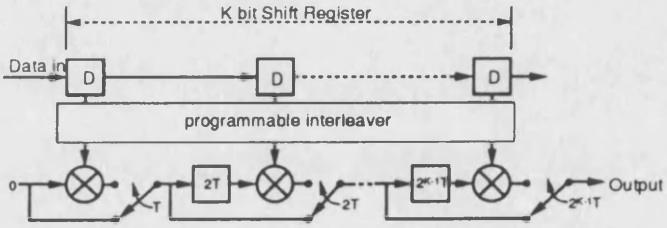

Figure 5b LROCC Encoder

In the receiver, the normal CDMA demodulator is replaced by modified form of Viterbi soft decision decoder which provide a maximum likelihood decision on the decoding of the i^{th} user[24]. Clearly, the performance of the LROCC-OFDM system is very much dependent upon the performance of the basic LROCC-CDMA system. Figure 6 provides a comparison of a conventional DS CDMA system and the LROCC system for the case of a system in which other-user noise is dominant and there are no channel imperfections.

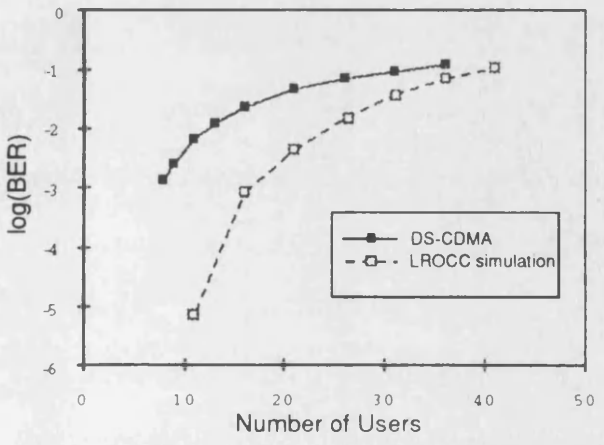

Figure 6a Comparison of DS-CDMA and LROCC system performance

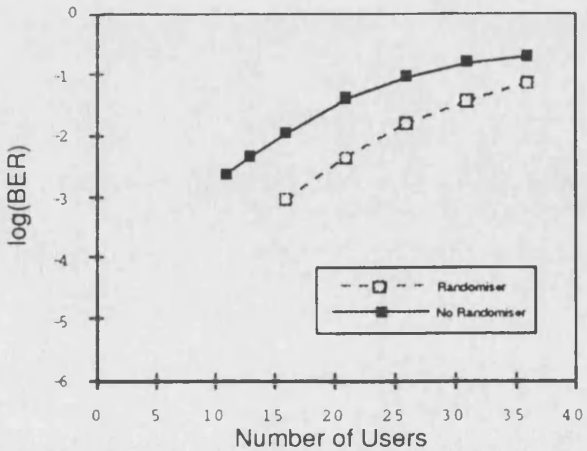

Figure 6b Effect of the randomiser on LROCC performance

In figure 6a the DS-CDMA system has a spreading sequence of 63 chips whilst the LROCC system uses a 64 chip Hadamard sequence. Channel imperfections are expected to be handled by the OFDM part of the system in a similar way to DS-CDMA-OFDM[20]. Clearly, LROCC outperforms the comparable DS-CDMA system, and so it is expected that the LROCC-OFDM system will provide similar performance improvements over CDMA-OFDM.

Acknowledgements
The authors are pleased to acknowledge the support of EPSRC for the provision of Research Contract No. GR/K27902 under which this work was carried out.

References

1. Gilhausen K S, Jacobs I M, Padovani R and Weaver, L A: "Increased capacity using CDMA for mobile satellite communications", IEEE J. Sel. Areas in Comms., Vol. SAC-8, pp 503-514, 1990.
2. Pickholtz, R L, Milstein, L B and Schilling, D L: "Spread-spectrum for mobile communications", IEEE Trans. Veh. Tech., Vol. VT-40, pp313-321, 1991.
3. Omura, J K, and Yang, P T: "Spread-spectrum S-CDMA for personal communications services", Proc. IEEE Milcom'92, pp 269-273, 1992.
4. Pursley, M B: "Effects of specular multipath fading on spread-spectrum communications ", New concepts in multi-user communications, J Skwirzynski, ed. NATO Adv. Study Inst., Sijthoff and Noordhoff, pp 481-505, 1981.
5. Turin, G L: "Introduction to spread-spectrum antimultipath techniques and their application to urban digital radio", Proc. IEEE, Vol. 68, pp 328-353, 1980.
6. Proakis, J G: "Digital Communications", McGraw Hill, New York, 1989.
7. For example: Alard, M and Lassalle, R: "Principles of modulation and channel coding for digital broadcasting for mobile receivers", EBU Review, pp47-69, August 1987.
8. Frazel, K, Kaiser, S, Robertson, P and Ruf, M J:" A concept of a reconfigurable digital-TV/HDTV transmission scheme with flexible channel coding & modulation for terestrial broadcasting", Proc Int. Workshop on HDTV, October 1994.
9. for example: Webb, W T and Hanzo, L:"Modern Quadrature Amplitude Modulation", Pentech Press/IEEE Press, 1994.
10. Zou, W Y and Wu, Y: "COFDM: an overview", IEEE Trans. on Broadcasting, Vol. 41, 1-8, 1995.
11. Sari, H, Karam, G and JeanClaude, I: "Channel equalisation and carrier synchronization in OFDM systems", Tirrienia Int Workshop on Digital Communications, Italy, 1993.
12. Sari, H, Karam, G and Jeanclaude, I: "An analysis of orthogonal frequency division multiplexing for mobile radio applications", IEEE Proc. 44th Vehicular Technology Conf., pp1635-1639, 1994.
13. Casas, E F and Leung, C: "OFDM for data communication over mobile radio FM channels - part 1", IEEE Trans. on Comms, Vol. 39, pp. 783-793, 1991.
14. Vahlin, A and Holte, N: "Use of a guard interval in OFDM on multipath channels", Electronics Letters, Vol. 30, pp. 2015-2016, 1994
15. Fettweis, G, Bahai, A S and Anvari, K: "On multicarrier code division multiple access (MC-CDMA) modem design", IEEE Proc. 44th Vehicular Technology Conf, pp 1670 - 1674, 1994.
16. Cimini, L C: "Analysis and simulation of a digital mobile channel using orthogonal frequency division multiplexing", IEEE Trans. on Comms., Vol. COM-33, pp665-675, 1985.
17. Fazel, K and Papke, L: On the performance of convolutionally-coded CDMA/OFDM for mobile communication system", Proc. PIMRC'93, Yokohama, D3.2.1-5, 1993.
18. Kaiser, S: "OFDM-CDMA vs DS-CDMA: preformance evaluation in fading channels", IEEE Proc., ICC'95, pp 1722-1726, 1995.
19. Sourour, E A and Nakagawa, M: "Performance of orthogonal multicarrier CDMA in a multipath fading channel", IEEE Trans. on Comms., Vol COM-44, pp 356-367, 1996.
20. Kondo, S and Milstein, LB: "Performance of multicarrier DS-CDMA Systems", IEEE Trans on Comms., Vol. COM-44, pp 238-246, 1996
21. Viterbi, A J: "Very low-rate convolutional codes for maximum theoretical performance of spread-spectrum multiple-access channels", IEEE Journal on SAC, Vol. 8, No.4, 1990
22. Monogioudis, P, Edmonds, R, Tafazolli, R and Evans, B G: "*Multirate 3rd generation CDMA systems*", IEEE International Conference on Communications, ICC'93, pp. 151-155, 1993
23. Ormondroyd, R F and Maxey, J J: "A high performance CDMA cellular radio system based on orthogonal low-rate convolutional coding", IEE International Conference on Radio Receivers and Associated Systems, Conference Proc. Vol. 414, pp. 17-21, 1995
24. Ormondroyd, R F and Maxey, J J: "Performance of low-rate orthogonal convolutional codes in DS-CDMA applications", To be published in IEEE Trans. on Vehicular Technology

VTC'97, Phoenix, Arizona, May 1997

NON-COHERENT DIFFERENTIAL ENCODED MULTI-CARRIER SS MODULATION SCHEMES USING LOW-RATE ORTHOGONAL CONVOLUTIONAL CODING IN FREQUENCY SELECTIVE RAYLEIGH FADING

J. J. Maxey and R. F. Ormondroyd

School of Electronic and Electrical Engineering
The University of Bath
Claverton Down, Bath, BA2 7AY, UK
e-mail: eepjjm@bath.ac.uk eesrfo@bath.ac.uk

BSTRACT - This paper investigates the performance enefits of applying convolutional coding and interleaving to non-coherent DS-CDMA system using OFDM to combat the it-error rate degradation suffered in a frequency selective ayleigh faded channel. The channel model is typical of the obile radio environment with Doppler effects and frequency elective Rayleigh fading. The paper also compares the erformance of the coded OFDM-CDMA system with a onventional single-carrier DS-CDMA system which uses a AKE receiver to combat fading. Finally, a comparison is ade between the performance of ordinary convolutional odes and low-rate orthogonal convolutional codes (LROCC). is found that the LROCC-OFDM system outperforms both e OFDM-CDMA and DS-CDMA RAKE systems quite ubstantially when interleaving is used.

I. INTRODUCTION

rthogonal frequency division multiplexing (OFDM) is urrently receiving considerable attention because it has been ound to give better performance over single carrier systems in e frequency selective fading environment of the mobile hannel. A reason for this is that in OFDM systems, both hannel equalisation and detector decisions are effectively erformed in the frequency domain, whereas in single-carrier ystems the receiver decisions and channel equalisation are ade in the time domain. The channel equalisation problem or OFDM designs is not eliminated, but simply shifted into e frequency domain. This allows relatively simple one-tap qualisation structures to be employed at the output of the FFT lgorithm in the receiver and, by using more sophisticated qualiser structures, the OFDM system actually enables the oppler spread of the channel to be equalised.

ecently, it has been proposed that CDMA multiplexing echniques should utilise OFDM modulation [1-3] to give ultiple access systems similar levels of resilience in ultipath fading to that provided for broadcast systems such s DAB and terrestrial HDTV. OFDM modulation uses an ntirely different approach than single carrier systems to olving the inter-symbol interference problem at high data ates which is based on sending many low-rate data channels in parallel to fight the frequency selectivity of the channel and to combat the distortions due to multipath propagation. To improve the detection of the wanted signals, either a highly efficient coding strategy or a good equaliser can be employed in the receiver. Further improvements in performance are obtained if a time guard band (or cyclic extension) [4,5] is used to maintain orthogonality of the sub-carriers.

Single carrier direct-sequence code division multiple-access (DS-CDMA) techniques provide a number of advantages over TDMA and FDMA methodologies in digital cellular radio applications, but are capacity limited by both "other-user" noise and the effects of severe multipath fading. The RAKE receiver attempts to overcome the multipath problem, but further resilience can be achieved by the use of a coding and interleaving strategy on the data of the DS-CDMA system. Conventional high rate convolutional codes, such as rate 1/2, rate 1/3 etc., can provide the necessary coding gain to give improved performance over Rayleigh faded channels, but strong interleaving between the data is necessary to make the effects of fading independent from one sub-channel to another. Multi-carrier modulation techniques give greater independence between the fading on each sub-channel and it is therefore possible to enhance the performance of the system without requiring too much coding gain. Therefore, the depth of interleaving does not need be as high as for conventional single-carrier DS-CDMA designs.

In this paper, a novel implementation of a multiple access OFDM system is presented which uses low-rate orthogonal convolutional codes (LROCC). This has been shown to offer worthwhile performance benefits [6-9]. In this approach, the conventional spreading process of direct sequence CDMA using high-speed PN sequence multiplication is now replaced by very low-rate convolutional codes of equal spreading ratio. This achieves not only diversity but also coding gain, without the rate penalty. This has the added advantage of providing a full coding gain at no cost of spectrum efficiency, and enables the interleaving depth of the modem to be reduced considerably.

II. TRANSMITTER AND RECEIVER STRUCTURES

In the methods proposed to date, each user's data is spread by a unique PN sequence, in the usual way to DS-CDMA. The chips are then mapped into complex valued symbols prior to being serial/parallel converted into a vector of N complex values. In the base station, each user's N value vector is summed at this point. The resulting vector is then orthogonally modulated onto the carrier, usually using the IFFT method [10,11]. Interleaving of the chips can also be used with this system.

The LROCC coding method effectively expands the data by a factor 2^K, where K is the constraint length of the convolutional encoder, before being modulated on $N=2^K$ orthogonal parallel carriers. With perfect synchronisation and no multipath, this enables several simultaneous users in the cellular structure to be isolated from one another in the time domain and through the use of orthogonally spaced carriers provides isolated data streams in the frequency domain. With OFDM, it is possible to separate each low bit-rate modulated carrier by as little as $1/2T_S$, where T_S is the period of the symbols, and still have no inter-symbol interference. Figs. 1 and 2 show a more detailed outline of the proposed transmitter and receiver structure.

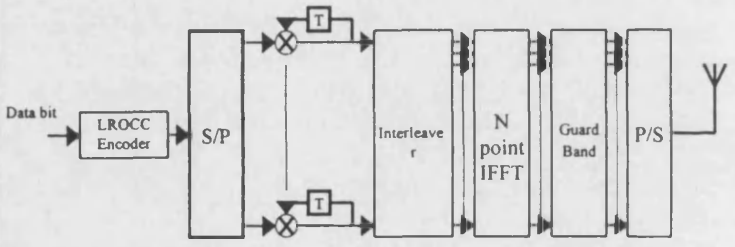

Fig. 1 Transmitter design using LROCC coding, differential encoding, interleaving and OFDM modulation

As the presence of multipath fading introduces amplitude and phase distortion on the signal, it is difficult to track the phase information without the use of a pilot tone. Therefore, a non-coherent modulation technique such as differential PSK is introduced, where the phase information in the demodulator is derived from the previous symbol. As long as the phase distortion factor due to multipath is nearly constant or at least slowly varying over the symbol duration T_S, a square law detector may be used for non-coherent demodulation.

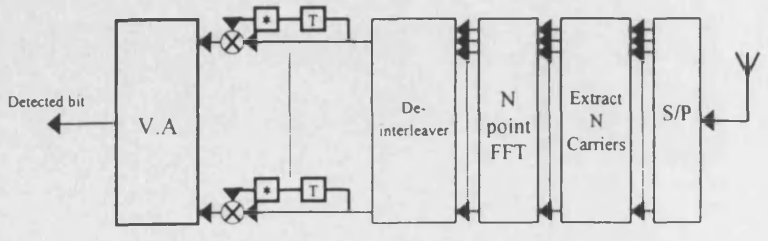

Fig. 2 Receiver design employing DPSK demodulation on each FFT output

III. THEORETICAL ANALYSIS

The theoretical performance of LROC codes in Rayleig faded channels has been analysed [12,13]. As this proces involves a maximum likelihood detection scheme, such as th Viterbi algorithm, it is possible to use conventional theoretic performance evaluation techniques for high-rate convolution codes to obtain an estimate for the upper-bound in Rayleig faded channels.

Each data bit of duration T_b is first encoded in the LROC coder where it is replaced with a corresponding chip sequen of length N, each chip having a duration T_c. The rate of th code is therefore $R=1/N$, where $N=2^K$ and K is the constrai length of the convolutional encoder. The chip sequence $y(n)$ then converted into a parallel block of N chips an differentially encoded on each arm of the modulator. Th input to the interleaver is then given as:

$$y(n) = y(n) \cdot y(n-N) \qquad n>N \tag{1}$$

Note that the delay term N represents the delay introduce through the serial-to-parallel conversion in the transmitt block.

This sequence is then interleaved and after the IFFT is give as:

$$x(k) = \frac{1}{N}\sum_{n=0}^{N-1} y(n)e^{j2\pi nk/N} \qquad k=0,1, \ldots N-1 \tag{2}$$
$$= \frac{1}{N}\sum_{n=0}^{N-1} y(n)e^{j2\pi f_n t_k}$$

where Δt is an arbitrarily chosen interval [11] and,

$$f_n = \frac{n}{N\Delta t} \text{ and } t_k = k\Delta t \tag{3}$$

This parallel sequence, including a time gu[illegible] band, is the converted into serial form and transmitted over the channel. I is assumed that the guard band is sufficiently larger than th channel impulse response. The multipath nature of the fadin channel will induce a phase and amplitude distortion on th original sequence and add AWGN. The DFT of the channe impulse response can be given as a complex channel fadin sequence:

$$h(n) = p(n)e^{j\phi(n)} \tag{4}$$

where $p(n)$ is the Rayleigh distributed attenuation coefficien and $\phi(n)$ represents the uniformly distributed phase distortion. The received signal will contain the frequency selective fade wanted signal and an additional AWGN term. The N chips pe block are extracted after the time guard band removal an then fed into the FFT algorithm, giving:

$$y(n) = \frac{1}{N}\sum_{k=0}^{N-1} H(k)Y(k)e^{j2\pi f_n t_k} + \mu(n) \qquad (5)$$
$$= h(n)y(n) + \mu(n)$$

where $\mu(n)$ is the complex Gaussian distributed noise term at the output of the FFT.

The sequence $g'(n)$ at the output of the DPSK demodulator is given as:

$$g'(n) = g(n) \cdot g^*(n-1)$$
$$= [h(n)y(n)+\mu(n)] \cdot [h^*(n-1)y^*(n-1)+)+\mu^*(n-1)] \qquad (6)$$

but,

$$g(n) = p(n)e^{j\phi(n)}$$
$$g^*(n-1) = p^*(n-1)e^{-j\phi(n-1)} \qquad (7)$$

Therefore,

$$g'(n) = p(n)e^{j\phi(n)}\, p^*(n-1)e^{-j\phi(n-1)}y(n)y^*(n-1)+$$
$$\mu(n)p^*(n-1)e^{-j\phi(n)}y^*(n-1)+$$
$$\mu^*(n-1)p(n)e^{j\phi(n)}y(n)+$$
$$\mu(n)\mu^*(n-1) \qquad (8)$$

For the ideal noiseless case $\mu(n)=\mu(n-1)=0$ and,

$$g'(n) = p(n)p^*(n-1)e^{j[\phi(n)-\phi(n-1)]}y(n)y^*(n-1)$$
$$= h(n)h^*(n-1)y(n)y^*(n-1) \qquad (9)$$

where $\phi(n)-\phi(n-1)$ is the phase difference. From (9), the mean value of $g'(n)$ is independent of the carrier phase and the output sequence can be detected correctly. Of course, for non-zero values of $\mu(n)$ the reliability of detection becomes worse as the background noise level increases.

The error detection performance of convolutional codes is evaluated by considering the different paths through the particular trellis structure of the code. The all-zero path is considered as the transmitted wanted path, and all other non-zero paths merging back to the wanted path are considered as the error paths. Therefore, to obtain an error bound on the performance of the LROCC structure, the generating transfer function of the convolutional code and its derivative will lead to an estimate of the upper bound on the error probability of the code The generating transfer function of the LROCC encoder is given by [12].:

$$T(W,B) = \frac{BW^K(1-W)}{1-W\left[1+B\left(1-W^{K-1}\right)\right]} \qquad (10)$$

where B denotes a transition in the trellis diagram caused by a data input of '1', W is a weight measurement for each branch metric and relates the average energy-per-bit to the noise density ratio per distance weight. For the AWGN channel:

$$W = Z^{\frac{1}{2r}} \qquad (11)$$

where r is the code rate and $Z = \exp(-E_b/N_0)$. For other channels, such as L-path Rayleigh fading, W follows a different statistic, and is given by [12]:

$$W = \left(\frac{1+U}{(1+(U/2))^2}\right)^L \qquad (12)$$

where L is the number of independently Rayleigh faded paths and U is the average signal-to-noise ratio per path.

In the receiver, to determine the upper bound for the bit-error rate of the LROCC code for any general class of channel, equation (10) must be differentiated with respect to B, and B then set to unity:

$$\left.\frac{dT(W,B)}{dB}\right|_{B=1} = \frac{W^K(1-W)^2}{\left(1-2W+W^K\right)^2} \qquad (13)$$

Equation (13) enables the BER performance of LROCC designs to be obtained in AWGN and L-path Rayleigh faded channels with independent fading on each path, and this is shown in Fig. 3.

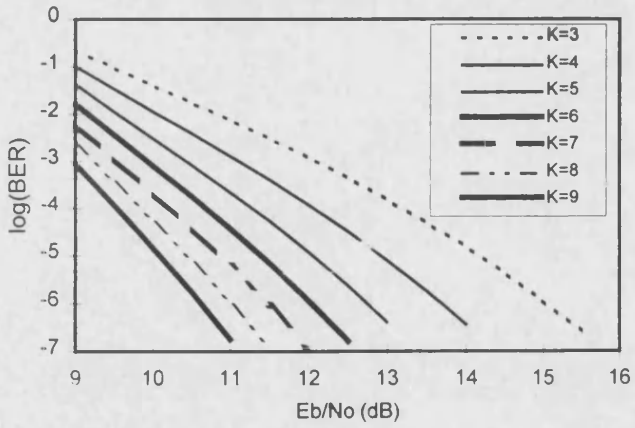

Fig. 3 LROCC performance in L-path Rayleigh fading

IV. SIMULATION RESULTS

The system design shown in Figs. 1 and 2 was simulated over a frequency selective Rayleigh faded channel using the LROC coding structure with and without an interleaver. The interleaver was chosen to be large enough to make successive block transmissions independent in the prevailing fading environment, therefore enhancing the decoder performance in

high interference and fading levels. In practice, interleaving of depth 160 symbols was found to provide independent fading for each symbol and for the OFDM design it effectively provides interleaving in the frequency domain.

The total bandwidth expansion (spreading factor) was set to 32 for all simulations (including code rate and PN sequence length, where each PN sequence was increased in length by a single chip inserted on the end of the sequence). The Rayleigh fading component on each multipath signal in the frequency selective channel model was statistically independent for each path of the channel with a total mean signal power of unity. The number of distinct Rayleigh faded paths, L, at the receiver was set to 4 and 7 paths with a Doppler frequency of f_d=300Hz, corresponding to a vehicle speed of 203km/h at a carrier frequency of 1.6GHz. Fig. 4 shows the performance for the uncoded and LROCC coded OFDM design. Increasing the number of multipath components in the channel from L=4 to L=7 can be seen to have little effect on the BER performance in a frequency selective Rayleigh faded channel, as the effective order of diversity for the OFDM design is very high (≈32). Since the non-coherent differential equalisation and demodulation procedure is effectively carried out in the frequency domain, the number of paths that can be resolved in the receiver is of a relatively high order, compared with a conventional DS-CDMA RAKE receiver, as seen later.

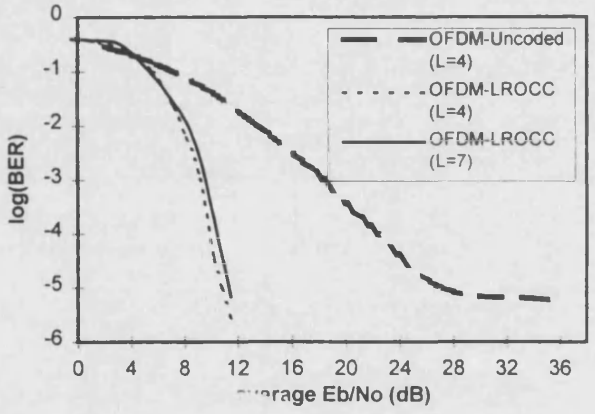

Fig. 4 Uncoded OFDM using Gold codes v. LROCC-OFDM in L-path frequency selective Rayleigh fading

Next, a comparison is drawn between conventional single carrier DS-CDMA designs using convolutional coding and RAKE receivers. The DS-CDMA RAKE design uses conventional convolutional coding of rate R=1/2, K=5 to encode the data bits together with Gold codes of length 15 to provide additional spreading in the transmitter. It can be seen that the OFDM-LROCC implementation shows considerable performance improvements at high signal-to-noise ratios (Figs. 5 and 6). Note that an increase in the number of multipath components in the channel has a much more dramatic effect on the BER performance of a DS-CDMA RAKE receiver than for OFDM coded designs. This is due to the fact that the non-coherent equalisation for the RAKE receiver is now performed in the time-domain, where t effects of Doppler and the high number of multipa components are much more difficult to resolve.

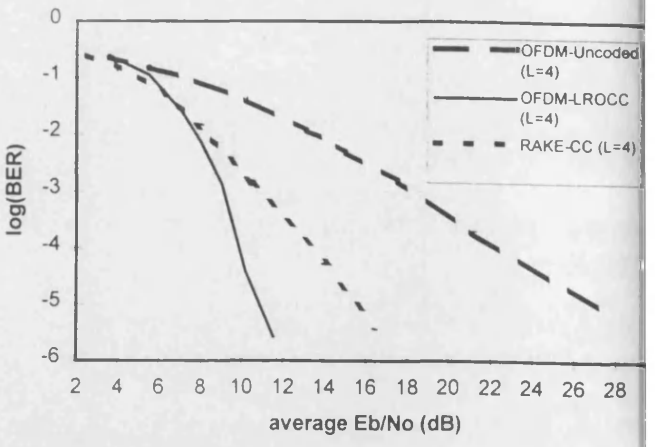

Fig. 5 Uncoded and coded OFDM compared with conventional coded RAKE design in 4-path fading

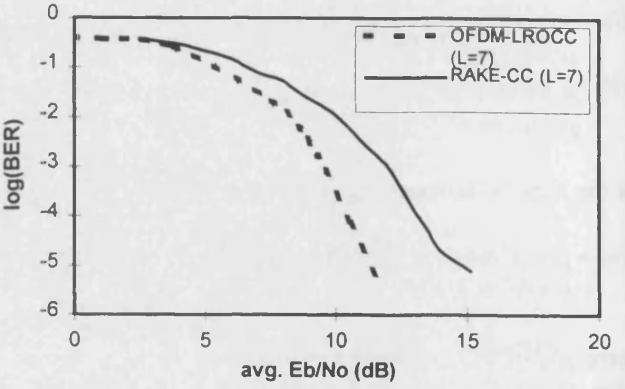

Fig. 6 LROCC-OFDM v. single carrier DS-CDMA RAK receiver employing rate R=1/2 convolutional coding

The multi-carrier OFDM system was also simulated over frequency selective Rayleigh faded channel with Doppl offsets of 50Hz, 100Hz, 200Hz, 300Hz. At a carrier frequenc of 1.6GHz this would correspond to mobile speeds of 34km/ 68km/h, 135km/h and 203km/h, respectively. The BE performance improvement found for a 6-path channel mod simulations (shown in Fig. 7) for higher values of Doppler as expected, since the convolutional coding strategy suffe more at low speeds than high vehicle speeds. This is due t the fact that the errors on the channel appear more bursty high vehicle speeds and enable the decoder to operate mo efficiently. At low vehicle speeds, the fading effects are mo clustered and hence strong interleaving would be require between the encoder and decoder.

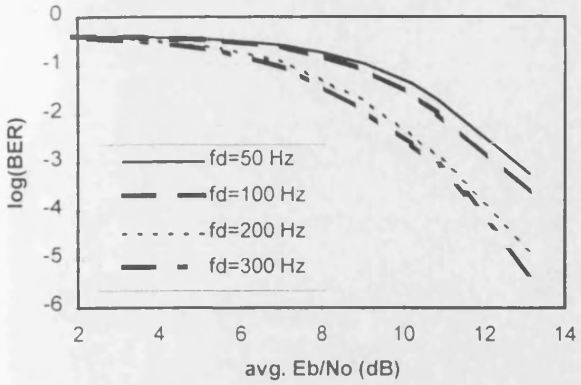

Fig. 7 BER performance of LROCC-OFDM design in 6-path frequency selective Rayleigh fading for different Doppler, f_d

V. CONCLUSIONS

he benefits of employing coding and interleaving in a non-oherent uplink channel for mobile radio, suffering from ultipath and frequency selective Rayleigh fading with oppler shift have been compared for OFDM and conven-onal single-carrier DS-CDMA designs. The importance of pplying adequate interleaving in frequency selective ayleigh faded channels has been shown. Considerable erformance improvements have been found with an LROCC rategy when applied to multi-carrier OFDM modulation with dequate interleaving to make the multipath fading effects ndependent on each channel. The LROCC-OFDM technique as been shown to provide considerable resilience to increases the number of multipaths representing the channel. Also, rough the use of non-coherent differential demodulation on ach output of the FFT in the OFDM receiver it is possible to esolve some of the frequency selective fading components in ie frequency domain.

VI. ACKNOWLEDGEMENTS

he authors are pleased to acknowledge EPSRC for their nancial support of the work reported through Contract No. iR/K27902 and also for their provision of a research udentship.

VII. REFERENCES

1] Kaiser, S; "OFDM-CDMA versus DS-CDMA: erformance Evaluation for Fading Channels"; IEEE nternational Conference on Communications (ICC'95), pp. 722-1726, June 1995.

2] Rowitch, D N and Milstein, L B; "Convolutional Coding or Direct Sequence Multicarrier CDMA"; IEEE Milcom'95, an Diego, 5-8th Nov, Vol. 1, pp.55-59, 1995.

[3] Sourour, E A and Nakagawa, M; "Performance of Orthogonal Multicarrier CDMA in a Multipath Fading Channel"; IEEE Transactions on Communications, Vol. 44, No.3, pp. 356-367, March 1996.

[4] Cimini, L J; "Analysis and Simulation of a Digital Mobile Channel Using Orthogonal Frequency Division Multiplexing"; IEEE Transactions on Communications, COM-33, No.7, pp. 665-675, July 1985.

[5] Vahlin, A and Holte, N; "Use of guard intervals in OFDM on multipath channels"; Electronics Letters, Vol.30, No.24, pp.2015-2016, 24th Nov. 1994.

[6] Maxey, J J and Ormondroyd, R F; "Optimisation of orthogonal low-rate convolutional codes in a DS-CDMA system"; IEEE/URSI Conference Proceedings of ISSSE'95, Vol. 95TH8047, pp. 493-496, 1995.

[7] Maxey, J J, Ormondroyd, R F and Edwards, K; "Evaluation of a fixed wireless access DS-CDMA system employing low-rate orthogonal convolutional codes"; 5th European Conference on Fixed Radio Systems and Networks, Bologna, Italy, 14-17th May, pp. 277-282, 1996.

[8] Ormondroyd, R F and Maxey, J J; "A high performance CDMA cellular radio system based on orthogonal low-rate convolutional coding"; IEE International Conference on Radio Receivers and Associated Systems, Conference Proc. Vol.414, pp.17-21, 1995.

[9] Viterbi, A J; "Very low-rate convolutional codes for maximum theoretical performance of spread-spectrum multiple-access channels"; IEEE Journal on SAC, Vol.8, No.4, 1990.

[10] Cimini, L J; "Analysis and Simulation of a Digital Mobile Channel Using Orthogonal Frequency Division Multiplexing"; IEEE Transactions on Communications, COM-33, No.7, pp. 665-675, July 1985.

[11] Weinstein, S B and Ebert, P M; "Data Transmission by Frequency-Division Multiplexing Using the Discrete Fourier Transform"; IEEE Transactions on Communication Technology, COM-19, No.5, pp. 628-635, Oct 1971.

[12] Viterbi, A J; "CDMA - Principles of Spread Spectrum Communication"; Addison-Wesley Wireless Communications Series, 1995.

[13] Maxey, J J and Ormondroyd, R F; "Low-Rate Orthogonal Convolutional Coded DS-CDMA using Non-Coherent Multi-Carrier Modulation over the AWGN and Rayleigh Faded Channel"; IEEE Conference Proceedings of ISSSTA'96, Vol. 2, pp.575-579, 1996.

IEEE 1st International Workshop on Multi-Carrier CDMA,
Oberpfaffenhofen, Germany, May 1997

MULTI-CARRIER CDMA USING CONVOLUTIONAL CODING AND INTERFERENCE CANCELLATION OVER FADING CHANNELS

J J Maxey and R F Ormondroyd

School of Electrical Engineering, The University of Bath, Bath, BA2 7AY, U.K
E-mail: eepjjm@bath.ac.uk and eesrfo@bath.ac.uk

ABSTRACT

OFDM DS-CDMA systems using convolutional coding techniques and multi-access interference (MAI) cancellation can be implemented effectively on the uplink of a mobile radio channel as long as the interference statistics are known at the receiver. The choice of the right equalisation technique is vital to maximise the SNR at the input to the detector. The use of maximum ratio combining (MRC) after MAI cancellation has been found to give good results. In this paper we compare the performance of MAI cancellation using zero-forcing equalisers and MRC with the performance of MAI cancellation using controlled equalisation paired with MRC. It is found that there are considerable performance improvements when controlled equalisation techniques are used for the initial estimate of the interfering user's data.

INTRODUCTION

Multi-Carrier OFDM techniques are increasingly gaining a wide interest in the field of mobile and fixed wireless communication systems using multiple access techniques such as DS-CDMA spread spectrum. Recently, a few papers have proposed the use of OFDM DS-CDMA for the uplink [1] in frequency selective faded channels with high interference. OFDM DS-CDMA can provide resilience to frequency selective faded channels by transforming high bit-rate data to multiple low-rate data streams, multiplexed over a wider bandwidth than the original data. This has the advantage of enabling the received data streams to appear as flat faded

data streams on each sub-carrier, and this enables the equaliser in the receiver to demodulate the data more effectively. A number of techniques have been proposed to combat these fading effects:

- Frequency- or time domain interleaving
- Convolutional coding architectures
- Guard-time interval insertion
- Equalisation structures
- MAI cancellation techniques (successive or parallel)

If the time-delay spread on the channel is large compared to the chip period it becomes necessary to make use of guard-intervals to reduce the effects of inter-symbol interference (ISI). No ISI will occur as long as the guard-interval length is greater than the maximum delay spread of the channel impulse response. Using DS-CDMA to spread the original bandwidth of the data enables the delay spread of the channel to be resolved more efficiently. Therefore DS-CDMA techniques can provide a robust multiple access scheme when many other users are transmitting over the same bandwidth in a faded channel.

Although the time guard-band limits the effect of ISI, there is still a need for channel equalisation. OFDM allows equalisation to be performed in the frequency domain at the output of the receiver FFT and this allows a simple one tap equalisation structure to be used, with its channel knowledge derived from the FFT of the channel impulse response. This can be measured using pilot channels or midambles inserted between the data. A number of techniques using equalisers of different complexity have been investigated [e.g. 2,3]. When the receiver has no knowledge of either the received SNR or the number of users using the channel, a relatively simple and effective equaliser that attempts to restore the orthogonality of the sub-channels is *controlled equalisation.* For more sophisticated receiver structures, the MMSE algorithm can provide considerable performance improvements. Sub-optimal MMSE algorithms can be employed through fixed estimates of the number of users present in the channel. This presents about 1dB loss in performance for the downlink channel.

For reception of the wanted data in other-user noise, maximum likelihood detection schemes give optimum performance. However, this can only be used if the spreading sequences of all users are relatively short since the complexity increases exponentially to the sequence length. The use of convolutional coding on the data provides BER performance benefits in memoryless and non-memoryless channels, yielding a coding gain larger than the bandwidth penalty. In Rayleigh faded channels, the coding gain can be further enhanced through strong interleaving in the time or frequency domain. For multi-user systems, the interference is dominated by "other-user" noise and this becomes the limiting factor on the performance. A variety of interference cancellation schemes can be used to remove this interference, as long as the spreading codes of all active users are known at the receiver.

This paper presents a comparison of different equalisation strategies used in conjunction with MAI cancellation. In particular, we consider zero-forcing equalisation, controlled equalisation and maximum ratio combing (MRC).

UPLINK DESIGN

There have been a number of papers reporting efficient uplink strategies for a cellular mobile radio system. The uplink design investigated here is based on a service provision of 32 kb/s for each user, using OFDM modulation and low-rate orthogonal convolutional (LROC) coding to provide the necessary spreading and coding. It is assumed that a small overhead is needed to provide the basestation with an estimate of the channel transfer function of each user. This allows the basestation to equalise each user's data more effectively. A diagram of the proposed transmitter and receiver is shown in figures 1 and 2. Here it assumed that the wanted user is user 1, and the interference effects of users 2 to L (where L is the total number of simultaneous users) are partially removed through interference cancellation.

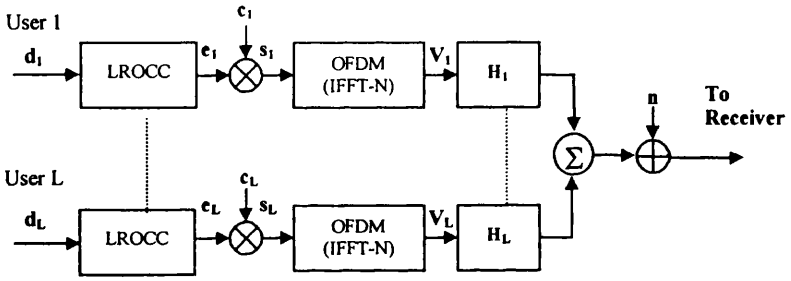

Figure 1. Simulation model of transmitter design for all uplink users and the channel model

Successive interference cancellation schemes are popular for designs that use no power control and perform best when all users in the system have geometrically distributed received powers. Parallel interference cancellation schemes, on the other hand, perform better when all users are assumed to be perfectly power controlled.

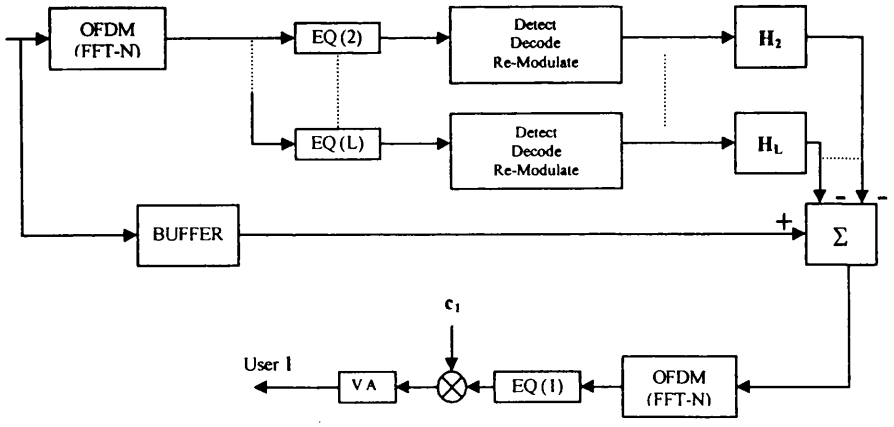

Figure 2. Basestation receiver structure to detect user 1

In the analysis we ignore the time index and consider the processing of a single block of data bits from user i. Each user transmits a data sequence d_i, where $i = 1,2 \ldots L$. Each data bit is of duration T_b seconds and is consequently coded in a convolutional encoder of rate $R=K/M$. The input sequence d_i of K data bits produces an output sequence e_i of length $n = [1 \ldots M]$, where each subsequent output symbol $e_i(n)$ is of duration $T_c=RT_b$. For LROCC codes the code rate is given as $R=1/M$, where M defines the spreading ratio of the user specific output sequence and is given as $M=2^K$. This equates to the bandwidth expansion factor. The encoded sequence consisting of orthogonal Walsh-Hadamard codes is further multiplied by a randomising sequence of equal length M, given as $c_i = [c_i^{(1)}, c_i^{(2)} \ldots c_i^{(M)}]^T$, where $[.]^T$ denotes the transposition of the matrix. Note that the randomising sequence c_i does not provide further spreading. The data is modulated as a block, hence for each block the input to the interleaver within the OFDM modulator block is given as:

$$s_i^{(n)} = e_i^{(n)} c_i^{(n)} \tag{1}$$

After OFDM modulation and interleaving, the output sequence may be represented by the complex vector sequence $V_i = [v_i^{(1)}, v_i^{(2)} \ldots v_i^{(M+\Delta)}]^T$ where Δ is the guard interval length. The guard interval forms a cyclic extension to the block sequence $[1 \ldots M]$ and reduces the effects of ISI due to the multipath spread in the fading channel. This can only be done effectively if the guard interval length is greater than the multipath spread length of the channel.

The output vector to be transmitted over the channel is represented by complex coefficients at the output of the IFFT in the modulator. Since each user communicating to the basestation experiences different independent fading statistics, the channel coefficients are different for each user. The channel may be described by a complex matrix $\mathbf{H}_i$ (in the frequency domain) of size $M \times M$ for each user, affecting the subcarriers $\mathbf{V}_i$ assigned to the transmitted sequence on the transmitter for user i. Since a perfect guard-interval length is assumed, the channel matrix $\mathbf{H}_i$ is a diagonal matrix with diagonal components $h_{n,n}$. The vector N represents the complex AWGN in the channel. Therefore, the received sequence at the output of the OFDM demodulator, assuming perfect interleaving and guard-band insertion, is given by:

$$R = \sum_{i}^{N_u} e_i \cdot c_i \cdot H_i + N \tag{2}$$

For this analysis we assume that the channel estimation is perfect. Using the complex channel estimates for each user we equalise the demodulated sequence for each user separately and obtain an estimate of the interference from other users. This is achieved through de-randomising the equalised signal by the user specific code c_i and performing maximum likelihood detection using the Viterbi algorithm. The estimated data sequences of all interfering users are re-modulated and re-encoded with the appropriate channel estimates and subsequently subtracted from the original

received sequence. Depending on the level of error in the estimation of the interfering user's data sequences, the bit-error performance of the wanted user can vary drastically.

The initial detection involves equalising structures that try to restore the shape of the signals in order to detect the other users' interference. The first stage of detection uses either zero forcing or controlled equalisation methods, as discussed in [4]. For zero-forcing equalisation, the effective coefficients are given as:

$$g_{n,n} = \frac{1}{h_{n,n}} = \frac{h_{n,n}^*}{|h_{n,n}|^2} \tag{3}$$

If controlled equalisation is used in the receiver, a rapid deep fade in the channel transfer function below a set threshold value will cause the receiver to switch to phase only equalisation on that particular carrier. The complex equalisation coefficient is then given by:

$$g_{n,n} = \frac{h_{n,n}^*}{|h_{n,n}|} \tag{4}$$

These enable the receiver to obtain an initial estimate of the interfering user's data sequences. When the interfering signals have been eliminated from the original received signal, it is then important to maximise the signal-to-noise ratio in the detector. For this reason it is of interest to use a combiner such as MRC. The complex equalisation coefficient is given in the frequency domain as:

$$g_{n,n} = h_{n,n}^* \tag{5}$$

MRC provides a signal estimate by combing the maximum signal-to-noise ratio of each faded sub-carrier and performs best on "clean" signals. Therefore this combining method is used on the second iteration. This provides an optimal equalisation strategy, since the "cleaned" signals are assumed to be relatively free of other-user interference.

SIMULATION RESULTS

The simulated uplink channel assumes a service provision of a 32 kb/s data stream for each user. A constraint length of K=5 provides a spreading ratio of 32 in the LROCC encoder and this is then randomised through the user-specific Gold code c_i of the same rate. This code provides no further additional spreading, but merely serves as a randomising sequence for the LROCC orthogonal code sets [5,6]. The number of sub-carriers is N=32 in a bandwidth of 1.028 MHz, and therefore each sub-carrier has a duration of 31.25μs. The simulated channel is based on the COST 207 frequency selective Rayleigh faded bad urban (BU) channel model [7]. The

Doppler frequency was set to 200Hz and perfect power control is assumed. Figure 3 shows the BER performance for different numbers of simultaneous users communicating with the basestation. The performance without MAI cancellation degrades significantly when more than 5 users are present. The use of MAI cancellation increases this to at least 10 users, and this is a significant gain in

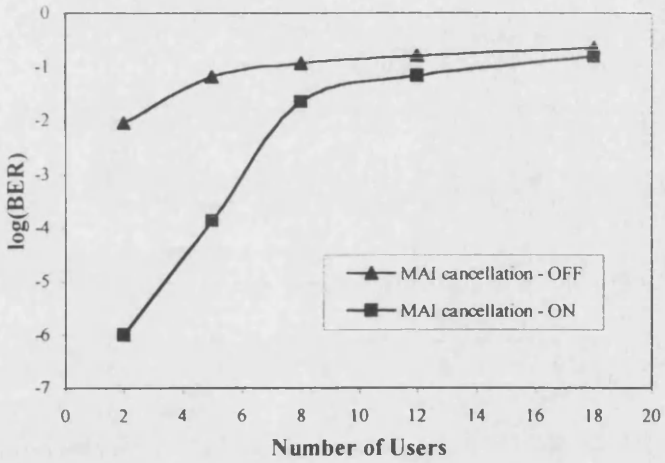

Figure 4. Uplink capacity comparison using zero forcing equalisation on the first iteration and MRC on the second detection stage

performance. Conversely, at low user numbers, the BER for 32 kb/s per user is substantially improved by MAI cancellation. Without MAI cancellation it is not possible to achieve an acceptable BER for any user numbers.

Controlled threshold equalisation tries to balance the disadvantages of zero forcing and phase only equalisation in fading conditions to provide an optimum balance of equalisation. The impact of threshold level on BER is shown in figure 4 using no MAI cancellation and 8 simultaneous users in the channel.

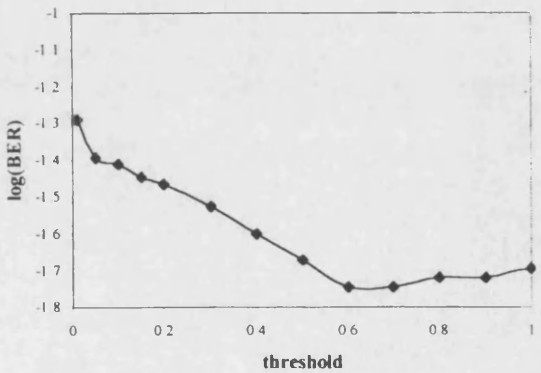

Figure 3. Optimum threshold value for controlled equalisation on initial detection

This figure suggests an optimum threshold value of about 0.6, and this value was subsequently used for the second type of receiver system that has been simulated which uses a controlled equaliser. The performance of this receiver is shown in figure 5.

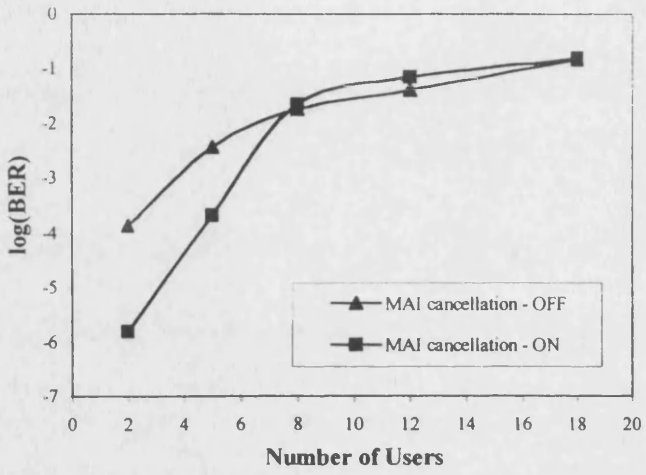

Figure 5. Uplink capacity comparison using controlled equalisation on the first iteration and MRC on the second detection stage

Compared with the method that uses the zero-forcing strategy on the initial iteration, described earlier, this technique shows a significant performance improvement when no MAI cancellation is used in other user noise environments, but a smaller performance improvement when MAI cancellation is used. At high user capacities (above 8 users typically) the performance gets worse compared with simple one stage detection schemes. The reason for this is that when the uplink channel is saturated with other user noise, the initial estimates of the first iteration become very unstable. This causes the interference estimates of all other interfering users to give a "dirty" signal that can actually degrade the bit-error rate performance.

The LROCC coding scheme relies primarily on independent errors to yield good results and it is therefore important to provide initial good estimates on the first iteration of interference estimation in the receiver and to use strong interleaving in heavily faded channels. The use of OFDM in frequency selective channels helps to further combat the fading effects and effectively provides independent fading on each sub-channel. Combing this modulation strategy with LROCC coding provides an ultimately robust transmission design for such channels.

CONCLUSIONS

The proposed transmitter and receiver design for the uplink channel of a mobile communication system in heavy frequency selective Rayleigh fading can be used to

combat the degradation effects through the use of LROC codes and controlled equalisation, providing a capacity gain of at least 25% at BER=10^{-3}. Of course, such gains will be degraded if the channel state information contains errors.

The use of zero forcing equalisers would not lead to a good performance without MAI cancellation, but through the use of MAI cancellation it is possible to combine zero-forcing algorithms with MRC on the final detection stage to give good results.

ACKNOWLEDGEMENTS

The authors are pleased to acknowledge the support of EPSRC for their support of this work through contract No. GR/K27902 and to NORTEL for their provision of CASE studentship support.

REFERENCES

[1] Y. Yukitoshi and M. Nakagawa, "A Multiuser Interference Cancellation Technique Utilizing Convolutional Codes and Orthogonal Multicarrier Modulation for Wireless Indoor Communications", *IEEE Journal on Selected Areas in Communications*, Vol. 14, No.8, October 1996

[2] K. Fazel, S. Kaiser and M. Schnell, "A Flexible and High Performance Cellular Mobile Communications System Based on Orthogonal Multi-Carrier SSMA", *Wireless Personal Communications*, Kluwer Academic Publishers, pp.121-144, 1995

[3] T. Mueller *et al*, "Comparison of different Detection Algorithms for OFDM-CDMA in Broadband Rayleigh Fading", *IEEE Conference Publication*, pp. 835-838, 1995.

[4] S. Kaiser, "OFDM-CDMA versus DS-CDMA: Performance evaluation for fading channels", *Proc. IEEE International Conference on Communications* (ICC'95), pp.1722-1726, June 1995.

[5] Maxey, J J and Ormondroyd, R F, "Optimisation of orthogonal low-rate convolutional codes in a DS-CDMA system", *IEEE/URSI Conference Proceedings of ISSSE'95*, Vol. 95TH8047, pp. 493-496, 1995

[6] Maxey, J J and Ormondroyd, R F, "Low-Rate Orthogonal Convolutional Coded DS-CDMA using Non-Coherent Multi-Carrier Modulation over the AWGN and Rayleigh Faded Channel", *IEEE Conference Proceedings of ISSSTA'96*, Vol. 2, pp.575-579, 1996

[7] COST 207: *Digital land mobile radio communications*, Final Report, Commission of the European Communities, Luxembourg 1989

Version submitted to JSAC'98, Special Issue on
Signal Processing

BROADBAND OFDM-CDMA MOBILE RADIO SYSTEM USING CONVOLUTIONAL CODING AND MULTI-USER INTERFERENCE CANCELLATION OVER FADING CHANNELS

J J Maxey and R F Ormondroyd

School of Electronic and Electrical Engineering
University of Bath, Claverton Down,
Bath, BA2 7AY, U.K.

Tel: (+44) 1225 826826 Fax: (+44) 1225 826305
e-mail: eepjjm@bath.ac.uk and eesrfo@bath.ac.uk

ABSTRACT

The performance of broadband OFDM-CDMA multiple-access mobile radio systems can be improved significantly using convolutional coding and multi-access interference (MAI) cancellation. However, effective MAI cancellation requires knowledge of both the interference statistics and the channel transfer functions of all the other-users in the cell with respect to the wanted-user so that effective equalisation can be applied in the receiver. In this paper, two OFDM-CDMA systems which make use of convolutional coding and parallel MAI cancellation are presented: one for the uplink and the other for the downlink. One of the chief aims of the paper is to show that the choice of equalisation strategy for the MAI cancellation receiver is extremely important if the signal to noise ratio at the input to the detector is to be maximised. It is found that controlled equalisation in conjunction with maximum ratio combining gives better performance than zero-forcing equalisation for both the uplink and downlink. However, to achieve this improvement the controlled equaliser threshold has to be optimised and it is found that the optimum value is not affected by the use of MAI cancellation. Finally, it is found that if the estimates of the channel statistics are in error, MAI cancellation can give a worse performance than using no MAI cancellation.

I INTRODUCTION

Orthogonal frequency division multiplexing (OFDM) techniques are now widely accepted as a means of providing reliable broadband data transmission over mobile and fixed wireless communication systems where time and frequency selective fading are dominant features of the channel transfer function. Recently, there have been a number of proposals to extend the use of OFDM modulation to multiple-access systems and a variety of techniques have been suggested. These include OFDMA [1] in which each user is allocated a number of OFDM sub-channels for the duration of the call and OFDM-CDMA [2,3], whereby CDMA multiple access methods are used in conjunction with OFDM modulation. There

are three main methods of achieving this. One method, proposed by Fazel [2,3], is to spread each user's data with a unique CDMA spreading code and to perform OFDM modulation on the CDMA chips. This method is commonly referred to as OFDM-CDMA. A second method, proposed by Kondo and Milstein [4], transmits a number of CDMA signals on relatively widely spaced separate carriers. The carriers may be orthogonal, but this is not essential and this system is usually referred to as multi-carrier CDMA (MC-CDMA). In the third system, proposed by Vandendorpe [5], the user data is first transformed using the inverse fast Fourier transform (IFFT) and the complex IFFT coefficients are then spread using the CDMA spreading code. This type of system is usually referred to as multi-tone CDMA.

The use of DS-CDMA techniques with OFDM gives added frequency diversity to each data bit and protects the system from deep fades in the frequency response of the channel. Using DS-CDMA to spread the original bandwidth of the data enables the delay spread of the channel to be resolved more efficiently. Therefore, OFDM-CDMA techniques can provide a robust multiple access scheme when many other users are transmitting over the same bandwidth in a faded channel with different user specific codes. In the limit, this has the advantage of enabling the received data streams to appear as flat faded data streams on each sub-carrier, and subsequently enables the equaliser at the receiver to demodulate the data more effectively. A number of techniques, such as (i) frequency- or time-domain interleaving, (ii) convolutional coding, (iii) guard-time insertion, (iv) frequency-domain equalisation and (v) MAI cancellation techniques (successive or parallel) have been proposed to combat these fading effects.

The system requirements of the uplink and downlink of a cellular radio system are essentially different. For the downlink, it is possible to ensure that all the users' signals are time aligned so that orthogonal coding and multiplexing achieves optimum performance. On the other hand, without very accurate delay management, the uplink effectively operates asynchronously. Consequently, different approaches must be used for the uplink and downlink to ensure that the overall system performance is not limited by a poor uplink performance. In this paper, the bit error-rate performance of multi-access OFDM systems are presented for the uplink and downlink using discrete-time computer simulations. For the downlink, an OFDM-CDMA approach is used. This design convolutionally codes and orthogonally spreads the user data, then sums all users before modulating them onto N OFDM sub-carriers. In contrast, the uplink simultaneously codes and spreads the user data using a low-rate orthogonal convolutional code (LROCC) [6,7] and then OFDM modulates the encoded signal. LROCC coding has been employed because it has been found to provide a higher processing gain under asynchronous conditions than convolutional coding combined with conventional spreading.

OFDM techniques are effective in multipath fading where the channel impulse response is significantly longer than the symbol period of the data being transmitted. In a conventional single carrier system, the impulse response gives rise to significant inter-symbol interference (ISI) that requires extremely complex time-domain adaptive equalisation structures. In an OFDM system, the ISI problem is transformed to an equivalent inter-carrier interference (ICI) problem, which is generally regarded as being much simpler to solve. Viewed in the time-domain, OFDM reduces ISI by transforming the data from a single high-rate symbol stream to many low rate symbol streams that are transmitted in parallel on separate sub-carriers. The duration of each parallel symbol (which defines the length of the OFDM frame) can be much longer than the channel impulse response simply by using many sub-carriers. The limit to the number of sub-carriers is set by the allowable frequency spacing between sub-carriers, which is determined by Doppler spread and local oscillator stability.

The optimum weights for the equaliser can be obtained either from decision directed methods or directly from the FFT of the channel impulse response. These can be measured using pilot channels or mid-ambles inserted between the data. A relatively simple and effective equalisation structure that attempts to restore the orthogonality of the sub-carriers is controlled equalisation [8] whereby the receiver has no knowledge of the received signal to noise ratio nor the number of users using the channel. A number of different equalisation techniques using structures of different complexity have been investigated [2,3]. For more sophisticated receiver structures, the MMSE algorithm can provide considerable performance improvements compared with conventional equalisers. Sub-optimal MMSE algorithms can be employed by using a fixed value for the estimated number of users in the channel. This presents about 1dB loss in performance for the downlink channel.

One method of countering the effects of the interference of the other co-channel users is to use maximum likelihood detection (MLD). These schemes can only be used if the spreading sequences of all users are relatively short. However, the complexity increases exponentially with the sequence length. The use of coding, nevertheless, provides considerable performance benefits in memoryless and non-memoryless channels. In Rayleigh faded channels, the coding gain can be further enhanced through strong interleaving in the time- or frequency domain. A variety of sub-optimal interference cancellation schemes can be used to remove this interference as long as the spreading codes of all active users are known at the receiver.

Power control methods are invariably used on the uplink of a cellular structure to reduce the interference effects from one cell to another and to reduce the near-far effect in the wanted cell. With this in mind, it is convenient to use parallel interference cancellation methods rather than successive interference

cancellation, since this requires geometrically distributed powers of different users in the cell, causing unnecessary inter-cell interference.

The work presented in this paper focuses on a novel MAI cancellation technique for the downlink and uplink of a mobile radio channel. Performance comparisons are shown for zero-forcing equalisation, controlled equalisation and maximum ratio combing (MRC) techniques.

II DOWNLINK MODEM DESIGN

The base station to mobile downlink offers a number of options for the most efficient detection process of the wanted-user. Orthogonal CDMA codes give the most robust distance separation in the code domain and will inherently give the best performance for time-aligned users in the base station transmitter. The introduction of convolutional coding can significantly improve the bit error rate (BER), depending on the operating E_b/N_o. This improvement is at the cost of bandwidth but, generally, the coding gain is larger than the bandwidth penalty. In AWGN channels, orthogonal codes give an optimum performance and no further improvements in BER can be gained through MAI cancellation techniques. However, in frequency selective faded channels, the performance of the system can be enhanced through parallel interference cancellation, which uses a two-stage detection process. This is the situation assumed in this paper.

A Base Station Transmitter

The downlink design is based closely on the system proposed by Fazel [2], shown in figure 1. In this system, the base station communicates with L users simultaneously. Walsh-Hadamard orthogonal codes are assumed for the CDMA spreading sequence and all data bits and spreading chips are assumed to be time-aligned. In order to shorten the length of the orthogonal spreading sequence of each user, and to allow more complex detection algorithms such as MLD to be employed, this transmitter architecture groups the L simultaneous users into D transmission blocks. Each of these blocks can be viewed as a 'mini CDMA' base station of only L/D users, rather than L users. Within this block, each user, i=1,2...L/D, transmits a data sequence, $d_i \in (-1,+1)$, clocked at a rate, $1/T_b$, and this is encoded using a convolutional encoder of rate R to produce a sequence of encoded symbols, e_i, each of duration $T_{cod}=RT_b$. The encoded symbols are then multiplied by the individual, user-specific, orthogonal spreading code, $c_i=[c_i(1),c_i(2)...c_i(L/D)]^T \in (-1,+1)$, where $[.]^T$ is the transposed matrix. Note that each block of L/D users employs the same set of orthogonal codes as the other (D-1) blocks. The overall spreading ratio for each data bit is therefore given as, $M=L(D.R)^{-1}$. Because orthogonal spreading codes have zero cross-correlation, the maximum capacity of the base station for all D blocks is $N_B=L$. The coded and spread data

is summed bit- and chip-synchronously with the other-users of the block and then buffered. In the analysis below we ignore the time index and consider the processing of a single block of data bits. Consequently, the transmission vector, $\boldsymbol{S}_d$, of the spread signals in the buffer of the d^{th} transmission block prior to interleaving and OFDM modulation is given by:

$$\boldsymbol{S}_d = \sum_{i=M(d-1)+1}^{Md} \boldsymbol{e}_i \boldsymbol{c}_i \tag{1}$$

To give some freedom to the number of sub-carriers that can be generated per data bit, each user can transmit Q data bits per OFDM symbol. Each of these are spread by the factor, M. Consequently, the size of each summing buffer is $Q.M$ and the total number of parallel inputs to the interleaver (and hence the size of the IFFT which performs the OFDM modulation) for all D blocks is thus $D.Q.M$.

After interleaving and OFDM modulation, the output sequence is represented by the complex vector sequence $V = [v_1, v_2 \ldots v_{D \cdot Q \cdot M+\Delta}]$. This vector contains Δ additional terms representing the guard interval that is inserted between adjacent OFDM frames. The guard interval forms a cyclic extension to the vector sequence V, whereby the first Δ elements of V are duplicated as the last Δ elements of V. This reduces the effects of ISI due to the multipath spread in the fading channel, and if the guard interval length is greater than the multipath spread length of the channel, the OFDM blocks are orthogonal. The output of the OFDM modulator may be expressed as:

$$x(t) = \sum_{q=0}^{Q-1} \sum_{d=0}^{D-1} \sum_{l=0}^{M-1} s_{q,d,l} \cdot e^{j2\pi f_{qDM+dM+l}} \qquad \text{for } -\Delta < t < T_t \tag{2}$$

where $s_{q,d,l}$ is the l^{th} component of $\boldsymbol{S}_d$ of the q^{th} data bit and the orthogonal sub-carrier frequency, $f_{qDM+dM+l}$ is given by:

$$f_{qDM+dM+l} = f_o + \frac{qDM + dM + l}{T_s} \tag{3}$$

where f_o is the lowest sub-carrier frequency and T_s is the symbol duration.

The output vector to be transmitted over the channel is represented by complex coefficients on the output of the IFFT in the modulator. Although all the users are orthogonally coded, because of the effect of the multipath channel, the wanted-user is corrupted by the other users. In this case, the channel has the same effect on the other-user interference as the wanted-user and so effective equalisation plays an important part in regaining orthogonality between the users in the received signal at any remote receiver. The amplitude and phase characteristics of the channel may be described by a complex matrix, $\boldsymbol{H}_d$, of size

$M \times M$ for the d^{th} transmission block. Since a perfect guard-interval length is assumed, the channel matrix $\boldsymbol{H}_d$ is a diagonal matrix with diagonal components $h_{n,n}$.

B Remote Receiver

In the remote receiver of the wanted-user, shown in figure 2, the multi-user OFDM signal is demodulated in the usual way using the FFT. As is often the case, we assume that the delay spread of the channel is less than the guard interval and that channel statistics can be considered stationary over the OFDM block duration, T (i.e. $T \ll 1/f_{dop}$ where f_{dop} is the Doppler frequency offset). The received signal is given by:

$$y(t) = \sum_{q=0}^{Q-1} \sum_{d=0}^{D-1} \sum_{l=0}^{M-1} h_{q,d,l} s_{q,d,l} \cdot e^{j2\pi f_{qDM+dM+l}} + n(t) \tag{4}$$

where $h_{q,d,l} = \rho_{q,d,l} e^{j\phi_{q,d,l}}$ is the complex channel fading characteristic with attenuation $\rho_{q,d,l}$ and phase shift $\phi_{q,d,l}$ at sub-carrier frequency $f_{q,d,l}$ and $n(t)$ is the additive noise. The received signal of the d^{th} transmission block after OFDM demodulation and can be represented as a vector $\boldsymbol{R}_d$:

$$\boldsymbol{R}_d = \boldsymbol{H}_d \boldsymbol{S}_d + \boldsymbol{N}_d \tag{5}$$

where $\boldsymbol{H}_d$ is the diagonal matrix representing the Rayleigh fading on the sub-carriers assigned to block d, assuming a guard-interval length which removes ISI or ICI. $\boldsymbol{N}_d$ represents the complex noise vector at the receiver.

Using an estimate of the channel frequency response, frequency domain equalisation is then carried out on all L sub-carriers to reduce the effect of multipath distortion and the symbols on the sub-carriers are then de-interleaved. After equalisation and de-interleaving, using the equalisation matrix of the first-stage equaliser, $\boldsymbol{G}_d(1)$, the signal before detection is given by:

$$\begin{aligned} \boldsymbol{R}'_d &= \boldsymbol{G}_d(1)(\boldsymbol{H}_d \boldsymbol{S}_d + \boldsymbol{N}_d) \\ &= \boldsymbol{G}_d(1)\boldsymbol{H}_d \boldsymbol{S}_d + \boldsymbol{G}_d(1)\boldsymbol{N}_d \end{aligned} \tag{6}$$

This signal is decoded and demodulated using a maximum likelihood detector such as the Viterbi algorithm to provide an estimate of the transmitted data bit d'_i. The estimated data bit is then re-encoded and re-modulated to form an estimate of the interference from the i^{th} user. This process is carried out for

all (L-1) interfering users. Assuming that the wanted-user is user 1, the estimated interference to user 1 is given as:

$$y'(t) = \sum_{q=0}^{Q-1} \sum_{d=0}^{D-1} \sum_{l=0}^{M-1} s'_{q,d,l} \cdot e^{j2\pi f_{qDM+dM+l}t} \quad \text{for } -\Delta<t<T_b \tag{7}$$

where $s'_{q,d,l}$ is the l^{th} estimate of S'_d of the q^{th} data bit, and,

$$S'_d = \sum_{\substack{i=M(d-1)+1 \\ i\neq 1}}^{Md} e'_i \, c_i \tag{8}$$

where e'_i is the estimated encoded output sequence of d'_i.

Therefore the wanted signal after MAI cancellation is now given by:

$$z(t) = y(t) - y'(t) \tag{9}$$

This signal is then demodulated and decoded for the wanted-user using the second stage complex equalisation matrix $G_d(2)$, where we now use a <u>different</u> equalisation algorithm to detect our wanted-user. This can be simplified to:

$$y'(t) = \sum_{q=0}^{Q-1} \sum_{d=0}^{D-1} \sum_{l=0}^{M-1} (s_{q,d,l} - s'_{q,d,l}) \cdot e^{j2\pi f_{qDM+dM+l}t} \quad \text{for } -\Delta<t<T_b \tag{10}$$

The received signal after OFDM demodulation and MAI cancellation is now given by:

$$R_d = G_d(2)[H_d(S_d - S'_d) + N_d] \tag{11}$$

This is then decoded with wanted-user's orthogonal sequence and detected using the Viterbi algorithm. Depending on the level of error in the estimation of the interfering user's data sequences, the bit-error performance of the wanted-user can vary drastically. In a channel of high other-user noise levels the BER performance will degrade quickly unless sophisticated interference cancellation techniques are employed.

C Equalisation Strategies

In this paper, the channel statistics are assumed to be perfectly known through the use of a pilot tone or a mid-amble training sequence. For the first stage of detection, equaliser $G_d(1)$ uses either zero forcing or controlled equalisation methods, as discussed in [2,3,8]. For zero-forcing equalisation, the complex-valued equaliser coefficients are given as:

$$g_{n.n} = \frac{1}{h_{n,n}} = \frac{h^*_{n.n}}{|h_{n,n}|^2} \tag{12}$$

where $h_{n,n}$ are the diagonal components of the channel matrix H_d. Controlled equalisers perform phase-only equalisation if the magnitude of the signal envelope drops below a set threshold value to prevent the channel noise being amplified. When the magnitude of the signal envelope is above the threshold, the effect of the noise is deemed to be acceptable and full advantage can be taken of zero-forcing equalisation. The assigned equalisation coefficients for controlled equalisation are:

$$g_{n,n} = \frac{1}{h_{n,n}} = \frac{h^*_{n,n}}{|h_{n,n}|^2} \qquad \text{for } |y(t)|^2 \geq \text{threshold}$$
$$= \frac{h^*_{n,n}}{|h_{n,n}|} \qquad \text{for } |y(t)|^2 < \text{threshold} \tag{13}$$

These enable the receiver to obtain an initial estimate of the interfering users' data sequences.

Maximum ratio combining (MRC) attempts to maximise the signal to noise ratio (SNR) of the multi-carrier signal by obtaining the maximum SNR of each faded sub-carrier. MRC removes the phase information from the sub-carrier and weights the received signal by the complex conjugate of the channel coefficients:

$$g_{n,n} = h^*_{n,n} \tag{14}$$

This type of strategy performs best on "clean" signals and is therefore used on the second stage, $G_d(2)$ after MAI cancellation only and provides an optimal combining strategy since the "cleaned" signals are assumed to be relatively free of other-user interference.

III DOWNLINK SIMULATION RESULTS

The bit error rate performance of the downlink was obtained using a discrete-time computer simulation written in C. The user data rate was set at 19 kb/ and the convolutional code was of rate R=1/2 and constraint length K=5. The encoded signals were spread using orthogonal Walsh-Hadamard sequences of length 16, giving a total bandwidth expansion factor of 32 and a maximum user capacity of 16 users per block. The total number of blocks was set to D=8 and Q=2 data bits of each user were transmitted per OFDM block. The number of sub-carriers is therefore $D.Q.M$ = 512, which results in a total bandwidth of 1.216 MHz and a sub-carrier spacing of 2.375kHz. The corresponding base station capacity is 16 x 8 =128 and these were represented in the simulation by randomly generated data bits.

Note that no further spreading is achieved through use of the randomising sequence, c_i.

After OFDM modulation and interleaving, the output sequence may be represented by the vector sequence $V_i = [v_i(1), v_i(2) \ldots v_i(M+\Delta)]$ where Δ is the guard interval length, as described earlier. The output vector to be transmitted over the channel is represented by complex coefficients on the output of the IFFT in the modulator.

B. Basestation receiver

The basestation receiver design can be seen in figure 7. Since each user communicating to the base station experiences different independent fading statistics, the channel coefficients are different for each user. The channel may be described by a complex matrix H_i (in the frequency domain) of size $M \times M$ for each user, effecting the sub-carriers V_i assigned to the transmitted sequence on the transmitter for user i. Since a perfect guard-interval length is assumed, the channel matrix H_i is a diagonal matrix with diagonal components $h_{n,n}$. The vector N represents the complex AWGN in the channel. Therefore, the received sequence at the output of the OFDM demodulator, assuming perfect interleaving and guard-band insertion, is given by:

$$R = \sum_{i}^{L} e_i \cdot c_i \cdot H_i + N \tag{15}$$

The base station receiver obtains information on the complex channel coefficients through the midambles inserted between symbol sequences. For the analysis of the uplink, we assume that the channel estimation is perfect. Using the complex channel estimates for each user we equalise the demodulated sequence for each user separately and obtain an estimate of the interference from other users. This is achieved through de-randomising the equalised signal by the user-specific code c_i and performing maximum likelihood detection using the Viterbi algorithm. The estimated data sequences of all interfering users are re-modulated and re-encoded with the appropriate channel equalisation estimate and these signals are subsequently subtracted from the original received sequence. Depending on the level of error in the estimation of the interfering user's data sequences the bit-error performance of the wanted-user can vary drastically. In a channel of high other-user noise levels the BER performance will degrade quickly unless sophisticated interference cancellation techniques are employed. The equalisation strategies that have been used are similar to those used for the downlink case. The first stage equalisers use either zero-forcing or controlled equalisation, whereas the second stage equaliser uses MRC.

V SIMULATION RESULTS

The simulated uplink channel assumes a service provision of a 32 kb/s data stream for each user. A constraint length of K=5 provides a spreading ratio of 32 in the LROCC encoder and is then randomised through the user-specific Gold code c_i of the same rate. This code provides no further additional spreading, but merely serves as a randomising sequence for the LROCC orthogonal code sets [6]. The number of sub-carriers is N=32 in a bandwidth of 1.028 MHz, and therefore the OFDM block period is 31.25μs. As for the downlink case, the channel is based on the COST 207 frequency selective Rayleigh faded bad urban (BU) channel model. The Doppler frequency was set to 200Hz and perfect power control is assumed.

Figure 8 shows the bit-error rate performance for different number of simultaneous users communicating with the base-station. The performance without interference cancellation can be seen to quickly degrade significantly when more than 5 users are present. The use of interference cancellation increases this to at least 10 users, and this is a significant gain in performance. Conversely, at low user numbers, the BER for 32 kb/s per user is substantially improved by MAI cancellation. Without MAI cancellation it is not possible to achieve an acceptable BER for any user numbers.

A more efficient equalisation scheme is based on controlled threshold equalisation. The threshold level displayed in figure 9 was estimated for the initial threshold detection strategy using no MAI cancellation and 8 simultaneous users in the channel. Figure 9 suggests an optimum threshold value of about 0.6 that was subsequently used for the equalisation structure employed in the Monte-Carlo simulations shown in figure 10. This technique shows a significant performance improvement for detection using no MAI cancellation in other-user noise environments but a smaller performance improvement using MAI cancellation compared to the zero-forcing strategy on the initial iteration, as shown earlier. At high user capacities (above 8 users typically) the performance gets worse compared to simple one stage detection schemes. When the uplink channel is saturated with other-user noise, the initial estimates on the first stage of MAI cancellation become very unstable. This causes the interference estimates of all other interfering users to give errors that propagate and actually harm the bit-error rate performance.

The LROCC coding scheme relies primarily on independent errors to yield good results and it is therefore important to provide initial good estimates on the first iteration of interference estimation in the receiver and to use strong interleaving in heavily faded channels. The use of OFDM in frequency selective channels helps to further combat the fading effects and effectively provides independent fading on each

sub-channel. Combing this modulation strategy with LROCC coding provides an ultimately robust transmission design for such channels.

VI. CONCLUSIONS

An uplink and downlink system design based on OFDM-CDMA have been proposed for a mobile communication system in a channel of heavy frequency selective Rayleigh fading. The use of LROCC and controlled equalisation with MAI cancellation in the uplink have been shown to provide a capacity gain of at least 25% at BER=10^{-3}, and likewise a 10dB gain in E_b/N_o in the downlink with rate R=1/2 convolutional codes. More realistic performance results with noisy channel estimates have found to provide a degradation of at least 6dB on this result, yielding a potential improvement of 4dB.

It has been established further, that the use of zero-forcing equalisers would not lead to a good performance without MAI cancellation, but through the use of MAI cancellation it is possible to combine zero-forcing algorithms with MRC on the final detection stage to give good results. It has been shown, however, that controlled equalisation for the first detection stage, in combination with MRC on the second detection stage outperforms the zero-forcing equaliser. This improvement is particularly noticeable for the system when MAI cancellation is not used.

VII. REFERENCES

[1] Rohling, H, *et al*, "Comparison of multiple access schemes for an OFDM downlink system", *Proc. First International Workshop on Multi-Carrier Spread-Spectrum*, DLR Oberpfaffenhofen, Germany, April 1997

[2] Fazel, K, "Performance of CDMA/OFDM for mobile communication systems", *IEEE 2nd International Conference on Universal Personal Communications (ICUPC) Proc.*, October 1993

[3] K. Fazel, S. Kaiser and M. Schnell, "A Flexible and High Performance Cellular Mobile Communications System Based on Orthogonal Multi-Carrier SSMA", *Wireless Personal Communications*, Kluwer Academic Publishers, pp.121-144, 1995

[4] Kondo, S and Milstein, L, "Performance of Multicarrier DS-CDMA Systems", *IEEE Transactions on Communications*, pp. 238-246, Vol. 44, No. 2, February 1996

[5] Vandendorpe, L, "Multitone Spread Spectrum Multiple Access Communications System in a Multipath Rician Fading Channel", *IEEE Transactions on Vehicular Technology*, pp. 327-337, Vol. 44, No. 2, May 1995

[6] Maxey, J J and Ormondroyd, R F, "Optimisation of orthogonal low-rate convolutional codes in a DS-CDMA system", *IEEE/URSI Conference Proceedings of ISSSE'95*, Vol. 95TH8047, pp. 493-496, 1995

[7] Maxey, J J and Ormondroyd, R F, "Low-Rate Orthogonal Convolutional Coded DS-CDMA using Non-Coherent Multi-Carrier Modulation over the AWGN and Rayleigh Faded Channel", *IEEE Conference Proceedings of ISSSTA'96*, Vol. 2, pp.575-579, 1996

[8] T. Mueller *et al,* "Comparison of different Detection Algorithms for OFDM-CDMA in Broadband Rayleigh Fading", *IEEE Conference Publication*, pp. 835-838, 1995.

[9] COST 207: *Digital land mobile radio communications*, Final Report, Commission of the European Communities, Luxembourg 1989

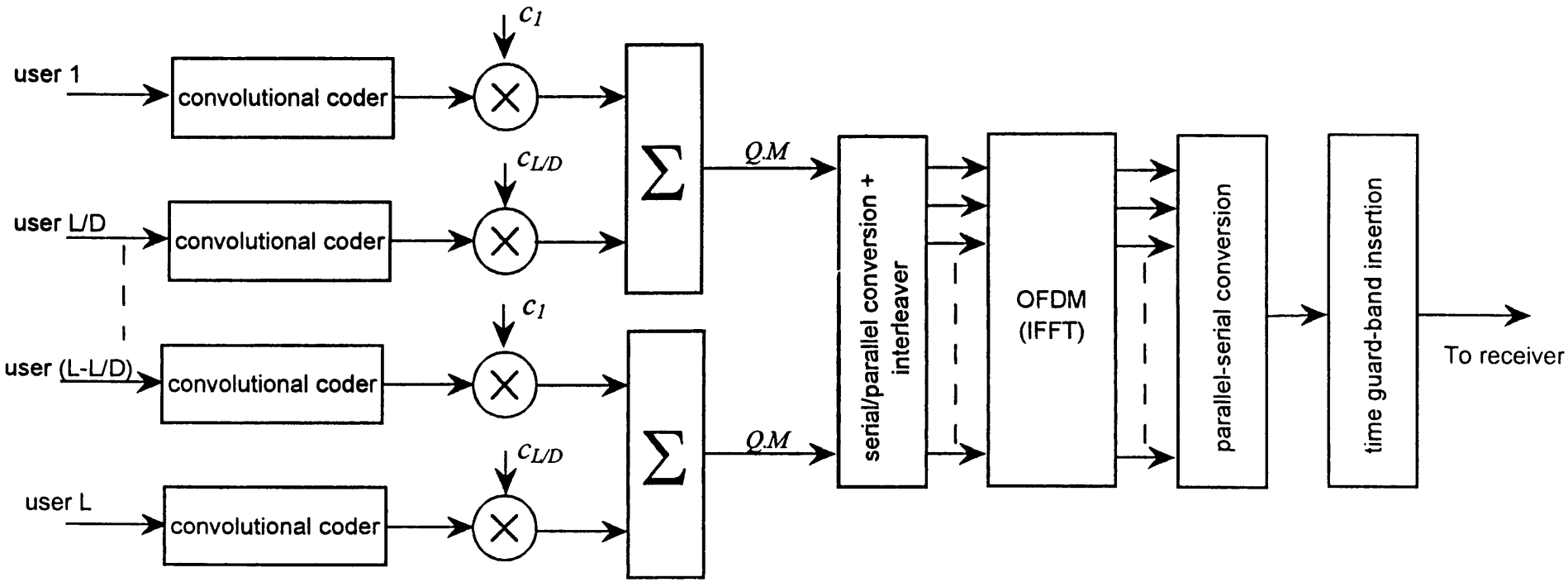

Figure 1 Convolutional coded OFDM-CDMA downlink base-station transmitter

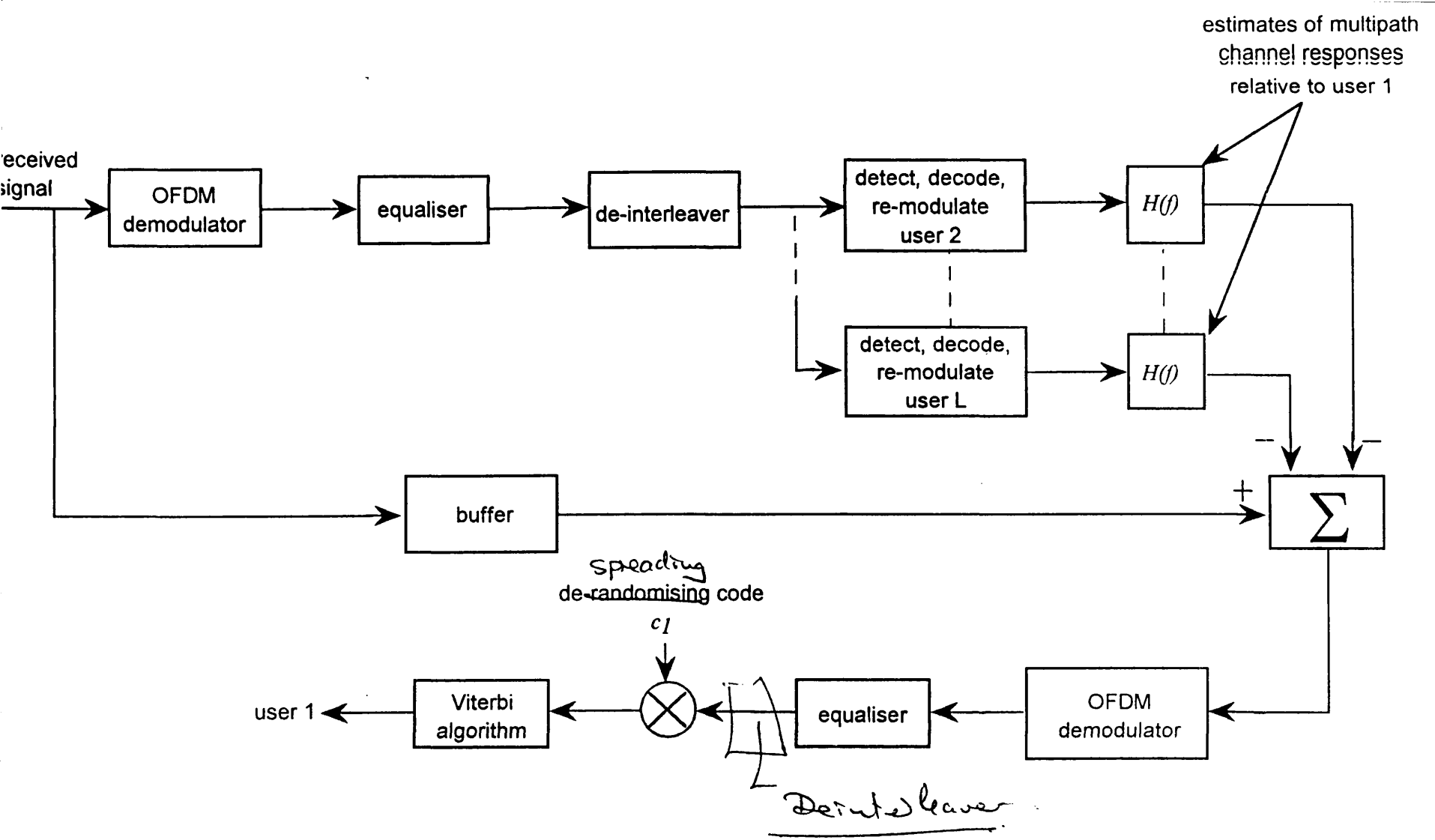

Figure 2 Subscriber receiver architecture for user 1

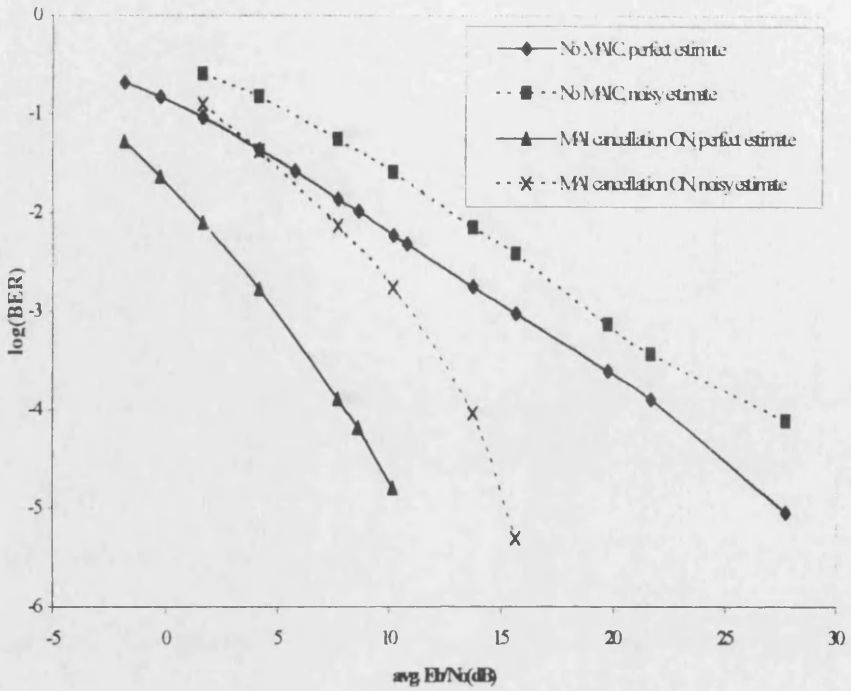

Figure 3. Performance using zero-forcing equalisation on the first iteration and MRC on the second detection (perfect channel estimates & noisy channel estimates)

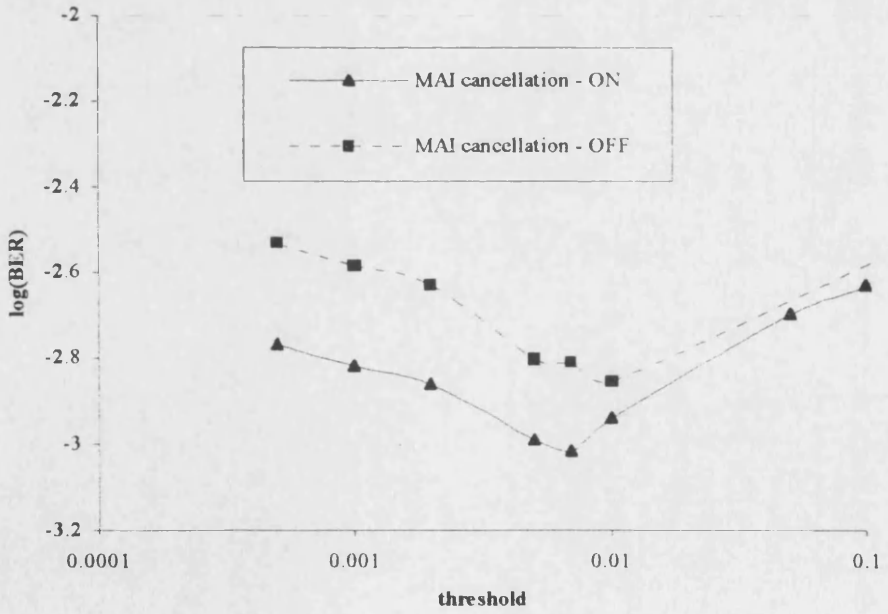

Figure 4. Optimum threshold value for controlled equalisation techniques on the downlink using MAI cancellation and no MAI cancellation

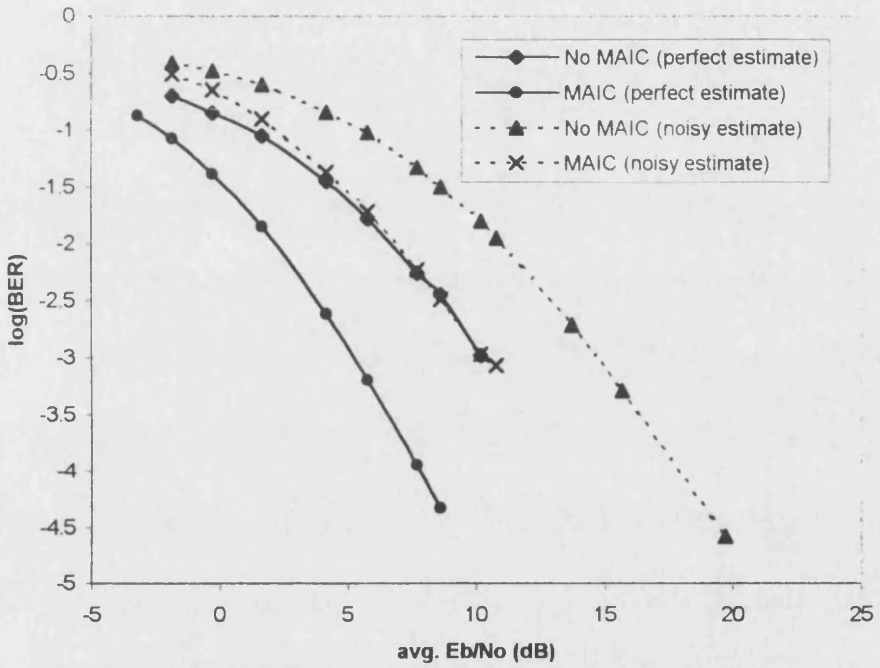

Figure 5. Performance using controlled equalisation on the first iteration and MRC on the second iteration

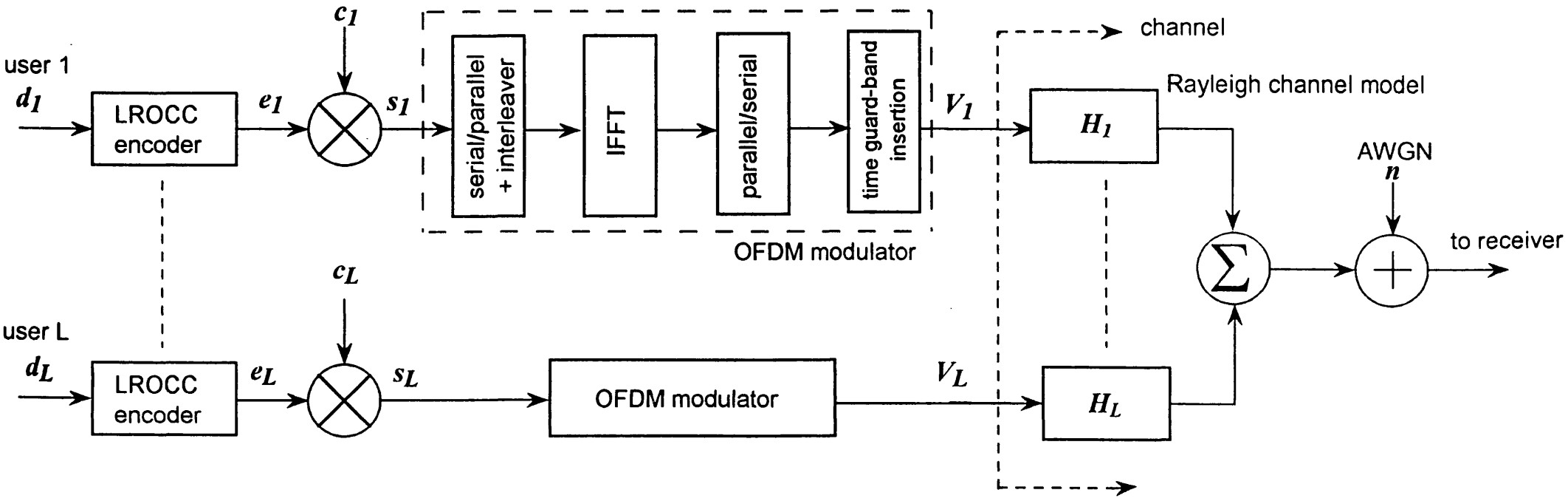

Figure 6. Model of the proposed transmitter for all uplink users and channel model

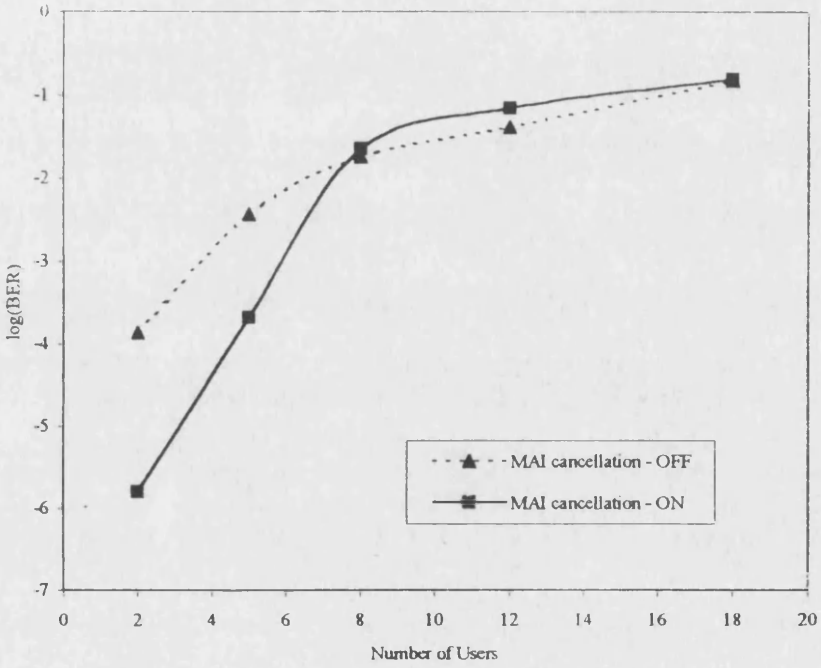

Figure 10. Uplink capacity comparison using controlled equalisation on the first iteration and MRC on the second detection stage

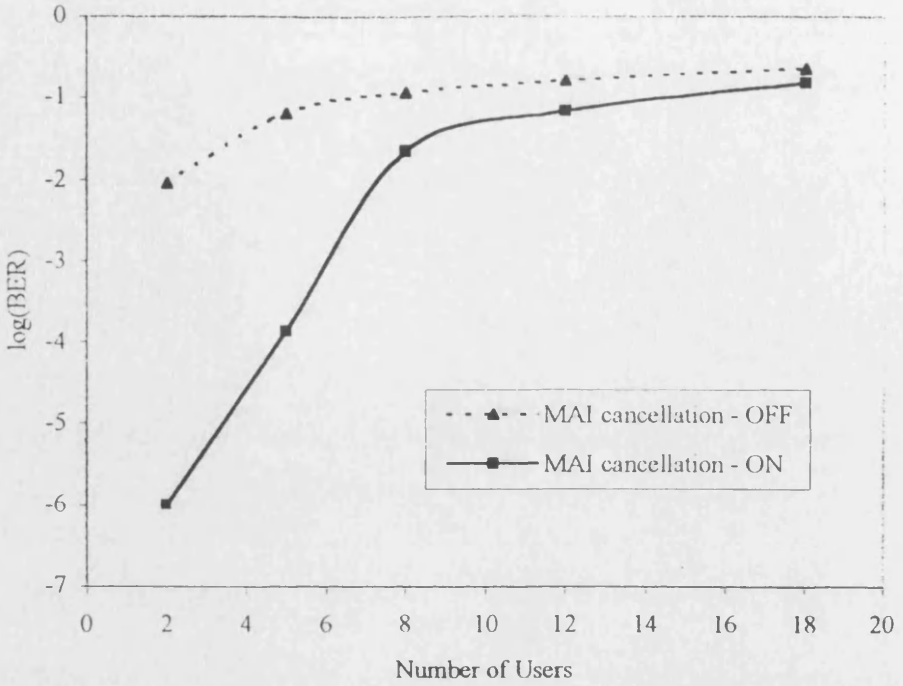

Figure 8. Uplink capacity comparison using zero-forcing equalisation on the first iteration and MRC on the second detection stage

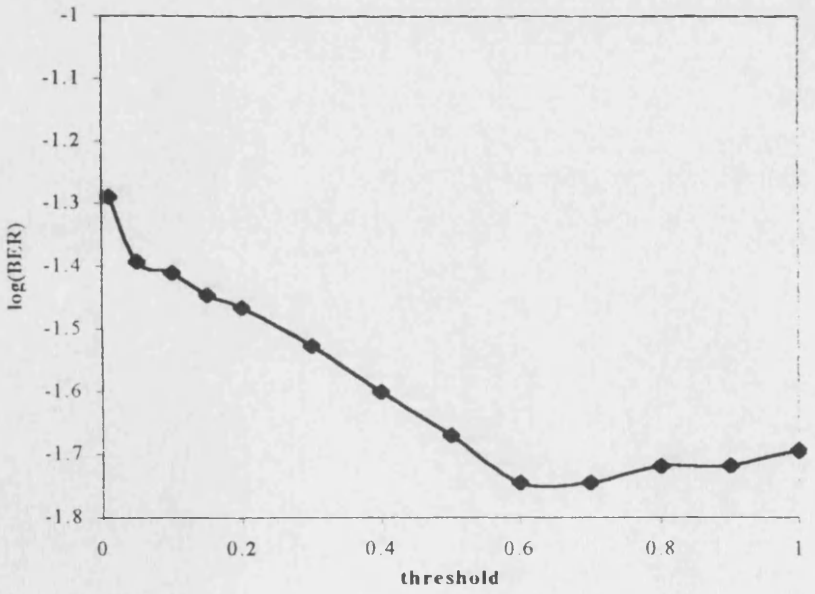

Figure 9. Optimum threshold value for controlled equalisation on initial detection